Lecture Notes for General Plasma Physics II

Matthew W. Kunz†

Department of Astrophysical Sciences, Princeton University, Peyton Hall, Princeton, NJ 08544
Princeton Plasma Physics Laboratory, PO Box 451, Princeton, NJ 08543

(compiled on 12 May 2026)

These are lecture notes for AST552: General Plasma Physics II, taught as part of the Program in Plasma Physics at Princeton University. Their creation has benefitted enormously from conversations with and lecture notes by Alex Schekochihin, Steve Balbus, Telemachos Mouschovias, Hantao Ji, Thomas Foster, and Rishin Madan. I am grateful to the Princeton graduate students who took this course in Spring 2026 and onwards for catching typos and suggesting places to improve the exposition.

These notes are continually undergoing edits, additions, and improvements, and are not guaranteed to be free of errors.

CONTENTS

† Email address for correspondence: mkunz@princeton.edu

PART I
Introduction

[in preparation]

PART II
Formulations of magnetohydrodynamics

To begin the course, we are going to obtain the equations of magnetohydrodynamics (MHD) three different ways. The first way will be via conservation laws and simple physical arguments. This way is the typical route to MHD via the theory of hydrodynamics, and should be familiar to you from GPPI. The second way will involve taking moments of the Vlasov–Landau equation and adopting certain assumptions to close the moment hierarchy that results. While less couched in physical reasoning, this route is useful because it better emphasizes the assumptions inherent to MHD. The third and final way will rely on a knowledge of charged particle drifts: we will make an explicit connection between guiding-center motion, particle drifts, and the momentum and induction equations of MHD, which unifies what the particles are doing with what the fluid elements are doing. Each route to the MHD equations has its utility.

II.1. Equations of hydrodynamics via conservation laws

This route uses things that every physicist should know: mass is conserved, Newton's second law (force equals mass times acceleration), and the first law of thermodynamics (energy is conserved).

II.1.1. *Mass is conserved: the continuity equation*

Consider a smooth gaseous fluid distributed according to its mass density ρ, which in general is a function of time t and position $\boldsymbol{r}$. Imagine an arbitrary fixed volume $\mathcal{V}$ enclosing some of that fluid. The mass inside of the volume is simply

$$M = \int_{\mathcal{V}} \mathrm{d}V\, \rho. \tag{II.1.1}$$

Now let's mathematize our intuition: within this fixed volume, the only way the enclosed mass can change is by material flowing in or out of its surface $\mathcal{S}$:

$$\frac{\mathrm{d}M}{\mathrm{d}t} \doteq \int_{\mathcal{V}} \mathrm{d}V\, \frac{\partial \rho}{\partial t} = -\int_{\mathcal{S}} \mathrm{d}\boldsymbol{S} \boldsymbol{\cdot} \rho \boldsymbol{u}, \tag{II.1.2}$$

where $\boldsymbol{u}$ is the flow velocity.

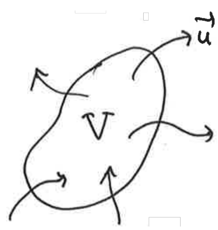

Gauss' theorem may be applied to rewrite the right-hand side of this equation as follows:

$$\int_{\mathcal{S}} \mathrm{d}\boldsymbol{S} \boldsymbol{\cdot} \rho \boldsymbol{u} = \int_{\mathcal{V}} \mathrm{d}V \, \boldsymbol{\nabla} \boldsymbol{\cdot} (\rho \boldsymbol{u}). \tag{II.1.3}$$

Because the volume under consideration is arbitrary, the integrands of the volume integrals in (II.1.2) and (II.1.3) must be the same. Therefore,

$$\boxed{\frac{\partial \rho}{\partial t} + \boldsymbol{\nabla} \boldsymbol{\cdot} (\rho \boldsymbol{u}) = 0} \tag{II.1.4}$$

This is the *continuity equation*; it's the differential form of mass conservation.

Exercise. Go to the bathroom and turn on the sink slowly to get a nice, laminar stream flowing down from the faucet. Go on, I'll wait. If you followed instructions, then you'll see that the stream becomes more narrow as it descends. Knowing that the density of water is very nearly constant, use the continuity equation to show that the cross-sectional area of the stream $A(z)$ as a function of distance from the faucet z is

$$A(z) = \frac{A_0}{\sqrt{1 + 2gz/v_0^2}},$$

where A_0 is the cross-sectional area of the stream upon exiting the faucet with velocity v_0 and g is the gravitational acceleration. If you turn the faucet to make the water flow faster, what happens to the tapering of the stream?

II.1.2. *Newton's second law: the momentum equation*

So far we have an equation for the evolution of the mass density ρ expressed in terms of the fluid velocity $\boldsymbol{u}$. How does the latter evolve? Newton's second law provides the answer: simply add up the accelerations, divide by the mass (density), and you've got the time rate of change of the velocity. But there is a subtlety here: there is a difference between the time rate of change of the velocity in the lab frame and the time rate of change of the velocity in the fluid frame. So which time derivative of $\boldsymbol{u}$ do we take? The key is in how the accelerations are expressed. Are these accelerations acting on a fixed point in space, or are they acting on an element of our fluid? It is much easier (and more physical) to think of these accelerations in the latter sense: given a deformable patch of the fluid – large enough in extent to contain a very large number of atoms but small enough that all the macroscopic variables such as density, velocity, and pressure have a unique value over the dimensions of the patch – what forces are acting on that patch? These are relatively simple to catalog, and we will do so in short order. But first, let's answer our original question: which time derivative of $\boldsymbol{u}$ do we take? Since we have committed to expressing the forces in the frame of the fluid element, the acceleration must likewise be expressed in this frame. The acceleration is *not*

$$\frac{\partial \boldsymbol{u}}{\partial t}. \tag{II.1.5}$$

Remember what a partial derivative means: something is being fixed! Here, it is the instantaneous position $\boldsymbol{r}$ of the fluid element. Equation (II.1.5) is the answer to the question, "how does the fluid velocity evolve at a fixed point in space?" Instead, we wish to fix our sights on the fluid element itself, which is moving. The acceleration we calculate must account for this frame transformation:

$$\boldsymbol{a} = \frac{\partial \boldsymbol{u}}{\partial t} + \frac{\mathrm{d}\boldsymbol{r}}{\mathrm{d}t} \boldsymbol{\cdot} \boldsymbol{\nabla} \boldsymbol{u}, \tag{II.1.6}$$

where $\mathrm{d}\boldsymbol{r}/\mathrm{d}t$ is the rate of change of the position of the fluid element, i.e., the velocity $\boldsymbol{u}(t,\boldsymbol{r})$. This combination of derivatives is so important that it has its own notation:

$$\frac{\mathrm{D}}{\mathrm{D}t} \doteq \frac{\partial}{\partial t} + \boldsymbol{u}\cdot\boldsymbol{\nabla}. \tag{II.1.7}$$

It is variously referred to as the *Lagrangian derivative*, or co-moving derivative, or convective derivative. By contrast, the expression given by (II.1.5) is the *Eulerian deriative*. Note that the continuity equation (II.1.4) may be expressed using the Lagrangian derivative as

$$\frac{\mathrm{D}\ln\rho}{\mathrm{D}t} = -\boldsymbol{\nabla}\cdot\boldsymbol{u}, \tag{II.1.8}$$

which states that incompressible flow corresponds to $\boldsymbol{\nabla}\cdot\boldsymbol{u} = 0$.

So, given some force $\boldsymbol{f}$ per unit volume that is acting on our fluid element, we now know how the fluid velocity evolves: force (per unit volume) equals mass (per unit volume) times acceleration (in the frame of the fluid element):

$$\boldsymbol{f} = \rho\frac{\mathrm{D}\boldsymbol{u}}{\mathrm{D}t}. \tag{II.1.9}$$

Now we need only catalog the relevant forces. This could be, say, gravity: $\rho\boldsymbol{g} = -\rho\boldsymbol{\nabla}\varPhi$. Or, if the fluid element is conducting, electromagnetic forces. But the most deserving of discussion at this point is the pressure force due to the internal thermal motions of the particles comprising the gas. For an ideal gas, the equation of state is

$$P = \frac{\rho k_{\mathrm{B}}T}{m} \doteq \rho C^2, \tag{II.1.10}$$

where T is the temperature in Kelvin, k_{B} is the Boltzmann constant, m is the mass per particle, and C is the speed of sound in an isothermal gas. Plasma physicists often drop Boltzmann's constant and register temperature in energy units (e.g., eV), and I will henceforth do the same in these notes. How does gas pressure due to microscopic particle motions exert a macroscopic force on a fluid element? First, the pressure must be spatially non-uniform: there must be more or less energetic content in the thermal motions of the particles in one region versus another, whether it be because the gas temperature varies in space or because there are more particles in one location as opposed to another. For example, the pressure force in the x direction in a slab of thickness $\mathrm{d}x$ and cross-sectional area $\mathrm{d}y\,\mathrm{d}z$ is

$$\big[P(t,x-\mathrm{d}x/2,y,z) - P(t,x+\mathrm{d}x/2,y,z)\big]\,\mathrm{d}y\,\mathrm{d}z = -\frac{\partial P}{\partial x}\,\mathrm{d}V. \tag{II.1.11}$$

Unless the thermal motions of the particles are not sufficiently randomized to be isotropic (e.g., if the collisional mean free path of the plasma is so long that inter-particle collisions cannot drive the system quickly enough towards local thermodynamic equilibrium), there is nothing particularly special about the x direction, and so the pressure force force acting on some differential volume $\mathrm{d}V$ is just $-\boldsymbol{\nabla}P\,\mathrm{d}V$.

Assembling the lessons we've learned here, we have the following force equation for our fluid:

$$\boxed{\rho\frac{\mathrm{D}\boldsymbol{u}}{\mathrm{D}t} \doteq \rho\left(\frac{\partial}{\partial t} + \boldsymbol{u}\cdot\boldsymbol{\nabla}\right)\boldsymbol{u} = -\boldsymbol{\nabla}P - \rho\boldsymbol{\nabla}\varPhi} \tag{II.1.12}$$

This equation is colloquially known as the *momentum equation*, even though it evolves the fluid velocity rather than its momentum density. To obtain an equation for the latter, the continuity equation (II.1.4) may be used to move the mass density into the time and space derivatives:

$$\frac{\partial(\rho\boldsymbol{u})}{\partial t} + \boldsymbol{\nabla\cdot}(\rho\boldsymbol{u}\boldsymbol{u}) = \frac{\partial\rho}{\partial t}\boldsymbol{u} + \rho\frac{\partial\boldsymbol{u}}{\partial t} + \rho\boldsymbol{u\cdot\nabla u} + \boldsymbol{\nabla\cdot}(\rho\boldsymbol{u})\boldsymbol{u}$$
$$= \left[\frac{\partial\rho}{\partial t} + \boldsymbol{\nabla\cdot}(\rho\boldsymbol{u})\right]\boldsymbol{u} + \rho\left(\frac{\partial}{\partial t} + \boldsymbol{u\cdot\nabla}\right)\boldsymbol{u}$$
$$= \left[\qquad 0 \qquad\right]\boldsymbol{u} + \rho\frac{\mathrm{D}\boldsymbol{u}}{\mathrm{D}t} = \boldsymbol{f}. \tag{II.1.13}$$

Thus, an equation for the momentum density:

$$\boxed{\frac{\partial(\rho\boldsymbol{u})}{\partial t} + \boldsymbol{\nabla\cdot}(\rho\boldsymbol{u}\boldsymbol{u}) = -\boldsymbol{\nabla}P - \rho\boldsymbol{\nabla}\Phi} \tag{II.1.14}$$

This form is particularly useful for deriving an evolution equation for the kinetic energy density. Dotting (II.1.14) with $\boldsymbol{u}$ and grouping terms,

$$\frac{\partial}{\partial t}\left(\frac{1}{2}\rho u^2\right) + \boldsymbol{\nabla\cdot}\left(\frac{1}{2}\rho u^2\boldsymbol{u}\right) = -\boldsymbol{u\cdot\nabla}P - \rho\boldsymbol{u\cdot\nabla}\Phi, \tag{II.1.15}$$

which is a statement that the kinetic energy of a fluid element changes as work is done by the forces.

Now, how do we know the pressure P? There's an equation for that...

II.1.3. *First law of thermodynamics: the internal energy equation*

There are several ways to go about obtaining an evolution equation for the pressure. One way is to introduce the *internal energy*,

$$e \doteq \frac{P}{\gamma - 1} \tag{II.1.16}$$

and use the first law of thermodynamics to argue that e is conserved but for $P\,\mathrm{d}V$ work:

$$\boxed{\frac{\partial e}{\partial t} + \boldsymbol{\nabla\cdot}(e\boldsymbol{u}) = -P\boldsymbol{\nabla\cdot u}} \tag{II.1.17}$$

This is the *internal energy* equation.

Yet another way of expressing the internal energy equation (II.1.17) is to write $e = \rho T/m(\gamma-1)$ and use the continuity equation (II.1.4) to eliminate the derivatives of the mass density. The result is

$$\frac{\mathrm{D}\ln T}{\mathrm{D}t} = -(\gamma-1)\boldsymbol{\nabla\cdot u}, \tag{II.1.18}$$

which states that the temperature of a fluid element is constant in an incompressible fluid (*viz.*, one with $\boldsymbol{\nabla\cdot u} = 0$). If this seems intuitively unfamiliar to you, consider this: the hydrodynamic entropy of a fluid element is given by

$$\sigma \doteq \frac{1}{\gamma-1}\ln P\rho^{-\gamma} = \frac{1}{\gamma-1}\ln T\rho^{1-\gamma}. \tag{II.1.19}$$

Taking the Lagrangian time derivative of the entropy along the path of a fluid element yields

$$\frac{\mathrm{D}\sigma}{\mathrm{D}t} = \frac{\mathrm{D}\ln T}{\mathrm{D}t} - (\gamma-1)\frac{\mathrm{D}\ln\rho}{\mathrm{D}t}. \tag{II.1.20}$$

It is then just a short trip back to (II.1.8) to see that (II.1.18) is, in fact, the second law of thermodynamics – entropy is conserved in the absence of sources or dissipative sinks:

$$\boxed{\frac{\mathrm{D}\sigma}{\mathrm{D}t} = 0} \tag{II.1.21}$$

In this sense, fluid elements in ideal hydrodynamics are thermodynamically isolated from one another.

II.1.4. *Total energy conservation*

Equation (II.1.17) may be used to derive a total (kinetic + internal + potential) energy equation for the fluid as follows. Do (II.1.15) + (II.1.17):

$$\begin{aligned}\frac{\partial}{\partial t}\left(\frac{1}{2}\rho u^2 + e\right) + \boldsymbol{\nabla}\cdot\left[\left(\frac{1}{2}\rho u^2 + e\right)\boldsymbol{u}\right] &= -\boldsymbol{\nabla}\cdot(P\boldsymbol{u}) - \rho\boldsymbol{u}\cdot\boldsymbol{\nabla}\varPhi,\\ &= -(\gamma-1)\boldsymbol{\nabla}\cdot(e\boldsymbol{u}) - \rho\boldsymbol{u}\cdot\boldsymbol{\nabla}\varPhi\end{aligned}$$

$$\implies \quad \frac{\partial}{\partial t}\left(\frac{1}{2}\rho u^2 + e\right) + \boldsymbol{\nabla}\cdot\left[\left(\frac{1}{2}\rho u^2 + \gamma e\right)\boldsymbol{u}\right] = -\rho\boldsymbol{u}\cdot\boldsymbol{\nabla}\varPhi. \tag{II.1.22}$$

Now use the continuity equation (II.1.4) to write

$$\frac{\partial(\rho\varPhi)}{\partial t} + \boldsymbol{\nabla}\cdot(\rho\varPhi\boldsymbol{u}) = \rho\boldsymbol{u}\cdot\boldsymbol{\nabla}\varPhi + \rho\frac{\partial\varPhi}{\partial t}. \tag{II.1.23}$$

Adding this equation to (II.1.22) yields the desired result:

$$\boxed{\frac{\partial}{\partial t}\left(\frac{1}{2}\rho u^2 + e + \rho\varPhi\right) + \boldsymbol{\nabla}\cdot\left[\left(\frac{1}{2}\rho u^2 + \gamma e + \rho\varPhi\right)\boldsymbol{u}\right] = \rho\frac{\partial\varPhi}{\partial t}} \tag{II.1.24}$$

The first term in parentheses under the time derivative is sometimes denoted by $\mathcal{E}$ – the total energy density of the system.

If the gravitational potential $\varPhi$ were due to self-gravity alone, then we could use Poisson's equation to perform the following manipulations to the gravitational energy density in (II.1.24)) and arrive at an equation for conservation of total energy:

$$\begin{aligned}\int \mathrm{d}\boldsymbol{r}\,\left[\text{LHS of (II.1.24)}\right] &= \frac{\mathrm{d}}{\mathrm{d}t}\int \mathrm{d}\boldsymbol{r}\,\left(\frac{1}{2}\rho u^2 + e + \rho\varPhi\right)\\ \int \mathrm{d}\boldsymbol{r}\,\left[\text{RHS of (II.1.24)}\right] &= \int \mathrm{d}\boldsymbol{r}\,\rho\frac{\partial\varPhi}{\partial t} = \int \mathrm{d}\boldsymbol{r}\,\rho(t,\boldsymbol{r})\,\frac{\partial}{\partial t}\left[-\mathrm{G}\int \mathrm{d}\boldsymbol{r}'\,\frac{\rho(t,\boldsymbol{r}')}{|\boldsymbol{r}-\boldsymbol{r}'|}\right]\\ &= -\mathrm{G}\int \mathrm{d}\boldsymbol{r}\int \mathrm{d}\boldsymbol{r}'\,\frac{\rho(t,\boldsymbol{r})}{|\boldsymbol{r}-\boldsymbol{r}'|}\frac{\partial\rho(t,\boldsymbol{r}')}{\partial t}\\ &= -\mathrm{G}\int \mathrm{d}\boldsymbol{r}'\int \mathrm{d}\boldsymbol{r}\,\frac{\rho(t,\boldsymbol{r}')}{|\boldsymbol{r}'-\boldsymbol{r}|}\frac{\partial\rho(t,\boldsymbol{r})}{\partial t} \quad \text{(switch } \boldsymbol{r} \text{ and } \boldsymbol{r}'\text{)}\\ &= \int \mathrm{d}\boldsymbol{r}\,\varPhi\frac{\partial\rho}{\partial t} = \frac{1}{2}\int \mathrm{d}\boldsymbol{r}\,\left(\varPhi\frac{\partial\rho}{\partial t} + \varPhi\frac{\partial\rho}{\partial t}\right) \quad \text{(symmetrize)}\\ &= \frac{1}{2}\int \mathrm{d}\boldsymbol{r}\,\left(\varPhi\frac{\partial\rho}{\partial t} + \rho\frac{\partial\varPhi}{\partial t}\right) = \frac{\mathrm{d}}{\mathrm{d}t}\int \mathrm{d}\boldsymbol{r}\,\frac{1}{2}\rho\varPhi.\end{aligned}$$

$$\implies \quad \boxed{\frac{\mathrm{d}\mathscr{E}}{\mathrm{d}t} \doteq \frac{\mathrm{d}}{\mathrm{d}t}\int \mathrm{d}\boldsymbol{r}\,\left(\frac{1}{2}\rho u^2 + e + \frac{1}{2}\rho\varPhi\right) = 0} \tag{II.1.25}$$

Note that the self-gravitational potential energy is negative:

$$\int \mathrm{d}\boldsymbol{r}\,\frac{1}{2}\rho\Phi = \int \mathrm{d}\boldsymbol{r}\,\frac{1}{2}\left(\frac{\nabla^2\Phi}{4\pi\mathrm{G}}\right)\Phi \overset{\text{bp}}{=} -\int \mathrm{d}\boldsymbol{r}\,\frac{1}{8\pi\mathrm{G}}\boldsymbol{\nabla}\Phi\boldsymbol{\cdot}\boldsymbol{\nabla}\Phi = -\int \mathrm{d}\boldsymbol{r}\,\frac{g^2}{8\pi\mathrm{G}} < 0,$$

where $\boldsymbol{g} = -\boldsymbol{\nabla}\Phi$ is the gravitational acceleration and $g \doteq |\boldsymbol{g}|$. Similar manipulations allow the gravitational force density in the momentum equation (II.1.14) to be written as a total momentum flux:

$$\begin{aligned}
\rho\boldsymbol{g} &= \left(-\frac{\boldsymbol{\nabla\cdot g}}{4\pi\mathrm{G}}\right)\boldsymbol{g} = -\frac{1}{4\pi\mathrm{G}}\Big[\boldsymbol{\nabla\cdot}(\boldsymbol{gg}) - \boldsymbol{g\cdot\nabla g}\Big] \\
&= -\frac{1}{4\pi\mathrm{G}}\left[\boldsymbol{\nabla\cdot}(\boldsymbol{gg}) - \frac{1}{2}\boldsymbol{\nabla}g^2\right] \quad \text{since } (\boldsymbol{g\cdot\nabla g})_i = g_k\partial_k(-\partial_i\Phi) = -g_k\partial_i\partial_k\Phi = g_k\partial_k g_k \\
&= \boldsymbol{\nabla\cdot}\left[\frac{1}{4\pi\mathrm{G}}\left(\frac{g^2}{2}\mathsf{\boldsymbol{I}} - \boldsymbol{gg}\right)\right] \doteq -\boldsymbol{\nabla\cdot}\boldsymbol{\mathcal{G}}
\end{aligned} \tag{II.1.26}$$

where $\mathsf{\boldsymbol{I}}$ is the unit dyadic. Thus,

$$\frac{\partial(\rho\boldsymbol{u})}{\partial t} = -\boldsymbol{\nabla\cdot}\left(\rho\boldsymbol{uu} + P\mathsf{\boldsymbol{I}} + \boldsymbol{\mathcal{G}}\right) \tag{II.1.27}$$

expresses conservation of momentum density.

Note that in all of these equations, we did not affix any species labels to any quantities, implicitly assuming that our hydrodynamics occurs on time scales much longer than the collisional equilibration times, so that all species are described by local Maxwellians with the same fluid velocities and scalar pressures. Not all terrestrial and astrophysical systems are so cooperative, and anisotropic pressures, velocity drifts between species, and dis-equilibration of species temperatures can often be the norm. You've been warned.

II.1.5. *The virial theorem*

Equation (II.1.27) is of the form

$$\frac{\partial(\rho\boldsymbol{u})}{\partial t} = -\boldsymbol{\nabla\cdot}\mathsf{\boldsymbol{T}}, \tag{II.1.28}$$

where $\mathsf{\boldsymbol{T}}$ is the total (Reynolds + pressure + gravitational) stress tensor. Let us use this tensor to figure out how the quantity

$$I = \int_{\mathcal{V}} \mathrm{d}\boldsymbol{r}\, r^2\rho \tag{II.1.29}$$

evolves. Namely, I is the moment of inertia of a continuum system with (fixed) volume $\mathcal{V}$, and which is subjected to stresses acting within its volume and on its surface $\mathcal{S}$:

$$\begin{aligned}
\frac{1}{2}\frac{\mathrm{d}^2 I}{\mathrm{d}t^2} &= \frac{1}{2}\int_{\mathcal{V}} \mathrm{d}\boldsymbol{r}\, r^2\frac{\partial^2\rho}{\partial t^2} = -\frac{1}{2}\int_{\mathcal{V}} \mathrm{d}\boldsymbol{r}\, r^2\frac{\partial}{\partial t}\boldsymbol{\nabla\cdot}(\rho\boldsymbol{u}) \overset{\text{bp}}{=} \int_{\mathcal{V}} \mathrm{d}\boldsymbol{r}\,\frac{\partial(\rho\boldsymbol{u})}{\partial t}\boldsymbol{\cdot r} \\
&= -\int_{\mathcal{V}} \mathrm{d}\boldsymbol{r}\,(\boldsymbol{\nabla\cdot}\mathsf{\boldsymbol{T}})\boldsymbol{\cdot r} = -\int_{\mathcal{V}} \mathrm{d}\boldsymbol{r}\,\big[\boldsymbol{\nabla\cdot}(\mathsf{\boldsymbol{T}}\boldsymbol{\cdot r}) - \mathsf{\boldsymbol{T}}\boldsymbol{:\nabla r}\big] \\
&= -\oint_{\mathcal{S}} \mathrm{d}\boldsymbol{S}\boldsymbol{\cdot}(\mathsf{\boldsymbol{T}}\boldsymbol{\cdot r}) + \int_{\mathcal{V}} \mathrm{d}\boldsymbol{r}\,\mathrm{tr}(\mathsf{\boldsymbol{T}}).
\end{aligned} \tag{II.1.30}$$

In order for the system to be in steady state, the stresses on the boundary must balance those acting on the volume:

$$\oint_{\mathcal{S}} \mathrm{d}\boldsymbol{S} \cdot (\boldsymbol{T} \cdot \boldsymbol{r}) = \int_{\mathcal{V}} \mathrm{d}\boldsymbol{r} \, \mathrm{tr}(\boldsymbol{T}) = \rho u^2 + 3P - \frac{g^2}{8\pi \mathrm{G}} \tag{II.1.31a}$$

$$\doteq 2\mathscr{E}_{\mathrm{kin}} + 3(\gamma - 1)\mathscr{E}_{\mathrm{th}} + \mathscr{E}_{\mathrm{grav}}, \tag{II.1.31b}$$

where we have introduced the total kinetic ($\mathscr{E}_{\mathrm{kin}}$), thermal ($\mathscr{E}_{\mathrm{th}}$), and gravitational ($\mathscr{E}_{\mathrm{grav}}$) energies. This steady-state system can only be self-confined – *viz.*, $\mathscr{E} < 0$ without any boundary stresses – if self-gravity is important. Indeed, setting (II.1.31b) to zero for self-confinement, the total energy can be made negative only via self-gravity:

$$\mathscr{E} = \mathscr{E}_{\mathrm{kin}} + \mathscr{E}_{\mathrm{th}} + \mathscr{E}_{\mathrm{grav}} = -\mathscr{E}_{\mathrm{kin}} - (3\gamma - 4)\mathscr{E}_{\mathrm{th}} < 0. \tag{II.1.32}$$

A weird consequence of this is that radiating stars heat up: as a star cools and loses pressure support, it must contract, but this contraction increases its gravitational potential energy (negatively), which in steady-state requires its thermal energy to increase. The result is that half of the radiated energy gets converted by gravitational contraction into thermal energy; put differently, self-gravitating systems have a negative heat capacity. Without self-gravity, the weighted sum of energies in (II.1.31b) is strictly positive, so confinement in this case requires stresses acting on the boundary of the system.

Magnetic fields will be added to this narrative in §II.3.7.

II.1.6. *Summary: adiabatic equations of hydrodynamics*

The adiabatic equations of hydrodynamics, written in conservative form, are:

$$\frac{\partial \rho}{\partial t} + \boldsymbol{\nabla} \cdot (\rho \boldsymbol{u}) = 0, \tag{II.1.33a}$$

$$\frac{\partial (\rho \boldsymbol{u})}{\partial t} + \boldsymbol{\nabla} \cdot (\rho \boldsymbol{u}\boldsymbol{u}) = -\boldsymbol{\nabla} P - \rho \boldsymbol{\nabla} \varPhi, \tag{II.1.33b}$$

$$\frac{\partial e}{\partial t} + \boldsymbol{\nabla} \cdot (e \boldsymbol{u}) = -P \boldsymbol{\nabla} \cdot \boldsymbol{u}. \tag{II.1.33c}$$

The left-hand sides of these equations express advection of, respectively, the mass density, the momentum density, and the internal energy density by the fluid velocity; the right-hand sides represents sources and sinks. If we instead write these equations in terms of the density, fluid velocity, and entropy and make use of the Lagrangian derivative (II.1.7), we have

$$\frac{\mathrm{D}\rho}{\mathrm{D}t} = -\rho \boldsymbol{\nabla} \cdot \boldsymbol{u}, \tag{II.1.34a}$$

$$\frac{\mathrm{D}\boldsymbol{u}}{\mathrm{D}t} = -\frac{1}{\rho} \boldsymbol{\nabla} P - \boldsymbol{\nabla} \varPhi, \tag{II.1.34b}$$

$$\frac{\mathrm{D}\sigma}{\mathrm{D}t} = 0, \tag{II.1.34c}$$

where $\sigma \doteq (\gamma - 1)^{-1} \ln P\rho^{-\gamma}$. The limit $\gamma \to \infty$, often of utility for describing liquids, corresponds to $\mathrm{D}\rho/\mathrm{D}t = 0$, i.e., incompressibility.

II.2. Mathematical matters

Theoretical investigations of fluid dynamics necessitate a working knowledge of vector calculus, and so we pause here briefly to review a few mathematical matters that will come in handy.

II.2.1. *Vector identities*

As a start to this section, let me advise you to brush up on your vector calculus...

$$
\begin{aligned}
\boldsymbol{A}\cdot(\boldsymbol{B}\times\boldsymbol{C}) &= \boldsymbol{B}\cdot(\boldsymbol{C}\times\boldsymbol{A}) = \boldsymbol{C}\cdot(\boldsymbol{A}\times\boldsymbol{B}),\\
\boldsymbol{A}\times(\boldsymbol{B}\times\boldsymbol{C}) &= \boldsymbol{B}(\boldsymbol{A}\cdot\boldsymbol{C}) - \boldsymbol{C}(\boldsymbol{A}\cdot\boldsymbol{B}),\\
\boldsymbol{\nabla}\cdot(\boldsymbol{A}\times\boldsymbol{B}) &= \boldsymbol{B}\cdot(\boldsymbol{\nabla}\times\boldsymbol{A}) - \boldsymbol{A}\cdot(\boldsymbol{\nabla}\times\boldsymbol{B}),\\
\boldsymbol{\nabla}\times(\boldsymbol{A}\times\boldsymbol{B}) &= (\boldsymbol{B}\cdot\boldsymbol{\nabla})\boldsymbol{A} - (\boldsymbol{A}\cdot\boldsymbol{\nabla})\boldsymbol{B} - \boldsymbol{B}(\boldsymbol{\nabla}\cdot\boldsymbol{A}) + \boldsymbol{A}(\boldsymbol{\nabla}\cdot\boldsymbol{B}),\\
\boldsymbol{A}\times(\boldsymbol{\nabla}\times\boldsymbol{B}) + \boldsymbol{B}\times(\boldsymbol{\nabla}\times\boldsymbol{A}) &= \boldsymbol{\nabla}(\boldsymbol{A}\cdot\boldsymbol{B}) - (\boldsymbol{A}\cdot\boldsymbol{\nabla})\boldsymbol{B} - (\boldsymbol{B}\cdot\boldsymbol{\nabla})\boldsymbol{A},\\
&\dots
\end{aligned}
$$

Fluid dynamics is full of these things, and you should either (i) commit them to memory, (ii) carry your NRL formulary with you everywhere, or (iii) know how to quickly derive them using things like

$$\epsilon_{kij}\epsilon_{k\ell m} = \delta_{i\ell}\delta_{jm} - \delta_{im}\delta_{j\ell},$$

where δ_{ij} is the Kronecker delta and ϵ_{ijk} is the Levi–Civita symbol.

II.2.2. *Leibniz's rule and the Lagrangian derivative of integrals*

In the proofs of many conservation laws, a Lagrangian time derivative is taken of a surface or volume integral whose integration limits are time-dependent. In this case, $\mathrm{D}/\mathrm{D}t$ does *not* commute with the integral sign. The trick to dealing with these situations is related to Leibniz's rule:

$$\frac{\mathrm{d}}{\mathrm{d}t}\int_{a(t)}^{b(t)}\mathrm{d}x\, f(t,x) = \int_{a(t)}^{b(t)}\mathrm{d}x\,\frac{\partial}{\partial t}f(t,x) + f(t,b(t))\frac{\mathrm{d}b}{\mathrm{d}t} - f(t,a(t))\frac{\mathrm{d}a}{\mathrm{d}t}. \tag{II.2.1}$$

The integral of a function can change in time because the end points of the integral move. In three dimensions, if we're taking the time derivative of a volume integral whose integration limits $\mathcal{V}(t)$ are time-dependent, the generalization of the above is

$$\frac{\mathrm{d}}{\mathrm{d}t}\int_{\mathcal{V}(t)}\mathrm{d}V\, f(t,\boldsymbol{r}) = \int_{\mathcal{V}(t)}\mathrm{d}V\,\frac{\partial}{\partial t}f(t,\boldsymbol{r}) + \oint_{\mathcal{S}(t)}\mathrm{d}\boldsymbol{S}\cdot\bigl[f(t,\boldsymbol{r})\boldsymbol{u}_{\mathrm{b}}(t,\boldsymbol{r})\bigr], \tag{II.2.2}$$

where $\boldsymbol{u}_{\mathrm{b}}$ is the velocity of the bounding surface $\mathcal{S}(t)$. This is known as the Reynolds transport theorem. In words, the time rate-of-change of a quantity positioned within a moving volume is a combination of the lab-frame rate-of-change of that quantity (i.e., the time derivative at fixed position $\boldsymbol{r}$ – note the partial derivative) and how much of that quantity flowed through the surface. When the velocity of the bounding surface equals the fluid velocity, $\boldsymbol{u}_{\mathrm{b}} = \boldsymbol{u}(t,\boldsymbol{r})$, so that each moving volume corresponds to that of a fluid element, we may replace $\mathrm{d}/\mathrm{d}t$ in (II.2.2) with the Lagrangian derivative $\mathrm{D}/\mathrm{D}t$:

$$\boxed{\frac{\mathrm{D}}{\mathrm{D}t}\int_{\mathcal{V}(t)}\mathrm{d}V\, f(t,\boldsymbol{r}) = \int_{\mathcal{V}(t)}\mathrm{d}V\,\frac{\partial}{\partial t}f(t,\boldsymbol{r}) + \oint_{\mathcal{S}(t)}\mathrm{d}\boldsymbol{S}\cdot\bigl[f(t,\boldsymbol{r})\boldsymbol{u}(t,\boldsymbol{r})\bigr]} \tag{II.2.3}$$

You've already encountered an example of this – mass conservation, in which the volume was a "material volume" moving with the fluid element itself:

$$0 = \frac{\mathrm{D}M}{\mathrm{D}t} \doteq \frac{\mathrm{D}}{\mathrm{D}t}\int_{\mathcal{V}(t)}\mathrm{d}V\,\rho = \int_{\mathcal{V}(t)}\mathrm{d}V\,\frac{\partial\rho}{\partial t} + \oint_{\mathcal{S}(t)}\mathrm{d}\boldsymbol{S}\cdot(\rho\boldsymbol{u}).$$

Using the divergence theorem on the final (surface-integral) term gives

$$0 = \int_{\mathcal{V}(t)}\mathrm{d}V\left[\frac{\partial\rho}{\partial t} + \boldsymbol{\nabla}\cdot(\rho\boldsymbol{u})\right],$$

which provides us with our continuity equation.

A similar rule to (II.2.3) is needed for time derivatives of surface integrals whose integration limits $\mathcal{S}(t)$ are time-dependent. For a vector field $\boldsymbol{F} = \boldsymbol{F}(t, \boldsymbol{r})$ and a bounding surface $\mathcal{S}(t)$ whose contour $\partial\mathcal{S}(t)$ moves with the fluid velocity $\boldsymbol{u} = \boldsymbol{u}(t, \boldsymbol{r})$, this is given by

$$\boxed{\frac{\mathrm{D}}{\mathrm{D}t}\int_{\mathcal{S}(t)} \mathrm{d}\boldsymbol{S}\cdot\boldsymbol{F} = \int_{\mathcal{S}(t)} \mathrm{d}\boldsymbol{S}\cdot\left[\frac{\partial \boldsymbol{F}}{\partial t} + (\boldsymbol{\nabla}\cdot\boldsymbol{F})\boldsymbol{u}\right] - \oint_{\partial\mathcal{S}(t)} \mathrm{d}\boldsymbol{\ell}\cdot(\boldsymbol{u}\times\boldsymbol{F})} \tag{II.2.4}$$

(By convention, the contour is taken in the counter-clockwise direction.) Note that $-\mathrm{d}\boldsymbol{\ell}\cdot(\boldsymbol{u}\times\boldsymbol{F}) = \boldsymbol{F}\cdot(\boldsymbol{u}\times\mathrm{d}\boldsymbol{\ell})$. In words, the co-moving change of the differential surface element $\mathrm{d}\boldsymbol{S}$ equals the amount of area swept out in a time $\mathrm{d}t$ via the advection of a differential line element $\mathrm{d}\boldsymbol{\ell}$ on $\partial\mathcal{S}$ by a distance $\boldsymbol{u}\,\mathrm{d}t$:

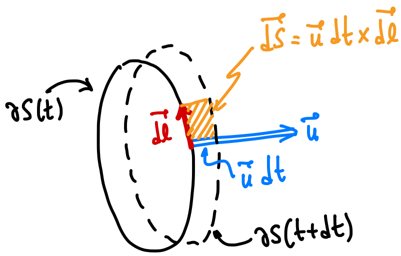

Equation (II.2.4) can be used to prove conservation of fluid vorticity (§II.2.5) and conservation of magnetic flux (§II.3.4).

II.2.3. $\boldsymbol{u}\cdot\boldsymbol{\nabla}\boldsymbol{u}$ *and curvilinear coordinates*

The nonlinear combination $\boldsymbol{u}\cdot\boldsymbol{\nabla}\boldsymbol{u}$ that features prominently in the Lagrangian time derivative can be complicated, particularly in curvilinear coordinates where the gradient operator within it acts on the unit vectors within $\boldsymbol{u}$. For example, in cylindrical coordinates (R, φ, z),

$$\begin{aligned}\boldsymbol{u}\cdot\boldsymbol{\nabla}\boldsymbol{u} &= \boldsymbol{u}\cdot\boldsymbol{\nabla}\big(u_R\hat{\boldsymbol{R}} + u_\varphi\hat{\boldsymbol{\varphi}} + u_z\hat{\boldsymbol{z}}\big)\\ &= (\boldsymbol{u}\cdot\boldsymbol{\nabla}u_R)\hat{\boldsymbol{R}} + (\boldsymbol{u}\cdot\boldsymbol{\nabla}u_\varphi)\hat{\boldsymbol{\varphi}} + (\boldsymbol{u}\cdot\boldsymbol{\nabla}u_z)\hat{\boldsymbol{z}} + \frac{u_\varphi^2}{R}\frac{\partial\hat{\boldsymbol{\varphi}}}{\partial\varphi} + \frac{u_R u_\varphi}{R}\frac{\partial\hat{\boldsymbol{R}}}{\partial\varphi}\\ &= (\boldsymbol{u}\cdot\boldsymbol{\nabla}u_i)\hat{\boldsymbol{e}}_i - \frac{u_\varphi^2}{R}\hat{\boldsymbol{R}} + \frac{u_R u_\varphi}{R}\hat{\boldsymbol{\varphi}},\end{aligned} \tag{II.2.5}$$

where, to obtain the final equality, we have used $\partial\hat{\boldsymbol{\varphi}}/\partial\varphi = -\hat{\boldsymbol{R}}$ and $\partial\hat{\boldsymbol{R}}/\partial\varphi = \hat{\boldsymbol{\varphi}}$; summation over the repeated index i is implied in the first term in the final line. A similar calculation in spherical coordinates (r, θ, φ) yields

$$\begin{aligned}\boldsymbol{u}\cdot\boldsymbol{\nabla}\boldsymbol{u} &= \left(u_r\frac{\partial}{\partial r} + \frac{u_\theta}{r}\frac{\partial}{\partial\theta} + \frac{u_\varphi}{r\sin\theta}\frac{\partial}{\partial\varphi}\right)\left(u_r\hat{\boldsymbol{r}} + u_\theta\hat{\boldsymbol{\theta}} + u_\varphi\hat{\boldsymbol{\varphi}}\right)\\ &= (\boldsymbol{u}\cdot\boldsymbol{\nabla}u_i)\hat{\boldsymbol{e}}_i - \frac{u_\theta^2 + u_\varphi^2}{r}\hat{\boldsymbol{r}} + \left(\frac{u_r u_\theta}{r} - \frac{u_\varphi^2\cot\theta}{r}\right)\hat{\boldsymbol{\theta}} + \left(\frac{u_\theta u_\varphi\cot\theta}{r} + \frac{u_r u_\varphi}{r}\right)\hat{\boldsymbol{\varphi}}\end{aligned} \tag{II.2.6}$$

The last two terms in the cylindrical $\boldsymbol{u}\cdot\boldsymbol{\nabla}\boldsymbol{u}$, equation (II.2.5), might look familiar to you from working in rotating frames. Indeed, let us write $\boldsymbol{u} = \boldsymbol{v} + R\Omega(R, z)\hat{\boldsymbol{\varphi}}$, where Ω

is an angular velocity, and substitute this decomposition into (II.2.5):

$$
\begin{aligned}
\boldsymbol{u}\cdot\boldsymbol{\nabla}\boldsymbol{u} &= \bigl[(\boldsymbol{v}+R\Omega\hat{\boldsymbol{\varphi}})\cdot\boldsymbol{\nabla}v_i\bigr]\hat{\boldsymbol{e}}_i + \bigl[(\boldsymbol{v}+R\Omega\hat{\boldsymbol{\varphi}})\cdot\boldsymbol{\nabla}(R\Omega)\bigr]\hat{\boldsymbol{\varphi}} \\
&\quad - \frac{(v_\varphi+R\Omega)^2}{R}\hat{\boldsymbol{R}} + \frac{v_R(v_\varphi+R\Omega)}{R}\hat{\boldsymbol{\varphi}} \\
&= \left[\left(\boldsymbol{v}\cdot\boldsymbol{\nabla}+\Omega\frac{\partial}{\partial\varphi}\right)v_i\right]\hat{\boldsymbol{e}}_i + \left[2\Omega\hat{\boldsymbol{z}}\times\boldsymbol{v} - R\Omega^2\hat{\boldsymbol{R}} + R\hat{\boldsymbol{\varphi}}(\boldsymbol{v}\cdot\boldsymbol{\nabla})\Omega\right] \\
&\quad + \left[\frac{v_R v_\varphi}{R}\hat{\boldsymbol{\varphi}} - \frac{v_\varphi^2}{R}\hat{\boldsymbol{R}}\right].
\end{aligned} \tag{II.2.7}
$$

Each of these terms has a straightforward physical interpretation. The first term in brackets represents advection by the flow and the rotation. The second term in brackets contains the Coriolis force, the centrifugal force, and “tidal” terms due to the differential rotation, in that order. (The “tidal” terms can be thought of the fictitious acceleration required for a fluid element to maintain its presence in the local rotating frame as it is displaced radially or vertically. They come from Taylor expanding the angular velocity about a point in the disk.) The third and final term is brackets are curvature terms due to the cylindrical geometry.

Exercise: Show that the $R\varphi$-component in cylindrical coordinates of the rate-of-strain tensor

$$W_{ij} \doteq \frac{\partial u_i}{\partial x_j} + \frac{\partial u_j}{\partial x_i} - \frac{2}{3}\delta_{ij}\frac{\partial u_k}{\partial x_k}$$

is given by

$$W_{R\varphi} = \frac{1}{R}\frac{\partial u_R}{\partial\varphi} + R\frac{\partial}{\partial R}\frac{u_\varphi}{R}.$$

Hint: $\partial u_i/\partial x_j = [(\hat{\boldsymbol{e}}_j\cdot\boldsymbol{\nabla})\boldsymbol{u}]\cdot\hat{\boldsymbol{e}}_i$ is coordinate invariant.

II.2.4. *Rotating reference frames*

The final calculation in the preceding section provides a natural segue into a discussion of fluid dynamics in rotating reference frames. To begin this discussion, let us first recall equation (II.2.5), in which the nonlinearity $\boldsymbol{u}\cdot\boldsymbol{\nabla}\boldsymbol{u}$ was written out in cylindrical coordinates for a fluid velocity $\boldsymbol{u}$ consisting of a cylindrical rotation $R\Omega\hat{\boldsymbol{\varphi}}$ with angular velocity $\Omega=\Omega(R,z)$ and a residual velocity $\boldsymbol{v}\doteq\boldsymbol{u}-R\Omega\hat{\boldsymbol{\varphi}}$:

$$
\begin{aligned}
\boldsymbol{u}\cdot\boldsymbol{\nabla}\boldsymbol{u} &= \left[\left(\boldsymbol{v}\cdot\boldsymbol{\nabla}+\Omega\frac{\partial}{\partial\varphi}\right)v_i\right]\hat{\boldsymbol{e}}_i + \left[2\Omega\hat{\boldsymbol{z}}\times\boldsymbol{v} - R\Omega^2\hat{\boldsymbol{R}} + R\hat{\boldsymbol{\varphi}}(\boldsymbol{v}\cdot\boldsymbol{\nabla})\Omega\right] \\
&\quad + \left[\frac{v_R v_\varphi}{R}\hat{\boldsymbol{\varphi}} - \frac{v_\varphi^2}{R}\hat{\boldsymbol{R}}\right].
\end{aligned}
$$

When this expansion was introduced in §II.2, each of its components were described physically: “The first term in brackets represents advection by the flow and the rotation. The second term in brackets contains the Coriolis force, the centrifugal force, and ‘tidal’ terms due to the differential rotation. . . The third and final term in brackets captures curvature effects due to the cylindrical geometry.” Let’s see these terms in action.

Using (II.2.5), we may express the equations of hydrodynamics (II.1.34) in cylindrical coordinates in a frame co-moving with the differential rotation. With

$$\frac{\mathrm{D}}{\mathrm{D}t} \to \frac{\partial}{\partial t} + \boldsymbol{v}\cdot\boldsymbol{\nabla} + \Omega\frac{\partial}{\partial\varphi} \tag{II.2.8}$$

to include advection by the rotation, we have

$$\frac{\mathrm{D}\rho}{\mathrm{D}t} = -\rho\boldsymbol{\nabla}\boldsymbol{\cdot}\boldsymbol{v}, \tag{II.2.9a}$$

$$\frac{\mathrm{D}v_R}{\mathrm{D}t} = \frac{1}{\rho}f_R + 2\Omega v_\varphi + R\Omega^2 + \frac{v_\varphi^2}{R}, \tag{II.2.9b}$$

$$\frac{\mathrm{D}v_\varphi}{\mathrm{D}t} = \frac{1}{\rho}f_\varphi - \frac{\kappa^2}{2\Omega}v_R - R\frac{\partial\Omega}{\partial z}v_z - \frac{v_R v_\varphi}{R}, \tag{II.2.9c}$$

$$\frac{\mathrm{D}v_z}{\mathrm{D}t} = \frac{1}{\rho}f_z, \tag{II.2.9d}$$

$$\frac{\mathrm{D}\sigma}{\mathrm{D}t} = 0, \tag{II.2.9e}$$

where

$$\boldsymbol{f} = -\boldsymbol{\nabla}P - \rho\boldsymbol{\nabla}\Phi \tag{II.2.10}$$

and the combination

$$\boxed{\kappa^2 \doteq 4\Omega^2 + \frac{\partial\Omega^2}{\partial\ln R} = \frac{1}{R^3}\frac{\partial(R^4\Omega^2)}{\partial R}} \tag{II.2.11}$$

is known as the (square of the) epicyclic frequency. Note that $R^4\Omega^2 = \ell^2$, the square of the specific angular momentum ℓ, and so κ^2 measures how much the specific angular momentum associated with the rotation increases or decreases outwards. For Keplerian rotation, $\kappa^2 = \Omega^2$.

In §IV.2, these equations will be used to obtain the so-called thermal wind equation, which describes the relationship between differential rotation and thermal stratification in steady state. They will also be used in §V.6 to investigate Rossby waves and inertial waves in rotating systems. In §II.3.8, these equations will be modified for the presence and evolution of magnetic fields, which will ultimately facilitate a derivation of the magnetorotational instability in §VI.8. Before moving on, however, there is one consequence of rotational flow that is worth mentioning at this point.

II.2.5. *Vorticity and circulation theorems*

With some vector identities in hand, let's take the curl of the force equation (II.1.34b):

$$\boldsymbol{\nabla}\times\left(\frac{\mathrm{D}\boldsymbol{u}}{\mathrm{D}t} = -\frac{1}{\rho}\boldsymbol{\nabla}P - \boldsymbol{\nabla}\Phi\right).$$

The potential term vanishes, since the curl of a gradient is zero. Likewise, the pressure term becomes

$$-\boldsymbol{\nabla}\frac{1}{\rho}\times\boldsymbol{\nabla}P = \frac{1}{\rho^2}\boldsymbol{\nabla}\rho\times\boldsymbol{\nabla}P.$$

As for the left-hand side, the gradient operator commutes with $\partial/\partial t$, but not with $\boldsymbol{u}\boldsymbol{\cdot}\boldsymbol{\nabla}$. Instead,

$$\boldsymbol{\nabla}\times\big[(\boldsymbol{u}\boldsymbol{\cdot}\boldsymbol{\nabla})\boldsymbol{u}\big] = \boldsymbol{\nabla}\times\left[\frac{1}{2}\boldsymbol{\nabla}u^2 - \boldsymbol{u}\times(\boldsymbol{\nabla}\times\boldsymbol{u})\right] = -\boldsymbol{\nabla}\times(\boldsymbol{u}\times\boldsymbol{\omega}),$$

where

$$\boldsymbol{\omega} \doteq \boldsymbol{\nabla}\times\boldsymbol{u} \tag{II.2.12}$$

is the *fluid vorticity*. The vorticity measures how much rotation a velocity field has (and its direction). Note that it is divergence free, which means that vortex lines cannot end within the fluid – they must either close on themselves (like a smoke ring) or intersect a boundary (like a tornado). Any fresh vortex lines that are made must be created as continuous curves that grow out of points or lines where the vorticity vanishes.

Assembling the above gives the *vorticity equation*,

$$\frac{\partial \boldsymbol{\omega}}{\partial t} - \boldsymbol{\nabla} \times (\boldsymbol{u} \times \boldsymbol{\omega}) = \frac{1}{\rho^2} \boldsymbol{\nabla} \rho \times \boldsymbol{\nabla} P. \tag{II.2.13}$$

Note that the right-hand side of this equation vanishes if the pressure is *barotropic*, i.e., if $P = P(\rho)$, so that surfaces of constant density and constant pressure coincide. If these surfaces do not coincide, then the fluid is said to have "baroclinicity" or to be "baroclinic". I'll demonstrate below using mathematics what (II.2.13) means physically, but you already know what the right-hand side means if you pay attention to the weather: areas of high atmospheric baroclinicity have frequent hurricanes and cyclones. In the parlance of fluid dynamics, this is called "baroclinic forcing". Now back to the math...

Dot (II.2.13) into a differential surface element $\mathrm{d}\boldsymbol{S}$ normal to the surface $\mathcal{S}$ of a fluid element, integrate over that surface, and use Stokes' theorem to replace the surface integral of a curl with a line integral over the surface boundary $\partial\mathcal{S}$:

$$\int_{\mathcal{S}} \frac{\partial \boldsymbol{\omega}}{\partial t} \cdot \mathrm{d}\boldsymbol{S} - \oint_{\partial\mathcal{S}} (\boldsymbol{u} \times \boldsymbol{\omega}) \cdot \mathrm{d}\boldsymbol{\ell} = \oint_{\partial\mathcal{S}} \left(-\frac{1}{\rho} \boldsymbol{\nabla} P \right) \cdot \mathrm{d}\boldsymbol{\ell} = -\oint_{\partial\mathcal{S}} \frac{\mathrm{d}P}{\rho}.$$

Using (II.2.4) to replace the left-hand side by the Lagrangian time derivative of $\boldsymbol{\omega} \cdot \mathrm{d}\boldsymbol{S}$ yields

$$\frac{\mathrm{D}}{\mathrm{D}t} \int_{\mathcal{S}} \boldsymbol{\omega} \cdot \mathrm{d}\boldsymbol{S} = -\oint_{\partial\mathcal{S}} \frac{\mathrm{d}P}{\rho}. \tag{II.2.14}$$

The surface integral on the left-hand side of this equation may be expressed using Stokes' theorem as the *circulation* $\mathit{\Gamma}$:

$$\int_{\mathcal{S}} \boldsymbol{\omega} \cdot \mathrm{d}\boldsymbol{S} = \oint_{\partial\mathcal{S}} \boldsymbol{u} \cdot \mathrm{d}\boldsymbol{\ell} \doteq \mathit{\Gamma}. \tag{II.2.15}$$

The circulation around the boundary $\partial\mathcal{S}$ can be thought of as the number of vortex lines that thread the enclosed area $\mathcal{S}$. Equation (II.2.14) then states that the circulation is conserved if the fluid is barotropic – Kelvin's circulation theorem:[1]

$$\boxed{\frac{\mathrm{D}\mathit{\Gamma}}{\mathrm{D}t} = -\oint_{\partial\mathcal{S}} \frac{\mathrm{d}P}{\rho} = 0 \quad \text{if } P = P(\rho)} \tag{II.2.16}$$

The figure below illustrates how baroclinic forcing generates vorticity.

[1]The above manipulations require that the surface is simply connected – that is, the region must be such that we can shrink the contour to a point without leaving the region. A region with a hole (like a bathtub drain) is not simply connected.

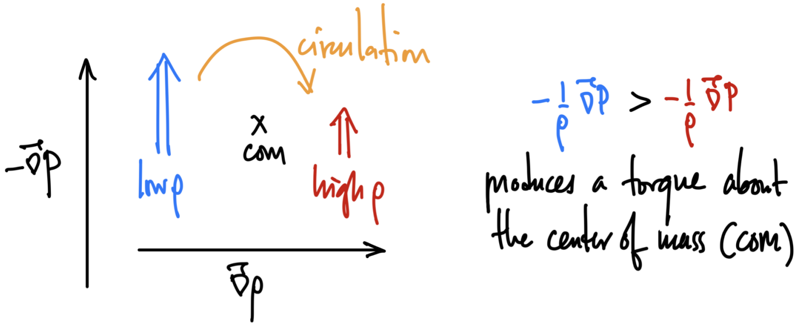

Another approach to proving (II.2.16) is to work with $\Gamma = \oint_{\partial\mathcal{S}} \boldsymbol{u}\cdot \mathrm{d}\boldsymbol{\ell}$ rather than $\int_{\mathcal{S}} \boldsymbol{\omega}\cdot\mathrm{d}\boldsymbol{S}$ and use the following for how an advected line element of $\partial\mathcal{S}$ changes in time:

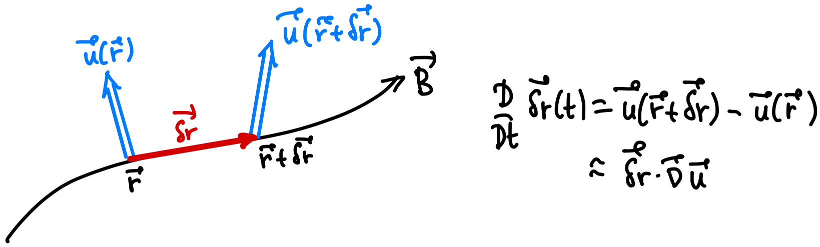

Exercise. The helicity of a region of fluid is defined to be $\mathcal{H} \doteq \int_{\mathcal{V}} \mathrm{d}V\, \boldsymbol{\omega}\cdot\boldsymbol{u}$, where the integral is taken over the volume of that region. Assume that $\Gamma = \text{const}$ and that $\boldsymbol{\omega}\cdot\hat{\boldsymbol{n}}$ vanishes when integrated over the surface bounding $\mathcal{V}$, where $\hat{\boldsymbol{n}}$ is the unit normal to that surface. Prove that the helicity $\mathcal{H}$ is conserved in a frame moving with the fluid, *viz.* $\mathrm{D}\mathcal{H}/\mathrm{D}t = 0$. Note that the fluid need not be incompressible for this property to hold.

The calculation leading to (II.2.16) can be repeated in a reference frame rotating at a constant angular velocity $\boldsymbol{\Omega}$, in which the fluid velocity is measured to be $\boldsymbol{v} = \boldsymbol{u} - \boldsymbol{\Omega}\times\boldsymbol{r}$ (here, $\boldsymbol{u}$ is the fluid velocity in the inertial frame; see §II.2.3). The associated vorticity in this rotating frame is

$$\boldsymbol{\omega}_{\mathrm{rot}} = \boldsymbol{\omega} - \boldsymbol{\nabla}\times(\boldsymbol{\Omega}\times\boldsymbol{r}) = \boldsymbol{\omega} - \boldsymbol{\Omega}(\boldsymbol{\nabla}\cdot\boldsymbol{r}) + (\boldsymbol{\Omega}\cdot\boldsymbol{\nabla})\boldsymbol{r} = \boldsymbol{\omega} - 3\boldsymbol{\Omega} + \boldsymbol{\Omega} = \boldsymbol{\omega} - 2\boldsymbol{\Omega}, \tag{II.2.17}$$

where $\boldsymbol{\omega} = \boldsymbol{\nabla}\times\boldsymbol{u}$. The circulation in the rotating reference frame is then given by

$$\begin{aligned}\Gamma_{\mathrm{rot}} &= \int_{\mathcal{S}} \boldsymbol{\omega}_{\mathrm{rot}}\cdot\mathrm{d}\boldsymbol{S} = \int_{\mathcal{S}} (\boldsymbol{\omega} - 2\boldsymbol{\Omega})\cdot\mathrm{d}\boldsymbol{S} \\ &= \oint_{\partial\mathcal{S}} \boldsymbol{u}\cdot\mathrm{d}\boldsymbol{\ell} - \int_{\mathcal{S}} 2\boldsymbol{\Omega}\cdot\mathrm{d}\boldsymbol{S} \\ &= \Gamma - \int_{\mathcal{S}} 2\boldsymbol{\Omega}\cdot\mathrm{d}\boldsymbol{S}. \end{aligned}\tag{II.2.18}$$

Kelvin's circulation theorem in this rotating frame is therefore

$$\frac{\mathrm{D}\Gamma_{\mathrm{rot}}}{\mathrm{D}t} = -\oint_{\partial\mathcal{S}} \frac{\mathrm{d}P}{\rho} - 2\Omega\frac{\mathrm{D}\mathcal{S}_{\mathrm{n}}}{\mathrm{D}t}, \tag{II.2.19}$$

where $\mathcal{S}_{\mathrm{n}}$ is component of the surface area oriented normally to $\boldsymbol{\Omega}$. In words, if the projected area of the vortex tube in the plane perpendicular to the rotation vector changes, then the circulation in the rotating frame must change to compensate (Bjerknes' circulation theorem). This is the origin of Rossby waves, something that will be discussed further in §V.6.

Finally, the *potential vorticity*

$$\mathrm{PV} \doteq \frac{\boldsymbol{\omega}}{\rho}\cdot\boldsymbol{\nabla}\sigma \tag{II.2.20}$$

is a conserved pseudoscalar even in the presence of baroclinic forcing:

$$\begin{aligned}\frac{\mathrm{D(PV)}}{\mathrm{D}t} &= -\mathrm{PV}\,\frac{\mathrm{D}\ln\rho}{\mathrm{D}t} + \frac{1}{\rho}\frac{\partial\boldsymbol{\omega}}{\partial t}\cdot\boldsymbol{\nabla}\sigma + \frac{\boldsymbol{\omega}}{\rho}\cdot\boldsymbol{\nabla}\frac{\partial\sigma}{\partial t} + \frac{\boldsymbol{u}}{\rho}\cdot\boldsymbol{\nabla}(\boldsymbol{\omega}\cdot\boldsymbol{\nabla}\sigma)\\
&= \mathrm{PV}\,\boldsymbol{\nabla}\cdot\boldsymbol{u} + \frac{1}{\rho}\left[\boldsymbol{\nabla}\times(\boldsymbol{u}\times\boldsymbol{\omega}) + \frac{1}{\rho^2}\boldsymbol{\nabla}\rho\times\boldsymbol{\nabla}P\right]\cdot\boldsymbol{\nabla}\sigma + \frac{\boldsymbol{\omega}}{\rho}\cdot\boldsymbol{\nabla}(-\boldsymbol{u}\cdot\boldsymbol{\nabla}\sigma)\\
&\quad + \frac{\boldsymbol{u}}{\rho}\cdot\boldsymbol{\nabla}(\boldsymbol{\omega}\cdot\boldsymbol{\nabla}\sigma)\\
&= \cancel{\mathrm{PV}\,\boldsymbol{\nabla}\cdot\boldsymbol{u}} + \frac{1}{\rho}\left[-\boldsymbol{u}\cdot\boldsymbol{\nabla}\boldsymbol{\omega} + \boldsymbol{\omega}\cdot\boldsymbol{\nabla}\boldsymbol{u} - \cancel{\boldsymbol{\omega}(\boldsymbol{\nabla}\cdot\boldsymbol{u})}\right]\cdot\boldsymbol{\nabla}\sigma + \frac{\boldsymbol{\omega}}{\rho}\cdot\boldsymbol{\nabla}(-\boldsymbol{u}\cdot\boldsymbol{\nabla}\sigma)\\
&\quad + \frac{\boldsymbol{u}}{\rho}\cdot\boldsymbol{\nabla}(\boldsymbol{\omega}\cdot\boldsymbol{\nabla}\sigma)\\
&= 0.\end{aligned} \tag{II.2.21}$$

To obtain the third equality above, we have used that

$$\frac{1}{\rho^2}\boldsymbol{\nabla}\rho\times\boldsymbol{\nabla}P = \frac{1}{\gamma\rho}\boldsymbol{\nabla}P\times\boldsymbol{\nabla}\ln\rho^{-\gamma} = \frac{1}{\gamma\rho}\boldsymbol{\nabla}P\times\boldsymbol{\nabla}\ln P\rho^{-\gamma} = \frac{\gamma-1}{\gamma\rho}\boldsymbol{\nabla}P\times\boldsymbol{\nabla}\sigma, \tag{II.2.22}$$

which is orthogonal to $\boldsymbol{\nabla}\sigma$. This theorem, due to Hans Ertel (Ertel 1942), does not hold in the presence of magnetic fields.

II.3. Equations of magnetohydrodynamics via conservation laws

II.3.1. *Newton's second law for perfect conductors*

Ideal MHD describes the hydrodynamics of a perfectly conducting fluid in the presence of electromagnetic fields. Mass is still conserved, so we still have the continuity equation (II.1.4):

$$\frac{\partial\rho}{\partial t} + \boldsymbol{\nabla}\cdot(\rho\boldsymbol{u}) = 0. \tag{II.3.1}$$

The first law of thermodynamics still holds, so we still have the internal energy equation (II.1.17):

$$\frac{\partial e}{\partial t} + \boldsymbol{\nabla}\cdot(e\boldsymbol{u}) = -P\boldsymbol{\nabla}\cdot\boldsymbol{u}. \tag{II.3.2}$$

And Newton's second law still governs the dynamics, so we still have the momentum equation (II.1.14):

$$\frac{\partial(\rho\boldsymbol{u})}{\partial t} + \boldsymbol{\nabla}\cdot(\rho\boldsymbol{u}\boldsymbol{u}) = \boldsymbol{f}. \tag{II.3.3}$$

But now we must supplement the force $\boldsymbol{f}$, which was equal to $-\boldsymbol{\nabla}P - \rho\boldsymbol{\nabla}\mathit{\Phi}$ in (II.1.14), with the force due to the electromagnetic fields on the conducting fluid elements. To do so, let us view our conducting fluid elements as a coherent collection of ions (with charge $q_\mathrm{i} = Ze > 0$) and electrons (with charge $q_\mathrm{e} = -e < 0$), and ask how electric and magnetic fields influence each of these species.

The electromagnetic force per unit volume on a collection of charges of species α is given by

$$\boldsymbol{f}_{\mathrm{EM}} = q_\alpha n_\alpha \left(\boldsymbol{E} + \frac{\boldsymbol{u}_\alpha}{c} \times \boldsymbol{B} \right), \tag{II.3.4}$$

where n_α is the number density of the species and $\boldsymbol{u}_\alpha$ is that species' bulk velocity. You can think of this simply as the Lorentz force $q_\alpha(\boldsymbol{E} + \boldsymbol{v} \times \boldsymbol{B}/c)$ integrated over the ensemble of α charges in each fluid element and divided by the volume of said fluid element. Separating (II.3.3) into its charged constituent parts, we then have the momentum equation for species α,

$$\frac{\partial(\rho_\alpha \boldsymbol{u}_\alpha)}{\partial t} + \boldsymbol{\nabla \cdot} (\rho_\alpha \boldsymbol{u}_\alpha \boldsymbol{u}_\alpha) = -\boldsymbol{\nabla} P_\alpha - \rho_\alpha \boldsymbol{\nabla} \varPhi + q_\alpha n_\alpha \left(\boldsymbol{E} + \frac{\boldsymbol{u}_\alpha}{c} \times \boldsymbol{B} \right). \tag{II.3.5}$$

At the moment, the trouble is that our continuity equation (II.3.1) and internal energy equation (II.3.2) make reference to the *total* mass density ρ, the *total* fluid velocity $\boldsymbol{u}$, the *total* pressure P, and the *total* internal energy e. The obvious thing to do, then, is to sum (II.3.5) over both species,

$$\sum_\alpha \left[\frac{\partial(\rho_\alpha \boldsymbol{u}_\alpha)}{\partial t} + \boldsymbol{\nabla \cdot} (\rho_\alpha \boldsymbol{u}_\alpha \boldsymbol{u}_\alpha) = -\boldsymbol{\nabla} P_\alpha - \rho_\alpha \boldsymbol{\nabla} \varPhi + q_\alpha n_\alpha \left(\boldsymbol{E} + \frac{\boldsymbol{u}_\alpha}{c} \times \boldsymbol{B} \right) \right], \tag{II.3.6}$$

and simplify each of the sums one by one. The first term in (II.3.6) becomes familiar after introducing the center-of-mass fluid velocity,

$$\boldsymbol{u} \doteq \frac{1}{\rho} \sum_\alpha \rho_\alpha \boldsymbol{u}_\alpha, \quad \text{where} \quad \rho \doteq \sum_\alpha \rho_\alpha. \tag{II.3.7}$$

The second term in (II.3.6) requires a bit more work. Write $\boldsymbol{u}_\alpha = \boldsymbol{u} + \varDelta \boldsymbol{u}_\alpha$, so that $\varDelta \boldsymbol{u}_\alpha$ measures the difference between the bulk flow of species α and the center-of-mass velocity $\boldsymbol{u}$. Then

$$\sum_\alpha \rho_\alpha \boldsymbol{u}_\alpha \boldsymbol{u}_\alpha = \rho \boldsymbol{u}\boldsymbol{u} + \boldsymbol{u} \cancelto{0}{\left(\sum_\alpha \rho_\alpha \varDelta \boldsymbol{u}_\alpha \right)} + \cancelto{0}{\left(\sum_\alpha \rho_\alpha \varDelta \boldsymbol{u}_\alpha \right)} \boldsymbol{u} + \sum_\alpha \rho_\alpha \varDelta \boldsymbol{u}_\alpha \varDelta \boldsymbol{u}_\alpha.$$

The first term here ($\rho \boldsymbol{u}\boldsymbol{u}$) should look familiar: it's the flux of momentum density associated with the total fluid, the same as was seen in §II.1.2. Moving the final term of the above expression to the right-hand side of (II.3.6) and writing $\sum_\alpha P_\alpha \doteq P$, we have a momentum equation that is starting to look more like (II.3.3):

$$\frac{\partial(\rho \boldsymbol{u})}{\partial t} + \boldsymbol{\nabla \cdot} (\rho \boldsymbol{u}\boldsymbol{u}) = -\boldsymbol{\nabla} P - \rho \boldsymbol{\nabla} \varPhi - \boldsymbol{\nabla \cdot} \left(\sum_\alpha \rho_\alpha \varDelta \boldsymbol{u}_\alpha \varDelta \boldsymbol{u}_\alpha \right) + \sum_\alpha q_\alpha n_\alpha \left(\boldsymbol{E} + \frac{\boldsymbol{u}_\alpha}{c} \times \boldsymbol{B} \right). \tag{II.3.8}$$

Now, this term involving $\varDelta \boldsymbol{u}_\alpha$ has nothing really to do with MHD, and was in fact implicitly discarded in §II.1.2, the reason being either that our fluid element is composed of a single species, or that collisions between different species keep their bulk flows very close to the center-of-mass velocity, or that the total mass density and total momentum density are completely dominated by a single species (e.g., the ions). In any of these cases, we may safely drop this term.

Almost there. All that remains to consider is

$$\sum_\alpha q_\alpha n_\alpha \left(\boldsymbol{E} + \frac{\boldsymbol{u}_\alpha}{c} \times \boldsymbol{B} \right).$$

In GPPI, you learned that the densities of the positive and negative charge carriers surrounding a point charge Q in a weakly coupled plasma satisfies

$$\sum_\alpha q_\alpha n_\alpha = \cancelto{0}{\sum_\alpha q_\alpha \overline{n}_\alpha} - \frac{Q}{4\pi\lambda_{\mathrm{D}}^3}\,\frac{\exp(-r/\lambda_{\mathrm{D}})}{r/\lambda_{\mathrm{D}}},$$

where $\overline{n}_\alpha$ is the mean density of species α, and therefore that the total charge density is extremely close to zero well outside of that charge's Debye sphere, i.e., the plasma is *quasi-neutral* on scales $r \gg \lambda_{\mathrm{D}}$. MHD concerns itself with just such scales, and so the total electric force on a fluid element in MHD vanishes under quasi-neutrality. This leaves the magnetic term, $(\sum_\alpha q_\alpha n_\alpha \boldsymbol{u}_\alpha) \times \boldsymbol{B}/c$. The sum in parentheses is equivalent to the *current density* of the plasma, $\boldsymbol{j}$, the amount of electric current flowing per unit cross-sectional area. We these principles implemented, our MHD momentum equation is finally here:

$$\boxed{\frac{\partial(\rho\boldsymbol{u})}{\partial t} + \boldsymbol{\nabla}\boldsymbol{\cdot}(\rho\boldsymbol{u}\boldsymbol{u}) = -\boldsymbol{\nabla}P - \rho\boldsymbol{\nabla}\varPhi + \frac{\boldsymbol{j}}{c}\times\boldsymbol{B}} \tag{II.3.9}$$

Another way to think of this additional term is by analogy with circuits: when a current $\boldsymbol{I}$ flows through a wire of length ℓ in the presence of a magnetic field $\boldsymbol{B}$, there is a force on the wire given by $\boldsymbol{I}\ell \times \boldsymbol{B}/c$. In the fluid context, the "wire" is the conducting fluid element through which electrons and ions move differentially.

We now have our continuity equation, internal energy equation, and MHD momentum equation. However, in deriving the latter, we have introduced two new variables, $\boldsymbol{j}$ and $\boldsymbol{B}$. The remaining tasks are then to express the current density $\boldsymbol{j}$ in terms of the magnetic field $\boldsymbol{B}$ (since by summing over the momentum equations of each species, we've lost information about each species' bulk flow), and to provide an equation for how the magnetic field evolves. Both of these tasks are solved via Maxwell's equations.

II.3.2. *Maxwell's equations for ideal MHD*

Maxwell's equations in their differential form are

$$\frac{\partial\boldsymbol{B}}{\partial t} = -c\boldsymbol{\nabla}\times\boldsymbol{E}, \quad \boldsymbol{\nabla}\boldsymbol{\cdot}\boldsymbol{B} = 0, \quad \frac{\partial\boldsymbol{E}}{\partial t} = c\boldsymbol{\nabla}\times\boldsymbol{B} - 4\pi\boldsymbol{j}, \quad \color{red}{\boldsymbol{\nabla}\boldsymbol{\cdot}\boldsymbol{E} = 4\pi\sum_\alpha q_\alpha n_\alpha}.$$

An important caveat here is that the final equation in red (Gauss' law) is rendered completely useless by the quasi-neutrality assumption, $\sum_\alpha q_\alpha n_\alpha \approx 0$. The other equations are (from left to right) Faraday's law of induction, Gauss' law for magnetism (no magnetic monopoles), and Maxwell's version of Ampère's law. No offense to Maxwell, but it turns out that the original Ampère's law,

$$\boldsymbol{j} = \frac{c}{4\pi}\boldsymbol{\nabla}\times\boldsymbol{B}, \tag{II.3.10}$$

is just fine for most of our purposes in this course. The displacement current, $(4\pi)^{-1}\partial\boldsymbol{E}/\partial t$, which mathematically and physically connects electromagnetism with the propagation of light, may be rigorously dropped if the fluid velocity satisfies $u^2 \ll c^2$. Why, you ask? Well, this brings us back to the first sentence of §II.3.1: we are interested in *perfect conductors*.

A perfect conductor is one that has exactly zero electrical resistance, and so by Ohm's law must have zero electrostatic field. But this doesn't necessarily mean that $\boldsymbol{E} = 0$, because an electric field can be induced by the motion of a conductor through a magnetic field (sometimes called the "motional emf"). What we mean by a perfect conductor is then that the electric field vanishes *in the frame of the conductor*, or

$$\boldsymbol{E} + \frac{\boldsymbol{u}}{c} \times \boldsymbol{B} = 0. \tag{II.3.11}$$

One way to think about this expression physically is that someone in the lab frame cannot tell the difference between a particle gyrating about a magnetic field in a train moving at speed $\boldsymbol{u}$, and a particle $E\times B$-drifting at speed $\boldsymbol{u}$:

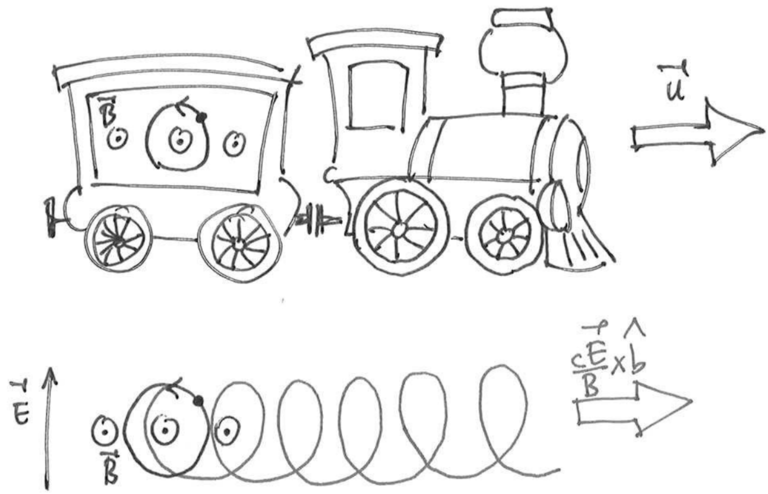

Inserting (II.3.11) into the Maxwell–Ampère law and ordering $\partial/\partial t \sim u/\ell$ for some characteristic bulk flow velocity u and gradient lengthscale ℓ, we find that the displacement current

$$\frac{\partial \boldsymbol{E}}{\partial t} \sim \frac{u^2}{c^2}\frac{cB}{\ell} \ll \frac{cB}{\ell} \sim c\boldsymbol{\nabla}\times\boldsymbol{B}$$

if the flow is non-relativistic. As claimed, the original Ampère's law is just fine.

Altogether then, we may close our MHD momentum equation with the following subset of Maxwell's equations:

$$\boxed{\frac{\partial \boldsymbol{B}}{\partial t} = \boldsymbol{\nabla}\times(\boldsymbol{u}\times\boldsymbol{B}), \quad \boldsymbol{\nabla}\cdot\boldsymbol{B} = 0, \quad \boldsymbol{j} = \frac{c}{4\pi}\boldsymbol{\nabla}\times\boldsymbol{B}} \tag{II.3.12}$$

These equations for the electromagnetic fields $\boldsymbol{B}$ and $\boldsymbol{j}$ – taken alongside (II.3.1), (II.3.2), and (II.3.8) specifying the evolution of the hydrodynamics variables (ρ, $\rho\boldsymbol{u}$, e) – constitute the equations of ideal MHD.

II.3.3. *Ideal MHD induction equation*

Using a particular vector identity (see §II.2.1), the ideal MHD induction equation may be written in the following form:

$$\frac{\partial \boldsymbol{B}}{\partial t} = \boldsymbol{\nabla}\times(\boldsymbol{u}\times\boldsymbol{B}) = -\boldsymbol{u}\cdot\boldsymbol{\nabla}\boldsymbol{B} + \boldsymbol{B}\cdot\boldsymbol{\nabla}\boldsymbol{u} - \boldsymbol{B}\boldsymbol{\nabla}\cdot\boldsymbol{u}. \tag{II.3.13}$$

Each of the terms on the right-hand side has a physical meaning. The first indicates that the magnetic field is advected (carried around by) the fluid flow; when placed on the left-hand side, we obtain the Lagrangian derivative of the magnetic field, $\mathrm{D}\boldsymbol{B}/\mathrm{D}t$, so that (II.3.13) becomes

$$\frac{\mathrm{D}\boldsymbol{B}}{\mathrm{D}t} = \boldsymbol{B}\cdot\boldsymbol{\nabla}\boldsymbol{u} - \boldsymbol{B}\boldsymbol{\nabla}\cdot\boldsymbol{u}. \tag{II.3.14}$$

In this Lagrangian frame, the magnetic field can evolve because of two effects. The first term on the right-hand side of (II.3.14), $\boldsymbol{B}\cdot\boldsymbol{\nabla}\boldsymbol{u}$, represents stretching of the magnetic field: if the fluid velocity has a gradient along the direction of the magnetic field, different parts of the field line will be carried along at different velocities, causing the field line to stretch. The final term, $-\boldsymbol{B}\boldsymbol{\nabla}\cdot\boldsymbol{u}$, corresponds to compression or rarefaction of the magnetic field. Indeed, with the continuity equation giving $-\boldsymbol{\nabla}\cdot\boldsymbol{u} = \mathrm{D}\ln\rho/\mathrm{D}t$, we see that co-moving increases (decreases) in the fluid density go hand-in-hand with increases (decreases) in the magnetic-field strength.

A rarely publicized but useful form of the induction equation (II.3.13) is obtained by defining the magnetic-field unit vector $\hat{\boldsymbol{b}} \doteq \boldsymbol{B}/B$ and writing separate equations for it and the magnetic-field strength B:

$$\frac{\mathrm{D}\ln B}{\mathrm{D}t} = \big(\hat{\boldsymbol{b}}\hat{\boldsymbol{b}} - \boldsymbol{I}\big) : \boldsymbol{\nabla}\boldsymbol{u} \quad \text{and} \quad \frac{\mathrm{D}\hat{\boldsymbol{b}}}{\mathrm{D}t} = \big(\boldsymbol{I} - \hat{\boldsymbol{b}}\hat{\boldsymbol{b}}\big) : \big(\hat{\boldsymbol{b}}\cdot\boldsymbol{\nabla}\boldsymbol{u}\big). \tag{II.3.15}$$

We'll need these in §IX.5.

II.3.4. *Flux freezing: Alfvén's theorem and Lundquist's theorem*

Arguably the most important prediction of the ideal MHD equations is that the magnetic flux Φ_B through the surface of any fluid element is exactly conserved as that element is advected and deformed by a flow $\boldsymbol{u} = \boldsymbol{u}(t,\boldsymbol{r})$. This is known as "Alfvén's theorem" or, more colloquially, *flux freezing*. Given Leibniz's rule regarding the time derivatives of surface integrals whose integrations limits $\mathcal{S}(t)$ are time-dependent (eq. (II.2.4)), the proof itself is trivial:

$$\begin{aligned}
\frac{\mathrm{D}\Phi_B}{\mathrm{D}t} \doteq \frac{\mathrm{D}}{\mathrm{D}t}\int_{\mathcal{S}(t)} \mathrm{d}\boldsymbol{S}\cdot\boldsymbol{B} &= \int_{\mathcal{S}(t)} \mathrm{d}\boldsymbol{S}\cdot\left[\frac{\partial\boldsymbol{B}}{\partial t} + (\boldsymbol{\nabla}\cdot\boldsymbol{B})\boldsymbol{u}\right] - \oint_{\partial\mathcal{S}(t)} \mathrm{d}\boldsymbol{\ell}\cdot(\boldsymbol{u}\times\boldsymbol{B}) \\
\text{(use equation (II.3.13))} &= \int_{\mathcal{S}(t)} \mathrm{d}\boldsymbol{S}\cdot\Big[\boldsymbol{\nabla}\times(\boldsymbol{u}\times\boldsymbol{B})\Big] - \oint_{\partial\mathcal{S}(t)} \mathrm{d}\boldsymbol{\ell}\cdot(\boldsymbol{u}\times\boldsymbol{B}) \\
\text{(use Stokes' theorem)} &= \oint_{\partial\mathcal{S}(t)} \mathrm{d}\boldsymbol{\ell}\cdot(\boldsymbol{u}\times\boldsymbol{B}) - \oint_{\partial\mathcal{S}(t)} \mathrm{d}\boldsymbol{\ell}\cdot(\boldsymbol{u}\times\boldsymbol{B}) \\
&= 0.
\end{aligned} \tag{II.3.16}$$

In words, the magnetic flux is conserved in a frame co-moving with a fluid element. (This is analogous to Kelvin's circulation theorem governing the circulation; cf. (II.2.16).)

An alternative description of flux freezing can be stated in terms of line tying: fluid elements that lie on a field line initially will remain on that field line (Lundquist 1951). Starting from the ideal induction equation (II.3.14), one may use the continuity equation to show that

$$\frac{\mathrm{D}}{\mathrm{D}t}\frac{\boldsymbol{B}}{\rho} = \frac{\boldsymbol{B}}{\rho}\cdot\boldsymbol{\nabla}\boldsymbol{u} - \frac{\boldsymbol{B}}{\rho}\boldsymbol{\nabla}\cdot\boldsymbol{u} + \frac{\boldsymbol{B}}{\rho}\boldsymbol{\nabla}\cdot\boldsymbol{u} = \frac{\boldsymbol{B}}{\rho}\cdot\boldsymbol{\nabla}\boldsymbol{u}. \tag{II.3.17}$$

This equation is formally equivalent to that describing the advection and stretching of a displacement vector $\boldsymbol{\xi}$ by a flow velocity $\boldsymbol{u}$, which is given by

$$\frac{\mathrm{D}\boldsymbol{\xi}}{\mathrm{D}t} = \boldsymbol{\xi}\cdot\boldsymbol{\nabla}\boldsymbol{u}. \tag{II.3.18}$$

Therefore, if two fluid elements are initially on the same field line, $\boldsymbol{\xi} = \text{const}\times(\boldsymbol{B}/\rho)$, then they will stay on that same field line.

II.3.5. *Lorentz force: magnetic pressure and tension*

We now know that perfectly conducting fluids advect, stretch, and compress magnetic fields while conserving magnetic flux. What is the effect of that flux on the dynamics of the fluid element itself? For that, we revisit the Lorentz force in the MHD momentum equation (II.3.9), and use Ampère's law to cast the current density in terms of the magnetic field:

$$\boldsymbol{f}_{\mathrm{M}} = \frac{\boldsymbol{j}}{c} \times \boldsymbol{B} = \frac{(\boldsymbol{\nabla} \times \boldsymbol{B}) \times \boldsymbol{B}}{4\pi} = -\boldsymbol{\nabla} \frac{B^2}{8\pi} + \frac{\boldsymbol{B} \cdot \boldsymbol{\nabla} \boldsymbol{B}}{4\pi}, \tag{II.3.19}$$

where to obtain the final equality we have used a well-known vector identity (see §II.2.1). Because $\boldsymbol{\nabla} \cdot \boldsymbol{B} = 0$, this can also be written as

$$\boldsymbol{f}_{\mathrm{M}} = -\boldsymbol{\nabla} \cdot \left[\frac{B^2}{8\pi} \mathsf{I} - \frac{\boldsymbol{B}\boldsymbol{B}}{4\pi} \right] = -\boldsymbol{\nabla} \cdot \mathsf{M}, \tag{II.3.20}$$

which implicitly defines the "Maxwell stress", M. This form of the magnetic force suggests a kind of elasticity. To further see this, use the definition of the magnetic unit vector $\hat{\boldsymbol{b}} \doteq \boldsymbol{B}/B$ to write

$$\boldsymbol{B} \cdot \boldsymbol{\nabla} \boldsymbol{B} = B \hat{\boldsymbol{b}} \cdot \boldsymbol{\nabla} (B \hat{\boldsymbol{b}}) = B^2 (\hat{\boldsymbol{b}} \cdot \boldsymbol{\nabla} \hat{\boldsymbol{b}}) + \hat{\boldsymbol{b}} \hat{\boldsymbol{b}} \cdot \boldsymbol{\nabla} \frac{B^2}{2}.$$

Using this in (II.3.19) and collecting terms yields

$$\boldsymbol{f}_{\mathrm{M}} = \frac{B^2}{4\pi} (\hat{\boldsymbol{b}} \cdot \boldsymbol{\nabla} \hat{\boldsymbol{b}}) - \left(\mathsf{I} - \hat{\boldsymbol{b}} \hat{\boldsymbol{b}} \right) \cdot \boldsymbol{\nabla} \frac{B^2}{8\pi}. \tag{II.3.21}$$

The first term here corresponds to a curvature force, with $\hat{\boldsymbol{b}} \cdot \boldsymbol{\nabla} \hat{\boldsymbol{b}} \doteq \boldsymbol{\kappa}_{\mathrm{c}}$ being the curvature of the field lines (see the diagram below). Note that $1/|\boldsymbol{\kappa}_{\mathrm{c}}|$ is the radius of curvature. When a field line is bent, there is a force pointing towards the local center of curvature that is trying to un-bend the field line and push the plasma towards a lower-energy state in which the magnetic field is straight. The second term in (II.3.21) corresponds to a magnetic pressure force acting perpendicular to the field (thus the projection of the gradient onto $\mathsf{I} - \hat{\boldsymbol{b}}\hat{\boldsymbol{b}}$). This term causes the magnetic-field strength to evolve towards being uniform across itself, again seeking a lower-energy state. Magnetic fields like to be straight and evenly spaced, and they will coerce the fluid to adopt motions that drive them towards being straight and evenly spaced.

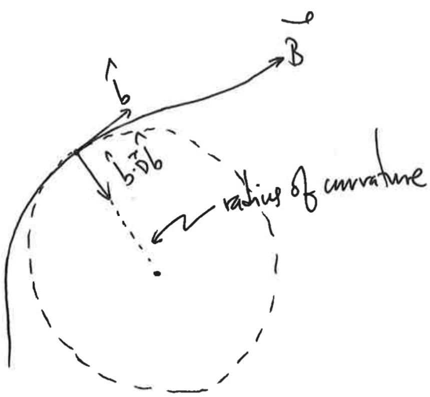

TENSION

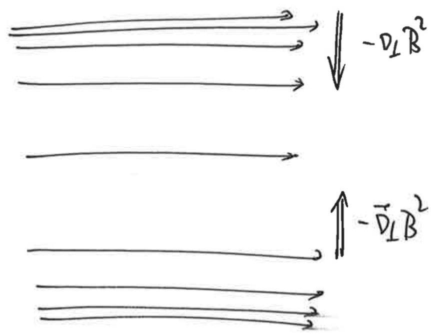

PRESSURE

II.3.6. *MHD energy equation*

In §II.1.3, we derived an evolution equation for the total energy of a neutral fluid, (II.1.24). Here we augment that equation for a perfectly conducting fluid to include the energy of the magnetic field, $B^2/8\pi$. Take the ideal MHD induction equation (II.3.13) and dot it with $\boldsymbol{B}/4\pi$:

$$
\begin{aligned}
\frac{\partial}{\partial t}\frac{B^2}{8\pi} &= \frac{\boldsymbol{B}}{4\pi}\boldsymbol{\cdot}\boldsymbol{\nabla}\times(\boldsymbol{u}\times\boldsymbol{B}) = \frac{B_i}{4\pi}\,\epsilon_{ijk}\frac{\partial}{\partial x_j}(\boldsymbol{u}\times\boldsymbol{B})_k \\
&= \epsilon_{ijk}\frac{\partial}{\partial x_j}\left[\frac{B_i}{4\pi}(\boldsymbol{u}\times\boldsymbol{B})_k\right] - \epsilon_{ijk}(\boldsymbol{u}\times\boldsymbol{B})_k\frac{\partial}{\partial x_j}\frac{B_i}{4\pi} \\
&= \epsilon_{ijk}\frac{\partial}{\partial x_j}\left[\frac{B_i}{4\pi}(\boldsymbol{u}\times\boldsymbol{B})_k\right] - \epsilon_{ijk}\epsilon_{k\ell m}u_\ell B_m\frac{\partial}{\partial x_j}\frac{B_i}{4\pi} \\
&= \epsilon_{ijk}\frac{\partial}{\partial x_j}\left[\frac{B_i}{4\pi}(\boldsymbol{u}\times\boldsymbol{B})_k\right] - (\delta_{i\ell}\delta_{jm}-\delta_{im}\delta_{j\ell})u_\ell B_m\frac{\partial}{\partial x_j}\frac{B_i}{4\pi} \\
&= -\boldsymbol{\nabla}\boldsymbol{\cdot}\left[\frac{\boldsymbol{B}\times(\boldsymbol{u}\times\boldsymbol{B})}{4\pi}\right] - \frac{\boldsymbol{u}\boldsymbol{B}\boldsymbol{:}\boldsymbol{\nabla}\boldsymbol{B}}{4\pi} + \boldsymbol{u}\boldsymbol{\cdot}\boldsymbol{\nabla}\frac{B^2}{8\pi}
\end{aligned}
$$

$$
\Longrightarrow\quad \frac{\partial}{\partial t}\frac{B^2}{8\pi} + \boldsymbol{\nabla}\boldsymbol{\cdot}\left[\frac{\boldsymbol{B}\times(\boldsymbol{u}\times\boldsymbol{B})}{4\pi}\right] = -\frac{\boldsymbol{u}\boldsymbol{B}\boldsymbol{:}\boldsymbol{\nabla}\boldsymbol{B}}{4\pi} + \boldsymbol{u}\boldsymbol{\cdot}\boldsymbol{\nabla}\frac{B^2}{8\pi}.
$$

Note that the quantity inside the divergence on the left-hand side of this equation equals $(c/4\pi)\boldsymbol{E}\times\boldsymbol{B} \doteq \boldsymbol{\mathcal{S}}$... the Poynting flux! In words, magnetic energy (as measured in the lab frame; note the partial time derivative) is transported by the Poynting flux. Those two terms on the right-hand side corresponding to will be cancelled by two equal-and-opposite terms found in the equation for the kinetic energy, obtained by dotting the momentum equation (II.3.9) with $\boldsymbol{u}$ and focusing on the Lorentz force:

$$
\boldsymbol{u}\boldsymbol{\cdot}\left(-\boldsymbol{\nabla}\frac{B^2}{8\pi} + \frac{\boldsymbol{B}\boldsymbol{\cdot}\boldsymbol{\nabla}\boldsymbol{B}}{4\pi}\right).
$$

Yep, they cancel. So, adding the total hydrodynamic energy equation including these Lorentz-force contributions to the magnetic energy equation leads to

$$
\boxed{\frac{\partial}{\partial t}\left(\frac{1}{2}\rho u^2 + e + \rho\Phi + \frac{B^2}{8\pi}\right) + \boldsymbol{\nabla}\boldsymbol{\cdot}\left[\left(\frac{1}{2}\rho u^2 + \gamma e + \rho\Phi\right)\boldsymbol{u} + \boldsymbol{\mathcal{S}}\right] = \rho\frac{\partial\Phi}{\partial t}} \qquad \text{(II.3.22)}
$$

But for the impact of a time-varying gravitational potential, the total MHD energy density $\mathcal{E} \doteq (1/2)\rho u^2 + e + \rho\Phi + B^2/8\pi$ is conserved.

II.3.7. *Virial theorem, revisited*

Now that our system has acquired an additional stress – the Maxwell stress $\boldsymbol{M}$ (II.3.20) – let us revisit the virial theorem from §II.1.5:

$$
\begin{aligned}
\frac{1}{2}\frac{\mathrm{d}^2 I}{\mathrm{d}t^2} = &-\oint_{\partial\mathcal{V}}\mathrm{d}\boldsymbol{S}\boldsymbol{\cdot}\left[\rho\boldsymbol{u}\boldsymbol{u} + \frac{\boldsymbol{g}\boldsymbol{g}}{4\pi\mathrm{G}} - \frac{\boldsymbol{B}\boldsymbol{B}}{4\pi} + \left(P - \frac{g^2}{8\pi\mathrm{G}} + \frac{B^2}{8\pi}\right)\boldsymbol{I}\right]\boldsymbol{\cdot}\boldsymbol{r} \\
&+ \int_{\mathcal{V}}\mathrm{d}\boldsymbol{r}\left(\rho u^2 + 3P - \frac{g^2}{8\pi\mathrm{G}} + \frac{B^2}{8\pi}\right).
\end{aligned} \qquad \text{(II.3.23)}
$$

The total energy is now

$$
\mathscr{E} \doteq \int\mathrm{d}\boldsymbol{r}\left(\frac{1}{2}\rho u^2 + e + \frac{1}{2}\rho\Phi + \frac{B^2}{8\pi}\right). \qquad \text{(II.3.24)}
$$

Recall from §II.1.5 that, in order for the system to be in steady state, the stresses on the boundary must balance those acting on the volume:

$$\oint_{\mathcal{S}} \mathrm{d}\boldsymbol{S} \cdot (\boldsymbol{T} \cdot \boldsymbol{r}) = \int_{\mathcal{V}} \mathrm{d}\boldsymbol{r} \, \mathrm{tr}(\boldsymbol{T}) = \rho u^2 + 3P - \frac{g^2}{8\pi \mathrm{G}} + \frac{B^2}{8\pi} \tag{II.3.25a}$$

$$\doteq 2\mathscr{E}_{\mathrm{kin}} + 3(\gamma - 1)\mathscr{E}_{\mathrm{th}} + \mathscr{E}_{\mathrm{grav}} + \mathscr{E}_{\mathrm{mag}}, \tag{II.3.25b}$$

where we have introduced the total magnetic energy $\mathscr{E}_{\mathrm{mag}}$. Again, this steady-state system can only be self-confined if self-gravity is important, but note that magnetic fields can provide support against gravitational collapse. One day I might add some things here about magnetohydrostatic equliibria of self-gravitating clouds.

The virial theorem demonstrates the impossibility of confining a plasma only with currents flowing within the plasma itself. To see this, note that $\mathscr{E} > 0$ without self-gravity, which implies that in steady state the stresses on the boundary must be positive as well:

$$\oint_{\mathcal{S}} \mathrm{d}\boldsymbol{S} \cdot \left[\rho \boldsymbol{u}\boldsymbol{u} - \frac{\boldsymbol{B}\boldsymbol{B}}{4\pi} + \left(P + \frac{B^2}{8\pi} \right) \boldsymbol{I} \right] \cdot \boldsymbol{r} > 0. \tag{II.3.26}$$

Let the volume be a sphere of radius r with $r \to \infty$. Because the plasma is entirely enclosed within $\mathcal{S}$, we have that $P = u = 0$ on the surface. And the magnetic field will decay at large radii at least as fast as a dipole field with $B \propto r^{-3}$. With $R \, \mathrm{d}S \propto R^3$ in spherical coordinates, there is no way for the surface integral to be positive and balance the volume integral.

II.3.8. *Curvilinear coordinates and rotating reference frames, revisited*

In §II.2.3, we examined the nonlinear combination $\boldsymbol{u} \cdot \boldsymbol{\nabla} \boldsymbol{u}$ in curvilinear coordinates, finding additional terms that stemmed from differentiating unit vectors and which included Coriolis, centrifugal, and tidal accelerations. Here we take a similar look at the combination $\boldsymbol{u} \cdot \boldsymbol{\nabla} \boldsymbol{B} - \boldsymbol{B} \cdot \boldsymbol{\nabla} \boldsymbol{u}$ that features in the induction equation (II.3.13).

First, cylindrical coordinates. Use $\partial \hat{\boldsymbol{\varphi}} / \partial \varphi = -\hat{\boldsymbol{R}}$ and $\partial \hat{\boldsymbol{R}} / \partial \varphi = \hat{\boldsymbol{\varphi}}$ in (II.3.13) to obtain

$$\frac{\partial \boldsymbol{B}}{\partial t} = (-\boldsymbol{u} \cdot \boldsymbol{\nabla} B_i) \hat{\boldsymbol{e}}_i + (\boldsymbol{B} \cdot \boldsymbol{\nabla} u_i) \hat{\boldsymbol{e}}_i + \frac{B_\varphi u_R - B_R u_\varphi}{R} \hat{\boldsymbol{\varphi}} - \boldsymbol{B} \boldsymbol{\nabla} \cdot \boldsymbol{u}$$

As in §II.2.4, if we then decompose the fluid velocity as $\boldsymbol{u} = \boldsymbol{v} + R\Omega(R, z)\hat{\boldsymbol{\varphi}}$, where Ω is an angular velocity, substitute this decomposition into the above equation, and re-group terms, we have

$$\frac{\mathrm{D}B_R}{\mathrm{D}t} = \boldsymbol{B} \cdot \boldsymbol{\nabla} v_R - B_R \boldsymbol{\nabla} \cdot \boldsymbol{v}, \tag{II.3.27a}$$

$$\frac{\mathrm{D}B_\varphi}{\mathrm{D}t} = \boldsymbol{B} \cdot \boldsymbol{\nabla} v_\varphi - B_\varphi \boldsymbol{\nabla} \cdot \boldsymbol{v} + B_R \frac{\partial \Omega}{\partial \ln R} + B_z R \frac{\partial \Omega}{\partial z} + \frac{B_\varphi v_R - B_R v_\varphi}{R}, \tag{II.3.27b}$$

$$\frac{\mathrm{D}B_z}{\mathrm{D}t} = \boldsymbol{B} \cdot \boldsymbol{\nabla} v_z - B_z \boldsymbol{\nabla} \cdot \boldsymbol{v}, \tag{II.3.27c}$$

with $\mathrm{D}/\mathrm{D}t \doteq \partial/\partial t + \boldsymbol{v} \cdot \boldsymbol{\nabla} + \Omega \, \partial/\partial \varphi$. Note that poloidal magnetic fields are sheared into the azimuthal direction by differential rotation. Likewise in cylindrical coordinates, the magnetic force becomes

$$\boldsymbol{f}_{\mathrm{M}} = -\boldsymbol{\nabla} \frac{B^2}{8\pi} + \frac{\boldsymbol{B} \cdot \boldsymbol{\nabla} B_i}{4\pi} \hat{\boldsymbol{e}}_i - \frac{B_\varphi^2}{4\pi R} \hat{\boldsymbol{R}} + \frac{B_R B_\varphi}{4\pi R} \hat{\boldsymbol{\varphi}} \tag{II.3.28}$$

Note the addition of an inwardly directed hoop stress caused by a magnetic field oriented in the azimuthal direction, and an azimuthally directed magnetic torque caused by $\partial \hat{\boldsymbol{R}} / \partial \hat{\boldsymbol{\varphi}} = \hat{\boldsymbol{\varphi}}$. The former guarantees that an azimuthal magnetic field satisfying

$B_\varphi \propto 1/R$ is force free. These equations will be used when deriving the magnetorotational instability.

For completeness, here are these same equations but in spherical coordinates (r, θ, φ) with $\Omega = \Omega(r, \theta)$:

$$\frac{\mathrm{D}B_r}{\mathrm{D}t} = \boldsymbol{B} \boldsymbol{\cdot} \boldsymbol{\nabla} v_r - B_r \boldsymbol{\nabla} \boldsymbol{\cdot} \boldsymbol{v}, \tag{II.3.29a}$$

$$\frac{\mathrm{D}B_\theta}{\mathrm{D}t} = \boldsymbol{B} \boldsymbol{\cdot} \boldsymbol{\nabla} v_\theta - B_\theta \boldsymbol{\nabla} \boldsymbol{\cdot} \boldsymbol{v} + \frac{v_r B_\theta - v_\theta B_r}{r}, \tag{II.3.29b}$$

$$\begin{aligned}\frac{\mathrm{D}B_\varphi}{\mathrm{D}t} &= \boldsymbol{B} \boldsymbol{\cdot} \boldsymbol{\nabla} v_\varphi - B_\varphi \boldsymbol{\nabla} \boldsymbol{\cdot} \boldsymbol{v} + \frac{v_r B_\varphi - v_\varphi B_r}{r} + \frac{(v_\theta B_\varphi - v_\varphi B_\theta)\cot\theta}{r} \\ &\quad + B_r \sin\theta \frac{\partial \Omega}{\partial \ln r} + B_\theta \sin\theta \frac{\partial \Omega}{\partial \theta},\end{aligned} \tag{II.3.29c}$$

$$\begin{aligned}\boldsymbol{f}_\mathrm{M} &= -\boldsymbol{\nabla}\frac{B^2}{8\pi} + \frac{\boldsymbol{B} \boldsymbol{\cdot} \boldsymbol{\nabla} B_i}{4\pi}\hat{\boldsymbol{e}}_i - \frac{B_\theta^2 + B_\varphi^2}{4\pi r}\hat{\boldsymbol{r}} + \frac{B_r B_\theta + B_\varphi^2 \cot\theta}{4\pi r}\hat{\boldsymbol{\theta}} \\ &\quad + \frac{B_r B_\varphi + B_\theta B_\varphi \cot\theta}{4\pi r}\hat{\boldsymbol{\varphi}}.\end{aligned} \tag{II.3.30}$$

These are useful for studying MHD in stars.

II.3.9. *Boundary conditions*

For a fixed boundary such as a solid wall, the normal component of the velocity must vanish:

$$\hat{\boldsymbol{n}} \boldsymbol{\cdot} \boldsymbol{u} = 0, \tag{II.3.31}$$

where $\hat{\boldsymbol{n}}$ is the unit vector normal to the boundary surface. For a free surface, the boundary simply deforms at the rate given by $\hat{\boldsymbol{n}} \boldsymbol{\cdot} \boldsymbol{u}$. The velocity in the tangential direction on a fixed boundary is only constrained if there is a "no-slip" condition:

$$\hat{\boldsymbol{n}} \times \boldsymbol{u} = 0. \tag{II.3.32}$$

As for the electromagnetic fields, the boundaries can be either perfectly conducting or insulating. For perfect conductors, Maxwell's equations dictate that the perpendicular magnetic field and the tangential electric field must vanish on the boundary:

$$\hat{\boldsymbol{n}} \boldsymbol{\cdot} \boldsymbol{B} = 0 \quad \text{and} \quad \hat{\boldsymbol{n}} \times \boldsymbol{E} = 0. \tag{II.3.33}$$

For insulating boundaries, the normal current density must vanish:

$$\hat{\boldsymbol{n}} \boldsymbol{\cdot} (\boldsymbol{\nabla} \times \boldsymbol{B}) = 0. \tag{II.3.34}$$

II.3.10. *Summary: adiabatic equations of ideal MHD*

The adiabatic equations of MHD, written in conservative form, are:

$$\frac{\partial \rho}{\partial t} + \boldsymbol{\nabla} \boldsymbol{\cdot} (\rho \boldsymbol{u}) = 0, \tag{II.3.35a}$$

$$\frac{\partial (\rho \boldsymbol{u})}{\partial t} + \boldsymbol{\nabla} \boldsymbol{\cdot} (\rho \boldsymbol{u}\boldsymbol{u}) = -\boldsymbol{\nabla} \boldsymbol{\cdot} \left[\left(P + \frac{B^2}{8\pi} \right) \boldsymbol{I} - \frac{\boldsymbol{B}\boldsymbol{B}}{4\pi} \right] - \rho \boldsymbol{\nabla} \Phi, \tag{II.3.35b}$$

$$\frac{\partial e}{\partial t} + \boldsymbol{\nabla} \boldsymbol{\cdot} (e \boldsymbol{u}) = -P \boldsymbol{\nabla} \boldsymbol{\cdot} \boldsymbol{u}, \tag{II.3.35c}$$

$$\frac{\partial \boldsymbol{B}}{\partial t} - \boldsymbol{\nabla} \times (\boldsymbol{u} \times \boldsymbol{B}) = 0. \tag{II.3.35d}$$

The left-hand sides of these equations express advection of, respectively, the mass density, the momentum density, the internal energy density, and the magnetic flux by the fluid velocity; the right-hand sides represents sources and sinks.

If we instead write these equations in terms of the density, fluid velocity, and entropy and make use of the Lagrangian derivative (II.1.7), we have

$$\frac{\mathrm{D}\rho}{\mathrm{D}t} = -\rho\boldsymbol{\nabla}\boldsymbol{\cdot}\boldsymbol{u}, \tag{II.3.36a}$$

$$\frac{\mathrm{D}\boldsymbol{u}}{\mathrm{D}t} = -\frac{1}{\rho}\boldsymbol{\nabla}\left(P+\frac{B^2}{8\pi}\right)+\frac{\boldsymbol{B}\boldsymbol{\cdot}\boldsymbol{\nabla}\boldsymbol{B}}{4\pi\rho}-\boldsymbol{\nabla}\Phi, \tag{II.3.36b}$$

$$\frac{\mathrm{D}\sigma}{\mathrm{D}t} = 0, \tag{II.3.36c}$$

$$\frac{\mathrm{D}\boldsymbol{B}}{\mathrm{D}t} = \boldsymbol{B}\boldsymbol{\cdot}\boldsymbol{\nabla}\boldsymbol{u}-\boldsymbol{B}\boldsymbol{\nabla}\boldsymbol{\cdot}\boldsymbol{u}, \tag{II.3.36d}$$

where $\sigma \doteq (\gamma-1)^{-1}\ln P\rho^{-\gamma}$.

II.4. Equations of magnetohydrodynamics via Vlasov–Landau

As promised, another way of obtaining the MHD equations is to start from the Vlasov–Landau kinetic equation, take moments, and impose some assumptions to close the resulting moment hierarchy. This is a purely formal approach, which has its own advantages over the more intuitive derivation in the preceding sections. It also has the utility of establishing some notation used later in the course.

II.4.1. *Vlasov–Landau in the co-moving fluid frame*

Start with the Vlasov–Landau equation for species α,

$$\dot{f}_\alpha \doteq \frac{\partial f_\alpha}{\partial t}+\boldsymbol{v}\boldsymbol{\cdot}\boldsymbol{\nabla}f_\alpha+\frac{q_\alpha}{m_\alpha}\left(\boldsymbol{E}+\frac{\boldsymbol{v}}{c}\times\boldsymbol{B}\right)\boldsymbol{\cdot}\frac{\partial f_\alpha}{\partial\boldsymbol{v}} = C[f_\alpha], \tag{II.4.1}$$

which governs the evolution of the one-particle distribution function $f_\alpha = f_\alpha(t,\boldsymbol{r},\boldsymbol{v})$ through phase space. Recall that f_α is the probability of finding a particle in a phase-space interval $\mathrm{d}\boldsymbol{r}\mathrm{d}\boldsymbol{v}$ about point $(\boldsymbol{r},\boldsymbol{v})$ at time t; that probability evolves because particles with velocity $\boldsymbol{v}$ move through real space at a rate $\mathrm{d}\boldsymbol{r}/\mathrm{d}t=\boldsymbol{v}$ and experience forces that change their velocities – in this case, because of electromagnetic fields that have been coarse-grained to filter out the spiky fields associated with the discrete nature of point particles. The effect of those spiky fields is encapsulated in the collision operator $C[f_\alpha]$ manifest on the right-hand side of (II.4.1), which accounts for the cumulative effect of many small-angle sub-Debye scatterings of particles on the probability of a given particle being found somewhere in phase space; it represents the effects of the two-particle distribution function on the one-particle distribution function (see Kunz's lecture notes for AST554).

Because we'll use quasi-neutrality to eliminate $\boldsymbol{E}$ at one point, it will be beneficial to add to (II.4.1) an additional force on the particles that is independent of q_α, such as that due to gravity, $m_\alpha\boldsymbol{g}$:

$$\dot{f}_\alpha \doteq \frac{\partial f_\alpha}{\partial t}+\boldsymbol{v}\boldsymbol{\cdot}\boldsymbol{\nabla}f_\alpha+\left[\frac{q_\alpha}{m_\alpha}\left(\boldsymbol{E}+\frac{\boldsymbol{v}}{c}\times\boldsymbol{B}\right)+\boldsymbol{g}\right]\boldsymbol{\cdot}\frac{\partial f_\alpha}{\partial\boldsymbol{v}} = C[f_\alpha]. \tag{II.4.2}$$

The velocity coordinate $\boldsymbol{v}$ could contain both random ("thermal") and mean velocities; because these two components might have very different magnitudes, it is useful to split them apart:

$$\boldsymbol{w} \doteq \boldsymbol{v}-\boldsymbol{u}_\alpha(t,\boldsymbol{r}), \tag{II.4.3}$$

where

$$\boldsymbol{u}_\alpha(t,\boldsymbol{r}) \doteq \frac{1}{n_\alpha}\int \mathrm{d}\boldsymbol{v}\,\boldsymbol{v}f_\alpha, \quad n_\alpha(t,\boldsymbol{r}) \doteq \int \mathrm{d}\boldsymbol{v}\, f_\alpha. \tag{II.4.4}$$

This split also makes the bookkeeping a bit easier. We then boost to the frame co-moving with the fluid flow $\boldsymbol{u}_\alpha(t,\boldsymbol{r})$ by means of a transformation of variables $f_\alpha(t,\boldsymbol{r},\boldsymbol{v}) \to f_\alpha(t,\boldsymbol{r},\boldsymbol{w})$, writing

$$\left.\frac{\partial}{\partial t}\right|_{\boldsymbol{v}} = \left.\frac{\partial}{\partial t}\right|_{\boldsymbol{w}} + \left.\frac{\partial \boldsymbol{w}}{\partial t}\right|_{\boldsymbol{v}} \cdot \frac{\partial}{\partial \boldsymbol{w}} = \left.\frac{\partial}{\partial t}\right|_{\boldsymbol{w}} - \frac{\partial \boldsymbol{u}_\alpha}{\partial t}\cdot\frac{\partial}{\partial \boldsymbol{w}}, \tag{II.4.5}$$

$$\left.\frac{\partial}{\partial \boldsymbol{r}}\right|_{\boldsymbol{v}} = \left.\frac{\partial}{\partial \boldsymbol{r}}\right|_{\boldsymbol{w}} + \left.\frac{\partial \boldsymbol{w}}{\partial \boldsymbol{r}}\right|_{\boldsymbol{v}} \cdot \frac{\partial}{\partial \boldsymbol{w}} = \left.\frac{\partial}{\partial \boldsymbol{r}}\right|_{\boldsymbol{w}} - \frac{\partial \boldsymbol{u}_\alpha}{\partial \boldsymbol{r}}\cdot\frac{\partial}{\partial \boldsymbol{w}}. \tag{II.4.6}$$

In this frame, equation (II.4.2) becomes

$$\frac{\mathrm{D}f_\alpha}{\mathrm{D}t_\alpha} + \boldsymbol{w}\cdot\boldsymbol{\nabla}f_\alpha + \Bigg[\underbrace{\frac{q_\alpha}{m_\alpha}\left(\boldsymbol{E}+\frac{\boldsymbol{v}}{c}\times\boldsymbol{B}\right)+\boldsymbol{g}-\frac{\mathrm{D}\boldsymbol{u}_\alpha}{\mathrm{D}t_\alpha}}_{\doteq\, \boldsymbol{a}_\alpha(t,\boldsymbol{r})} - \boldsymbol{w}\cdot\boldsymbol{\nabla}\boldsymbol{u}_\alpha\Bigg]\cdot\frac{\partial f_\alpha}{\partial \boldsymbol{w}} = C[f_\alpha], \tag{II.4.7}$$

where

$$\frac{\mathrm{D}}{\mathrm{D}t_\alpha} \doteq \frac{\partial}{\partial t} + \boldsymbol{u}_\alpha\cdot\boldsymbol{\nabla} \tag{II.4.8}$$

is the usual Lagrangian time derivative. The additional acceleration terms in (II.4.7) that result from the frame transformation, *viz.* $\mathrm{D}\boldsymbol{u}_\alpha/\mathrm{D}t_\alpha$ and $\boldsymbol{w}\cdot\boldsymbol{\nabla}\boldsymbol{u}_\alpha$, are the result of boosting to a time- and space-dependent frame. The former term is fairly self-explanatory – particles must be accelerated so as to continue residing in the “fluid element” they comprise, which is itself being accelerated by various (magneto)hydrodynamic forces that result in $\mathrm{D}\boldsymbol{u}_\alpha/\mathrm{D}t_\alpha$ – but the latter deserves some discussion. Imagine you are trying to walk at constant velocity $\boldsymbol{w} = w\hat{\boldsymbol{x}}$ across several layers of differentially moving conveyor belts with velocities $\boldsymbol{u} = u(x)\hat{\boldsymbol{y}}$, as in the figure below. In your frame (and the frame of the conveyor belts), your velocity will always be $w\hat{\boldsymbol{x}}$. But, in the lab frame, your velocity will include the velocity of the conveyor belts. This means that, every time you step onto a new conveyor belt that has some velocity oriented in the y direction that is different from that of the last conveyor belt, you will be accelerating in the lab frame. That is, your velocity in the lab frame will change over an interval of time from one conveyor belt to the next. Mathematically, the figure below corresponds to an acceleration $w\Delta u_y/\Delta x$ every time you step from one conveyor belt at position x with velocity $u\hat{\boldsymbol{y}}$ to another conveyor belt at position $x+\Delta x$ with velocity $(u+\Delta u)\hat{\boldsymbol{y}}$. The difference between these two points of view is enacted by adding $-\boldsymbol{w}\cdot\boldsymbol{\nabla}\boldsymbol{u}_\alpha$ to the acceleration term of (II.4.7).

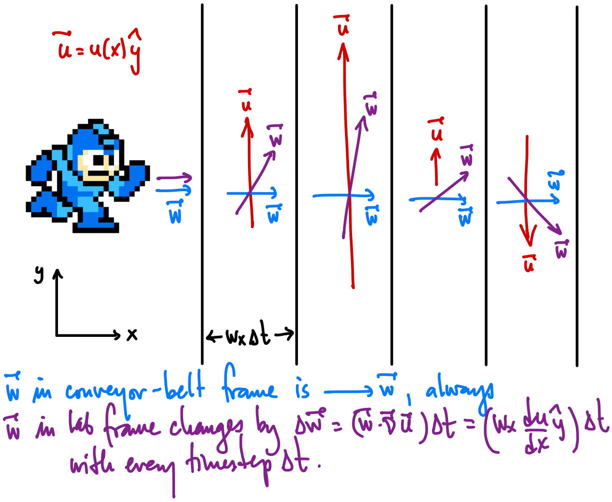

II.4.2. *Moments of the kinetic equation*

With velocity-space coordinates anchored in the co-moving fluid frame, taking moments is straightforward. The zeroth moment of (II.4.7) is

$$\int \mathrm{d}\boldsymbol{w}\,(\text{II.4.7}):\quad \frac{\mathrm{D}}{\mathrm{D}t_\alpha}\cancelto{n_\alpha}{\int \mathrm{d}\boldsymbol{w}\, f_\alpha} + \cancelto{0}{\int \mathrm{d}\boldsymbol{w}\,\boldsymbol{w}\cdot\boldsymbol{\nabla} f_\alpha} + \boldsymbol{a}_\alpha\cdot\cancelto{0}{\int \mathrm{d}\boldsymbol{w}\,\frac{\partial f_\alpha}{\partial \boldsymbol{w}}}$$

$$-\underbrace{\int \mathrm{d}\boldsymbol{w}\,(\boldsymbol{w}\cdot\boldsymbol{\nabla}\boldsymbol{u}_\alpha)\cdot\frac{\partial f_\alpha}{\partial \boldsymbol{w}}}_{\overset{\mathrm{bp}}{=}\,-(\boldsymbol{\nabla}\cdot\boldsymbol{u}_\alpha)\cancelto{n_\alpha}{\int \mathrm{d}\boldsymbol{w}\, f_\alpha}} = \cancelto{0}{\int \mathrm{d}\boldsymbol{w}\, C[f_\alpha]}$$

$$\Longrightarrow \quad \boxed{\frac{\mathrm{D}n_\alpha}{\mathrm{D}t_\alpha} + n_\alpha\boldsymbol{\nabla}\cdot\boldsymbol{u}_\alpha = 0} \quad \text{(continuity equation for species } \alpha\text{)} \qquad \text{(II.4.9)}$$

The first moment is

$$\int \mathrm{d}\boldsymbol{w}\, m_\alpha\boldsymbol{w}(\text{II.4.7}):\quad \frac{\mathrm{D}}{\mathrm{D}t_\alpha}\cancelto{0}{\int \mathrm{d}\boldsymbol{w}\, m_\alpha\boldsymbol{w} f_\alpha} + \int \mathrm{d}\boldsymbol{w}\, m_\alpha\boldsymbol{w}\boldsymbol{w}\cdot\boldsymbol{\nabla} f_\alpha + m_\alpha\boldsymbol{a}_\alpha\cdot\underbrace{\int \mathrm{d}\boldsymbol{w}\,\boldsymbol{w}\frac{\partial f_\alpha}{\partial \boldsymbol{w}}}_{\overset{\mathrm{bp}}{=}\,-n_\alpha\boldsymbol{I}}$$

$$-\cancelto{0}{\int \mathrm{d}\boldsymbol{w}\, m_\alpha\boldsymbol{w}(\boldsymbol{w}\cdot\boldsymbol{\nabla}\boldsymbol{u}_\alpha)\cdot\frac{\partial f_\alpha}{\partial \boldsymbol{w}}} = \int \mathrm{d}\boldsymbol{w}\, m_\alpha\boldsymbol{w} C[f_\alpha]$$

$$\Longrightarrow \quad \boxed{\boldsymbol{\nabla}\cdot\boldsymbol{P}_\alpha - m_\alpha n_\alpha\boldsymbol{a}_\alpha = \int \mathrm{d}\boldsymbol{w}\, m_\alpha\boldsymbol{w} C[f_\alpha] \doteq \boldsymbol{R}_\alpha} \quad \text{(force equation for species } \alpha\text{)} \qquad \text{(II.4.10)}$$

where

$$\boxed{\boldsymbol{P}_\alpha \doteq \int \mathrm{d}\boldsymbol{w}\, m_\alpha\boldsymbol{w}\boldsymbol{w} f_\alpha} \qquad \text{(II.4.11)}$$

is the thermal pressure tensor of species α and $\boldsymbol{R}_\alpha$ is the friction force on species α (recall Newton's third law, $\sum_\alpha \boldsymbol{R}_\alpha = 0$). Equation (II.4.10) may of course be rewritten in the following, more familiar, form:

$$m_\alpha n_\alpha \frac{\mathrm{D}\boldsymbol{u}_\alpha}{\mathrm{D}t_\alpha} = m_\alpha n_\alpha \left[\frac{q_\alpha}{m_\alpha} \left(\boldsymbol{E} + \frac{\boldsymbol{v}}{c} \times \boldsymbol{B} \right) + \boldsymbol{g} \right] - \boldsymbol{\nabla} \cdot \boldsymbol{\mathsf{P}}_\alpha + \boldsymbol{R}_\alpha. \tag{II.4.12}$$

If we sum (II.4.12) over species, the electric-field term vanishes by quasineutrality, $\sum_\alpha q_\alpha n_\alpha = 0$. Then, defining the total mass density $\rho \doteq \sum_\alpha m_\alpha n_\alpha$ and the mean center-of-mass velocity $\boldsymbol{u} \doteq \rho^{-1} \sum_\alpha m_\alpha n_\alpha \boldsymbol{u}_\alpha$, equation (II.4.12) implies

$$\rho \left(\frac{\partial}{\partial t} + \boldsymbol{u} \cdot \boldsymbol{\nabla} \right) \boldsymbol{u} = \rho \boldsymbol{g} - \boldsymbol{\nabla} \cdot (\boldsymbol{\mathsf{P}} + \boldsymbol{\mathsf{D}}), \tag{II.4.13}$$

where $\boldsymbol{\mathsf{P}} \doteq \sum_\alpha \boldsymbol{\mathsf{P}}_\alpha$ is the total pressure tensor and

$$\boldsymbol{\mathsf{D}} \doteq \sum_\alpha m_\alpha n_\alpha \Delta\boldsymbol{u}_\alpha \Delta\boldsymbol{u}_\alpha \tag{II.4.14}$$

is a tensor composed of species drifts relative to the center-of-mass velocity,

$$\Delta\boldsymbol{u}_\alpha \doteq \boldsymbol{u}_\alpha - \boldsymbol{u}. \tag{II.4.15}$$

(Note that $\sum_\alpha m_\alpha n_\alpha \Delta\boldsymbol{u}_\alpha = 0$, by definition.) The second moment is

$$\begin{aligned} \int \mathrm{d}\boldsymbol{w}\, m_\alpha w_i w_j (\text{II.4.7}) : \quad & \frac{\mathrm{D}}{\mathrm{D}t_\alpha} \underbrace{\int \mathrm{d}\boldsymbol{w}\, m_\alpha w_i w_j}_{= P_{\alpha,ij}} + \int \mathrm{d}\boldsymbol{w}\, m_\alpha w_i w_j \boldsymbol{w} \cdot \boldsymbol{\nabla} f_\alpha \\ & + m_\alpha a_{\alpha,k} \cancelto{0}{\int \mathrm{d}\boldsymbol{w}\, w_i w_j \frac{\partial f_\alpha}{\partial w_k}} - \int \mathrm{d}\boldsymbol{w}\, m_\alpha w_i w_j (\boldsymbol{w} \cdot \boldsymbol{\nabla} u_{\alpha,\ell}) \frac{\partial f_\alpha}{\partial w_\ell} \\ & = \int \mathrm{d}\boldsymbol{w}\, m_\alpha w_i w_j C[f_\alpha]. \end{aligned} \tag{II.4.16}$$

Define the heat flux tensor for species α:

$$\boldsymbol{\mathsf{Q}}_\alpha \doteq \int \mathrm{d}\boldsymbol{w}\, m_\alpha \boldsymbol{w}\boldsymbol{w}\boldsymbol{w} f_\alpha. \tag{II.4.17}$$

Then, equation (II.4.16) becomes, after integrating by parts the final term on its left-hand side,

$$\boxed{\frac{\mathrm{D}P_{\alpha,ij}}{\mathrm{D}t_\alpha} + (\boldsymbol{\nabla} \cdot \boldsymbol{\mathsf{Q}}_\alpha)_{ij} + \big(\delta_{i\ell} P_{\alpha,jk} + \delta_{j\ell} P_{\alpha,ik} + \delta_{k\ell} P_{\alpha,ij} \big) \frac{\partial u_{\alpha,\ell}}{\partial r_k} = \int \mathrm{d}\boldsymbol{w}\, m_\alpha w_i w_j C[f_\alpha]} \tag{II.4.18}$$

Usually the trace of this equation is taken, with the scalar (isotropic) pressure being given by

$$P_\alpha \doteq \frac{1}{3} \mathrm{tr}\, \boldsymbol{\mathsf{P}}_\alpha. \tag{II.4.19}$$

Then (II.4.18) provides an evolutionary equation for the internal energy:

$$\frac{3}{2} \frac{\mathrm{D}P_\alpha}{\mathrm{D}t_\alpha} + \boldsymbol{\nabla} \cdot \boldsymbol{q}_\alpha + \frac{3}{2} P_\alpha \boldsymbol{\nabla} \cdot \boldsymbol{u}_\alpha + \boldsymbol{\mathsf{P}}_\alpha \,\boldsymbol{:}\, \boldsymbol{\nabla} \boldsymbol{u}_\alpha = Q_\alpha, \tag{II.4.20}$$

where

$$\boldsymbol{q}_\alpha \doteq \int \mathrm{d}\boldsymbol{w}\, \frac{1}{2} m_\alpha w^2 \boldsymbol{w} f_\alpha \tag{II.4.21}$$

is the conductive heat flux of species α and

$$Q_\alpha \doteq \int \mathrm{d}\boldsymbol{w}\, \frac{1}{2} m_\alpha w^2 C[f_\alpha] \tag{II.4.22}$$

is the collisional energy exchange between species. Further writing

$$\boxed{\mathsf{\boldsymbol{P}}_\alpha \doteq P_\alpha \mathsf{\boldsymbol{I}} + \boldsymbol{\mathit{\Pi}}_\alpha,} \tag{II.4.23}$$

where $\boldsymbol{\mathit{\Pi}}_\alpha$ is the viscous stress tensor of species α and using (II.4.9) to replace $\boldsymbol{\nabla}\cdot\boldsymbol{u}_\alpha$ in (II.4.20) by $\mathrm{D}\ln n_\alpha/\mathrm{D}t$, the internal energy equation (II.4.20) provides an equation for the hydrodynamic entropy:

$$\boxed{\frac{3}{2} P_\alpha \frac{\mathrm{D}}{\mathrm{D}t_\alpha} \ln \frac{P_\alpha}{n_\alpha^{5/3}} = -\boldsymbol{\nabla}\cdot\boldsymbol{q}_\alpha - \boldsymbol{\mathit{\Pi}}_\alpha \boldsymbol{:} \boldsymbol{\nabla}\boldsymbol{u}_\alpha + Q_\alpha} \tag{II.4.24}$$

Note that, in the absence of conductive heat fluxes, viscous stresses, and energy exchange amongst species, the hydrodynamic entropy of a fluid element is conserved (as it should be). Finally, using (II.4.23), the force equation (II.4.12) becomes

$$m_\alpha n_\alpha \frac{\mathrm{D}\boldsymbol{u}_\alpha}{\mathrm{D}t_\alpha} = m_\alpha n_\alpha \left[\frac{q_\alpha}{m_\alpha} \left(\boldsymbol{E} + \frac{\boldsymbol{v}}{c} \times \boldsymbol{B} \right) + \boldsymbol{g} \right] - \boldsymbol{\nabla} P_\alpha - \boldsymbol{\nabla}\cdot\boldsymbol{\mathit{\Pi}}_\alpha + \boldsymbol{R}_\alpha, \tag{II.4.25}$$

giving our final form of the momentum equation for species α.

II.4.3. *Dimensionless free parameters and the reduction to ideal MHD*

To arrive at our ideal-MHD equations, two reductions to the above equations must be performed. The first reduction is to sum over all species, leading to a "single-fluid" framework with $\rho \doteq \sum_\alpha \rho_\alpha$, $P \doteq \sum_\alpha P_\alpha$, $\boldsymbol{u} \doteq \rho^{-1} \sum_\alpha \rho_\alpha \boldsymbol{u}_\alpha$, etc. The only place where this is a non-trivial exercise is in the momentum equation. As mentioned earlier (after (II.3.8)), the drift that appears between $\boldsymbol{u}_\alpha$ and the center-of-mass velocity $\boldsymbol{u} = \boldsymbol{u}_\alpha - \Delta\boldsymbol{u}_\alpha$ can usually be neglected, e.g., if collisions between different species keep their bulk flows very close to the center-of-mass velocity, or if the total mass density and total momentum density are dominated by a single species. The latter situation is a statement about the mass ratio of the constituent species (e.g., $m_\mathrm{e}/m_\mathrm{i} \ll 1$ in an ion-electron plasma). This means that, so far, we've accumulated two dimensionless free parameters. In AST554, you will obtain expressions for $\boldsymbol{\mathit{\Pi}}_\alpha$ and $\boldsymbol{q}_\alpha$ for a collisional plasma; that procedure introduces additional dimensionless free parameters.

For an electron-ion plasma with a single species of ion, exhibiting characteristic scales along ($L_\parallel$) and across ($L_\perp$) a magnetic field, here is a list of possible free parameters:

$$\mathrm{M} \doteq \frac{U}{C}, \quad \frac{m_\mathrm{e}}{m_\mathrm{i}}, \quad \beta \doteq \frac{P}{B^2/8\pi} \left(\text{or } \frac{U}{v_\mathrm{A}} \right), \quad \frac{\lambda_\mathrm{mfp}}{L_\parallel}, \quad \frac{r_\mathrm{gyro}}{L_\perp}, \quad \frac{L_\parallel}{L_\perp}.$$

The first is the Mach number – the ratio of the characteristic fluid velocity U to the sound speed C – which features in various "high-flow" or "low-flow" orderings employed in magnetized plasmas (e.g., Braginskii 1965; Mikhailovskii & Tsypin 1971, 1984). The second is the electron-to-ion mass ratio, a natural expansion parameter in much of plasma physics. The third is the plasma beta parameter – the ratio of the gas pressure to the magnetic pressure. There are various orderings that involve combinations of β and $m_\mathrm{i}/m_\mathrm{e}$, or β and M; in the latter case, one can alternatively specify the Alfvén Mach number, $\mathrm{M_A} \doteq U/v_\mathrm{A}$, where $v_\mathrm{A} \doteq B/\sqrt{4\pi\rho}$ is the Alfvén speed. The fourth free parameter is the ratio of collisional mean free path (λ_mfp) to the characteristic gradient scale along the magnetic-field direction, $L_\parallel$. This parameter being small allows one to obtain expressions for $\boldsymbol{\Pi}_\alpha$ and $\boldsymbol{q}_\alpha$ in terms of the lower-order moments, thereby closing the "fluid" equations. The idea is that a short mean free path constraints the velocity distribution function of the particles to be nearly Maxwellian in all velocity coordinates. The fifth free parameter is the ratio of the charged particles' gyroradii to the characteristic gradient scale across the magnetic-field direction, $L_\perp$. Magnetized fluids generally have $r_{\rm gyro} \ll \lambda_{\rm mfp} \ll L_\parallel \sim L_\perp$, although the ratio $L_\parallel/L_\perp$ can be large or order unity (in a magnetized plasma it's never really small, because the magnetic field constrains particle motion across it).

Single-fluid ideal MHD generally employs the following ordering: $M \sim \beta \sim L_\parallel/L_\perp \sim 1$ and $(m_{\rm e}/m_{\rm i},\ \lambda_{\rm mfp}/L_\parallel,\ r_{\rm gyro}/L_\perp) \to 0$. The latter ensures that the electron mass, the collisional mean free path, and the gyro-radius never appear in the equations. With $\beta \sim 1$, $r_{\rm gyro}/L_\perp \to 0$ also means that the ion inertial length (i.e., skin depth) $d_{\rm i}$ cannot make an appearance. Extensions of single-fluid ideal MHD might include finite-Larmor-radius effects (with $r_{\rm gyro}/L_\perp$ small but finite) and diffusive transport (with $\lambda_{\rm mfp}/L_\parallel$ small but finite). Other extensions may be obtained from the electron momentum equation after using the smallness of the electron mass to drop the inertial term :

$$0 = -en_{\rm e}\left(\boldsymbol{E} + \frac{\boldsymbol{u}_{\rm e}}{c}\times\boldsymbol{B}\right) - \boldsymbol{\nabla}\cdot\boldsymbol{P}_{\rm e} + \boldsymbol{R}_{\rm e}. \tag{II.4.26}$$

With the current density for a quasi-neutral plasma satisfying $\boldsymbol{j} = en_{\rm e}(\boldsymbol{u}_{\rm i} - \boldsymbol{u}_{\rm e}) = (c/4\pi)\boldsymbol{\nabla}\times\boldsymbol{B}$, this equation may be re-arranged to obtain

$$\boldsymbol{E} + \frac{\boldsymbol{u}_{\rm i}}{c}\times\boldsymbol{B} = \frac{(\boldsymbol{\nabla}\times\boldsymbol{B})\times\boldsymbol{B}}{4\pi en_{\rm e}} - \frac{\boldsymbol{\nabla}\cdot\boldsymbol{P}_{\rm e}}{en_{\rm e}} + \frac{\boldsymbol{R}_{\rm e}}{en_{\rm e}}. \tag{II.4.27}$$

This expression is a generalized Ohm's law for the electric field, written in the frame of the ion flow. The first-term on its right-hand side corresponds to the "Hall effect", which is analyzed and discussed in §X; one may estimate its size in an electron–ion plasma by comparing it to the ideal electric field with $u_{\rm i} \sim v_{\rm A}$:

$$\frac{c}{v_{\rm A}B}\frac{(\boldsymbol{\nabla}\times\boldsymbol{B})\times\boldsymbol{B}}{4\pi en_{\rm e}} \sim \frac{d_{\rm i}}{L},$$

showing that it is a finite-$d_{\rm i}$ term. One may drop finite-Larmor-radius effect but include the Hall effect if the plasma beta parameter is sufficiently small, since $r_{\rm gyro,i} = \sqrt{\beta_{\rm i}}d_{\rm i}$. The importance of the other two terms in (II.4.27) may likewise be estimated:

$$\frac{c}{v_{\rm A}B}\frac{\boldsymbol{\nabla}\cdot\boldsymbol{P}_{\rm e}}{en_{\rm e}} \sim \beta_{\rm e}\frac{d_{\rm i}}{L} \quad \text{and} \quad \frac{c}{v_{\rm A}B}\frac{\boldsymbol{R}_{\rm e}}{en_{\rm e}} \sim (\Omega_{\rm e}\tau_{\rm ei})^{-1}\frac{d_{\rm i}}{L}.$$

Again, finite-$d_{\rm i}$ terms, but ones that may become large depending upon $\beta_{\rm e}$ and the magnetization $\Omega_{\rm e}\tau_{\rm ei}$.

II.5. Equations of magnetohydrodynamics via charged-particle drifts

The final means of arriving at the MHD equations involves calculating the currents associated with the guiding-center drifts of the constituent particles. From GPPI, you should know that the single-particle guiding-center drifts are the $E\times B$ drift, the grad-B drift, the curvature drift, and the polarization drift:

$$\boldsymbol{v}_E = \frac{c}{B}\boldsymbol{E}\times\hat{\boldsymbol{b}}, \quad \boldsymbol{v}_{\nabla B} = \frac{w_\perp^2}{2\Omega_\alpha}\hat{\boldsymbol{b}}\times\boldsymbol{\nabla}\ln B, \quad \boldsymbol{v}_{\rm c} = \frac{v_\parallel^2}{\Omega_\alpha}\hat{\boldsymbol{b}}\times(\hat{\boldsymbol{b}}\cdot\boldsymbol{\nabla}\hat{\boldsymbol{b}}), \quad \boldsymbol{v}_{\rm pol} = \frac{1}{\Omega_\alpha}\frac{c}{B}\frac{\partial\boldsymbol{E}_\perp}{\partial t}. \tag{II.5.1a,b,c,d}$$

The latter two are part of a more general "acceleration" drift,

$$\frac{\hat{\boldsymbol{b}}}{\Omega} \times \frac{\mathcal{D}}{\mathcal{D}t}(v_\parallel \hat{\boldsymbol{b}} + \boldsymbol{v}_E), \quad \text{where} \quad \frac{\mathcal{D}}{\mathcal{D}t} \doteq \frac{\partial}{\partial t} + (v_\parallel \hat{\boldsymbol{b}} + \boldsymbol{v}_E)\cdot\boldsymbol{\nabla}$$

is the Lagrangian time derivative in the parallel-streaming and $E\times B$-drifting frame. Note that all of these drifts are perpendicular to the magnetic field. To make a connection between these single-particle drifts and the MHD equations, we actually need something additional called the *magnetization current*. Before getting to that (it will be discussed in §II.5.2), let us compute the currents associated with the above drifts. As you surely know by now, the $E\times B$ drift is species independent, and thus contributes no current in a quasi-neutral plasma. What about the others?

II.5.1. *Guiding-center drift currents*

To compute the perpendicular currents associated with the particle drifts, $\boldsymbol{j}_{\perp,\mathrm{dr}}$, we imagine a plasma whose particles' velocities are distributed according to a distribution function $f_\alpha(t,\boldsymbol{r},\boldsymbol{v})$ for each species α. The perpendicular current is then obtained by affixing a species label α to the drifts we computed, multiplying each of them by q_α, summing over species, and integrating over the velocity space after weighting each drift by f_α, *viz.*

$$\begin{aligned}
\boldsymbol{j}_{\perp,\mathrm{dr}} &= \sum_\alpha q_\alpha \int \mathrm{d}\boldsymbol{v}\, \boldsymbol{v}_{\mathrm{dr},\alpha} f_\alpha \\
&= \sum_\alpha q_\alpha \int \mathrm{d}\boldsymbol{v} \left[\frac{w_\perp^2}{2\Omega_\alpha}\hat{\boldsymbol{b}}\times\boldsymbol{\nabla}\ln B + \frac{\hat{\boldsymbol{b}}}{\Omega_\alpha}\times\frac{\mathcal{D}}{\mathcal{D}t}(v_\parallel\hat{\boldsymbol{b}} + \boldsymbol{v}_\mathrm{E})\right] f_\alpha \\
&= \frac{c}{B}\hat{\boldsymbol{b}}\times\boldsymbol{\nabla}\ln B \sum_\alpha \int \mathrm{d}\boldsymbol{v}\,\frac{1}{2}m_\alpha w_\perp^2 f_\alpha + \frac{c}{B}\hat{\boldsymbol{b}}\times(\hat{\boldsymbol{b}}\cdot\boldsymbol{\nabla}\hat{\boldsymbol{b}})\sum_\alpha\int \mathrm{d}\boldsymbol{v}\, m_\alpha v_\parallel^2 f_\alpha \\
&\quad + \frac{c}{B}\hat{\boldsymbol{b}}\times\left(\frac{\partial\hat{\boldsymbol{b}}}{\partial t} + \boldsymbol{v}_E\cdot\boldsymbol{\nabla}\hat{\boldsymbol{b}} + \hat{\boldsymbol{b}}\cdot\boldsymbol{\nabla}\boldsymbol{v}_E\right)\sum_\alpha\int\mathrm{d}\boldsymbol{v}\, m_\alpha v_\parallel f_\alpha \\
&\quad + \frac{c}{B}\hat{\boldsymbol{b}}\times\left(\frac{\partial\boldsymbol{v}_E}{\partial t} + \boldsymbol{v}_E\cdot\boldsymbol{\nabla}\boldsymbol{v}_E\right)\sum_\alpha\int\mathrm{d}\boldsymbol{v}\, m_\alpha f_\alpha.
\end{aligned} \tag{II.5.2}$$

Each of the above integrals over the distribution function f_α have a name: $\int \mathrm{d}\boldsymbol{v}\, m_\alpha f_\alpha = m_\alpha n_\alpha$ is the mass density, $\int \mathrm{d}\boldsymbol{v}\, m_\alpha v_\parallel f_\alpha = m_\alpha n_\alpha u_{\parallel\alpha}$ is the parallel component of the bulk momentum density, and

$$\int \mathrm{d}\boldsymbol{v}\,\frac{1}{2}m_\alpha w_\perp^2 f_\alpha = P_{\perp\alpha}, \qquad \int\mathrm{d}\boldsymbol{v}\, m_\alpha v_\parallel^2 f_\alpha = P_{\parallel\alpha} + m_\alpha n_\alpha u_{\parallel\alpha}^2$$

are measures of the particle energies perpendicular and parallel to the magnetic-field direction. Namely, $P_{\perp\alpha}$ ($P_{\parallel\alpha}$) measures the energetic content of the random ("thermal") motions of the particles of species α in the direction perpendicular (parallel) to the local magnetic field; for a collisional plasma in which collisions fully isotropize the particles' random motions, $P_{\perp\alpha} = P_{\|\alpha} = P_\alpha$. Substituting these expressions into (II.5.2) yields

$$\frac{B}{c}\boldsymbol{j}_{\perp,\mathrm{dr}} = \sum_\alpha P_{\perp\alpha}\hat{\boldsymbol{b}}\times\boldsymbol{\nabla}\ln B + \sum_\alpha \Big(P_{\|\alpha} + m_\alpha n_\alpha u_{\|\alpha}^2\Big)\hat{\boldsymbol{b}}\times(\hat{\boldsymbol{b}}\boldsymbol{\cdot}\boldsymbol{\nabla}\hat{\boldsymbol{b}})$$
$$+ \sum_\alpha m_\alpha n_\alpha \hat{\boldsymbol{b}}\times\left[u_{\|\alpha}\frac{\partial\hat{\boldsymbol{b}}}{\partial t} + u_{\|\alpha}\boldsymbol{v}_E\boldsymbol{\cdot}\boldsymbol{\nabla}\hat{\boldsymbol{b}} + u_{\|\alpha}\hat{\boldsymbol{b}}\boldsymbol{\cdot}\boldsymbol{\nabla}\boldsymbol{v}_E + \frac{\partial\boldsymbol{v}_E}{\partial t} + \boldsymbol{v}_E\boldsymbol{\cdot}\boldsymbol{\nabla}\boldsymbol{v}_E\right]. \tag{II.5.3}$$

This may be further simplified using $\hat{\boldsymbol{b}}\times\hat{\boldsymbol{b}} = 0$ and recalling the definition of the Lagrangian time derivative

$$\frac{\mathrm{D}}{\mathrm{D}t_\alpha} \doteq \frac{\partial}{\partial t} + \boldsymbol{u}_\alpha\boldsymbol{\cdot}\boldsymbol{\nabla}, \quad \text{where } \boldsymbol{u}_\alpha \doteq u_{\|\alpha}\hat{\boldsymbol{b}} + \boldsymbol{v}_{\mathrm{E}}. \tag{II.5.4}$$

The result is that

$$\frac{B}{c}\boldsymbol{j}_{\perp,\mathrm{dr}} = \sum_\alpha P_{\perp\alpha}\hat{\boldsymbol{b}}\times\boldsymbol{\nabla}\ln B + \sum_\alpha P_{\|\alpha}\hat{\boldsymbol{b}}\times(\hat{\boldsymbol{b}}\boldsymbol{\cdot}\boldsymbol{\nabla}\hat{\boldsymbol{b}}) + \sum_\alpha m_\alpha n_\alpha\hat{\boldsymbol{b}}\times\frac{\mathrm{D}\boldsymbol{u}_\alpha}{\mathrm{D}t_\alpha}. \tag{II.5.5}$$

So there are currents associated with the grad-B drift, the curvature drift, and the acceleration drifts (which include the polarization drift). We return to this formula in §II.5.3 after discussing the magnetization current.

II.5.2. *Magnetization current*

Plasmas are diamagnetic, a fact made manifest in μ conservation: the greater the plasma (perpendicular) thermal energy, the more it excludes the magnetic field. There is a macroscopic current, not caused by single-particle drifts, associated with this property. Essentially, because a magnetized plasma may be thought of as being composed of magnetic dipoles, each of which being associated with a gyro-orbiting particle, a plasma may be considered as a magnetic material. From basic electromagnetism, the current of a magnetic material in which the magnetization is non-uniform is given by $\boldsymbol{j}_M = c\boldsymbol{\nabla}\times\boldsymbol{M}$, where $\boldsymbol{M}$ is the magnetization per unit volume due to these magnetic dipoles. The latter may be obtained by integrating up all the magnetic moments of each of the particles, $-\mu\hat{\boldsymbol{b}}$ where $\mu \doteq mw_\perp^2/2B$, weighted by the particle distribution function:

$$\boldsymbol{M} = -\hat{\boldsymbol{b}}\sum_\alpha\int \mathrm{d}\boldsymbol{v}\,\mu_\alpha f_\alpha = -\frac{\hat{\boldsymbol{b}}}{B}\sum_\alpha\int\mathrm{d}\boldsymbol{v}\,\frac{1}{2}m_\alpha w_\perp^2 f_\alpha = -\frac{\hat{\boldsymbol{b}}}{B}\sum_\alpha P_{\perp\alpha}. \tag{II.5.6}$$

The resulting current is

$$\boldsymbol{j}_M = c\boldsymbol{\nabla}\times\boldsymbol{M} = -c\boldsymbol{\nabla}\times\left(\frac{\hat{\boldsymbol{b}}}{B}\sum_\alpha P_{\perp\alpha}\right). \tag{II.5.7}$$

The figure below illustrates the origin of this current. In this example, there are more ions gyrating about the (uniform) magnetic field in the center of the plasma than near the edge, and so there is a density (and thus pressure) gradient pointing inwards (indicated by the blue arrows). Therefore, there are more particles whose field-perpendicular velocities are oriented clockwise along the red dashed line than there are particles whose velocities are oriented counter-clockwise. The difference results in a current that flows as indicated, in the $\hat{\boldsymbol{b}}\times\boldsymbol{\nabla}n$ direction. A similar effect occurs if the density of guiding centers is uniform but the particles' perpendicular velocities are larger in some region of space than they are elsewhere. Alternatively, one may think of the magnetization current in terms of diamagnetism: if the perpendicular thermal energy of the particles is larger in one region than in another, the ability of the plasma to exclude magnetic fields is inhomogeneous. This produces a current.

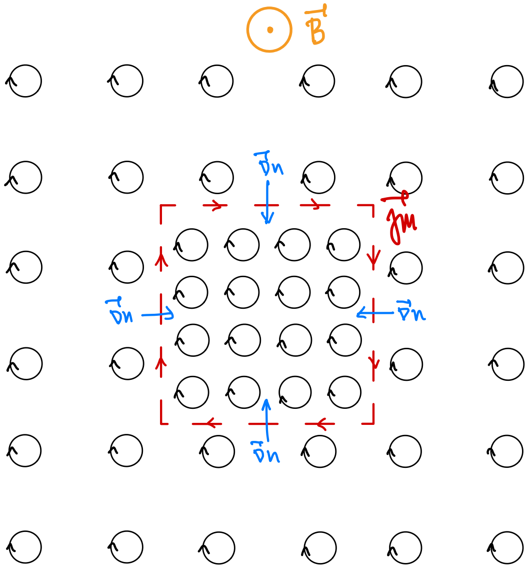

II.5.3. *Total plasma current, momentum equation, and diamagnetic flow*

Let us add up all the perpendicular currents we have discussed thus far:

$$\begin{aligned}\boldsymbol{j}_\perp &= \boldsymbol{j}_M + \boldsymbol{j}_{\perp,\mathrm{dr}} \\ &= -c\boldsymbol{\nabla}\times\left(\frac{\hat{\boldsymbol{b}}}{B}\sum_\alpha P_{\perp\alpha}\right) + \frac{c}{B}\sum_\alpha P_{\perp\alpha}\hat{\boldsymbol{b}}\times\boldsymbol{\nabla}\ln B + \frac{c}{B}\sum_\alpha P_{\parallel\alpha}\hat{\boldsymbol{b}}\times(\hat{\boldsymbol{b}}\cdot\boldsymbol{\nabla}\hat{\boldsymbol{b}}) \\ &\quad + \frac{c}{B}\sum_\alpha m_\alpha n_\alpha \hat{\boldsymbol{b}}\times\frac{\mathrm{D}\boldsymbol{u}_\alpha}{\mathrm{D}t_\alpha}. \end{aligned} \tag{II.5.8}$$

The first two terms may be combined to yield

$$\frac{B}{c}\boldsymbol{j}_\perp = -\boldsymbol{\nabla}\times\left(\hat{\boldsymbol{b}}\sum_\alpha P_{\perp\alpha}\right) + \sum_\alpha P_{\parallel\alpha}\hat{\boldsymbol{b}}\times(\hat{\boldsymbol{b}}\cdot\boldsymbol{\nabla}\hat{\boldsymbol{b}}) + \sum_\alpha m_\alpha n_\alpha\hat{\boldsymbol{b}}\times\frac{\mathrm{D}\boldsymbol{u}_\alpha}{\mathrm{D}t_\alpha}. \tag{II.5.9}$$

This next step will be made clearer later in the course, but for now let use simply introduce the tensor

$$\boldsymbol{P}_\alpha = P_{\perp\alpha}(\boldsymbol{I}-\hat{\boldsymbol{b}}\hat{\boldsymbol{b}}) + P_{\parallel\alpha}\hat{\boldsymbol{b}}\hat{\boldsymbol{b}}, \tag{II.5.10}$$

where $\boldsymbol{I}$ is the unit dyadic. (This is the form of the thermal pressure tensor in a magnetized plasma.) Noting that $\boldsymbol{\nabla}\times\hat{\boldsymbol{b}} - \hat{\boldsymbol{b}}\cdot(\hat{\boldsymbol{b}}\cdot\boldsymbol{\nabla}\hat{\boldsymbol{b}}) = \hat{\boldsymbol{b}}\hat{\boldsymbol{b}}\cdot(\boldsymbol{\nabla}\times\hat{\boldsymbol{b}})$ is parallel to $\hat{\boldsymbol{b}}$, equation (II.5.9) becomes simply

$$\frac{B}{c}\boldsymbol{j}_\perp = \hat{\boldsymbol{b}}\times\sum_\alpha\left(\boldsymbol{\nabla}\cdot\boldsymbol{P}_\alpha + m_\alpha n_\alpha\frac{\mathrm{D}\boldsymbol{u}_\alpha}{\mathrm{D}t_\alpha}\right). \tag{II.5.11}$$

Taking $\hat{\boldsymbol{b}}\times$ (II.5.11) and using the vector identity $\hat{\boldsymbol{b}}\times(\hat{\boldsymbol{b}}\times\boldsymbol{A}) = -\boldsymbol{A}_\perp$, we obtain

$$\sum_\alpha\left(m_\alpha n_\alpha\frac{\mathrm{d}\boldsymbol{u}_\alpha}{\mathrm{d}t_\alpha} + \boldsymbol{\nabla}\cdot\boldsymbol{P}_\alpha\right)_\perp = \frac{\boldsymbol{j}\times\boldsymbol{B}}{c}. \tag{II.5.12}$$

Voila, the perpendicular component of the momentum equation! To go from here to the single-fluid, ideal-MHD momentum equation, one simply takes the pressure tensor to be isotropic, $\boldsymbol{P} = P\boldsymbol{I}$, and further sets $\boldsymbol{D} = 0$ (see (II.4.14)). All the single-particle drifts are contained in MHD.

Allow me to close by pointing out that the quantity

$$\boldsymbol{u}_{\mathrm{dia},\alpha} \doteq \frac{\hat{\boldsymbol{b}}}{\Omega_\alpha} \times \frac{\boldsymbol{\nabla\cdot P}_\alpha}{m_\alpha n_\alpha} \tag{II.5.13}$$

that appears implicitly in (II.5.11) has a name – it is referred to as the *diamagnetic flow velocity* of species α.[2] It is *not* a particle drift, but rather refers to net flux of gyrating particles passing through a reference surface due to an inhomogeneous distribution of guiding centers.

[2]I am deliberately *not* calling it the "diamagnetic drift velocity", as some are wont to do. Nothing is actually drifting, so this moniker makes no sense! One may show that the diamagnetic flow is what one obtains when Taylor-expanding an equilibrium distribution $f(\mathcal{E}, \mu, \boldsymbol{R})$ that is a function of the particle energy $\mathcal{E}$, magnetic moment μ, and guiding-position $\boldsymbol{R}$ about the particle position $\boldsymbol{r} \doteq \boldsymbol{R} + \boldsymbol{\rho}$ and computing its first velocity-space moment.

PART III

Magnetostatics

III.1. Magnetic surfaces, coordinates, and representations

A magnetic surface or "flux surface" is a surface that is covered completely by a magnetic-field line. Alternatively, given a smooth surface $\mathcal{S}$ with normal vector $\hat{\boldsymbol{n}}$, that surface is a flux surface if $\boldsymbol{B} \cdot \hat{\boldsymbol{n}} = 0$ everywhere on $\mathcal{S}$. In this case, the magnetic surface defined by $\psi(\boldsymbol{r}) = \text{const}$ satisfies

$$\boldsymbol{B} \cdot \boldsymbol{\nabla} \psi(\boldsymbol{r}) = 0. \tag{III.1.1}$$

This, and other functions $f(\boldsymbol{r})$ that satisfy $\boldsymbol{B} \cdot \boldsymbol{\nabla} f(\boldsymbol{r}) = 0$ everywhere on $\mathcal{S}$, are called "flux functions", and can be used to label the flux surfaces. In an MHD equilibrium between the pressure and Lorentz forces, we have that

$$0 = -\boldsymbol{\nabla} P + \frac{\boldsymbol{j} \times \boldsymbol{B}}{c} \quad \Longrightarrow \quad \boldsymbol{B} \cdot \boldsymbol{\nabla} P = 0 \quad \text{and} \quad \boldsymbol{j} \cdot \boldsymbol{\nabla} P = 0. \tag{III.1.2}$$

The first of these indicates that P is a flux function, and therefore can be used to label the surfaces. The second indicates that P is also constant along surfaces defined by the current density $\boldsymbol{j}$, i.e., $\boldsymbol{j} \cdot \hat{\boldsymbol{n}} = 0$ on $\mathcal{S}$ defines a current surface. Physically, current flows between, and not across, isobars; but because isobars are also flux surfaces, current flows between, and not across, flux surfaces. (While $\boldsymbol{j}$ and $\boldsymbol{B}$ lie on flux surfaces, this does not imply that they are parallel to one another.)

In devices like tokamaks, flux surfaces (and therefore isobars) are generally nested tori:

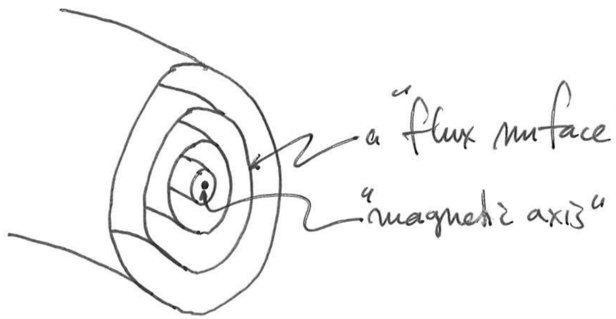

Indeed, the Hopf–Poincaré theorem states that a non-vanishing, continuous tangential vector field cannot lie on a sphere in 3D, and so flux surfaces cannot be spherical surfaces. But it is important to emphasize the adverbs "completely" and "everywhere" (on $\mathcal{S}$) in the preceding paragraph, which are absolutely crucial to the definition of a flux surface. For example, suppose that there is a field line wrapped around a torus on which $\boldsymbol{B} \cdot \boldsymbol{\nabla} P = 0$, but that that field line bites its tail after some distance (i.e., closes in on itself after a finite number of toroidal and poloidal circuits around the torus). Then all we know is that $P = \text{const}$ on the entirety of that "rational" field line, not that $P = \text{const}$ defines a *surface*. Indeed, there could be a neighboring rational field line lying on the same torus that also satisfies $\boldsymbol{B} \cdot \boldsymbol{\nabla} P = 0$, but for a different pressure P. It is only if the field line fills a surface (i.e., is "irrational") that the surface is covered completely by the field line and thus the quantity P can be considered a label of that surface. In general, there are many more irrational field lines than rational field lines. That is a good thing, because rational field lines can break the nested, clean, torus-shaped flux surfaces that are desirable for confinement.

Now, suppose we have a set of flux surfaces. One may define magnetic fluxes through these surfaces. For example, the poloidal flux is defined by

$$\Psi_\mathrm{p} \doteq \int_{\mathcal{S}_\mathrm{p}} \mathrm{d}\boldsymbol{S} \cdot \boldsymbol{B}, \tag{III.1.3}$$

where $\mathcal{S}_\mathrm{p}$ is a ring-shaped ribbon stretched between the magnetic axis and the flux surface; Ψ_p counts how many field lines pierce this surface. Likewise, we can define a toroidal flux:

$$\Psi_\mathrm{t} \doteq \int_{\mathcal{S}_\mathrm{t}} \mathrm{d}\boldsymbol{S} \cdot \boldsymbol{B}, \tag{III.1.4}$$

where $\mathcal{S}_\mathrm{t}$ is a poloidal cross-section of the flux surface. These cross-sections are shown in the figure below:

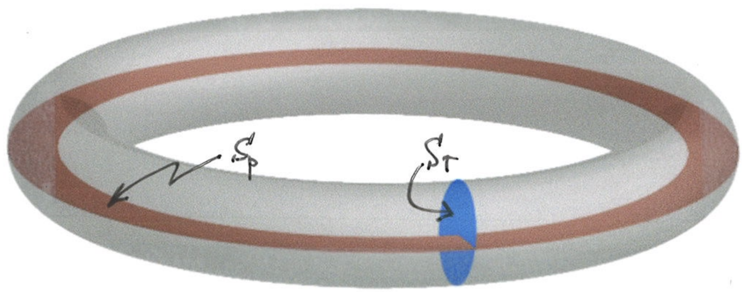

With Ψ_p and Ψ_t being flux-surface labels, we can bake that knowledge into our choice of coordinate system. In toroidal geometry, we may introduce the triad (ψ, θ, ζ), where $\psi = \psi(\boldsymbol{r})$ specifies the "radial" location of the flux surface away from the magnetic axis, $\theta = \theta(\boldsymbol{r})$ specifies the "poloidal" angle around the surface, and $\zeta = \zeta(\boldsymbol{r})$ specifies the toroidal angle around the "azimuthal" extent of the surface:

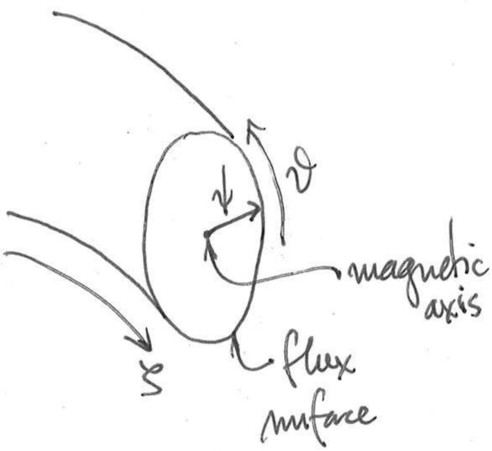

Note that these surfaces do not have to conform to perfect tori in order to establish this "general toroidal coordinate system", only that $\psi(\boldsymbol{r})$, $\theta(\boldsymbol{r})$ and $\zeta(\boldsymbol{r})$ must be smooth functions with the Jacobian

$$\mathcal{J} \doteq \boldsymbol{\nabla}\psi \cdot (\boldsymbol{\nabla}\theta \times \boldsymbol{\nabla}\zeta) \tag{III.1.5}$$

being positive and finite everywhere. For example:

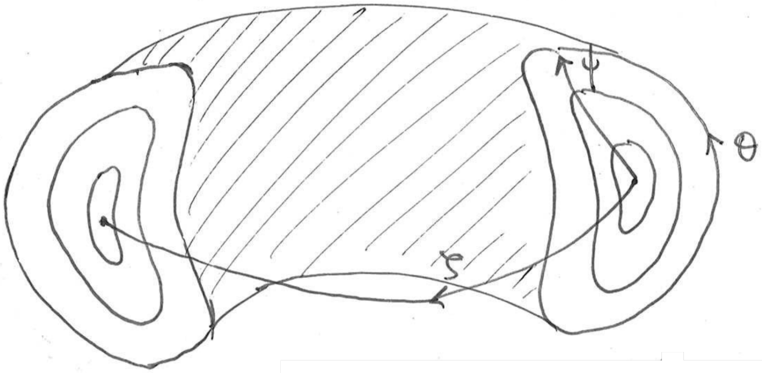

That being said, it is useful to establish a link between these coordinates and the more standard ones for the case of a perfect torus, in which $(\psi, \theta, \zeta) \to (r_0, \theta_0, \zeta_0)$ with

$$r_0 = \sqrt{(R - R_0)^2 + z^2}, \quad \theta_0 = \tan^{-1}\left(\frac{z}{R - R_0}\right), \quad \zeta_0 = -\varphi. \tag{III.1.6}$$

These are labelled in the figure below:

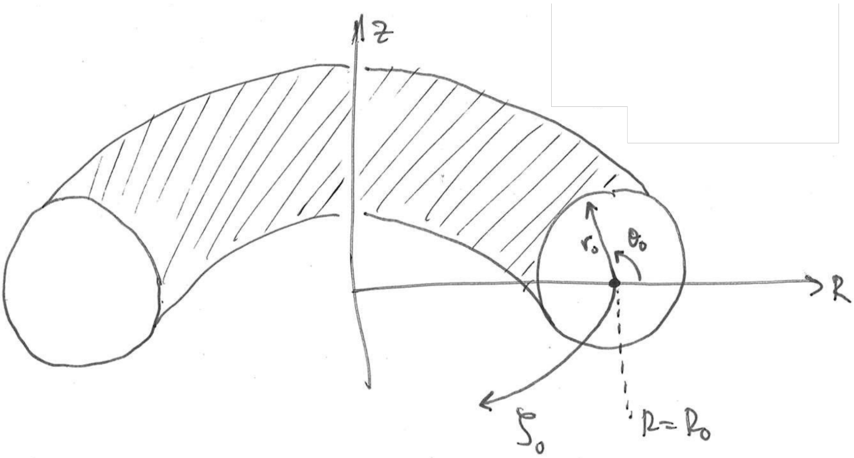

Note that

$$\theta(r_0, \theta_0 + 2\pi m, \zeta_0 + 2\pi n) = \theta(r_0, \theta_0, \zeta_0) + 2\pi m, \tag{III.1.7}$$
$$\zeta(r_0, \theta_0 + 2\pi m, \zeta_0 + 2\pi n) = \zeta(r_0, \theta_0, \zeta_0) + 2\pi n \tag{III.1.8}$$

for any integers m and n. In words, θ and ζ are arbitrary poloidal and toroidal angles such that θ increases by 2π when the the torus is traversed the short way around (the poloidal direction), and φ increases by 2π the long way around (the toroidal direction). The generalized radial coordinate $\psi(\boldsymbol{r})$ must be single-valued:

$$\psi(r_0, \theta_0 + 2\pi m, \zeta_0 + 2\pi n) = \psi(r_0, \theta_0, \zeta_0). \tag{III.1.9}$$

In this case, $\psi = \text{const}$ defines a set of nested tori.

We may make a direct connection between the flux surfaces and these magnetic coordinates by using Gauss' law to write the poloidal flux (III.1.3) in terms of the volume enclosed by the surface $\mathcal{S}_\text{p}$:

$$2\pi\Psi_\text{p} = 2\pi \int_{\mathcal{S}_\text{p}} \mathrm{d}\boldsymbol{S} \cdot \boldsymbol{B} = \oint_{\partial\mathcal{V}} \mathrm{d}\boldsymbol{S} \cdot \boldsymbol{B}\theta = \int_{\mathcal{V}} \mathrm{d}\boldsymbol{r}\, \boldsymbol{\nabla} \cdot (\boldsymbol{B}\theta) = \int_{\mathcal{V}} \mathrm{d}\boldsymbol{r}\, \boldsymbol{B} \cdot \boldsymbol{\nabla}\theta. \tag{III.1.10}$$

The key step is the second equality, which imagines that the surface $\mathcal{S}_{\rm p}$, shown as the red ribbon in the figure above, is actually two neighboring surfaces created by radial cuts from the magnetic axis outwards to the flux surface: one at $\theta = 0$ and one at $\theta = 2\pi$. The volume between these two surfaces that span the discontinuity in θ from $\theta = 0$ to $\theta = 2\pi$ is denoted by $\mathcal{V}$. We may perform a similar calculation for the toroidal flux (III.1.4), now imagining the blue cross-sectional area in the figure above as being composed of two neighboring surfaces created by slicing normally through the torus $\zeta = 0$ and bounding the volume of the flux tube within:

$$2\pi \varPsi_{\rm t} = 2\pi \int_{\mathcal{S}_{\rm t}} {\rm d}\boldsymbol{S} \boldsymbol{\cdot} \boldsymbol{B} = \oint_{\partial\mathcal{V}} {\rm d}\boldsymbol{S} \boldsymbol{\cdot} \boldsymbol{B}\zeta = \int_{\mathcal{V}} {\rm d}\boldsymbol{r}\, \boldsymbol{\nabla} \boldsymbol{\cdot} (\boldsymbol{B}\zeta) = \int_{\mathcal{V}} {\rm d}\boldsymbol{r}\, \boldsymbol{B} \boldsymbol{\cdot} \boldsymbol{\nabla}\zeta. \tag{III.1.11}$$

The quantities in (III.1.10) and (III.1.11) occur sufficiently frequently that carrying around the 2π becomes cumbersome:[3]

$$\psi \doteq \frac{\varPsi_{\rm p}}{2\pi} = \frac{1}{(2\pi)^2} \int_{\mathcal{V}} {\rm d}\boldsymbol{r}\, \boldsymbol{B} \boldsymbol{\cdot} \boldsymbol{\nabla}\theta, \tag{III.1.12}$$

$$\chi \doteq \frac{\varPsi_{\rm t}}{2\pi} = \frac{1}{(2\pi)^2} \int_{\mathcal{V}} {\rm d}\boldsymbol{r}\, \boldsymbol{B} \boldsymbol{\cdot} \boldsymbol{\nabla}\zeta, \tag{III.1.13}$$

Note that we've used the symbol ψ twice in two different contexts: first, as the "radial" location of the flux surface away from the magnetic axis, and now as the poloidal flux (divided by 2π). But this is by design: we can label the "radial" location of the surfaces by the amount of flux that penetrates them. From this association follows a general representation of the magnetic field expressed in terms of these flux functions and the generalized angles:

$$\boldsymbol{B} = \boldsymbol{\nabla}\zeta \times \boldsymbol{\nabla}\psi + \boldsymbol{\nabla}\chi \times \boldsymbol{\nabla}\theta + \boldsymbol{\nabla}\chi \times \boldsymbol{\nabla}\lambda, \tag{III.1.14}$$

where $\lambda = \lambda(\chi, \theta, \zeta)$ is a function that is 2π-periodic in the two angles θ and ζ so that its contribution to the integrals in (III.1.12) and (III.1.13) vanishes by periodicity. Indeed, inserting this expression into (III.1.12) gives

$$\begin{aligned}
\psi &= \frac{1}{(2\pi)^2} \int_{\mathcal{V}} {\rm d}\boldsymbol{r}\, (\boldsymbol{\nabla}\zeta \times \boldsymbol{\nabla}\psi + \boldsymbol{\nabla}\chi \times \boldsymbol{\nabla}\theta + \boldsymbol{\nabla}\chi \times \boldsymbol{\nabla}\lambda) \boldsymbol{\cdot} \boldsymbol{\nabla}\theta \\
&= \frac{1}{(2\pi)^2} \int_{\mathcal{V}} {\rm d}\boldsymbol{r}\, \boldsymbol{\nabla}\psi \boldsymbol{\cdot} (\boldsymbol{\nabla}\theta \times \boldsymbol{\nabla}\zeta) + \frac{1}{(2\pi)^2} \int_{\mathcal{V}} {\rm d}\boldsymbol{r}\, \boldsymbol{\nabla}\lambda \boldsymbol{\cdot} (\boldsymbol{\nabla}\theta \times \boldsymbol{\nabla}\chi) \\
&= \frac{1}{(2\pi)^2} \int_{\mathcal{V}} {\rm d}\psi\, {\rm d}\theta\, {\rm d}\zeta \left(1 - \frac{\partial\lambda}{\partial\zeta} \frac{{\rm d}\chi}{{\rm d}\psi}\right) = \psi + 0 = \psi.
\end{aligned} \tag{III.1.15}$$

Likewise for (III.1.13) with χ:

$$\begin{aligned}
\chi &= \frac{1}{(2\pi)^2} \int_{\mathcal{V}} {\rm d}\boldsymbol{r}\, (\boldsymbol{\nabla}\zeta \times \boldsymbol{\nabla}\psi + \boldsymbol{\nabla}\chi \times \boldsymbol{\nabla}\theta + \boldsymbol{\nabla}\chi \times \boldsymbol{\nabla}\lambda) \boldsymbol{\cdot} \boldsymbol{\nabla}\zeta \\
&= \frac{1}{(2\pi)^2} \int_{\mathcal{V}} {\rm d}\boldsymbol{r}\, \boldsymbol{\nabla}\chi \boldsymbol{\cdot} (\boldsymbol{\nabla}\theta \times \boldsymbol{\nabla}\zeta) + \frac{1}{(2\pi)^2} \int_{\mathcal{V}} {\rm d}\boldsymbol{r}\, \boldsymbol{\nabla}\lambda \boldsymbol{\cdot} (\boldsymbol{\nabla}\zeta \times \boldsymbol{\nabla}\chi) \\
&= \frac{1}{(2\pi)^2} \int_{\mathcal{V}} {\rm d}\chi\, {\rm d}\theta\, {\rm d}\zeta \left(1 + \frac{\partial\lambda}{\partial\theta}\right) = \chi + 0 = \chi.
\end{aligned} \tag{III.1.16}$$

[3] Warning! Some fusion practitioners use ψ and χ to mean the poloidal and toroidal flux functions, respectively; others flip the definitions so that ψ is the toroidal flux function. The latter is more often associated with those who work on stellarators. For example, the review by Helander (2014) defines ψ (χ) as the toroidal (poloidal) flux. Sometimes even the direction of ζ is flipped to make the coordinate system left-handed instead of right-handed. Yikes! Be careful.

We can exploit the freedom in choosing λ to insist that

$$\frac{\mathrm{d}\theta}{\mathrm{d}\lambda} = \frac{\mathrm{d}\psi}{\mathrm{d}\chi} - 1, \tag{III.1.17}$$

which relates the coordinates to the poloidal and toroidal fluxes. The utility of this choice is apparent if we define $\vartheta \doteq \theta + \lambda$, for which (III.1.14) becomes

$$\boxed{\boldsymbol{B} = \boldsymbol{\nabla}\zeta \times \boldsymbol{\nabla}\psi + \boldsymbol{\nabla}\chi \times \boldsymbol{\nabla}\vartheta} \tag{III.1.18}$$

and (III.1.17) gives

$$\boxed{\frac{\mathrm{d}\vartheta}{\mathrm{d}\zeta} = \frac{\mathrm{d}\psi}{\mathrm{d}\chi} = \frac{\boldsymbol{\nabla}\psi\boldsymbol{\cdot}(\boldsymbol{\nabla}\vartheta\times\boldsymbol{\nabla}\zeta)}{\boldsymbol{\nabla}\chi\boldsymbol{\cdot}(\boldsymbol{\nabla}\vartheta\times\boldsymbol{\nabla}\zeta)} = \frac{(\boldsymbol{\nabla}\zeta\times\boldsymbol{\nabla}\psi)\boldsymbol{\cdot}\boldsymbol{\nabla}\vartheta}{(\boldsymbol{\nabla}\chi\times\boldsymbol{\nabla}\vartheta)\boldsymbol{\cdot}\boldsymbol{\nabla}\zeta} = \frac{\boldsymbol{B}\boldsymbol{\cdot}\boldsymbol{\nabla}\vartheta}{\boldsymbol{B}\boldsymbol{\cdot}\boldsymbol{\nabla}\zeta} \doteq \iota(\psi)} \tag{III.1.19}$$

In these (ϑ, ζ) coordinates, the average pitch of the field lines on a surface as calculated from the fluxes and the local pitch of the field lines on that surface are equal to one another. As a result, the magnetic-field lines expressed in these new "straight-field-line coordinates" (ψ, ϑ, ζ) are straight lines on each flux surface ψ with a constant *rotational transform* $\iota = \iota(\psi)$:

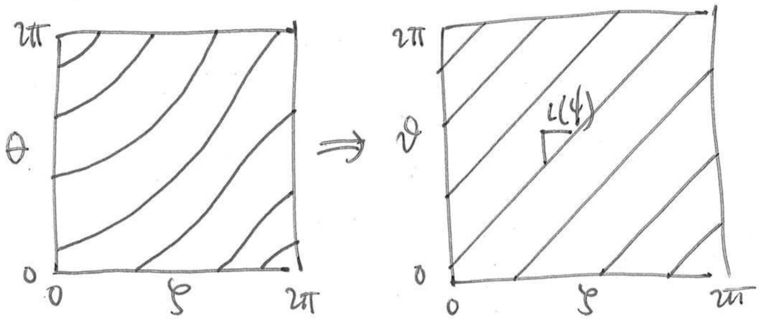

In this sense, λ is the function that describes the difference between the local pitch of the field lines (as measured in the general toroidal coordinates system) and the average pitch of the field lines. Using $\iota = \mathrm{d}\psi/\mathrm{d}\chi$ from (III.1.19), we may then rewrite (III.1.18) as

$$\boxed{\boldsymbol{B} = \boldsymbol{\nabla}\chi \times \boldsymbol{\nabla}(\vartheta - \iota\zeta) = \boldsymbol{\nabla}(\zeta - q\vartheta) \times \boldsymbol{\nabla}\psi} \tag{III.1.20}$$

where

$$q(\psi) \doteq \frac{\mathrm{d}\chi}{\mathrm{d}\psi} = \frac{\mathrm{d}\zeta}{\mathrm{d}\vartheta} = \frac{1}{\iota(\psi)} \tag{III.1.21}$$

is called the *safety factor*.

Before continuing, a few words on the physical interpretation of ι and q. The former (ι) is the average change in poloidal angle per single transit in the toroidal direction, or the number of poloidal turns in one toroidal turn for a field line. Likewise, the safety factor q indicates how many toroidal turns a field line makes during each poloidal turn around the flux surface. Namely, if $q = n/m$ with both m and n integers, a field line will return in its original position after n toroidal and m poloidal transits around the torus. If the value of q is irrational, the magnetic surface is covered ergodically by the field line. An example of a torus with a field line having $q = 3/2$:

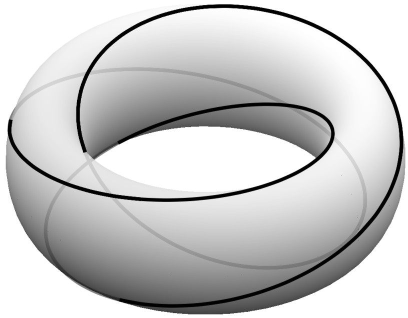

This quantity is called the safety factor because $q > 1$ is the Kruskal–Shafranov stability condition for the toroidal field to stabilize the plasma against the kink mode (about which we'll learn in §VI.9).

To work with straight-field-line coordinates, analytic modeling of stellarators often defines the angle

$$\alpha \doteq \vartheta - \iota\zeta \quad \text{such that (III.1.20) reads} \quad \boldsymbol{B} = \boldsymbol{\nabla}\chi \times \boldsymbol{\nabla}\alpha. \tag{III.1.22}$$

Tokamak modeling more often uses q than ι, and so one can similarly define

$$\alpha \doteq \zeta - q\vartheta \quad \text{such that (III.1.20) reads} \quad \boldsymbol{B} = \boldsymbol{\nabla}\alpha \times \boldsymbol{\nabla}\psi. \tag{III.1.23}$$

In both cases, $\boldsymbol{B} \boldsymbol{\cdot} \boldsymbol{\nabla}\alpha = 0$ and α is constant along the magnetic field. Then each magnetic-field line can be identified by two coordinates, α and ψ (or α and χ). Indeed, we follow a field line once around the torus toroidally, the poloidal angle changes by $\vartheta \to \vartheta + 2\pi\,\iota$, so that (ψ, α) and $(\psi, \alpha + 2\pi\,\iota)$ label the same field line.

The representation of a magnetic field as the cross product of the gradients of two potential fields is known as the *Clebsch representation*. It is a general way of (locally) writing divergence-free vector fields (even those that do not possess flux surfaces). Given two scalar functions $\psi(\boldsymbol{r})$ and $\alpha(\boldsymbol{r})$ such that $\boldsymbol{B} = \boldsymbol{\nabla}\alpha \times \boldsymbol{\nabla}\psi$, any magnetic-field line can be described by the equations $\alpha = \text{const}$, $\psi = \text{const}$. Moreover, if $\boldsymbol{B}$ evolves according to the ideal induction equation (i.e., flux freezing), then

$$\begin{aligned}
\frac{\partial \boldsymbol{B}}{\partial t} = \boldsymbol{\nabla}\alpha \times \boldsymbol{\nabla}\frac{\partial \psi}{\partial t} - \boldsymbol{\nabla}\psi \times \boldsymbol{\nabla}\frac{\partial \alpha}{\partial t} &= \boldsymbol{\nabla} \times (\boldsymbol{u} \times \boldsymbol{B}) \\
&= \boldsymbol{\nabla} \times \big[\boldsymbol{u} \times (\boldsymbol{\nabla}\alpha \times \boldsymbol{\nabla}\psi)\big] \\
&= \boldsymbol{\nabla} \times \big[\boldsymbol{\nabla}\alpha\,(\boldsymbol{u} \boldsymbol{\cdot} \boldsymbol{\nabla}\psi) - \boldsymbol{\nabla}\psi\,(\boldsymbol{u} \boldsymbol{\cdot} \boldsymbol{\nabla}\alpha)\big] \\
&= -\boldsymbol{\nabla}\alpha \times \boldsymbol{\nabla}(\boldsymbol{u} \boldsymbol{\cdot} \boldsymbol{\nabla}\psi) + \boldsymbol{\nabla}\psi \times \boldsymbol{\nabla}(\boldsymbol{u} \boldsymbol{\cdot} \boldsymbol{\nabla}\alpha)
\end{aligned}$$

$$\Longrightarrow \quad \frac{\mathrm{D}\alpha}{\mathrm{D}t} = \frac{\partial \alpha}{\partial t} + \boldsymbol{u} \boldsymbol{\cdot} \boldsymbol{\nabla}\alpha = 0 \quad \text{and} \quad \frac{\mathrm{D}\psi}{\mathrm{D}t} = \frac{\partial \psi}{\partial t} + \boldsymbol{u} \boldsymbol{\cdot} \boldsymbol{\nabla}\psi = 0. \tag{III.1.24}$$

This is an alternate way of expressing flux freezing: the field line lying at the intersection of two magnetic surfaces is advected by the plasma and therefore moves with the plasma flow.

III.2. Hamiltonian structure of field lines

Magnetic-field lines are a Hamiltonian system. To see this, start with the poloidal-toroidal Clebsch representation of the magnetic field:

$$\boldsymbol{B} = \boldsymbol{\nabla}\zeta \times \boldsymbol{\nabla}\psi + \boldsymbol{\nabla}\chi \times \boldsymbol{\nabla}\vartheta. \tag{III.2.1}$$

By definition, magnetic-field lines are specified by $\boldsymbol{B}\cdot\mathrm{d}\boldsymbol{\ell}=0$, where $\mathrm{d}\boldsymbol{\ell}$ is an element along the field line. Choosing to label our flux surfaces using the potential χ, this definition implies the following equalities:

$$\frac{\mathrm{d}\chi}{\boldsymbol{B}\cdot\boldsymbol{\nabla}\chi}=\frac{\mathrm{d}\vartheta}{\boldsymbol{B}\cdot\boldsymbol{\nabla}\vartheta}=\frac{\mathrm{d}\zeta}{\boldsymbol{B}\cdot\boldsymbol{\nabla}\zeta}. \tag{III.2.2}$$

Upon substituting in our Clebsch decomposition, these equalities may be re-arranged to obtain

$$\frac{\mathrm{d}\vartheta}{\mathrm{d}\zeta}=\frac{\mathrm{d}\psi}{\mathrm{d}\chi}\quad\text{and}\quad\frac{\mathrm{d}\chi}{\mathrm{d}\zeta}=-\frac{\mathrm{d}\psi}{\mathrm{d}\vartheta} \tag{III.2.3}$$

These are Hamilton's equations if we adopt $\psi=\psi(\chi,\vartheta,\zeta)$ as our Hamiltonian and ζ as our time coordinate, the latter of which requiring ζ to be non-singular. Where does this come from?

Recall from classical mechanics that magnetic fields contribute to the Lagrangian of a system the following term:

$$\mathcal{L}_{\mathrm{em}}=\boldsymbol{v}\cdot\boldsymbol{A}, \tag{III.2.4}$$

where $\boldsymbol{A}$ is the vector potential (we have set the "charge" to unity). A vector potential corresponding to (III.2.1) is

$$\boldsymbol{A}=-\psi\boldsymbol{\nabla}\zeta+\chi\boldsymbol{\nabla}\vartheta; \tag{III.2.5}$$

note that I didn't say *the* vector potential, because of gauge freedom. Substituting (III.2.5) into (III.2.4) and writing $\boldsymbol{v}=\mathrm{d}\boldsymbol{\ell}/\mathrm{d}\zeta$ (because we are considering ζ as our time coordinate), we find that

$$\mathcal{L}_{\mathrm{em}}=\mathrm{d}\ell\left(\chi\frac{\mathrm{d}\vartheta}{\mathrm{d}\zeta}-\psi\right). \tag{III.2.6}$$

Dropping the arbitrary pre-factor of $\mathrm{d}\ell$ and the no-longer-accurate "em" subscript on $\mathcal{L}$, we have

$$\mathcal{L}(\zeta,\vartheta,\dot{\theta})=\chi\frac{\mathrm{d}\vartheta}{\mathrm{d}\zeta}-\psi\quad\Longrightarrow\quad\mathcal{H}=\psi(\zeta,\vartheta,\chi), \tag{III.2.7}$$

where ϑ is playing the role of the generalized coordinate q and χ is playing the role of the conjugate momentum p. Evidently, the flux function ψ is our Hamiltonian. This only works if the variational principle from which the Lagrangian $\mathcal{L}$ is derived involves finding the path along which the action

$$S=\int\mathrm{d}\boldsymbol{\ell}\cdot\boldsymbol{A}=\int\left(-\psi\,\mathrm{d}\zeta+\chi\,\mathrm{d}\vartheta\right)=\int\mathrm{d}\zeta\left(-\psi+\chi\frac{\mathrm{d}\vartheta}{\mathrm{d}\zeta}\right) \tag{III.2.8}$$

is stationary. In other words, magnetic-field lines are the paths that extremize S. One way to visualize this[4] is to start from the definition of the action and relate it to magnetic flux by integrating around a closed loop:

$$\oint\mathrm{d}\boldsymbol{\ell}\cdot\boldsymbol{A}=\int\mathrm{d}\boldsymbol{S}\cdot\boldsymbol{B}. \tag{III.2.9}$$

To extremize the action, the curve should lie along the local magnetic field, otherwise a magnetic flux will be produced through the enclosed surface.

One consequence of this perspective is that axisymmetric fields are associated with an integrable Hamiltonian: $\mathrm{d}\vartheta/\mathrm{d}\zeta=\mathrm{d}\chi/\mathrm{d}\zeta=0$ in (III.2.3) implies that each field line lies on a flux surface given by $\psi=\psi(\chi,\vartheta)=\text{const}$ (or $\chi=\text{const}$ for that matter). In this sense,

[4] I learned this from Thomas Foster.

our magnetic surfaces are tori, and the trajectories of the associated Hamiltonian lie on nested toroidal surfaces defined by values of the "energy" ψ. (Recall that symmetries are associated with conserved quantities.) Another consequence is that the equation for the poloidal angle reduces to

$$\frac{\mathrm{d}\vartheta}{\mathrm{d}\zeta} = \iota(\chi) = \frac{1}{q(\psi)} \quad \Longrightarrow \quad \vartheta(\zeta) = \vartheta_0 + \iota\zeta = \vartheta_0 - \zeta/q. \tag{III.2.10}$$

So, indeed, if the safety factor $q = m/n$ is rational, then ϑ returns to its initial value ϑ_0 (mod 2π) after a finite number of toroidal circuits, with each field line on the rational surface being closed.

Suppose the axisymmetry is broken by a perturbation, such that

$$\psi(\chi, \vartheta, \zeta) = \psi_0(\chi) + \sum_{m,n\neq 0} \psi_{mn}(\chi)\, \mathrm{e}^{\mathrm{i}(m\vartheta - n\zeta)}. \tag{III.2.11}$$

Then Hamilton's equations (III.2.3) read

$$\frac{\mathrm{d}\vartheta}{\mathrm{d}\zeta} = \frac{\mathrm{d}\psi}{\mathrm{d}\chi} = \iota(\chi) + \sum_{m,n\neq 0} \psi'_{mn}(\chi)\, \mathrm{e}^{\mathrm{i}(m\vartheta - n\zeta)}, \tag{III.2.12a}$$

$$-\frac{\mathrm{d}\chi}{\mathrm{d}\zeta} = \frac{\mathrm{d}\psi}{\mathrm{d}\vartheta} = \sum_{m,n\neq 0} \mathrm{i}m\, \psi_{mn}(\chi)\, \mathrm{e}^{\mathrm{i}(m\vartheta - n\zeta)} \tag{III.2.12b}$$

with $\iota = \mathrm{d}\psi_0/\mathrm{d}\chi$. Take $\psi_{mn} \ll \psi_0$ so that we may take the perturbation to be linear, corresponding to the magnetic field *almost* possessing good flux surfaces. Then (III.2.12) become

$$\vartheta \simeq \vartheta_0 + \iota(\chi_0)\zeta, \tag{III.2.13a}$$

$$\chi \simeq \chi_0 + \sum_{m,n\neq 0} \frac{m\, \psi_{mn}(\chi_0)}{n - m\iota(\chi_0)}\, \mathrm{e}^{\mathrm{i}[m\vartheta_0 - (n - m\iota(\chi_0))\zeta]}. \tag{III.2.13b}$$

Note the singularity at $\iota(\chi_0) = n/m$, which is a rational surface. It is around these rational surfaces that magnetic islands can form. If such islands become wide enough to overlap with one another, then the magnetic field can become chaotic and will not possess nested flux surfaces everywhere in the plasma. (The island width is $\varDelta\chi \sim \sqrt{\psi_{mn}/\iota'(\chi_0)}$, where ι' denotes the shear in the pitch of the magnetic field from one flux surface to the next; strong shear limits the width of the islands.) These islands may be removed by adding a current, with a magnitude chosen to cancel the rotational transform and thus unwind the twisted magnetic field within the island. That's all for now.

III.3. Hamada and Boozer coordinates

Instead of adding $\nabla\chi \times \nabla\lambda$ with $\lambda = \lambda(\chi, \theta, \zeta)$ in (III.1.14), one could have instead added $\nabla\lambda \times \nabla\psi$ with $\lambda = \lambda(\psi, \theta, \zeta)$, again without changing ψ or χ. Then instead of introducing $\vartheta \doteq \theta + \lambda$, one would define $\xi \doteq \zeta + \lambda$ to obtain the representations

$$\boldsymbol{B} = \nabla\xi \times \nabla\psi + \nabla\chi \times \nabla\theta = \nabla\chi \times \nabla(\theta - \iota\xi) = \nabla(\xi - q\theta) \times \nabla\psi,$$

with

$$\frac{\mathrm{d}\chi}{\mathrm{d}\psi} = \frac{\mathrm{d}\xi}{\mathrm{d}\theta} = q(\psi) = \frac{1}{\iota(\psi)}.$$

In this case, (θ, ξ) is a perfectly valid straight-field-line coordinate system. The difference between this representation and equations (III.1.18) and (III.1.20) is only in how one moves to straight-field-line coordinates: by using λ to adjust θ, or by using λ to adjust ζ. As long as the field lines remain straight in the new coordinate system, one may even introduce two different λ functions and adjust both:

$$\boldsymbol{B} = \boldsymbol{\nabla}(\zeta + \lambda_\psi) \times \boldsymbol{\nabla}\psi + \boldsymbol{\nabla}\chi \times \boldsymbol{\nabla}(\theta + \lambda_\chi).$$

with $\lambda_\psi = \lambda_\psi(\psi, \theta, \zeta)$ and $\lambda_\chi = \lambda_\chi(\chi, \theta, \zeta)$. The standard convention (used in §§III.1 and III.2) is to set $\lambda_\psi = 0$ and use $\lambda_\chi = \lambda$ to adjust θ such that $\mathrm{d}\theta/\mathrm{d}\lambda = \iota - 1$. But suppose we were to choose

$$\lambda_\chi = \lambda - \iota\omega \quad \text{and} \quad \lambda_\psi = -\omega,$$

where $\omega(\chi, \vartheta, \zeta)$ is well behaved and 2π-periodic in the poloidal and toroidal directions. Then $\boldsymbol{B}$ would be unchanged from the standard straight-field-line coordinates:

$$\boldsymbol{B} = \boldsymbol{\nabla}(\zeta - \omega) \times \boldsymbol{\nabla}\psi + \boldsymbol{\nabla}\chi \times \boldsymbol{\nabla}(\theta + \lambda - \iota\omega) = \boldsymbol{\nabla}\zeta \times \boldsymbol{\nabla}\psi + \boldsymbol{\nabla}\chi \times \boldsymbol{\nabla}\vartheta.$$

Let us use this freedom to introduce $\zeta' \doteq \zeta - \omega$ and $\vartheta' \doteq \vartheta - \iota\omega$, and write

$$\boldsymbol{B} = \boldsymbol{\nabla}\zeta' \times \boldsymbol{\nabla}\psi + \boldsymbol{\nabla}\chi \times \boldsymbol{\nabla}\vartheta'. \tag{III.3.1}$$

Our first goal is to choose ω such that the streamlines of the current density are also straight lines in our coordinate system. We'll start by using (χ, ϑ, ζ) coordinates, in which our magnetic-field lines are already straight.

The manipulations we employed to arrive at our straight-field-line coordinate system began with calculating the poloidal and toroidal magnetic fluxes through $\mathcal{S}_\mathrm{p}$ and $\mathcal{S}_\mathrm{t}$, and then demanding that the new coordinates make the local pitch of the magnetic-field lines on a flux surface equal to their average pitch on that flux surface. For the current density, we work instead with the poloidal and toroidal currents:

$$I_\mathrm{p} \doteq \int_{\mathcal{S}_\mathrm{t}} \mathrm{d}\boldsymbol{S} \boldsymbol{\cdot} \boldsymbol{j} = \frac{c}{4\pi} \oint_{\partial\mathcal{S}_\mathrm{t}} \mathrm{d}\boldsymbol{\ell} \boldsymbol{\cdot} \boldsymbol{B}, \tag{III.3.2}$$

$$I_\mathrm{t} \doteq \int_{\mathcal{S}_\mathrm{p}} \mathrm{d}\boldsymbol{S} \boldsymbol{\cdot} \boldsymbol{j} = \frac{c}{4\pi} \oint_{\partial\mathcal{S}_\mathrm{p}} \mathrm{d}\boldsymbol{\ell} \boldsymbol{\cdot} \boldsymbol{B}, \tag{III.3.3}$$

where the closed contours are taken around the toroidal and poloidal cross-sections, respectively. Because $\boldsymbol{\nabla} \boldsymbol{\cdot} \boldsymbol{j} = 0$, we can play the same game with $\boldsymbol{j}$ as we did with $\boldsymbol{B}$ (cf. (III.1.12) and (III.1.13)) to write

$$G \doteq \frac{I_\mathrm{p}}{2\pi} = \frac{1}{(2\pi)^2} \int_{\mathcal{V}} \mathrm{d}\boldsymbol{r}\, \boldsymbol{j} \boldsymbol{\cdot} \boldsymbol{\nabla}\vartheta, \tag{III.3.4}$$

$$I \doteq \frac{I_\mathrm{t}}{2\pi} = \frac{1}{(2\pi)^2} \int_{\mathcal{V}} \mathrm{d}\boldsymbol{r}\, \boldsymbol{j} \boldsymbol{\cdot} \boldsymbol{\nabla}\zeta. \tag{III.3.5}$$

Then, following (III.1.14), we may write

$$\boldsymbol{j} = \boldsymbol{\nabla} I \times \boldsymbol{\nabla}\vartheta + \boldsymbol{\nabla} G \times \boldsymbol{\nabla}\zeta + \boldsymbol{\nabla} K \times \boldsymbol{\nabla}\chi, \tag{III.3.6}$$

where $K = K(\chi, \vartheta, \zeta)$ is a function (just like λ) that is 2π-periodic in ϑ and ζ. The idea is to choose K such that the pitch of the local current streamlines on a flux surface matches the average pitch of the current streamlines on that surface, and then relate the gauge function K to the other gauge function ω. This task is performed by first using (III.3.6) to recover an alternative representation of the magnetic field:

$$\boldsymbol{j} = \frac{c}{4\pi} \boldsymbol{\nabla} \times \boldsymbol{B} \quad \Longrightarrow \quad \frac{c}{4\pi} \boldsymbol{B} = I \boldsymbol{\nabla}\vartheta + G \boldsymbol{\nabla}\zeta + K \boldsymbol{\nabla}\chi + \boldsymbol{\nabla} H,$$

where $H = H(\chi, \vartheta, \zeta)$ is a gauge function. Substituting in the latest set of coordinates,

$\zeta = \zeta' + \omega$ and $\vartheta = \vartheta' + \iota\omega$, yields

$$\begin{aligned}\frac{c}{4\pi}\boldsymbol{B} &= I\boldsymbol{\nabla}(\vartheta' + \iota\omega) + G\boldsymbol{\nabla}(\zeta' + \omega) + K\boldsymbol{\nabla}\chi + \boldsymbol{\nabla}H \\ &= I\boldsymbol{\nabla}\vartheta' + G\boldsymbol{\nabla}\zeta' + \left[K - \omega\frac{\mathrm{d}}{\mathrm{d}\chi}(\iota I + G)\right]\boldsymbol{\nabla}\chi + \boldsymbol{\nabla}\left[H + \omega(\iota I + G)\right] \\ &\doteq I\boldsymbol{\nabla}\vartheta' + G\boldsymbol{\nabla}\zeta' + K'\boldsymbol{\nabla}\chi + \boldsymbol{\nabla}H'. \end{aligned} \tag{III.3.7}$$

If we then choose $K' = 0$ by setting $K = \omega(\mathrm{d}/\mathrm{d}\chi)(\iota I + G)$, then

$$\frac{c}{4\pi}\boldsymbol{B} = I\boldsymbol{\nabla}\vartheta' + G\boldsymbol{\nabla}\zeta' + \boldsymbol{\nabla}H' \quad\Longrightarrow\quad \boxed{\boldsymbol{j} = \boldsymbol{\nabla}I\times\boldsymbol{\nabla}\vartheta' + \boldsymbol{\nabla}G\times\boldsymbol{\nabla}\zeta'} \tag{III.3.8}$$

This choice of $K' = 0$ results in what is known as *Hamada coordinates*, in which the streamlines of both $\boldsymbol{B}$ and $\boldsymbol{j}$ are straight lines but with different rotational transforms. Indeed, by introducing

$$\tilde{\iota} = \frac{1}{\tilde{q}} = -\frac{\mathrm{d}G}{\mathrm{d}I}, \tag{III.3.9}$$

we may write the current density in Clebsch form:

$$\boldsymbol{j} = \boldsymbol{\nabla}I\times\boldsymbol{\nabla}(\vartheta' - \tilde{\iota}\zeta') = \boldsymbol{\nabla}G\times\boldsymbol{\nabla}(\zeta' - \tilde{q}\vartheta'). \tag{III.3.10}$$

Hamada coordinates are especially good for simplifying MHD stability analyses, calculating neoclassical transport, and offering good convergence in Fourier space when analyzing stellarators or low-aspect-ratio, strongly shaped tokamaks.

The reason to set $K' = 0$ in (III.3.7) was so that only a full gradient ($\boldsymbol{\nabla}H'$) remained to join the desired current terms, $I\boldsymbol{\nabla}\vartheta' + G\boldsymbol{\nabla}\zeta'$. That gradient is then annihilated by taking the curl to obtain the current density. But this choice isn't unique. The so-called *Boozer coordinates* result by instead choosing $H' = 0$ by setting $H = -\omega(\iota I + G)$. In this case,

$$\frac{4\pi}{c}\boldsymbol{B} = I\boldsymbol{\nabla}\vartheta' + G\boldsymbol{\nabla}\zeta' + K'\boldsymbol{\nabla}\chi, \tag{III.3.11}$$

thus providing the magnetic field in a relatively simple, covariant representation. Another utility of Boozer coordinates is seen by crossing $\boldsymbol{\nabla}\chi$ with (III.3.11) to obtain

$$\frac{4\pi}{c}\boldsymbol{\nabla}\chi\times\boldsymbol{B} = \boldsymbol{\nabla}\chi\times\big(I\boldsymbol{\nabla}\vartheta' + G\boldsymbol{\nabla}\zeta'\big) = I\boldsymbol{\nabla}\chi\times\boldsymbol{\nabla}\left(\vartheta' + \frac{G}{I}\zeta'\right), \tag{III.3.12}$$

thus eliminating K' (a useful simplification because K' is an arbitrary function of all three coordinates). If the electrostatic potential is a flux function (which it usually is to lowest order because charges can rapidly move along field lines and short out potential differences), then the electric field is a "radial" electric field pointing along $\boldsymbol{\nabla}\chi$. In this case, Boozer coordinates transform the streamlines of the $\boldsymbol{E}\times\boldsymbol{B}$ drift into straight lines (not necessarily perpendicular to the straight magnetic-field lines in this coordinate system). Boozer coordinates are useful in analyzing stellarators (which generally have $G \gg I$), especially in quasi-axisymmetric configurations, i.e., those for which the magnetic-field strength $B(\chi, \vartheta', \zeta')$ is independent of ζ'.

III.4. MHD equilibria in cylindrical geometry

Imagine a straight, cylindrical (R, φ, z) plasma in magnetohydrostatic equilibrium with the fields depending only upon the cylindrical radius R:

$$0 = \boldsymbol{\nabla}P - \frac{\boldsymbol{j}\times\boldsymbol{B}}{c} \quad\Longrightarrow\quad 0 = \frac{\mathrm{d}}{\mathrm{d}R}\left(P + \frac{B_\varphi^2 + B_z^2}{8\pi}\right) + \frac{B_\varphi^2}{4\pi R}. \tag{III.4.1}$$

Here we have used the fact that the solenoidality constraint on the magnetic field implies zero radial magnetic field:

$$0 = \boldsymbol{\nabla} \boldsymbol{\cdot} \boldsymbol{B} = \frac{1}{R}\frac{\mathrm{d}(RB_R)}{\mathrm{d}R} \quad \Longrightarrow \quad B_R = 0.$$

Note that (III.4.1) may be also written as

$$0 = \frac{\mathrm{d}}{\mathrm{d}R}\left(P + \frac{B_z^2}{8\pi}\right) + \frac{B_\varphi}{4\pi R}\frac{\mathrm{d}(RB_\varphi)}{\mathrm{d}R}. \tag{III.4.2}$$

This configuration, in which the current satisfies

$$j_\varphi = -\frac{c}{4\pi}\frac{\mathrm{d}B_z}{\mathrm{d}R} = \frac{cB_z}{B^2}\frac{\mathrm{d}P}{\mathrm{d}R} \quad \text{and} \quad j_z = \frac{c}{4\pi R}\frac{\mathrm{d}(RB_\varphi)}{\mathrm{d}R} = -\frac{cB_\varphi}{B^2}\frac{\mathrm{d}P}{\mathrm{d}R}, \tag{III.4.3}$$

is known as a *screw pinch*, diagrammed below:

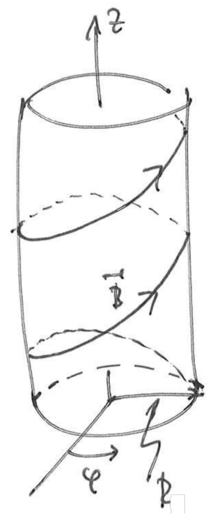

The field lines spiral while residing on a cylindrical surface. Indeed, making the replacements $\zeta \to z$ and $\vartheta \to \varphi$ in (III.1.18) yields the following expression for the magnetic field:

$$\boldsymbol{B} = \hat{\boldsymbol{z}} \times \boldsymbol{\nabla}\psi + \boldsymbol{\nabla}\chi \times \frac{\hat{\boldsymbol{\varphi}}}{R} = \frac{\mathrm{d}\psi}{\mathrm{d}R}\hat{\boldsymbol{\varphi}} + \frac{1}{R}\frac{\mathrm{d}\chi}{\mathrm{d}R}\hat{\boldsymbol{z}}, \tag{III.4.4}$$

where ψ and χ are the fluxes associated with B_φ and B_z, respectively. Using these coordinates to compute the safety factor (III.1.21) yields

$$q(R) \doteq \frac{\mathrm{d}\chi}{\mathrm{d}\psi} = \frac{RB_z(R)}{B_\varphi(R)}. \tag{III.4.5}$$

This will become useful in the next section.

Note that we may multiply (III.4.1) by R^2 and integrate from $R = 0$ to the pinch's radius a to obtain the following:

$$\begin{aligned}
0 &= \int_0^a \mathrm{d}R\, R^2 \frac{\mathrm{d}}{\mathrm{d}R}\left(P + \frac{B_\varphi^2 + B_z^2}{8\pi}\right) + \int_0^a \mathrm{d}R\, R^2 \frac{B_\varphi^2}{4\pi R} \\
&\overset{\text{bp}}{=} a^2\left(P + \frac{B_\varphi^2 + B_z^2}{8\pi}\right)_{R=a} - \int_0^a \mathrm{d}R\, 2R\left(P + \frac{B_\varphi^2 + B_z^2}{8\pi}\right) + \int_0^a \mathrm{d}R\, 2R \frac{B_\varphi^2}{8\pi} \\
\Longrightarrow 0 &= \left(\frac{B_\varphi^2 + B_z^2}{8\pi}\right)_{R=a} - \underbrace{\frac{1}{\pi a^2}\int_0^a \mathrm{d}R\, 2\pi R\left(P + \frac{B_z^2}{8\pi}\right)}_{\doteq \langle P\rangle + \langle B_z^2\rangle/8\pi} .
\end{aligned}$$

Then we may define the quantity

$$\beta_\mathrm{p} \doteq \frac{8\pi\langle P\rangle}{B_\varphi^2(a)} = 1 + \frac{B_z^2(a) - \langle B_z^2\rangle}{B_\varphi^2(a)}. \tag{III.4.6}$$

Freidberg (2014) calls this the "poloidal beta", except that for the pinch it certainly looks like the *toroidal* beta: the magnetic energy referenced is the azimuthal magnetic field evaluated at the surface of the pinch. The reason it's "poloidal" is because, when viewed with one's eyes oriented from above (pointing towards $-z$), the φ direction is oriented in the poloidal direction. To make a tokamak, one simply takes a screw pinch and wraps it back onto itself periodically in a toroidal geometry; in this case, the toroidal direction is actually along the (now-bent) z axis (thus our associations $\zeta \to z$ and $\vartheta \to \varphi$). Again, more on this in the next section. For now, simply note that

$$\begin{aligned}
\beta_\mathrm{p} < 1 &: \langle B_z^2\rangle > B_z^2(a) \quad \text{“paramagnetic”} \\
\beta_\mathrm{p} > 1 &: \langle B_z^2\rangle < B_z^2(a) \quad \text{“diamagnetic”}
\end{aligned}$$

The situation $\beta_\mathrm{p} > 1$ is diamagnetic in the sense that the average field inside the z-pinch is less than the field on the surface (where the pressure vanishes); this occurs because the internal plasma pressure pushes outwards against the confining azimuthal field. As β_p increases, the plasma becomes better at excluding the magnetic field from its interior.

There are two limiting cases of the screw pinch: one called the θ-pinch when $j = j_\varphi$ and $B_\varphi = 0$ (despite "θ" not being $\varphi\ldots$), and the other called the z-pinch when $j = j_z$ and $B_z = 0$. The θ-pinch is just a cylinder with the magnetic field oriented along its symmetry axis:

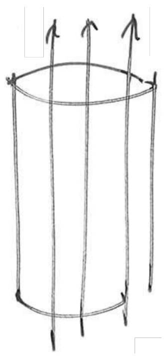

Force balance across field lines gives $P + B_z^2/8\pi = \text{const}$: either the plasma is confined by a magnetic field (i.e., diamagnetic), or the magnetic field is confined by a plasma (i.e., paramagnetic):

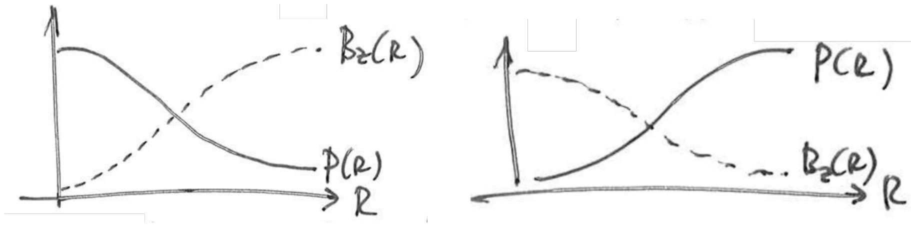

We will show later in the course that this configuration is stable.

The z-pinch is a cylinder with the magnetic field oriented in solely in the azimuthal direction:

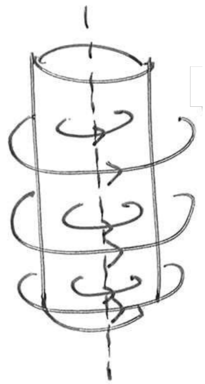

In this case, force balance is given by

$$0 = \frac{\mathrm{d}P}{\mathrm{d}R} + \frac{B_\varphi}{4\pi R}\frac{\mathrm{d}(RB_\varphi)}{\mathrm{d}R}, \tag{III.4.7}$$

which implies $\beta_\mathrm{p} = 1$. To obtain this configuration, it is the current that is usually supplied rather than the azimuthal field, and so

$$B_\varphi(R) = \frac{4\pi}{cR}\int_0^R \mathrm{d}R'\, R' j_z(R'). \tag{III.4.8}$$

This configuration is an equilibrium because the field loops want to contract inwards in the direction of their curvature $\boldsymbol{\kappa} = -\hat{\boldsymbol{R}}/R$, but the magnetic pressure (and the plasma pressure) prevent this. While this configuration confines the plasma, it is unfortunately horribly unstable. There is more in HW02 on the pinch, including the so-called *Bennett relation* and the use of z-pinches for magneto-inertial fusion (e.g., Sandia's Z machine). Some amount of B_z can help stabilize the z-pinch, and so $\boldsymbol{B} = B_\varphi(R)\hat{\boldsymbol{\varphi}} + B_z\hat{\boldsymbol{z}}$ is often investigated (see §VI.9).

The main trouble with all pinch devices for confinement is the loss of plasma at the ends of the cylinder, which is why this configuration was bent into a torus for axial confinement…

III.5. MHD equilibria in toroidal geometry

Take a screw pinch and wrap it into a torus with major radius R_0.

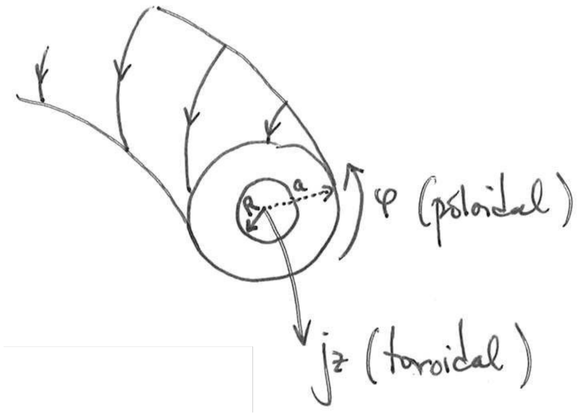

[in progress – see HW02 for more]

III.6. Grad–Shafranov equation

Suppose we were given a plasma pressure profile and a current density distribution. What would be the magnetic geometry that would satisfy the equilibrium

$$\boldsymbol{\nabla}P = \frac{\boldsymbol{j}\times\boldsymbol{B}}{c} \quad \text{with} \quad \boldsymbol{j} = \frac{c}{4\pi}\boldsymbol{\nabla}\times\boldsymbol{B} \quad \text{and} \quad \boldsymbol{\nabla}\boldsymbol{\cdot}\boldsymbol{B} = 0? \tag{III.6.1}$$

Alternatively, suppose we were given a magnetic-field geometry and the currents consistent with that geometry. What would be the equilibrium pressure profile? Both questions are answered by the solution to the Grad–Shafranov (GS) equation.

III.6.1. *GS equation when $\partial/\partial z = 0$*

To derive the GS equation, let's start simple. Suppose I have a plasma that is translationally symmetric, with $\partial/\partial z = 0$. We can use the fact that z is a symmetry direction alongside $\boldsymbol{\nabla}\boldsymbol{\cdot}\boldsymbol{B} = 0$ to write

$$\boldsymbol{B} = \boldsymbol{\nabla}\psi\times\hat{\boldsymbol{z}} + B_z\hat{\boldsymbol{z}}, \tag{III.6.2}$$

where $\psi = \psi(x,y)$ is a scalar potential and $B_z = B_z(x,y)$. By Ampère's law, the current satisfies

$$\frac{4\pi}{c}\boldsymbol{j} = \boldsymbol{\nabla}\times\boldsymbol{B} = (-\nabla^2\psi)\hat{\boldsymbol{z}} - \hat{\boldsymbol{z}}\times\boldsymbol{\nabla}B_z. \tag{III.6.3}$$

We've already seen that P is a flux function, $\boldsymbol{B}\boldsymbol{\cdot}\boldsymbol{\nabla}P = 0$, and so can be used to label the flux surfaces: $P = P(\psi)$. What of B_z? Force balance also implies $\boldsymbol{j}\boldsymbol{\cdot}\boldsymbol{\nabla}P = 0$, from which follows

$$(-\hat{\boldsymbol{z}}\times\boldsymbol{\nabla}B_z)\boldsymbol{\cdot}\boldsymbol{\nabla}P = \hat{\boldsymbol{z}}\boldsymbol{\cdot}(\boldsymbol{\nabla}P\times\boldsymbol{\nabla}B_z) = 0 \quad\Longrightarrow\quad B_z = B_z(P) = B_z(\psi).$$

So both P and B_z are flux functions. Accordingly, force balance becomes

$$\begin{aligned}\boldsymbol{\nabla}P = \frac{\boldsymbol{j}\times\boldsymbol{B}}{c} &= \frac{1}{4\pi}\Big[(-\nabla^2\psi)\hat{\boldsymbol{z}}\times(\boldsymbol{\nabla}\psi\times\hat{\boldsymbol{z}}) + (\boldsymbol{\nabla}B_z\times\hat{\boldsymbol{z}})\times(B_z\hat{\boldsymbol{z}})\Big]\\ &= -\frac{1}{4\pi}\Big[(\nabla^2\psi)\boldsymbol{\nabla}\psi + B_z\boldsymbol{\nabla}B_z\Big].\end{aligned} \tag{III.6.4}$$

The key step in the GS formalism is to express P and B_z as functions of ψ, so that

$$\boldsymbol{\nabla}P = \frac{\mathrm{d}P}{\mathrm{d}\psi}\boldsymbol{\nabla}\psi \quad \text{and} \quad \boldsymbol{\nabla}B_z^2 = \frac{\mathrm{d}B_z^2}{\mathrm{d}\psi}\boldsymbol{\nabla}\psi. \tag{III.6.5}$$

Substituting (III.6.5) into (III.6.4) and rearranging leads to

$$\boxed{-\nabla^2\psi = \frac{4\pi}{c} j_z = 4\pi \frac{\mathrm{d}P}{\mathrm{d}\psi} + \frac{1}{2}\frac{\mathrm{d}B_z^2}{\mathrm{d}\psi}} \tag{III.6.6}$$

This is the GS equation for translationally symmetric plasmas.

There are a few simple solutions to this equation. For the first, set $P = \text{const}$ and $B_z(\psi)/\sqrt{4\pi} = \alpha\psi$. Then we have

$$-\nabla^2\psi = \alpha^2\psi \quad \Longrightarrow \quad \psi = \psi_0 \cos(\alpha x)\cos(\alpha y)$$

in Cartesian geometry. Another simple solution involves a linear pressure profile, $\mathrm{d}(P + B_z^2/8\pi)/\mathrm{d}\psi = \text{const}$. Then

$$-\nabla^2\psi = C \quad \Longrightarrow \quad \psi = \frac{C}{4}(x^2+y^2) + \chi(x,y),$$

where χ is any harmonic function satisfying $\nabla^2\chi = 0$, e.g.,

$$\chi = A(x^2-y^2) + Bxy + Cx + Dy.$$

This solution is the Cartesian analogue of the so-called *Solov'ev solution*, which is discussed briefly in the next section and featured in HW02.

III.6.2. *GS equation when $\partial/\partial\varphi = 0$*

Next suppose that the plasma is azimuthally symmetric, with $\partial/\partial\varphi = 0$ in cylindrical coordinates (R,φ,z). We can use the fact that φ is a symmetry direction alongside $\boldsymbol{\nabla}\cdot\boldsymbol{B} = 0$ to write

$$\boldsymbol{B} = \boldsymbol{\nabla}\psi \times \boldsymbol{\nabla}\varphi + RB_\varphi \boldsymbol{\nabla}\varphi \tag{III.6.7}$$

where $\psi = \psi(R,z)$ and $B_\varphi = B_\varphi(R,z)$. By Ampère's law, the current satisfies

$$\frac{4\pi}{c}\boldsymbol{j} = \boldsymbol{\nabla}\times\boldsymbol{B} = -\underbrace{\left[\frac{\partial^2\psi}{\partial z^2} + R\frac{\partial}{\partial R}\left(\frac{1}{R}\frac{\partial\psi}{\partial R}\right)\right]}_{= R^2\,\boldsymbol{\nabla}\cdot\left(\frac{\boldsymbol{\nabla}\psi}{R^2}\right) \doteq \Delta^*\psi} \boldsymbol{\nabla}\varphi + \boldsymbol{\nabla}(RB_\varphi)\times\boldsymbol{\nabla}\varphi \tag{III.6.8}$$

Because $\boldsymbol{j}\cdot\boldsymbol{\nabla}P = 0$ and $P = P(\psi)$, this equation implies

$$\big[\boldsymbol{\nabla}(RB_\varphi)\times\boldsymbol{\nabla}\varphi\big]\cdot\boldsymbol{\nabla}P = \boldsymbol{\nabla}\varphi\cdot\big[\boldsymbol{\nabla}P\times\boldsymbol{\nabla}(RB_\varphi)\big] = 0 \quad \Longrightarrow \quad RB_\varphi \doteq (RB_\varphi)(\psi).$$

With both ψ and RB_φ being flux functions, force balance (with $\boldsymbol{\nabla}\varphi = \hat{\boldsymbol{\varphi}}/R$) becomes

$$\boldsymbol{\nabla}P = \frac{\boldsymbol{j}\times\boldsymbol{B}}{c} = -\frac{1}{4\pi R^2}\Big[(\Delta^*\psi)(\boldsymbol{\nabla}\psi) + RB_\varphi\boldsymbol{\nabla}(RB_\varphi)\Big]. \tag{III.6.9}$$

Now we express P and B_φ as functions of ψ:

$$\boldsymbol{\nabla}P = \frac{\mathrm{d}P}{\mathrm{d}\psi}\boldsymbol{\nabla}\psi \quad \text{and} \quad \boldsymbol{\nabla}(RB_\varphi) = \frac{\mathrm{d}(RB_\varphi)}{\mathrm{d}\psi}\boldsymbol{\nabla}\psi. \tag{III.6.10}$$

Substituting (III.6.10) into (III.6.9) and rearranging leads to

$$\boxed{-\Delta^*\psi = \frac{4\pi}{c}Rj_\varphi = 4\pi R^2\frac{\mathrm{d}P}{\mathrm{d}\psi} + \frac{1}{2}\frac{\mathrm{d}(RB_\varphi)^2}{\mathrm{d}\psi}} \tag{III.6.11}$$

This is the GS equation for axisymmetric plasmas. Sometimes the combination RB_φ is replaced by the symbol F, which is proportional to the poloidal current:

$$2\pi RB_\varphi = -\frac{4\pi}{c} I_\mathrm{p} \doteq 2\pi F \quad \Longrightarrow \quad \boxed{-\Delta^*\psi = 4\pi R^2 \frac{\mathrm{d}P}{\mathrm{d}\psi} + \frac{1}{2}\frac{\mathrm{d}F^2}{\mathrm{d}\psi}} \tag{III.6.12}$$

This form is useful when it is the current that is being supplied rather than the azimuthal field.

A special class of solutions to (III.6.11) are due to Solov'ev (1968), in which

$$4\pi \frac{\mathrm{d}P}{\mathrm{d}\psi} = -C \quad \text{and} \quad \frac{1}{2}\frac{\mathrm{d}F^2}{\mathrm{d}\psi} = A, \tag{III.6.13}$$

where A and C are constant parameters. These are explored in HW02.

III.6.3. *GS equation for $\varepsilon \ll 1$ and $\beta_\mathrm{p} \sim 1$*

[in progress]

III.7. Wöltjer–Taylor relaxation and force-free states

In some systems (e.g., the solar corona, experiments in plasma confinement using a toroidal pinch), the plasma evolves towards a preferred configuration known as a "relaxed state". This state is in a configuration of minimum magnetic energy, but a minimum energy subject to the constraint that the global magnetic helicity $\mathcal{H}_0 \doteq \int_{\mathcal{V}_0} \mathrm{d}\boldsymbol{r}\, \boldsymbol{A}\cdot\boldsymbol{B}$ is conserved during relaxation. Here, $\boldsymbol{A}$ is the vector potential satisfying $\boldsymbol{B} = \boldsymbol{\nabla}\times\boldsymbol{A}$ and $\mathcal{V}_0$ is the total volume of the isolated plasma under consideration. One can show that magnetic energy decays faster than magnetic helicity when both the magnetic energy and fractional magnetic helicity decrease with increasing wavenumber k and if the magnetic energy spectrum is not too steep (Blackman 2004). Helicity can be interpreted in a topological sense as the number of linkages of magnetic flux tubes ($\mathcal{T}$) with one another:

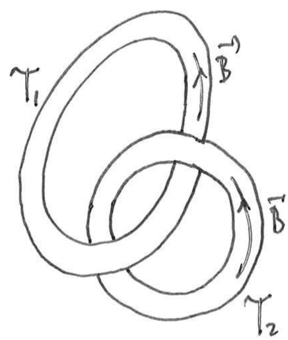

$$\begin{aligned}\mathcal{H}_1 &= \int_{\mathcal{T}_1} \mathrm{d}\boldsymbol{r}\, \boldsymbol{A}\cdot\boldsymbol{B} = \int_{\mathcal{T}_1} \underbrace{\mathrm{d}\boldsymbol{\ell}}_{\mathrm{d}\ell\,\hat{\boldsymbol{b}}} \cdot \underbrace{\mathrm{d}\boldsymbol{S}}_{\mathrm{d}S\,\hat{\boldsymbol{b}}}\, \boldsymbol{A}\cdot \underbrace{\boldsymbol{B}}_{=B\hat{\boldsymbol{b}}} = \int_{\mathcal{T}_1} \left(\mathrm{d}\ell\, \boldsymbol{A}\cdot\hat{\boldsymbol{b}}\right)\left(\mathrm{d}S\,\hat{\boldsymbol{b}}\cdot B\hat{\boldsymbol{b}}\right) \\ &= \int_{\mathcal{T}_1} (\boldsymbol{A}\cdot\mathrm{d}\boldsymbol{\ell})\,(\boldsymbol{B}\cdot\mathrm{d}\boldsymbol{S}) = \underbrace{\Phi_1}_{\text{flux through tube 1}} \underbrace{\int_{\mathcal{T}_1} \boldsymbol{A}\cdot\mathrm{d}\boldsymbol{\ell}}_{\text{flux through hole in tube 1}} = \Phi_1 \underbrace{\Phi_2}_{\text{flux through tube 2}} .\end{aligned} \tag{III.7.1}$$

For a system with many linked flux tubes, the helicity of tube i is

$$\mathcal{H}_i = \Phi_i \, \Phi_{\text{through } i\text{'s hole}} = \Phi_i \sum_j \Phi_j N_{ij}, \tag{III.7.2}$$

where N_{ij} is the number of times tube j passes through the hole in tube i. The total helicity of all of the flux tubes is then

$$\mathcal{H}_0 = \sum_{i,j} \Phi_i \Phi_j N_{ij}, \tag{III.7.3}$$

i.e., the number of linkages of flux tubes. Even when the plasma is not ideal, helicity conservation seems to remain a fairly good approximation.[5]

While $\boldsymbol{A} \cdot \boldsymbol{B}$ is not gauge invariant, its integral within a flux tube is. Let $\boldsymbol{A} \to \boldsymbol{A} + \boldsymbol{\nabla}\psi$. Then, with $\boldsymbol{B} = \boldsymbol{\nabla} \times \boldsymbol{A}$, the combination

$$\boldsymbol{A} \cdot \boldsymbol{B} \to (\boldsymbol{A} + \boldsymbol{\nabla}\psi) \cdot \boldsymbol{B} = \boldsymbol{A} \cdot \boldsymbol{B} + \boldsymbol{\nabla}\psi \cdot \boldsymbol{B} \tag{III.7.4}$$

is not gauge invariant. But if we take its integral within a flux tube of volume $\mathcal{V}$,

$$\begin{aligned}
\int_{\mathcal{V}} \mathrm{d}\boldsymbol{r}\, \boldsymbol{A} \cdot \boldsymbol{B} \to \int_{\mathcal{V}} \mathrm{d}\boldsymbol{r}\, \boldsymbol{A} \cdot \boldsymbol{B} + \int_{\mathcal{V}} \mathrm{d}\boldsymbol{r}\, \boldsymbol{\nabla}\psi \cdot \boldsymbol{B} \\
= \int_{\mathcal{V}} \mathrm{d}\boldsymbol{r}\, \boldsymbol{A} \cdot \boldsymbol{B} + \int_{\mathcal{V}} \mathrm{d}\boldsymbol{r}\, \boldsymbol{\nabla} \cdot (\boldsymbol{B}\psi) \\
= \int_{\mathcal{V}} \mathrm{d}\boldsymbol{r}\, \boldsymbol{A} \cdot \boldsymbol{B} + \oint_{\partial\mathcal{V}} \mathrm{d}\boldsymbol{S} \cdot \boldsymbol{B}\psi,
\end{aligned} \tag{III.7.5}$$

we see that the helicity stays invariant provided that $\boldsymbol{B}$ at the boundary of the flux tube is parallel to the boundary (i.e., no field lines stick out of the volume). For $\mathcal{H}_0$ to be a gauge invariant then, the total volume of the isolated plasma must enclose all of the magnetic-field lines.

$\mathcal{H}_0$ is a conserved quantity in ideal MHD (but not in resistive MHD). In resistive MHD,

$$\frac{\partial \boldsymbol{B}}{\partial t} = \boldsymbol{\nabla} \times (\boldsymbol{u} \times \boldsymbol{B} - \eta \boldsymbol{\nabla} \times \boldsymbol{B}) \quad \Longrightarrow \quad \frac{\partial \boldsymbol{A}}{\partial t} = \boldsymbol{u} \times \boldsymbol{B} - \eta \boldsymbol{\nabla} \times \boldsymbol{B} + \boldsymbol{\nabla}\chi \tag{III.7.6}$$

for some scalar function χ. Thus,

$$\begin{aligned}
\frac{\partial}{\partial t} \boldsymbol{A} \cdot \boldsymbol{B} &= \big(\cancel{\boldsymbol{u} \times \boldsymbol{B}} - \eta \boldsymbol{\nabla} \times \boldsymbol{B} + \boldsymbol{\nabla}\chi\big) \cdot \boldsymbol{B} + \boldsymbol{A} \cdot \big[\boldsymbol{\nabla} \times (\boldsymbol{u} \times \boldsymbol{B} - \eta \boldsymbol{\nabla} \times \boldsymbol{B})\big] \\
&= -\eta \boldsymbol{B} \cdot (\boldsymbol{\nabla} \times \boldsymbol{B}) + \Big[\boldsymbol{\nabla} \cdot (\boldsymbol{B}\chi) - \cancel{\chi \boldsymbol{\nabla} \cdot \boldsymbol{B}}\Big] \\
&\quad + \Big\{-\boldsymbol{\nabla} \cdot \big[\boldsymbol{A} \times (\boldsymbol{u} \times \boldsymbol{B} - \eta \boldsymbol{\nabla} \times \boldsymbol{B})\big] + (\cancel{\boldsymbol{u} \times \boldsymbol{B}} - \eta \boldsymbol{\nabla} \times \boldsymbol{B}) \cdot \underbrace{(\boldsymbol{\nabla} \times \boldsymbol{A})}_{= \boldsymbol{B}}\Big\} \\
&= \boldsymbol{\nabla} \cdot \big[\boldsymbol{B}\chi - \boldsymbol{u} \boldsymbol{A} \cdot \boldsymbol{B} + \boldsymbol{B} \boldsymbol{A} \cdot \boldsymbol{u} + \eta \boldsymbol{A} \times (\boldsymbol{\nabla} \times \boldsymbol{B})\big] - 2\eta \boldsymbol{B} \cdot (\boldsymbol{\nabla} \times \boldsymbol{B}).
\end{aligned} \tag{III.7.7}$$

---

[5]Some history: Wöltjer (1958) showed that there are an infinite number of integral invariants in ideal MHD: $\mathcal{H}_i \doteq \int_{\mathcal{V}_i} \mathrm{d}\boldsymbol{r}\, \boldsymbol{A} \cdot \boldsymbol{B} = \text{const}$ on each and every flux tube $\mathcal{V}_i$ in the system. These invariants are related to the well-known property that the magnetic field is frozen into an ideally conducting plasma. J.B. Taylor (1974) realized that, in a slightly resistive turbulent plasma contained within a perfectly conducting boundary, the only flux tube to retain its integrity is that which contains the entire plasma. Then, only $\mathcal{H}_0$ will remain invariant. Taylor's conjecture is that MHD systems tend to minimize their magnetic energy subject to the constraint that the *total* magnetic helicity remains constant. This is what this section and the next are all about.

Integrating this over $\mathcal{V}_0$ and using Gauss' law gives

$$\frac{\mathrm{d}}{\mathrm{d}t}\int_{\mathcal{V}_0}\mathrm{d}\boldsymbol{r}\,\boldsymbol{A}\cdot\boldsymbol{B}=\oint_{\partial\mathcal{V}_0}\mathrm{d}\boldsymbol{S}\cdot\left[\boldsymbol{B}\chi-\boldsymbol{u}\boldsymbol{A}\cdot\boldsymbol{B}+\boldsymbol{B}\boldsymbol{A}\cdot\boldsymbol{u}+\eta\boldsymbol{A}\times(\boldsymbol{\nabla}\times\boldsymbol{B})\right]\\ -2\eta\int_{\mathcal{V}_0}\mathrm{d}\boldsymbol{r}\,\boldsymbol{B}\cdot(\boldsymbol{\nabla}\times\boldsymbol{B}). \tag{III.7.8}$$

The surface integral vanishes if and only if both $\boldsymbol{u}$ and $\boldsymbol{B}$ are parallel to the boundary $\partial\mathcal{V}_0$; physically, no magnetic fields can stick out and no flow can cross the boundary. Neglecting the η term in the surface integral is perhaps a bit more subtle, but it clearly vanishes if there are no currents on $\partial\mathcal{V}_0$; this may be accomplished by arranging $\mathcal{V}_0$ appropriately (e.g., placing it far away) or simply by taking $\eta\to 0$. Thus,

$$\boxed{\frac{\mathrm{d}\mathcal{H}_0}{\mathrm{d}t}=-2\eta\int_{\mathcal{V}_0}\mathrm{d}\boldsymbol{r}\,\boldsymbol{B}\cdot(\boldsymbol{\nabla}\times\boldsymbol{B})} \tag{III.7.9}$$

$\mathcal{H}_0$ is conserved in ideal MHD.

Because helicity is generally better conserved than magnetic energy, the game here is to minimize magnetic energy subject to constant helicity. This can be accomplished using the variational principle:

$$\delta\int_{\mathcal{V}}\mathrm{d}\boldsymbol{r}\left(B^2-\alpha\boldsymbol{A}\cdot\boldsymbol{B}\right)=0, \tag{III.7.10}$$

where α is the Lagrange multiplier introduced to enforce the constant-helicity constraint. The first (B^2) term in (III.7.10) is

$$\delta\int_{\mathcal{V}}\mathrm{d}\boldsymbol{r}\,B^2=2\int_{\mathcal{V}}\mathrm{d}\boldsymbol{r}\,\boldsymbol{B}\cdot\delta\boldsymbol{B}=2\int_{\mathcal{V}}\mathrm{d}\boldsymbol{r}\,\boldsymbol{B}\cdot(\boldsymbol{\nabla}\times\delta\boldsymbol{A})\\ =2\int_{\mathcal{V}}\mathrm{d}\boldsymbol{r}\left[-\boldsymbol{\nabla}\cdot(\boldsymbol{B}\times\delta\boldsymbol{A})+(\boldsymbol{\nabla}\times\boldsymbol{B})\cdot\delta\boldsymbol{A}\right]\\ =-2\int_{\partial\mathcal{V}}\mathrm{d}\boldsymbol{S}\cdot(\boldsymbol{B}\times\delta\boldsymbol{A})+2\int_{\mathcal{V}}\mathrm{d}\boldsymbol{r}\,(\boldsymbol{\nabla}\times\boldsymbol{B})\cdot\delta\boldsymbol{A}. \tag{III.7.11}$$

The second ($\alpha\boldsymbol{A}\cdot\boldsymbol{B}$) term in (III.7.10) is

$$\delta\int_{\mathcal{V}}\mathrm{d}\boldsymbol{r}\,\alpha\boldsymbol{A}\cdot\boldsymbol{B}=\alpha\int_{\mathcal{V}}\mathrm{d}\boldsymbol{r}\,(\delta\boldsymbol{A}\cdot\boldsymbol{B}+\boldsymbol{A}\cdot\delta\boldsymbol{B})=\alpha\int_{\mathcal{V}}\mathrm{d}\boldsymbol{r}\left[\delta\boldsymbol{A}\cdot\boldsymbol{B}+\boldsymbol{A}\cdot(\boldsymbol{\nabla}\times\delta\boldsymbol{A})\right]\\ =\alpha\int_{\mathcal{V}}\mathrm{d}\boldsymbol{r}\left[\delta\boldsymbol{A}\cdot\boldsymbol{B}-\boldsymbol{\nabla}\cdot(\boldsymbol{A}\times\delta\boldsymbol{A})+\underbrace{(\boldsymbol{\nabla}\times\boldsymbol{A})}_{=\boldsymbol{B}}\cdot\delta\boldsymbol{A}\right]\\ =2\alpha\int_{\mathcal{V}}\mathrm{d}\boldsymbol{r}\,\boldsymbol{B}\cdot\delta\boldsymbol{A}-\alpha\int_{\partial\mathcal{V}}\mathrm{d}\boldsymbol{S}\cdot(\boldsymbol{A}\times\delta\boldsymbol{A}). \tag{III.7.12}$$

Subtracting (III.7.12) from (III.7.11), equation (III.7.10) becomes

$$2\int_{\mathcal{V}}\mathrm{d}\boldsymbol{r}\left(\boldsymbol{\nabla}\times\boldsymbol{B}-\alpha\boldsymbol{B}\right)\cdot\delta\boldsymbol{A}+\int_{\partial\mathcal{V}}\mathrm{d}\boldsymbol{S}\cdot\left[(\alpha\boldsymbol{A}-2\boldsymbol{B})\times\delta\boldsymbol{A}\right]=0. \tag{III.7.13}$$

To simplify the surface integral in (III.7.13), one may use the linearized induction equation written in terms of the Lagrangian displacement $\boldsymbol{\xi}$ of a fluid element into which the magnetic field is frozen: $\delta\boldsymbol{B}=\boldsymbol{\nabla}\times(\boldsymbol{\xi}\times\boldsymbol{B})$ – see §V. This equation implies

$\delta\boldsymbol{A} = \boldsymbol{\xi}\times\boldsymbol{B} + \boldsymbol{\nabla}\chi$ for some gauge function χ, and so

$$\boldsymbol{A}\times\delta\boldsymbol{A} = \boldsymbol{A}\times(\boldsymbol{\xi}\times\boldsymbol{B}) + \boldsymbol{A}\times\boldsymbol{\nabla}\chi = \boldsymbol{\xi}(\boldsymbol{A}\cdot\boldsymbol{B}) - \boldsymbol{B}(\boldsymbol{A}\cdot\boldsymbol{\xi}) + \boldsymbol{A}\times\boldsymbol{\nabla}\chi,$$
$$\boldsymbol{B}\times\delta\boldsymbol{A} = \boldsymbol{B}\times(\boldsymbol{\xi}\times\boldsymbol{B}) + \boldsymbol{B}\times\boldsymbol{\nabla}\chi = \boldsymbol{\xi}B^2 - \boldsymbol{B}(\boldsymbol{B}\cdot\boldsymbol{\xi}) + \boldsymbol{B}\times\boldsymbol{\nabla}\chi.$$

The surface integral thus vanishes if $\boldsymbol{\xi}$ and $\boldsymbol{B}$ are parallel to the boundary $\partial\mathcal{V}$, i.e., if there are no displacements and magnetic-field lines through the boundary. This leaves the volume integral,

$$2\int_{\mathcal{V}} \mathrm{d}\boldsymbol{r}\,\big(\boldsymbol{\nabla}\times\boldsymbol{B} - \alpha\boldsymbol{B}\big)\cdot\delta\boldsymbol{A} = 0,$$

which implies that $\boldsymbol{B}$ is a linear force-free field:

$$\boxed{\boldsymbol{\nabla}\times\boldsymbol{B} = \alpha\boldsymbol{B}} \tag{III.7.14}$$

so called because $\boldsymbol{j}\times\boldsymbol{B} = 0$. Taking the curl of (III.7.14) and using $\boldsymbol{\nabla}\cdot\boldsymbol{B} = 0$ gives the Helmholtz equation:

$$\big(\nabla^2 + \alpha^2\big)\boldsymbol{B} = 0. \tag{III.7.15}$$

We explore some important solutions to this equation below.

Before obtaining some force-free fields, it is worth noting two things. First, when α is a constant, the force-free relation $\boldsymbol{\nabla}\times\boldsymbol{B} = \alpha\boldsymbol{B}$ implies $\boldsymbol{B} = \alpha\boldsymbol{A} + \boldsymbol{\nabla}\chi$, where χ is a gauge field. As a result, the helicity density

$$h \doteq \boldsymbol{A}\cdot\boldsymbol{B} = \frac{B^2}{\alpha} - \frac{\boldsymbol{B}}{\alpha}\cdot\boldsymbol{\nabla}\chi. \tag{III.7.16}$$

Then

$$\mathcal{H}_0 = \int \mathrm{d}\boldsymbol{r}\,\frac{1}{\alpha}\big(B^2 - \chi\boldsymbol{B}\cdot\boldsymbol{\nabla}\ln\alpha\big) - \oint \mathrm{d}\boldsymbol{S}\cdot\boldsymbol{B}\,\frac{\chi}{\alpha} = \int \mathrm{d}\boldsymbol{r}\,\frac{B^2}{\alpha}, \tag{III.7.17}$$

where the final equality follows from (III.7.18) and $\hat{\boldsymbol{n}}\cdot\boldsymbol{B} = 0$. Thus, when $\alpha = \text{const}$, the total helicity is proportional to the magnetic energy.

The second thing to note is that α can be promoted to being a function of space (or even time) and any magnetic field satisfying $\boldsymbol{\nabla}\times\boldsymbol{B} = \alpha\boldsymbol{B}$ is still force-free. In such "nonlinear force-free states", the parameter α can be used to label the flux surfaces: taking the divergence of both sides of (III.7.14) and using $\boldsymbol{\nabla}\cdot\boldsymbol{B} = 0$ implies

$$\boldsymbol{B}\cdot\boldsymbol{\nabla}\alpha = 0. \tag{III.7.18}$$

This is nice. Unfortunately, force-free fields cannot have simple structure. For example, it is not possible for a force-free field to contain a set of nested field lines that all lie on a common surface. The proof is by contradiction. Suppose a set of nested field lines does exist on a surface $\mathcal{S}$. If one such field line runs along a closed contour $\varGamma$ on the surface $\mathcal{S}$, then by Stokes' theorem,

$$\oint_{\varGamma} \mathrm{d}\boldsymbol{\ell}\cdot\boldsymbol{B} = \int_{\mathcal{S}} \mathrm{d}S\,\hat{\boldsymbol{n}}\cdot(\boldsymbol{\nabla}\times\boldsymbol{B}) = \frac{4\pi}{c}\int_{\mathcal{S}} \mathrm{d}S\,\hat{\boldsymbol{n}}\cdot\boldsymbol{j}.$$

But because the field is force-free, $\boldsymbol{j}$ is parallel to $\boldsymbol{B}$, in which case $\hat{\boldsymbol{n}}\cdot\boldsymbol{B} = 0$ (i.e., $\boldsymbol{B}$ lies on the surface) implies $\hat{\boldsymbol{n}}\cdot\boldsymbol{j} = 0$. Hence the right-hand side of the above equation is zero. However, we began by assuming that the configuration is such that the left-hand side of the same equation is nonzero: the field lines reside on the surface. Contradiction.

III.8. Force-free magnetic configurations

For our first example of a linear force-free magnetic field, let us work in Cartesian coordinates. Consider a field configuration that is uniform in the y direction, sinusoidal in the x direction with wavenumber k_x, and exponentially decaying over a lengthscale k_z^{-1} in the $z > 0$ direction, with $\alpha^2 < k_x^2$:

$$B_x = B_{x0}\sin(k_x x)\mathrm{e}^{-k_z z}, \quad B_y = B_{y0}\sin(k_x x)\mathrm{e}^{-k_z z}, \quad B_z = B_0\cos(k_x x)\mathrm{e}^{-k_z z}. \tag{III.8.1}$$

The coefficients B_{x0}, B_{y0}, and B_0 may be related by imposing $\boldsymbol{\nabla}\times\boldsymbol{B} = \alpha\boldsymbol{B}$:

$$k_z B_{y0} = \alpha B_{x0}, \quad -k_z B_{x0} + k_x B_0 = \alpha B_{y0}, \quad k_x B_{y0} = \alpha B_0, \tag{III.8.2}$$

which are readily solved to obtain

$$\frac{B_x k_x}{k_z} = \frac{B_y k_x}{\alpha} = B_0\sin(k_x x)\mathrm{e}^{-k_z z}, \quad B_z = B_0\cos(k_x x)\mathrm{e}^{-k_z z}, \tag{III.8.3}$$

with $k_z^2 = k_x^2 - \alpha^2 > 0$. These formulae correspond to sinusoidally arched fields line in the x-z plane whose projection onto the x-y plane are parallel straight lines given by $\mathrm{d}y/\mathrm{d}x = \alpha/k_z$. Indeed, using $\mathrm{d}x/B_x = \mathrm{d}y/B_y = \mathrm{d}z/B_z$, we can obtain the parametric equations

$$x(s) = s, \quad y(s) = y_0 + \frac{\alpha}{k_z}(s - x_0), \quad z(s) = z_0 + \frac{1}{k_z}\ln\frac{\sin(k_x s)}{\sin(k_x x_0)}. \tag{III.8.4}$$

Sturrock (1994) describes this as follows [with his notation changed to suit these notes]: "…begin with a potential field of the form shown in (III.8.3) with $\alpha = 0$… then shear the x-y plane in such a way that strips parallel to the y-axis are displaced in the y-direction. This shear is uniform… increasing the shear amounts to increasing α." An image taken from his text is provided below:

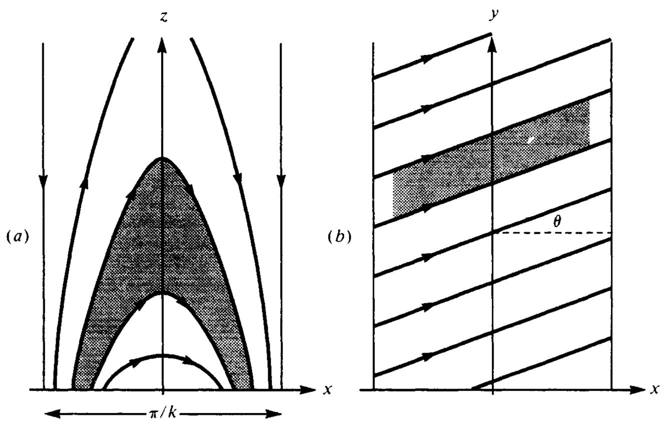

Fig. 13.3. Panel (a) shows the projection in the x–z plane of the force-free field defined by (13.3.4). Panel (b) shows the projection in the x–y plane. (Figure reproduced with kind permission from Priest 1982.)

Next, consider a relaxed, force-free field having cylindrical symmetry: $\partial/\partial\varphi = \partial/\partial z = 0$. In this case, the z and φ components of $\boldsymbol{\nabla}\times\boldsymbol{B} = \alpha(R)\boldsymbol{B}$ are

$$\frac{1}{R}\frac{\mathrm{d}}{\mathrm{d}R}(RB_\varphi) = \alpha(R)B_z \quad\text{and}\quad -\frac{\mathrm{d}B_z}{\mathrm{d}R} = \alpha(R)B_\varphi. \tag{III.8.5}$$

Combining these leads to

$$\frac{1}{R}\frac{\mathrm{d}}{\mathrm{d}R}\left(R\frac{\mathrm{d}B_z}{\mathrm{d}R}\right) = \frac{\mathrm{d}^2 B_z}{\mathrm{d}R^2} + \frac{1}{R}\frac{\mathrm{d}B_z}{\mathrm{d}R} = -\alpha^2 B_z + \frac{\mathrm{d}\ln\alpha}{\mathrm{d}R}\frac{\mathrm{d}B_z}{\mathrm{d}R}$$
$$\Longrightarrow \quad \frac{\mathrm{d}^2 B_z}{\mathrm{d}R^2} + \left(1 - \frac{\mathrm{d}\ln\alpha}{\mathrm{d}\ln R}\right)\frac{1}{R}\frac{\mathrm{d}B_z}{\mathrm{d}R} + \alpha^2 B_z = 0. \tag{III.8.6}$$

First, suppose that $\alpha = \text{const}$, in which case (III.8.6) is a Bessel equation in R for B_z with solution

$$B_z = B_0\,\mathrm{J}_0(\alpha R) \quad \text{and} \quad B_\varphi = B_0\,\mathrm{J}_1(\alpha R), \tag{III.8.7}$$

where J_n is the nth Bessel function and B_0 is some (arbitrary) constant (the solution for B_φ follows from the identity $\mathrm{J}_0' = -\mathrm{J}_1$). Equation (III.8.6) corresponds to a field twisted about a cylindrical surface, with the pitch of the field (i.e., the safety factor) $q \doteq RB_z/B_\varphi = R\mathrm{J}_0/\mathrm{J}_1$ being a function of cylindrical radius. On the symmetry axis, $q = 2/\alpha$; away from the axis, q varies from ∞ to $-\infty$ as αR progresses through the various zeros of the Bessel function J_1. Demanding that the cylinder have finite radial extent requires an external pressure. Here are some field lines on three flux surfaces ($R = 1, 2, 3$) for this force-free pinch with $\alpha = 2$:

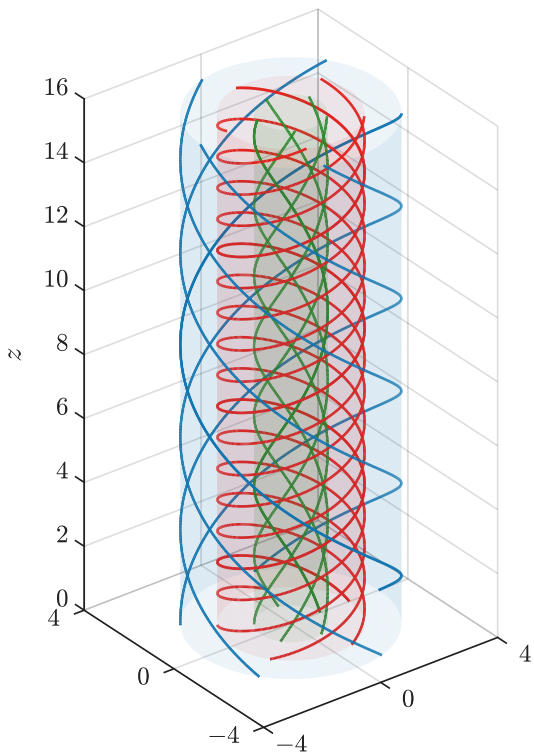

and the pitch angle of the field versus radius:

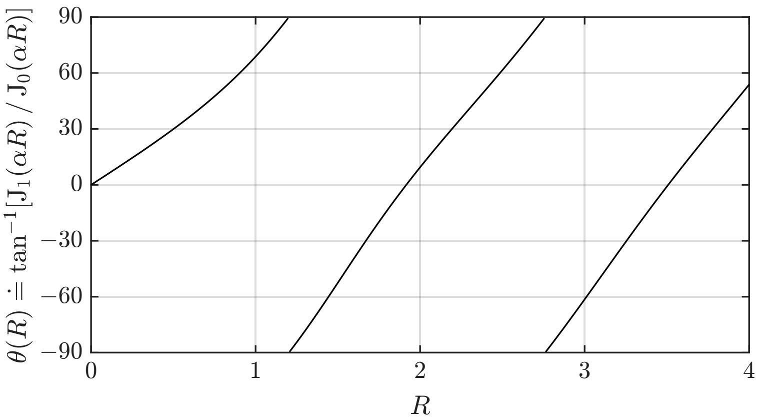

Provided that $\hat{\boldsymbol{n}} \cdot \boldsymbol{B} = 0$ on the surface, the magnetic helicity enclosed within a cylindrical volume $\mathcal{V}_0 = \pi a^2 L_z$ for this configuration is

$$\text{constant } \alpha : \quad \mathcal{H}_0 = \frac{B_0^2}{\alpha} \int_{\mathcal{V}_0} \mathrm{d}\boldsymbol{r}\ \left[\mathrm{J}_0^2(\alpha R) + \mathrm{J}_1^2(\alpha R)\right]$$
$$= \frac{B_0^2}{\alpha^2} \mathcal{V}_0 \left[J_0(\alpha a) + 2J_1^2(\alpha a) + J_2^2(\alpha a) - \frac{2}{\alpha a} J_1(\alpha a) J_2(\alpha a) \right]. \quad \text{(III.8.8)}$$

One can then solve implicitly for $\alpha = \alpha(\mathcal{H}_0)$, which provides an expression for the magnetic field in terms of its helicity.

One obtains a different solution if the safety factor is taken to be a constant, in which case

$$\alpha(R) = -\frac{q}{R}\frac{\mathrm{d}\ln B_z}{\mathrm{d}R} = -q\frac{\alpha(R)q - 2}{R^2} \quad \Longrightarrow \quad \alpha(R) = \frac{2q}{q^2 + R^2}. \quad \text{(III.8.9)}$$

Our equation for B_z then becomes

$$\frac{\mathrm{d}\ln B_z}{\mathrm{d}R} = -\frac{2R}{q^2 + R^2} = -\frac{\mathrm{d}\ln(q^2 + R^2)}{\mathrm{d}R} \quad \Longrightarrow \quad B_z = \frac{qB_\varphi}{R} = \frac{B_0 q^2}{q^2 + R^2}. \quad \text{(III.8.10)}$$

The vector potential corresponding to (III.8.10) is readily obtained by integrating $B_\varphi = -\mathrm{d}A_z/\mathrm{d}R$ and $B_z = R^{-1}\mathrm{d}(RA_\varphi)/\mathrm{d}R$:

$$A_\varphi = \frac{q^2 B_0}{2R} \ln(q^2 + R^2), \quad A_z = -\frac{qB_0}{2} \ln(q^2 + R^2).$$

Then $h = \boldsymbol{A} \cdot \boldsymbol{B} = 0$. But the field lines are clearly twisted! *Question.* What's going on?

The above cylindrical solutions are symmetric about the z-axis and constant along z. More general solutions for $\alpha = \text{const}$ may be obtained by solving

$$(\nabla^2 + \alpha^2) B_z = \frac{1}{R}\frac{\partial}{\partial R}\left(R\frac{\partial B_z}{\partial R}\right) + \alpha^2 B_z + \frac{1}{R^2}\frac{\partial^2 B_z}{\partial \varphi^2} + \frac{\partial^2 B_z}{\partial z^2} = 0 \quad \text{(III.8.11)}$$

using separation of variables (e.g., Chandrasekhar & Kendall 1957). First, write

$$B_z(\boldsymbol{r}) = \sum_{m,k_z} f_{m,k_z}(R)\, \mathrm{e}^{-\mathrm{i}m\varphi + \mathrm{i}k_z z} \quad \text{(III.8.12)}$$

for mode numbers m and k_z. Then define $x^2 \doteq (\alpha^2 - k_z^2)R^2$ with $\alpha > k_z$ and re-arrange (III.8.11) to obtain the following Bessel equation for $f_m(x)$:

$$x^2 \frac{\mathrm{d}^2 f_m}{\mathrm{d}x^2} + x\frac{\mathrm{d}f_m}{\mathrm{d}x} + (x^2 - m^2) f_m = 0 \quad \Longrightarrow \quad f_m = B_0 \mathrm{J}_m(x). \quad \text{(III.8.13)}$$

Taking the real part of the solution provides

$$B_z(x, \varphi, z) = B_0 \sum_{m,k_z} \mathrm{J}_m(x) \cos(m\varphi + k_z z). \tag{III.8.14}$$

Use the R and φ components of $\boldsymbol{\nabla} \times \boldsymbol{B} = \alpha \boldsymbol{B}$ to match the Fourier harmonics:

$$\begin{aligned}
\alpha B_{R;m,k_z} + \mathrm{i} k_z B_{\varphi;m,k_z} &= \mathrm{i} m B_0 \sqrt{\alpha^2 - k_z^2}\, \frac{J_m(x)}{x} \\
\alpha B_{\varphi;m,k_z} - \mathrm{i} k_z B_{R;m,k_z} &= -B_0 \sqrt{\alpha^2 - k_z^2}\, J'_m(x).
\end{aligned}$$

Adding and subtracting these and then taking the real part leads to

$$B_R(x, \varphi, z) = -B_0 \sum_{m,k_z} \frac{1}{\sqrt{\alpha^2 - k_z^2}} \left[k_z J'_m(x) + m\alpha \frac{\mathrm{J}_m(x)}{x} \right] \sin(m\varphi + k_z z), \tag{III.8.15}$$

$$B_\varphi(x, \varphi, z) = -B_0 \sum_{m,k_z} \frac{1}{\sqrt{\alpha^2 - k_z^2}} \left[\alpha J'_m(x) + m k_z \frac{\mathrm{J}_m(x)}{x} \right] \cos(m\varphi + k_z z). \tag{III.8.16}$$

This solution is valid if $B_R(a) = 0$.

As a last remark on the subject of relaxation to force-free states, boundary conditions can change the relaxation. For example, at a perfectly conducting boundary, the normal component of the magnetic field B_n is fixed and so the toroidal flux in the plasma is invariant. Expressed in terms of the vector potential, the loop integrals $\oint \boldsymbol{A} \boldsymbol{\cdot} \mathrm{d}\boldsymbol{\ell}$ and $\oint \boldsymbol{A} \boldsymbol{\cdot} \mathrm{d}\boldsymbol{S}$ (the toroidal flux) taken along closed paths the long and short way around the toroidal boundary should be fixed. In this case, it is convenient to work instead with

$$\mathcal{H} = \int \mathrm{d}\boldsymbol{r}\, \boldsymbol{A} \boldsymbol{\cdot} \boldsymbol{B} - \left(\oint \mathrm{d}\boldsymbol{\ell} \boldsymbol{\cdot} \boldsymbol{A} \right) \left(\oint \mathrm{d}\boldsymbol{S} \boldsymbol{\cdot} \boldsymbol{A} \right),$$

which is manifestly gauge invariant when a complete conducting shell surrounds the plasma, even for multivalued gauge potentials (Taylor 1980). If the boundary of the plasma is not a flux surface, then the helicity is gauge dependent and therefore not well defined.

If you're interested in learning more, consult the review by Taylor (1986) and the textbook by Marsh (1996).

PART IV
Steady flows

IV.1. Taylor–Couette flow

A Taylor–Couette flow is a solution for a hydrodynamic fluid enclosed within two concentric, rotating, cylindrical walls. Let the radius of the inner cylinder be $R_1 > 0$ and that of the outer cylinder be $R_2 > R_1$. The inner (outer) cylinder rotates with an angular frequency $\mathit{\Omega}_1$ ($\mathit{\Omega}_2$). Radial force balance for the rotating fluid between the two cylindrical walls is simply

$$0 = -\frac{1}{\rho}\frac{\mathrm{d}P}{\mathrm{d}R} + \mathit{\Omega}^2 R. \tag{IV.1.1}$$

But what causes the fluid to rotate? If the walls were perfectly frictionless, the fluid would remain stationary if initiated at rest. The trick is that viscous stresses at the walls enforce a no-slip condition, which torques the fluid just inside the walls into co-rotation with its confining wall. The fluid interior to these co-rotating layers rotates because of viscous coupling to this rotating boundary-layer fluid. In steady state, the flux of angular momentum from the walls, from radial shell to radial shell of the fluid, must vanish. To determine the resulting rotation profile, we examine the azimuthal component of the momentum equation with $\boldsymbol{u} = R\mathit{\Omega}(R)\hat{\boldsymbol{\varphi}}$ (see (II.2.9c) with $\boldsymbol{v} = 0$), being sure to include the additional stress from the fluid viscosity ν (taken here to be constant):

$$0 = -\frac{1}{\rho R}\frac{\mathrm{d}P}{\mathrm{d}\varphi} + \frac{\nu}{R^2}\frac{\mathrm{d}}{\mathrm{d}R}\left(R^3\frac{\mathrm{d}\mathit{\Omega}}{\mathrm{d}R}\right). \tag{IV.1.2}$$

The viscous term here comes from the divergence of the viscous stress:

$$\begin{aligned}
-\boldsymbol{\nabla}\boldsymbol{\cdot}\boldsymbol{\mathit{\Pi}} = -\boldsymbol{\nabla}\boldsymbol{\cdot}(-\nu\boldsymbol{W}) &\doteq -\boldsymbol{\nabla}\boldsymbol{\cdot}\left\{-\nu\left[\boldsymbol{\nabla}\boldsymbol{u} + (\boldsymbol{\nabla}\boldsymbol{u})^T - \frac{2}{3}(\boldsymbol{\nabla}\boldsymbol{\cdot}\boldsymbol{u})\boldsymbol{I}\right]\right\} \\
&= \nu\,\boldsymbol{\nabla}\boldsymbol{\cdot}\left[\frac{\mathrm{d}\mathit{\Omega}}{\mathrm{d}\ln R}\big(\hat{\boldsymbol{R}}\hat{\boldsymbol{\varphi}} + \hat{\boldsymbol{\varphi}}\hat{\boldsymbol{R}}\big)\right] = \nu\frac{\mathrm{d}}{\mathrm{d}R}\frac{\mathrm{d}\mathit{\Omega}}{\mathrm{d}\ln R} + \frac{2\nu}{R}\frac{\mathrm{d}\mathit{\Omega}}{\mathrm{d}\ln R} \\
&= \frac{\nu}{R^2}\frac{\mathrm{d}}{\mathrm{d}R}\left(R^3\frac{\mathrm{d}\mathit{\Omega}}{\mathrm{d}R}\right).
\end{aligned} \tag{IV.1.3}$$

In axisymmetry, the solution to (IV.1.2) is

$$\mathit{\Omega} = a + \frac{b}{R^2}, \tag{IV.1.4}$$

with a and b being constants set by boundary conditions on the inner and outer surfaces:

$$a = \frac{\mathit{\Omega}_2 R_2^2 - \mathit{\Omega}_1 R_1^2}{R_2^2 - R_1^2} \quad\text{and}\quad b = \frac{(\mathit{\Omega}_1 - \mathit{\Omega}_2)R_1^2 R_2^2}{R_2^2 - R_1^2}. \tag{IV.1.5}$$

IV.2. Thermal wind equation and baroclinic forcing

In steady state with $\boldsymbol{v} = 0$, the radial and vertical components of the momentum equation, equations (II.2.9b) and (II.2.9d) respectively, become

$$0 = -\frac{1}{\rho}\frac{\partial P}{\partial R} - \frac{\partial \mathit{\Phi}}{\partial R} + R\mathit{\Omega}^2 \quad\text{and}\quad 0 = -\frac{1}{\rho}\frac{\partial P}{\partial z} - \frac{\partial \mathit{\Phi}}{\partial z}. \tag{IV.2.1}$$

Taking $\partial/\partial z$ of the first equation, using the second equation, and rearranging yields

$$R\frac{\partial \Omega^2}{\partial z} = \frac{\hat{\boldsymbol{\varphi}}}{\rho^2} \cdot (\boldsymbol{\nabla} P \times \boldsymbol{\nabla} \rho). \tag{IV.2.2}$$

This is the $\hat{\boldsymbol{\varphi}}$ component of the vorticity equation. Note that, if ρ is constant or if $P = P(\rho)$, then the angular velocity Ω must be constant on cylinders; this is a version of the *Taylor–Proudman theorem*. Now, let us recall the definition of the hydrodynamic entropy, $\sigma = (\gamma - 1)^{-1} \ln P\rho^{-\gamma}$ and use it to replace $\boldsymbol{\nabla} \ln \rho$. The result is

$$R\frac{\partial \Omega^2}{\partial z} = \frac{\gamma - 1}{\gamma} \hat{\boldsymbol{\varphi}} \cdot \left(\boldsymbol{\nabla} \sigma \times \frac{1}{\rho} \boldsymbol{\nabla} P \right) = \hat{\boldsymbol{\varphi}} \cdot \left(\frac{1}{\rho} \boldsymbol{\nabla} P \times \boldsymbol{\nabla} \ln T \right). \tag{IV.2.3}$$

In the Sun, $\boldsymbol{g} = (1/\rho)\boldsymbol{\nabla} P$ is an excellent approximation, with only a tiny angular component due to centrifugal effects. Adopting this simplification and working in spherical coordinates (r, θ, φ), equation (IV.2.3) becomes

$$\boxed{R\frac{\partial \Omega^2}{\partial z} = \frac{\gamma - 1}{\gamma} \frac{g}{r} \frac{\partial \sigma}{\partial \theta}} \tag{IV.2.4}$$

where $g = GM/r^2$. [The right-hand side of (IV.2.4) can also be written as $-(g/r)\partial \ln T/\partial \theta$.] Equation (IV.2.4) is known as the *thermal wind equation*. It is used often in geophysical applications (e.g., longitudinal entropy gradients driven by temperature differences cause wind shear) and to understand the rotation profile in the convection zone of the Sun.

IV.3. The Parker solar wind

It's common knowledge these days that the Sun produces a wind; solar storms, coronal mass ejections, and the aurorae they produce are routinely covered by news outlets. But before deriving a physical model for this wind, it helps to understand why such a wind should exist at all. Indeed, when Eugene Parker proposed the existence of the solar wind in his groundbreaking 1958 paper, the manuscript was initially rejected by The Astrophysical Journal, with one of the reviewers calling it "utter nonsense". Fortunately, the ApJ Editor-in-Chief S. Chandrasekhar knew better, overruled the reviewers, and published it. The very next year (1959), the Luna 1 satellite launched by the USSR measured energetic particles streaming from the Sun; a few years later (1962), those observations were confirmed by NASA's Mariner 2 spacecraft, which also detected two distinct streams of solar wind, a slow stream at $\sim$0.1 km s^{-1} and a fast stream traveling at approximately twice that speed.

The origin of the wind can be understood as follows. Suppose a hydrostatic equilibrium between the thermal pressure of the solar atmosphere and spherical gravity from a point mass M:

$$\frac{1}{\rho}\frac{\mathrm{d}P}{\mathrm{d}r} = -\frac{\mathrm{G}M}{r^2}. \tag{IV.3.1}$$

For simplicity, adopt a power law for the temperature beyond the solar surface at $r = r_0$:

$$T(r) = T_0 \left(\frac{r_0}{r} \right)^{1-\alpha}. \tag{IV.3.2}$$

An isothermal atmosphere corresponds to $\alpha = 1$. The temperature should fall off with distance (i.e., $\alpha < 1$), however, if anything because thermal conduction would carry heat from the solar surface out into the interplanetary medium. Substituting this power law into (IV.3.1) and integrating from r_0 out to r yields

$$P(r) = P_0 \exp\left\{-\frac{GMm}{\alpha r_0 T_0}\left[1 - \left(\frac{r_0}{r}\right)^\alpha\right]\right\}. \tag{IV.3.3}$$

Note that there is a finite pressure at infinity. Let's put in some numbers. The typical number density and temperature at the base of the solar corona at $r_0 \sim 10^6$ km are $n_0 \sim 3\times10^7$ cm^{-3} and $T_0 = T_{\rm i0} + T_{\rm e0} \sim 200$ eV, respectively. The mass of the Sun is $\mathrm{M}_\odot \approx 2\times10^{33}$ g. Setting $\alpha \lesssim 1$ yields $P(r\to\infty) \lesssim 10^{-3}P_0$. With $P_0 \approx 0.01$ dyne cm^{-3}, this gives $P(r\to\infty) \lesssim 10^{-5}$ dyne cm^{-3}. This is to be contrasted with the gas pressure of the interstellar medium (ISM), which may be estimated using the mean density $n_{\rm ISM} \sim 1$ cm^{-3} and mean temperature $T_{\rm ISM} \sim 0.5$ eV of the ISM to find $P_{\rm ISM} \sim 10^{-12}$ dyne cm^{-3}. This is clearly many orders of magnitude less than $P(r\to\infty)$, the implication being that the solar atmosphere is vastly over-pressured compared to its surroundings. This is what lead E. Parker to conclude "that probably it is not possible for the solar corona, or, indeed, perhaps the atmosphere of any star, to be in complete hydrostatic equilibrium out to large distances. We expect always to find some continued outward hydrodynamic expansion of gas." Let us calculate that expansion.

Consider a steady, gravitationally unbound, spherical flow away from a central mass M, with the sound speed being $c_{\rm s0}$ at the base of the solar corona r_0 and the flow velocity tending to v_∞ at infinity. The radial equation of motion is

$$u\frac{{\rm d}u}{{\rm d}r} = -\frac{1}{\rho}\frac{{\rm d}P}{{\rm d}r} - \frac{GM}{r^2}. \tag{IV.3.4}$$

Adopting an adiabatic equation of state, for which the pressure $P = K\rho^\gamma$ with $\gamma > 1$, provides

$$\frac{1}{\rho}\frac{{\rm d}P}{{\rm d}r} = \frac{\rm d}{{\rm d}r}\left(\frac{K^{1/\gamma}P^{1-1/\gamma}}{1-1/\gamma}\right) = \frac{\rm d}{{\rm d}r}\left(\frac{\gamma K\rho^{\gamma-1}}{\gamma-1}\right) = \frac{\rm d}{{\rm d}r}\left(\frac{c_{\rm s}^2}{\gamma-1}\right), \tag{IV.3.5}$$

where $c_{\rm s}^2 \doteq {\rm d}P/{\rm d}\rho = \gamma K\rho^{\gamma-1}$. Then (IV.3.4) may be integrated to obtain what amounts to Bernoulli's equation:

$$\frac{u^2}{2} + \frac{c_{\rm s}^2}{\gamma-1} - \frac{GM}{r} = \text{const}. \tag{IV.3.6}$$

The constant on the right-hand side can be evaluated both at the base of the corona (where $u = 0$) and at infinity (where $c_{\rm s}^2 = 0$) to obtain an expression for the asymptotic wind speed:

$$\text{const} = \frac{c_{\rm s0}^2}{\gamma-1} - \frac{GM}{r_0} = \frac{u_\infty^2}{2} \quad\Longrightarrow\quad u_\infty^2 = 2\left(\frac{c_{\rm s0}^2}{\gamma-1} - \frac{GM}{r_0}\right). \tag{IV.3.7}$$

Note that a nearly isothermal gas (i.e., $\gamma = 1^+$) can have a sound speed that is a small fraction of the escape velocity and still become unbound. The radius at which the outflow speed u reaches the sound speed (the so-called "sonic point") may be calculated from (IV.3.6) by setting $u = c_{\rm s}$ and solving for $r = r_{\rm s}$:

$$r_{\rm s} = 2GM\left(\frac{\gamma+1}{\gamma-1}\,c_{\rm s}^2 - u_\infty^2\right)^{-1}. \tag{IV.3.8}$$

Note that this is currently an implicit equation because $c_{\rm s}^2$ evaluated at $r = r_{\rm s}$ is unknown.

Returning to (IV.3.4)...

$$u\frac{\mathrm{d}u}{\mathrm{d}r}+\frac{\mathrm{G}M}{r^2}=-\frac{1}{\rho}\frac{\mathrm{d}P}{\mathrm{d}r}=-\frac{\mathrm{d}}{\mathrm{d}r}\left(\frac{c_{\mathrm{s}}^2}{\gamma-1}\right)=c_{\mathrm{s}}^2\,\frac{\mathrm{d}\ln(r^2u)}{\mathrm{d}r}. \tag{IV.3.9}$$

To obtain the final equality, we used the continuity equation to write

$$\frac{1}{\gamma-1}\frac{\mathrm{d}\ln c_{\mathrm{s}}^2}{\mathrm{d}r}=\frac{\mathrm{d}\ln\rho}{\mathrm{d}r}=-\frac{\mathrm{d}\ln(r^2u)}{\mathrm{d}r}. \tag{IV.3.10}$$

Upon rearrangement, equation (IV.3.9) leads to

$$u\frac{\mathrm{d}u}{\mathrm{d}r}=\frac{u^2}{r}\left(\frac{2c_{\mathrm{s}}^2-\mathrm{G}M/r}{u^2-c_{\mathrm{s}}^2}\right). \tag{IV.3.11}$$

This equation indicates that the sonic point r_{s} can only be crossed if $2c_{\mathrm{s}}^2=\mathrm{G}M/r_{\mathrm{s}}$ at the radius where $u^2=c_{\mathrm{s}}^2$, so that the numerator and denominator vanish together. Combining this requirement with the Bernoulli relation (IV.3.8) yields an expression for the sound speed at the sonic point,

$$c_{\mathrm{s}}^2(r=r_{\mathrm{s}})=\frac{\gamma-1}{5-3\gamma}\,u_\infty^2<u_\infty^2, \tag{IV.3.12}$$

with the inequality arising because the velocity must rise monotonically beyond the sonic point. This requires $\gamma<3/2$ for a wind solution to exist. Equation (IV.3.8) can then be evaluated to determine r_{s}:

$$r_{\mathrm{s}}=\frac{5-3\gamma}{\gamma-1}\,\frac{\mathrm{G}M}{2u_\infty^2}. \tag{IV.3.13}$$

Integrating (IV.3.10) from the sonic point r_{s} to any other radius r provides

$$\frac{c_{\mathrm{s}}^2(r)}{c_{\mathrm{s}}^2(r_{\mathrm{s}})}=\left[\frac{\rho(r)}{\rho(r_{\mathrm{s}})}\right]^{\gamma-1}=\left[\frac{r_{\mathrm{s}}^2}{r^2}\frac{c_{\mathrm{s}}(r_{\mathrm{s}})}{u(r)}\right]^{\gamma-1}. \tag{IV.3.14}$$

Feeding this profile into (IV.3.6) provides a solution for the wind speed. The steps to obtain the full solution are then: (i) use (IV.3.7) to calculate u_∞^2 using quantities evaluated at the base of the wind; (ii) use this quantity in (IV.3.12) and (IV.3.13) to calculate the sound speed at and location of the sonic point; (iii) use these to determine the radial profile of the sound speed with (IV.3.14); and (iv) substitute this profile into (IV.3.6) to determine the radial profile of the wind speed.

Following the same procedure for an isothermal wind ($\gamma=1$) results in the following expressions:

$$\frac{u^2}{c_{\mathrm{s}}^2}-1-\ln\left(\frac{r^4}{r_{\mathrm{s}}^4}\frac{u^2}{c_{\mathrm{s}}^2}\right)=4\left(\frac{r_{\mathrm{s}}}{r}-1\right),\quad r_{\mathrm{s}}=\frac{\mathrm{G}M}{2c_{\mathrm{s}}^2}. \tag{IV.3.15}$$

This solution is shown in the diagram below:

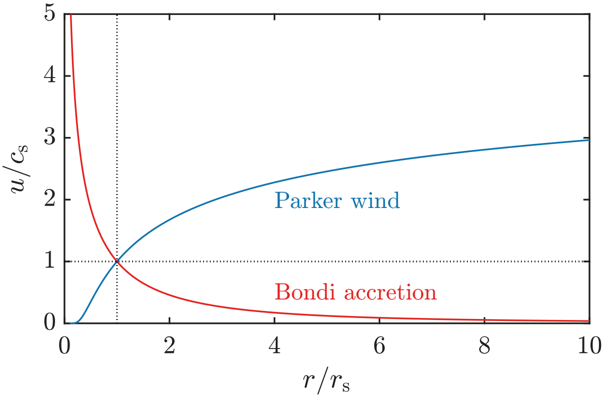

Note that there is an additional solution to (IV.3.15), traced by the red line and marked "Bondi accretion" (Bondi 1952). This solution corresponds to mass accretion of material starting at large distances and small velocities, accelerating in through the sonic point, and accreting onto the central massive object with a supersonic radial velocity.

While the solar wind is directed radially outwards, this is only true in the frame of the Sun. With the Sun rotating every ≈24 days at the equator, the solar wind in the "lab" frame sweeps back into a spiral (as if from a rotating lawn sprinkler). This spiral is now referred to as the "Parker spiral," the trajectory of which in the equatorial plane is given by

$$\frac{u_\varphi}{u_R} = \frac{R\Omega}{u} = R\,\frac{\mathrm{d}\varphi}{\mathrm{d}R} \quad \Longrightarrow R - R_\odot = \frac{u}{\Omega}(\varphi - \varphi_0), \tag{IV.3.16}$$

where Ω is the angular velocity at the solar surface $R_\odot$, and φ_0 is the angular location from which a particular solar-wind stream is launched. By the time the solar wind reaches the Earth's orbit (at $\simeq 215\ R_\odot$) the angle is roughly 45°, becoming more azimuthal farther out away from the Sun.

This flow entrains the interplanetary magnetic field and, assuming ideal-MHD evolution, coerces it to follow the stream lines (at least at distances greater than the Alfvén radius, beyond which the solar-wind speed is larger than the local Alfvén speed; this Alfvén radius varies between $\approx 15\ R_\odot$ and $30\ R_\odot$, depending on the solar cycle). The result is that $B_\varphi/B_R = u_\varphi/u_R = R\Omega/u$. With the radial component of the (solenoidal) magnetic field decreasing from B_0 at $R = R_\odot$ following

$$B_R(R) = B_0\left(\frac{R_\odot}{R}\right)^2, \tag{IV.3.17}$$

the azimuthal magnetic field then follows:

$$B_\varphi(R) = B_0\,\frac{\Omega R_\odot}{u}\,\frac{R_\odot}{R}. \tag{IV.3.18}$$

Note that the pitch angle

$$\frac{B_\varphi(R)}{B_R(R)} = \frac{R\Omega}{u} \approx \left(\frac{R}{1\ \mathrm{au}}\right)\left(\frac{T_{\mathrm{rot},\odot}}{24\ \mathrm{days}}\right)^{-1}\left(\frac{u}{400\ \mathrm{km\ s^{-1}}}\right)^{-1} \tag{IV.3.19}$$

increases with distance.

PART V

MHD waves

V.1. Linear theory: Alfvén, magnetosonic, and entropy modes

Consider a uniform, stationary, ideal-MHD, non-self-gravitating fluid, threaded by a uniform magnetic field $\boldsymbol{B}_0$. To orient our coordinate system, we choose the magnetic field to lie along the z axis, so that $\boldsymbol{B}_0 = B_0\hat{\boldsymbol{z}}$. Then the perpendicular direction (denoted by a subscript $\perp$) lies in the x-y plane. We perturb the fluid with small displacements, which we take to be sinusoidal:

$$\begin{array}{rcccl} \rho(t,\boldsymbol{r}) & = & \rho_0 & + & \delta\rho \exp(\mathrm{i}\boldsymbol{k}\cdot\boldsymbol{r}-\mathrm{i}\omega t), \\ \boldsymbol{u}(t,\boldsymbol{r}) & = & 0 & + & \delta\boldsymbol{u} \exp(\mathrm{i}\boldsymbol{k}\cdot\boldsymbol{r}-\mathrm{i}\omega t), \\ \boldsymbol{B}(t,\boldsymbol{r}) & = & B_0\hat{\boldsymbol{z}} & + & \delta\boldsymbol{B} \exp(\mathrm{i}\boldsymbol{k}\cdot\boldsymbol{r}-\mathrm{i}\omega t), \\ P(t,\boldsymbol{r}) & = & P_0 & + & \delta P \exp(\mathrm{i}\boldsymbol{k}\cdot\boldsymbol{r}-\mathrm{i}\omega t). \end{array} \tag{V.1.1}$$

In general, the wavevector $\boldsymbol{k} = k_\parallel\hat{\boldsymbol{z}} + \boldsymbol{k}_\perp$ has components along ($\parallel$) and across ($\perp$) the background magnetic field. Because ideal MHD has no dissipation or dispersion, and because we took the background to be uniform and stationary, the wave frequency ω is purely real, corresponding to a plane-wave oscillation; more generally, ω can be complex, allowing for growing or decaying solutions.

If you paid close attention, you noticed that I qualified the perturbations as being "small". *Small*? What's "small"? I mean that all nonlinearities that result when perturbing our equations will be dropped, leaving behind a set of linear equations for which the sinusoidal form adopted above represents exact solutions. The result is *linear theory*, from which one may obtain the relation between ω and $\boldsymbol{k}$ called the *dispersion relation*. It's important to bear in mind, however, that when substituting the eigenvalues $\omega = \omega(\boldsymbol{k})$ back into the linear equations to compute the eigenvectors, one must take the real parts to obtain actual observable quantities. Now down to business.

Substituting (V.1.1) into the ideal, adiabatic MHD equations (see (II.3.36)) and retaining only those terms proportional to δ leads, after some re-arrangement, to the following set:

$$-\mathrm{i}\omega\frac{\delta\rho}{\rho_0} = -\mathrm{i}\boldsymbol{k}\cdot\delta\boldsymbol{u}, \tag{V.1.2a}$$

$$-\mathrm{i}\omega\delta\boldsymbol{u} = -\mathrm{i}\boldsymbol{k}\left(c_\mathrm{s}^2\frac{\delta P}{\gamma P_0} + v_\mathrm{A}^2\frac{\delta B_\parallel}{B_0}\right) + \mathrm{i}k_\parallel v_\mathrm{A}^2\frac{\delta\boldsymbol{B}}{B_0}, \tag{V.1.2b}$$

$$-\mathrm{i}\omega\left(\frac{\delta P}{P_0} - \gamma\frac{\delta\rho}{\rho_0}\right) = 0, \tag{V.1.2c}$$

$$-\mathrm{i}\omega\frac{\delta\boldsymbol{B}}{B_0} = \mathrm{i}k_\parallel\delta\boldsymbol{u} - \hat{\boldsymbol{z}}\,\mathrm{i}\boldsymbol{k}\cdot\delta\boldsymbol{u}, \tag{V.1.2d}$$

where $v_\mathrm{A}^2 \doteq B_0^2/(4\pi\rho_0)$ is the Alfvén speed and $c_\mathrm{s}^2 \doteq \gamma P_0/\rho_0$ is the adiabatic sound speed, both evaluated in the background state. Before crunching on this, note that (V.1.2c) has two solutions: $\delta P = c_\mathrm{s}^2\delta\rho$ and $\omega = 0$. The former is the familiar adiabatic relation between the perturbed pressure and perturbed density. The latter is commonly referred to as the "entropy mode", which in the ideal case corresponds to an inconsequential relabeling of fluid elements that preserves the entropy of the system. When conductive mixing of fluid elements is allowed, this mode acquires a non-zero frequency.

As a first pass, set $\boldsymbol{k} = k_\parallel\hat{\boldsymbol{z}}$, in which case the divergence-free constraints on the magnetic field, $\boldsymbol{\nabla}\cdot\delta\boldsymbol{B} = 0$, guarantees that $\delta B_\parallel = 0$. The parallel and perpendicular components of the equations then separate cleanly:

$$-\mathrm{i}\omega\frac{\delta\rho}{\rho_0} = -\mathrm{i}k_\parallel \delta u_\parallel \tag{V.1.3a}$$

$$-\mathrm{i}\omega\delta u_\parallel = -\mathrm{i}k_\parallel c_\mathrm{s}^2 \frac{\delta P}{\gamma P_0} \tag{V.1.3b}$$

$$\delta B_\parallel = 0 \tag{V.1.3c}$$

$$-\mathrm{i}\omega\left(\frac{\delta P}{P_0} - \gamma\frac{\delta\rho}{\rho_0}\right) = 0 \tag{V.1.3d}$$

$$-\mathrm{i}\omega\delta \boldsymbol{u}_\perp = \mathrm{i}k_\parallel v_\mathrm{A}^2 \frac{\delta \boldsymbol{B}_\perp}{B_0} \tag{V.1.4a}$$

$$-\mathrm{i}\omega\frac{\delta \boldsymbol{B}_\perp}{B_0} = \mathrm{i}k_\parallel \delta \boldsymbol{u}_\perp \tag{V.1.4b}$$

On the left are equations describing compressive fluctuations: the entropy mode ($\omega = 0$) and a parallel-propagating sound wave. The dispersion relation for the latter is obtained by setting $\delta P = c_\mathrm{s}^2 \delta\rho$ and combining the continuity and parallel momentum equations to find

$$\omega = \pm k_\parallel c_\mathrm{s} \quad \text{with} \quad \frac{\delta\rho}{\rho_0} = \pm\frac{\delta u_\parallel}{c_\mathrm{s}}. \tag{V.1.5}$$

With $k_\parallel > 0$, these represent forward-propagating (+ sign) and backward-propagating (− sign) sound waves. The equations on the right side of (V.1.4) describe incompressible fluctuations called shear Alfvén waves:

$$\omega = \pm k_\parallel v_\mathrm{A} \quad \text{with} \quad \frac{\delta \boldsymbol{B}_\perp}{B_0} = \mp\frac{\delta \boldsymbol{u}_\perp}{v_\mathrm{A}}. \tag{V.1.6}$$

These waves are not associated with any motion along the field nor any changes in density. The fluid motion here is exactly the $E\times B$ velocity, which is what it needs to be for the perturbed magnetic field to remain frozen into the fluid.

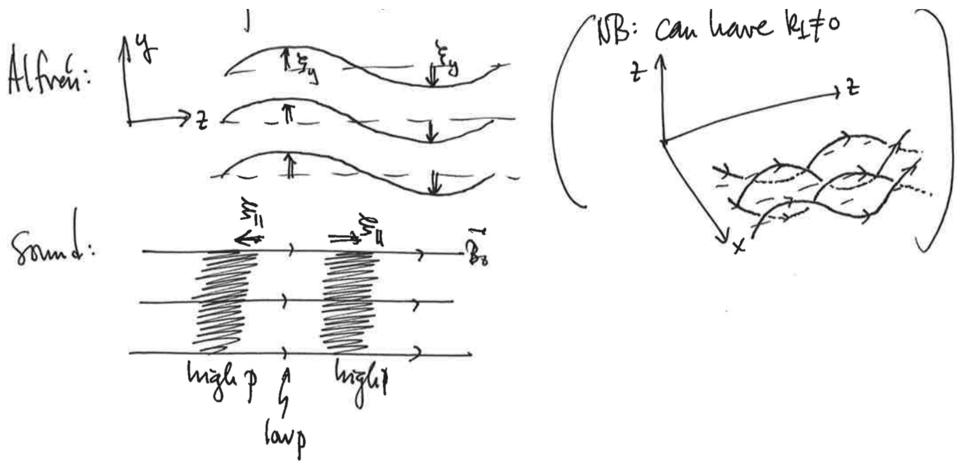

Now for the general case. Start by splitting (V.1.2b) and (V.1.2d) into their parallel and perpendicular parts:

$$-\mathrm{i}\omega\delta u_\parallel = -\mathrm{i}k_\parallel c_\mathrm{s}^2 \frac{\delta P}{\gamma P_0} \tag{V.1.7a}$$

$$-\mathrm{i}\omega\frac{\delta B_\parallel}{B_0} = -\mathrm{i}\boldsymbol{k}_\perp \boldsymbol{\cdot} \delta\boldsymbol{u}_\perp \tag{V.1.7b}$$

$$-\mathrm{i}\omega\delta \boldsymbol{u}_\perp = -\mathrm{i}\boldsymbol{k}_\perp \left(c_\mathrm{s}^2\frac{\delta P}{\gamma P_0} + v_\mathrm{A}^2\frac{\delta B_\parallel}{B_0}\right) + \mathrm{i}k_\parallel v_\mathrm{A}^2 \frac{\delta \boldsymbol{B}_\perp}{B_0} \tag{V.1.8a}$$

$$-\mathrm{i}\omega\frac{\delta \boldsymbol{B}_\perp}{B_0} = \mathrm{i}k_\parallel \delta \boldsymbol{u}_\perp \tag{V.1.8b}$$

Do $k_\parallel$(V.1.7a) + $\boldsymbol{k}_\perp \cdot$(V.1.8$a$) and use (V.1.2$a$) and (V.1.2$c$) to replace $\boldsymbol{k}\cdot\delta\boldsymbol{u}$ with $\omega(\delta P/\gamma P_0)$ to find that

$$\left(\omega^2 - k^2 c_\mathrm{s}^2\right)\frac{\delta P}{\gamma P_0} = k^2 v_\mathrm{A}^2 \frac{\delta B_\parallel}{B_0}. \tag{V.1.9}$$

Solve this expression for the pressure perturbation and substitute it back into (V.1.8a) and re-arrange to obtain

$$\left(\omega^2 - k_\parallel^2 v_\mathrm{A}^2\right)\frac{\delta \boldsymbol{B}_\perp}{B_0} = -k_\parallel \boldsymbol{k}_\perp v_\mathrm{A}^2 \left(\frac{\omega^2}{\omega^2 - k^2 c_\mathrm{s}^2}\right)\frac{\delta B_\parallel}{B_0}. \tag{V.1.10}$$

Finally, use $\boldsymbol{k}\cdot\delta\boldsymbol{B} = 0$ to eliminate $\delta B_\parallel$ in favor of $-(\boldsymbol{k}_\perp/k_\parallel)\cdot\delta\boldsymbol{B}_\perp$:

$$\left[\left(\omega^2 - k_\parallel^2 v_\mathrm{A}^2\right)\boldsymbol{I} - \boldsymbol{k}_\perp\boldsymbol{k}_\perp v_\mathrm{A}^2\left(\frac{\omega^2}{\omega^2 - k^2 c_\mathrm{s}^2}\right)\right]\cdot\frac{\delta\boldsymbol{B}_\perp}{B_0} = 0. \tag{V.1.11}$$

Taking the determinant and setting it to zero gives the dispersion relation

$$\boxed{\left(\omega^2 - k_\parallel^2 v_\mathrm{A}^2\right)\left[\omega^2 - k_\parallel^2 v_\mathrm{A}^2 - k_\perp^2 v_\mathrm{A}^2\left(\frac{\omega^2}{\omega^2 - k^2 c_\mathrm{s}^2}\right)\right] = 0} \tag{V.1.12}$$

Before proceeding with the analysis, I'll note that the factor in square brackets is often written instead as

$$\omega^4 - \omega^2 k^2 (c_\mathrm{s}^2 + v_\mathrm{A}^2) + k^2 c_\mathrm{s}^2 k_\parallel^2 v_\mathrm{A}^2$$

after multiplying through by $\omega^2 - k^2 c_\mathrm{s}^2$, but I like it as written in the boxed equation because one can more easily take limits in large or small $\beta \doteq (2/\gamma)(c_\mathrm{s}^2/v_\mathrm{A}^2)$.

Equation (V.1.12) admits six roots; the entropy mode ($\omega = 0$) discussed earlier in this section was lost when we set $\delta P = c_\mathrm{s}^2\delta\rho$. Two of these roots are clearly the forward- and backward-propagating shear Alfvén waves, $\omega = \pm k_\parallel v_\mathrm{A}$. The remaining four roots are

$$\omega^2 = \omega_\mathrm{fast}^2 \doteq \frac{k^2(c_\mathrm{s}^2 + v_\mathrm{A}^2)}{2} + \sqrt{\frac{k^4(c_\mathrm{s}^2 + v_\mathrm{A}^2)^2}{4} - k^2 c_\mathrm{s}^2 k_\parallel^2 v_\mathrm{A}^2}, \tag{V.1.13}$$

$$\omega^2 = \omega_\mathrm{slow}^2 \doteq \frac{k^2(c_\mathrm{s}^2 + v_\mathrm{A}^2)}{2} - \sqrt{\frac{k^4(c_\mathrm{s}^2 + v_\mathrm{A}^2)^2}{4} - k^2 c_\mathrm{s}^2 k_\parallel^2 v_\mathrm{A}^2}. \tag{V.1.14}$$

These are "magneto-sonic" modes, so called because they combine the effects of the magnetic field and the fluid pressure. Two of these modes are labelled "fast" and two are labelled "slow"; each pair corresponds to a set of forward- and backwards-propagating waves. The names "fast" and "slow" are assigned because of the + and − signs; clearly, $\omega_\mathrm{fast}^2 > \omega_\mathrm{slow}^2$.

Take the limit $\beta \gg 1$. Then $\omega_\mathrm{fast}^2 \approx k^2 c_\mathrm{s}^2$ and $\omega_\mathrm{slow}^2 \approx k_\parallel^2 v_\mathrm{A}^2$. The former is proportional to k^2 because, when the sound speed is much faster than the Alfvén speed, the main restoring force is the (isotropic) pressure. The latter is sometimes called "pseudo-Alfvén" wave, because its dispersion relation matches that of a shear Alfvén wave but its polarization is different. Take the limit $\beta \ll 1$. Then $\omega_\mathrm{fast}^2 \approx k^2 v_\mathrm{A}^2$ and $\omega_\mathrm{slow}^2 \approx k_\parallel^2 c_\mathrm{s}^2$. The latter is a sound wave propagating along straight field lines.

Another set of limits that are useful to examine concern the wavevector orientation. The sketch below illustrates a fast mode with $k_\parallel = 0$, which is powered by a combination of increased gas and magnetic pressure in regions of compression (where $\boldsymbol{\nabla}\cdot\boldsymbol{\xi} < 0$):

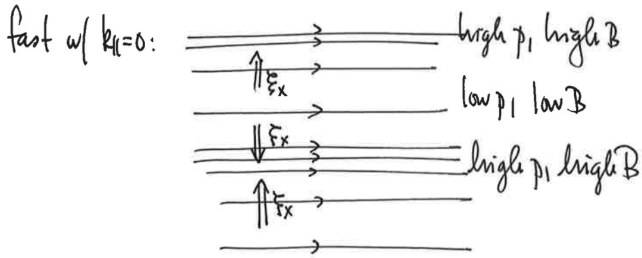

When $k_\parallel \neq 0$ but satisfies $k_\parallel/k_\perp \ll 1$, corresponding to scales along the background magnetic field being much larger than scales across the magnetic field, the magnetosonic waves become $\omega^2_{\rm fast} \approx k^2_\perp(c^2_{\rm s} + v^2_{\rm A})$ and $\omega^2_{\rm slow} \approx k^2_\parallel v^2_{\rm A}(1 + v^2_{\rm A}/c^2_{\rm s})^{-1}$, the difference being whether the gas pressure and magnetic pressure are in phase or out of phase:

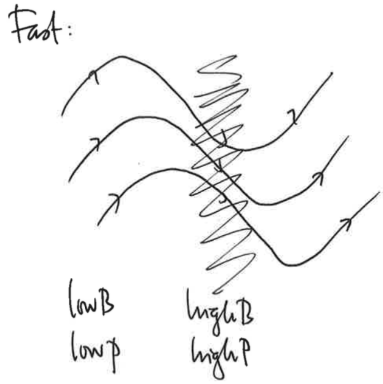

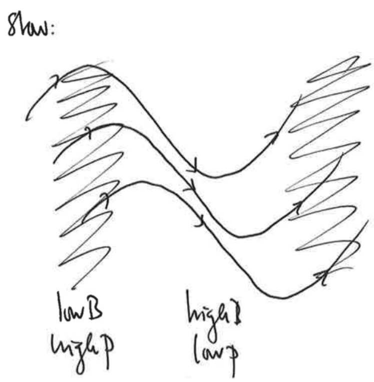

Recall from (V.1.9) that

$$\frac{\delta P}{\gamma P_0} + \frac{k^2 v^2_{\rm A}}{k^2 c^2_{\rm s} - \omega^2}\frac{\delta B_\parallel}{B_0} = 0.$$

With $k_\parallel \ll k_\perp$ and $\omega^2 = \omega^2_{\rm slow} \approx k^2_\parallel v^2_{\rm A}(1 + v^2_{\rm A}/c^2_{\rm s})^{-1}$, this becomes

$$\frac{\delta P}{\gamma P_0} + \frac{k^2_\perp v^2_{\rm A}}{k^2_\perp c^2_{\rm s} - k^2_\parallel v^2_{\rm A}(1 + v^2_{\rm A}/c^2_{\rm s})^{-1}}\frac{\delta B_\parallel}{B_0}, \tag{V.1.15}$$

or

$$\delta P + \frac{B_0 \delta B_\parallel}{4\pi} \approx 0. \tag{V.1.16}$$

This is just a statement of total pressure balance. Visually:

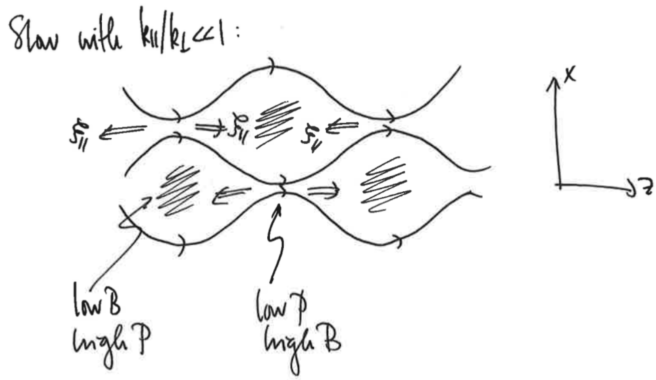

V.2. Lagrangian versus Eulerian perturbations

Before proceeding to study more waves, and even the possibility of instabilities, it is worth discussing a different approach to perturbation theory. Just as there is an Eulerian time derivative and a Lagrangian time derivative, there is Eulerian perturbation theory and Lagrangian perturbation theory. The former, in which perturbations are denoted by a δ, measures the change in a quantity at a particular point in space. For example, if the equilibrium density at $\boldsymbol{r}$, $\rho(\boldsymbol{r})$, is changed at time t by some disturbance to become $\rho'(t,\boldsymbol{r})$, then we denote the Eulerian perturbation of the density by

$$\rho'(t,\boldsymbol{r}) - \rho(\boldsymbol{r}) \doteq \delta\rho \ll \rho(\boldsymbol{r}). \tag{V.2.1}$$

Again, these perturbations are taken *at fixed position*. The latter – Lagrangian perturbation theory – concerns the evolution of small perturbations about a background state *within a particular fluid element* as it undergoes a displacement $\boldsymbol{\xi}$. For example, if a particularly fluid element is displaced from its equilibrium position $\boldsymbol{r}$ to position $\boldsymbol{r}+\boldsymbol{\xi}$, then the density of that fluid element changes by an amount

$$\rho'(t,\boldsymbol{r}+\boldsymbol{\xi}) - \rho(\boldsymbol{r}) \doteq \varDelta\rho. \tag{V.2.2}$$

This is a Lagrangian perturbation. To linear order, δ and $\varDelta$ are related by

$$\varDelta\rho \simeq \rho'(t,\boldsymbol{r}) + \boldsymbol{\xi}\cdot\boldsymbol{\nabla}\rho(\boldsymbol{r}) - \rho(\boldsymbol{r}) = \delta\rho + \boldsymbol{\xi}\cdot\boldsymbol{\nabla}\rho. \tag{V.2.3}$$

There are many situations in which a Lagrangian approach is easier to use than an Eulerian approach; there are also some situations in which doing so is absolutely necessary (e.g., see §IIIe of Balbus (1988) and §Ic of Balbus & Soker (1989) for discussions of the perils of using Eulerian perturbations in the context of local thermal instability).

Question: It is possible to have zero Eulerian perturbation and yet have finite Lagrangian perturbation. What does this mean physically? Is there a physical change in the system?

The Lagrangian velocity perturbation $\varDelta\boldsymbol{u}$ is given by

$$\varDelta\boldsymbol{u} \doteq \frac{\mathrm{D}\boldsymbol{\xi}}{\mathrm{D}t} = \left(\frac{\partial}{\partial t} + \boldsymbol{u}\cdot\boldsymbol{\nabla}\right)\boldsymbol{\xi}, \tag{V.2.4}$$

where $\boldsymbol{u}$ is the background velocity. It is the instantaneous time rate of the displacement of a fluid element, taken relative to the unperturbed flow. Because $\varDelta\boldsymbol{u} = \delta\boldsymbol{u} + \boldsymbol{\xi}\cdot\boldsymbol{\nabla}\boldsymbol{u}$, we have

$$\delta\boldsymbol{u} = \frac{\partial\boldsymbol{\xi}}{\partial t} + \boldsymbol{u}\cdot\boldsymbol{\nabla}\boldsymbol{\xi} - \boldsymbol{\xi}\cdot\boldsymbol{\nabla}\boldsymbol{u}. \tag{V.2.5}$$

Note the additional $\boldsymbol{\xi}\cdot\boldsymbol{\nabla}\boldsymbol{u}$ term, representing a measurement of the background fluid gradients by the fluid displacement.

Exercise. Let $\boldsymbol{u} = R\varOmega(R)\hat{\boldsymbol{\varphi}}$, as in a differentially rotating disk in cylindrical coordinates. Consider a displacement $\boldsymbol{\xi}$ with radial and azimuthal components ξ_R and ξ_φ, each depending upon R and φ. Show that

$$\frac{\mathrm{D}\xi_R}{\mathrm{D}t} = \delta u_R \quad\text{and}\quad \frac{\mathrm{D}\xi_\varphi}{\mathrm{D}t} = \delta u_\varphi + \xi_R\frac{\mathrm{d}\varOmega}{\mathrm{d}\ln R}. \tag{V.2.6}$$

The second term in the latter equation accounts for the stretching of radial displacements into the azimuthal direction by the differential rotation.

You can think of both δ and Δ as difference operators, since we're only working to linear order in the perturbation amplitude: e.g.,

$$\delta\left(\frac{1}{\rho}\right) = \frac{1}{\rho+\delta\rho} - \frac{1}{\rho} \simeq -\frac{\delta\rho}{\rho^2}.$$

But you must be very careful when mixing Eulerian and Lagrangian points of view. Prove the following commutation relations:

$$\begin{aligned}
&(i) \quad \left[\delta, \frac{\partial}{\partial t}\right] = 0;\\
&(ii) \quad \left[\delta, \frac{\partial}{\partial x_i}\right] = 0;\\
&(iii) \quad \left[\Delta, \frac{\partial}{\partial t}\right] = -\frac{\partial \xi_j}{\partial t}\frac{\partial}{\partial x_j};\\
&(iv) \quad \left[\Delta, \frac{\partial}{\partial x_i}\right] = -\frac{\partial \xi_j}{\partial x_i}\frac{\partial}{\partial x_j};\\
&(v) \quad \left[\Delta, \frac{\mathrm{D}}{\mathrm{D}t}\right] = 0;\\
&(vi) \quad \left[\delta, \frac{\mathrm{D}}{\mathrm{D}t}\right] = -\xi_j \frac{\partial}{\partial x_j}\frac{\mathrm{D}}{\mathrm{D}t};\\
&(vii) \quad \left[\frac{\partial}{\partial x_i}, \frac{\mathrm{D}}{\mathrm{D}t}\right] = \frac{\partial u_j}{\partial x_i}\frac{\partial}{\partial x_j}.
\end{aligned}$$

We can use these to obtain linearized versions of the continuity equation, momentum equation, induction equation, and entropy equation expressed in terms of Lagrangian perturbations.

First, apply a Lagrangian perturbation to the continuity equation:

$$\Delta\left[\frac{\mathrm{D}\ln\rho}{\mathrm{D}t} = -\boldsymbol{\nabla}\cdot\boldsymbol{u}\right].$$

The left-hand side is straightforward, because Δ commutes with $\mathrm{D}/\mathrm{D}t$:

$$\Delta\left[\frac{\mathrm{D}\ln\rho}{\mathrm{D}t}\right] = \frac{\mathrm{D}}{\mathrm{D}t}\Delta\ln\rho = \frac{\mathrm{D}}{\mathrm{D}t}\frac{\Delta\rho}{\rho}.$$

The right-hand side can be cleaned up using the commutation rules above:

$$\begin{aligned}
\Delta\Big[-\boldsymbol{\nabla}\cdot\boldsymbol{u}\Big] &= -\Delta\frac{\partial}{\partial x_i}u_i \overset{(iv)}{=} -\left(\frac{\partial}{\partial x_i}\Delta - \frac{\partial \xi_j}{\partial x_i}\frac{\partial}{\partial x_j}\right)u_i = -\frac{\partial}{\partial x_i}\frac{\mathrm{D}\xi_i}{\mathrm{D}t} + \frac{\partial \xi_j}{\partial x_i}\frac{\partial u_i}{\partial x_j}\\
&\overset{(vii)}{=} -\left(\frac{\mathrm{D}}{\mathrm{D}t}\frac{\partial}{\partial x_i} + \frac{\partial u_j}{\partial x_i}\frac{\partial}{\partial x_j}\right)\xi_i + \frac{\partial \xi_j}{\partial x_i}\frac{\partial u_i}{\partial x_j} = -\frac{\mathrm{D}}{\mathrm{D}t}\boldsymbol{\nabla}\cdot\boldsymbol{\xi}
\end{aligned}$$

Combining the left- and right-hand sides provides

$$\frac{\mathrm{D}}{\mathrm{D}t}\left[\frac{\Delta\rho}{\rho} + \boldsymbol{\nabla}\cdot\boldsymbol{\xi} = 0\right] \quad \Longrightarrow \quad \boxed{\Delta\rho = -\rho\boldsymbol{\nabla}\cdot\boldsymbol{\xi}} \tag{V.2.7}$$

Now let's run the same procedure on the entropy equation:

$$0 = \Delta\left[\frac{\mathrm{D}s}{\mathrm{D}t}\right] \overset{(v)}{=} \frac{\mathrm{D}}{\mathrm{D}t}\Big[\Delta s\Big] = \frac{\mathrm{D}}{\mathrm{D}t}\left[\frac{\Delta P}{P} - \gamma\frac{\Delta\rho}{\rho}\right] = \frac{\mathrm{D}}{\mathrm{D}t}\left[\frac{\Delta T}{T} - (\gamma-1)\frac{\Delta\rho}{\rho}\right].$$

Using the continuity equation for $\Delta\rho$ yields

$$\boxed{\frac{\Delta P}{P} = -\gamma \nabla \cdot \boldsymbol{\xi}} \qquad \text{or} \qquad \boxed{\frac{\Delta T}{T} = -(\gamma - 1) \nabla \cdot \boldsymbol{\xi}} \tag{V.2.8}$$

The ideal induction equation requires more work, but it's made a bit easier by writing it in the form of (II.3.17):

$$\Delta\left[\frac{\mathrm{D}}{\mathrm{D}t}\frac{\boldsymbol{B}}{\rho} = \frac{\boldsymbol{B}}{\rho} \cdot \nabla \boldsymbol{u}\right].$$

As with the continuity equation, the left-hand side is straightforward:

$$\Delta\left[\frac{\mathrm{D}}{\mathrm{D}}\frac{\boldsymbol{B}}{\rho}\right] \overset{(v)}{=} \frac{\mathrm{D}}{\mathrm{D}t}\Delta\left[\frac{\boldsymbol{B}}{\rho}\right] = \frac{\mathrm{D}}{\mathrm{D}t}\left[\frac{\Delta \boldsymbol{B}}{\rho} - \frac{\boldsymbol{B}}{\rho}\frac{\Delta\rho}{\rho}\right] = \frac{\mathrm{D}}{\mathrm{D}t}\left[\frac{\Delta \boldsymbol{B} + \boldsymbol{B}(\nabla \cdot \boldsymbol{\xi})}{\rho}\right],$$

where the linearized continuity equation was used in the final step. For the right-hand side, use the chain rule and several commutation rules to re-arrange as follows:

$$\begin{aligned}
\Delta\left[\frac{\boldsymbol{B}}{\rho} \cdot \nabla \boldsymbol{u}\right] &= \Delta\left[\frac{\boldsymbol{B}}{\rho}\right] \cdot \nabla \boldsymbol{u} + \frac{B_i}{\rho}\Delta\left[\frac{\partial}{\partial x_i}\boldsymbol{u}\right] \overset{(iv)}{=} \Delta\left[\frac{\boldsymbol{B}}{\rho}\right] \cdot \nabla \boldsymbol{u} + \frac{B_i}{\rho}\left(\frac{\partial}{\partial x_i}\Delta \boldsymbol{u} - \frac{\partial \xi_j}{\partial x_i}\frac{\partial \boldsymbol{u}}{\partial x_j}\right) \\
&= \Delta\left[\frac{\boldsymbol{B}}{\rho}\right] \cdot \nabla \boldsymbol{u} + \frac{B_i}{\rho}\frac{\partial}{\partial x_i}\frac{\mathrm{D}\boldsymbol{\xi}}{\mathrm{D}t} - \frac{B_i}{\rho}\frac{\partial \xi_j}{\partial x_i}\frac{\partial \boldsymbol{u}}{\partial x_j} \\
&\overset{(vii)}{=} \Delta\left[\frac{\boldsymbol{B}}{\rho}\right] \cdot \nabla \boldsymbol{u} + \underbrace{\frac{B_i}{\rho}\left(\frac{\mathrm{D}}{\mathrm{D}t}\frac{\partial \boldsymbol{\xi}}{\partial x_i} + \frac{\partial u_j}{\partial x_i}\frac{\partial \boldsymbol{\xi}}{\partial x_j}\right)}_{= \frac{\mathrm{D}}{\mathrm{D}t}\left(\frac{\boldsymbol{B}}{\rho} \cdot \nabla \boldsymbol{\xi}\right) - \frac{\partial \boldsymbol{\xi}}{\partial x_i}\frac{\mathrm{D}}{\mathrm{D}t}\frac{B_i}{\rho} + \frac{B_i}{\rho}\frac{\partial u_j}{\partial x_i}\frac{\partial \boldsymbol{\xi}}{\partial x_j}} - \frac{B_i}{\rho}\frac{\partial \xi_j}{\partial x_i}\frac{\partial \boldsymbol{u}}{\partial x_j} \\
&= \left[\frac{\Delta \boldsymbol{B} + \boldsymbol{B}(\nabla \cdot \boldsymbol{\xi})}{\rho}\right] \cdot \nabla \boldsymbol{u} + \frac{\mathrm{D}}{\mathrm{D}t}\left(\frac{\boldsymbol{B}}{\rho} \cdot \nabla \boldsymbol{\xi}\right) - \frac{B_i}{\rho}\frac{\partial \xi_j}{\partial x_i}\frac{\partial \boldsymbol{u}}{\partial x_j} \\
&= \left[\frac{\Delta \boldsymbol{B} + \boldsymbol{B}(\nabla \cdot \boldsymbol{\xi}) - (\boldsymbol{B} \cdot \nabla)\boldsymbol{\xi}}{\rho}\right] \cdot \nabla \boldsymbol{u} + \frac{\mathrm{D}}{\mathrm{D}t}\left(\frac{\boldsymbol{B}}{\rho} \cdot \nabla \boldsymbol{\xi}\right).
\end{aligned}$$

Moving the $\mathrm{D}/\mathrm{D}t$ term to the left-hand side results in

$$\frac{\mathrm{D}}{\mathrm{D}t}\left[\frac{\Delta \boldsymbol{B} + \boldsymbol{B}(\nabla \cdot \boldsymbol{\xi}) - (\boldsymbol{B} \cdot \nabla)\boldsymbol{\xi}}{\rho}\right] = \left[\frac{\Delta \boldsymbol{B} + \boldsymbol{B}(\nabla \cdot \boldsymbol{\xi}) - (\boldsymbol{B} \cdot \nabla)\boldsymbol{\xi}}{\rho}\right] \cdot \nabla \boldsymbol{u}.$$

This is just the equation for a vector being advected and stretched by a flow velocity $\boldsymbol{u}$, written in the Lagrangian frame: $\mathrm{D}\boldsymbol{x}/\mathrm{D}t = (\boldsymbol{x} \cdot \nabla)\boldsymbol{u}$ (recall (II.3.18)). The general solution to this equation is

$$\boxed{\Delta \boldsymbol{B} = (\boldsymbol{B} \cdot \nabla)\boldsymbol{\xi} - \boldsymbol{B}(\nabla \cdot \boldsymbol{\xi})} \tag{V.2.9}$$

The boxed equations are particularly useful for linear analyses, so let us collect them here, written in terms of both Lagrangian and Eulerian perturbations:

$$\begin{aligned}
\Delta\rho &= -\rho(\nabla \cdot \boldsymbol{\xi}) & \delta\rho &= -\nabla \cdot (\rho\boldsymbol{\xi}) \\
\Delta P &= -\gamma P(\nabla \cdot \boldsymbol{\xi}) & \delta P &= -\nabla \cdot (P\boldsymbol{\xi}) - (\gamma - 1)P(\nabla \cdot \boldsymbol{\xi}) \\
\Delta \boldsymbol{B} &= (\boldsymbol{B} \cdot \nabla)\boldsymbol{\xi} - \boldsymbol{B}(\nabla \cdot \boldsymbol{\xi}) & \delta \boldsymbol{B} &= \nabla \times (\boldsymbol{\xi} \times \boldsymbol{B})
\end{aligned}$$

The utility of these equations are that they are expressed in terms of the displacement $\boldsymbol{\xi}$; in some cases, this facilitates a clearer physical picture of what's going on.

Finally, the momentum equation. Denoting all the forces on its right-hand side by $\boldsymbol{f}$, we have

$$\Delta\left[\frac{\mathrm{D}\boldsymbol{u}}{\mathrm{D}t}\right] \overset{(v)}{=} \frac{\mathrm{D}}{\mathrm{D}t}\left[\Delta\boldsymbol{u}\right] = \frac{\mathrm{D}^2\boldsymbol{\xi}}{\mathrm{D}t^2} = \Delta\left[\frac{\boldsymbol{f}}{\rho}\right] = \frac{\Delta\boldsymbol{f}}{\rho} - \frac{\boldsymbol{f}}{\rho}(\boldsymbol{\nabla\cdot\xi}).$$

If we are perturbing about an equilibrium in which the sum of all the forces vanishes everywhere, $\boldsymbol{f} = 0$, then the final term on the right-hand side vanishes and $\Delta\boldsymbol{f} = \delta\boldsymbol{f}$, leaving

$$\boxed{\rho\frac{\mathrm{D}^2\boldsymbol{\xi}}{\mathrm{D}t^2} = \delta\boldsymbol{f} = -\boldsymbol{\nabla}\left(\delta P + \frac{\boldsymbol{B\cdot}\delta\boldsymbol{B}}{4\pi}\right) + \frac{\delta\boldsymbol{B\cdot\nabla B}}{4\pi} + \frac{\boldsymbol{B\cdot\nabla}\delta\boldsymbol{B}}{4\pi} - \delta\rho\boldsymbol{\nabla}\varPhi} \tag{V.2.10}$$

Just remember that there's a $\boldsymbol{u\cdot\nabla}$ inside of that $\mathrm{D}/\mathrm{D}t$.

V.3. Lagrangian MHD

The above equations for governing the evolution of Lagrangian perturbation are part of a more general Lagrangian MHD framework, due to Newcomb (1962). This framework is presented here and then linearized to afford an alternative route to our Lagrangian perturbation equations.

At $t = 0$, label each fluid element by its position $\boldsymbol{r}_0$. At any future time, the location of those fluid elements can be obtained, provided that their displacements $\boldsymbol{\xi}(t, \boldsymbol{r}_0)$ are also known:

$$\boldsymbol{r}(t, \boldsymbol{r}_0) = \boldsymbol{r}_0 + \boldsymbol{\xi}(t, \boldsymbol{r}_0).$$

You can think of $\boldsymbol{r}_0$ as a label that a fluid element carries around with it, marking the location from which it began its journey. In this sense, $\boldsymbol{r}_0$ is a Lagrangian label; by contrast, $\boldsymbol{r}(t, \boldsymbol{r}_0)$ is a Eulerian label that states where in the lab frame that particular fluid element has ended up after some time t.

Because mass is conserved, the amount of material in an infinitesimal volume element as it moves around must be constant:

$$\rho_0(\boldsymbol{r}_0)\mathrm{d}\boldsymbol{r}_0 = \rho(\boldsymbol{r}(t, \boldsymbol{r}_0))\mathrm{d}\boldsymbol{r} \doteq \rho_L(t, \boldsymbol{r}_0)\mathrm{d}\boldsymbol{r}. \tag{V.3.1}$$

On the left-hand side is the mass enclosed in the initial volume of the fluid element at $t = 0$. Because this mass must be constant as it moves around, it will equal the amount of material located at $\boldsymbol{r}$ within volume $\mathrm{d}\boldsymbol{r}$ if that volume were connected back to its initial position at $\boldsymbol{r}_0$ via $\boldsymbol{\xi}(t, \boldsymbol{r}_0)$. The notation on the right-hand size of this equation makes the Lagrangian viewpoint clear: $\rho_L(t, \boldsymbol{r}_0)$ is the density of the fluid element starting from $\boldsymbol{r}_0$, which is found at $\boldsymbol{r}(t, \boldsymbol{r}_0)$ at time t. The volume element $\mathrm{d}\boldsymbol{r}_0$ is connected to $\mathrm{d}\boldsymbol{r}$ through the determinant of the Jacobian:

$$\mathrm{d}\boldsymbol{r} = \mathcal{J}(t, \boldsymbol{r}_0)\mathrm{d}\boldsymbol{r}_0, \quad \text{where} \quad \mathcal{J} \doteq \left|\frac{\partial\boldsymbol{r}}{\partial\boldsymbol{r}_0}\right| = \frac{1}{6}\epsilon_{ijk}\epsilon_{lmn}\frac{\partial r_i}{\partial r_{0l}}\frac{\partial r_j}{\partial r_{0m}}\frac{\partial r_k}{\partial r_{0n}}. \tag{V.3.2}$$

Mass continuity is then

$$\rho_L(t, \boldsymbol{r}_0) = \frac{\rho_0(\boldsymbol{r}_0)}{\mathcal{J}(t, \boldsymbol{r}_0)}. \tag{V.3.3}$$

Before obtaining the other MHD equations within this Lagrangian viewpoint, let us take the displacement $\boldsymbol{\xi}$ to be small, in which case $\mathcal{J} \doteq |\boldsymbol{I} + \partial\boldsymbol{\xi}/\partial\boldsymbol{r}_0| \simeq 1 + \boldsymbol{\nabla}_0\boldsymbol{\cdot\xi}$ to leading order in $\boldsymbol{\xi}$. Then

$$\Delta\rho \doteq \rho_L(t, \boldsymbol{r}_0) - \rho_0(\boldsymbol{r}_0) \simeq -\rho_0(\boldsymbol{r}_0)(\boldsymbol{\nabla}_0\boldsymbol{\cdot\xi}), \tag{V.3.4}$$

exactly what we found in §V.2 (see (V.2.7)). Applying this methodology to pressure is trivial given the assumed adiabatic equation of state:

$$P_L(t,\boldsymbol{r}_0)=\frac{P_0(\boldsymbol{r}_0)}{\mathcal{J}^\gamma(t,\boldsymbol{r}_0)}\quad\Longrightarrow\quad \Delta P\doteq P_L(t,\boldsymbol{r}_0)-P_0(\boldsymbol{r}_0)\simeq-\gamma P_0(\boldsymbol{r}_0)(\boldsymbol{\nabla}_0\boldsymbol{\cdot}\boldsymbol{\xi}),\tag{V.3.5}$$

just as in (V.2.8).

For the ideal induction equation, we follow a similar strategy as in §V.2 by working with the equation for $(\mathrm{D}/\mathrm{D}t)(\boldsymbol{B}/\rho)$ (see (II.3.17)):

$$\frac{\mathrm{D}}{\mathrm{D}t}\frac{\boldsymbol{B}_L}{\rho_L}=\frac{\boldsymbol{B}_L}{\rho_L}\boldsymbol{\cdot}\boldsymbol{\nabla}\boldsymbol{u}=\frac{\boldsymbol{B}_L}{\rho_L}\boldsymbol{\cdot}\frac{\partial\boldsymbol{r}_0}{\partial\boldsymbol{r}}\boldsymbol{\cdot}\boldsymbol{\nabla}_0\boldsymbol{u}=\frac{\boldsymbol{B}_L}{\rho_L}\boldsymbol{\cdot}\frac{\partial\boldsymbol{r}_0}{\partial\boldsymbol{r}}\boldsymbol{\cdot}\boldsymbol{\nabla}_0\frac{\mathrm{D}\boldsymbol{r}}{\mathrm{D}t}\tag{V.3.6}$$

The solution to this equation that satisfies $\boldsymbol{B}_L/\rho_L=\boldsymbol{B}_0/\rho_0$ at $t=0$ is

$$\frac{\boldsymbol{B}_L}{\rho_L}=\frac{\boldsymbol{B}_0}{\rho_0}\boldsymbol{\cdot}\boldsymbol{\nabla}\boldsymbol{r}\quad\Longrightarrow\quad\boldsymbol{B}_L(t,\boldsymbol{r}_0)=\frac{\boldsymbol{B}_0(\boldsymbol{r}_0)\boldsymbol{\cdot}\boldsymbol{\nabla}_0\boldsymbol{r}(t,\boldsymbol{r}_0)}{\mathcal{J}(t,\boldsymbol{r}_0)}.\tag{V.3.7}$$

Again taking the displacement $\boldsymbol{\xi}$ to be small, and using (V.3.4) to replace ρ_L, leads to

$$\Delta\boldsymbol{B}\doteq\boldsymbol{B}_L(t,\boldsymbol{r}_0)-\boldsymbol{B}_0(\boldsymbol{r}_0)\simeq\boldsymbol{B}_0(\boldsymbol{r}_0)\boldsymbol{\cdot}\boldsymbol{\nabla}_0\boldsymbol{\xi}-\boldsymbol{B}_0(\boldsymbol{r}_0)(\boldsymbol{\nabla}_0\boldsymbol{\cdot}\boldsymbol{\xi}).\tag{V.3.8}$$

This matches (V.2.9).

Nothing particularly educational is gained by spelling out the derivation of the momentum equation in the Lagrangian picture, and nothing particularly useful beyond (V.2.10) is gained by having the answer. But here it is:

$$\frac{\rho_0}{\mathcal{J}}\frac{\mathrm{D}^2\boldsymbol{r}}{\mathrm{D}t^2}=-\left(\frac{\partial\boldsymbol{r}_0}{\partial\boldsymbol{r}}\right)\boldsymbol{\cdot}\boldsymbol{\nabla}_0\left(\frac{P_0}{\mathcal{J}^\gamma}+\frac{|\boldsymbol{B}_0\boldsymbol{\cdot}\boldsymbol{\nabla}_0\boldsymbol{r}|^2}{8\pi\mathcal{J}^2}\right)+\frac{\boldsymbol{B}_0}{4\pi\mathcal{J}}\boldsymbol{\cdot}\boldsymbol{\nabla}_0\frac{\boldsymbol{B}_0}{\mathcal{J}}\boldsymbol{\cdot}\frac{\partial\boldsymbol{r}}{\partial\boldsymbol{r}_0}.\tag{V.3.9}$$

V.4. Nonlinear MHD waves

It is worth noting that some waves in ideal MHD are exact nonlinear solutions to the equations. For example, a shear-Alfvén wave with

$$\boldsymbol{B}=B_0\hat{\boldsymbol{z}}+B_\perp\sin\bigl[k(z-v_\mathrm{A}t)\bigr]\hat{\boldsymbol{x}}\quad\text{and}\quad\boldsymbol{u}_\perp=-v_\mathrm{A}\frac{B_\perp}{B_0}\sin\bigl[k(z-v_\mathrm{A}t)\bigr]\hat{\boldsymbol{x}}\tag{V.4.1}$$

satisfies $\boldsymbol{u}\boldsymbol{\cdot}\boldsymbol{\nabla}\boldsymbol{u}=\boldsymbol{u}\boldsymbol{\cdot}\boldsymbol{\nabla}\boldsymbol{B}=0$ and is an exact nonlinear solution if the pressure satisfies

$$P+\frac{B_\perp^2}{8\pi}\sin^2\bigl[k(z-v_\mathrm{A}t)\bigr]=\text{const}.\tag{V.4.2}$$

In principle, such a pressure profile could be arranged, but it seems a bit contrived. A more natural nonlinear solution for an Alfvén wave applies when the wave is circularly polarized:

$$\boldsymbol{B}_\perp=-\sqrt{4\pi\rho}\,\boldsymbol{u}_\perp=B_\perp\cos[k(z-v_\mathrm{A}t)]\hat{\boldsymbol{x}}+B_\perp\sin[k(z-v_\mathrm{A}t)]\hat{\boldsymbol{y}}.\tag{V.4.3}$$

For this polarization, the total field strength satisfies $B^2=B_0^2+B_\perp^2=\text{const}$, and so the background pressure can remain constant.

A set of equations for nonlinear Alfvén waves can be constructed following Elsasser (1950). Assume incompressibility with $\rho=\text{const}$, and define the Elsasser fields

$$\boldsymbol{Z}^\pm\doteq\boldsymbol{u}\pm\frac{\boldsymbol{B}}{\sqrt{4\pi\rho}}.\tag{V.4.4}$$

Take the incompressible momentum and induction equations in the following forms:

$$\frac{\partial \boldsymbol{u}}{\partial t} + \boldsymbol{u}\cdot\boldsymbol{\nabla}\boldsymbol{u} = \frac{\boldsymbol{B}\cdot\boldsymbol{\nabla}\boldsymbol{B}}{4\pi\rho} - \frac{1}{\rho}\boldsymbol{\nabla}\left(P + \frac{B^2}{8\pi}\right) \tag{V.4.5}$$

$$\frac{\partial \boldsymbol{B}}{\partial t} + \boldsymbol{u}\cdot\boldsymbol{\nabla}\boldsymbol{B} = \boldsymbol{B}\cdot\boldsymbol{\nabla}\boldsymbol{u}. \tag{V.4.6}$$

Divide the latter by $\sqrt{4\pi\rho}$, and add and subtract the equations:

$$\frac{\partial \boldsymbol{Z}^{\pm}}{\partial t} + \boldsymbol{u}\cdot\boldsymbol{\nabla}\boldsymbol{Z}^{\pm} = \pm\frac{\boldsymbol{B}}{\sqrt{4\pi\rho}}\cdot\boldsymbol{\nabla}\boldsymbol{Z}^{\pm} - \frac{1}{\rho}\boldsymbol{\nabla}\left(P + \frac{B^2}{8\pi}\right). \tag{V.4.7}$$

Defining $\widetilde{h} \doteq (P + B^2/8\pi)/\rho$ and re-arranging, we obtain

$$\boxed{\frac{\partial \boldsymbol{Z}^{\pm}}{\partial t} + \boldsymbol{Z}^{\mp}\cdot\boldsymbol{\nabla}\boldsymbol{Z}^{\pm} = -\boldsymbol{\nabla}\widetilde{h}} \tag{V.4.8}$$

Note that $\boldsymbol{Z}^{\pm}$ is advected by $\boldsymbol{Z}^{\mp}$, a feature that is extremely important for theories of MHD turbulence. Because $\boldsymbol{\nabla}\cdot\boldsymbol{Z}^{\pm} = 0$, $\widetilde{h}$ is determined by

$$\nabla^2\widetilde{h} = -\boldsymbol{\nabla}\boldsymbol{\nabla} : \boldsymbol{Z}^{+}\boldsymbol{Z}^{-}. \tag{V.4.9}$$

This is the pressure required to ensure incompressibility.

It will prove beneficial to split the magnetic field into its background and perturbed parts, so that

$$\boldsymbol{Z}^{\pm} = \pm v_{\mathrm{A}}\hat{\boldsymbol{z}} + \delta\boldsymbol{Z}^{\pm}. \tag{V.4.10}$$

Then (V.4.8) becomes

$$\boxed{\frac{\partial \delta\boldsymbol{Z}^{\pm}}{\partial t} \mp v_{\mathrm{A}}\frac{\partial \delta\boldsymbol{Z}^{\pm}}{\partial z} + \delta\boldsymbol{Z}^{\mp}\cdot\boldsymbol{\nabla}\delta\boldsymbol{Z}^{\pm} = -\boldsymbol{\nabla}\widetilde{h}} \tag{V.4.11}$$

We'll explore this equation more in the next section, and further on when discussing MHD turbulence, but there are a few things to note now while I have your attention. First, if $\delta\boldsymbol{Z}^{-} = 0$, then $\delta\boldsymbol{Z}^{+}$ satisfies a linear equation representing the propagation of an Alfvén-wave packet at velocity $v_{\mathrm{A}}\hat{\boldsymbol{z}}$. Likewise, if $\delta\boldsymbol{Z}^{+} = 0$, then $\delta\boldsymbol{Z}^{-}$ satisfies a linear equation representing the propagation of an Alfvén-wave packet at speed $-v_{\mathrm{A}}\hat{\boldsymbol{z}}$. Therefore,

$$\delta\boldsymbol{Z}^{\pm} = \boldsymbol{f}(\boldsymbol{r} \pm v_{\mathrm{A}}t\hat{\boldsymbol{z}}), \quad \delta\boldsymbol{Z}^{\mp} = 0, \tag{V.4.12}$$

where $\boldsymbol{f}$ is an arbitrary function, are exact nonlinear solutions of incompressible MHD. Such isolated Alfvén-wave packets, called "Elsasser states" never interact with one another, because they all travel at the same velocity ($\pm v_{\mathrm{A}}\hat{\boldsymbol{z}}$) and so can never catch up with one another. But if both Elsasser states are active, then these counter-propagating Alfvén-wave packets can nonlinearly interact through the term $\delta\boldsymbol{Z}^{\mp}\cdot\boldsymbol{\nabla}\delta\boldsymbol{Z}^{\pm}$ in (V.4.11) and distort one another. Despite this interaction, however, there are certain conserved quantities.

Equations (V.4.8) independently conserve the total energy,

$$\frac{\mathrm{d}}{\mathrm{d}t}\int \mathrm{d}\boldsymbol{r}\,\frac{1}{2}\left(\frac{|\boldsymbol{Z}^{+}|^2}{2} + \frac{|\boldsymbol{Z}^{-}|^2}{2}\right) = \frac{\mathrm{d}}{\mathrm{d}t}\int \mathrm{d}\boldsymbol{r}\left(\frac{u^2}{2} + \frac{B^2}{8\pi\rho}\right) = 0, \tag{V.4.13}$$

and the *cross-helicity*:

$$\boxed{\frac{\mathrm{d}}{\mathrm{d}t}\int \mathrm{d}\boldsymbol{r}\,\frac{1}{2}\left(\frac{|\boldsymbol{Z}^{+}|^2}{2} - \frac{|\boldsymbol{Z}^{-}|^2}{2}\right) = \frac{\mathrm{d}}{\mathrm{d}t}\int \mathrm{d}\boldsymbol{r}\,\boldsymbol{u}\cdot\frac{\boldsymbol{B}}{\sqrt{4\pi\rho}} = 0} \tag{V.4.14}$$

The cross-helicity is sometimes called the *imbalance*, because it measures the difference in energies between the counter-propagating Alfvénic fluctuations. In the solar wind, there is significantly more energy in Alfvénic fluctuations propagating away from the Sun than towards it, increasingly so nearer to the corona (e.g., Wicks *et al.* 2013).

V.5. Reduced MHD

Reduced MHD (RMHD) is a nonlinear system of fluid equations used to describe anisotropic fluctuations in magnetized plasmas at lengthscales $\ell \gg r_{\rm gyro,i}$ and frequencies $\omega \ll \Omega_{\rm i}$, where $r_{\rm gyro,i}$ and $\Omega_{\rm i}$ are the ion Larmor radius and frequency, respectively. It was initially used to model elongated structures in tokamaks (Kadomtsev & Pogutse 1974; Strauss 1976, 1977), but has since become a standard paradigm in astrophysical contexts such as solar-wind turbulence (Zank & Matthaeus 1992*a*,*b*; Bhattacharjee *et al.* 1998) and the solar corona (Oughton *et al.* 2003; Perez & Chandran 2013).

While one may formulate different versions of RMHD, here I will confine the discussion solely to ideally conducting fluids whose equilibrium state is homogeneous ($\rho_0 = {\rm const}$, $P_0 = {\rm const}$), stationary ($\boldsymbol{u}_0 = 0$), and threaded by a uniform mean magnetic field oriented along the z axis ($\boldsymbol{B}_0 = B_0\hat{\boldsymbol{z}}$). The fluid is perturbed with small displacements, which we take to satisfy the ordering

$$\frac{\delta\rho}{\rho_0} \sim \frac{\delta P}{P_0} \sim \frac{u_\perp}{c_{\rm s}} \sim \frac{u_\parallel}{c_{\rm s}} \sim \frac{\delta B_\perp}{B_0} \sim \frac{\delta B_\parallel}{B_0} \sim \frac{k_\parallel}{k_\perp} \doteq \epsilon \ll 1, \tag{V.5.1}$$

where the sound speed $c_{\rm s} \doteq (\gamma P_0/\rho_0)^{1/2}$ is of order the Alfvén speed $v_{\rm A} \doteq B_0/(4\pi\rho_0)^{1/2}$. In other words, the plasma beta parameter

$$\beta \doteq \frac{8\pi P_0}{B_0^2} = \frac{2}{\gamma}\frac{c_{\rm s}^2}{v_{\rm A}^2} \tag{V.5.2}$$

is taken to be of order unity; subsidiary limits in high and low β may be taken after the ϵ expansion is performed. The fluctuations are therefore sub-sonic, sub-Alfvénic, and spatially anisotropic with respect to the magnetic-field direction, with a characteristic length scale parallel to the field ($\sim k_\parallel^{-1}$) that is much larger than across the field ($\sim k_\perp^{-1}$). Because our focus is on Alfvén-wave fluctuations, the characteristic frequency of the fluctuations is taken to satisfy $\omega \sim k_\parallel v_{\rm A}$, so that $\omega \sim \epsilon k_\perp v_{\rm A}$. As a result of this ordering, fast magnetosonic modes are ordered out of the equations. The ordering (V.5.1) is applied to each of the ideal MHD equations and the result examined order by order in ϵ. Before doing so, note that the Lagrangian derivative

$$\frac{\rm D}{{\rm D}t} = \underbrace{\frac{\partial}{\partial t}}_{\sim\omega} + \underbrace{u_\parallel\nabla_\parallel}_{\sim\epsilon\omega} + \underbrace{\boldsymbol{u}_\perp\boldsymbol{\cdot}\boldsymbol{\nabla}_\perp}_{\sim\omega} = \frac{\partial}{\partial t} + \boldsymbol{u}_\perp\boldsymbol{\cdot}\boldsymbol{\nabla}_\perp + \mathcal{O}(\epsilon\omega),$$

so that fluctuations are nonlinearly advected to leading order by the $\boldsymbol{E}\times\boldsymbol{B}$ flow. This is important, as it indicates that, while the fluctuations are assumed small, they are *not* infinitesimally small. Let us proceed.

First, the continuity equation:

$$\underbrace{\frac{\rm D}{{\rm D}t}\frac{\delta\rho}{\rho_0}}_{1} = -\underbrace{\nabla_\parallel u_\parallel}_{1} - \underbrace{\boldsymbol{\nabla}_\perp\boldsymbol{\cdot}\boldsymbol{u}_\perp}_{0},$$

where the order in ϵ at which each term enters relative to ω is indicated. To leading order, we have

$$\boxed{\boldsymbol{\nabla}_\perp \boldsymbol{\cdot} \boldsymbol{u}_\perp = 0} \tag{V.5.3}$$

i.e., the perpendicular dynamics is incompressible. This implies that $\boldsymbol{u}_\perp$ can be written in terms of a stream function:

$$\boldsymbol{u}_\perp = \hat{\boldsymbol{z}} \times \boldsymbol{\nabla}_\perp \varPhi. \tag{V.5.4}$$

Likewise, the solenoidality constraint on the magnetic field allows us to write $\delta\boldsymbol{B}_\perp$ in terms of a flux function:

$$\frac{\delta\boldsymbol{B}_\perp}{\sqrt{4\pi\rho_0}} = \hat{\boldsymbol{z}} \times \boldsymbol{\nabla}_\perp \varPsi. \tag{V.5.5}$$

Thus, the Alfvénic fluctuations can be described in terms of two scalar functions, $\varPhi$ and $\varPsi$. (The compressive fluctuations involve the higher-order terms in the continuity equation, and are discussed below.)

The evolution equations for $\varPhi$ and $\varPsi$ are obtained by applying the RMHD ordering (V.5.1) to the ideal-MHD induction equation:

$$\underbrace{\frac{\mathrm{D}}{\mathrm{D}t}\frac{\delta\boldsymbol{B}}{B_0}}_{①} = \underbrace{\frac{\partial\boldsymbol{u}}{\partial z}}_{①} + \underbrace{\left(\frac{\delta\boldsymbol{B}_\perp}{B_0}\boldsymbol{\cdot}\boldsymbol{\nabla}_\perp\right)\boldsymbol{u}}_{①} + \underbrace{\left(\frac{\delta B_\parallel}{B_0}\nabla_\parallel\right)\boldsymbol{u}}_{②} - \underbrace{\hat{\boldsymbol{z}}(\boldsymbol{\nabla}\boldsymbol{\cdot}\boldsymbol{u})}_{①} - \underbrace{\frac{\delta\boldsymbol{B}}{B_0}(\boldsymbol{\nabla}\boldsymbol{\cdot}\boldsymbol{u})}_{②}.$$

To leading order, the perpendicular magnetic-field fluctuations satisfy

$$\frac{\mathrm{D}}{\mathrm{D}t}\frac{\delta\boldsymbol{B}_\perp}{B_0} = \left(\frac{\partial}{\partial z} + \frac{\delta\boldsymbol{B}_\perp}{B_0}\boldsymbol{\cdot}\boldsymbol{\nabla}_\perp\right)\boldsymbol{u}_\perp. \tag{V.5.6}$$

The term in parentheses in (V.5.6) is just $\hat{\boldsymbol{b}}\boldsymbol{\cdot}\boldsymbol{\nabla}$ written out to $\mathcal{O}(\epsilon k_\perp)$, and so field-parallel gradients in the perpendicular flow drive (Lagrangian) changes in the perpendicular magnetic-field fluctuations. Using the expressions (V.5.4) and (V.5.5) for $\boldsymbol{u}_\perp$ and $\delta\boldsymbol{B}_\perp$, respectively, equation (V.5.6) implies

$$\boxed{\frac{\partial\varPsi}{\partial t} + \{\varPhi,\varPsi\} = v_{\mathrm{A}}\frac{\partial\varPhi}{\partial z}} \tag{V.5.7}$$

where the Poisson bracket

$$\{\varPhi,\varPsi\} \doteq \hat{\boldsymbol{z}}\boldsymbol{\cdot}(\boldsymbol{\nabla}_\perp\varPhi\times\boldsymbol{\nabla}_\perp\varPsi) = \frac{\partial\varPhi}{\partial x}\frac{\partial\varPsi}{\partial y} - \frac{\partial\varPhi}{\partial y}\frac{\partial\varPsi}{\partial x}. \tag{V.5.8}$$

The evolution equation for $\varPhi$ is obtained from the perpendicular component of the momentum equation (II.3.8):

$$\begin{aligned}\underbrace{\frac{\mathrm{D}\boldsymbol{u}_\perp}{\mathrm{D}t}}_{①} + \underbrace{(u_\parallel\nabla_\parallel)\boldsymbol{u}_\perp}_{②} + \underbrace{\frac{\delta\rho}{\rho_0}\frac{\mathrm{D}\boldsymbol{u}_\perp}{\mathrm{D}t}}_{②} + \underbrace{\frac{\delta\rho}{\rho_0}(u_\parallel\nabla_\parallel)\boldsymbol{u}_\perp}_{③} &= \underbrace{-\boldsymbol{\nabla}_\perp\left(c_{\mathrm{s}}^2\frac{\delta P}{\gamma P_0} + v_{\mathrm{A}}^2\frac{\delta B_\parallel}{B_0}\right)}_{⓪} \\ &\quad - \underbrace{v_{\mathrm{A}}^2\boldsymbol{\nabla}_\perp\frac{|\delta\boldsymbol{B}|^2}{2B_0^2}}_{①} + \underbrace{v_{\mathrm{A}}^2\frac{\partial}{\partial z}\frac{\delta\boldsymbol{B}_\perp}{B_0}}_{①} + \underbrace{v_{\mathrm{A}}^2\left(\frac{\delta\boldsymbol{B}_\perp}{B_0}\boldsymbol{\cdot}\boldsymbol{\nabla}_\perp\right)\frac{\delta\boldsymbol{B}_\perp}{B_0}}_{①} + \underbrace{v_{\mathrm{A}}^2\left(\frac{\delta B_\parallel}{B_0}\nabla_\parallel\right)\frac{\delta\boldsymbol{B}_\perp}{B_0}}_{②},\end{aligned} \tag{V.5.9}$$

where the order in ϵ at which each term enters relative to ωc_{s} is indicated. At $\mathcal{O}(1)$, we have perpendicular pressure balance:

$$-\nabla_\perp\left(c_s^2\frac{\delta P}{\gamma P_0}+v_A^2\frac{\delta B_\parallel}{B_0}\right)=0\quad\Longrightarrow\quad\frac{\delta P}{P_0}=-\frac{2}{\beta}\frac{\delta B_\parallel}{B_0}=-\gamma\frac{v_A^2}{c_s^2}\frac{\delta B_\parallel}{B_0}.\tag{V.5.10}$$

At $\mathcal{O}(\epsilon)$,

$$\frac{\mathrm{D}\boldsymbol{u}_\perp}{\mathrm{D}t}=-\nabla_\perp\left(c_s^2\frac{\delta P_2}{\gamma P_0}+v_A^2\frac{|\delta\boldsymbol{B}|^2}{2B_0^2}\right)+v_A^2\frac{\partial}{\partial z}\frac{\delta\boldsymbol{B}_\perp}{B_0}+v_A^2\left(\frac{\delta\boldsymbol{B}_\perp}{B_0}\cdot\nabla_\perp\right)\frac{\delta\boldsymbol{B}_\perp}{B_0},\tag{V.5.11}$$

where δP_2 is the second-order pressure fluctuation. Fortunately, δP_2 need not be determined, since its only role is to enforce incompressibility, equation (V.5.3). Indeed, taking the curl of (V.5.11) eliminates the entire pressure term, leaving

$$\nabla_\perp\times\left[\frac{\mathrm{D}\boldsymbol{u}_\perp}{\mathrm{D}t}=v_A^2\frac{\partial}{\partial z}\frac{\delta\boldsymbol{B}_\perp}{B_0}+v_A^2\left(\frac{\delta\boldsymbol{B}_\perp}{B_0}\cdot\nabla_\perp\right)\frac{\delta\boldsymbol{B}_\perp}{B_0}\right]\tag{V.5.12}$$

Noting that

$$\begin{aligned}\nabla_\perp\times(\hat{\boldsymbol{z}}\times\nabla_\perp\Phi)&=\hat{\boldsymbol{z}}\,\nabla_\perp^2\Phi,\\ \nabla_\perp\times(\hat{\boldsymbol{z}}\times\nabla_\perp\Psi)&=\hat{\boldsymbol{z}}\,\nabla_\perp^2\Psi,\\ \nabla_\perp\times\big[(\hat{\boldsymbol{z}}\times\nabla_\perp\Phi)\cdot\nabla_\perp(\hat{\boldsymbol{z}}\times\nabla_\perp\Phi)\big]&=\hat{\boldsymbol{z}}\,\hat{\boldsymbol{z}}\cdot(\nabla_\perp\Phi\times\nabla_\perp\nabla_\perp^2\Phi),\\ \nabla_\perp\times\big[(\hat{\boldsymbol{z}}\times\nabla_\perp\Psi)\cdot\nabla_\perp(\hat{\boldsymbol{z}}\times\nabla_\perp\Psi)\big]&=\hat{\boldsymbol{z}}\,\hat{\boldsymbol{z}}\cdot(\nabla_\perp\Psi\times\nabla_\perp\nabla_\perp^2\Psi),\end{aligned}$$

the $\hat{\boldsymbol{z}}$ component of (V.5.12) may be written as

$$\boxed{\frac{\partial}{\partial t}\nabla_\perp^2\Phi+\left\{\Phi,\nabla_\perp^2\Phi\right\}=v_A\frac{\partial}{\partial z}\nabla_\perp^2\Psi+\left\{\Psi,\nabla_\perp^2\Psi\right\}}\tag{V.5.13}$$

This is essentially an equation for the flow vorticity.

Equations (V.5.7) and (V.5.13) form a closed set of equations for the Alfvénic fluctuations:

$$\frac{\mathrm{D}\Psi}{\mathrm{D}t}=v_A\frac{\partial\Phi}{\partial z},\tag{V.5.14a}$$

$$\frac{\mathrm{D}}{\mathrm{D}t}\nabla_\perp^2\Phi=v_A\hat{\boldsymbol{b}}\cdot\nabla\nabla_\perp^2\Psi,\tag{V.5.14b}$$

where

$$\frac{\mathrm{D}}{\mathrm{D}t}=\frac{\partial}{\partial t}+\{\Phi,\dots\}\quad\text{and}\quad\hat{\boldsymbol{b}}\cdot\nabla=\frac{\partial}{\partial z}+\frac{1}{v_A}\{\Psi,\dots\}.\tag{V.5.15}$$

Note that the compressive fluctuations make no appearance in the equations for the Alfvénic fluctuations, and so the former exert no influence on the latter.

Finally, there is an advantageous combination of (V.5.14) that makes clear the foundation of theories of Alfvén-wave turbulence. Define the Elsässer potentials

$$\zeta^\pm\doteq\Phi\pm\Psi.\tag{V.5.16}$$

Then $\Phi=(\zeta^++\zeta^-)/2$ and $\Psi=(\zeta^+-\zeta^-)/2$, and so (V.5.14) may be written as

$$\frac{\partial}{\partial t}\left(\frac{\zeta^+-\zeta^-}{2}\right)+\left\{\frac{\zeta^++\zeta^-}{2},\frac{\zeta^+-\zeta^-}{2}\right\}=v_A\frac{\partial}{\partial z}\left(\frac{\zeta^++\zeta^-}{2}\right)\tag{V.5.17a}$$

$$\begin{aligned}\frac{\partial}{\partial t}\nabla_\perp^2\left(\frac{\zeta^++\zeta^-}{2}\right)+\left\{\frac{\zeta^++\zeta^-}{2},\nabla_\perp^2\frac{\zeta^++\zeta^-}{2}\right\}&=v_A\frac{\partial}{\partial z}\nabla_\perp^2\left(\frac{\zeta^+-\zeta^-}{2}\right)\\&\quad+\left\{\frac{\zeta^+-\zeta^-}{2},\nabla_\perp^2\frac{\zeta^+-\zeta^-}{2}\right\}.\end{aligned}\tag{V.5.17b}$$

Noting that $\{\zeta^\pm, \zeta^\pm\} = 0$ and taking $\nabla_\perp^2$ of (V.5.17a), these become

$$\frac{\partial}{\partial t}\nabla_\perp^2(\zeta^+ - \zeta^-) + \frac{1}{2}\nabla_\perp^2\Big(\{\zeta^-, \zeta^+\} - \{\zeta^+, \zeta^-\}\Big) = v_\mathrm{A}\frac{\partial}{\partial z}\nabla_\perp^2(\zeta^+ + \zeta^-),$$
$$\frac{\partial}{\partial t}\nabla_\perp^2(\zeta^+ + \zeta^-) + \frac{1}{2}\Big(\{\zeta^+, \nabla_\perp^2\zeta^-\} + \{\zeta^-, \nabla_\perp^2\zeta^+\}\Big) = v_\mathrm{A}\frac{\partial}{\partial z}\nabla_\perp^2(\zeta^+ - \zeta^-)$$
$$- \frac{1}{2}\Big(\{\zeta^+, \nabla_\perp^2\zeta^-\} + \{\zeta^-, \nabla_\perp^2\zeta^+\}\Big),$$

which may be added to and subtracted from one another to obtain

$$\boxed{\frac{\partial}{\partial t}\nabla_\perp^2\zeta^\pm \mp v_\mathrm{A}\frac{\partial}{\partial z}\nabla_\perp^2\zeta^\pm = -\frac{1}{2}\Big(\{\zeta^+, \nabla_\perp^2\zeta^-\} + \{\zeta^-, \nabla_\perp^2\zeta^+\} \mp \nabla_\perp^2\{\zeta^+, \zeta^-\}\Big)} \tag{V.5.18}$$

The left-hand side of this equation captures the propagation of linear Alvén waves: $\zeta^\pm = f^\pm(x, y, z \mp v_\mathrm{A} t)$. What is notable is that these solutions are also exact *nonlinear* solutions if either $\zeta^- = 0$ or $\zeta^+ = 0$, since the nonlinearities on the right-hand side of (V.5.18) then vanish. In fact, in this case the fluctuation (or, indeed, wave packet) may be of arbitrary shape and magnitude, simply propagating along the mean magnetic field at the Alfvén speed. The key here is that only *counterpropagating* fluctuations can interact (Kraichnan 1965). They do so by scattering off each other without exchanging energy; indeed, it is easy to show by multiplying (V.5.18) by $\rho_0\zeta^\pm$ and integrating by parts that the nonlinear Alfvén-wave energy

$$W_\mathrm{AW}^\pm \doteq \frac{1}{2}\int \mathrm{d}^3\boldsymbol{r}\,\rho_0|\boldsymbol{\nabla}_\perp\zeta^\pm|^2 \tag{V.5.19}$$

is conserved. This conservation law plays an important role in theories of Alfvén-wave turbulence, particularly the fact that, whatever the compressive fluctuations are doing, they are doing it independently of the Alfvén-wave cascade.

Now, the evolution equations for the compressive fluctuations will be derived and analyzed by you in a problem set. But let me state them here without proof:

$$\frac{\mathrm{D}}{\mathrm{D}t}\frac{\delta\sigma}{\sigma_0} = 0, \tag{V.5.20}$$
$$\frac{\mathrm{D}}{\mathrm{D}t}\frac{\delta\rho}{\rho_0} = -\frac{1}{1 + c_\mathrm{s}^2/v_\mathrm{A}^2}\hat{\boldsymbol{b}}\boldsymbol{\cdot}\boldsymbol{\nabla}u_\parallel, \tag{V.5.21}$$
$$\frac{\mathrm{D}}{\mathrm{D}t}\frac{\delta B_\parallel}{B_0} = \frac{1}{1 + v_\mathrm{A}^2/c_\mathrm{s}^2}\hat{\boldsymbol{b}}\boldsymbol{\cdot}\boldsymbol{\nabla}u_\parallel, \tag{V.5.22}$$
$$\frac{\mathrm{D}}{\mathrm{D}t}u_\parallel = v_\mathrm{A}^2\hat{\boldsymbol{b}}\boldsymbol{\cdot}\boldsymbol{\nabla}\frac{\delta B_\parallel}{B_0}, \tag{V.5.23}$$

where $\sigma \doteq (\gamma - 1)^{-1}\ln p\rho^{-\gamma}$ is the specific entropy. Equations (V.5.21)–(V.5.23) describe the slow-wave-polarized fluctuations, for which perpendicular pressure balance (equation (V.5.10)) holds. Equation (V.5.20) describes the zero-frequency entropy mode. Note that the only nonlinearities in these equations are via the derivatives defined in (V.5.15). Question: What does the imply about the relationship between the compressive fluctuations and the Alfvénic ones?

V.6. Waves in rotating systems

V.6.1. *Rossby waves*

Consider a two-dimensional, incompressible fluid on the surface of uniformly rotating sphere (e.g., a planetary atmosphere). For a constant density or a barotropic equation of state, equation (II.2.19) describing Kelvin's circulation theorem becomes

$$\frac{\mathrm{D}}{\mathrm{D}t}\left(\mathit{\Gamma}_{\mathrm{rot}} + 2\mathit{\Omega}\mathcal{S}\cos\theta\right) = 0, \tag{V.6.1}$$

where θ is the angle between the rotation vector and the surface oriented normal to the fluid element. (Note that incompressibility assures $\mathcal{S} = \text{const.}$) This equation states that, as a fluid element makes its way from the equator northwards (*viz.*, from $\theta = \pi/2$ towards $\theta = 0$), its circulation as measured in the rotating frame must decrease. This means that the element must then rotate in the clockwise direction. Likewise, a fluid element that starts at the north pole and moves southwards towards the equator (*viz.*, from $\theta = 0$ towards $\theta = \pi/2$) increases its relative vorticity and thus rotates in the counterclockwise direction.

With this behavior in mind, let's now imagine a small-amplitude, wave-like disturbance at constant latitude (see diagram below). Northward displacements in this wave acquire negative relative vorticity and rotate clockwise; southward displacements acquire positive relative vorticity and rotate counterclockwise. These changes in the velocity of the disturbance actually feed back on the wave itself to make it travel westward; in effect, the wave is advecting itself to the west.

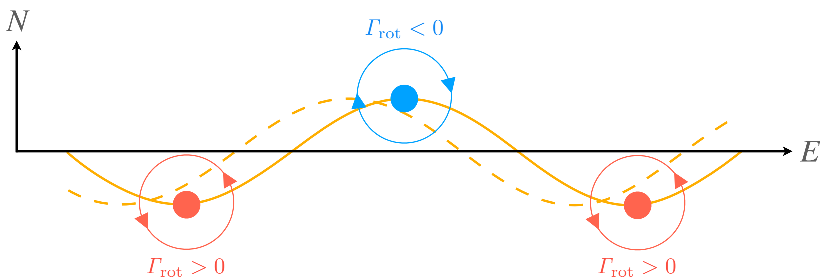

The relationship between the frequency ω and wavevector $\boldsymbol{k}$ for this wave – the *dispersion relation* – is given by

$$\omega = -\frac{k_y}{k_x^2 + k_y^2}\,\frac{2\mathit{\Omega}\sin\theta}{r}, \tag{V.6.2}$$

where x denotes the local poloidal direction (pointing southward), y denotes the local azimuthal direction (pointing eastward), and r the spherical radial distance. With $\mathit{\Omega} > 0$ and $k_y > 0$, the phase velocity of the wave $\omega/k_y < 0$, i.e., the wave travels westward. Note that the group velocity, $\partial\omega/\partial k_y$, can be either positive or negative; in general, shorter wavelengths (higher k) have an eastward group velocity and longer wavelengths (smaller k) have a westward group velocity.

These waves are named after the meteorologist Carl Rossby, who derived the mathematics governing this phenomenon in 1939 while at MIT (after which he became assistant director of research at the U.S. Weather Bureau and then moved to University of Chicago as Chair of the Department of Meteorology).[6]

[6] See https://elischolar.library.yale.edu/journal_of_marine_research/516.

V.6.2. *Spiral density waves and inertial waves*

In rotating disks, there are effects that modify the standard MHD waves and effects that introduce new kinds of oscillations. These effects are explored in this section. We first neglect magnetic effects and work in ideal hydrodynamics.

We work in cylindrical polar coordinates (R, φ, z) with z oriented along the axis of a differentially rotating disk with angular frequency $\Omega\hat{\boldsymbol{z}}$. For simplicity, we'll take the background pressure to be barotropic, in which case $\Omega = \Omega(R)$ only (remember §IV.2?), but allow for radial and vertical stratification in the density, $\rho = \rho(R, z)$. Starting from (II.2.9), the linearized equations are

$$\left(\frac{\partial}{\partial t} + \Omega\frac{\partial}{\partial\varphi}\right)\frac{\delta\rho}{\rho} = -\frac{1}{R}\frac{\partial(R\delta v_R)}{\partial R} - \frac{1}{R}\frac{\partial\delta v_\varphi}{\partial\varphi} - \frac{\partial\delta v_z}{\partial z} - \delta v_R\frac{\partial\ln\rho}{\partial R} - \delta v_z\frac{\partial\ln\rho}{\partial z}, \tag{V.6.3a}$$

$$\left(\frac{\partial}{\partial t} + \Omega\frac{\partial}{\partial\varphi}\right)\delta v_R = -\frac{\partial\delta h}{\partial R} + 2\Omega\delta v_\varphi, \tag{V.6.3b}$$

$$\left(\frac{\partial}{\partial t} + \Omega\frac{\partial}{\partial\varphi}\right)\delta v_\varphi = -\frac{1}{R}\frac{\partial\delta h}{\partial\varphi} - \frac{\kappa^2}{2\Omega}\delta v_R, \tag{V.6.3c}$$

$$\left(\frac{\partial}{\partial t} + \Omega\frac{\partial}{\partial\varphi}\right)\delta v_z = -\frac{\partial\delta h}{\partial z}, \tag{V.6.3d}$$

where $\delta h \doteq \delta P/\rho = c_{\rm s}^2\,\delta\rho/\rho$ is the enthalpy. Working in the WKB limit, we may adopt solutions of the form $\exp(-{\rm i}\omega t + {\rm i}m\varphi + {\rm i}k_R R + {\rm i}k_z z)$; the idea is that the perturbations vary on lengthscales much shorter than those characterizing the background disk, *viz.*, $k_R L_R \sim k_R R \gg 1$ and $k_z L_z \gg 1$, where L_R (L_z) is the characteristic disk lengthscale in the radial (vertical) direction. Substituting in this plane-wave solution yields the following set of equations for the perturbations' Fourier amplitudes:

$$-{\rm i}\varpi\frac{\delta\rho}{\rho} = -{\rm i}k_R\delta v_R - {\rm i}\frac{m}{R}\delta v_\varphi - {\rm i}k_z\delta v_z, \tag{V.6.4a}$$

$$-{\rm i}\varpi\delta v_R = -{\rm i}k_R c_{\rm s}^2\frac{\delta\rho}{\rho} + 2\Omega\delta v_\varphi, \tag{V.6.4b}$$

$$-{\rm i}\varpi\delta v_\varphi = -{\rm i}\frac{m}{R}c_{\rm s}^2\frac{\delta\rho}{\rho} - \frac{\kappa^2}{2\Omega}\delta v_R, \tag{V.6.4c}$$

$$-{\rm i}\varpi\delta v_z = -{\rm i}k_z c_{\rm s}^2\frac{\delta\rho}{\rho}, \tag{V.6.4d}$$

where $\varpi \doteq \omega - m\Omega$ is the Doppler-shifted frequency.

In the "tightly wound" limit in which $k_R, k_z \gg m/R$, these equations may be straightforwardly combined to obtain the following dispersion relation:

$$\varpi^4 - \varpi^2\big(\kappa^2 + k^2c_{\rm s}^2\big) + \kappa^2k_z^2c_{\rm s}^2 = 0, \tag{V.6.5}$$

where $k^2 = k_R^2 + k_z^2$. Another way to write this result is

$$\varpi^2 - k^2c_{\rm s}^2 = \frac{\kappa^2k_R^2c_{\rm s}^2}{\varpi^2 - \kappa^2}, \tag{V.6.6}$$

which has the usual sound-wave dispersion relation on the left-hand side (except that $\omega^2 \to \varpi^2$) and has a right-hand side that includes effects associated with the differential rotation.

Consider first the case $k_z = 0$. The result is the dispersion relation for *spiral density* *waves*:

$$\overline{\omega}^2 = \kappa^2 + k^2 c_s^2. \tag{V.6.7}$$

Such waves are thought to be particularly important in theories of galactic structure and protostellar disks, especially when a $-4\pi G\rho$ is appended to the right-hand side to account for the disk's own self-gravity. Note that rotation is a stabilizing influence and boosts the frequency of the wave, as is differential rotation as long as $\kappa^2 > 0$ (the usual situation in astrophysical disks). This is because the angular momentum of a displaced fluid element is conserved: as the fluid element is compressed in the sound wave it spins up, and the accompanying centrifugal force resists the contraction and thereby boosts the frequency of the oscillation.

Now take $k_z c_s \gg \kappa$ in (V.6.6) to obtain the dispersion relation for *inertial waves*:

$$\overline{\omega}^2 = \frac{k_z^2}{k^2}\kappa^2.$$

These waves are essentially incompressible, and are the only fluctuations in a polytropic, non-self-gravitating disk having frequencies less than κ. Note the dependence on k_z, which in concert with their incompressible nature tells us that the fluid displacements in this wave are primarily in the disk plane. The force responsible for this wave is the Coriolis force, which arises from the geometric terms in $\boldsymbol{u}\cdot\boldsymbol{\nabla}\boldsymbol{u}$ – thus the moniker "inertial wave". Inertial waves are basically epicycles that have been modified by pressure forces.

Finally, let us obtain a general equation *without* adopting the WKB approximation. Take the perturbations in (V.6.3) to have the form $f(R,z)\exp(-i\omega t + im\varphi)$. After much work, the following linear wave equation for the potential $\delta h \doteq \delta P/\rho$ emerges:

$$\left[\frac{1}{R}\frac{\partial}{\partial R}\left(\frac{R\rho}{D}\frac{\partial}{\partial R}\right) - \frac{1}{\overline{\omega}^2}\frac{\partial}{\partial z}\left(\rho\frac{\partial}{\partial z}\right) - \frac{m^2\rho}{R^2 D} + \frac{1}{\overline{\omega}R}\frac{\partial}{\partial R}\left(\frac{2\Omega m\rho}{D}\right)\right]\delta h = -\delta\rho, \tag{V.6.8}$$

where $D \doteq \kappa^2 - \overline{\omega}^2$ Note the resonances at $D = 0$ and $\overline{\omega} = 0$, which are referred to as the *Lindblad resonance* and the *corotation resonance*, respectively. Near these resonances, the waves couple strongly to the disk. (The WKB treatment formally breaks down at the Lindblad resonance, at which k_R must vanish.) These resonances are important in the study of tidally driven waves and planetary migration. For more on this topic, see Goldreich & Tremaine (1979, 1980) and Balbus (2003).

Including magnetic fields will change the dynamics completely when $\Omega = \Omega(R)$, driving the disk linearly unstable in what is now known as the magnetorotational instability. We'll come to that in §VI.8. For now, let us only consider the case of rigid rotation ($\kappa^2 = 4\Omega^2$) and a magnetic field aligned with the rotation axis of the disk ($\boldsymbol{B} = B_0\hat{\boldsymbol{z}} + \delta\boldsymbol{B}$).

Equations (V.6.3) then become

$$\left(\frac{\partial}{\partial t}+\Omega\frac{\partial}{\partial\varphi}\right)\frac{\delta\rho}{\rho} = -\frac{1}{R}\frac{\partial(R\delta v_R)}{\partial R}-\frac{1}{R}\frac{\partial\delta v_\varphi}{\partial\varphi}-\frac{\partial\delta v_z}{\partial z}-\delta v_R\frac{\partial\ln\rho}{\partial R}-\delta v_z\frac{\partial\ln\rho}{\partial z}, \tag{V.6.9a}$$

$$\left(\frac{\partial}{\partial t}+\Omega\frac{\partial}{\partial\varphi}\right)\delta v_R = -\frac{\partial\delta h}{\partial R}+2\Omega\delta v_\varphi+\frac{B_0}{4\pi\rho}\frac{\partial\delta B_R}{\partial z}, \tag{V.6.9b}$$

$$\left(\frac{\partial}{\partial t}+\Omega\frac{\partial}{\partial\varphi}\right)\delta v_\varphi = -\frac{1}{R}\frac{\partial\delta h}{\partial\varphi}-2\Omega\delta v_R+\frac{B_0}{4\pi\rho}\frac{\partial\delta B_\varphi}{\partial z}, \tag{V.6.9c}$$

$$\left(\frac{\partial}{\partial t}+\Omega\frac{\partial}{\partial\varphi}\right)\delta v_z = -\frac{\partial\delta h}{\partial z}+\frac{B_0}{4\pi\rho}\frac{\partial\delta B_z}{\partial z}, \tag{V.6.9d}$$

$$\left(\frac{\partial}{\partial t}+\Omega\frac{\partial}{\partial\varphi}\right)\delta B_R = B_0\frac{\partial\delta v_R}{\partial z}, \tag{V.6.9e}$$

$$\left(\frac{\partial}{\partial t}+\Omega\frac{\partial}{\partial\varphi}\right)\delta B_\varphi = B_0\frac{\partial\delta v_\varphi}{\partial z}, \tag{V.6.9f}$$

$$\left(\frac{\partial}{\partial t}+\Omega\frac{\partial}{\partial\varphi}\right)\delta B_z = -\frac{B_0}{R}\frac{\partial(R\delta v_R)}{\partial R}-\frac{B_0}{R}\frac{\partial\delta v_\varphi}{\partial\varphi}. \tag{V.6.9g}$$

Following the same process as earlier in this section, the WKB dispersion relation in the tightly wound limit ($k_R, k_z \gg m/R$) is

$$\big(\varpi^2-k_\parallel^2v_{\rm A}^2\big)\big[\varpi^4-\varpi^2k^2(c_{\rm s}^2+v_{\rm A}^2)+k^2c_{\rm s}^2k_\parallel^2v_{\rm A}^2\big] = 4\Omega^2\varpi^2\big(\varpi^2-k_z^2c_{\rm s}^2\big). \tag{V.6.10}$$

Note that the rotation has coupled the Alfvén and magnetosonic branches. In the limit $k^2c_{\rm s}^2 \gg \varpi^2$, which has the effect of enforcing incompressibility, this dispersion relation becomes

$$\big(\varpi^2-k_\parallel^2v_{\rm A}^2\big)^2 = 4\Omega^2\varpi^2\frac{k_z^2}{k^2}, \tag{V.6.11}$$

which provides the following four roots describing *magneto-Coriolis waves*:

$$\varpi_{\rm fast} = \pm\Omega\frac{|k_z|}{k}\pm\sqrt{\Omega^2\frac{k_z^2}{k^2}+k_\parallel^2v_{\rm A}^2} \quad \text{and} \quad \varpi_{\rm slow} = \mp\Omega\frac{|k_z|}{k}\pm\sqrt{\Omega^2\frac{k_z^2}{k^2}+k_\parallel^2v_{\rm A}^2}. \tag{V.6.12}$$

When the two signs are the same, the Lorentz force and Coriolis force work reinforce one another, boosting the wave frequency. This is essentially an inertial wave modified by the magnetic force. When the two signs are opposite, the Lorentz force and Coriolis force oppose one another; these waves are sometimes called magnetostrophic waves.

PART VI

MHD instabilities

With some waves under our belts and now equipped with both Eulerian and Lagrangian viewpoints, let's do some MHD linear instabilities. The program is to set up some equilibria and then subject them to small-amplitude perturbations in the fluid and magnetic field. There are a few different ways of doing this and assessing whether the system is stable or unstable to these perturbations. There's something called the MHD Energy Principle, which will tell you whether a given set of perturbations about some equilibrium state will bring the system profitably to a lower energy state. There's something called Eulerian perturbation theory, where you subject the equilibrium state to small-amplitude perturbations, formulate those perturbations in the lab frame, and ask whether the perturbations oscillate, grow, or decay (this is the approach we took to studying the MHD waves). And there's something called Lagrangian perturbation theory, which is same as Eulerian perturbation theory but is formulated in the frame of fluid (thus the groundwork laid in the last chapter). Each of these has its advantages depending on the equilibrium state, boundary conditions, and questions being asked. Eulerian perturbation theory is the most straightforward procedure, so we'll start there.

VI.1. A primer on instability

Before attacking the MHD equations, let's do something simple to establish notation and learn the procedure. Consider the following ordinary differential equation:

$$\frac{\mathrm{d}^2x}{\mathrm{d}t^2} + 2\nu\frac{\mathrm{d}x}{\mathrm{d}t} + \varOmega^2(x - x_0) = 0, \tag{VI.1.1}$$

where ν and $\varOmega > 0$ are constants. You may recognize this as the equation for a damped simple harmonic oscillator of natural frequency $\varOmega$ whose velocity along the x axis is damped at a rate $\nu > 0$. But let's not yet commit to any particular sign of ν. First, the equilibrium state. This is easy: the oscillator is at rest at $x = x_0$. We now displace the oscillator by a small amount ξ, so that $x(t) = x_0 + \xi(t)$. The equation governing this displacement is

$$\frac{\mathrm{d}^2\xi}{\mathrm{d}t^2} + 2\nu\frac{\mathrm{d}\xi}{\mathrm{d}t} + \varOmega^2\xi = 0. \tag{VI.1.2}$$

This equation admits solutions $\xi \sim \exp(-\mathrm{i}\omega t)$, where ω is a complex frequency that satisfies the *dispersion relation*

$$\omega^2 + 2\mathrm{i}\omega\nu - \varOmega^2 = 0 \quad\Longrightarrow\quad \omega = -\mathrm{i}\nu \pm \sqrt{\varOmega^2 - \nu^2}. \tag{VI.1.3}$$

How do we assess stability? If the imaginary part of ω is positive, then $-\mathrm{i}\omega$ has a positive real part, and the displacements will grow exponentially in time. If the imaginary part of ω is negative, then $-\mathrm{i}\omega$ has a negative real part, and this corresponds to exponential decay of the perturbation. If ω additionally has a real part, then this represents a growing or decaying oscillator. It's clear from a cursory glance at the dispersion relation (VI.1.3) that the perturbations oscillate and decay exponentially if $\varOmega > \nu > 0$. If $\nu > \varOmega > 0$, then the perturbations decay without oscillating. But if $\nu < 0$, then there is always an exponentially growing solution. Thus, $\nu > 0$ is the *stability criterion* for this system.

Now, suppose the equation of interest were instead

$$\frac{\mathrm{d}^2x}{\mathrm{d}t^2} + 2\nu\frac{\mathrm{d}x}{\mathrm{d}t} + \varOmega^2\sin(x - x_0) = 0. \tag{VI.1.4}$$

The equilibrium is still the same, but if we want simple harmonic oscillator solutions, we're only going to get them if the displacement is small, i.e., $|\xi| \ll x_0$. In that case, we can Taylor expand $\sin(x - x_0) \approx \xi - \xi^3/6 + \dots$. To leading order in ξ, we're back to where we started with (VI.1.2). This is *linear theory*: identify an equilibrium, perturb the system about that equilibrium, and drop all terms nonlinear in the perturbation amplitude.

Note that we are not solving an initial value problems. We are agnostic about the initial conditions and only ask whether some disturbance will ultimately grow or decay. In some situations (most notably, Landau damping), solving the initial value problem is absolutely essential to obtain the full solution and all the physics involved. But if you just want to calculate the wave-like response of a system to infinitesimally small perturbations and learn whether such a response grows or decays, you need only adopt solutions $\sim \exp(-\mathrm{i}\omega t)$, find the dispersion relation for ω vs $\boldsymbol{k}$, and examine the sign of its imaginary part. (The difference is related to a Laplace vs a Fourier transform in time.)

VI.2. Linearized MHD equations

Take (II.3.36) and write

$$\rho = \rho_0(\boldsymbol{r}) + \delta\rho(t,\boldsymbol{r}), \quad \boldsymbol{u} = \delta\boldsymbol{u}(t,\boldsymbol{r}), \quad P = P_0(\boldsymbol{r}) + \delta P(t,\boldsymbol{r}), \quad \boldsymbol{B} = \boldsymbol{B}_0(\boldsymbol{r}) + \delta\boldsymbol{B}(t,\boldsymbol{r});$$

i.e., consider a stratified, stationary equilibrium state threaded by a magnetic field and subject it to perturbations. Never mind how the equilibrium is set up – it is what it is, and we'll perturb it. Neglecting all terms quadratic in δ, equations (II.3.36) become

$$\frac{\partial \delta\rho}{\partial t} = -(\delta\boldsymbol{u}\cdot\boldsymbol{\nabla})\rho_0 - \rho_0(\boldsymbol{\nabla}\cdot\delta\boldsymbol{u}), \tag{VI.2.1}$$

$$\frac{\partial \delta\boldsymbol{u}}{\partial t} = -\frac{1}{\rho_0}\boldsymbol{\nabla}\left(\delta P + \frac{\boldsymbol{B}_0\cdot\delta\boldsymbol{B}}{4\pi}\right) + \frac{\delta\rho}{\rho_0^2}\boldsymbol{\nabla}\left(P_0 + \frac{B_0^2}{8\pi}\right) + \frac{(\boldsymbol{B}_0\cdot\boldsymbol{\nabla})\delta\boldsymbol{B}}{4\pi\rho_0} + \frac{(\delta\boldsymbol{B}\cdot\boldsymbol{\nabla})\boldsymbol{B}_0}{4\pi\rho_0} - \frac{\delta\rho}{\rho_0^2}\frac{(\boldsymbol{B}_0\cdot\boldsymbol{\nabla})\boldsymbol{B}_0}{4\pi} - \boldsymbol{\nabla}\delta\varPhi, \tag{VI.2.2}$$

$$\frac{\partial \delta\boldsymbol{B}}{\partial t} = -(\delta\boldsymbol{u}\cdot\boldsymbol{\nabla})\boldsymbol{B}_0 + (\boldsymbol{B}_0\cdot\boldsymbol{\nabla})\delta\boldsymbol{u} - \boldsymbol{B}_0(\boldsymbol{\nabla}\cdot\delta\boldsymbol{u}), \tag{VI.2.3}$$

$$\frac{\partial}{\partial t}\left(\frac{\delta P}{P_0} - \gamma\frac{\delta\rho}{\rho_0}\right) = -\delta\boldsymbol{u}\cdot\boldsymbol{\nabla}\ln\frac{P_0}{\rho_0^\gamma}. \tag{VI.2.4}$$

(Again, a quick way of getting these is to think of δ as a difference operator that commutes with partial differentiation.) If the equilibrium state satisfies

$$0 = -\boldsymbol{\nabla}\left(P_0 + \frac{B_0^2}{8\pi}\right) + \frac{(\boldsymbol{B}_0\cdot\boldsymbol{\nabla})\boldsymbol{B}_0}{4\pi} - \rho_0\boldsymbol{\nabla}\varPhi_0,$$

then the linearized momentum equation (VI.2.2) reduces to

$$\frac{\partial \delta\boldsymbol{u}}{\partial t} = -\frac{1}{\rho_0}\boldsymbol{\nabla}\left(\delta P + \frac{\boldsymbol{B}_0\cdot\delta\boldsymbol{B}}{4\pi}\right) - \frac{\delta\rho}{\rho_0}\boldsymbol{\nabla}\varPhi_0 + \frac{(\boldsymbol{B}_0\cdot\boldsymbol{\nabla})\delta\boldsymbol{B}}{4\pi\rho_0} + \frac{(\delta\boldsymbol{B}\cdot\boldsymbol{\nabla})\boldsymbol{B}_0}{4\pi\rho_0} - \boldsymbol{\nabla}\delta\varPhi. \tag{VI.2.5}$$

Pretty much every gradient of an equilibrium quantity here will give an instability (otherwise, you just get back simple linear waves on a homogeneous background). So let's not analyze this all at once. But I write this system of equations here for two important reasons: (i) it makes clear that we can adopt solutions $\delta \sim \exp(-\mathrm{i}\omega t)$ for the perturbations, since the equations are linear in the fluctuation amplitudes and the background is time-independent; (ii) we can only adopt full plane-wave solutions

$\delta \sim \exp(-\mathrm{i}\omega t + \mathrm{i}\boldsymbol{k}\cdot\boldsymbol{r})$ if the fluctuations vary on length scales much smaller than that over which the background varies (the so-called WKB approximation). Otherwise, we have to worry about the exact structure of the background gradients and their boundary conditions. In some cases, we'll do just that. So these are the themes of most linear stability analyses: a WKB approximation whereby plane-wave solutions are assumed on top of a background state that is slowly varying, and a focus only on whether fluctuations grow or decay rather than their specific spatio-temporal evolution from a set of initial conditions.

Now to calculate something... I'll start with two simple instabilities, the first of which (Jeans instability) will be analyzed using Eulerian perturbation theory, and the second of which (Kelvin–Helmholtz instability) will be analyzed using Lagrangian perturbation theory. Hopefully you'll see why one approach is sometimes easier than the other.

VI.3. Self-gravity: Jeans instability

One of the simplest hydrodynamical waves is a small-amplitude sound wave propagating on an infinite, homogeneous background. Take (II.3.36), set $\boldsymbol{B}_0 = 0$, and assume ρ_0 and P_0 to be constant. The resulting linearized equations are

$$\frac{\partial}{\partial t}\frac{\delta\rho}{\rho_0} = -\boldsymbol{\nabla}\cdot\delta\boldsymbol{u}, \quad \frac{\partial\delta\boldsymbol{u}}{\partial t} = -\frac{1}{\rho_0}\boldsymbol{\nabla}\delta P - \boldsymbol{\nabla}\delta\varPhi, \quad \frac{\partial}{\partial t}\left(\frac{\delta P}{P_0} - \gamma\frac{\delta\rho}{\rho_0}\right) = 0. \tag{VI.3.1a}$$

I've retained the perturbed gravitational potential $\delta\varPhi$ in the second equation, because we're going to assume that the fluid is self-gravitating with a potential that obey's Poisson's equation:[7]

$$\nabla^2\delta\varPhi = 4\pi G\delta\rho. \tag{VI.3.1b}$$

These equations are linear in δ, and so we may adopt plane-wave solutions, $\delta \sim \exp(-\mathrm{i}\omega t + \mathrm{i}\boldsymbol{k}\cdot\boldsymbol{r})$. Substituting this form into (VI.3.1) gives

$$-\mathrm{i}\omega\frac{\delta\rho}{\rho_0} = -\mathrm{i}\boldsymbol{k}\cdot\delta\boldsymbol{u}, \quad -\mathrm{i}\omega\delta\boldsymbol{u} = -\mathrm{i}\boldsymbol{k}\frac{\delta P}{\rho_0} - \mathrm{i}\boldsymbol{k}\delta\varPhi, \quad -\mathrm{i}\omega\left(\frac{\delta P}{P_0} - \gamma\frac{\delta\rho}{\rho_0}\right) = 0, \tag{VI.3.2a}$$

$$-k^2\delta\varPhi = 4\pi G\delta\rho. \tag{VI.3.2b}$$

Taking $\boldsymbol{k}\,\boldsymbol{\cdot}$ the second equation and using the other three yields the dispersion relation

$$\omega\big(\omega^2 - k^2c_\mathrm{s}^2 + 4\pi G\rho_0\big) = 0, \tag{VI.3.3}$$

where $c_\mathrm{s}^2 \doteq \gamma P_0/\rho_0$. The $\omega = 0$ root comes from the perturbed entropy equation, and corresponds to a isentropic relabelling of the fluid elements; its name is the 'entropy mode'. The other two roots correspond to forward- and backward-propagating sound waves under the influence of their own self-gravity:

$$\omega = \pm ka\sqrt{1 - \frac{4\pi G\rho_0}{k^2a^2}} \tag{VI.3.4}$$

Self-gravity reduces the speed of the wave for wavenumbers satisfying $kc_\mathrm{s} > (4\pi G\rho_0)^{1/2}$, for which the (expansive) pressure force is greater than the (attractive) gravitational force. At $kc_\mathrm{s} = (4\pi G\rho_0)^{1/2}$, these two forces balance exactly, and the mode is neutrally

[7]Wouldn't an infinite, homogeneous, self-gravitating fluid collapse under its own weight? Indeed it would. Ignoring this inconvenience is known as the *Jeans swindle*. Following Binney & Tremaine (1987): 'it is a swindle because in general there is no formal justification for discarding the unperturbed gravitational field'.

stable. But for $kc_{\rm s} < (4\pi G\rho_0)^{1/2}$, the wavelength is long enough to include a sufficiently large amount of mass in the perturbation to overwhelm the pressure force. Instability ensues, and the mode grows without propagating. This is the *Jeans instability*, named after Sir James Jeans (although Sir Isaac Newton understood the concept over 200 years before the calculation). The critical wavelength

$$\lambda_{\rm J} = c_{\rm s}\sqrt{\frac{\pi}{G\rho_0}} \tag{VI.3.5}$$

is referred to as the *Jeans length.*

Some astrophysics propaganda: For an isothermal ($\gamma = 1$) molecular cloud of temperature 10 K, number density 200 cm^{-3}, and mean mass per particle $2.33m_{\rm p}$, the Jeans length is $\simeq$1.5 pc. The corresponding *Jeans mass* enclosed within a spherical volume with $\lambda_{\rm J}$ as its diameter is

$$M_{\rm J} = \frac{\pi}{6}\rho_0\lambda_{\rm J}^3 = 20.3\left(\frac{T_0}{10~{\rm K}}\right)^{3/2}\left(\frac{n}{200~{\rm cm}^{-3}}\right)^{-1/2}~{\rm M}_\odot. \tag{VI.3.6}$$

Giant molecular clouds with these parameters have typical masses $\gtrsim$$10^4$ M$_\odot$, indicating that more must be going on than just thermal pressure support against self-gravity (see: magnetic fields and turbulence). Note that $M_{\rm J} = M_\odot$ at a density $n \simeq 8.2\times10^4$ cm^{-3}.

VI.4. Shear: Kelvin–Helmholtz instability

Consider two uniform fluids separated by a discontinuous interface at $z = 0$, as in the figure below:

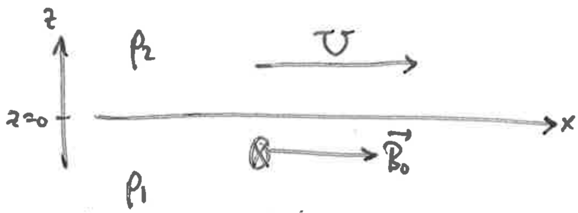

The fluid above the interface ($z > 0$) has density ρ_2 and equilibrium velocity $\boldsymbol{u}_0 = U\hat{\boldsymbol{x}}$. The fluid below the interface ($z < 0$) has density ρ_1 and is stationary. (We can always transform to a frame in which this fluid is stationary, so why not take advantage of that?) There is a uniform magnetic field $\boldsymbol{B}_0 = B_{0x}\hat{\boldsymbol{x}} + B_{0y}\hat{\boldsymbol{y}}$ oriented parallel to the interface that permeates all of the fluid, which we take to be perfectly conducting. For simplicity, take the fluid to be incompressible, *viz.* $\boldsymbol{\nabla}\cdot\boldsymbol{u} = 0$.

We seek the dispersion relation governing small-amplitude perturbations. It turns out that this problem is most easily analyzed using Lagrangian perturbations rather than Eulerian perturbations – the reason being that the interface and the interfacial pressure between the two fluids must remain continuous as the fluid is perturbed, and it's easier to measure this interface in the frame of the fluid element than in the lab frame.

Take the momentum equation in each of the fluids, above and below, and apply the difference operator $\varDelta \doteq \delta + \boldsymbol{\xi}\cdot\boldsymbol{\nabla}$ while recalling that $[\varDelta, {\rm D}/{\rm D}t] = 0$ and $\varDelta\boldsymbol{u} = {\rm D}\boldsymbol{\xi}/{\rm D}t$:

$$\varDelta\left[\rho\frac{{\rm D}\boldsymbol{u}}{{\rm D}t} = -\boldsymbol{\nabla}\left(P + \frac{B^2}{8\pi}\right) + \frac{\boldsymbol{B}\cdot\boldsymbol{\nabla}\boldsymbol{B}}{4\pi}\right]$$
$$\Longrightarrow\quad \rho\frac{{\rm D}^2\boldsymbol{\xi}}{{\rm D}t^2} = -\boldsymbol{\nabla}\delta\left(P + \frac{B^2}{8\pi}\right) + \frac{\boldsymbol{B}_0\cdot\boldsymbol{\nabla}\delta\boldsymbol{B}}{4\pi}, \tag{VI.4.1}$$

the form of the right-hand side following because $\boldsymbol{\nabla} B_0 = \boldsymbol{\nabla} P_0 = 0$. Use the linearized induction equation (V.2.9) with $\boldsymbol{\nabla} B_0 = 0$, which reads $\delta \boldsymbol{B} = (\boldsymbol{B}_0 \boldsymbol{\cdot} \boldsymbol{\nabla})\boldsymbol{\xi}$, and rearrange to obtain

$$\left[\frac{\mathrm{D}^2}{\mathrm{D}t^2} - \frac{(\boldsymbol{B}_0 \boldsymbol{\cdot} \boldsymbol{\nabla})^2}{4\pi\rho}\right]\boldsymbol{\xi} = -\frac{1}{\rho}\boldsymbol{\nabla}\delta\left(P + \frac{B^2}{8\pi}\right) \doteq -\frac{1}{\rho}\boldsymbol{\nabla}\delta\varPi. \tag{VI.4.2}$$

Note that taking the divergence of this equation and using $\boldsymbol{\nabla}\boldsymbol{\cdot}\boldsymbol{\xi} = 0$ (incompressibility) implies that the total perturbed pressure $\varPi$ satisfies

$$\nabla^2 \delta\varPi = 0. \tag{VI.4.3}$$

With the x and y directions being infinite in extent and the background state possessing no structure in those directions, we may write $\delta\varPi = \delta\varPi(z)\exp(\mathrm{i}k_x x + \mathrm{i}k_y y)$ to find

$$\left(-k^2 + \frac{\mathrm{d}^2}{\mathrm{d}z^2}\right)\delta\varPi(z) = 0 \quad \Longrightarrow \quad \delta\varPi(z) \propto \exp(-|kz|), \quad k \equiv \sqrt{k_x^2 + k_y^2}. \tag{VI.4.4}$$

The absolute value in the argument of the exponential indicates that the perturbation must die off as $z \to \pm\infty$. We may now adopt solutions of the form $\exp(-\mathrm{i}\omega t)$ and evaluate the z component of (VI.4.2) above and below the interface:

$$\left[(-\mathrm{i}\omega + \mathrm{i}k_x U)^2 + \frac{(\boldsymbol{k}\boldsymbol{\cdot}\boldsymbol{B}_0)^2}{4\pi\rho_2}\right]\xi_{z2} = +\frac{1}{\rho_2}|k|\delta\varPi_2, \tag{VI.4.5a}$$

$$\left[(-\mathrm{i}\omega \qquad\quad)^2 + \frac{(\boldsymbol{k}\boldsymbol{\cdot}\boldsymbol{B}_0)^2}{4\pi\rho_1}\right]\xi_{z1} = -\frac{1}{\rho_1}|k|\delta\varPi_1, \tag{VI.4.5b}$$

respectively. At the interface, $\xi_{z1} = \xi_{z2}$ and $\Delta\varPi_1 = \Delta\varPi_2$, i.e., the two fluids must move together at the interface and their pressures must hold continuous as they are perturbed. Because $\boldsymbol{\nabla} B_0 = \boldsymbol{\nabla} P_0 = 0$, the latter implies $\delta\varPi_1 = \delta\varPi_2$. Using this information to match (VI.4.5a) and (VI.4.5b) leads to

$$(\omega - k_x U)^2 \rho_2 + \omega^2 \rho_1 = \frac{(\boldsymbol{k}\boldsymbol{\cdot}\boldsymbol{B}_0)^2}{2\pi} \tag{VI.4.6}$$

$$\Longrightarrow \quad \boxed{\omega = \frac{k_x U}{2}\frac{\overline{\rho}}{\rho_1}\left\{1 \pm \mathrm{i}\sqrt{\frac{\rho_1}{\rho_2}\left[1 - \frac{(\boldsymbol{k}\boldsymbol{\cdot}\boldsymbol{B}_0)^2}{\pi\overline{\rho}k_x^2 U^2}\right]}\right\}} \tag{VI.4.7}$$

where $\overline{\rho} \doteq 2\rho_1\rho_2/(\rho_1 + \rho_2)$ is the reduced mass density. For

$$\frac{(\boldsymbol{k}\boldsymbol{\cdot}\boldsymbol{B}_0)^2}{4\pi\overline{\rho}} < \left(\frac{k_x U}{2}\right)^2, \tag{VI.4.8}$$

the discriminant is positive and there is a growing (and propagating) mode whose growth rate is proportional to the wavenumber and the velocity shear across the interface. Note that, for $\rho_1 = \rho_2 = \rho$, we have $\overline{\rho} = \rho$, and then (VI.4.7) becomes

$$\omega = \frac{k_x U}{2}\left[1 \pm \mathrm{i}\sqrt{1 - \frac{(\boldsymbol{k}\boldsymbol{\cdot}\boldsymbol{B}_0)^2}{\pi\rho k_x^2 U^2}}\right];$$

for $U = 0$, this returns a stably propagating shear Alfvén wave, $\omega = \mp(\boldsymbol{k}\boldsymbol{\cdot}\boldsymbol{v}_\mathrm{A})$. This indicates that it is the tension in the magnetic-field lines that is responsible for stabilizing the instability. That being said, if the magnetic field is oriented such that $B_{0x} = 0$, then (VI.4.8) can always be satisfied for small enough $|k_y/k_x|$, no matter how strong is B_{0y}.

The physics is as follows. An upwardly displaced distortion of the interface into region 2 causes a constriction of the velocity there, and the fluid must move faster to conserve its mass. But when it moves faster, the pressure must drop (Bernoulli!). The opposite happens below the interface. Now there is a pressure gradient pushing upwards, reinforcing the displacement, and the process runs away (unless the magnetic tension can stabilize the displacements and propagate them away as Alfvén waves). That's why pressure perturbations were vital in (VI.4.2).

Question: Does this instability occur in a simple linear shear flow, e.g., $\boldsymbol{u}_0 = Sz\hat{\boldsymbol{x}}$? No! The proof goes as follows. Drop the magnetic field for simplicity. With $\boldsymbol{u}_0 = u_0(z)\hat{\boldsymbol{x}}$, one can show using $\boldsymbol{\nabla\cdot\xi} = 0$ and the momentum equation that

$$\frac{\mathrm{d}^2\xi_z}{\mathrm{d}z^2} - k_x^2\xi_z = \frac{ku_0''}{\omega - k_x u_0}\xi_z.$$

Multiply this by ξ_z^* (the '$*$' denotes the complex conjugate) and integrate between the upper and lower boundaries $z = \pm L$ to obtain

$$\int_{-L}^{L}\mathrm{d}z\left(\xi_z^*\xi_z'' - k_x^2|\xi_z|^2\right) = \int_{-L}^{L}\mathrm{d}z\,\frac{k_x u_0''}{\omega - k_x u_0}|\xi_z|^2.$$

The first term on the left-hand side may be simplified using integration by parts and assuming either periodicity or that ξ_z or ξ_z' vanish at the boundaries. Then

$$\int_{-L}^{L}\mathrm{d}z\left(-|\xi_z'|^2 - k_x^2|\xi_z|^2\right) = \int_{-L}^{L}\mathrm{d}z\,\frac{k_x u_0''}{\omega - k_x u_0}|\xi_z|^2,$$

If the system is unstable, then ω must have an imaginary part, ω_I. Writing $\omega = \omega_\mathrm{R} + \mathrm{i}\omega_\mathrm{I}$, the imaginary part of the above equation is simply

$$\omega_\mathrm{I}\int_{-L}^{L}\mathrm{d}z\,\frac{k_x u_0''}{|\omega - k_x u_0|^2}|\xi_z|^2 = 0.$$

This states that u_0'' must be positive over part of the integration range, and negative over the remainder, i.e., u_0'' must pass through zero. Thus, instability requires an *inflection point* (Rayleigh 1880). (Note that the converse is not true: a velocity profile *with* an inflection point is not necessarily unstable.)

VI.5. Buoyancy: Rayleigh–Taylor instability

Using Lagrangian perturbation theory, it is easy to generalize the calculation in the previous section (§VI.4) to include gravity. Again, let the fluid above the interface ($z > 0$) have uniform density ρ_2, and the fluid below the interface ($z < 0$) have uniform density ρ_1. Include the same uniform background magnetic field as before, $\boldsymbol{B}_0 = B_{0x}\hat{\boldsymbol{x}} + B_{0y}\hat{\boldsymbol{y}}$. But now place these fluids in a constant gravitational field $\boldsymbol{g} = -g\hat{\boldsymbol{z}}$, with the gas pressure either side of the interface satisfying hydrostatic equilibrium in the vertical direction:

$$g = -\frac{1}{\rho_1}\frac{\mathrm{d}P_1}{\mathrm{d}z} = -\frac{1}{\rho_2}\frac{\mathrm{d}P_2}{\mathrm{d}z}.$$

The entire calculation goes through as before, but with the following additions and modifications. First, we must include the perturbed gravitational force in the momentum equation (VI.4.1), *viz.* $\varDelta(\rho\boldsymbol{g}) = -(\varDelta\rho)g\hat{\boldsymbol{z}}$. Secondly, because of the background pressure gradient in each of the fluids, we no longer have that $\varDelta(\boldsymbol{\nabla}P) = \boldsymbol{\nabla}\delta P$, but rather that $\varDelta(\boldsymbol{\nabla}P) = \boldsymbol{\nabla}\delta P + \boldsymbol{\xi\cdot\nabla}(\boldsymbol{\nabla}P)$. Using hydrostatic equilibrium, this may equivalently be written as $\Delta(\boldsymbol{\nabla}P) = \boldsymbol{\nabla}\delta P - \boldsymbol{\xi}\cdot\boldsymbol{\nabla}(\rho g\hat{\boldsymbol{z}})$. Making these two changes in (VI.4.1) leads to

$$\rho\frac{\mathrm{D}^2\boldsymbol{\xi}}{\mathrm{D}t^2} = -\boldsymbol{\nabla}\delta\left(P + \frac{B^2}{8\pi}\right) + \frac{\boldsymbol{B}_0\cdot\boldsymbol{\nabla}\delta\boldsymbol{B}}{4\pi} - (\Delta\rho)g\hat{\boldsymbol{z}} + \boldsymbol{\xi}\cdot\boldsymbol{\nabla}(\rho g\hat{\boldsymbol{z}}). \tag{VI.5.1}$$

Despite this extra work, however, those two additional terms cancel one another if the fluid is incompressible and the density is constant in each region, since then $\Delta\rho - \boldsymbol{\xi}\cdot\boldsymbol{\nabla}\rho = \delta\rho = 0$. As a result, the *only* difference between this calculation and the Kelvin–Helmholtz calculation in §VI.4 is that the imposition of pressure continuity at the perturbed interface does not imply that $\delta\Pi_1 = \delta\Pi_2$, but rather

$$\Delta\Pi_1 = \Delta\Pi_2 \implies \delta\Pi_1 - \xi_{z1}\rho_1 g = \delta\Pi_2 - \xi_{z2}\rho_2 g \implies \delta\Pi_2 - \delta\Pi_1 = \xi_z(\rho_2 - \rho_1)g.$$

We may then use this in (VI.4.5) to jump straight to the dispersion relation (cf. (VI.4.6))

$$(\omega - k_x U)^2\rho_2 + \omega^2\rho_1 = \frac{(\boldsymbol{k}\cdot\boldsymbol{B}_0)^2}{2\pi} + |k|g(\rho_1 - \rho_2), \tag{VI.5.2}$$

whose solutions are (cf. (VI.4.7))

$$\omega = \frac{k_x U}{2}\frac{\bar{\rho}}{\rho_1}\left\{1 \pm \mathrm{i}\sqrt{\frac{\rho_1}{\rho_2}\left[1 + \frac{2|k|g}{k_x^2U^2}\frac{\rho_2-\rho_1}{\bar{\rho}} - \frac{(\boldsymbol{k}\cdot\boldsymbol{B}_0)^2}{\pi\bar{\rho}k_x^2U^2}\right]}\right\}. \tag{VI.5.3}$$

By design, this has both Kelvin–Helmholtz and Rayleigh–Taylor in it; let's set $U = 0$ to eliminate the former, in which case

$$\boxed{\omega = \pm\mathrm{i}\sqrt{|k|g\frac{\rho_2-\rho_1}{\rho_1+\rho_2} - \frac{(\boldsymbol{k}\cdot\boldsymbol{B}_0)^2}{2\pi(\rho_1+\rho_2)}}} \tag{VI.5.4}$$

This equation states that linear instability requires $\rho_2 > \rho_1$ (heavy on top, light on the bottom), with the difference between the densities being large enough for the destabilizing pressure gradient (Bernoulli!) to overcome the stabilizing magnetic tension. Note that, if $\boldsymbol{B}_0$ is not oriented along the interface, no amount of magnetic field can stabilize the system.

Usually a physical explanation of the Rayleigh–Taylor instability isn't provided in derivations of its linear theory; indeed, the fact that heavy stuff falls down if given the opportunity to do so is fairly obvious. But it's worth thinking about the physics a little harder, and connecting this intuition back to the math. Let's return to (VI.5.1) with $U = 0$ and $\boldsymbol{B} = 0$ in order to isolate the Rayleigh–Taylor physics, and take curl of this equation:

$$\boldsymbol{\nabla}\times\left(\rho\frac{\mathrm{D}^2\boldsymbol{\xi}}{\mathrm{D}t^2}\right) = 0.$$

Chain-ruling the curl, dividing through by ρ, and using (VI.5.1) to eliminate $\mathrm{D}^2\boldsymbol{\xi}/\mathrm{D}t^2$ yields

$$\frac{\mathrm{D}^2}{\mathrm{D}t^2}\boldsymbol{\nabla}\times\boldsymbol{\xi} = \frac{1}{\rho^2}\boldsymbol{\nabla}\rho\times\boldsymbol{\nabla}\delta P.$$

If you read §II.2.5, you'll recognize this as an equation for the vorticity, which is being baroclinically forced by the misalignment between the background density gradient and the *perturbed* pressure gradient. Because of the rippled interface, this perturbed pressure gradient has a component in the x direction, which points from regions where $\xi_z > 0$ towards regions where $\xi_z < 0$. With $\boldsymbol{\nabla}\rho$ pointing upwards (in the unstable situation), the baroclinic forcing is pointing in just the right direction to accentuate the vorticity in the original perturbation. See the figure below.

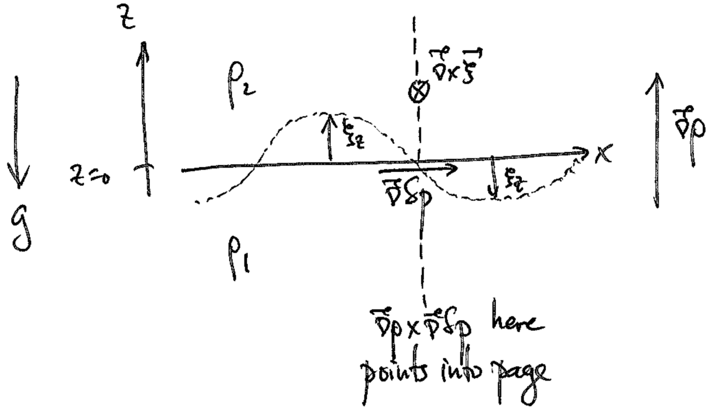

VI.6. Buoyancy: Convective (Schwarzschild) instability

Next up: stratification. Henceforth, ignore self-gravity. Suppose our plasma is immersed in a constant, externally imposed gravitational field $\boldsymbol{g} = -g\hat{\boldsymbol{z}}$ and that its thermal-pressure gradient balances the gravitational acceleration to produce a stationary, equilibrium state. Ignoring for the moment magnetic fields, this hydrostatic equilibrium is described by the equation

$$\frac{1}{\rho_0}\frac{\mathrm{d}P_0}{\mathrm{d}z} = g = \text{const}, \tag{VI.6.1}$$

where $\rho_0 = \rho_0(z)$. The hydrodynamic equations linearized about this equilibrium are

$$\frac{\partial}{\partial t}\frac{\delta\rho}{\rho_0} + \boldsymbol{\nabla\cdot}\delta\boldsymbol{u} + \delta u_z\frac{\mathrm{d}\ln\rho_0}{\mathrm{d}z} = 0, \tag{VI.6.2}$$

$$\frac{\partial\delta\boldsymbol{u}}{\partial t} = -\frac{1}{\rho_0}\boldsymbol{\nabla}\delta P - \frac{\delta\rho}{\rho_0}g\hat{\boldsymbol{z}}, \tag{VI.6.3}$$

$$\frac{\partial}{\partial t}\left(\frac{\delta P}{P_0} - \gamma\frac{\delta\rho}{\rho_0}\right) + \delta u_z\frac{\mathrm{d}}{\mathrm{d}z}\ln\frac{P_0}{\rho_0^\gamma} = 0. \tag{VI.6.4}$$

Solutions to this set of equations are $\propto \exp(-\mathrm{i}\omega t)$:

$$-\mathrm{i}\omega\frac{\delta\rho}{\rho_0} + \boldsymbol{\nabla\cdot}\delta\boldsymbol{u} + \delta u_z\frac{\mathrm{d}\ln\rho_0}{\mathrm{d}z} = 0, \tag{VI.6.5}$$

$$-\mathrm{i}\omega\delta\boldsymbol{u} = -\frac{1}{\rho_0}\boldsymbol{\nabla}\delta P - \frac{\delta\rho}{\rho_0}g\hat{\boldsymbol{z}}, \tag{VI.6.6}$$

$$-\mathrm{i}\omega\left(\frac{\delta P}{P_0} - \gamma\frac{\delta\rho}{\rho_0}\right) + \delta u_z\frac{\mathrm{d}}{\mathrm{d}z}\ln\frac{P_0}{\rho_0^\gamma} = 0. \tag{VI.6.7}$$

Continued on hand-written notes…

In general, we cannot Fourier transform these eqns. in z, because the coefficients in front of the perturbed quantities are z-dependent. But we can do so in the horizontal (say, x) direction:

$$-i\omega \frac{\delta\rho}{\rho_0} + ik_x \delta u_x + \frac{d\,\delta u_z}{dz} + \delta u_z \frac{d\ln\rho_0}{dz} = 0,$$

$$-i\omega \delta u_x = -ik_x \frac{\delta p}{\rho_0},$$

$$-i\omega \delta u_z = -\frac{1}{\rho_0}\frac{d\,\delta p}{dz} - \frac{\delta\rho}{\rho_0} g,$$

$$-i\omega \left(\frac{\delta p}{p_0} - \gamma \frac{\delta\rho}{\rho_0} \right) + \delta u_z \frac{d\ln p_0\rho_0^{-\gamma}}{dz} = 0,$$

where now the fluctuations are z-dependent Fourier amplitudes. Denoting $\vec{\delta u} = -i\omega\vec{\xi}$, and dropping the equilibrium "0" subscripts for notational ease, we have

(A) $$\frac{\delta\rho}{\rho} + ik_x\xi_x + \xi_z' + \xi_z \frac{d\ln\rho}{dz} = 0,$$

(B) $$-\omega^2 \xi_x = -ik_x \frac{\delta p}{\rho},$$

(C) $$-\omega^2 \xi_z = -\frac{1}{\rho}\frac{d}{dz}\delta p - \frac{\delta\rho}{\rho} g,$$

(D) $$\frac{\delta p}{p} = \gamma\frac{\delta\rho}{\rho} - \xi_z \frac{d\ln p\rho^{-\gamma}}{dz}.$$

(B) and (D) $\Rightarrow$ $-\omega^2 \xi_x = -ik_x \frac{P}{\rho}\left[\gamma \frac{\delta\rho}{\rho} - \xi_z \frac{d\ln P\rho^{-\gamma}}{dz}\right]$

and (A) $\Rightarrow$ $$-\omega^2 \xi_x = +ik_x \frac{P}{\rho}\gamma\left[+ik_x\xi_x + \xi_z' + \xi_z \frac{d\ln\rho}{dz}\right] + ik_x\frac{P}{\rho}\xi_z\frac{d\ln P\rho^{-\gamma}}{dz}$$

$\Rightarrow (-\omega^2 + k_x^2 a^2)\xi_x = ik_x a^2 \xi_z' + \frac{ik_x a^2}{\gamma}\frac{d\ln P}{dz}\xi_z$,

where $a^2 \equiv \gamma P/\rho$. Note: $g = -\frac{a^2}{\gamma}\frac{d\ln P}{dz}$, so this is

$$\boxed{(-\omega^2 + k_x^2 a^2)\xi_x = ik_x a^2 \xi_z' - ik_x \xi_z g}$$

(A) $\Rightarrow$ $$\frac{\delta\rho}{\rho} = -\xi_z' - \xi_z\frac{d\ln\rho}{dz} - \frac{ik_x\left[ik_x a^2\xi_z' - ik_x\xi_z g\right]}{-\omega^2 + k_x^2 a^2}$$

$\Rightarrow$ $$\boxed{\frac{\delta\rho}{\rho} = \frac{\omega^2\xi_z' + \left[(\omega^2 - k_x^2 a^2)\frac{d\ln\rho}{dz} - k_x^2 g\right]\xi_z}{k_x^2 a^2 - \omega^2}}$$ (a)

$\Rightarrow$ $$\frac{\delta P}{P} = \frac{1}{k_x^2 a^2 - \omega^2}\left[\gamma\omega^2\xi_z' + \gamma\left((\omega^2 - k_x^2 a^2)\frac{d\ln\rho}{dz} - k_x^2 g\right)\xi_z + (\omega^2 - k_x^2 a^2)\frac{d\ln P\rho^{-\gamma}}{dz}\xi_z\right]$$

$$= \frac{1}{k_x^2 a^2 - \omega^2}\left[\gamma\omega^2\xi_z' + \omega^2\frac{d\ln P}{dz}\xi_z\right]$$

$$= \frac{\omega^2}{k_x^2 a^2 - \omega^2}\left[\gamma\xi_z' + \frac{d\ln P}{dz}\xi_z\right]$$ (★)

into (c):

$$+\omega^2 \xi_z = +g\left[\frac{\omega^2 \xi_z' + (\omega^2 - k_x^2 a^2)\frac{d\ln p}{dz}\xi_z - k_x^2 g \xi_z}{k_x^2 a^2 - \omega^2}\right]$$

$$+ \frac{1}{\rho}\frac{d}{dz}\left[\frac{\omega^2 p}{k_x^2 a^2 - \omega^2}\left(\xi_z' \gamma + \xi_z \frac{d\ln p}{dz}\right)\right]$$

$$= \frac{\frac{\omega^2}{\rho}\frac{dp}{dz}\left(\xi_z'\gamma + \xi_z \frac{d\ln p}{dz}\right)}{k_x^2 a^2 - \omega^2} + \frac{p}{\rho}\frac{\omega^2}{k_x^2 a^2 - \omega^2}\left(\gamma \xi_z'' + \xi_z' \frac{d\ln p}{dz} + \xi_z \frac{d^2 \ln p}{dz^2}\right)$$

$$- \frac{\omega^2 p}{\rho}\frac{k_x^2}{(k_x^2 a^2 - \omega^2)^2}\frac{da^2}{dz}\left(\xi_z'\gamma + \xi_z \frac{d\ln p}{dz}\right)$$

$$\Rightarrow \omega^2 \xi_z = \frac{g}{k_x^2 a^2 - \omega^2}\left[\omega^2 \xi_z' - k_x^2 g \xi_z + (\omega^2 - k_x^2 a^2)\frac{d\ln p}{dz}\xi_z\right]$$

$$+ \frac{\omega^2}{k_x^2 a^2 - \omega^2}(-g)\left[\xi_z'\gamma + \xi_z \frac{d\ln p}{dz}\right]$$

$$+ \left(\frac{a^2}{\gamma}\right)\frac{\omega^2}{k_x^2 a^2 - \omega^2}\left[\xi_z''\gamma + \xi_z' \frac{d\ln p}{dz} + \xi_z \frac{g\gamma}{a^2}\frac{d\ln T}{dz}\right]$$

$$- \frac{\omega^2}{\gamma}\frac{a^2 k_x^2 a^2}{(k_x^2 a^2 - \omega^2)^2}\frac{d\ln T}{dz}\left[\xi_z'\gamma + \xi_z \frac{d\ln p}{dz}\right]$$

Multiply by $\frac{k_x^2 a^2 - \omega^2}{\omega^2 a^2}$ and group:

ξ_z'': 1.

$$\xi_z' : \cancel{\frac{g}{a^2}} - \frac{g\gamma}{a^2} + \cancel{\frac{1}{\gamma}\frac{d\ln p}{dz}} - \frac{k_x^2 a^2}{\cancel{\gamma}}\frac{1}{(k_x^2a^2-\omega^2)}\frac{d\ln T}{dz}\cancel{\gamma}$$

$$= \frac{d\ln p}{dz} - \left(\frac{k_x^2a^2}{k_x^2a^2-\omega^2}\right)\frac{d\ln T}{dz} = \frac{d\ln p/dz}{k_x^2a^2-\omega^2}\left[k_x^2a^2-\omega^2 - k_x^2a^2\frac{d\ln T}{d\ln p}\right]$$

$$= \frac{d\ln p/dz}{k_x^2a^2-\omega^2}\left[-\omega^2 + k_x^2a^2\frac{d\ln p}{d\ln p}\right] = \frac{\omega^2\frac{d\ln p}{dz} - k_x^2a^2\frac{d\ln p}{dz}}{\omega^2-k_x^2a^2}$$

$$\xi_z : -\frac{(k_x^2a^2-\omega^2)}{a^2} - \frac{k_x^2g^2}{\omega^2a^2} - g\frac{d\ln p}{dz}\frac{k_x^2a^2\cancel{-\omega^2}}{\omega^2a^2}$$

$$-\cancel{\frac{g}{a^2}\frac{d\ln p}{dz}} + \cancel{\frac{a^2}{\gamma}\frac{1}{a^2}\frac{g\gamma}{a^2}\frac{d\ln T}{dz}} - \frac{k_x^2a^2}{\gamma(k_x^2a^2-\omega^2)}\frac{d\ln T}{dz}\frac{d\ln p}{dz}$$

$$= \frac{-1}{k_x^2a^2-\omega^2}\left[\frac{k_x^2a^2}{\gamma}\frac{d\ln T}{dz}\frac{d\ln p}{dz} + \frac{gk_x^2}{\omega^2}\frac{d\ln p}{dz}(k_x^2a^2-\omega^2) + \frac{k_x^2g^2}{a^2\omega^2}(k_x^2a^2-\omega^2) + \frac{(k_x^2a^2-\omega^2)^2}{a^2}\right]$$

$$= \frac{1}{\omega^2-k_x^2a^2}\left[\frac{\omega^4}{a^2} - 2\omega^2k_x^2 + k_x^4a^2 - \frac{k_x^2g^2}{a^2} - \cancel{gk_x^2\frac{d\ln p}{dz}} + \frac{k_x^2a^2}{\gamma}\frac{d\ln T}{dz}\frac{d\ln p}{dz} + \frac{gk_x^4a^2}{\omega^2}\frac{d\ln p}{dz} + \frac{k_x^4\cancel{a^2}g^2}{\cancel{a^2}\omega^2}\right]$$

$$-k_x^2 g\left(\frac{d\ln p}{dz} - \cancel{\frac{d\ln p}{dz}}\right)$$

So,

$$\boxed{\xi_z'' + \xi_z' \left[\frac{\omega^2 \frac{d\ln p}{dz} - k_x^2 a^2 \frac{d\ln \rho}{dz}}{\omega^2 - k_x^2 a^2} \right] + \xi_z \frac{1}{\omega^2 - k_x^2 a^2} \left[\frac{\omega^4}{a^2} - 2\omega^2 k_x^2 + k_x^4 a^2 - k_x^2 g \frac{d\ln p}{dz}\left(1 - \frac{1}{\gamma}\right) + g \frac{k_x^4 a^2}{\omega^2} \frac{d\ln \rho}{dz} + \frac{k_x^4 g^2}{\omega^2} \right] = 0.}$$

This is UGLY!!! And we can't solve it analytically anyhow. It's just a stratified fluid — why is it so complicated?! The reason is twofold: (1) this equation mixes up buoyancy and sound waves — distinct physical effects; and (2) the sound and buoyancy frequencies are functions of height. Let's fix this by adopting an <u>ordering</u>: let

$$\frac{d\xi_z}{dz} \sim i k_z \xi_z = i k_z H \left(\frac{\xi_z}{H}\right) \gg \frac{\xi_z}{H},$$

where $H \equiv \left|\frac{dz}{d\ln p}\right| \sim \left|\frac{dz}{d\ln \rho}\right|$. In other words, we assume that ξ_z varies on a scale $\ll$ the scale of the background. This is a WKB approach. So...

Let $\epsilon \equiv \frac{1}{k_z H} \ll 1$. Also, $k_x \sim k_z$. Now, we must make a decision about the size of ω, by comparing it with

$$\frac{a}{H} = \frac{\gamma g}{a} = \sqrt{\frac{\gamma g}{H}}.$$ There are two choices of interest:

(i) $\omega \sim a/H$

(ii) $\omega \sim ka \sim \underbrace{(a/H)}_{\epsilon} \gg \dfrac{a}{H}$.

First, write $\dfrac{d\xi_z}{dz} = i k_z \xi_z$ with $k_z H \equiv \dfrac{1}{\epsilon}$;  becomes

$$-k_z^2 \xi_z + i k_z \xi_z \left[\frac{\omega^2 \frac{d\ln p}{dz} - k_x^2 a^2 \frac{d\ln \rho}{dz}}{\omega^2 - k_x^2 a^2} \right]$$

$$+ \frac{\xi_z}{\omega^2 - k_x^2 a^2} \left[\frac{\omega^4}{a^2} - 2\omega^2 k_x^2 + k_x^4 a^2 - k_x^2 g \frac{d\ln p}{dz}\left(1 - \frac{1}{\gamma}\right) \right.$$

$$\left. + \frac{g k_x^4 a^2}{\omega^2} \frac{d\ln \rho}{dz} + \frac{k_x^4 g^2}{\omega^2} \right] = 0.$$

Now, (i) $\omega \sim a/H$ gives $k_x^2 a^2 \gg \omega^2$ and so the dominant terms are

$$-k_z^2 \xi_z + \xi_z(-k_x^2) - \xi_z \frac{g k_x^2}{\omega^2} \frac{d\ln \rho}{dz} - \xi_z \frac{k_x^2 g^2}{a^2 \omega^2} = 0$$

$$\Rightarrow \quad k^2 + \frac{g k_x^2}{\omega^2} \underbrace{\left[\frac{d\ln \rho}{dz} + \frac{g}{a^2} \right]}_{\frac{d\ln \rho}{dz} - \frac{1}{\gamma}\frac{d\ln p}{dz} = -\frac{1}{\gamma}\frac{d\ln p\rho^{-\gamma}}{dz}} = 0.$$

$$\Rightarrow \boxed{\begin{aligned}\omega^2 &= \frac{k_x^2}{k^2}\frac{g}{\gamma}\frac{d\ln p\rho^{-\gamma}}{dz} \\ &= -\frac{k_x^2}{k^2}\frac{1}{\gamma\rho}\frac{dp}{dz}\frac{d\ln p\rho^{-\gamma}}{dz} \equiv \frac{k_x^2}{k^2}N^2\end{aligned}}$$

where N^2 is the square of the Brunt – Väisälä frequency.
If $N^2>0$, these are called <u>internal waves</u> or <u>g-modes</u>.

Note that different wavenumbers have different velocities (i.e., dispersion) and that ω depends on the direction of $\vec{k}$: $\dfrac{\partial\omega}{\partial\vec{k}} = \dfrac{\omega}{k^2}\dfrac{k_z}{k_x}\left(k_z\hat{x}-k_x\hat{z}\right)$, so that $\vec{k}\cdot\dfrac{\partial\omega}{\partial\vec{k}}=0$.

We'll return to the physical cause of these waves later, after the "Boussinesq approximation" is introduced, but, for now, note that $N^2<0$ (i.e., upwardly decreasing entropy) gives instability. Go boil some water and think about it.

(ii) $\omega \sim ka \gg a/H$. This gives the following dominant terms:

$$-k_z^2 + \frac{1}{\omega^2-k_x^2a^2}\Big[\underbrace{\frac{\omega^4}{a^2} - 2\omega^2k_x^2 + k_x^4a^2}_{(\omega^2-k_x^2a^2)^2/a^2}\Big]=0$$

$$\Rightarrow \boxed{\omega^2 = (k_x^2+k_z^2)\,a^2}$$ <u>Sound waves!</u>

Now, sound waves are often a nuisance in many calculations. They mostly play a rather boring role, and often serve only to make the algebra more tedious. There is something called the <u>Boussinesq approximation</u>, which rigorously filters out sound waves. Let's see how this works in our convection problem...

Return to ⊛ with $\omega \sim \epsilon k a$:

$$\frac{\delta p}{p} \simeq \frac{\omega^2}{k_x^2 a^2} i k_z \xi_z \gamma \quad \text{if } k_z \neq 0;$$

$$\simeq \underbrace{\frac{\omega^2}{k_x^2 a^2}}_{\sim \epsilon^2 \ll 1} \frac{d\ln p}{dz} \xi_z \quad \text{otherwise.}$$

So, perhaps we should have dropped perturbations to the gas pressure at some point. Where? In the momentum equation? Hmm... careful. Consider (B) with $\frac{\delta p}{p} \simeq \frac{\omega^2}{k_x^2 a^2} i k_z \xi_z \gamma$

$\Rightarrow \xi_x = -\xi_z \frac{k_z}{k_x}$, or $\vec{k} \cdot \vec{\xi} = 0$. Looks like pressure fluctuations are enforcing (near) incompressibility. Best not to drop them! And (C)?

$$\underbrace{-\omega^2 \xi_z = -i k_z \frac{p}{\rho} \frac{\omega^2}{k_x^2 a^2}}_{\text{same order!}} i k_z \xi_z \gamma - \frac{\delta\rho}{\rho} g$$

Okay. So, pressure fluctuations are small, but not so small that they can be dropped from the momentum eqn. What about the entropy eqn?

(D) $\Longrightarrow$ $$\frac{\delta P}{P} = \gamma\frac{\delta\rho}{\rho} - \xi_z \frac{d\ln P\rho^{-\gamma}}{dz}$$

$\sim \frac{\xi_z}{H}\frac{\omega^2}{k_x^2 a^2}$ $\sim \frac{\xi_z}{H}$, required for internal waves

or $\sim i k_z \xi_z \gamma \frac{\omega^2}{k_x^2 a^2}$, either way... it's small. So, drop δP from entropy equation! What does that leave us with?

$$\gamma\frac{\delta\rho}{\rho} \simeq \xi_z \frac{d\ln P\rho^{-\gamma}}{dz}$$

$\Longrightarrow \frac{\delta\rho}{\rho} \sim \frac{\xi_z}{H}$. Ah! Look at (A): $\frac{\delta\rho}{\rho} + ik_z\xi_z + ik_x\xi_x + \xi_z\frac{d\ln\rho}{dz} = 0$

$\sim \frac{\xi_z}{H}$ $\sim k\xi_z$ $\sim \frac{\xi_z}{H}$

So, to leading order, we have $\vec{k}\cdot\vec{\xi} = 0$ — incompressibility! Okay, things are consistent, and we have the Boussinesq approx:

$$\frac{\delta P}{P} \sim \frac{1}{kH}\frac{\delta p}{p} \ll \frac{\delta\rho}{\rho} \sim \frac{\delta u}{a} \ll \frac{k\,\delta u}{\omega} \sim k\xi \sim (kH)\frac{\delta u}{a}.$$

Or, defining the Mach number $\mathcal{M}$ and taking it to be small ($\sim \epsilon$),

$$\frac{\delta u}{a} \sim \frac{\delta\rho}{\rho} \sim \frac{\delta T}{T} \sim \frac{1}{\mathcal{M}}\frac{\delta p}{p} \sim \frac{1}{kH} \sim \epsilon \ll 1.$$

In practice, this means:

1) Assume (near) incompressibility ($\vec{\nabla}\cdot\vec{\delta u} = 0$)

2) Drop δp everywhere EXCEPT the momentum eqn. They are enforcing (near) incompressibility.

3) Keep $\delta\rho$ everywhere EXCEPT the continuity eqn. They interact with gravity to give buoyancy.

Watch how much simpler this is...

Ⓐ $\longrightarrow \quad ik_x\xi_x + ik_z\xi_z = 0$

Ⓑ $\longrightarrow \quad -\omega^2\xi_x = -ik_x\frac{\delta p}{\rho}$

$$\longrightarrow \quad \frac{\delta p}{\rho} = \frac{i\omega^2 k_z}{k_x^2}\xi_z$$

Ⓒ $\longrightarrow \quad -\omega^2\xi_z = -ik_z\frac{\delta p}{\rho} - \frac{\delta\rho}{\rho}g$

$$\longrightarrow \quad \omega^2\xi_z = \frac{k_x^2}{k^2}g\frac{\delta\rho}{\rho}$$

Ⓓ $\longrightarrow \quad 0 = \gamma\frac{\delta\rho}{\rho} - \xi_z\frac{d\ln p\rho^{-\gamma}}{dz}$

$$\omega^2 = \frac{k_x^2}{k^2}N^2. \quad \text{Done!}$$

What we've done here is eliminated the restoring pressure forces that drive sound waves, essentially by assuming that a^2 is so large that sound waves propagate instantaneously. When the restoring force is purely external (e.g., gravity), the flow behaves as though it were incompressible (nearly). Physically, a slow-moving fluid element remains in pressure balance with its surroundings. This readjustment is what makes buoyancy waves and convection possible. Let us see that explicitly.

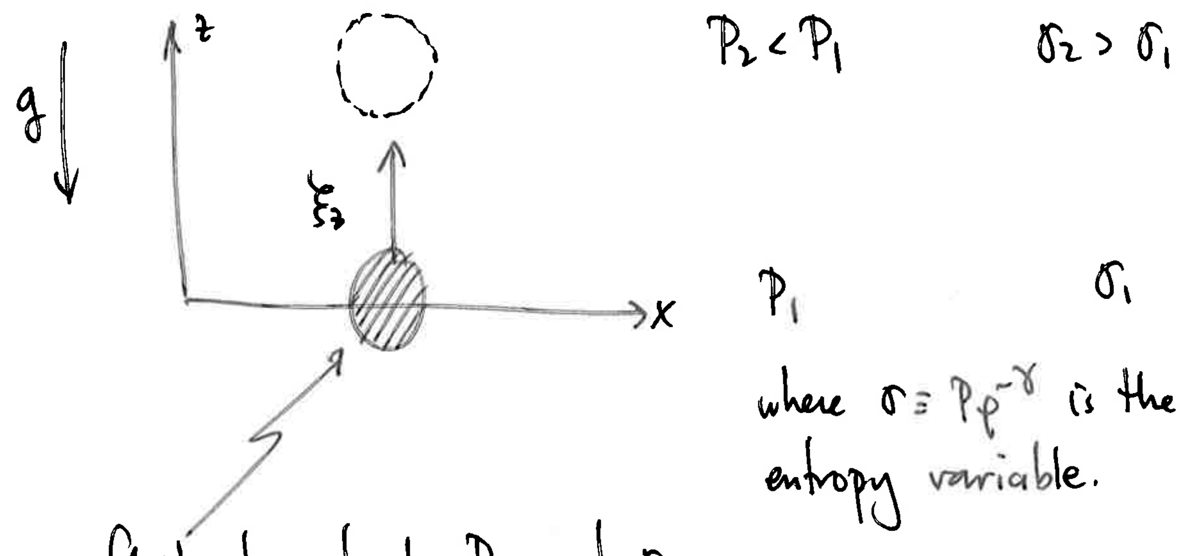

where $\sigma \equiv P\rho^{-\gamma}$ is the entropy variable.

fluid element at P_1 and σ_1

Displace fluid element upwards while conserving its entropy. Now it has less entropy than its surroundings. With pressure balance holding, this means that it is also denser than its surroundings. It must fall back to its equilibrium position. Overshooting, it will oscillate at frequency N. (Mathematically, $\Delta\sigma = 0 \Rightarrow \Delta p/p = \gamma\, \Delta\rho/\rho \Rightarrow \vec{\xi}\cdot\vec{\nabla}\ln p = \gamma \frac{\delta\rho}{\rho} + \gamma\, \vec{\xi}\cdot\vec{\nabla}\ln\rho \Rightarrow \frac{\delta\rho}{\rho} = \frac{N^2}{g}\xi_z$.)

Now, consider $\sigma_2 < \sigma_1$. Our upwardly displaced fluid element has more entropy than its surroundings, and it will continue to rise $\longrightarrow$ convective instability. The (Karl) Schwarzschild criterion for convective stability is $\boxed{N^2 > 0}$.

Bonus: Exact solution to  for an isothermal atmosphere.

Suppose $\frac{d\ln p}{dz} = \frac{d\ln \rho}{dz}$ ($T = \text{const}$). Then $\frac{d\ln p}{dz} = -\frac{\gamma g}{a^2} = \text{const}$.

$\Rightarrow p = p_0 \exp(-z/H)$ with $H \equiv a^2/\gamma g$. Then we have

$$\xi_z'' - \frac{\xi_z'}{H} + \left[\frac{\omega^2 - k_x^2 a^2}{a^2} + \frac{k_x^2 g}{H}\left(1 - \frac{1}{\gamma}\right)\frac{1}{\omega^2}\right]\xi_z = 0.$$

Let $\xi_z = f(z)\exp\left(\frac{z}{2H}\right)$. Then

$$\xi_z' = f' e^{z/2H} + \frac{f}{2H} e^{z/2H} = f' e^{z/2H} + \xi_z/2H$$

$$\xi_z'' = f'' e^{z/2H} + \frac{f'}{H} e^{z/2H} + \frac{\xi_z}{(2H)^2}$$

$$f'' + \frac{f'}{H} + \frac{f}{(2H)^2} - \frac{f'}{H} - \frac{f}{2H^2} + [\ldots] f = 0.$$

$$f'' + \underbrace{\left[-\frac{1}{4H^2} + \frac{\omega^2 - k_x^2 a^2}{a^2} + \frac{k_x^2 a^2}{\gamma H^2}\left(1 - \frac{1}{\gamma}\right)\frac{1}{\omega^2}\right]}_{=\text{const.}} f = 0.$$

bracket

$\Rightarrow f = \exp(\pm i k_z z)$ with $k_z^2 =$

$$\to -k_z^2 - \frac{1}{4H^2} + \frac{\omega^2 - k_x^2 a^2}{a^2} + \frac{k_x^2 a^2}{\omega^2 H^2}\left(\frac{\gamma-1}{\gamma^2}\right) = 0.$$

Mult. by $\omega^2 a^2$ and regroup terms:

$$\omega^4 + \omega^2\left[-k_z^2 a^2 - \frac{a^2}{4H^2} - k_x^2 a^2\right] + k_x^2 a^2 \left(\frac{a^2}{H^2}\right)\left(\frac{\gamma-1}{\gamma^2}\right) = 0.$$

$$\Rightarrow \omega^2 = \frac{k^2 a^2 + \frac{a^2}{4H^2}}{2} \pm \frac{1}{2}\left[\left(k^2 a^2 + \frac{a^2}{4H^2}\right)^2 - 4k_x^2 a^2 \left(\frac{a^2}{H^2}\right)\left(\frac{\gamma-1}{\gamma^2}\right)\right]^{1/2}.$$

Note that $N^2 = \frac{g}{\gamma}\frac{d\ln P\rho^{-\gamma}}{dz} = \left(\frac{1-\gamma}{\gamma}\right) g \frac{d\ln\rho}{dz} = \frac{a^2}{H^2}\left(\frac{\gamma-1}{\gamma^2}\right).$

So,

$$\boxed{\omega^2 = \frac{k^2 a^2 + \frac{a^2}{4H^2}}{2} \pm \frac{1}{2}\left[\left(k^2 a^2 + \frac{a^2}{4H^2}\right)^2 - 4k_x^2 a^2 N^2\right]^{1/2}.}$$

If $(kH)^2 \gg 1$, this becomes $\omega^2 = k^2 a^2$ for the sound wave (+ sign) and $\omega^2 = \frac{k_x^2 N^2}{k_z^2 + k_x^2}$ for the g-mode (− sign).

The final term in the square root captures the coupling between these modes.

VI.7. Buoyancy: Parker instability

Continued on hand-written notes...

- A related problem is the <u>Parker Instability</u>, or "magnetic Rayleigh-Taylor instability" (although it is different in detail from RTI and is closer to Schwarzschild Convection). Consider an atmosphere similar to that in our convective instability calculation, but with a magnetic field oriented perpendicularly to gravity with a z-dependence: $\vec{B}_0 = B_0(z)\hat{x}$. The force balance in the equilibrium state now includes a contribution from the magnetic pressure: $g = -\frac{1}{\rho}\left(\frac{dp}{dz} + \frac{1}{8\pi}\frac{dB_0^2}{dz}\right) = \text{const.}$, or

$$\frac{g}{a^2} = -\frac{1}{\gamma}\frac{d\ln P}{dz} - \frac{v_{A0}^2}{a^2}\frac{d\ln B_0}{dz}.$$

Our equations are almost the same:

$$\frac{\delta\rho}{\rho} + ik_x\xi_x + \xi_z' + \xi_z\frac{d\ln\rho}{dz} = 0,$$

$$-\omega^2\xi_x = -ik_x\left(\frac{\delta p}{\rho} + \frac{B_0\,\delta B_x}{4\pi\rho}\right) + \frac{ik_xB_0}{4\pi\rho}\delta B_x + \frac{\delta B_z}{4\pi\rho}\frac{dB_0}{dz},$$

$$-\omega^2\xi_z = -\frac{1}{\rho}\frac{d}{dz}\left(\delta p + \frac{B_0\,\delta B_x}{4\pi}\right) - \frac{\delta\rho}{\rho}g + \frac{ik_xB_0}{4\pi\rho}\delta B_z,$$

$$\frac{\delta p}{p} = \gamma\frac{\delta\rho}{\rho} - \xi_z\frac{d\ln p\rho^{-\gamma}}{dz},$$

but now with magnetic-field perturbations and gradients. The former are given by $\vec{\delta B} = \nabla\times(\vec{\xi}\times\vec{B}_0) \Rightarrow \delta B_x = -\frac{d}{dz}(\xi_z B_0)$

$$\delta B_z = ik_xB_0\xi_z$$

First, note that $\dfrac{\delta p + B_0 \delta B_x / 4\pi}{\rho}$

$$= a^2 \frac{\delta\rho}{\rho} - \frac{a^2}{\gamma} \frac{d\ln p\rho^{-\gamma}}{dz} \xi_z + \frac{B_0}{4\pi\rho}\left(-\frac{d}{dz}\right)(\xi_z B_0)$$

$$= a^2\left[-ik_x\xi_x - \xi_z' - \xi_z \frac{d\ln\rho}{dz} - \frac{1}{\gamma}\frac{d\ln p\rho^{-\gamma}}{dz}\xi_z - \frac{V_{A0}^2}{a^2}\left(\xi_z' + \xi_z \frac{d\ln B_0}{dz}\right)\right]$$

$$= a^2\left[-ik_x\xi_x - \xi_z'\left(1+\frac{V_{A0}^2}{a^2}\right) + \frac{g}{a^2}\xi_z\right].$$

Then

$$-\omega^2\xi_x = -ik_x a^2\left[-ik_x\xi_x - \xi_z'\left(1+\frac{V_{A0}^2}{a^2}\right) + \frac{g}{a^2}\xi_z\right] + \frac{ik_x B_0}{4\pi\rho}\left[-\xi_z' B_0 - \xi_z B_0 \frac{d\ln B_0}{dz}\right] + \frac{ik_x B_0}{4\pi\rho}\xi_z \frac{dB_0}{dz}$$

$$\Rightarrow (-\omega^2 + k_x^2 a^2)\xi_x = ik_x a^2 \xi_z'\left(1+\cancel{\frac{V_{A0}^2}{a^2}}\right) - ik_x g\xi_z - \cancel{ik_x V_{A0}^2 \xi_z'} - \cancel{ik_x V_{A0}^2 \frac{d\ln B_0}{dz}}\xi_z + \cancel{ik_x V_{A0}^2 \frac{d\ln B_0}{dz}}\xi_z$$

$$\Rightarrow \boxed{(-\omega^2 + k_x^2 a^2)\xi_x = ik_x a^2 \xi_z' - ik_x \xi_z g}$$

Same as # w/o B field!

$$\Rightarrow \frac{\delta\rho}{\rho} = -\xi_z' - \xi_z \frac{d\ln\rho}{dz} - ik_x \frac{\left[ik_x a^2 \xi_z' - ik_x \xi_z g\right]}{(-\omega^2 + k_x^2 a^2)}$$

$$\boxed{\frac{\delta\rho}{\rho} = \frac{\omega^2 \xi_z' + \left[(\omega^2 - k_x^2 a^2)\frac{d\ln p}{dz} - k_x^2 g\right]\xi_z}{k_x^2 a^2 - \omega^2}}$$

same as ◎ w/o B field!

Buoyancy is fundamentally the same as in the hydro case.
Plugging all of this into the z-component of the momentum eqn. gives $\left(\text{with } \frac{\delta p + \delta B^2/8\pi}{p} = \frac{\omega^2}{\omega^2 - k_x^2 a^2}\left[\frac{\gamma g}{a^2}\xi_z - \gamma \xi_z'\right] - \frac{\gamma v_{A0}^2}{a^2}\xi_z'\right)$

$$-\omega^2 \xi_z = -\frac{1}{\rho}\frac{d}{dz}\left[\frac{p\,\omega^2}{\omega^2 - k_x^2 a^2}\left(\frac{\gamma g}{a^2}\xi_z - \gamma \xi_z'\right) - \frac{B_0^2}{4\pi}\xi_z'\right]$$

$$- g\left\{\frac{\omega^2 \xi_z' + \left[(\omega^2 - k_x^2 a^2)\frac{d\ln p}{dz} - k_x^2 g\right]\xi_z}{k_x^2 a^2 - \omega^2}\right\}$$

$$+ \frac{i k_x B_0}{4\pi\rho}\left(i k_x B_0 \xi_z\right)$$

$$\Rightarrow \left(-\omega^2 + k_x^2 v_{A0}^2\right)\xi_z = -\frac{a^2}{\gamma}\frac{d\ln p}{dz}\frac{\omega^2}{\omega^2 - k_x^2 a^2}\left(\frac{\gamma g \xi_z}{a^2} - \gamma \xi_z'\right)$$

$$- \frac{a^2}{\gamma}\frac{\omega^2 k_x^2 a^2}{(\omega^2 - k_x^2 a^2)^2}\frac{d\ln T}{dz}\left(\frac{\gamma g \xi_z}{a^2} - \gamma \xi_z'\right) + v_{A0}^2 \xi_z'' + \xi_z' v_{A0}^2 \frac{d\ln B_0^2}{dz}$$

$$- \frac{a^2}{\gamma}\frac{\omega^2}{\omega^2 - k_x^2 a^2}\left(\cancel{\frac{\gamma g}{a^2}\xi_z'} - \frac{\gamma g}{a^2}\xi_z \frac{d\ln T}{dz} - \gamma \xi_z''\right)$$

$$+ \frac{g}{\omega^2 - k_x^2 a^2}\left\{\cancel{\omega^2 \xi_z'} + \left[(\omega^2 - k_x^2 a^2)\frac{d\ln p}{dz} - k_x^2 g\right]\xi_z\right\}$$

After some straightforward algebra, we find

$$\xi_z'' \left(V_{A0}^2 + \frac{a^2\omega^2}{\omega^2 - k_x^2 a^2} \right)$$

$$+ \xi_z' \left[V_{A0}^2 \frac{d\ln B_0^2}{dz} + \frac{a^2\omega^2}{(\omega^2 - k_x^2 a^2)^2} \left(\omega^2 \frac{d\ln p}{dz} - k_x^2 a^2 \frac{d\ln \rho}{dz} \right) \right]$$

$$+ \xi_z \left[\frac{g}{\gamma} \frac{k_x^2 a^2}{\omega^2 - k_x^2 a^2} \left(\frac{d\ln p\rho^{-\gamma}}{dz} + \frac{\gamma V_{A0}^2}{a^2} \frac{d\ln B_0}{dz} \right) - \frac{g\,\omega^2 k_x^2 a^2}{(\omega^2 - k_x^2 a^2)^2} \frac{d\ln T}{dz} \right.$$
$$\left. + \omega^2 - k_x^2 V_{A0}^2 \right]$$

All extra terms are $\propto V_{A0}^2$. For $k_z \to 0$, $k_x^2 a^2 \gg 1$, this becomes

$$\boxed{\omega^2 \simeq \underbrace{k_x^2 V_{A0}^2}_{\text{magnetic tension}} + \frac{g}{\gamma}\left(\underbrace{\frac{d\ln p\rho^{-\gamma}}{dz}}_{\text{thermal buoyancy}} + \underbrace{\frac{1}{\beta}\frac{d\ln B_0^2}{dz}}_{\text{magnetic buoyancy}} \right)} \quad \text{w/} \quad \beta = \frac{B_0^2}{8\pi p}.$$

Now, $\frac{d\ln p\rho^{-\gamma}}{dz} + \frac{1}{\beta}\frac{d\ln B_0^2}{dz} > 0$ for stability. But the physics is the same as in Schwarzschild convection — just the pressure balance is different. Can also see this by rephrasing in terms of $\delta\Pi = \delta p + \frac{\vec{B}\cdot\delta\vec{B}}{4\pi}$ and imposing total pressure balance, $\delta\Pi = 0$...

$$\frac{\delta\Pi}{\rho} = \frac{a^2}{\gamma}\left\{ \frac{\omega^2}{\omega^2-k_x^2a^2}\left[\frac{\gamma g}{a^2}\xi_z - \gamma\xi_z'\right] - \frac{\gamma v_A^2}{a^2}\xi_z' \right\}$$

$$= \frac{\omega^2}{\omega^2-k_x^2a^2}\, g\,\xi_z - \left[\frac{a^2\omega^2}{\omega^2-k_x^2a^2} + v_A^2\right]\xi_z'$$

$$\frac{d}{dz}\left(\frac{\delta\Pi}{\rho}\right) = \left(\frac{d}{dz}\frac{g\omega^2}{\omega^2-k_x^2a^2}\right)\xi_z + \left(\frac{\omega^2 g}{\omega^2-k_x^2a^2}\right)\xi_z'$$

$$- \left(\frac{a^2\omega^2}{\omega^2-k_x^2a^2} + v_A^2\right)\xi_z'' - \left(\frac{d}{dz}\frac{a^2\omega^2}{\omega^2-k_x^2a^2} + \frac{d}{dz}v_A^2\right)\xi_z'$$

Use disp. rel. to replace ξ_z'' w/

$$-\left(v_A^2 + \frac{a^2\omega^2}{\omega^2-k_x^2a^2}\right)^{-1}\left\{ \xi_z'\left[v_A^2\frac{d\ln B^2}{dz} + \frac{a^2\omega^2}{(\omega^2-k_x^2a^2)^2}\left(\omega^2\frac{d\ln p}{dz} - k_x^2a^2\frac{d\ln\rho}{dz}\right)\right]\right.$$

$$+\xi_z\left[\omega^2 - k_x^2v_A^2 - \frac{g\omega^2k_x^2a^2}{(\omega^2-k_x^2a^2)^2}\frac{d\ln T}{dz}\right.$$

$$\left.\left. + \frac{g}{\gamma}\frac{k_x^2a^2}{\omega^2-k_x^2a^2}\left(\frac{d\ln p\rho^{-\gamma}}{dz} + \frac{\gamma v_A^2}{a^2}\frac{d\ln B}{dz}\right)\right]\right\}$$

$$\Rightarrow \frac{d}{dz}\left(\frac{\delta\Pi}{\rho}\right) = \xi_z\left[\cancel{\frac{d}{dz}\frac{g\omega^2}{\omega^2-k_x^2a^2}} + \omega^2 - k_x^2v_A^2 - \cancel{\frac{g\omega^2k_x^2a^2}{(\omega^2-k_x^2a^2)^2}\frac{d\ln T}{dz}}\right.$$

$$\left. + \frac{g}{\gamma}\frac{k_x^2a^2}{\omega^2-k_x^2a^2}\left(\frac{d\ln p\rho^{-\gamma}}{dz} + \frac{v_A^2\gamma}{a^2}\frac{d\ln B}{dz}\right)\right]$$

$$+\xi_z'\left[\frac{\omega^2 g}{\omega^2-k_x^2a^2} - \frac{d}{dz}\frac{a^2\omega^2}{\omega^2-k_x^2a^2} - \frac{dv_A^2}{dz}\right.$$

$$\left. + v_A^2\frac{d\ln B^2}{dz} + \frac{a^2\omega^2}{(\omega^2-k_x^2a^2)^2}\left(\omega^2\frac{d\ln p}{dz} - k_x^2a^2\frac{d\ln\rho}{dz}\right)\right]$$

$$\frac{d}{dz}\left(\frac{\delta\Pi}{\rho}\right) = \xi_z\left[\omega^2 - k_x^2 V_A^2 + \frac{g}{\gamma}\frac{k_x^2 a^2}{\omega^2 - k_x^2 a^2}\left(\frac{d\ln p\rho^{-\gamma}}{dz} + \frac{V_A^2\gamma}{a^2}\frac{d\ln B}{dz}\right)\right]$$

$$+ \xi_z'\left[V_A^2\left(\cancel{\frac{d\ln B^2}{dz}} - \cancel{\frac{d\ln B^2}{dz}} + \frac{d\ln\rho}{dz}\right)\right.$$

$$+ \frac{\omega^2}{\omega^2 - k_x^2 a^2}\left(g - \cancel{a^2\frac{d\ln T}{dz}} + \cancel{\frac{a^2(-k_x^2 a^2)}{\omega^2 - k_x^2 a^2}}\frac{d\ln T}{dz}\right.$$

$$\left.\left. + \frac{a^2}{\omega^2 - k_x^2 a^2}\left(\cancel{\omega^2\frac{d\ln T}{dz}} + \omega^2\frac{d\ln\rho}{dz} - k_x^2 a^2\frac{d\ln\rho}{dz}\right)\right)\right]$$

$$= \xi_z\left[\ldots\right] + \left[V_A^2\frac{d\ln\rho}{dz} + \frac{\omega^2}{\omega^2 - k_x^2 a^2}\left(g + a^2\frac{d\ln\rho}{dz}\right)\right]\xi_z'$$

$$= \xi_z\left[\ldots\right] + \left[V_A^2\frac{d\ln\rho}{dz} + \frac{a^2\omega^2}{\omega^2 - k_x^2 a^2}\left(-\frac{1}{\gamma}\frac{d\ln P}{dz} - \frac{V_A^2}{a^2}\frac{d\ln B}{dz} + \frac{d\ln\rho}{dz}\right)\right]\xi_z'$$

$$= -\frac{1}{\gamma}\frac{d\ln P\rho^{-\gamma}}{dz} - \frac{V_A^2}{a^2}\frac{d\ln B}{dz}$$

$$= \xi_z\left[\omega^2 - k_x^2 V_A^2 + \frac{g}{\gamma}\frac{k_x^2 a^2}{\omega^2 - k_x^2 a^2}\left(\frac{d\ln p\rho^{-\gamma}}{dz} + \frac{\gamma V_A^2}{a^2}\frac{d\ln B}{dz}\right)\right]$$

$$+ \xi_z'\left[V_A^2\frac{d\ln\rho}{dz} - \frac{a^2\omega^2}{\omega^2 - k_x^2 a^2}\frac{1}{\gamma}\left(\frac{d\ln p\rho^{-\gamma}}{dz} + \frac{\gamma V_A^2}{a^2}\frac{d\ln B}{dz}\right)\right]$$

$$\xi_z' = \left(-\frac{\delta\Pi}{\rho} + \frac{\omega^2 g\,\xi_z}{\omega^2 - k_x^2 a^2}\right)\Big/\left(\frac{a^2\omega^2}{\omega^2 - k_x^2 a^2} + V_A^2\right)$$

$$\frac{d}{dz}\left(\frac{\delta\pi}{\rho}\right) = \frac{\delta}{\xi_z}\Bigg[\omega^2 - k_x^2 V_A^2 + \frac{g}{\gamma}\frac{k_x^2 a^2}{\omega^2 - k_x^2 a^2}(\ldots)$$

$$+ \frac{\omega^2 g}{\omega^2 - k_x^2 a^2}\left(\frac{a^2\omega^2}{\omega^2 - k_x^2 a^2} + V_A^2\right)^{-1} V_A^2 \frac{d\ln\rho}{dz}$$

$$- \frac{\omega^2 g}{\omega^2 - k_x^2 a^2}\left(\frac{a^2\omega^2}{\omega^2 - k_x^2 a^2} + V_A^2\right)^{-1} \frac{a^2\omega^2}{\omega^2 - k_x^2 a^2}\frac{1}{\gamma}(\ldots)\Bigg]$$

$$- \frac{\delta\pi}{\rho}\left(\frac{a^2\omega^2}{\omega^2 - k_x^2 a^2} + V_A^2\right)^{-1}\left[V_A^2 \frac{d\ln\rho}{dz} - \frac{a^2\omega^2}{\omega^2 - k_x^2 a^2}\frac{1}{\gamma}(\ldots)\right]$$

Sps. pressure balance ... $\delta\pi/\rho = 0$. Dispersion relation is then

$$\omega^2 - k_x^2 V_A^2 + \frac{g}{\gamma}\frac{1}{\omega^2 - k_x^2 a^2}\left(\frac{a^2\omega^2}{\omega^2 - k_x^2 a^2} + V_A^2\right)^{-1}$$

$$\cdot\Bigg[k_x^2 a^2\left(\frac{a^2\omega^2}{\omega^2 - k_x^2 a^2} + V_A^2\right)(\ldots) + \gamma V_A^2 \omega^2 \frac{d\ln\rho}{dz}$$

$$- \frac{\omega^2 a^2 \omega^2}{\omega^2 - k_x^2 a^2}(\ldots)\Bigg] = 0.$$

$$\left(-a^2\omega^2 + k_x^2 a^2 V_A^2\right)(\ldots) + \gamma V_A^2 \omega^2 \frac{d\ln\rho}{dz}$$

$$0 = (\omega^2 - k_x^2 V_A^2)\left[\omega^2\left(1+\frac{V_A^2}{a^2}\right) - k_x^2 V_A^2\right]$$

$$- \frac{g}{\gamma}\left(\frac{d\ln P\rho^{-\gamma}}{dz} + \frac{1}{\beta}\frac{d\ln B^2}{dz}\right)(\omega^2 - k_x^2 V_A^2) + g\frac{V_A^2}{a^2}\frac{d\ln\rho}{dz}\,\omega^2$$

$$\boxed{\begin{aligned} 0 = {} & (\omega^2 - k_x^2 V_A^2)\left[\omega^2\left(\frac{V_A^2}{a^2}+1\right) - k_x^2 V_A^2 - \frac{g}{\gamma}\left(\frac{d\ln P\rho^{-\gamma}}{dz} + \frac{1}{\beta}\frac{d\ln B^2}{dz}\right)\right] \\ & + g\frac{d\ln\rho}{dz}\,\omega^2\frac{V_A^2}{a^2} \end{aligned}}$$

NB: if $k_x = 0$, this $= \omega^2\left[\frac{V_A^2}{a^2} g\frac{d\ln\rho}{dz} + \omega^2\left(\frac{V_A^2}{a^2}+1\right) - \frac{g}{\gamma}\frac{d\ln P\rho^{-\gamma}}{dz} - \frac{g}{\gamma\beta}\frac{d\ln B^2}{dz}\right]$

$$0 = \omega^2\left[\omega^2\left(\frac{V_A^2}{a^2}+1\right) - \frac{g}{\gamma}\left(\frac{d\ln P\rho^{-\gamma}}{dz} + \gamma V_A^2\frac{d\ln B\rho^{-1}}{dz}\right)\right]$$

$$\Rightarrow \omega^2 = 0 \text{ and } \frac{g}{\gamma}\left(\frac{d\ln P\rho^{-\gamma}}{dz} + \gamma V_A^2\frac{d\ln B\rho^{-1}}{dz}\right)\Big/\left(1+\frac{V_A^2}{a^2}\right)$$

When $N^2 = 0$, this is the <u>interchange instability</u>, and involves the exchange of flux tubes in height when $\frac{d\ln B\rho^{-1}}{dz} < 0$.

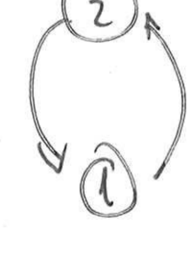

switch them ... $\Phi_2 = \int B_2\, da = B_2 A_2$ $\quad \Phi_1 = \int B_1\, da = B_1 A_1$

$M_2 = \left(\frac{\rho}{B}\right)_2 \Phi_2 \quad M_1 = \left(\frac{\rho}{B}\right)_1 \Phi_1$

But $\Phi_1 = \Phi_2 \Rightarrow M_{\frac{1}{2}} = \left(\frac{\rho}{B}\right)_{\frac{1}{2}} \Phi$. So if (ρ/B) increases upwards, then there's more mass on top
$\Rightarrow$ energetically favorable to switch them to liberate gravitational potential energy.

If $k_x \neq 0$, this gives Parker instability.

One can obtain an exact solution for an isothermal atmosphere, just like in the hydro case.

$$\frac{d\ln T}{dz} = 0 \;; \quad \frac{d\ln B^2}{dz} = \frac{d\ln\rho}{dz} = \frac{d\ln P}{dz} = -\frac{1}{H}$$

Write $\xi_z \propto e^{\pm i k_z z + z/2H}$ and set

$$k_z^2 \equiv -\frac{1}{4H^2} + \frac{(\omega^2 - k_x^2 v_A^2)(\omega^2 - k_x^2 a^2) + k_x^2 a^2 N_{ms}^2}{\omega^2 (a^2 + v_A^2) - k_x^2 a^2 v_A^2}$$

w/ $N_{ms}^2 \equiv \frac{g}{\gamma}\left(\frac{d\ln P\rho^{-\gamma}}{dz} + \frac{1}{\beta}\frac{d\ln B^2}{dz}\right)$. Dispersion relation is then

$$\omega^4 - \omega^2\left(k^2 + \frac{1}{4H^2}\right)v_{ms}^2 + k_x^2 a^2\left[k_z^2 a^2 + \frac{v_A^2}{4H^2} + N_{ms}^2\right] = 0$$

with $v_{ms}^2 \equiv a^2 + v_A^2$ the magnetosonic speed (squared).

NB: A cold atmosphere ($a^2 \to 0$) with support only from $B(z)$ has

$$\omega^4 - \omega^2\left(k^2 + \frac{1}{4H^2}\right)v_A^2 - k_x^2 v_A^2 \frac{g}{H} = 0 ,$$

which is unstable.

The idea is that the supporting magnetic pressure gradient wants to relax (B^2 likes being constant), and it can do so by offloading mass sinusoidally:

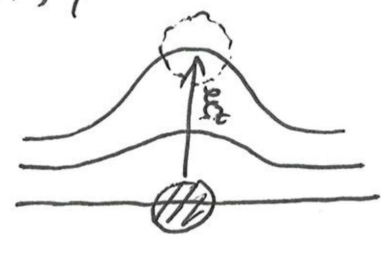

VI.8. Rotation: Rayleigh and Magnetorotational instabilities

In §II.2.4, we wrote down the equations of hydrodynamics in a rotating frame – see (II.2.9). Here we do the same for the equations of MHD. With $\boldsymbol{v} = \boldsymbol{u} - R\Omega(R,z)\hat{\boldsymbol{\varphi}}$ and

$$\frac{\mathrm{D}}{\mathrm{D}t} \doteq \frac{\partial}{\partial t} + \boldsymbol{v}\cdot\boldsymbol{\nabla} + \Omega\frac{\partial}{\partial\varphi},$$

the continuity and force equations are the same,

$$\frac{\mathrm{D}\rho}{\mathrm{D}t} = -\rho\boldsymbol{\nabla}\cdot\boldsymbol{v}, \tag{VI.8.1}$$

$$\frac{\mathrm{D}v_R}{\mathrm{D}t} = f_R + 2\Omega v_\varphi + R\Omega^2 + \frac{v_\varphi^2}{R}, \tag{VI.8.2}$$

$$\frac{\mathrm{D}v_\varphi}{\mathrm{D}t} = f_\varphi - \frac{\kappa^2}{2\Omega}v_R - R\frac{\partial\Omega}{\partial z}v_z - \frac{v_R v_\varphi}{R}, \tag{VI.8.3}$$

$$\frac{\mathrm{D}v_z}{\mathrm{D}t} = f_z, \tag{VI.8.4}$$

but with the addition of the Lorentz force:

$$\boldsymbol{f} = -\frac{1}{\rho}\boldsymbol{\nabla}\left(P + \frac{B^2}{8\pi}\right) + \frac{\boldsymbol{B}\cdot\boldsymbol{\nabla}B_i}{4\pi\rho}\,\hat{\boldsymbol{e}}_i + \frac{B_R B_\varphi}{4\pi\rho R}\hat{\boldsymbol{\varphi}} - \frac{B_\varphi^2}{4\pi\rho R}\hat{\boldsymbol{R}} - \boldsymbol{\nabla}\Phi. \tag{VI.8.5}$$

Note the additional geometric terms $\propto B^2/R$; these are tension forces associated with the bend in the magnetic-field lines as they follow the azimuthal direction. To these equations we must append the induction equation:

$$\frac{\mathrm{D}B_R}{\mathrm{D}t} = -B_R\boldsymbol{\nabla}\cdot\boldsymbol{v} + \boldsymbol{B}\cdot\boldsymbol{\nabla}v_R, \tag{VI.8.6}$$

$$\frac{\mathrm{D}B_\varphi}{\mathrm{D}t} = -B_\varphi\boldsymbol{\nabla}\cdot\boldsymbol{v} + \boldsymbol{B}\cdot\boldsymbol{\nabla}v_\varphi + \frac{\partial\Omega}{\partial\ln R}B_R + R\frac{\partial\Omega}{\partial z}B_z, \tag{VI.8.7}$$

$$\frac{\mathrm{D}B_z}{\mathrm{D}t} = -B_z\boldsymbol{\nabla}\cdot\boldsymbol{v} + \boldsymbol{B}\cdot\boldsymbol{\nabla}v_z. \tag{VI.8.8}$$

With the exception of advection by the differential rotation, the only additions to the induction equation beyond its more customary Cartesian form appear in its azimuthal component: $+\,R\boldsymbol{B}\cdot\boldsymbol{\nabla}\Omega$ on the right-hand side. This corresponds to stretching of the flux-frozen magnetic field by the differential rotation.

In the hand-written pages that follow, these equations are used to describe the evolution of small fluctuations about a homogeneous, differentially rotating disk with $\Omega = \Omega(R)$, in which the centrifugal acceleration $R\Omega^2$ is balanced by gravity $-\partial\Phi/\partial R$. If the latter is dominated by that of a central point mass M, we have $\Phi = -GM/R$ and so $\Omega = (GM/R^3)^{1/2}$ – i.e., Keplerian rotation.

Before proceeding, I'll write down the linearized MHD equations written in cylindrical coordinates (R,φ,z) in a rotating frame with $\boldsymbol{\Omega} = \Omega(R,z)\hat{\boldsymbol{z}}$. The only assumptions here are that the background magnetic field is uniform, and that the equilibrium state arises from a balance between the centrifugal force and gravity plus thermal-pressure gradients (i.e., we allow for density and pressure stratification in the background state). We also neglect curvature terms of order $\sim(v_\mathrm{A}^2/R)(\delta B/B)$, as these are small compared to the other terms unless the toroidal magnetic field is super-thermal by a factor $\sim(R/H)^{1/2}$, where $H\sim c_\mathrm{s}/\Omega$ is the disk thickness and c_s is the sound speed – an atypical situation.

Without further ado...

$$\left(\frac{\partial}{\partial t}+\Omega\frac{\partial}{\partial\varphi}\right)\delta\rho=-(\delta\boldsymbol{v}\boldsymbol{\cdot}\boldsymbol{\nabla})\rho-\rho(\boldsymbol{\nabla}\boldsymbol{\cdot}\delta\boldsymbol{v}), \tag{VI.8.9}$$

$$\begin{aligned}\left(\frac{\partial}{\partial t}+\Omega\frac{\partial}{\partial\varphi}\right)\delta v_R=&-\frac{1}{\rho}\frac{\partial}{\partial R}\left(\delta P+\frac{\boldsymbol{B}\boldsymbol{\cdot}\delta\boldsymbol{B}}{4\pi}\right)+\frac{\delta\rho}{\rho^2}\frac{\partial P}{\partial R}+\frac{(\boldsymbol{B}\boldsymbol{\cdot}\boldsymbol{\nabla})\delta B_R}{4\pi\rho}-\frac{\partial\delta\Phi}{\partial R}\\&-2\Omega\delta v_\varphi,\end{aligned} \tag{VI.8.10}$$

$$\begin{aligned}\left(\frac{\partial}{\partial t}+\Omega\frac{\partial}{\partial\varphi}\right)\delta v_\varphi=&-\frac{1}{\rho R}\frac{\partial}{\partial\varphi}\left(\delta P+\frac{\boldsymbol{B}\boldsymbol{\cdot}\delta\boldsymbol{B}}{4\pi}\right)+\frac{\delta\rho}{\rho}\frac{1}{\rho R}\frac{\partial P}{\partial\varphi}+\frac{(\boldsymbol{B}\boldsymbol{\cdot}\boldsymbol{\nabla})\delta B_\varphi}{4\pi\rho}-\frac{1}{R}\frac{\partial\delta\Phi}{\partial\varphi}\\&+\frac{\kappa^2}{2\Omega}\delta v_R+R\frac{\partial\Omega}{\partial z}\delta v_\varphi,\end{aligned} \tag{VI.8.11}$$

$$\left(\frac{\partial}{\partial t}+\Omega\frac{\partial}{\partial\varphi}\right)\delta v_z=-\frac{1}{\rho}\frac{\partial}{\partial z}\left(\delta P+\frac{\boldsymbol{B}\boldsymbol{\cdot}\delta\boldsymbol{B}}{4\pi}\right)+\frac{\delta\rho}{\rho^2}\frac{\partial P}{\partial z}+\frac{(\boldsymbol{B}\boldsymbol{\cdot}\boldsymbol{\nabla})\delta B_z}{4\pi\rho}-\frac{\partial\delta\Phi}{\partial z} \tag{VI.8.12}$$

$$\left(\frac{\partial}{\partial t}+\Omega\frac{\partial}{\partial\varphi}\right)\delta B_R=(\boldsymbol{B}\boldsymbol{\cdot}\boldsymbol{\nabla})\delta v_R-B_R(\boldsymbol{\nabla}\boldsymbol{\cdot}\delta\boldsymbol{v}), \tag{VI.8.13}$$

$$\left(\frac{\partial}{\partial t}+\Omega\frac{\partial}{\partial\varphi}\right)\delta B_\varphi=(\boldsymbol{B}\boldsymbol{\cdot}\boldsymbol{\nabla})\delta v_\varphi-B_\varphi(\boldsymbol{\nabla}\boldsymbol{\cdot}\delta\boldsymbol{v})+\frac{\partial\Omega}{\partial\ln R}\delta B_R+R\frac{\partial\Omega}{\partial z}\delta B_z, \tag{VI.8.14}$$

$$\left(\frac{\partial}{\partial t}+\Omega\frac{\partial}{\partial\varphi}\right)\delta B_z=(\boldsymbol{B}\boldsymbol{\cdot}\boldsymbol{\nabla})\delta v_z-B_z(\boldsymbol{\nabla}\boldsymbol{\cdot}\delta\boldsymbol{v}), \tag{VI.8.15}$$

$$\left(\frac{\partial}{\partial t}+\Omega\frac{\partial}{\partial\varphi}\right)\delta\sigma=-\delta v_R\frac{\partial\ln P\rho^{-\gamma}}{\partial R}-\delta v_z\frac{\partial\ln P\rho^{-\gamma}}{\partial z}, \tag{VI.8.16}$$

where $\delta\sigma\doteq\delta P/P-\gamma\delta\rho/\rho$.

- Rotational and magnetorotational instability.

Accretion disks are ubiquitous in astrophysics, and they get their namesake by actually facilitating mass accretion onto compact objects like young protostars, neutron stars, black holes, etc. But for this to happen, angular momentum must be redistributed, and it turns out that this is frustratingly difficult in Keplerian disks. The problem is that, hydrodynamically, Keplerian flows are quite stable (we'll show below that they are linearly stable; there is no proof that they are nonlinearly stable, but experimental efforts to find nonlinear instability in hydrodynamic, differentially rotating flows have so far failed). Fluid elements do not like to give up their angular momentum. The culprit is the Coriolis force, a surprisingly strong stabilizing effect. (Indeed, planar shear flows without rotation quite easily disrupt so long as the viscosity is not too large.) Another issue is that the molecular viscosity, which might transport angular momentum purely by frictional means, is absolutely negligible in most all astrophysical fluids. One way out is to posit some anomalous viscosity via (unknown) turbulence. This is the route taken in the classic Shakura & Sunyaev

(1973) paper — assume turbulent transport, characterize it by a scalar viscosity, and take that viscous stress to be proportional to the gas pressure:

$$T_{R\varphi} = \alpha_{ss}\, p$$

p ← gas pressure

α_{ss} ← proportionality constant

$T_{R\varphi}$ ← R-φ component of the stress tensor, responsible for transporting φ momentum in the R direction.

This led to the "α-disk" framework of accretion disks, which has been extremely profitable, but woefully unsatisfying. This changed in 1991.

Let's pause here and explore the above claims a bit further. I said a Keplerian disk is hydrodynamically stable to small disturbances. Let's prove it. There are two ways to do this — using point masses in orbits, and using the full hydro eqns. in a rotating frame. Here's the first:

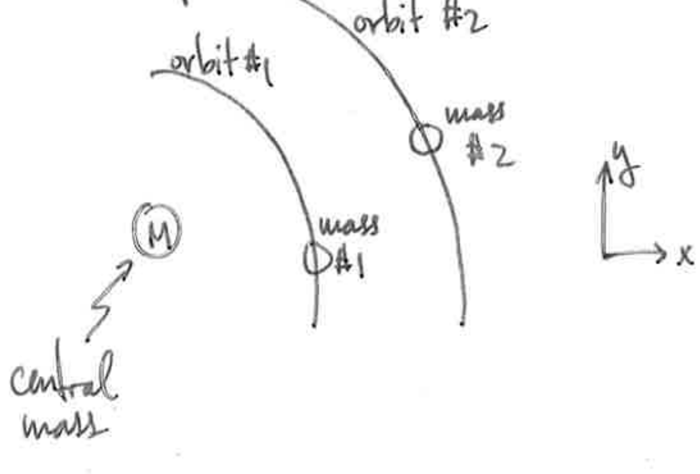

The eqns. of motion for these masses are

$$\ddot{x} - 2\Omega\dot{y} = -\frac{d\Omega^2}{d\ln R}\, x$$

$$\ddot{y} + 2\Omega\dot{x} = 0$$

These are called the "Hill equations" (Hill 1878). They include the Coriolis force and an extra term in the "radial" equation for the x displacement that accounts for the "tidal" force (the local difference between the centrifugal force and gravity). And they are local — note the Cartesian coordinate system with x pointing locally radial and y pointing locally azimuthal. Take solutions $x, y \sim e^{i\omega t}$ to compute the normal modes of this system:

$$\begin{bmatrix} -\omega^2 + \frac{d\Omega^2}{d\ln R} & 2\Omega i\omega \\ -2\Omega i\omega & -\omega^2 \end{bmatrix} \begin{bmatrix} x \\ y \end{bmatrix} = 0 \Rightarrow \omega^2\left(\omega^2 - \frac{d\Omega^2}{d\ln R}\right) = 4\Omega^2\omega^2$$

$$\Rightarrow \omega^2 - \underbrace{\left(4\Omega^2 + \frac{d\Omega^2}{d\ln R}\right)}_{\equiv \kappa^2} = 0 \Rightarrow \boxed{\omega = \pm\kappa}$$

κ ← "epicyclic frequency"

These are epicyclic oscillations when $\kappa^2 > 0$, and exponentially growing disturbances when $\kappa^2 < 0$.

Note that $4\Omega^2 + \frac{d\Omega^2}{d\ln R} = \frac{1}{R^3}\frac{d\ell^2}{dR}$, where $\ell = \Omega R^2$ is the (specific) angular momentum. Thus,

$$\boxed{\frac{d\ell^2}{d\ln R} > 0 \Leftrightarrow \text{linear stability}}$$

"Rayleigh criterion"

The fluid way: Let's assume incompressibility for simplicity. Going back to our hydrodynamic equs., with gravity from a central point mass and $\vec{u} = \vec{v} + R\Omega\hat{\varphi}$, we have

$$\left(\frac{\partial}{\partial t} + \Omega\frac{\partial}{\partial\varphi}\right) v_R + \vec{v}\cdot\vec{\nabla} v_R - 2\Omega v_\varphi - R\Omega^2 - \frac{v_\varphi^2}{R}$$

$$= -\frac{\partial p}{\partial R}\frac{1}{\rho} + g_R,$$

$$\left(\frac{\partial}{\partial t} + \Omega\frac{\partial}{\partial\varphi}\right) v_\varphi + \vec{v}\cdot\vec{\nabla} v_\varphi + 2\Omega v_R + v_R\frac{d\Omega}{d\ln R} + \frac{v_R v_\varphi}{R}$$

$$= -\frac{1}{R}\frac{\partial p}{\partial\varphi}\frac{1}{\rho},$$

where $g_R = -\frac{GM}{R^2}$. Our equilibrium state is $\vec{v}=0$, p = constant, and $g_R = -R\Omega^2 \Rightarrow \Omega^2 = \frac{GM}{R^3}$, a Keplerian orbit. Writing $\vec{v} = 0 + \vec{\delta v}$ and $p = p_0 + \delta p$, our equations to linear order in δ are

$$\left(\frac{\partial}{\partial t} + \Omega\frac{\partial}{\partial\varphi}\right)\delta v_R - 2\Omega\,\delta v_\varphi = -\frac{1}{\rho}\frac{\partial}{\partial R}\delta p,$$

$$\left(\frac{\partial}{\partial t} + \Omega\frac{\partial}{\partial\varphi}\right)\delta v_\varphi + 2\Omega\,\delta v_R + \frac{d\Omega}{d\ln R}\delta v_R = -\frac{1}{\rho}\frac{1}{R}\frac{\partial\,\delta p}{\partial\varphi}.$$

For simplicity, let us neglect the $\partial/\partial\varphi$ derivatives and let $\delta \sim \exp(-i\omega t + i k_R R + i k_z z)$. Then, with

$\vec{\nabla}\cdot\vec{\delta v} = 0 \Rightarrow k_R \delta v_R = -k_z \delta v_z$ and $\frac{\partial}{\partial t}\delta v_z = -\frac{1}{\rho}\frac{\partial}{\partial z}\delta p$,

we find $\frac{\delta p}{\rho} = -\frac{k_R}{k_z^2}\omega\,\delta v_R$ and so

$$\begin{bmatrix} -i\omega \frac{k^2}{k_z^2} & -2\Omega \\ \frac{\kappa^2}{2\Omega} & -i\omega \end{bmatrix}\begin{bmatrix} \delta v_R \\ \delta v_\varphi \end{bmatrix} = 0 \Rightarrow \boxed{\omega^2 = \frac{k_z^2}{k^2}\kappa^2}$$

$\frac{\kappa^2}{2\Omega} = 2\Omega + \frac{d\Omega}{d\ln R}$

Same stability criterion as before, $\kappa^2 > 0$.

Physically, what's going on? Take a fluid element at orbit #1 and displace it outwards to orbit #2 while maintaining a constant ang. momentum. Since $\ell_2 > \ell_1$, the fluid element cannot stay in its new orbit and must return back to orbit #1.

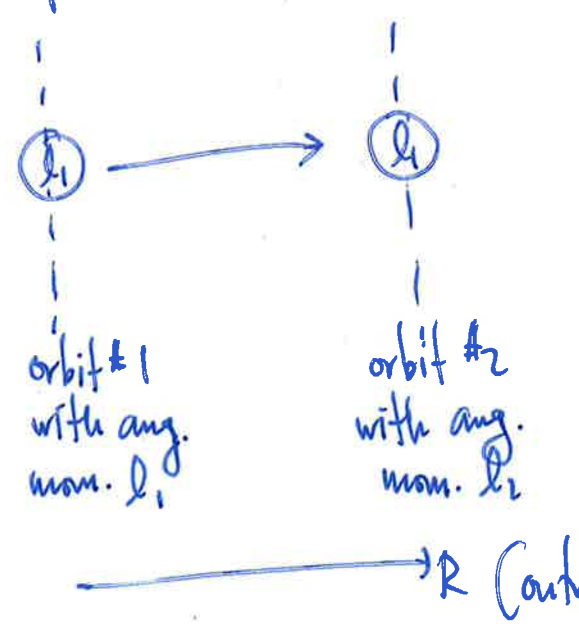

$\Rightarrow$ STABLE.

Now, back to 1991 ...

Steve Balbus and John Hawley, then both at Univ. of Virginia, found by a straightforward linear analysis and clever use of 90's supercomputers, that a small but finite magnetic field is all that is required to linearly destabilize Keplerian rotation. How could this be missed? The answer is complicated. The instability — at first known as the "Balbus–Hawley instability" but now goes by the moniker "magnetorotational instability" (MRI) — appeared in a little-known Russian paper by Velikhov in 1959, and 2 years later made its way into Chandrasekhar's classic text on "hydrodynamic and hydromagnetic stability". But there it appeared in a rather odd guise, at least to an astronomer thinking about accretion disks — Couette flow, i.e., rotational flow excited by placing a (conducting) fluid between two cylindrical walls rotating at different speeds. It wasn't until B&H rediscovered it and placed it in the astrophysical context that the instability became appreciated as a possible solution to the accretion problem. What followed was an industry of linear analysis and nonlinear numerical simulations aiming to characterize the MRI in a wide variety of disk systems. But let's go back to the beginning:

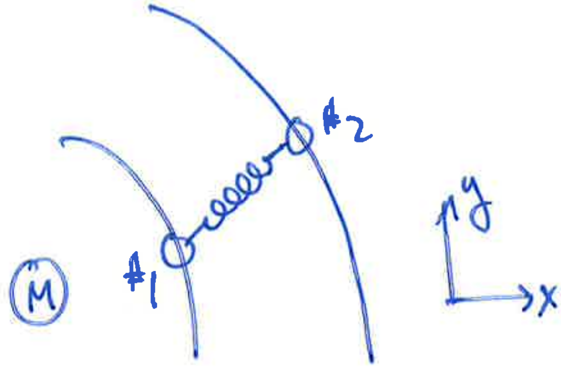

Take the Hill system but attach a spring between the two masses — magnetic fields act as springs, so you can imagine this being a field line threading two fluid elements. Add Hooke's law to the eqns. of motion:

$$\ddot{x} - 2\Omega\dot{y} = -\frac{d\Omega^2}{d\ln R}x - Kx$$

$$\ddot{y} + 2\Omega\dot{x} = -Ky$$

w/ K = spring constant

$x, y \sim e^{-i\omega t}$ $\Rightarrow \begin{bmatrix} -\omega^2 + \frac{d\Omega^2}{d\ln R} + K & 2\Omega i\omega \\ -2\Omega i\omega & -\omega^2 + K \end{bmatrix} \begin{bmatrix} x \\ y \end{bmatrix} = 0$

$$\Rightarrow \left(\omega^2 - \frac{d\Omega^2}{d\ln R} - K\right)\left(\omega^2 - K\right) = 4\Omega^2\omega^2$$

$$\Rightarrow \left(\omega^2 - \underbrace{K}_{\text{extra}}\right)\left(\omega^2 - \underbrace{K}_{\text{extra}} - 4\Omega^2 - \frac{d\Omega^2}{d\ln R}\right) = 4\Omega^2 \underbrace{K}_{\text{extra}}$$

Solutions are $\omega^2 - K = \frac{\kappa^2}{2} \pm \sqrt{\left(\frac{\kappa^2}{2}\right)^2 + 4\Omega^2 K}$,

whose $(-)$ solution is unstable if $\boxed{K + \frac{d\Omega^2}{d\ln R} < 0}$

This is important, because Keplerian disks have $\frac{d\Omega^2}{d\ln R} < 0$! Note that the spring cannot be too strong here. Interestingly,

$$\boxed{\frac{d\ell^2}{d\ln R} > 0 \text{ for hydro stability} \longrightarrow \frac{d\Omega^2}{d\ln R} > 0 \text{ for MHD stability}}$$

One can show that the Lagrangian change in the ang. mom. of a fluid element as it is displaced is given by

$$\frac{\Delta \ell}{\ell} = \frac{x}{R}\left(\frac{\kappa^2}{2\Omega^2} - \frac{i\omega}{\Omega}\frac{y}{x}\right)$$

$$= -\frac{x}{R}\left(\frac{2K}{\omega^2 - K}\right)$$

the spring broke conservation of angular momentum!

If $K \ll |\omega^2| \sim \Omega^2$, then outward displacements $(x>0)$ gain angular momentum as they are torqued by the spring (NB: $\omega^2 < 0$ corresponds to growth, so $\Delta \ell \propto (x/R)$).

At max. growth (take $\frac{\partial}{\partial K}$ of disp. relation and find extrema of ω^2), the growth rate $-i\omega = \frac{1}{2}\left|\frac{d\Omega}{d\ln R}\right|$ and

$$\left.\frac{\Delta l}{l}\right|_{max} = \frac{2x}{R}\left(1 - \frac{1}{4}\left|\frac{d\Omega}{d\ln R}\right|\right).$$

Now the fluid picture: (let $\vec{B}_0 = B_0\hat{z}$ for simplicity)

$$\left(\frac{\partial}{\partial t} + \Omega\frac{\partial}{\partial\varphi}\right)\delta v_R - 2\Omega\,\delta v_\varphi = -\frac{1}{\rho}\frac{\partial}{\partial R}\left(\delta p + \frac{\vec{B}_0\cdot\delta\vec{B}}{4\pi}\right) + \frac{\vec{B}_0\cdot\vec{\nabla}\,\delta B_R}{4\pi\rho},$$

$$\left(\frac{\partial}{\partial t} + \Omega\frac{\partial}{\partial\varphi}\right)\delta v_\varphi + \frac{\kappa^2}{2\Omega}\,\delta v_R = -\frac{1}{\rho}\frac{1}{R}\frac{\partial}{\partial\varphi}\left(\delta p + \frac{\vec{B}_0\cdot\delta\vec{B}}{4\pi}\right) + \frac{\vec{B}_0\cdot\vec{\nabla}\,\delta B_\varphi}{4\pi\rho}.$$

We need equs. for δB_R and δB_φ (δB_z is determined from $\vec{\nabla}\cdot\delta\vec{B} = 0$). So, take the induction equ. and write it in cylindrical coordinates w/ $\vec{u} = \vec{v} + R\Omega\hat{\varphi}$:

$$\left(\vec{B}\cdot\vec{\nabla}\vec{u} = \hat{e}_i\,\vec{B}\cdot\vec{\nabla}v_i + \frac{v_R B_\varphi}{R}\hat{\varphi} - \frac{v_\varphi B_\varphi}{R}\hat{R} - \Omega B_\varphi\hat{R} + \hat{\varphi}B_R\left(\Omega + \frac{d\Omega}{d\ln R}\right)\right)$$

$$\Rightarrow \left(\frac{\partial}{\partial t} + \Omega\frac{\partial}{\partial\varphi}\right)\delta B_R = \vec{B}_0\cdot\vec{\nabla}\,\delta v_R,$$

$$\left(\frac{\partial}{\partial t} + \Omega\frac{\partial}{\partial\varphi}\right)\delta B_\varphi = \vec{B}_0\cdot\vec{\nabla}\,\delta v_\varphi + \delta B_R\frac{d\Omega}{d\ln R}.$$

Again, take $\partial/\partial\varphi = 0$ and let $\delta \sim \exp\left(-i\omega t + ik_R R + ik_z z\right)$.

$$\left.\begin{aligned} \vec{\nabla}\cdot\vec{\delta v} = 0 &\longrightarrow \delta v_z = -\frac{k_R}{k_z}\,\delta v_R \\ \vec{\nabla}\cdot\vec{\delta B} = 0 &\longrightarrow \delta B_z = -\frac{k_R}{k_z}\,\delta B_R \end{aligned}\right\} \quad \frac{\partial}{\partial t}\delta v_z = -\frac{1}{\rho}\frac{\partial}{\partial z}\left(\delta p + \frac{\vec{B}_0\cdot\vec{\delta B}}{4\pi}\right) + \frac{\vec{B}_0\cdot\vec{\nabla}\,\delta B_z}{4\pi\rho}$$

$$\Rightarrow \frac{\delta p}{\rho} + \frac{\vec{B}_0\cdot\vec{\delta B}}{4\pi\rho} = \frac{-\omega k_R}{k_z^2}\delta v_R - \frac{\vec{k}\cdot\vec{B}_0}{4\pi\rho}\frac{k_R}{k_z^2}\delta B_R$$

$$\Rightarrow \left\{\begin{aligned} -i\omega\,\delta v_R - 2\Omega\,\delta v_\varphi &= -ik_R\left[-\frac{\omega k_R}{k_z^2}\delta v_R - \frac{\vec{k}\cdot\vec{B}_0}{4\pi\rho}\frac{k_R}{k_z^2}\delta B_R\right] + \frac{i\vec{k}\cdot\vec{B}_0}{4\pi\rho}\delta B_R \\ -i\omega\,\delta v_\varphi + \frac{\kappa^2}{2\Omega}\delta v_R &= \frac{i\vec{k}\cdot\vec{B}_0}{4\pi\rho}\delta B_\varphi \end{aligned}\right.$$

$$\Rightarrow \left\{\begin{aligned} -i\omega\frac{k^2}{k_z^2}\delta v_R - 2\Omega\,\delta v_\varphi &= \frac{i\vec{k}\cdot\vec{B}_0}{4\pi\rho}\frac{k^2}{k_z^2}\delta B_R \\ \frac{\kappa^2}{2\Omega}\delta v_R - i\omega\,\delta v_\varphi &= \frac{i\vec{k}\cdot\vec{B}_0}{4\pi\rho}\delta B_\varphi \end{aligned}\right.$$

and
$$\left\{\begin{aligned} -i\omega\,\delta B_R &= i\vec{k}\cdot\vec{B}_0\,\delta v_R \\ -i\omega\,\delta B_\varphi &= i\vec{k}\cdot\vec{B}_0\,\delta v_\varphi + \delta B_R\frac{d\Omega}{d\ln R} \end{aligned}\right\}$$

solve these for $\vec{\delta v}$ and plug into these

$$\left[\begin{array}{l} -i\omega \dfrac{k^2}{k_z^2}\left(\dfrac{-i\omega\, \delta B_R}{i\mathbf{k}\cdot\mathbf{B}_0}\right) - 2\Omega\left(\dfrac{-i\omega\,\delta B_\phi - \delta B_R\, d\Omega/d\ln R}{i\mathbf{k}\cdot\mathbf{B}_0}\right) = \dfrac{i\mathbf{k}\cdot\mathbf{B}_0}{4\pi\rho}\dfrac{k^2}{k_z^2}\,\delta B_R \\[3ex] \dfrac{\kappa^2}{2\Omega}\left(\dfrac{-i\omega\,\delta B_R}{i\mathbf{k}\cdot\mathbf{B}_0}\right) - i\omega\left(\dfrac{-i\omega\,\delta B_\phi - \delta B_R\, d\Omega/d\ln R}{i\mathbf{k}\cdot\mathbf{B}_0}\right) = \dfrac{i\mathbf{k}\cdot\mathbf{B}_0}{4\pi\rho}\,\delta B_\phi \end{array}\right.$$

Cleaning up...

$$\begin{bmatrix} -\omega^2 + (\mathbf{k}\cdot\mathbf{v}_A)^2 - \dfrac{k_z^2}{k^2}\dfrac{d\Omega^2}{d\ln R} & 2\Omega i\omega\dfrac{k_z^2}{k^2} \\[2ex] -2\Omega i\omega & -\omega^2 + (\mathbf{k}\cdot\mathbf{v}_A)^2 \end{bmatrix}\begin{bmatrix} \delta B_R \\[2ex] \delta B_\phi \end{bmatrix} = 0.$$

Look familiar? $K \rightarrow (\mathbf{k}\cdot\mathbf{v}_A)^2$! Magnetic tension is a spring. Dispersion relation:

$$\left[\omega^2 - (\mathbf{k}\cdot\mathbf{v}_A)^2\right]\left[\omega^2 - (\mathbf{k}\cdot\mathbf{v}_A)^2 - \kappa^2\frac{k_z^2}{k^2}\right] = 4\Omega^2(\mathbf{k}\cdot\mathbf{v}_A)^2$$

$$\Rightarrow \quad \omega^2 - (\mathbf{k}\cdot\mathbf{v}_A)^2 = \frac{\kappa^2}{2} \pm \sqrt{\left(\frac{\kappa^2}{2}\right)^2 + 4\Omega^2(\mathbf{k}\cdot\mathbf{v}_A)^2}$$

unstable if $\boxed{(\mathbf{k}\cdot\mathbf{v}_A)^2 + \dfrac{d\Omega^2}{d\ln R} < 0}$

Note: Can write discriminant as $\left[\dfrac{\kappa^2}{2} + (\mathbf{k}\cdot\mathbf{v}_A)^2\right]^2 - (\mathbf{k}\cdot\mathbf{v}_A)^2\left[(\mathbf{k}\cdot\mathbf{v}_A)^2 + \kappa^2 - 4\Omega^2\right]$

$$= \left[\frac{\kappa^2}{2} + (\mathbf{k}\cdot\mathbf{v}_A)^2\right]^2 - (\mathbf{k}\cdot\mathbf{v}_A)^2\left[(\mathbf{k}\cdot\mathbf{v}_A)^2 + \frac{d\Omega^2}{d\ln R}\right]$$

This means Keplerian disks are linearly unstable, provided the magnetic field isn't so strong that all the wavenumbers $k_z = 2\pi/\lambda_z$ that can fit within the height of the disk satisfy $k_z^2 v_{Az}^2 > \left|\frac{d\Omega^2}{d\ln R}\right|$ — then tension stabilizes all relevant modes.

See Balbus & Hawley 1998 Rev. Mod. Phys. for more.

VI.9. Instabilities of a pinch

Turning now towards more fusion-relevant equilibria, we consider the stability of the Z-pinch and θ-pinch. Because they are both cylindrical configurations but with differing magnetic geometries, we'll keep our equations general at first. In this sense, we'll be targeting the stability of a screw pinch. But the fully general equations get rather unwieldy, and simplifications will have to be made to obtain analytic solutions that are physically informative. It will help to keep the Parker instability calculation in the back of your head, because it's similar except for the cylindrical geometry. Speaking of cylindrical geometry, we must be careful because the unit vectors in this coordinate system depend on space; for example,

$$\boldsymbol{B}\cdot\boldsymbol{\nabla}\boldsymbol{A} = \hat{\boldsymbol{e}}_i\boldsymbol{B}\cdot\boldsymbol{\nabla}A_i - \frac{B_\varphi A_\varphi}{R}\hat{\boldsymbol{R}} + \frac{B_\varphi A_R}{R}\hat{\boldsymbol{\varphi}}$$

for some vector $\boldsymbol{A}$. It is because of these extra curvature terms that the equilibrium configuration must account for the hoop stress:

$$0 = -\frac{\mathrm{d}}{\mathrm{d}R}\left(P + \frac{B_\varphi^2 + B_z^2}{8\pi}\right) - \frac{B_\varphi^2}{4\pi R} = -\frac{\mathrm{d}}{\mathrm{d}R}\left(P + \frac{B_z^2}{8\pi}\right) - \frac{B_\varphi}{4\pi R}\frac{\partial(RB_\varphi)}{\partial R}. \tag{VI.9.1}$$

To remind you: $B_z = 0$ and $B_\varphi = B_\varphi(R)$ gives the standard Z-pinch; $B_z = B_z(R)$ and $B_\varphi = 0$ gives the standard θ-pinch; and the combination of them gives a screw pinch.

Equipped with an equilibrium state, we allow perturbations in all quantities:

$$\rho = \rho(R) + \delta\rho, \quad P = P(R) + \delta P, \quad \boldsymbol{B} = B_\varphi(R)\hat{\boldsymbol{\varphi}} + B_z(R)\hat{\boldsymbol{z}} + \delta\boldsymbol{B}, \quad \boldsymbol{u} = \delta\boldsymbol{u} = \frac{\mathrm{D}\boldsymbol{\xi}}{\mathrm{D}t}.$$

The calculation proceeds much as in the Parker instability. The perturbed momentum equation governing the evolution of the displacement vector $\boldsymbol{\xi}$ is (see (V.2.10))

$$\rho\frac{\mathrm{D}^2\boldsymbol{\xi}}{\mathrm{D}t^2} = -\boldsymbol{\nabla}\left(\delta P + \frac{\boldsymbol{B}\cdot\delta\boldsymbol{B}}{4\pi}\right) + \frac{\delta\boldsymbol{B}\cdot\boldsymbol{\nabla}\boldsymbol{B}}{4\pi} + \frac{\boldsymbol{B}\cdot\boldsymbol{\nabla}\delta\boldsymbol{B}}{4\pi}.$$

We take all perturbations δ to have the form $\delta(R)\exp(-\mathrm{i}\omega t + \mathrm{i}\boldsymbol{k}\cdot\boldsymbol{r})$ with the wavevector $\boldsymbol{k} = (m/R)\hat{\boldsymbol{\varphi}} + k_z\hat{\boldsymbol{z}}$. Accounting for the curvature terms arising from $\boldsymbol{B}\cdot\boldsymbol{\nabla}\delta\boldsymbol{B}$, this equation written in component form provides

$$-\omega^2\xi_R = -\frac{1}{\rho}\frac{\mathrm{d}}{\mathrm{d}R}\left(\delta P + \frac{\boldsymbol{B}\cdot\delta\boldsymbol{B}}{4\pi}\right) - \frac{2B_\varphi\delta B_\varphi}{4\pi\rho R} + \frac{\mathrm{i}(\boldsymbol{k}\cdot\boldsymbol{B})}{4\pi\rho}\delta B_R, \tag{VI.9.2a}$$

$$-\omega^2\xi_\varphi = -\frac{\mathrm{i}m}{\rho R}\left(\delta P + \frac{\boldsymbol{B}\cdot\delta\boldsymbol{B}}{4\pi}\right) + \frac{\delta B_R}{4\pi\rho R}\frac{\mathrm{d}}{\mathrm{d}R}(RB_\varphi) + \frac{\mathrm{i}(\boldsymbol{k}\cdot\boldsymbol{B})}{4\pi\rho}\delta B_\varphi, \tag{VI.9.2b}$$

$$-\omega^2\xi_z = -\frac{\mathrm{i}k_z}{\rho}\left(\delta P + \frac{\boldsymbol{B}\cdot\delta\boldsymbol{B}}{4\pi}\right) + \frac{\delta B_R}{4\pi\rho}\frac{\mathrm{d}B_z}{\mathrm{d}R} + \frac{\mathrm{i}(\boldsymbol{k}\cdot\boldsymbol{B})}{4\pi\rho}\delta B_z. \tag{VI.9.2c}$$

The linearized induction equation $\delta\boldsymbol{B} = \boldsymbol{\nabla}\times(\boldsymbol{\xi}\times\boldsymbol{B})$ written in component form is

$$\delta B_R = \mathrm{i}(\boldsymbol{k}\cdot\boldsymbol{B})\xi_R, \tag{VI.9.3a}$$

$$\delta B_\varphi = \mathrm{i}(\boldsymbol{k}\cdot\boldsymbol{B})\xi_\varphi - \xi_R R\frac{\mathrm{d}}{\mathrm{d}R}\left(\frac{B_\varphi}{R}\right) - B_\varphi(\boldsymbol{\nabla}\cdot\boldsymbol{\xi}), \tag{VI.9.3b}$$

$$\delta B_z = \mathrm{i}(\boldsymbol{k}\cdot\boldsymbol{B})\xi_z - \xi_R\frac{\mathrm{d}B_z}{\mathrm{d}R} - B_z(\boldsymbol{\nabla}\cdot\boldsymbol{\xi}). \tag{VI.9.3c}$$

Finally, the perturbed gas pressure satisfies

$$\delta P = -\xi_R\frac{\mathrm{d}P}{\mathrm{d}R} - \gamma P(\boldsymbol{\nabla}\cdot\boldsymbol{\xi}), \tag{VI.9.4}$$

which when combined with the perturbed magnetic pressure results in

$$\frac{1}{\rho}\left(\delta P+\frac{\boldsymbol{B}\cdot\delta\boldsymbol{B}}{4\pi}\right)=\mathrm{i}(\boldsymbol{k}\cdot\boldsymbol{v}_{\mathrm{A}})(\boldsymbol{v}_{\mathrm{A}}\cdot\boldsymbol{\xi})+v_{\mathrm{A}\varphi}^2\frac{2\xi_R}{R}-\left(c_{\mathrm{s}}^2+v_{\mathrm{A}}^2\right)(\boldsymbol{\nabla}\cdot\boldsymbol{\xi}), \tag{VI.9.5}$$

where $c_{\mathrm{s}}^2 \doteq \gamma P/\rho$, $v_{\mathrm{A}}^2 \doteq B^2/4\pi\rho$, and $v_{\mathrm{A}\varphi}^2 \doteq B_\varphi^2/4\pi\rho$. The reason we have left the compressibility

$$\boldsymbol{\nabla}\cdot\boldsymbol{\xi}=\frac{1}{R}\frac{\mathrm{d}(R\xi_R)}{\mathrm{d}R}+\mathrm{i}(\boldsymbol{k}\cdot\boldsymbol{\xi}) \tag{VI.9.6}$$

unexpanded in (VI.9.2)–(VI.9.5) is because one of the limits we will take is the incompressible limit, in which $\boldsymbol{\nabla}\cdot\boldsymbol{\xi}=0$. Keeping this term compact will make it easy to drop later.

As declared at the start of this section, the calculation that follows by combining (VI.9.2)–(VI.9.6) is rather long and, as far as I can tell, is analytically intractable in full generality, at least without prescribing a particularly simple magnetic-field profile and some restricted set of radial boundary conditions. (The general screw-pinch eigenmode equation is called the "Hain–Lüst equation"; Hain & Lüst 1958.) There are, however, some limiting cases in which analytic progress can be made (with some effort). These are:

(i) axisymmetry, $m=0$. This eliminates an important instability called the "kink instability", but simplifies the algebra and allows us to derive an important instability generally referred to as the "sausage instability". Note that, for $B_z=0$, $m=0$ implies $k_\parallel=0$ – such a perturbation is customarily referred to as a 'flute mode', because cylindrical magnetic flux tubes subject to such perturbations resemble fluted columns popular in Greek and Roman architecture.

(ii) incompressibility, $\boldsymbol{\nabla}\cdot\boldsymbol{\xi}=0$. This limit eliminates the sausage instability, but otherwise often filters out all but the fastest-growing instabilities.

(iii) $v_{\mathrm{A}\varphi}=AR$, $v_{\mathrm{A}z}=\mathrm{const}$, $\rho=\mathrm{const}$. In this restrictive case, the equilibrium satisfies $\mathrm{d}\ln B_\varphi/\mathrm{d}\ln R=1$ and $P(R)=P_S+A^2(R_S^2-R^2)$ where the subscript 'S' denotes the values at the surface of the cylinder. Note that the combination $\boldsymbol{k}\cdot\boldsymbol{v}_{\mathrm{A}}$ is constant in this case, which simplifies the mathematics a great deal.

(iv) $v_{\mathrm{A}\varphi}=0$, for which the equilibrium is $P+B_z^2/8\pi=\mathrm{const}$ – the classic θ-pinch.

These calculations follow in the hand-written notes. One of the lessons here is that continuing to take the route we've been taking – assessing stability by linearizing, calculating the dispersion relation, and examining the eigenvectors – is becoming an increasingly tedious exercise. If all one is concerned about is stability or lack thereof, there is a much faster way, which follows in the next section.

$$\hat{R}: \quad -\omega^2 \rho \xi_R = -\frac{d}{dR}\delta\Pi + \frac{B\cdot ik}{4\pi}\delta B_R - \frac{2B_\varphi \delta B_\varphi}{4\pi R}$$

$$= -\frac{d}{dR}\delta\Pi - \frac{(k\cdot B)^2}{4\pi}\xi_R - \frac{2B_\varphi}{4\pi R}\Big[-\xi_R B_\varphi' + ik\cdot B\,\xi_\varphi + \frac{B_\varphi \xi_R}{R} - B_\varphi D\cdot\xi\Big]$$

$$\Big[-\omega^2 + (k\cdot V_A)^2 - \frac{2V_{A\varphi}^2}{R^2}\frac{d\ln B_\varphi}{d\ln R} + \frac{2V_{A\varphi}^2}{R^2}\Big]\xi_R$$

$$= \frac{-1}{\rho}\frac{d}{dR}\delta\Pi - 2V_{A\varphi}\, ik\cdot V_A \frac{\xi_\varphi}{R} + \frac{2V_{A\varphi}^2}{R} D\cdot\xi$$

$$\hat{\varphi}: \quad -\omega^2\rho\xi_\varphi = -\frac{im}{R}\delta\Pi + \frac{ik\cdot B}{4\pi}\delta B_\varphi + \frac{\delta B_R}{4\pi}B_\varphi' + \frac{B_\varphi \delta B_R}{4\pi R}$$

$$= -\frac{im}{R}\delta\Pi + \frac{ik\cdot B}{4\pi}\Big[\cancel{-\xi_R B_\varphi'} + ik\cdot B\,\xi_\varphi + \frac{B_\varphi \xi_R}{R} - B_\varphi D\cdot\xi\Big]$$

$$+ \cancel{\frac{ik\cdot B}{4\pi}\xi_R B_\varphi'} + \frac{B_\varphi}{4\pi R} ik\cdot B\,\xi_R$$

$$\Big[-\omega^2 + (k\cdot V_A)^2\Big]\xi_\varphi = -\frac{im}{\rho R}\delta\Pi + 2ik\cdot V_A V_{A\varphi}\frac{\xi_R}{R} - ik\cdot V_A V_{A\varphi} D\cdot\xi$$

$$\hat{z}: \quad -\omega^2\rho\xi_z = -ik_z\delta\Pi + \frac{ik\cdot B}{4\pi}\delta B_z + \frac{\delta B_R}{4\pi}B_z'$$

$$= -ik_z\delta\Pi + \frac{ik\cdot B}{4\pi}\Big[\cancel{-\xi_R B_z'} + ik\cdot B\,\xi_z - B_z \vec{D}\cdot\vec{\xi}\Big]$$

$$+ \cancel{\frac{ik\cdot B}{4\pi}\xi_R B_z'}$$

$$\Big[-\omega^2 + (k\cdot V_A)^2\Big]\xi_z = -\frac{ik_z}{\rho}\delta\Pi - ik\cdot V_A V_{Az} D\cdot\xi$$

$\boxed{\text{Axisymmetry, } m=0}$ $\quad k\cdot V_A = k_z V_{Az}, \quad \nabla\cdot\xi = \frac{1}{R}(R\xi_R)' + ik_z\xi_z$

$$\left[-\omega^2 + (k\cdot V_A)^2 + \frac{2V_{A\varphi}^2}{R^2}\left(1 - \frac{d\ln B_\varphi}{d\ln R}\right)\right]\xi_R = -\frac{1}{\rho}\frac{d}{dR}\delta\Pi - 2V_{A\varphi}\, i k\cdot V_A \frac{\xi_\varphi}{R}$$
$$+ \frac{2V_{A\varphi}^2}{R}\left[\frac{1}{R}(R\xi_R)' + ik_z\xi_z\right]$$

$$\left[-\omega^2 + (k\cdot V_A)^2\right]\xi_\varphi = 2ik\cdot V_A V_{A\varphi}\frac{\xi_R}{R} - ik\cdot V_A V_{A\varphi}\left[\frac{1}{R}(\xi_R R)' + ik_z\xi_z\right]$$

$$\left[-\omega^2 + (k\cdot V_A)^2\right]\xi_z = -ik_z\frac{\delta\Pi}{\rho} - ik\cdot V_A V_{Az}\left[\frac{1}{R}(R\xi_R)' + ik_z\xi_z\right]$$

$$\frac{\delta\Pi}{\rho} = -(a^2+V_A^2)\left[\frac{1}{R}(R\xi_R)' + ik_z\xi_z\right] + 2\xi_R\frac{V_{A\varphi}^2}{R} + ik\cdot V_A V_A\cdot\xi$$

$$\xi_\varphi = \frac{ik\cdot V_A V_{A\varphi}}{(-\varpi^2)}\frac{\xi_R}{R} - \frac{ik\cdot V_A V_{A\varphi}}{(-\varpi^2)}\xi_R' + \frac{k_z V_{A\varphi}\, k\cdot V_A}{(-\varpi^2)}\xi_z$$

with $\varpi^2 \equiv \omega^2 - (k\cdot V_A)^2$

into
$$\frac{\delta\Pi}{\rho} = \left[-(a^2+V_A^2) + 2V_{A\varphi}^2\right]\frac{\xi_R}{R} - (a^2+V_A^2)\xi_R' + \left[\begin{array}{l}-ik_z(a^2+V_A^2)\\ \quad + ik\cdot V_A V_{Az}\end{array}\right]\xi_z$$
$$+ \frac{ik\cdot V_A V_{A\varphi}}{(-\varpi^2)}\left[ik\cdot V_A V_{A\varphi}\left(\frac{\xi_R}{R} - \xi_R'\right) + k_z V_{A\varphi}\, k\cdot V_A\,\xi_z\right]$$
$$= \left[-(a^2+V_A^2) + 2V_{A\varphi}^2 + \frac{(k\cdot V_A)^2 V_{A\varphi}^2}{\varpi^2}\right]\frac{\xi_R}{R}$$
$$+ \left[-(a^2+V_A^2) - \frac{(k\cdot V_A)^2 V_{A\varphi}^2}{\varpi^2}\right]\xi_R' + ik_z\left[\begin{array}{l}-(a^2+V_A^2) + k\cdot V_A V_{Az}/k_z\\ -(k\cdot V_A)^2 V_{A\varphi}^2/\varpi^2\end{array}\right]\xi_z$$

into ξ_z eqn:

$$-\varpi^2\xi_z = -ik_z\left\{\left[-(a^2+V_A^2) + 2V_{A\varphi}^2 + \frac{V_{A\varphi}^2(k\cdot V_A)^2}{\varpi^2}\right]\frac{\xi_R}{R}\right.$$
$$-\left[a^2+V_A^2+\frac{(k\cdot V_A)^2 V_{A\varphi}^2}{\varpi^2}\right]\xi_R'$$
$$\left.-ik_z\left[a^2+V_A^2+\frac{(k\cdot V_A)^2 V_{A\varphi}^2}{\varpi^2} - k\cdot V_A\frac{V_{Az}}{k_z}\right]\xi_z\right\}$$
$$+k_z k\cdot V_A V_{Az}\xi_z - ik\cdot V_A V_{Az}\frac{1}{R}\left(\xi_R + R\xi_R'\right)$$

$$\left[-\varpi^2 - k_z k\cdot V_A V_{Az} + k_z^2(a^2+V_A^2) + k_z^2(k\cdot V_A)^2\frac{V_{A\varphi}^2}{\varpi^2} - \frac{k_z^2}{k_z}k\cdot V_A V_{Az}\right]\xi_z$$

$$= \left[-\omega^2 + k_z^2a^2 + \frac{1}{\varpi^2}\left(\overset{\omega^2k_z^2V_{A\varphi}^2}{\cancel{\omega^2k_z^2V_A^2}} - \cancel{(k\cdot V_A)^2k_z^2V_A^2} + \cancel{k_z^2V_{A\varphi}^2(k\cdot V_A)^2} - \cancel{k_z k\cdot V_A V_{Az}\omega^2} + \cancel{(k\cdot V_A)^3k_zV_{Az}}\right)\right]\xi_z$$

$$= \left[-\omega^2 + k_z^2a^2 + \frac{\omega^2}{\varpi^2}k_z^2V_{A\varphi}^2\right]\xi_z = \frac{\xi_z}{\varpi^2}\left[\omega^2k_z^2V_{A\varphi}^2 + \omega^2k_z^2a^2 - (k\cdot V_A)^2k_z^2a^2 - \omega^4 + \omega^2(k\cdot V_A)^2\right]$$

$$= -\frac{\xi_z}{\varpi^2}\left[\omega^4 - \omega^2k_z^2(a^2+V_A^2) + k_z^2a^2(k\cdot V_A)^2\right]$$

$$= \frac{ik_z\xi_R'}{\varpi^2}\left[(k\cdot V_A)^2V_{A\varphi}^2 + \varpi^2(a^2+V_A^2) - \frac{k\cdot V_A V_{Az}\varpi^2}{k_z}\right] \leftarrow \omega^2V_{A\varphi}^2 + \varpi^2a^2$$

$$+\frac{ik_z}{\varpi^2}\frac{\xi_R}{R}\left[(a^2+V_A^2)\varpi^2 - 2V_{A\varphi}^2\varpi^2 - V_{A\varphi}^2(k\cdot V_A)^2 - \frac{k\cdot V_A V_{Az}\varpi^2}{k_z}\right] \leftarrow \varpi^2a^2 - \omega^2V_{A\varphi}^2$$

Define $\tilde{\omega}^4 \equiv \omega^4 - \omega^2 k_z^2 (a^2 + V_A^2) + k_z^2 a^2 (k \cdot V_A)^2$

$$\Rightarrow \xi_z = -\frac{\cancel{\varpi^2}}{\tilde{\omega}^4}\left(\omega^2 V_{A\varphi}^2 + \varpi^2 a^2\right) \frac{i k_z \xi_R'}{\cancel{\varpi^2}}$$

$$- \frac{\cancel{\varpi^2}}{\tilde{\omega}^4}\left(\varpi^2 a^2 - \omega^2 V_{A\varphi}^2\right) \frac{i k_z \xi_R}{\cancel{\varpi^2} R}$$

Back into $\delta\Pi$:

$$\frac{\delta\Pi}{\rho} = \Bigg[-(a^2 + V_A^2) + 2V_{A\varphi}^2 + \frac{(k\cdot V_A)^2 V_{A\varphi}^2}{\varpi^2}$$

$$- \frac{i k_z}{\varpi^2}\left(a^2\varpi^2 + V_{A\varphi}^2 \omega^2\right)\left(-\frac{i k_z}{\tilde{\omega}^4}\right)\left(\varpi^2 a^2 - \omega^2 V_{A\varphi}^2\right)\Bigg] \frac{\xi_R}{R}$$

$$+ \Bigg[-(a^2 + V_A^2) - \frac{(k\cdot V_A)^2 V_{A\varphi}^2}{\varpi^2}$$

$$- \frac{i k_z}{\varpi^2}\left(a^2\varpi^2 + V_{A\varphi}^2 \omega^2\right)\left(-\frac{i k_z}{\tilde{\omega}^4}\right)\left(\varpi^2 a^2 + \omega^2 V_{A\varphi}^2\right)\Bigg] \xi_R'$$

$$= \left[-(a^2 + V_{Az}^2) + \frac{\omega^2 V_{A\varphi}^2}{\varpi^2} - \frac{k_z^2}{\varpi^2}\left(\frac{a^4\varpi^4 - \omega^4 V_{A\varphi}^4}{\tilde{\omega}^4}\right)\right] \frac{\xi_R}{R}$$

$$+ \left[-(a^2 + V_{Az}^2) - \frac{\omega^2 V_{A\varphi}^2}{\varpi^2} - \frac{k_z^2}{\varpi^2}\frac{(a^2\varpi^2 + V_{A\varphi}^2\omega^2)^2}{\tilde{\omega}^4}\right] \xi_R'$$

into the ξ_R eqn:

$$\left[-\varpi^2 + \frac{2V_{A\varphi}^2}{R^2}\left(1-\frac{d\ln B_\varphi}{d\ln R}\right)\right]\xi_R$$

$$\frac{2V_{A\varphi}^2}{R}\, ik_z\xi_z\,\frac{\omega^2}{\varpi^2}$$

$$= \frac{2V_{A\varphi}^2}{R}\, ik_z\xi_z - 2ik\cdot V_A\frac{V_{A\varphi}}{R}\,\frac{k_z V_{A\varphi} k\cdot V_A}{(-\varpi^2)}\,\xi_z$$

$$- 2ik\cdot V_A\frac{V_{A\varphi}}{R}\,\frac{ik\cdot V_A V_{A\varphi}}{(-\varpi^2)}\left(\frac{\xi_R}{R}+\xi_R'\right) + \frac{2V_{A\varphi}^2}{R^2}\,(R\xi_R)'$$

$$-\frac{1}{\rho}\frac{d}{dR}\left(\rho\frac{\delta\Pi}{\rho}\right)$$

$$= \frac{2V_{A\varphi}^2}{R}\,\frac{ik_z\omega^2}{\varpi^2}\left(-\frac{ik_z}{\tilde\omega^4}\right)\left[\left(\omega^2V_{A\varphi}^2+\varpi^2a^2\right)\xi_R' + \left(\varpi^2a^2-\omega^2V_{A\varphi}^2\right)\frac{\xi_R}{R}\right]$$

$$+ \frac{2V_{A\varphi}^2}{R}\left[\xi_R' + \frac{\xi_R}{R}\right]\left[1-\frac{(k\cdot V_A)^2}{\varpi^2}\right]$$

$$-\left(\frac{1}{\rho}\frac{d\rho}{dR}+\frac{d}{dR}\right)\left\{\frac{\xi_R}{R}\left[-(a^2+V_{Az}^2)+\frac{\omega^2V_{A\varphi}^2}{\varpi^2}-\frac{k_z^2}{\varpi^2}\,\frac{a^4\varpi^4-\omega^4V_{A\varphi}^4}{\tilde\omega^4}\right]\right.$$

$$\left. + \xi_R'\left[-(a^2+V_{Az}^2)-\frac{\omega^2V_{A\varphi}^2}{\varpi^2}-\frac{k_z^2}{\varpi^2}\,\frac{(a^2\varpi^2+V_{A\varphi}^2\omega^2)^2}{\tilde\omega^4}\right]\right\}$$

$$\left[-\varpi^2 + \frac{2V_{A\varphi}^2}{R^2}\left(1-\frac{d\ln B_\varphi}{d\ln R}\right) - \frac{2V_{A\varphi}^2}{R^2}\left(1-\frac{(k\cdot V_A)^2}{\varpi^2}\right)\right.$$

$$\left. -\frac{2V_{A\varphi}^2}{R^2}\,\frac{k_z^2\omega^2}{\varpi^2\tilde\omega^4}\left(\varpi^2a^2-\omega^2V_{A\varphi}^2\right)\right]\xi_R$$

$$+\left[-\frac{2V_{A\varphi}^2}{R}\,\frac{k_z^2\omega^2}{\varpi^2\tilde\omega^4}\left(\omega^2V_{A\varphi}^2+\varpi^2a^2\right) - \frac{2V_{A\varphi}^2}{R}\left(1-\frac{(k\cdot V_A)^2}{\varpi^2}\right)\right]\xi_R'$$

$$= -\left(\frac{d\ln\rho}{dR}+\frac{d}{dR}\right)\left\{\ldots\right\}$$

Anticipate fastest-growing modes having $k_R \ll k_z$ w/ $\omega^2 \ll k_z^2(a^2+V_A^2)$. Then $\tilde{\omega}^4 \approx -k_z^2(a^2\varpi^2 + V_A^2\omega^2)$ ...

$$\left[-\varpi^2 + \frac{2V_{A\varphi}^2}{R^2}\left(-\frac{d\ln B_\varphi}{d\ln R} + \frac{(k\cdot V_A)^2}{\varpi^2} + \frac{\cancel{k_z^2}\,\omega^2(\varpi^2 a^2 - \omega^2 V_{A\varphi}^2)}{\varpi^2\cancel{k_z^2}(\varpi^2 a^2 + \omega^2 V_A^2)}\right)\right]\xi_R$$

$$+\left[-\frac{2V_{A\varphi}^2}{R}\right]\left[\frac{-\cancel{k_z^2}\,\omega^2(\omega^2 V_{A\varphi}^2 + \varpi^2 a^2)}{\varpi^2\cancel{k_z^2}(a^2\varpi^2 + V_A^2\omega^2)} + 1 - \frac{(k\cdot V_A)^2}{\varpi^2}\right]\xi_R'$$

$$\approx -\left(\frac{d\ln\rho}{dR} + \frac{d}{dR}\right)\left\{\frac{\xi_R}{R}\left[-(a^2+V_{Az}^2) + \frac{\omega^2 V_{A\varphi}^2}{\varpi^2} + \frac{a^4\varpi^4 - \omega^4 V_{A\varphi}^4}{\varpi^2(a^2\varpi^2 + V_A^2\omega^2)}\right]\right.$$

$$\left. + \xi_R'\left[-(a^2+V_{Az}^2) - \frac{\omega^2 V_{A\varphi}^2}{\varpi^2} + \frac{(a^2\varpi^2 + V_{A\varphi}^2\omega^2)^2}{\varpi^2(a^2\varpi^2 + V_A^2\omega^2)}\right]\right\}$$

(i) Take $B_z = 0$: in this case, $k\cdot V_A = 0$ and much simplifies...

$$\left[-\omega^2 + \frac{2V_{A\varphi}^2}{R^2}\left(-\frac{d\ln B_\varphi}{d\ln R} + \frac{a^2 - V_{A\varphi}^2}{a^2 + V_{A\varphi}^2}\right)\right]\xi_R + [0]\,\xi_R'$$

$$\approx -\left(\frac{d\ln\rho}{dR} + \frac{d}{dR}\right)\left\{\frac{\xi_R}{R}\left[-a^2 + V_{A\varphi}^2 + \frac{a^4 - V_{A\varphi}^4}{a^2 + V_A^2}\right]\right.$$

$$\left. + \xi_R'\left[-a^2 - V_{A\varphi}^2 + a^2 + V_{A\varphi}^2\right]\right\} = 0.$$

$$\Rightarrow \boxed{\begin{aligned}\omega^2 &\approx \frac{2V_{A\varphi}^2}{R^2}\left(-\frac{d\ln B_\varphi}{d\ln R} + \frac{a^2 - V_{A\varphi}^2}{a^2 + V_{A\varphi}^2}\right)\\ &= -\frac{2V_{A\varphi}^2}{R^2}\left(\frac{d\ln B_\varphi}{d\ln R} + \frac{1 - \beta\gamma/2}{1 + \beta\gamma/2}\right)\end{aligned}} \qquad \left(\beta \equiv \frac{2}{\gamma}\frac{a^2}{V_{A\varphi}^2}\right)$$

This mode is <u>stable</u> if

$$\frac{1-\beta\gamma/2}{1+\beta\gamma/2} \le -\frac{d\ln B_\varphi}{d\ln R}.$$

(Note that $\beta \to 0$, such that there is no plasma, says a wire's magnetic field $B_\varphi = I/2\pi R$ is stable.) If this criterion is not satisfied, instability is possible. What would this instability look like? Well, $\vec{\nabla}\cdot\vec{\xi} = \frac{1}{R}(R\xi_R)' + ik_z\xi_z$

$$= \frac{1}{R}(R\xi_R)' + \frac{k_z^2}{\tilde{\omega}^4}\left[\omega^2 v_{A\varphi}^2\left(\xi_R' - \frac{\xi_R}{R}\right) + \tilde{\omega}^2 c^2\left(\xi_R' + \frac{\xi_R}{R}\right)\right]$$

$$\approx \frac{2}{1+\beta\gamma/2}\frac{\xi_R}{R}$$ $\Rightarrow$ moving outwards dilutes the field, moving inwards compresses it.

and $\xi_z \sim \frac{i\xi_R}{k_z R} \ll \xi_R$

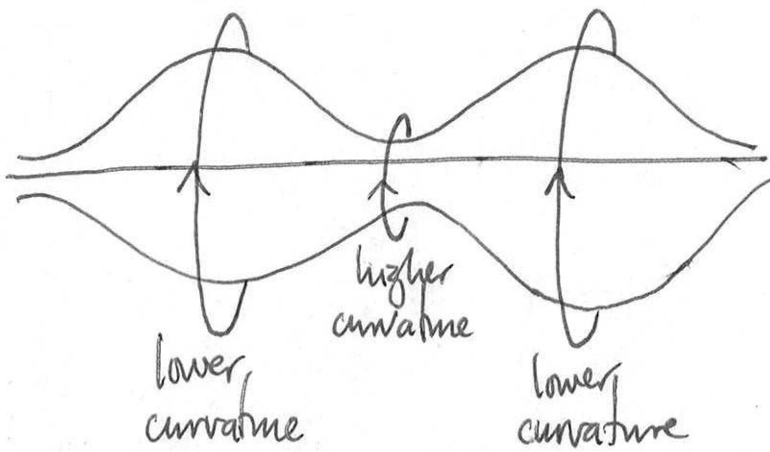

"Sausage instability"

necessary (but not sufficient) condition is

$$-\frac{d\ln B_\varphi}{d\ln R} < \frac{1-\beta\gamma/2}{1+\beta\gamma/2}$$

$\frac{\delta\Pi}{\rho} \approx 2v_{A\varphi}^2\xi_R'$ is small, meaning that the pressure can't compensate for the increased hoop stress in regions of higher curvature $\Rightarrow$ runs away.

(ii) $B_z^2/B_\varphi^2 \ll 1$ but $(k\cdot V_A)^2 \sim \frac{V_{A\varphi}^2}{R^2} \sim \omega^2$. In this limit, the RHS of our equation for ξ_R still goes to zero (this time, to $O(B_z/B_\varphi)^2$), and we get

$$\xi_R\left[-\varpi^2 + \frac{2V_{A\varphi}^2}{R^2}\left(-\frac{d\ln B_\varphi}{d\ln R} + \frac{(k\cdot V_A)^2}{\varpi^2} + \frac{\omega^2}{\varpi^2}\,\frac{\varpi^2 a^2 - \omega^2 V_{A\varphi}^2}{\varpi^2 a^2 + \omega^2 V_{A\varphi}^2}\right)\right]$$

$$-\frac{2V_{A\varphi}^2}{R^2}\left[-\frac{2(k\cdot V_A)^2}{\varpi^2}\right] R\xi_R' \approx 0$$

Drop ξ_R' by assuming $k_R R \ll \left(\frac{B_\varphi}{B_z}\frac{1}{k_z R}\right)^2$. Let

$$\omega_0^2 \equiv \frac{2V_{A\varphi}^2}{R^2}\left(-\frac{d\ln B_\varphi}{d\ln R} + \frac{a^2 - V_{A\varphi}^2}{a^2 + V_{A\varphi}^2}\right)$$ be the solution from

case (i). After some algebra,

$$\omega^2 \approx \underbrace{\omega_0^2}_{\text{if this is } <0 \text{ (unstable)}} + \underbrace{(k\cdot V_A)^2\left[1 + \frac{4V_{A\varphi}^2}{R^2}\frac{a^4}{(a^2+V_{A\varphi}^2)(\varpi^2 a^2+\omega^2 V_{A\varphi}^2)}\right]}_{\text{this is stabilizing}}$$

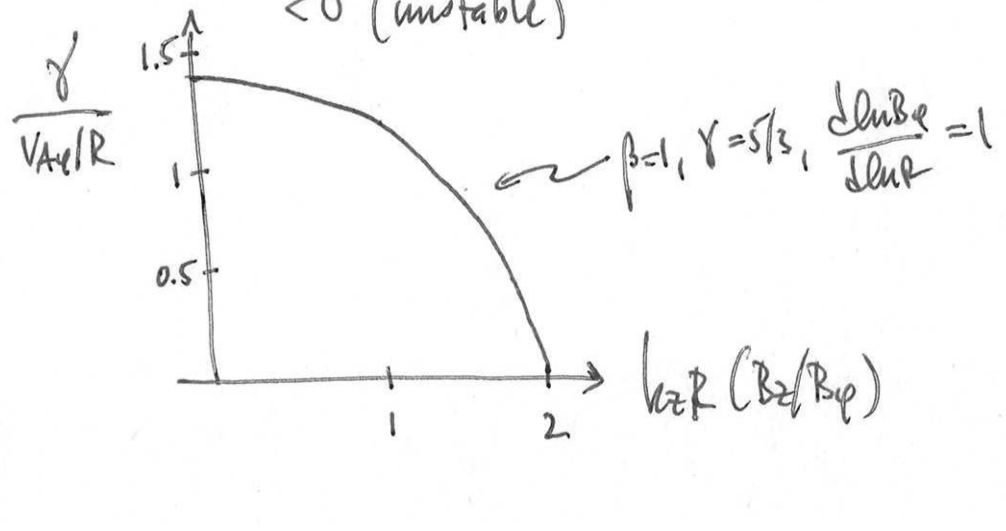

Note that the sausage can be stabilized by having B_z due to magn. tension.

$$\boxed{\text{Incompressible, } \vec{\nabla}\cdot\vec{\xi} = 0} \qquad \xi_z = -\frac{1}{R}\frac{d}{dR}(R\xi_R)\frac{1}{ik_z} - \frac{m}{k_z R}\xi_\varphi$$

$$\left[-\varpi^2 + \frac{2V_{A\varphi}^2}{R^2}\left(1 - \frac{d\ln B_\varphi}{d\ln R}\right)\right]\xi_R = -\frac{1}{\rho}\frac{d}{dR}\delta\Pi - 2i\,k\cdot V_A\,\frac{V_{A\varphi}}{R}\xi_\varphi$$

$$-\varpi^2\xi_\varphi = -\frac{im}{R}\frac{\delta\Pi}{\rho} + 2i\,k\cdot V_A\,V_{A\varphi}\frac{\xi_R}{R}$$

$$-\varpi^2\xi_z = -ik_z\frac{\delta\Pi}{\rho}$$

$$\nabla\cdot\xi = 0$$

$$+\frac{1}{R}(R\xi_R)' + \frac{im}{R}\xi_\varphi = \frac{k_z^2}{\varpi^2}\frac{\delta\Pi}{\rho}$$

$$-\varpi^2\xi_\varphi - 2i\,k\cdot V_A V_{A\varphi}\frac{\xi_R}{R} = \frac{-im}{R}\frac{\varpi^2}{k_z^2}\left[\frac{1}{R}(R\xi_R)' + \frac{im}{R}\xi_\varphi\right]$$

$$-\varpi^2\Big(\underbrace{1 + \frac{m^2}{k_z^2}}_{k^2/k_z^2}\Big)\xi_\varphi = 2i\,k\cdot V_A V_{A\varphi}\frac{\xi_R}{R} - \frac{im}{R}\frac{\varpi^2}{k_z^2}\frac{1}{R}(R\xi_R)'$$

Back into $\frac{\delta\Pi}{\rho}$: $\frac{1}{R}(R\xi_R)' + \frac{im}{R}\left[2i\,k\cdot V_A V_{A\varphi}\frac{\xi_R}{R} - \frac{im}{R}\frac{\varpi^2}{k_z^2}\frac{1}{R}(R\xi_R)'\right]$

$$\cdot\left[\frac{k_z^2}{k^2}\frac{1}{\varpi^2}(-1)\right]$$

$$= \frac{k_z^2}{\varpi^2}\frac{\delta\Pi}{\rho}$$

$$\Rightarrow \frac{\delta\Pi}{\rho} = \frac{\cancel{\varpi^2}}{\cancel{k_z^2}}\left(-\frac{\cancel{k_z^2}}{k^2}\right)\left(\frac{1}{\cancel{\varpi^2}}\right)\frac{m^2}{R^2}\frac{\varpi^2}{k_z^2}\xi_R' + \frac{\varpi^2}{k_z^2}\xi_R'$$

$$+\xi_R\left[\frac{\varpi^2}{k_z^2}\frac{\xi_R}{R} + \frac{1}{k^2}\frac{m}{R}2\,k\cdot V_A V_{A\varphi}\frac{\xi_R}{R} - \frac{1}{k^2}\frac{m^2}{R^2}\frac{\varpi^2}{k_z^2}\frac{\xi_R}{R}\right]$$

$$= \frac{\varpi^2}{\cancel{k_z^2}}\xi_R'\frac{\cancel{k_z^2}}{k^2} + \frac{\xi_R}{R}\left[\frac{\varpi^2}{\cancel{k_z^2}}\frac{\cancel{k_z^2}}{k^2} + \frac{2mV_{A\varphi}\,k\cdot V_A}{R k^2}\right]$$

into ξ_R equ:

$$\left[-\varpi^2 + \frac{2V_{A\varphi}^2}{R^2}\left(1 - \frac{d\ln B_\varphi}{d\ln R}\right)\right]\xi_R = -2i\,\mathbf{k}\cdot\mathbf{V}_A \frac{V_{A\varphi}}{R}\frac{k_z^2}{k^2}\left(-\frac{1}{\varpi^2}\right)$$

$$\cdot\left[2i\,\mathbf{k}\cdot\mathbf{V}_A V_{A\varphi}\frac{\xi_R}{R} - \frac{im\varpi^2}{R\,k_z^2}\left(\xi_R' + \frac{\xi_R}{R}\right)\right]$$

$$-\frac{1}{\rho}\frac{d}{dR}\left[\rho\left(\frac{\varpi^2}{k^2}\xi_R' + \frac{1}{k^2}\frac{\xi_R}{R}\left(\varpi^2 + \frac{2mV_{A\varphi}\mathbf{k}\cdot\mathbf{V}_A}{R}\right)\right)\right]$$

$$\left[-\varpi^2 + \frac{2V_{A\varphi}^2}{R^2}\left(1 - \frac{d\ln B_\varphi}{d\ln R}\right) + \frac{4(\mathbf{k}\cdot\mathbf{V}_A)^2}{\varpi^2}\frac{V_{A\varphi}^2}{R^2}\frac{k_z^2}{k^2} - \frac{2m}{R}\frac{1}{k^2}\frac{\mathbf{k}\cdot\mathbf{V}_A V_{A\varphi}}{R^2}\right.$$

$$\left.+\frac{1}{\rho}\frac{d}{dR}\left(\frac{\rho}{k^2 R}\left(\varpi^2 + \frac{2mV_{A\varphi}\mathbf{k}\cdot\mathbf{V}_A}{R}\right)\right)\right]\xi_R$$

$$= \left[\cancel{\frac{2m}{R}\mathbf{k}\cdot\mathbf{V}_A\frac{V_{A\varphi}}{R}\frac{k_z^2}{k^2}\frac{1}{k_z^2}} - \frac{1}{\rho}\frac{d}{dR}\left(\frac{\rho\varpi^2}{k^2}\right) - \frac{\varpi^2}{k^2 R}\right.$$

$$\left.-\cancel{\frac{2m}{R}V_{A\varphi}\mathbf{k}\cdot\mathbf{V}_A\frac{1}{k^2 R}}\right]\xi_R' - \frac{\varpi^2}{k^2}\xi_R''$$

$$\xi_R'' R^2 + \frac{k^2}{\varpi^2}R^2\xi_R'\left[\frac{\varpi^2}{k^2 R} + \frac{1}{\rho}\frac{d}{dR}\left(\frac{\rho\varpi^2}{k^2}\right)\right]$$

$$+\frac{k^2}{\varpi^2}R^2\xi_R\left[-\varpi^2 + \frac{2V_{A\varphi}^2}{R^2}\left(1 - \frac{d\ln B_\varphi}{d\ln R}\right) + \ldots\right] = 0.$$

Solving this for a general profile can only be done numerically, so we'll take two approaches:

(i) $k_R R \ll m \ll k_z R$, as in the Parker instability;

(ii) adopt a special profile. First, (i)...

$$\xi_R'' R^2 + \xi_R' R\left[1 + R\frac{d}{dR}\ln\left(\frac{\rho\varpi^2}{k^2}\right)\right]$$

$$+ \xi_R\left[-k^2R^2 + \frac{2k^2V_{A\varphi}^2}{\varpi^2}\left(1 - \frac{d\ln B_\varphi}{d\ln R} + \frac{2(k\cdot V_A)^2}{\varpi^2}\frac{k_z^2}{k^2}\right)\right.$$

$$- \frac{2m}{R}\frac{k\cdot V_A V_{A\varphi}}{\varpi^2} + R\frac{d}{dR}\ln\left(\frac{\rho\varpi^2}{k^2R}\right)$$

$$\left. + \frac{k^2R^2}{\varpi^2\rho}\frac{d}{dR}\left(\rho\frac{2m}{R}\frac{k\cdot V_A V_{A\varphi}}{k^2R}\right)\right] \simeq 0.$$

limit gives $$-1 + \frac{2V_{A\varphi}^2}{\varpi^2R^2}\left(1 - \frac{d\ln B_\varphi}{d\ln R} + \frac{2(k\cdot V_A)^2}{\varpi^2}\right) \simeq 0$$

$$\Rightarrow \varpi^4 - \varpi^2\frac{2V_{A\varphi}^2}{R^2}\left(1 - \frac{d\ln B_\varphi}{d\ln R}\right) - \frac{4V_{A\varphi}^2(k\cdot V_A)^2}{R^2} \simeq 0$$

$$\Rightarrow \omega^4 - \omega^2\left[\frac{2V_{A\varphi}^2}{R^2}\left(1 - \frac{d\ln B_\varphi}{d\ln R}\right) + 2(k\cdot V_A)^2\right]$$

$$+ (k\cdot V_A)^2\left[(k\cdot V_A)^2 - \frac{2V_{A\varphi}^2}{R^2}\left(1 + \frac{d\ln B_\varphi}{d\ln R}\right)\right] \simeq 0.$$

Clearly, the magnetic tension is stabilizing. Stability requires all coefficients to be ≥ 0. The more restrictive condition concerns C_0 $\Rightarrow$ $$(k\cdot V_A)^2 - \frac{2V_{A\varphi}^2}{R^2}\left(1 + \frac{d\ln B_\varphi}{d\ln R}\right) \geq 0$$

$$\Rightarrow \boxed{\frac{d\ln B_\varphi}{d\ln R} \leq \frac{R^2(\vec{k}\cdot\vec{V}_A)^2}{2V_{A\varphi}^2} - 1 \quad \text{STABLE}}$$

Most restrictive case is $B_z = 0$, in which case the RHS of this inequality $= \frac{m^2}{2} - 1$.

When this criterion is not satisfied, one may get the <u>kink instability</u>.

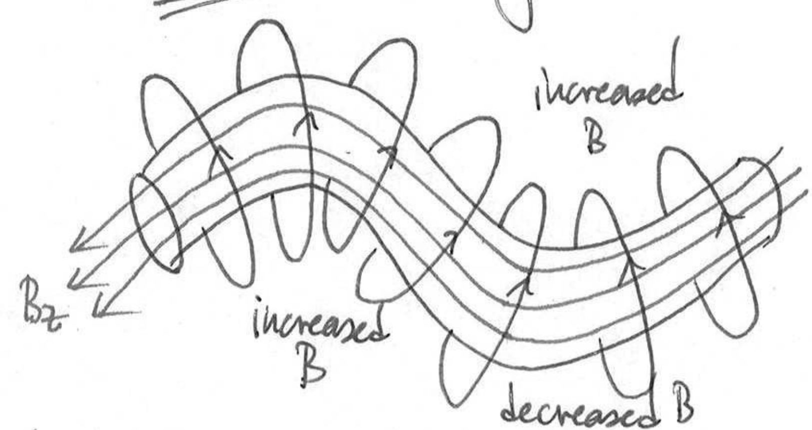

Flux surfaces are bent, with a twist to remain incompressible. The bending makes B go up (down) in the concave (convex) parts, which pushes the plasma in a way so as to amplify the perturbation.

Having a B_z is stabilizing via tension.

$$\xi_z = \frac{i k_z}{k^2}\left[\frac{2k\cdot v_A m v_{A\varphi}}{\varpi^2}\frac{\xi_R}{R} + \frac{1}{R}(R\xi_R)'\right]$$

$$\sim O\left(\frac{1}{k_z R}\right)\xi_R \ll \xi_R$$

$$\xi_\varphi = \frac{i m}{k^2 R}\left[\frac{-2k\cdot v_A m v_{A\varphi}}{\varpi^2}\frac{k_z^2 R^2}{m^2}\frac{\xi_R}{R} + \frac{1}{R}(R\xi_R)'\right] \simeq \frac{-2k\cdot v_A v_{A\varphi}}{\varpi^2} i\xi_R$$

$$\sim i\xi_R$$

Note: before the $k_R R \ll m \ll k_z R$ limit is taken, one can regroup terms to obtain

$$\frac{d}{dR}\left[\frac{\rho\varpi^2}{k^2 R}(R\xi_R)'\right] + \xi_R\left[\frac{\rho\varpi^2}{k^2R^2}(1 - k^2R^2) + R\frac{d}{dR}\left(\frac{2m\rho}{R}\frac{k\cdot v_A v_{A\varphi}}{k^2R^2}\right) + \frac{2\rho v_{A\varphi}^2}{R^2}\left(1 - \frac{d\ln B_\varphi}{d\ln R} + \frac{2k_\parallel^2 v_A^2 k_z^2}{\varpi^2 k^2}\right)\right] = 0,$$

which helps b/c

$$\delta\Pi = \frac{\rho\varpi^2}{k^2 R}(R\xi_R)' + 2\rho\frac{m}{R}v_{A\varphi}\frac{k_\parallel \xi_R}{k^2 R}.$$

Now, rather than take limits, let's adopt a simple profile: $\frac{B_\varphi}{\sqrt{4\pi\rho}} = AR$, $B_z = \text{const.}$, $\rho = \text{const.}$

$\Rightarrow$ $\mathbf{k}\cdot\mathbf{v}_A = k_z v_{Az} + \frac{m}{R} AR = \text{const.}$

Loads of manipulation on a separate 3 pages led me to

$$\delta\Pi'' + \frac{1}{R}\delta\Pi' - \left(\frac{m^2}{R^2} + \kappa^2\right)\delta\Pi = 0$$

with $\kappa^2 \equiv k_z^2\left[1 - \frac{4 v_{A\varphi}^2 (\mathbf{k}\cdot\mathbf{v}_A)^2}{R^2 \varpi^4}\right]$ and

$$\frac{\delta\Pi}{\rho} = \frac{2m}{R} v_{A\varphi}\, \mathbf{k}\cdot\mathbf{v}_A \left(\frac{\xi_R}{k^2 R}\right) + \frac{\varpi^2}{k^2}\frac{1}{R}(R\xi_R)'.$$

Bessel's equation! Solution is $\propto I_m(\kappa R)$. To fix proportionality coefficient, note that the external solution must be $\propto K_m(k_z R)$ so that it falls away @ ∞. Then impose continuity of ξ_R at the cylinder's surface, $R = R_s$.

$$\boxed{V_{A\varphi} = 0, \quad p + B_z^2/8\pi = \text{const.}}$$

$$-\omega^2 \xi_R = -\frac{1}{\rho}\frac{d}{dR}\delta\pi + \frac{i k\cdot B}{4\pi\rho}\underbrace{\delta B_R}_{= i k\cdot B\,\xi_R}$$

$$-\omega^2 \xi_\varphi = -\frac{im}{\rho R}\delta\pi + \frac{i k\cdot B}{4\pi\rho}\underbrace{\delta B_\varphi}_{= i k\cdot B\,\xi_\varphi}$$

$$-\omega^2 \xi_z = -i\frac{k_z}{\rho}\delta\pi + \frac{\delta B_R}{4\pi\rho}B_z' + \frac{i k\cdot B}{4\pi\rho}\underbrace{\delta B_z}_{= i k\cdot B\,\xi_z - \xi_R B_z' - B_z(\nabla\cdot\xi)}$$

$$\frac{\delta\pi}{\rho} = i k\cdot V_A V_{Az}\xi_z - (a^2 + V_{Az}^2)\,\nabla\cdot\xi$$

$$-\varpi^2 \xi_z = -i k_z \frac{\delta\pi}{\rho} - \frac{i k\cdot V_A V_{Az}}{a^2+V_{Az}^2}\left[i k\cdot V_A V_{Az}\xi_z - \frac{\delta\pi}{\rho}\right]$$

w/ $\varpi^2 \equiv \omega^2 - (k\cdot V_A)^2$.

$$\Rightarrow \left[-\varpi^2 - \frac{(k\cdot V_A)^2 V_{Az}^2}{a^2+V_{Az}^2}\right]\xi_z = \frac{\delta\pi}{\rho}(-ik_z)\left[\underbrace{1 - \frac{V_{Az}^2}{a^2+V_{Az}^2}}_{=\frac{a^2}{a^2+V_{Az}^2}}\right]$$

$$\Rightarrow \left[\underbrace{-\varpi^2(a^2+V_{Az}^2) - V_{Az}^2(k\cdot V_A)^2}_{= -\omega^2(a^2+V_{Az}^2) + (k\cdot V_A)^2 a^2}\right]\xi_z = -ik_z a^2 \frac{\delta\pi}{\rho}$$

$$\Rightarrow \left[\omega^2\left(1 + \frac{V_{Az}^2}{a^2}\right) - (k\cdot V_A)^2\right]\xi_z = ik_z\frac{\delta\pi}{\rho}.$$

ξ_φ eqn. $\Rightarrow$ $\quad -\varpi^2 \xi_\varphi = -\frac{im}{\rho R}\,\delta\Pi$

ξ_R eqn. $\Rightarrow$ $\quad -\varpi^2 \xi_R = -\frac{1}{\rho}\frac{d}{dR}\,\delta\Pi$

Now we have $\vec{\xi}$ in terms of $\delta\Pi$. Put into $\delta\Pi$ eqn. using $\vec{\nabla}\cdot\vec{\xi} = \frac{1}{R}(R\xi_R)' + i\vec{k}\cdot\vec{\xi}$:

$$\frac{\delta\Pi}{\rho} = i k\cdot V_A V_{Az}\left[ik_z\frac{\delta\Pi}{\rho}\right] \Big/ \left[\omega^2\left(1+\frac{V_{Az}^2}{a^2}\right) - (k\cdot V_A)^2\right]$$

$$-\left(a^2+V_{Az}^2\right)\frac{1}{R}\frac{d}{dR}\left[R\,\frac{1}{\rho}\frac{d\delta\Pi}{dR}\Big/\varpi^2\right]$$

$$-\left(a^2+V_{Az}^2\right)\frac{im}{R}\left[\frac{im}{\rho R}\delta\Pi\Big/\varpi^2\right]$$

$$-\left(a^2+V_{Az}^2\right) ik_z\left[ik_z\,\delta\Pi/\rho\right] \Big/ \left[\omega^2\left(1+\frac{V_{Az}^2}{a^2}\right) - (k\cdot V_A)^2\right]$$

$$\Rightarrow \delta\Pi\left[1 + \frac{\cancel{(k\cdot V_A)^2} - k_z^2a^2 - \cancel{(k\cdot V_A)^2}}{\omega^2\left(1+\frac{V_{Az}^2}{a^2}\right) - (k\cdot V_A)^2} - \frac{m^2}{R^2}\left(\frac{a^2+V_{Az}^2}{\varpi^2}\right)\right]$$

$$= -\rho\left(a^2+V_{Az}^2\right)\frac{1}{R}\frac{d}{dR}\left[\frac{R}{\rho\varpi^2}\frac{d\delta\Pi}{dR}\right]$$

$$= \varpi^2 + \omega^2\frac{V_{Az}^2}{a^2} = \varpi^2\left(1+\frac{V_{Az}^2}{a^2}\right) + (k\cdot V_A)^2\frac{V_{Az}^2}{a^2}.$$

Mult. by $\dfrac{\varpi^2}{a^2+V_{Az}^2}\cdot R^2$:

$$R^2\cdot\frac{\varpi^2\rho}{R}\frac{d}{dR}\left[\frac{R}{\rho\varpi^2}\frac{d}{dR}\delta\Pi\right]+\left[\kappa^2R^2-m^2\right]\delta\Pi=0$$

$$\text{w/}\quad \kappa^2\equiv\frac{\varpi^2}{a^2+V_{Az}^2}\left[1-\frac{k_z^2a^2}{\varpi^2\left(1+\frac{V_{Az}^2}{a^2}\right)+(k\cdot V_A)^2\frac{V_{Az}^2}{a^2}}\right]$$

This is like a Bessel equation, but we don't know the profiles yet of V_{Az}^2, a^2, ρ, so the parameter $\kappa^2=\kappa^2(R)$ in general. It turns out that the Θ-pinch investigated here is always stable, with a local dispersion relation given by $\kappa^2=\frac{m^2}{R^2}\rightarrow\ \frac{m^2}{R^2}(a^2+V_{Az}^2)=\varpi^2\left[1-\frac{k_z^2a^2}{\varpi^2\left(1+\frac{V_{Az}^2}{a^2}\right)+(k\cdot V_A)^2\frac{V_{Az}^2}{a^2}}\right]$

$$\rightarrow\quad \varpi^4+\varpi^2\left[V_{Az}^2\left(k_z^2-\frac{m^2}{R^2}\right)-a^2\left(k_z^2+\frac{m^2}{R^2}\right)\right]-\frac{m^2}{R^2}k_z^2V_{Az}^4=0.$$

$$\rightarrow\quad \omega^4-\omega^2k^2(a^2+V_{Az}^2)+(k\cdot V_A)^2k^2a^2=0.$$ Magnetosonic waves!

For more on stability, stay tuned...

VI.10. The "standard" energy principle

As demonstrated by the many calculations above, one may assess the linear stability of a given equilibrium state by perturbing all the fields, writing down a set of linearized equations describing those perturbed fields, assuming plane-wave solutions (to the extent one can), obtaining the dispersion relation and eigenfunctions, and examining what kind of equilibrium states and linear displacements cause a mode's frequency to become imaginary. We saw that this is often a lengthy process. This section presents an alternative approach, in which linear stability can be assessed directly without the need to calculate explicitly a dispersion relation and its eigenfunctions. The basic idea is to ask whether a given displacement allows the system to achieve a state with lower energy.

The approach taken here, following Bernstein *et al.* (1958) and Bernstein (1983), requires that the background has zero equilibrium flow (any steady, uniform flow can be removed by a Galilean transform).[8] In this case,

$$\Delta\boldsymbol{u} = \delta\boldsymbol{u} \quad\Longleftrightarrow\quad \frac{\mathrm{D}\boldsymbol{\xi}}{\mathrm{D}t} = \frac{\partial\boldsymbol{\xi}}{\partial t}$$

and the linearized momentum equation (V.2.10) becomes[9]

$$\rho\frac{\partial^2\boldsymbol{\xi}}{\partial t^2} = \boldsymbol{f}[\boldsymbol{\xi}] = -\boldsymbol{\nabla}\delta P + \frac{\boldsymbol{j}\times\delta\boldsymbol{B}}{c} + \frac{(\boldsymbol{\nabla}\times\delta\boldsymbol{B})\times\boldsymbol{B}}{4\pi} - \delta\rho\boldsymbol{\nabla}\Phi. \tag{VI.10.1}$$

As usual, these Eulerian perturbations may be expressed in terms of the displacement $\boldsymbol{\xi}$ via the continuity equation, the entropy equation, and the induction equation:

$$\delta\rho = -\boldsymbol{\nabla}\boldsymbol{\cdot}(\rho\boldsymbol{\xi}), \quad \delta P = -\gamma P(\boldsymbol{\nabla}\boldsymbol{\cdot}\boldsymbol{\xi}) - \boldsymbol{\xi}\boldsymbol{\cdot}\boldsymbol{\nabla}P, \quad \text{and} \quad \delta\boldsymbol{B} = \boldsymbol{\nabla}\times(\boldsymbol{\xi}\times\boldsymbol{B}).$$

The program going forward is to calculate the total energy of the perturbed system,

$$\mathscr{E} = \int \mathrm{d}\boldsymbol{r}\left(\frac{1}{2}\rho u^2 + e + \frac{1}{2}\rho\Phi + \frac{B^2}{8\pi}\right) \doteq \int \mathrm{d}\boldsymbol{r}\,\frac{1}{2}\rho u^2 + W, \tag{VI.10.2}$$

and examine how energy is redistributed between the kinetic energy and the potential energy (the latter denoted by W) while keeping the total energy constant.

Expanding (VI.10.2) in $\boldsymbol{\xi}$ about $\boldsymbol{\xi} = 0$ leads to

$$\mathscr{E} = \int \mathrm{d}\boldsymbol{r}\,\frac{1}{2}\rho\left|\frac{\partial\boldsymbol{\xi}}{\partial t}\right|^2 + W_0 + \delta W_1[\boldsymbol{\xi}] + \delta W_2[\boldsymbol{\xi},\boldsymbol{\xi}] + \dots, \tag{VI.10.3}$$

where W_0 is the equilibrium part of W (i.e., its value when $\boldsymbol{\xi} = 0$), W_1 is the first-order (linear) part of W, and W_2 is the second-order part of W, and so on; $W_0 = 0$ for the system to be in equilibrium. Energy must be conserved to all orders, and so the time derivative of $\mathscr{E}$ must vanish at each order independently:

$$\frac{\mathrm{d}\mathscr{E}}{\mathrm{d}t} = \int \mathrm{d}\boldsymbol{r}\,\rho\frac{\partial^2\boldsymbol{\xi}}{\partial t^2}\boldsymbol{\cdot}\frac{\partial\boldsymbol{\xi}}{\partial t} + \delta W_1\left[\frac{\partial\boldsymbol{\xi}}{\partial t}\right] + \delta W_2\left[\frac{\partial\boldsymbol{\xi}}{\partial t},\boldsymbol{\xi}\right] + \delta W_2\left[\boldsymbol{\xi},\frac{\partial\boldsymbol{\xi}}{\partial t}\right] + \dots = 0, \tag{VI.10.4}$$

Because the perturbed kinetic energy is quadratic in the displacement, the only first-order

[8] Versions of what follows that include an equilibrium flow may be found in Frieman & Rotenberg (1960).

[9] The Lorentz force in this equation is written in a slightly different form than found in (V.2.10), where it was expanded out into its pressure and tension components – the reason being that the form here is more useful for manipulations performed later in this section.

term is associated with δW_1. As a result,

$$\delta W_1\left[\frac{\partial \boldsymbol{\xi}}{\partial t}\right] = 0, \tag{VI.10.5}$$

i.e., there are no first-order changes in the potential energy of the system when it is perturbed. At second order in $\boldsymbol{\xi}$, we have that

$$\int \mathrm{d}\boldsymbol{r}\, \rho \frac{\partial^2 \boldsymbol{\xi}}{\partial t^2} \boldsymbol{\cdot} \frac{\partial \boldsymbol{\xi}}{\partial t} = -\delta W_2\left[\frac{\partial \boldsymbol{\xi}}{\partial t}, \boldsymbol{\xi}\right] - \delta W_2\left[\boldsymbol{\xi}, \frac{\partial \boldsymbol{\xi}}{\partial t}\right]. \tag{VI.10.6}$$

Using (VI.10.1) to introduce $\boldsymbol{f}[\boldsymbol{\xi}]$ and denoting $\partial \boldsymbol{\xi}/\partial t$ by $\boldsymbol{\eta}$ yields

$$\int \mathrm{d}\boldsymbol{r}\, \boldsymbol{f}[\boldsymbol{\xi}] \boldsymbol{\cdot} \boldsymbol{\eta} = -\delta W_2[\boldsymbol{\eta}, \boldsymbol{\xi}] - \delta W_2[\boldsymbol{\xi}, \boldsymbol{\eta}]. \tag{VI.10.7}$$

This is just a work–energy theorem: the work done against the forces is equivalent to the change in the potential energy of the system. This provides a scheme for calculating the change in energy needed to assess stability: take the right-hand side of (VI.10.1), dot it with $\partial \boldsymbol{\xi}/\partial t$, and integrate over space. In fact, we can do something even simpler, because (VI.10.7) is true for arbitrary $\boldsymbol{\eta}$. Note that the right-hand side of this equation is symmetric under interchange of $\boldsymbol{\xi}$ and $\boldsymbol{\eta}$, which implies that the force $\boldsymbol{f}[\boldsymbol{\xi}]$ is a self-adjoint operator:

$$\int \mathrm{d}\boldsymbol{r}\, \boldsymbol{f}[\boldsymbol{\xi}] \boldsymbol{\cdot} \boldsymbol{\eta} = \int \mathrm{d}\boldsymbol{r}\, \boldsymbol{f}[\boldsymbol{\eta}] \boldsymbol{\cdot} \boldsymbol{\xi}. \tag{VI.10.8}$$

Some implications of $\boldsymbol{f}$ being self-adjoint are discussed in the next paragraph, but the immediate implication is that

$$\boxed{\delta W_2[\boldsymbol{\xi}, \boldsymbol{\xi}] = -\frac{1}{2} \int \mathrm{d}\boldsymbol{r}\, \boldsymbol{f}[\boldsymbol{\xi}] \boldsymbol{\cdot} \boldsymbol{\xi}} \tag{VI.10.9}$$

This equation states that, in order to assess whether the change in the potential energy of the system is positive or negative (or zero), we must calculate the volume integral of the force dotted into the displacement. Before doing so, back to $\boldsymbol{f}$ being self-adjoint...

Because $\boldsymbol{f}[\boldsymbol{\xi}]$ is self-adjoint, its eigenvalues $\{\omega_n^2\}$ are real and their associated eigenmodes $\{\boldsymbol{\xi}_n\}$ are orthogonal. This means that any instability of this ideal MHD system will give rise to purely growing modes, i.e., there are no overstabilities (growing oscillations). Mathematically,

$$\boldsymbol{\xi}(t, \boldsymbol{r}) = \sum_n \boldsymbol{\xi}_n(\boldsymbol{r}) \mathrm{e}^{-\mathrm{i}\omega_n t} \quad \Longrightarrow \quad \boldsymbol{f}[\boldsymbol{\xi}_n] = -\rho_0 \omega_n^2 \boldsymbol{\xi}_n,$$

with ω_n being purely real or purely imaginary. When $\omega_n^2 > 0$ the frequency is real and the mode is purely oscillatory; when $\omega_n^2 < 0$ the frequency is imaginary and the mode undergoes exponential amplification. The marginal point $\omega_n^2 = 0$ separates stable from unstable solutions. The *Energy Principle* is

$$\boxed{\delta W_2[\boldsymbol{\xi}, \boldsymbol{\xi}] \geqslant 0 \text{ for all } \boldsymbol{\xi} \quad \Longleftrightarrow \quad \text{equilibrium is stable}} \tag{VI.10.10}$$

The '$\Longleftrightarrow$' indicates that this is a necessary and sufficient condition for stability. Its proof goes as follows.

First, suppose that $\delta W_2 \geqslant 0$. Then by (VI.10.3), we have that

$$0 \leqslant \int \mathrm{d}\boldsymbol{r}\, \frac{1}{2} \rho \left|\frac{\partial \boldsymbol{\xi}}{\partial t}\right|^2 = \mathscr{E}_2 - \delta W_2 \leqslant \mathscr{E}_2.$$

Thus, the kinetic energy of the perturbations is bounded from above, so the system must be stable. To show that stability implies $\delta W_2 \geqslant 0$, suppose that any displacement at any given time t can be decomposed as

$$\boldsymbol{\xi}(t,\boldsymbol{r}) = \sum_n a_n(t)\boldsymbol{\xi}_n(\boldsymbol{r}),$$

so that the energy perturbation (VI.10.9) is

$$\begin{aligned}\delta W_2[\boldsymbol{\xi},\boldsymbol{\xi}] &= -\frac{1}{2}\int \mathrm{d}\boldsymbol{r}\, \boldsymbol{f}[\boldsymbol{\xi}]\cdot\boldsymbol{\xi} = -\frac{1}{2}\sum_{n,m} a_n a_m \int \mathrm{d}\boldsymbol{r}\, \boldsymbol{f}[\boldsymbol{\xi}_m]\cdot\boldsymbol{\xi}_n \\ &= \frac{1}{2}\sum_{n,m} a_n a_m \omega_m^2 \int \mathrm{d}\boldsymbol{r}\, \rho_0 \boldsymbol{\xi}_n\cdot\boldsymbol{\xi}_m = \frac{1}{2}\sum_n a_n^2\omega_n^2 \int \mathrm{d}\boldsymbol{r}\, \rho_0 |\boldsymbol{\xi}_n|^2,\end{aligned} \tag{VI.10.11}$$

where the final equality follows from the orthogonality of the eigenvectors. If the system is stable, then all eigenvalues $\omega_n^2 \geqslant 0$, and so $\delta W_2[\boldsymbol{\xi},\boldsymbol{\xi}] \geqslant 0$ by (VI.10.11). If you're grumpy about the assumption of completeness when writing the displacement as a sum of all the normal modes, consult pp. 45–47 of Manheimer & Lashmore-Davies (1984).

Now, all that remains is to calculate δW_2:

$$\delta W_2[\boldsymbol{\xi},\boldsymbol{\xi}] = -\frac{1}{2}\int \mathrm{d}\boldsymbol{r}\left[-\boldsymbol{\nabla}\delta P + \frac{\boldsymbol{j}\times\delta\boldsymbol{B}}{c} + \frac{(\boldsymbol{\nabla}\times\delta\boldsymbol{B})\times\boldsymbol{B}}{4\pi} - \delta\rho\boldsymbol{\nabla}\Phi\right]\cdot\boldsymbol{\xi}. \tag{VI.10.12}$$

Using the linearized equations, some integration by parts, and Gauss' theorem to convert some volume integrals of fluxes into surface integrals, each of the terms can be re-arranged as follows:

$$\begin{aligned}
\int \mathrm{d}\boldsymbol{r}\,(-\boldsymbol{\nabla}\delta P)\cdot\boldsymbol{\xi} &\overset{\text{bp}}{=} \int \mathrm{d}\boldsymbol{r}\,(\boldsymbol{\nabla}\cdot\boldsymbol{\xi})\,\delta P - \oint \mathrm{d}\boldsymbol{S}\cdot\boldsymbol{\xi}\,\delta P \\
&= \int \mathrm{d}\boldsymbol{r}\,(\boldsymbol{\nabla}\cdot\boldsymbol{\xi})\big[-\gamma P(\boldsymbol{\nabla}\cdot\boldsymbol{\xi}) - \boldsymbol{\xi}\cdot\boldsymbol{\nabla}P\big] - \oint \mathrm{d}\boldsymbol{S}\cdot\boldsymbol{\xi}\,\delta P \\
\int \mathrm{d}\boldsymbol{r}\,\frac{\boldsymbol{j}\times\delta\boldsymbol{B}}{c}\cdot\boldsymbol{\xi} &= -\int \mathrm{d}\boldsymbol{r}\,\frac{\boldsymbol{j}\cdot(\boldsymbol{\xi}\times\delta\boldsymbol{B})}{c} \\
\int \mathrm{d}\boldsymbol{r}\,\frac{(\boldsymbol{\nabla}\times\delta\boldsymbol{B})\times\boldsymbol{B}}{4\pi}\cdot\boldsymbol{\xi} &= -\int \mathrm{d}\boldsymbol{r}\,\frac{(\boldsymbol{\nabla}\times\delta\boldsymbol{B})\cdot(\boldsymbol{\xi}\times\boldsymbol{B})}{4\pi} \\
&\overset{\text{bp}}{=} -\int \mathrm{d}\boldsymbol{r}\,\frac{(\delta\boldsymbol{B}\times\boldsymbol{\nabla})\cdot(\boldsymbol{\xi}\times\boldsymbol{B})}{4\pi} - \oint \mathrm{d}\boldsymbol{S}\cdot\frac{\delta\boldsymbol{B}\times(\boldsymbol{\xi}\times\boldsymbol{B})}{4\pi} \\
&= -\int \mathrm{d}\boldsymbol{r}\,\frac{\delta\boldsymbol{B}\cdot[\boldsymbol{\nabla}\times(\boldsymbol{\xi}\times\boldsymbol{B})]}{4\pi} - \oint \mathrm{d}\boldsymbol{S}\cdot\boldsymbol{\xi}\,\frac{\boldsymbol{B}\cdot\delta\boldsymbol{B}}{4\pi} \\
&= -\int \mathrm{d}\boldsymbol{r}\,\frac{|\delta\boldsymbol{B}|^2}{4\pi} - \oint \mathrm{d}\boldsymbol{S}\cdot\boldsymbol{\xi}\,\frac{\boldsymbol{B}\cdot\delta\boldsymbol{B}}{4\pi} \\
\int \mathrm{d}\boldsymbol{r}\,(-\delta\rho)\boldsymbol{\nabla}\Phi\cdot\boldsymbol{\xi} &= \int \mathrm{d}\boldsymbol{r}\,\boldsymbol{\nabla}\cdot(\rho\boldsymbol{\xi})(\boldsymbol{\xi}\cdot\boldsymbol{\nabla}\Phi) \doteq -\int \mathrm{d}\boldsymbol{r}\,(\boldsymbol{\xi}\cdot\boldsymbol{g})\boldsymbol{\nabla}\cdot(\rho\boldsymbol{\xi})
\end{aligned}$$

Assembling all the terms, equation (VI.10.12) becomes

$$\boxed{\begin{aligned}&\delta W_2[\boldsymbol{\xi},\boldsymbol{\xi}]\\&=\frac{1}{2}\int\mathrm{d}\boldsymbol{r}\left[\gamma P(\boldsymbol{\nabla\cdot\xi})^2+(\boldsymbol{\xi\cdot\nabla}P)(\boldsymbol{\nabla\cdot\xi})+\frac{\boldsymbol{j}\boldsymbol{\cdot}(\boldsymbol{\xi}\times\delta\boldsymbol{B})}{c}+\frac{|\delta\boldsymbol{B}|^2}{4\pi}+(\boldsymbol{\xi\cdot g})\boldsymbol{\nabla\cdot}(\rho\boldsymbol{\xi})\right]\\&+\frac{1}{2}\oint\mathrm{d}\boldsymbol{S\cdot\xi}\left[-\gamma P(\boldsymbol{\nabla\cdot\xi})-\boldsymbol{\xi\cdot\nabla}P+\frac{\boldsymbol{B\cdot}\delta\boldsymbol{B}}{4\pi}\right]\end{aligned}} \tag{VI.10.13}$$

Stability is therefore assessed by evaluating δW_2 for a given equilibrium state and investigating whether there are any perturbations for which $\delta W_2 < 0$. With $\gamma P(\boldsymbol{\nabla\cdot\xi})^2$ and $|\delta\boldsymbol{B}|^2/4\pi$ being non-negative, a necessary (but not sufficient) condition for instability is obtained by evaluating the other terms and demanding they be negative.

Freidberg (2014) refers to this as the 'standard form' of δW_2; note that the expression is not unique because one can do various integrations by parts to move terms between the volume and surface integrals. Moreover, if the boundary were to be a perfectly conducting wall, or if we had the freedom to move the boundary to infinity (e.g., if there were no surrounding vacuum region), then the surface integral in (VI.10.13) would vanish. An alternative form of δW_2 is often reported, which, although being more tedious to evaluate, nevertheless is more physically transparent. Reported first by Furth (1965) and Greene & Johnson (1968), this version involves splitting the displacement $\boldsymbol{\xi}$ and the magnetic perturbation $\delta\boldsymbol{B}$ into their components across and along the equilibrium magnetic field and using force balance in the equilibrium state to re-arrange some terms into more readily interpretable portions. The procedure goes as follows.

VI.11. The "intuitive" energy principle

First, split up the magnetic perturbation into its perpendicular and parallel parts, noting that only the perpendicular component of $\boldsymbol{\xi}$ enters into the linearized induction equation:

$$\delta\boldsymbol{B}=\delta\boldsymbol{B}_\perp+\delta B_\parallel\hat{\boldsymbol{b}}=\big[\hat{\boldsymbol{b}}\times\boldsymbol{\nabla}\times(\boldsymbol{\xi}_\perp\times\boldsymbol{B})\big]\times\hat{\boldsymbol{b}}+\big[\hat{\boldsymbol{b}}\boldsymbol{\cdot\nabla}\times(\boldsymbol{\xi}_\perp\times\boldsymbol{B})\big]\hat{\boldsymbol{b}}. \tag{VI.11.1}$$

Then use various vector identities, Ampère's law, and force balance to write $\delta B_\parallel$ in terms of $\boldsymbol{\nabla\cdot\xi}_\perp$ and the pressure and potential gradients:

$$\begin{aligned}\delta B_\parallel&=\hat{\boldsymbol{b}}\boldsymbol{\cdot}\big[\boldsymbol{\nabla}\times(\boldsymbol{\xi}_\perp\times\boldsymbol{B})\big]\\&=-\boldsymbol{\nabla\cdot}\big[\hat{\boldsymbol{b}}\times(\boldsymbol{\xi}_\perp\times\boldsymbol{B})\big]\quad+(\boldsymbol{\nabla}\times\hat{\boldsymbol{b}})\boldsymbol{\cdot}(\boldsymbol{\xi}_\perp\times\boldsymbol{B})\\&=-\boldsymbol{\nabla\cdot}(B\boldsymbol{\xi}_\perp)\qquad+\frac{1}{B}(\boldsymbol{\nabla}\times\boldsymbol{B}+\hat{\boldsymbol{b}}\times\boldsymbol{\nabla}B)\boldsymbol{\cdot}(\boldsymbol{\xi}_\perp\times\boldsymbol{B})\\&=-B\boldsymbol{\nabla\cdot\xi}_\perp-\boldsymbol{\xi}_\perp\boldsymbol{\cdot\nabla}B\quad+\frac{1}{B}(\boldsymbol{\nabla}\times\boldsymbol{B})\boldsymbol{\cdot}(\boldsymbol{\xi}_\perp\times\boldsymbol{B})-\boldsymbol{\xi}_\perp\boldsymbol{\cdot\nabla}B\\&=-B\boldsymbol{\nabla\cdot\xi}_\perp-2\boldsymbol{\xi}_\perp\boldsymbol{\cdot\nabla}B-\frac{4\pi}{cB}\boldsymbol{\xi}_\perp\boldsymbol{\cdot}(\boldsymbol{j}\times\boldsymbol{B})\qquad\text{(by Ampère's law)}\\&=-B\boldsymbol{\nabla\cdot\xi}_\perp-2\boldsymbol{\xi}_\perp\boldsymbol{\cdot\nabla}B-\frac{4\pi}{B}\boldsymbol{\xi}_\perp\boldsymbol{\cdot}(\boldsymbol{\nabla}P+\rho\boldsymbol{\nabla}\varPhi)\qquad\text{(by force balance)}\end{aligned} \tag{VI.11.2}$$

Introduce the magnetic curvature vector $\boldsymbol{\kappa}_{\rm c}$ and use force balance in it as well:

$$\begin{aligned}\boldsymbol{\kappa}_{\rm c} \doteq \hat{\boldsymbol{b}}\boldsymbol{\cdot}\boldsymbol{\nabla}\hat{\boldsymbol{b}} &= \frac{\boldsymbol{B}\boldsymbol{\cdot}\boldsymbol{\nabla}\boldsymbol{B}}{B^2} - \hat{\boldsymbol{b}}\hat{\boldsymbol{b}}\boldsymbol{\cdot}\boldsymbol{\nabla}\ln B \\ &= \frac{4\pi}{B^2}(\boldsymbol{\nabla}P + \rho\boldsymbol{\nabla}\Phi) + \boldsymbol{\nabla}\ln B - \hat{\boldsymbol{b}}\hat{\boldsymbol{b}}\boldsymbol{\cdot}\boldsymbol{\nabla}\ln B.\end{aligned} \tag{VI.11.3}$$

Take the dot product of the curvature vector with $B\boldsymbol{\xi}_\perp$:

$$2B\boldsymbol{\xi}_\perp\boldsymbol{\cdot}\boldsymbol{\kappa}_{\rm c} = \frac{8\pi}{B}\boldsymbol{\xi}_\perp\boldsymbol{\cdot}(\boldsymbol{\nabla}P + \rho\boldsymbol{\nabla}\Phi) + 2\boldsymbol{\xi}_\perp\boldsymbol{\cdot}\boldsymbol{\nabla}B. \tag{VI.11.4}$$

Combine (VI.11.2) and (VI.11.4) to arrive at a new expression for the parallel magnetic-field perturbation:

$$\delta B_\parallel = -B\boldsymbol{\nabla}\boldsymbol{\cdot}\boldsymbol{\xi}_\perp - 2B\boldsymbol{\xi}_\perp\boldsymbol{\cdot}\boldsymbol{\kappa}_{\rm c} + \frac{4\pi}{B}\boldsymbol{\xi}_\perp\boldsymbol{\cdot}(\boldsymbol{\nabla}P + \rho\boldsymbol{\nabla}\Phi). \tag{VI.11.5}$$

Next, split apart the Lorentz-force term as follows:

$$\frac{\boldsymbol{j}\boldsymbol{\cdot}(\boldsymbol{\xi}\times\delta\boldsymbol{B})}{c} = \frac{\boldsymbol{j}_\parallel\boldsymbol{\cdot}(\boldsymbol{\xi}\times\delta\boldsymbol{B})}{c} + \frac{\boldsymbol{j}_\perp\boldsymbol{\cdot}(\boldsymbol{\xi}\times\delta\boldsymbol{B})}{c}. \tag{VI.11.6}$$

For the second term in this equation, use force balance to replace $\boldsymbol{j}_\perp$ with the pressure and potential gradients so that it becomes

$$\begin{aligned}\left[\frac{\hat{\boldsymbol{b}}}{B}\times(\boldsymbol{\nabla}P + \rho\boldsymbol{\nabla}\Phi)\right]\boldsymbol{\cdot}(\boldsymbol{\xi}\times\delta\boldsymbol{B}) &= \xi_\parallel\frac{\delta\boldsymbol{B}}{B}\boldsymbol{\cdot}(\boldsymbol{\nabla}P + \rho\boldsymbol{\nabla}\Phi) - \frac{\delta B_\parallel}{B}\boldsymbol{\xi}\boldsymbol{\cdot}(\boldsymbol{\nabla}P + \rho\boldsymbol{\nabla}\Phi) \\ &= \xi_\parallel\frac{\delta\boldsymbol{B}_\perp}{B}\boldsymbol{\cdot}(\boldsymbol{\nabla}P + \rho\boldsymbol{\nabla}\Phi) - \frac{\delta B_\parallel}{B}\boldsymbol{\xi}_\perp\boldsymbol{\cdot}(\boldsymbol{\nabla}P + \rho\boldsymbol{\nabla}\Phi).\end{aligned} \tag{VI.11.7}$$

Combine this with (VI.11.5) to obtain

$$\begin{aligned}\frac{\boldsymbol{j}_\perp\boldsymbol{\cdot}(\boldsymbol{\xi}\times\delta\boldsymbol{B})}{c} &= \left[\xi_\parallel\frac{\delta\boldsymbol{B}_\perp}{B} - (\boldsymbol{\nabla}\boldsymbol{\cdot}\boldsymbol{\xi}_\perp)\boldsymbol{\xi}_\perp - 2(\boldsymbol{\xi}_\perp\boldsymbol{\cdot}\boldsymbol{\kappa}_{\rm c})\boldsymbol{\xi}_\perp\right]\boldsymbol{\cdot}(\boldsymbol{\nabla}P + \rho\boldsymbol{\nabla}\Phi) \\ &\quad - \frac{(\delta B_\parallel)^2}{4\pi} + \frac{B^2}{4\pi}\bigl(\boldsymbol{\nabla}\boldsymbol{\cdot}\boldsymbol{\xi}_\perp + 2\boldsymbol{\xi}_\perp\boldsymbol{\cdot}\boldsymbol{\kappa}_{\rm c}\bigr)^2.\end{aligned} \tag{VI.11.8}$$

These manipulations place the volume integral of (VI.10.13) in the following form:

$$\begin{aligned}\frac{1}{2}\int{\rm d}\boldsymbol{r}\,\Biggl\{&\gamma P(\boldsymbol{\nabla}\boldsymbol{\cdot}\boldsymbol{\xi})^2 + \frac{|\delta\boldsymbol{B}_\perp|^2}{4\pi} + \frac{B^2}{4\pi}\bigl(\boldsymbol{\nabla}\boldsymbol{\cdot}\boldsymbol{\xi}_\perp + 2\boldsymbol{\xi}_\perp\boldsymbol{\cdot}\boldsymbol{\kappa}_{\rm c}\bigr)^2 \\ &+ \frac{\boldsymbol{j}_\parallel\boldsymbol{\cdot}(\boldsymbol{\xi}\times\delta\boldsymbol{B})}{c} - 2(\boldsymbol{\xi}_\perp\boldsymbol{\cdot}\boldsymbol{\kappa}_{\rm c})\boldsymbol{\xi}_\perp\boldsymbol{\cdot}(\boldsymbol{\nabla}P + \rho\boldsymbol{\nabla}\Phi) \\ &+ \left[\xi_\parallel\frac{\delta\boldsymbol{B}_\perp}{B} - (\boldsymbol{\nabla}\boldsymbol{\cdot}\boldsymbol{\xi}_\perp)\boldsymbol{\xi}_\perp\right]\boldsymbol{\cdot}(\boldsymbol{\nabla}P + \rho\boldsymbol{\nabla}\Phi) + (\boldsymbol{\xi}\boldsymbol{\cdot}\boldsymbol{\nabla}P)(\boldsymbol{\nabla}\boldsymbol{\cdot}\boldsymbol{\xi}) + (\boldsymbol{\xi}\boldsymbol{\cdot}\boldsymbol{g})\boldsymbol{\nabla}\boldsymbol{\cdot}(\rho\boldsymbol{\xi})\Biggr\}.\end{aligned} \tag{VI.11.9}$$

Note that the top row is non-negative, indicating physics that is ultimately responsible for stabilizing the system: compressing the plasma, bending the magnetic-field lines, and compressing the magnetic field. The middle row includes terms involving gradients in the equilibrium state and therefore can possess either sign; aside from what will be a small edit to write $\boldsymbol{j}_\parallel\boldsymbol{\cdot}(\boldsymbol{\xi}\times\delta\boldsymbol{B})$ instead as $-\boldsymbol{\xi}\boldsymbol{\cdot}(\boldsymbol{j}_\parallel\times\delta\boldsymbol{B})$, the terms in this row are in their final form. The terms on the third and final row still require some work.

Take the last three terms in the final line above, use the fact that $\hat{\boldsymbol{b}}\cdot(\boldsymbol{\nabla}P+\rho\boldsymbol{\nabla}\Phi)=\hat{\boldsymbol{b}}\cdot(\boldsymbol{j}\times\boldsymbol{B})/c=0$, recall that $c_{\rm s}^2\doteq\gamma P/\rho$, and practice some adroit grouping of terms:

$$
\begin{aligned}
&-(\boldsymbol{\nabla}\cdot\boldsymbol{\xi}_\perp)\underbrace{\boldsymbol{\xi}_\perp\cdot(\boldsymbol{\nabla}P+\rho\boldsymbol{\nabla}\Phi)}_{=\,\boldsymbol{\xi}\cdot\boldsymbol{\nabla}P+\boldsymbol{\xi}\cdot(\rho\boldsymbol{\nabla}\Phi)}+\underbrace{(\boldsymbol{\xi}\cdot\boldsymbol{\nabla}P)(\boldsymbol{\nabla}\cdot\boldsymbol{\xi})}_{(\boldsymbol{\xi}\cdot\boldsymbol{\nabla}P)[\boldsymbol{\nabla}\cdot\boldsymbol{\xi}_\perp+\boldsymbol{\nabla}\cdot(\xi_\parallel\hat{\boldsymbol{b}})]}-\underbrace{\boldsymbol{\nabla}\cdot(\rho\boldsymbol{\xi})(\boldsymbol{\nabla}\Phi\cdot\boldsymbol{\xi})}_{(\boldsymbol{\nabla}\cdot\boldsymbol{\xi}+\boldsymbol{\xi}\cdot\boldsymbol{\nabla}\ln\rho)\,\boldsymbol{\xi}\cdot(\rho\boldsymbol{\nabla}\Phi)}\\
&=-2(\boldsymbol{\nabla}\cdot\boldsymbol{\xi})\,\boldsymbol{\xi}\cdot(\rho\boldsymbol{\nabla}\Phi)-(\boldsymbol{\xi}\cdot\boldsymbol{\nabla}\ln\rho)\,\boldsymbol{\xi}\cdot(\rho\boldsymbol{\nabla}\Phi)+\boldsymbol{\nabla}\cdot(\xi_\parallel\hat{\boldsymbol{b}})\,\boldsymbol{\xi}\cdot(\boldsymbol{\nabla}P+\rho\boldsymbol{\nabla}\Phi)\\
&=\left[\gamma P\left(\boldsymbol{\nabla}\cdot\boldsymbol{\xi}-\frac{\boldsymbol{\xi}\cdot\boldsymbol{\nabla}\Phi}{c_{\rm s}^2}\right)^2-\gamma P(\boldsymbol{\nabla}\cdot\boldsymbol{\xi})^2\right]-\boldsymbol{\xi}\cdot(\rho\boldsymbol{\nabla}\Phi)\left(\boldsymbol{\xi}\cdot\boldsymbol{\nabla}\ln\rho+\frac{\boldsymbol{\xi}\cdot\boldsymbol{\nabla}\Phi}{c_{\rm s}^2}\right)\\
&\quad+\boldsymbol{\nabla}\cdot(\xi_\parallel\hat{\boldsymbol{b}})\,\boldsymbol{\xi}_\perp\cdot(\boldsymbol{\nabla}P+\rho\boldsymbol{\nabla}\Phi)\\
&=\left[\gamma P\left(\boldsymbol{\nabla}\cdot\boldsymbol{\xi}-\frac{\boldsymbol{\xi}\cdot\boldsymbol{\nabla}\Phi}{c_{\rm s}^2}\right)^2-\gamma P(\boldsymbol{\nabla}\cdot\boldsymbol{\xi})^2\right]+\boldsymbol{\xi}\cdot(\rho\boldsymbol{\nabla}\Phi)\,\frac{1}{\gamma}\,\boldsymbol{\xi}\cdot\boldsymbol{\nabla}\ln\frac{P}{\rho^\gamma}\\
&\quad+\left[\boldsymbol{\nabla}\cdot(\xi_\parallel\hat{\boldsymbol{b}})-\frac{\boldsymbol{\xi}\cdot\boldsymbol{\nabla}\Phi}{c_{\rm s}^2}\right]\boldsymbol{\xi}_\perp\cdot(\boldsymbol{\nabla}P+\rho\boldsymbol{\nabla}\Phi).
\end{aligned}
\tag{VI.11.10}
$$

Then write

$$
\begin{aligned}
\delta\boldsymbol{B}_\perp\cdot(\boldsymbol{\nabla}P+\rho\boldsymbol{\nabla}\Phi)&=\big[\boldsymbol{\nabla}\times(\boldsymbol{\xi}_\perp\times\boldsymbol{B})\big]\cdot(\boldsymbol{\nabla}P+\rho\boldsymbol{\nabla}\Phi)\\
&=\boldsymbol{\nabla}\cdot\big[(\boldsymbol{\xi}_\perp\times\boldsymbol{B})\times(\boldsymbol{\nabla}P+\rho\boldsymbol{\nabla}\Phi)\big]\\
&\quad+\big[\boldsymbol{\nabla}\times(\boldsymbol{\nabla}P+\rho\boldsymbol{\nabla}\Phi)\big]\cdot(\boldsymbol{\xi}_\perp\times\boldsymbol{B})\\
&=\boldsymbol{\nabla}\cdot\big[\boldsymbol{B}\,\boldsymbol{\xi}_\perp\cdot(\boldsymbol{\nabla}P+\rho\boldsymbol{\nabla}\Phi)-\boldsymbol{\xi}_\perp\,\cancelto{0}{\boldsymbol{B}\cdot(\boldsymbol{\nabla}P+\rho\boldsymbol{\nabla}\Phi)}\big]\\
&\quad+(\boldsymbol{\nabla}\rho\times\boldsymbol{\nabla}\Phi)\cdot(\boldsymbol{\xi}_\perp\times\boldsymbol{B})\\
&=\boldsymbol{\nabla}\cdot\big[\boldsymbol{B}\,\boldsymbol{\xi}_\perp\cdot(\boldsymbol{\nabla}P+\rho\boldsymbol{\nabla}\Phi)\big]+(\boldsymbol{\nabla}\rho\times\boldsymbol{\nabla}\Phi)\cdot(\boldsymbol{\xi}_\perp\times\boldsymbol{B}),
\end{aligned}
\tag{VI.11.11}
$$

from which follows that

$$
\begin{aligned}
\xi_\parallel\frac{\delta\boldsymbol{B}_\perp}{B}\cdot(\boldsymbol{\nabla}P+\rho\boldsymbol{\nabla}\Phi)&=\boldsymbol{\nabla}\cdot\big[\xi_\parallel\hat{\boldsymbol{b}}\,\boldsymbol{\xi}_\perp\cdot(\boldsymbol{\nabla}P+\rho\boldsymbol{\nabla}\Phi)\big]-\boldsymbol{\nabla}\cdot(\xi_\parallel\hat{\boldsymbol{b}})\,\boldsymbol{\xi}_\perp\cdot(\boldsymbol{\nabla}P+\rho\boldsymbol{\nabla}\Phi)\\
&\quad+\xi_\parallel(\boldsymbol{\nabla}\rho\times\boldsymbol{\nabla}\Phi)\cdot(\boldsymbol{\xi}_\perp\times\hat{\boldsymbol{b}}).
\end{aligned}
\tag{VI.11.12}
$$

Combining these findings, replacing $\boldsymbol{\nabla}\Phi$ with $-\boldsymbol{g}$ for brevity, and using Gauss' theorem on the perfect divergence in (VI.11.11) allows us to rewrite (VI.10.13) as

$$
\boxed{
\begin{aligned}
&\delta W_2[\boldsymbol{\xi},\boldsymbol{\xi}]\\
&=\frac{1}{2}\int{\rm d}\boldsymbol{r}\left\{\gamma P(\boldsymbol{\nabla}\cdot\boldsymbol{\xi}-2\boldsymbol{\xi}\cdot\boldsymbol{\kappa}_{\rm g})^2+\frac{|\delta\boldsymbol{B}_\perp|^2}{4\pi}+\frac{B^2}{4\pi}\big(\boldsymbol{\nabla}\cdot\boldsymbol{\xi}_\perp+2\boldsymbol{\xi}_\perp\cdot\boldsymbol{\kappa}_{\rm c}\big)^2\right.\\
&\qquad\left.-\,\boldsymbol{\xi}\cdot\left[\frac{\boldsymbol{j}_\parallel\times\delta\boldsymbol{B}}{c}+2(\boldsymbol{\kappa}_{\rm c}+\boldsymbol{\kappa}_{\rm g})\,\boldsymbol{\xi}_\perp\cdot(\boldsymbol{\nabla}P-\rho\boldsymbol{g})+\rho\boldsymbol{g}\,\frac{1}{\gamma}\boldsymbol{\xi}\cdot\boldsymbol{\nabla}\ln\frac{P}{\rho^\gamma}\right]\right\}\\
&+\frac{1}{2}\oint{\rm d}\boldsymbol{S}\cdot\boldsymbol{\xi}\left[-\gamma P(\boldsymbol{\nabla}\cdot\boldsymbol{\xi})-\boldsymbol{\xi}\cdot\boldsymbol{\nabla}P+\frac{\boldsymbol{B}\cdot\delta\boldsymbol{B}}{4\pi}\right]
\end{aligned}
}
\tag{VI.11.13}
$$

To keep the notation compact, we have introduced the gravitational 'curvature' vector

$$
\boldsymbol{\kappa}_{\rm g}\doteq\frac{\boldsymbol{\nabla}\Phi}{2c_{\rm s}^2}=-\frac{\boldsymbol{g}}{2c_{\rm s}^2},
\tag{VI.11.14}
$$

which measures the characteristic scale of the gravitational potential, namely, the pressure scale height of a stratified atmosphere in hydrostatic equilibrium.

In this 'intuitive' form, each of the terms in (VI.11.13) is readily interpretable. The entire first row consists of non-negative terms, and therefore is stabilizing. These terms include the work done against: compression of the hot plasma, the bending of the magnetic-field lines, and the compression of the (flux-frozen) magnetic field. To understand the inclusion of the curvature vector $\boldsymbol{\kappa}_{\rm g}$ in the first term of (VI.11.13), note that this term vanishes when

$$\boldsymbol{\nabla}\cdot\boldsymbol{\xi} = 2\boldsymbol{\xi}\cdot\boldsymbol{\kappa}_{\rm g} \quad \Longrightarrow \quad \frac{\Delta\rho}{\rho} = \boldsymbol{\xi}\cdot\frac{\boldsymbol{g}}{c_{\rm s}^2}. \tag{VI.11.15}$$

For adiabatic displacements $\Delta\sigma \doteq \Delta\ln(P/\rho^\gamma) = 0$ in a hydrostatic atmosphere with $\boldsymbol{\nabla}P = \rho\boldsymbol{g}$, this relation implies

$$\Delta P = \cancelto{0}{P\Delta\sigma} + \gamma P\frac{\Delta\rho}{\rho} = \boldsymbol{\xi}\cdot(\rho\boldsymbol{g}) = \boldsymbol{\xi}\cdot\boldsymbol{\nabla}P \quad \Longrightarrow \quad \delta P = 0, \tag{VI.11.16}$$

i.e., fluid elements maintain pressure balance with the surrounding fluid as they are displaced. As a result, no sound waves are radiated away, which would otherwise cost energy that might otherwise go into powering convectively unstable motions. In this simplest of cases, we have rediscovered what we had learned in §VI.6: provided that $\boldsymbol{\xi}\cdot{\rm d}\boldsymbol{S} = 0$ (i.e., the boundary of the volume is placed far enough away), the only remaining term in δW_2 for this hydrodynamic case is

$$-\frac{1}{2}\int {\rm d}\boldsymbol{r}\,\boldsymbol{\xi}\cdot(\rho\boldsymbol{g})\,\frac{1}{\gamma}\boldsymbol{\xi}\cdot\boldsymbol{\nabla}\ln\frac{P}{\rho^\gamma} = \int {\rm d}\boldsymbol{r}\,\frac{1}{2}\rho\xi_z^2\,\frac{g}{\gamma}\frac{\rm d}{{\rm d}z}\ln\frac{P}{\rho^\gamma} = \int {\rm d}\boldsymbol{r}\,\frac{1}{2}\rho\xi_z^2\,N^2, \tag{VI.11.17}$$

where N^2 is the square of the Brunt–Väisälä frequency. In words, the sign of the entropy gradient determines the stability of the fluid: σ must be constant or increase upwards for stability, *viz.* $N^2 \geqslant 0$. Similar considerations explain the $+2\boldsymbol{\xi}_\perp\cdot\boldsymbol{\kappa}_{\rm c}$ in the final term of the first row of (VI.11.13). Using (VI.11.5), the change in the magnetic pressure is given by

$$\frac{\delta B^2}{8\pi} = \frac{B\delta B_\parallel}{4\pi} = -\frac{B^2}{4\pi}\big(\boldsymbol{\nabla}\cdot\boldsymbol{\xi}_\perp + 2\boldsymbol{\xi}_\perp\cdot\boldsymbol{\kappa}_{\rm c}\big) + \boldsymbol{\xi}_\perp\cdot(\boldsymbol{\nabla}P - \rho\boldsymbol{g}). \tag{VI.11.18}$$

Minimizing $\boldsymbol{\nabla}\cdot\boldsymbol{\xi}_\perp + 2\boldsymbol{\xi}_\perp\cdot\boldsymbol{\kappa}_{\rm c}$ minimizes the change in the magnetic pressure, and therefore the energetic cost of moving perpendicular to the equilibrium magnetic field.

All of the terms on the second row of (VI.11.13) are sign-indefinite and therefore have the potential to drive instabilities. We have already mentioned the final term: the sign of the entropy gradient determines stability in a hydrostatic equilibrium. As for the other two terms, the first involves the parallel current density $\boldsymbol{j}_\parallel$; in the pinch geometry of §VI.9, it becomes

$$-\boldsymbol{\xi}\cdot\frac{\boldsymbol{j}_\parallel\times\delta\boldsymbol{B}}{c} = \frac{1}{4\pi}\left[B_\varphi\frac{{\rm d}B_z}{{\rm d}R} - B_z\frac{1}{R}\frac{{\rm d}(RB_\varphi)}{{\rm d}R}\right](\boldsymbol{\xi}\times\hat{\boldsymbol{b}})\cdot\delta\boldsymbol{B}. \tag{VI.11.19}$$

Note that both an azimuthal and axial magnetic field are required for this term to operate. The second term in the second row of (VI.11.13) involves the sum of the magnetic and gravitational curvature vectors, $\boldsymbol{\kappa}_{\rm c}+\boldsymbol{\kappa}_{\rm g}$. For a hydrostatic equilibrium, this term vanishes because $\boldsymbol{\nabla}P = \rho\boldsymbol{g}$. In a magnetohydrostatic equilibrium, it becomes proportional to the perpendicular current:

$$-2\boldsymbol{\xi}\cdot(\boldsymbol{\kappa}_{\rm c}+\boldsymbol{\kappa}_{\rm g})\,\boldsymbol{\xi}_\perp\cdot(\boldsymbol{\nabla}P - \rho\boldsymbol{g}) = -2\boldsymbol{\xi}\cdot(\boldsymbol{\kappa}_{\rm c}+\boldsymbol{\kappa}_{\rm g})\,\boldsymbol{\xi}_\perp\cdot\frac{\boldsymbol{j}_\perp\times\boldsymbol{B}}{c}. \tag{VI.11.20}$$

In the pinch geometry of §VI.9, this term reads

$$-\frac{1}{4\pi}\left[B_z\frac{\mathrm{d}B_z}{\mathrm{d}R}+B_\varphi\frac{1}{R}\frac{\mathrm{d}(RB_\varphi)}{\mathrm{d}R}\right]\frac{2b_\varphi^2}{R}\,\xi_R^2, \tag{VI.11.21}$$

which for outwardly increasing field strengths is negative. Put differently, when the field-line curvature vector and the thermal pressure gradient are oriented in the same direction, this term is negative definite and can cause pressure-driven instabilities, corresponding to a situation often referred to as 'bad curvature'. In the Parker-instability geometry of §VI.7, equation (VI.11.20) is instead

$$+\frac{\rho g}{\gamma\beta}\frac{\mathrm{d}\ln B^2}{\mathrm{d}z}\,\xi_z^2, \tag{VI.11.22}$$

which for upwardly decreasing field strengths is negative. This agrees with the previous linear calculations. Let's now see if the details check out...

VI.12. Convective and pinch instabilities, revisited

With the intuitive form of the energy principle in hand, let us revisit the linear stability analyses from earlier in this Chapter and make sure we recover the same stability criteria. First, the Parker instability. With the plane-parallel, magnetohydrostatic atmosphere having

$$\boldsymbol{\kappa}_\mathrm{c}=\boldsymbol{j}_\parallel=\boldsymbol{0}\quad\text{and}\quad\boldsymbol{\nabla}P-\rho\boldsymbol{g}=-\frac{\mathrm{d}}{\mathrm{d}z}\frac{B^2}{8\pi}\hat{\boldsymbol{z}},$$

equation (VI.11.13) becomes

$$\delta W_2=\frac{1}{2}\int\mathrm{d}\boldsymbol{r}\left\{\gamma P\left(\boldsymbol{\nabla\cdot\xi}-\xi_z\frac{g}{c_\mathrm{s}^2}\right)^2+\frac{|\delta\boldsymbol{B}_\perp|^2}{4\pi}+\frac{B^2}{4\pi}\left(\boldsymbol{\nabla\cdot\xi}_\perp\right)^2\right.$$
$$\left.+\frac{\rho g}{\gamma}\left(\frac{1}{\beta}\frac{\mathrm{d}\ln B^2}{\mathrm{d}z}+\frac{\mathrm{d}\ln P\rho^{-\gamma}}{\mathrm{d}z}\right)\xi_z^2\right\}. \tag{VI.12.1}$$

From this expression, it is immediately clear that a sufficient condition for stability is

$$\frac{1}{\beta}\frac{\mathrm{d}\ln B^2}{\mathrm{d}z}+\frac{\mathrm{d}\ln P\rho^{-\gamma}}{\mathrm{d}z}\geqslant 0. \tag{VI.12.2}$$

Instability may be assessed by first minimizing δW_2 with respect to $\eta\doteq\boldsymbol{\nabla\cdot\xi}$ after using $\delta\boldsymbol{B}_\perp=\mathrm{i}k_xB\xi_z\hat{\boldsymbol{z}}$ and $\boldsymbol{\nabla\cdot\xi}_\perp=\xi_z'$ where the $'$ denotes differentiation with respect to z:

$$\frac{\partial[\text{integrand}]}{\partial\eta}=2\gamma P\left(\eta-\xi_z\frac{g}{c_\mathrm{s}^2}\right)=0\quad\Longrightarrow\quad\eta=\frac{g}{c_\mathrm{s}^2}\xi_z. \tag{VI.12.3}$$

Substituting this expression for η back into (VI.12.1) gives

$$\delta W_2=\frac{1}{2}\int\mathrm{d}\boldsymbol{r}\left\{\frac{k_x^2B^2}{4\pi}|\xi_z|^2+\frac{B^2}{4\pi}|\xi_z'|^2+\frac{\rho g}{\gamma}\left(\frac{1}{\beta}\frac{\mathrm{d}\ln B^2}{\mathrm{d}z}+\frac{\mathrm{d}\ln P\rho^{-\gamma}}{\mathrm{d}z}\right)|\xi_z|^2\right\}. \tag{VI.12.4}$$

To minimize the stabilizing terms, seek modes for which $k_z\to 0$ and $\delta W_2<0$:

$$k_x^2v_\mathrm{A}^2+\frac{g}{\gamma}\left(\frac{1}{\beta}\frac{\mathrm{d}\ln B^2}{\mathrm{d}z}+\frac{\mathrm{d}\ln P\rho^{-\gamma}}{\mathrm{d}z}\right)<0\qquad\text{(Parker instability criterion)} \tag{VI.12.5}$$

This agrees with our linear calculation in (VI.7). Good.

Next, let us investigate the Z-pinch with $B_z = \text{const}$, for which

$$\boldsymbol{\kappa}_\mathrm{g} = \boldsymbol{j}_\parallel = \boldsymbol{0}, \quad \boldsymbol{\kappa}_\mathrm{c} = -\frac{b_\varphi^2}{R}\hat{\boldsymbol{R}}, \quad \boldsymbol{\nabla} P = -\frac{1}{8\pi R^2}\frac{\mathrm{d}(RB_\varphi)^2}{\mathrm{d}R}\hat{\boldsymbol{R}}.$$

Equation (VI.11.13) becomes

$$\delta W_2 = \frac{1}{2}\int \mathrm{d}\boldsymbol{r}\left\{\gamma P(\boldsymbol{\nabla\cdot\xi})^2 + \frac{|\delta\boldsymbol{B}_\perp|^2}{4\pi} + \frac{B^2}{4\pi}\left(\boldsymbol{\nabla\cdot\xi}_\perp - \xi_R\frac{2b_\varphi^2}{R}\right)^2 - \frac{B_\varphi}{4\pi R}\frac{\mathrm{d}(RB_\varphi)}{\mathrm{d}R}\frac{2b_\varphi^2}{R}\,\xi_R^2\right\}. \tag{VI.12.6}$$

To investigate the most unstable sausage mode, set $m = B_z = 0$. Then $\delta\boldsymbol{B}_\perp = \mathrm{i}(\boldsymbol{k\cdot B})\boldsymbol{\xi}_\perp = 0$ because $\boldsymbol{k}$ has no component along $\hat{\boldsymbol{b}}$, and $\boldsymbol{\nabla\cdot\xi}_\perp = \boldsymbol{\nabla\cdot\xi}$. Denoting $\eta \doteq \boldsymbol{\nabla\cdot\xi}$, we have that

$$\delta W_2 = \frac{1}{2}\int \mathrm{d}\boldsymbol{r}\left\{\gamma P\,\eta^2 + \frac{B^2}{4\pi}\left(\eta - \xi_R\frac{2}{R}\right)^2 - \frac{B_\varphi}{4\pi R}\frac{\mathrm{d}(RB_\varphi)}{\mathrm{d}R}\frac{2}{R}\,\xi_R^2\right\}. \tag{VI.12.7}$$

As with the Parker instability, minimize δW_2 with respect to η:

$$\frac{\partial[\text{integrand}]}{\partial\eta} = 2\gamma P\eta + 2\frac{B^2}{4\pi}\left(\eta - \xi_R\frac{2}{R}\right) = 0 \quad\Longrightarrow\quad \eta = \frac{2}{1+\gamma\beta/2}\frac{\xi_R}{R}. \tag{VI.12.8}$$

Substituting this expression back into (VI.12.7) and rearranging yields

$$\delta W_2 = -\int \mathrm{d}\boldsymbol{r}\,\frac{B^2}{4\pi}\left(\frac{1-\gamma\beta/2}{1+\gamma\beta/2} + \frac{\mathrm{d}\ln B_\varphi}{\mathrm{d}\ln R}\right)\frac{|\xi_R|^2}{R^2}, \tag{VI.12.9}$$

which provides a necessary condition for instability:

$$\frac{\mathrm{d}\ln B_\varphi}{\mathrm{d}\ln R} + \frac{1-\gamma\beta/2}{1+\gamma\beta/2} > 0 \qquad (Z\text{-pinch sausage instability criterion}) \tag{VI.12.10}$$

This matches the criterion obtained in §VI.9. Restoring $m \neq 0$ and $B_z \neq 0$ but setting $\boldsymbol{\nabla\cdot\xi} = 0$ will let us investigate the kink mode. In this case, equation (VI.11.13) reduces to

$$\delta W_2 = \frac{1}{2}\int \mathrm{d}\boldsymbol{r}\left\{\frac{|\delta\boldsymbol{B}_\perp|^2}{4\pi} + \frac{B^2}{4\pi}\left(\boldsymbol{\nabla\cdot\xi}_\parallel + \xi_R\frac{2b_\varphi^2}{R}\right)^2 - \frac{B_\varphi}{4\pi R}\frac{\mathrm{d}(RB_\varphi)}{\mathrm{d}R}\frac{2b_\varphi^2}{R}\,\xi_R^2\right\}. \tag{VI.12.11}$$

Already from here, it's clear that a necessary (but not sufficient) condition for instability is that RB_φ increase outwards. To go further, write $\boldsymbol{\xi} \to \sum_{m,k_z}\boldsymbol{\xi}(R)\exp(\mathrm{i}m\varphi + \mathrm{i}k_z z)$ and expand each of the terms. To keep things manageable for this first pass, take $B_z/B_\varphi \ll 1$ but $\boldsymbol{k\cdot B}$ finite (as in §VI.9). Then

$$\frac{|\delta\boldsymbol{B}_\perp|^2}{B^2} \simeq k_\parallel^2\big(|\xi_R|^2 + |\xi_z|^2\big), \quad \xi_\parallel = \frac{1}{k_\parallel}\left[\frac{\mathrm{i}}{R}\frac{\mathrm{d}(R\xi_R)}{\mathrm{d}R} - k_z\xi_z\right].$$

Substituting these into (VI.12.11) and minimizing δW_2 with respect to ξ_z^*, we find after some straightforward algebra that

$$\frac{\partial[\text{integrand}]}{\partial\xi_z^*} = 0 \quad\Longrightarrow\quad \xi_z \simeq \frac{\mathrm{i}k_z}{k^2}\left[\frac{1}{R}\frac{\mathrm{d}(R\xi_R)}{\mathrm{d}R} - 2\frac{\xi_R}{R}\right] \tag{VI.12.12}$$

with $k^2 = k_z^2 + (m/R)^2$, and so

$$\delta W_2 \simeq \sum_{m,k_z} \pi L_z \int_0^\infty \mathrm{d}R\, R\, \frac{B^2}{4\pi} \left\{ \left[k_\parallel^2 R^2 - 2\left(1 + \frac{\mathrm{d}\ln B_\varphi}{\mathrm{d}\ln R}\right)\right] \frac{|\xi_R|^2}{R^2} + \frac{k_\parallel^2}{k^2} \left| \frac{1}{R}\frac{\mathrm{d}(R\xi_R)}{\mathrm{d}R} - \frac{2m}{k_\parallel R}\frac{\xi_R}{R} \right|^2 \right\} \tag{VI.12.13}$$

by Parseval's theorem. The term on the bottom row is positive and therefore stabilizing, so to minimize its influence we take the limit $m^2 \ll k_z^2 R^2$, so that $k_\parallel^2/k^2 \ll 1$. Then the remaining terms will afford the possibility that $\delta W_2 < 0$ (instability) if

$$\frac{\mathrm{d}\ln B_\varphi}{\mathrm{d}\ln R} > \frac{k_\parallel^2 R^2}{2} - 1 \qquad (Z\text{-pinch kink instability criterion}) \tag{VI.12.14}$$

Note that $k_\parallel = (m/R)b_\varphi + k_z b_z$, and so the axial magnetic field is stabilizing, just as we found in §VI.9.

Now the θ-pinch with $B_z = B_z(R)$ and $B_\varphi = 0$, for which

$$\boldsymbol{\kappa}_\mathrm{g} = \boldsymbol{\kappa}_\mathrm{c} = \boldsymbol{j}_\parallel = \boldsymbol{0}, \quad \boldsymbol{\nabla} P = -\frac{1}{8\pi}\frac{\mathrm{d}B_z^2}{\mathrm{d}R}\hat{\boldsymbol{R}}.$$

Already it's obvious from the energy principle that this system is stable: all of the sign-indefinite terms vanish under these conditions, and all that remains are non-negative terms:

$$\delta W_2 = \frac{1}{2}\int \mathrm{d}\boldsymbol{r} \left\{ \gamma P (\boldsymbol{\nabla\cdot\xi})^2 + \frac{|\delta \boldsymbol{B}_\perp|^2}{4\pi} + \frac{B_z^2}{4\pi}(\boldsymbol{\nabla\cdot\xi}_\perp)^2 \right\} \geqslant 0. \tag{VI.12.15}$$

One may determine what the least stable configuration is by minimizing δW_2. As usual, this is aided by adopting incompressibility, for which $\boldsymbol{\nabla\cdot\xi}_\perp = -\mathrm{i}k_z\xi_z$. Using $|\delta\boldsymbol{B}_\perp|^2 = (\boldsymbol{k\cdot B})^2(|\xi_R|^2 + |\xi_\varphi|^2)$ then provides

$$\delta W_2 \to \int \mathrm{d}\boldsymbol{r}\, \frac{1}{2}\rho v_{\mathrm{A}z}^2\, k_\parallel^2 |\boldsymbol{\xi}|^2, \tag{VI.12.16}$$

again demonstrating stability but indicating that the least stable modes are those having the longest wavelengths (which produce the least amount of magnetic tension and pressure).

Finally, all the incompressible pinch results may be obtained in full generality by examining the screw pinch with $B_\varphi = B_\varphi(R)$ and $B_z = B_z(R)$. In this case, $\boldsymbol{\kappa}_\mathrm{g} = 0$ and

$$\boldsymbol{j}_\parallel = \frac{c}{4\pi}\left[\frac{b_z}{R}\frac{\mathrm{d}(RB_\varphi)}{\mathrm{d}R} - b_\varphi \frac{\mathrm{d}B_z}{\mathrm{d}R}\right]\hat{\boldsymbol{b}}, \quad \boldsymbol{\kappa}_\mathrm{c} = -\frac{b_\varphi^2}{R}\hat{\boldsymbol{R}}, \quad \boldsymbol{\nabla}P = -\left[\frac{\mathrm{d}}{\mathrm{d}R}\frac{B_z^2}{8\pi} + \frac{B_\varphi}{4\pi R}\frac{\mathrm{d}(RB_\varphi)}{\mathrm{d}R}\right]\hat{\boldsymbol{R}}.$$

With $\boldsymbol{\nabla\cdot\xi} = 0$ implying $\boldsymbol{\nabla\cdot\xi}_\perp = -\boldsymbol{\nabla\cdot\xi}_\parallel$, equation (VI.11.13) becomes

$$\delta W_2 = \frac{1}{2}\int \mathrm{d}\boldsymbol{r} \left\{ \frac{|\delta\boldsymbol{B}_\perp|^2}{4\pi} + \frac{B^2}{4\pi}\left(\boldsymbol{\nabla\cdot\xi}_\parallel + \xi_R \frac{2b_\varphi^2}{R}\right)^2 + \frac{j_\parallel}{c}\hat{\boldsymbol{b}}\boldsymbol{\cdot}(\boldsymbol{\xi}\times\delta\boldsymbol{B}) + \frac{2b_\varphi^2}{R}\frac{\mathrm{d}P}{\mathrm{d}R}\xi_R^2 \right\}. \tag{VI.12.17}$$

With the magnetic field oriented in a spiral, it is convenient to orient our coordinate system with a tetrad given by $\hat{\boldsymbol{R}}$, $\hat{\boldsymbol{b}}$, and the mutually orthogonal direction $\hat{\boldsymbol{\eta}} \doteq \hat{\boldsymbol{R}}\times\hat{\boldsymbol{b}}$.

The translation between these coordinates and the usual cylindrical ones is afforded by

$$\xi_\parallel \doteq \boldsymbol{\xi}\cdot\hat{\boldsymbol{b}} = b_\varphi\xi_\varphi + b_z\xi_z \quad \text{and} \quad \xi_\eta \doteq \boldsymbol{\xi}\cdot\hat{\boldsymbol{\eta}} = -b_z\xi_\varphi + b_\varphi\xi_z, \tag{VI.12.18}$$

$$\delta\boldsymbol{B}_\perp = \mathrm{i}k_\parallel B\xi_R\,\hat{\boldsymbol{R}} + \left\{\mathrm{i}k_\parallel B\xi_\eta + \left[b_z\frac{\mathrm{d}(B_\varphi/R)}{\mathrm{d}\ln R} - b_\varphi\frac{\mathrm{d}B_z}{\mathrm{d}R}\right]\xi_R\right\}\hat{\boldsymbol{\eta}}. \tag{VI.12.19}$$

Incompressibility provides

$$\xi_\parallel = \frac{\mathrm{i}}{k_\parallel}\left[\frac{1}{R}\frac{\mathrm{d}(R\xi_R)}{\mathrm{d}R} + \mathrm{i}k_\eta\xi_\eta\right]. \tag{VI.12.20}$$

Substituting these expressions into (VI.12.17), minimizing the result with respect to ξ_η^*, and praying that all goes well ultimately leads to

$$\xi_\eta = \frac{\mathrm{i}k_\eta}{k^2R}\left[\frac{\mathrm{d}(R\xi_R)}{\mathrm{d}R} - 2\frac{k_zb_\varphi}{k_\eta}\xi_R\right] \tag{VI.12.21}$$

and

$$\delta W_2 = \sum_{m,k_z}\pi L_z\int_0^\infty \mathrm{d}R\,R\,\frac{B^2}{4\pi}\left\{\left[k_\parallel^2R^2 - 2b_\varphi^2\left(1+\frac{\mathrm{d}\ln B_\varphi}{\mathrm{d}\ln R}\right)\right]\frac{|\xi_R|^2}{R^2} + \frac{k_\parallel^2}{k^2}\left|\frac{1}{R}\frac{\mathrm{d}(R\xi_R)}{\mathrm{d}R} - \frac{2b_\varphi m}{k_\parallel R}\frac{\xi_R}{R}\right|^2\right\}, \tag{VI.12.22}$$

Somewhere there needs to be a note about $k_\parallel \neq 0$.
Suydam's criterion (1958) for stability:

$$1 + 4\frac{8\pi P'q^2}{RB_z^2q'^2} > 0 \quad RB_z^2\left(\frac{q'}{q}\right)^2 + 32\pi P' > 0.$$

$q = (R/R_0)(B_z/B_\varphi)$. Destabilizing term is bad curvature of B_φ field. Stabilizing term represents work done bending the magnetic-field lines when interchanging two flux tubes in a system with shear.

The "straight tokamak": cylindrical column of length $2\pi R_0$ with $B_\varphi/B_z \sim \epsilon$, $q \sim 1$, $\beta_z \sim \epsilon^2$, with $\epsilon \doteq a/R_0 \ll 1$.

VI.13. Ballooning modes

In preparation

PART VII
MHD discontinuities and shocks

Everything included in the last two Parts of these lecture notes focused solely on the linear evolution of perturbations, i.e., evolution in which nonlinearities affecting a single wave are ignored and any nonlinear couplings between different wave modes are ignored. This is usually justified by stating that the perturbation amplitudes are "sufficiently small." But there is actually more that is required. Even for small-amplitude perturbations, nonlinearities can accumulate over time and cause effects not described by linear theory. In the presence of multiple fluctuations, these nonlinearities can transfer energy amongst the modes, sending energy to smaller or larger scales in what is commonly referred to as a cascade. But even for single fluctuations, nonlinearities do interesting things. For example, nonlinearities can cause a fluctuation to steepen into a sawtooth-like, rather than sinusoidal, profile (§VII.1). The resulting discontinuity at the front of the sawtooth profile triggers dissipative or dispersive effects whose job it is to smooth the profile over what is called a boundary layer. Nevertheless, there remains a relatively sharp transition between conditions just ahead of the boundary layer and just behind the boundary layer. Even though this transition often involves irreversible dissipation and the conversion of bulk flow energy into thermal energy, one may relate these two regions – upstream and downstream – via the conservation of mass, momentum, total energy, and, when magnetic fields are present, magnetic flux. These relations are called the Rankine–Hugoniot jump conditions, the topic of §VII.2. But such discontinuities and the jump conditions that describe them apply more broadly than to the products of nonlinear wave steepening. Anything that generates a time-steady, discontinuous change in the state of the plasma can be described by the Rankine–Hugoniot jump conditions. The classic example of this is the shock, which occurs when an object or disturbance moves faster than information can propagate into the surrounding fluid or plasma. The lack of causal connection with the surrounding medium means that it cannot react and thus gets swept up and compressed. With multiple speeds characterizing a hot, magnetized plasma – sound, Alfvén, fast and slow magnetosonic – it is therefore not surprising that there are multiple types of shocks. Additional non-ideal physics, such as radiative cooling, anisotropic pressure, or two-fluid effects like ambipolar diffusion, make the study of MHD shocks all the more rich and rewarding.

VII.1. Wave steepening

The process of wave steepening applies to a variety of linear waves, but for this presentation we focus solely on an adiabatic sound wave, in which case the only nonlinearity is from the Reynolds stress that provides the by-now-familiar $\boldsymbol{u}\cdot\boldsymbol{\nabla}\boldsymbol{u}$ term. Estimating its size as $\sim k(\delta u)^2$ for a fluctuation of wavenumber k and amplitude δu, it is clear that this term becomes important when its time-integrated size becomes large enough to compete with the linear-in-δu inertial term:

$$\delta u \sim k(\delta u)^2 t_{\rm nl}, \tag{VII.1.1}$$

where $t_{\rm nl}$ the nonlinear timescale over which such nonlinear effects accumulate. This is readily solved to find that

$$t_{\rm nl} \sim (k\delta u)^{-1}. \tag{VII.1.2}$$

For a small-amplitude wave, this can be a long time, but the steepening is inevitable unless some self-organizational process acts to minimize the dot product between $\boldsymbol{u}$ and its gradient $\boldsymbol{\nabla u}$. But why "steepening"? The reason is that, as the sound wave propagates, the parts of the wave having larger density also have a larger sound speed, and vice versa for the parts with smaller density. With the sound speed being the characteristic speed at which the wave travels, this means that the peaks travel at a slightly larger speed than do the troughs. As those peaks advance ahead of the average wave speed, they gradually catch up to the troughs, causing the gradients in the density, and thus the flow, to get progressively larger. In a time $t_{\rm nl}$, those gradients become large enough for the "linear" wave to no longer look like a linear wave: the sinusoidal variation of the density and flow has been replaced by a profile that is more like a sawtooth. Let us mathematize this physical reasoning.

Start with the continuity and momentum equations for the density and flow velocity:

$$\frac{\partial \rho}{\partial t} + \boldsymbol{u}\boldsymbol{\cdot}\boldsymbol{\nabla}\rho = -\rho\boldsymbol{\nabla}\boldsymbol{\cdot}\boldsymbol{u} \quad \text{and} \quad \frac{\partial \boldsymbol{u}}{\partial t} + \boldsymbol{u}\boldsymbol{\cdot}\boldsymbol{\nabla}\boldsymbol{u} = -c_{\rm s}^2\frac{\boldsymbol{\nabla}\rho}{\rho}. \tag{VII.1.3}$$

Here we have taken the equation of state to be adiabatic, with the pressure $P = \rho c_{\rm s}^2/\gamma$ for an adiabatic sound speed $c_{\rm s} \doteq (\gamma P/\rho)^{1/2}$. This adiabatic assumption will fail eventually, once the nonlinearity leads to gradients sharp enough to trigger dissipation, but let's run with it for now. Use $P = P_0(\rho/\rho_0)^\gamma$ to replace ρ in (VII.1.3) with $c_{\rm s} = c_{\rm s0}(\rho/\rho_0)^{(\gamma-1)/2}$ for some background $c_{\rm s0}$ and ρ_0:

$$\frac{2}{\gamma-1}\left(\frac{\partial c_{\rm s}}{\partial t} + \boldsymbol{u}\boldsymbol{\cdot}\boldsymbol{\nabla}c_{\rm s}\right) = -c_{\rm s}\boldsymbol{\nabla}\boldsymbol{\cdot}\boldsymbol{u} \quad \text{and} \quad \frac{\partial \boldsymbol{u}}{\partial t} + \boldsymbol{u}\boldsymbol{\cdot}\boldsymbol{\nabla}\boldsymbol{u} = -\frac{2}{\gamma-1}c_{\rm s}\boldsymbol{\nabla}c_{\rm s}. \tag{VII.1.4}$$

Restricting attention to the one-dimensional problem (without loss of generality) and re-arranging terms, we find

$$\frac{2}{\gamma-1}\frac{\partial c_{\rm s}}{\partial t} + c_{\rm s}\frac{\partial u}{\partial x} = -\frac{2}{\gamma-1}u\frac{\partial c_{\rm s}}{\partial x} \quad \text{and} \quad \frac{\partial u}{\partial t} + u\frac{\partial u}{\partial x} = -\frac{2}{\gamma-1}c_{\rm s}\frac{\partial c_{\rm s}}{\partial x}. \tag{VII.1.5}$$

The symmetry of these equations is suggestive... add them and subtract them:

$$\frac{\partial}{\partial t}\left(u \pm \frac{2}{\gamma-1}c_{\rm s}\right) + (u \pm c_{\rm s})\frac{\partial}{\partial x}\left(u \pm \frac{2}{\gamma-1}c_{\rm s}\right) = 0. \tag{VII.1.6}$$

This equation states that the quantities

$$J_\pm \doteq u \pm \frac{2}{\gamma-1}c_{\rm s} \tag{VII.1.7}$$

are constant along the characteristics $v_\pm \doteq u \pm c_{\rm s}$. Given any initial conditions, we can compute $J_\pm$ and simply advect those quantities along ${\rm d}x/{\rm d}t = v_\pm$.

Consider initial conditions corresponding to the eigenvector of a linear sound wave having wavenumber k and propagating in the $+x$ direction:

$$\frac{\delta\rho}{\rho_0} = \frac{\delta u}{c_{\rm s0}} = \frac{2}{\gamma-1}\frac{\delta c_{\rm s}}{c_{\rm s0}}. \tag{VII.1.8}$$

The corresponding values of $J_\pm$ are

$$J_+ = \delta u + \frac{2}{\gamma-1}(c_{\rm s0} + \delta c_{\rm s}) = 2\,\delta u + \frac{2}{\gamma-1}c_{\rm s0}, \tag{VII.1.9}$$

$$J_- = \delta u - \frac{2}{\gamma-1}(c_{\rm s0} + \delta c_{\rm s}) = \qquad -\frac{2}{\gamma-1}c_{\rm s0}. \tag{VII.1.10}$$

With $\delta u = (1/2)(J_+ + J_-)$ and $c_{\rm s0} + \delta c_{\rm s} = [(\gamma-1)/4](J_+ - J_-)$, the characteristic velocity expressed in terms of the invariants is

$$v = \frac{1}{2}(J_+ + J_-) + \frac{\gamma - 1}{4}(J_+ - J_-) = \frac{\gamma + 1}{4} J_+ + \frac{3 - \gamma}{4} J_- . \tag{VII.1.11}$$

With J_- constant and independent of position, and J_+ constant along the characteristic, the characteristic velocity is constant along the characteristic. Substituting in the eigenvector $\delta u = A\, c_{s0} \cos kx$ with amplitude A, we have

$$v = c_{s0}\left(1 + A\,\frac{1+\gamma}{2}\cos kx_0\right) \quad\Longrightarrow\quad x(t, x_0) = c_{s0}\left(1 + A\,\frac{1+\gamma}{2}\cos kx_0\right) t + x_0 . \tag{VII.1.12}$$

The characteristics have different slopes depending on their origin x_0, and fluid elements issuing from different values of x_0 can end up at the same location. The condition for this to occur is that characteristics issuing from x_0 and $x_1 > x_0$ ultimately share the same $x(t_{\rm nl})$ after the nonlinear time $t_{\rm nl}$, or

$$c_{s0}\left(1 + A\,\frac{1+\gamma}{2}\cos kx_0\right) t_{\rm nl} + x_0 = c_{s0}\left(1 + A\,\frac{1+\gamma}{2}\cos kx_1\right) t_{\rm nl} + x_1 \tag{VII.1.13}$$

$$\Longrightarrow \quad c_{s0} t_{\rm nl} = \frac{2}{\gamma+1}\frac{(x_1 - x_0)}{A(\cos kx_0 - \cos kx_1)} \approx \frac{2}{\gamma+1}\frac{1}{Ak\sin kx_0} \tag{VII.1.14}$$

when x_1 and x_0 are close. This matches our heuristic argument in (VII.1.2). An example of such characteristics (for $A = 0.1$, $\gamma = 5/3$, $k = 2\pi$) is shown in the figure below, which an intersection of characteristics highlighted:

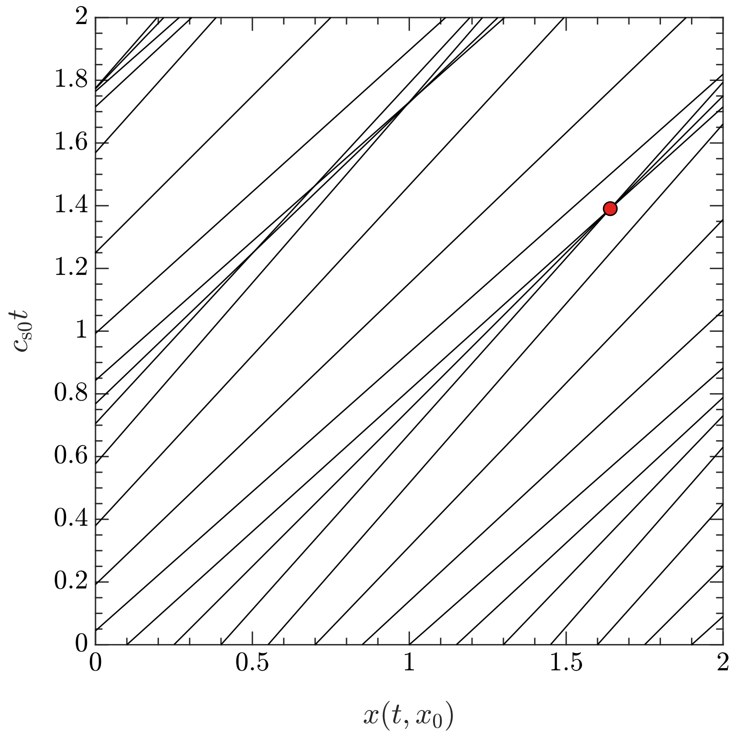

VII.2. Rankine–Hugoniot jump conditions

Once a shock is established and evolves into a steady state, can the characteristics of the downstream plasma be expressed solely in terms of the conditions found upstream? The answer, supplied by the *Rankine–Hugoniot jump conditions*, is yes. For an MHD plasma, these conditions are obtained by taking the equations of mass continuity, momentum, total energy, and magnetic induction, setting their time derivatives equal to zero, and integrating the result across the shock front. When supplemented by the solenoidality constraint on the magnetic field, the result is a set of equations expressing continuity of the fluxes across the shock interface. This procedure is most easily done in the frame of the shock, such that the shock is a stationary boundary across which the fluid variables change discontinuously. The convention in what follows is that the upstream plasma enters from the shock front from the left, gets processed, and exits to the right. The calculation is also eased when the steady-state equations are written in conservative form:

$$\nabla\cdot(\rho\boldsymbol{u}) = 0, \tag{VII.2.1}$$

$$\nabla\cdot\left[\rho\boldsymbol{u}\boldsymbol{u} + \left(p + \frac{B^2}{8\pi}\right)\mathsf{I} - \frac{\boldsymbol{B}\boldsymbol{B}}{4\pi}\right] = 0, \tag{VII.2.2}$$

$$\nabla\cdot\left[\left(\frac{1}{2}\rho u^2 + \frac{\gamma P}{\gamma-1} + \frac{B^2}{4\pi}\right)\boldsymbol{u} - \frac{(\boldsymbol{B}\cdot\boldsymbol{u})\boldsymbol{B}}{4\pi}\right] = 0, \tag{VII.2.3}$$

$$\nabla\cdot(\boldsymbol{u}\boldsymbol{B} - \boldsymbol{B}\boldsymbol{u}) = 0, \tag{VII.2.4}$$

$$\nabla\cdot\boldsymbol{B} = 0. \tag{VII.2.5}$$

Note that we are using here an equation for the total energy; the equation governing the internal energy (or the entropy) is useless here, because dissipation within the shock causes the fluid to jump to a different adiabat as it crosses through. Even though no time derivatives appear in the above equations, there is a sense of irreversibility, which in the fluid case is enabled by viscosity within the shock transition converting kinetic energy into internal energy.

VII.2.1. *General derivation of the jump conditions*

To obtain the jump conditions, we integrate the above conservation laws over a volume centered about the shock front having infinitesimal thickness, and use Gauss' law to turn the divergences into surface integrals. Evaluating those surface integrals just upstream of the shock (subscript "1") and just downstream of the shock (subscript "2") leads to the following set of difference equations:

$$\big[\rho u_n\big]_{12} = 0, \tag{VII.2.6}$$

$$\left[\rho u_n\boldsymbol{u} + \left(P + \frac{B^2}{8\pi}\right)\hat{\boldsymbol{n}} - \frac{B_n\boldsymbol{B}}{4\pi}\right]_{12} = 0, \tag{VII.2.7}$$

$$\left[\left(\frac{1}{2}\rho u^2 + \frac{\gamma P}{\gamma-1} + \frac{B^2}{4\pi}\right)u_n - \frac{(\boldsymbol{B}\cdot\boldsymbol{u})B_n}{4\pi}\right]_{12} = 0, \tag{VII.2.8}$$

$$\big[u_n\boldsymbol{B} - B_n\boldsymbol{u}\big]_{12} = 0, \tag{VII.2.9}$$

$$\big[B_n\big]_{12} = 0, \tag{VII.2.10}$$

where $[\dots]_{12}$ denotes the difference in the quantity in brackets between the two regions. A schematic is shown here with all quantities labeled:

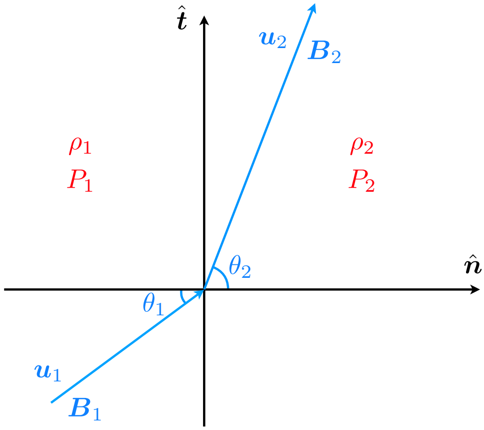

Equation (VII.2.6) states that whatever mass flows into the shock must exit the shock in steady state:

$$\rho_1 u_{n1} = \rho_2 u_{n2} \quad \Longrightarrow \quad \frac{u_{n1}}{u_{n2}} = \frac{\rho_2}{\rho_1} \doteq R. \tag{VII.2.11}$$

In the final line, we have followed standard practice in denoting the density ratio by R, a quantity that obviously must be >1 for there to be a shock. Our task is then to express the ratios of all other quantities (e.g., P_2/P_1, B_2/B_1) in terms of R, and then solve a polynomial equation for R to close the system.

The component of (VII.2.7) along the shock normal is

$$\rho_1 u_{n1}^2 + P_1 + \frac{B_1^2}{8\pi} - \frac{B_{n1}^2}{4\pi} = \rho_2 u_{n2}^2 + P_2 + \frac{B_2^2}{8\pi} - \frac{B_{n2}^2}{4\pi} \tag{VII.2.12}$$

With (VII.2.10) guaranteeing that $B_{n2} = B_{n1}$, the only component of the magnetic field that enters this equation is the tangential component, B_t. Dividing this equation through by $\rho_1 u_{n1}^2$ and defining the Mach number via $M^2 \doteq u_{\rm n1}^2/c_{\rm s1}^2$, where $c_{\rm s1} \doteq (\gamma P_1/\rho_1)^{1/2}$ is the adiabatic sound speed in the upstream fluid, we find that

$$1 + \frac{1}{\gamma M^2}\left(1 + \frac{B_{t1}^2}{8\pi P_1}\right) = \frac{1}{R} + \frac{1}{\gamma M^2}\left(\frac{P_2}{P_1} + \frac{B_{t2}^2}{8\pi P_1}\right) \tag{VII.2.13}$$

Note that the magnetic field tangential to the shock front acts to enhance the pressure, making it more difficult for the shock to increase the density. At this point one might be tempted to introduce the plasma beta parameter in the upstream fluid, $\beta \doteq 8\pi P_1/B_1^2$, but it turns out to be more natural in shock problems to compare the magnetic energy not to the thermal pressure but rather to the ram pressure. So let us define the Alfvén Mach number $M_{\rm A} \doteq u_{n1}/v_{\rm A1}$, where $v_{\rm A1} \doteq B_1/(4\pi\rho_1)^{1/2}$ is the upstream Alfvén speed. To indicate that only the tangential component of the magnetic field enters, we also define the geometric factor $T \doteq B_{t1}^2/B_1^2$, in which case (VII.2.13) becomes

$$1 + \frac{1}{\gamma M^2} + \frac{T}{2M_{\rm A}^2} = \frac{1}{R} + \frac{1}{\gamma M^2}\frac{P_2}{P_1} + \frac{T}{2M_{\rm A}^2}\frac{B_{t2}^2}{B_{t1}^2}. \tag{VII.2.14}$$

The next step is to eliminate B_{t2}/B_{t1} using the tangential component of the steady-state induction equation (VII.2.9), which provides

$$u_{n1}\boldsymbol{B}_{t1} - B_{n1}\boldsymbol{u}_{t1} = u_{n2}\boldsymbol{B}_{t2} - B_{n2}\boldsymbol{u}_{t2} \quad \Longrightarrow \quad \frac{1}{R}\frac{\boldsymbol{B}_{t2}}{B_{n1}} - \frac{\boldsymbol{B}_{t1}}{B_{n1}} = \frac{\boldsymbol{u}_{t2}}{u_{n1}} - \frac{\boldsymbol{u}_{t1}}{u_{n1}}. \tag{VII.2.15}$$

The right-hand side of this equation may be readily obtained from the tangential component of the momentum equation (VII.2.7):

$$\rho_1 u_{n1}\boldsymbol{u}_{t1} - \frac{B_{n1}\boldsymbol{B}_{t1}}{4\pi} = \rho_2 u_{n2}\boldsymbol{u}_{t2} - \frac{B_{n2}\boldsymbol{B}_{t2}}{4\pi} \quad \Longrightarrow \quad \frac{\boldsymbol{u}_{t2}}{u_{n1}} - \frac{\boldsymbol{u}_{t1}}{u_{n1}} = \frac{N}{M_{\rm A}^2}\left(\frac{\boldsymbol{B}_{t2}}{B_{n1}} - \frac{\boldsymbol{B}_{t1}}{B_{n1}}\right) \tag{VII.2.16}$$

To obtain the final equality, we have used that $B_{n2} = B_{n1}$ and defined the geometric factor $N \doteq B_{n1}^2/B_1^2 = 1 - T$. Combining (VII.2.15) and (VII.2.16) then affords expressions for the tangential component of the magnetic field,

$$\boldsymbol{B}_{t2} = \left(\frac{R - RN/M_{\rm A}^2}{1 - RN/M_{\rm A}^2}\right)\boldsymbol{B}_{t1}, \tag{VII.2.17}$$

and the tangential component of the velocity,

$$\frac{\boldsymbol{u}_{t2}}{u_{n1}} = \frac{\boldsymbol{u}_{t1}}{u_{n1}} + \frac{N}{M_{\rm A}^2}\left(\frac{R-1}{1 - RN/M_{\rm A}^2}\right)\frac{\boldsymbol{B}_{t1}}{B_{n1}}. \tag{VII.2.18}$$

Note that $N = 0$ ensures $B_{t2}/B_{t1} = R$, so that the strength of the tangential field increases in proportion to the density (as expected from flux freezing). Note also the pole at $R = M_{\rm A}^2/N$, a feature to which we shall return in due course (§VII.2.5). With (VII.2.17) in hand, we can now revisit (VII.2.14), eliminate B_{t2}^2/B_{t1}^2, and re-arrange to obtain an expression for the pressure ratio:

$$\frac{1}{\gamma M^2}\frac{P_2}{P_1} = 1 - \frac{1}{R} + \frac{1}{\gamma M^2} + \frac{T}{2M_{\rm A}^2}\left[1 - \left(\frac{R - RN/M_{\rm A}^2}{1 - RN/M_{\rm A}^2}\right)^2\right]. \tag{VII.2.19}$$

With everything now expressed in terms of the unknown density enhancement R, we obtain our polynomial equation for R by substituting (VII.2.11) and (VII.2.17)–(VII.2.19) into the total energy equation (VII.2.8), or

$$\left(\frac{1}{2}\rho_1 u_1^2 + \frac{\gamma P_1}{\gamma - 1} + \frac{B_{t1}^2}{4\pi}\right)u_{n1} - \frac{B_{n1}\boldsymbol{B}_{t1}\boldsymbol{\cdot}\boldsymbol{u}_{t1}}{4\pi} = \left(\frac{1}{2}\rho_2 u_2^2 + \frac{\gamma P_2}{\gamma - 1} + \frac{B_{t2}^2}{4\pi}\right)u_{n2} - \frac{B_{n2}\boldsymbol{B}_{t2}\boldsymbol{\cdot}\boldsymbol{u}_{t2}}{4\pi}. \tag{VII.2.20}$$

Writing $u_1^2 = u_{n1}^2 + u_{t1}^2$ and dividing through by $(1/2)\rho_1 u_{n1}^3$ leads, after some straightforward algebra and re-organization, to the following equation for R:

$$\boxed{\begin{aligned} &\left(1 - \frac{RN}{M_{\rm A}^2}\right)^2\left[R^2\left(1 + \frac{2}{\gamma-1}\frac{1}{M^2}\right) - R\frac{2}{\gamma-1}\left(\gamma + \frac{1}{M^2}\right) + \frac{\gamma+1}{\gamma-1}\right] \\ &= \frac{RT}{M_{\rm A}^2}\left[-R^3\frac{N}{M_{\rm A}^2} + R^2\left(\frac{\gamma-2}{\gamma-1} + \frac{N}{M_{\rm A}^2}\frac{2\gamma}{\gamma-1}\right) - R\left(2 + \frac{N}{M_{\rm A}^2}\frac{\gamma+1}{\gamma-1}\right) + \frac{\gamma}{\gamma-1}\right]\end{aligned}} \tag{VII.2.21}$$

The subsequent subsections analyze this equation in a variety of limits.

Before proceeding, however, it is instructive to take the limit $R \to 1$, in which case (VII.2.21) returns

$$N = M_{\rm A}^2 \quad \text{and} \quad N = M^2 + M_{\rm A}^2 - M^2 M_{\rm A}^2. \tag{VII.2.22}$$

Re-arranging these and casting them in more familiar variables, we find

$$u_{n1}^2 = v_{\rm A1}^2 N \quad \text{and} \quad u_{n1}^2 = \frac{c_{\rm s1}^2 + v_{\rm A1}^2}{2} \pm \sqrt{\left(\frac{c_{\rm s1}^2 + v_{\rm A1}^2}{2}\right)^2 - c_{\rm s1}^2 v_{\rm A1}^2 N}, \qquad \text{(VII.2.23)}$$

i.e., the squares of the Alfvén and (fast and slow) magnetosonic speeds. In this sense, one may consider the various MHD shocks that are analyzed below as nonlinear versions of the usual MHD waves. It will turn out that $B_{t2} > B_{t1}$ for a fast shock, $B_{t2} < B_{t1}$ for a slow shock, and $B_{t2} \to -B_{t1}$ for an Alfvénic (sometimes called "intermediate") shock in the limit. Let us proceed.

VII.2.2. *HD and parallel MHD shocks*

Suppose there were no magnetic field (i.e., $M_{\rm A} \to \infty$). In this case, equation (VII.2.21) reduces to

$$R^2 \left(1 + \frac{2}{\gamma - 1}\frac{1}{M^2}\right) - R\,\frac{2}{\gamma - 1}\left(\gamma + \frac{1}{M^2}\right) + \frac{\gamma + 1}{\gamma - 1} = 0, \qquad \text{(VII.2.24)}$$

which may be readily solved to find

$$R = \frac{\gamma + 1}{\gamma - 1 + 2/M^2}. \qquad \text{(VII.2.25)}$$

This expression for R may then be substituted into the following expressions to obtain the jump ratios

$$\frac{\rho_2}{\rho_1} = \frac{u_{n1}}{u_{n2}} = R, \quad \frac{P_2}{P_1} = 1 + \gamma M^2 \left(1 - \frac{1}{R}\right) = 1 + \frac{2\gamma}{\gamma + 1}(M^2 - 1), \quad \boldsymbol{u}_{t2} = \boldsymbol{u}_{t1}. \qquad \text{(VII.2.26)}$$

Note that M must be greater than unity, or else the pressure would have to decrease across the shock; doing so would violate the second law of thermodynamics, as it would imply that heat energy is converted into ordered kinetic energy, with the pressure gradient accelerating the flow. The case $M = 1$ is of course a trivial solution, in which there is no discontinuity in any of the flow variables. The Mach number downstream of the shock may be obtained from $u_2/u_1 = 1/R$ and $c_{\rm s2}/c_{\rm s1} = (T_2/T_1)^{1/2} = (1/R)^{1/2}(P_2/P_1)^{1/2}$, or

$$M_2 \doteq \frac{u_2}{c_{\rm s2}} = \sqrt{\frac{(\gamma - 1) + 2/M^2}{2\gamma - (\gamma - 1)/M^2}} < 1. \qquad \text{(VII.2.27)}$$

The downstream flow is subsonic. Finally, it will be useful to have a general expression for the change in entropy $\sigma \doteq \ln(P/\rho^\gamma)$ across the shock front:

$$\sigma_2 - \sigma_1 = \ln\frac{P_2}{P_1} - \gamma \ln\frac{\rho_2}{\rho_1} = \ln\left[1 + \frac{2\gamma}{\gamma + 1}(M^2 - 1)\right] + \gamma \ln\left(\frac{\gamma - 1 + 2/M^2}{\gamma + 1}\right). \qquad \text{(VII.2.28)}$$

At $M = 1$, $\sigma_2 - \sigma_1 = 0$ because there is no shock. For $M > 1$, entropy increases and the fluid rapidly jumps to a different adiabat.

It is instructive to exam the two limiting cases of a strong shock ($M^2 \gg 1$) and a weak shock ($M^2 - 1 \ll 1$). The former can be easily read off:

$$\text{strong HD shock:} \quad R \approx \frac{\gamma + 1}{\gamma - 1}, \quad \frac{P_2}{P_1} \approx \frac{2\gamma}{\gamma + 1}M^2, \quad M_2 \approx \sqrt{\frac{\gamma - 1}{2\gamma}}. \qquad \text{(VII.2.29)}$$

Note that R asymptotes to a value that is independent of the Mach number (one that is worth committing to memory). For a monatomic gas with $\gamma = 5/3$, this implies a maximum compression ratio $R_{\max} = 4$, a pressure ratio $P_2/P_1 \approx (5/4)M^2$, a temperature ratio $T_2/T_1 \approx (5/16)M^2$, and a Mach number $M_2 \approx 0.45$. The reason for this asymptotic result is that the downstream pressure continues to increase as M^2, and so the fluid gets more and more difficult to compress as M increases. Despite the compression factor asymptoting to an order-unity number, the entropy increases without bound (see (VII.2.28)):

$$\sigma_2 - \sigma_1 \approx \ln\frac{2\gamma M^2}{\gamma+1} + \gamma\ln\frac{\gamma-1}{\gamma+1}. \tag{VII.2.30}$$

This makes sense – more and more irreversible dissipation of the kinetic energy must occur as M increases in order keep the compression ratio fixed. In the opposite limit of a weak shock, we may expand (VII.2.25) in $\epsilon \doteq M^2 - 1 \ll 1$ to find

$$\text{weak HD shock:} \quad R \approx 1 + \frac{2}{\gamma+1}\,\epsilon, \quad \frac{P_2}{P_1} \approx 1 + \frac{2\gamma}{\gamma+1}\,\epsilon, \quad M_2 \approx 1 - \frac{\epsilon}{2}. \tag{VII.2.31}$$

Obtaining the entropy change in this case requires expanding (VII.2.28) to $\mathcal{O}(\epsilon^3)$:

$$\sigma_2 - \sigma_1 \approx \frac{2\gamma(\gamma-1)}{3(\gamma+1)^2}\,\epsilon^3 \tag{VII.2.32}$$

So, indeed, entropy increases (though barely!).

Let us restore the magnetic field, but take $N = 1$ ($T = 0$) so that the magnetic field is oriented along the shock normal. In this case, the entire right-hand side of (VII.2.21) vanishes and we recover the hydrodynamic result (VII.2.25) times an Alfvénic root at $R = M_{\rm A}^2$. This makes sense, because the shock occurs while sliding along an unperturbed magnetic field oriented parallel to the flow – a "parallel MHD shock."

VII.2.3. *Perpendicular MHD shocks*

If the upstream magnetic field is instead oriented perpendicularly to the shock normal ($N = 0$, $T = 1$), then (VII.2.21) becomes

$$R^2\left(1 + \frac{2}{\gamma-1}\frac{1}{M^2}\right) - R\,\frac{2}{\gamma-1}\left(\gamma + \frac{1}{M^2}\right) + \frac{\gamma+1}{\gamma-1} = \frac{R}{M_{\rm A}^2}\left(R^2\,\frac{\gamma-2}{\gamma-1} - 2R + \frac{\gamma}{\gamma-1}\right), \tag{VII.2.33}$$

whose (cubic) solutions provide

$$\frac{P_2}{P_1} = 1 + \gamma M^2\left(1 - \frac{1}{R}\right) - \frac{1}{\beta}(R^2 - 1), \quad \boldsymbol{B}_{t2} = R\boldsymbol{B}_{t1}, \quad \boldsymbol{u}_{t2} = \boldsymbol{u}_{t1}. \tag{VII.2.34}$$

The minus sign in the final $(1/\beta)$ term in the pressure ratio, combined with the need for $(R^2 - 1)$ to be positive, indicates that the magnetic pressure relieves some of the burden on the gas pressure in supporting the shock. But for that to be true, the incoming flow must be at least super-Alfvénic, so that any magnetic compression cannot be radiated away as a wave. In the hydrodynamic (or parallel MHD) case, we required $M > 1$ for there to be a shock. What is the criterion here? Rather than solve this cubic for R and demand that $R > 1$, a simpler route is to write $R = 1 + \epsilon$ with $|\epsilon| \ll 1$, demand that ϵ be positive, and solve for M in terms of $M_{\rm A}$. The result is that

$$1 > \frac{1}{M^2} + \frac{1}{M_{\rm A}^2} \quad \Longrightarrow \quad u_1^2 > c_{\rm s1}^2 + v_{\rm A1}^2; \tag{VII.2.35}$$

i.e., the shock speed must exceed the fast magnetosonic speed ahead of the shock. Because of this, perpendicular shocks are often referred to as "fast-mode shocks."

Again without solving (VII.2.33) exactly, we may determine the effect of the magnetic field on the shock by writing $R = R_{\rm HD}(1+M_{\rm A}^{-2}\,\imath)$ with $R_{\rm HD}$ being the hydrodynamic solution (VII.2.25), and solving perturbatively for the correction $\imath$ assuming that $M_{\rm A}^2 \gg 1$ (equivalently, $\beta M^2 \gg 1$). After some algebra and adroit consolidation of terms, we find to $\mathcal{O}(M_{\rm A}^{-2})$ that

$$R = R_{\rm HD}\left\{1 - M_{\rm A}^{-2}\frac{2-(2-\gamma)/M^2-\gamma/M^4}{[(\gamma-1)+2/M^2][(\gamma-1)+(3-\gamma)/M^2-2/M^4]}\right\}. \qquad \text{(VII.2.36)}$$

In both the limits of $M^2 \gg 1$ and $(M^2-1) \ll 1$, the magnetic field acts to reduce the compression ratio:

$$\text{strong shock with } M_{\rm A}^2 \gg 1: \quad R \approx R_{\rm HD}\left[1 - M_{\rm A}^{-2}\frac{2}{(\gamma-1)^2}\right],$$

$$\text{weak shock with } M_{\rm A}^2 \gg 1: \quad R \approx R_{\rm HD}\left[1 - \frac{2}{\gamma\beta}\frac{\gamma+2}{(\gamma+1)^2}\right]. \qquad \text{(VII.2.37)}$$

This makes sense physically, because some of the kinetic energy must go into compressing the magnetic field. More general solutions of (VII.2.33) are obtained numerically and given in the figure below for different $\beta = (2/\gamma)(M_{\rm A}/M)^2$:

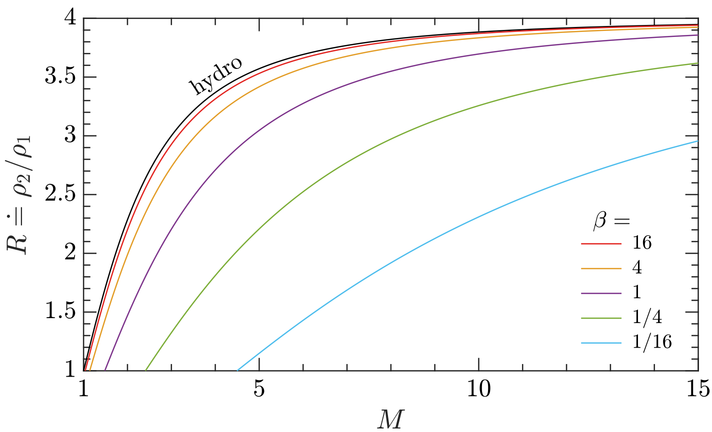

Stronger magnetic fields perpendicular to the shock normal reduce the compression ratio from its hydrodynamic value, while increasing the threshold Mach number for the shock to form.

VII.2.4. *Oblique MHD shocks*

When the upstream magnetic field and/or the incoming flow is oriented at an oblique angle with respect to the shock front, the situation becomes more complex. The field and flow can be refracted by the shock, with the angle of incidence being different on either side of the interface. As a first pass through this calculation, let us first drop the magnetic field and ask what would happen in a hydrodynamic setting if the incoming flow were at an angle. Equation (VII.2.16) states that $\boldsymbol{u}_{t2} = \boldsymbol{u}_{t1}$ in this case, and we know that $u_{n2} = u_{n1}/R$. Combining these, we see that $\tan\theta_2 \doteq u_{t2}/u_{n2} = R\,u_{t1}/u_{n1} \doteq R\tan\theta_1$, indicating that the flow changes direction in the downstream to become canted towards the plane of the shock. When an oblique magnetic field is also present, this increase in the angle θ across the shock is accompanied by a sharp bend in the magnetic-field lines, whose tension then affects the jump conditions by transferring momentum in the tangential direction.

An apparent complication from the conservation laws is that both $\boldsymbol{u}_{t1}$ and $\boldsymbol{B}_{t1}$ appear as initial conditions, implying that there are two independent angles to worry about, one related to u_{t1}^2/u_{n1}^2 and one related to $B_{t1}^2/B_{n1}^2 = T/N = 1/N - 1$. But the polynomial equation for R that we obtained (VII.2.21) only makes reference to the latter. The reason why is because one may boost to a frame in which $\boldsymbol{u}_1 \times \boldsymbol{B}_1 = \boldsymbol{0}$, in which the upstream flow and field are aligned. This frame is referred to as the *de Hoffmann–Teller frame* (De Hoffmann & Teller 1950). The idea is that, if $\boldsymbol{u}_1$ and $\boldsymbol{B}_1$ weren't aligned, then there would be a motional electric field corresponding to a conductor moving at the $\boldsymbol{E} \times \boldsymbol{B}$ drift velocity. By boosting to that $\boldsymbol{E} \times \boldsymbol{B}$-drifting frame, we can eliminate the electric field and have $\boldsymbol{u}_1 \times \boldsymbol{B}_1 = \boldsymbol{0}$ in that frame. It then follows from the jump condition (VII.2.9) that $\boldsymbol{u}_2 \times \boldsymbol{B}_2 = \boldsymbol{0}$; i.e., if we work in a frame in which the upstream flow is parallel to the upstream magnetic field, then the downstream flow is also parallel to the downstream magnetic field. The velocity of this "dH–T" frame is not unique; one can add any field-aligned vector to the $\boldsymbol{E} \times \boldsymbol{B}$ drift velocity without changing the physics:

$$\boldsymbol{u}_{\text{dH–T}} = \frac{\boldsymbol{B}_1 \times (\boldsymbol{u}_1 \times \boldsymbol{B}_1)}{B_1^2} + \lambda \boldsymbol{B}_1, \quad \lambda = \text{const.} \tag{VII.2.38}$$

For example,

$$\boldsymbol{u}_{\text{dH–T}} = \hat{\boldsymbol{n}} \times \left(\boldsymbol{u}_1 \times \frac{\boldsymbol{B}_1}{B_{1n}} \right), \tag{VII.2.39}$$

where $\hat{\boldsymbol{n}}$ denotes the shock normal, also works.

The figure below shows the compression ratio, calculated by solving (VII.2.21) numerically, for a strong oblique shock with $\gamma = 5/3$, $M = 10$, and $\beta \in \{1/4, 1, 4\}$, at a variety of angles $\theta_1 \doteq \cos^{-1}(B_{n1}/B_1)$:

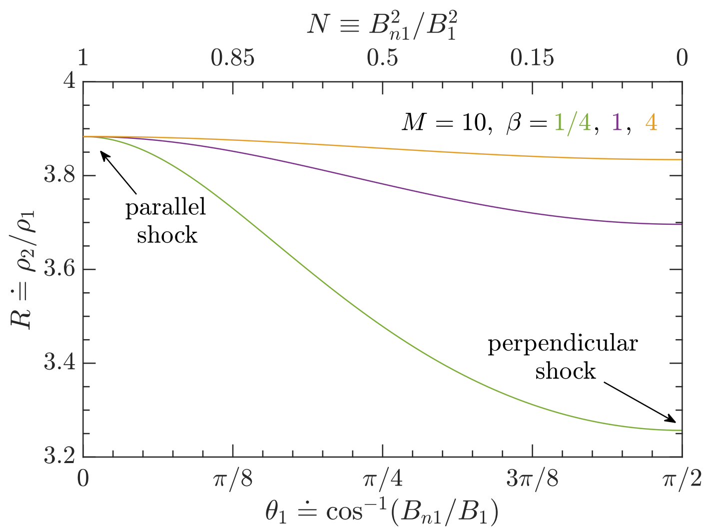

As expected (see (VII.2.37)), the value of R decreases as the shock goes from parallel to perpendicular. Here is the angle $\theta_2 \doteq \cos^{-1}(B_{n2}/B_2)$ that the downstream magnetic field makes with respect to the shock normal:

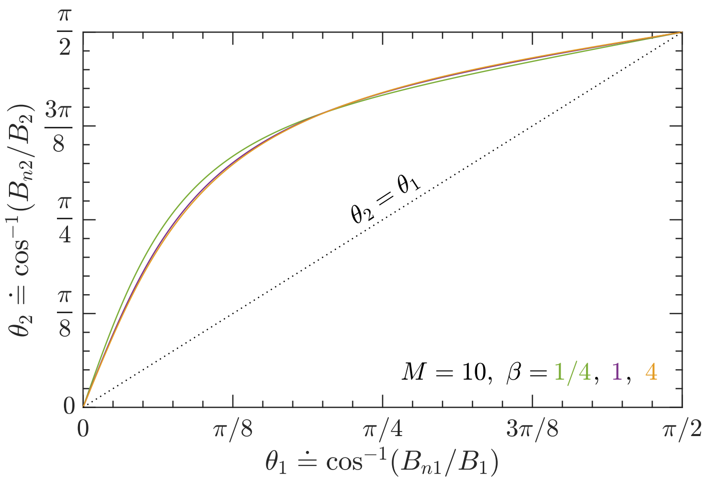

Note that $\theta_2 > \theta_1$ for $\theta_1 \in (0, \pi/2)$, indicating that the downstream magnetic field is canted upwards towards the shock interface in an oblique fast-mode shock. This makes physical sense: a super-Alfvénic shock can sweep up the tangential component of the magnetic field and compress it without the field having time to rarify to produce a magneto-sonic wave, thereby driving the orientation of the magnetic field towards the shock interface.

Here is the same set of plots but for a weak oblique shock with $M = 2$:

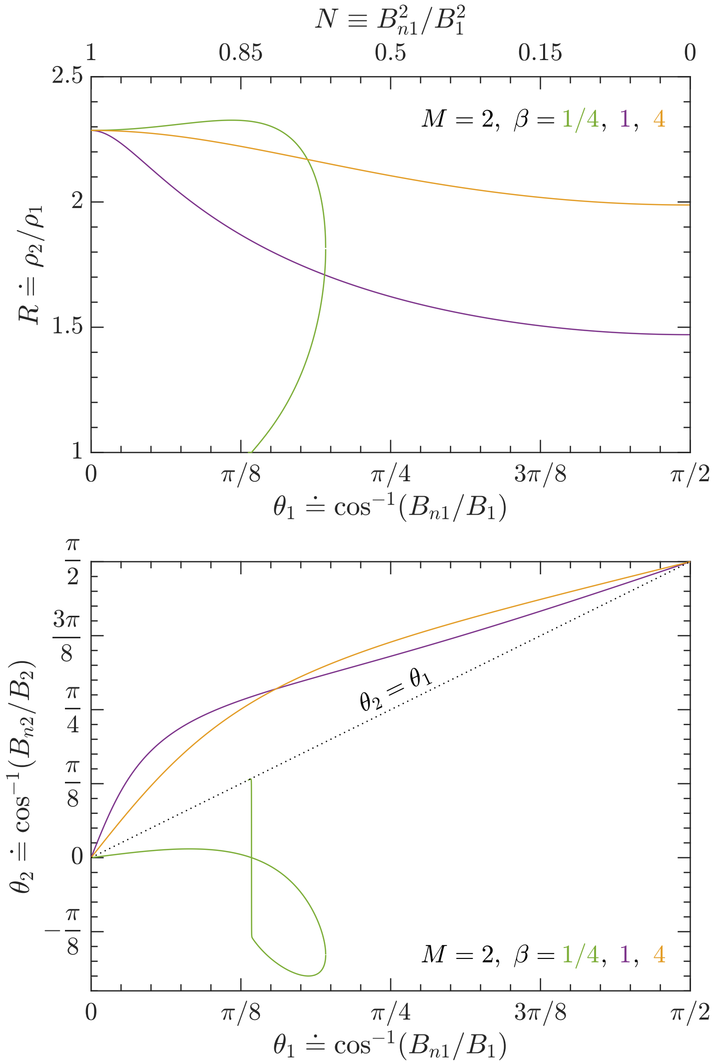

The behavior at $\beta = 1$ ($M_{\text{A}} \simeq 1.8$) and $\beta = 4$ ($M_{\text{A}} \simeq 3.7$) is qualitatively similar to what was seen for the strong shock: the compression ratio decreases as the shock becomes more perpendicular, and the angle of the magnetic field increases across the shock. But at $\beta = 1/4$ ($M_{\text{A}} \simeq 0.9$), everything seems to change. The branch that starts at $N = 1$ where the parallel shocks live turns upwards towards larger compression factors, ultimately taking a dive towards small R and even becoming double-valued. To make this feature clearer, the following plots show R and θ_2 only for $\beta = 1/4$, but with the different branches traced in blue and red:

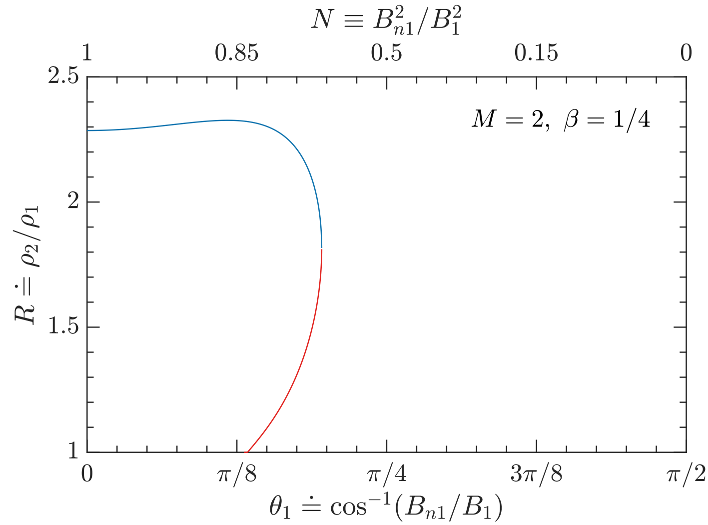

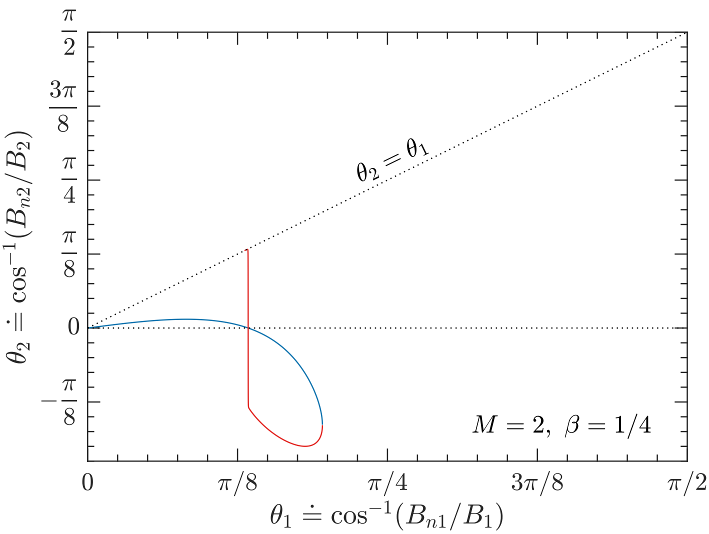

What's going on?

In general, R satisfies a fourth-order polynomial equation. Let's count the roots. One root is trivial, at $R = 1$. One root is the standard solution for a parallel and perpendicular shock, with a smooth interpolation between them at intermediate angles. The final two roots are the lines traced in blue and red. When the upstream magnetic field has a small tangential component, the blue root satisfies $\theta_2 < \theta_1$, indicating that the downstream magnetic field is oriented *closer* to the shock normal than in the upstream. The value of θ_2 actually passes through zero at $N = M_{\rm A}^2 = (\gamma\beta/2)M^2$, or $\theta_1 = \cos^{-1}(M\sqrt{\gamma\beta/2})$, and then goes negative (!), corresponding to B_{t2} having the opposite sign as B_{t1}. The red root does so as well, jumping off the trivial $R = 1$, $\theta_2 = \theta_1$ solution as N approaches $M_{\rm A}^2$ from above, and diving through zero and into negative territory for $N < M_{\rm A}^2$. This root ultimately connects to the blue root at the maximum value of θ_1 for which a shock solution exists.

The reason for this strange behavior is that the combination of $M = 2$ and $\beta = 1/4$ places the shock speed below the fast speed but above the slow speed for all N. As a result, the downstream magnetic field has the freedom to orient itself in different ways.

In particular, when $N < M_{\rm A}^2$, the shock speed is super-Alfvénic and the tangential component of the magnetic field can flip its sign. This flipping of signs is related to a phenomenon know as a "switch-off" shock, our final stop on this tour of MHD shocks...

VII.2.5. *Switch-off (and switch-on) shocks*

A "switch-off" shock occurs when an oblique shock with $B_{t1}, u_{t1} \neq 0$ leads to a purely normal field and flow in the downstream, $B_{t2} = u_{t2} = 0$. Under these conditions, equations (VII.2.15) and (VII.2.16) demand that $N = M_{\rm A}^2 < 1$. In words, the incoming flow and magnetic field must be oriented with respect to the shock front at a precise angle that depends only on the Alfvén Mach number of the shock, and the incoming flow must be precisely Alfvénic (meaning that $u_{n1}^2 = v_{\rm A1}^2 N$ – see (VII.2.23)). In this case, the compression ratio satisfies

$$R^2\left(\frac{2}{M^2}+\frac{\gamma-1}{M_{\rm A}^2}\right)-\gamma R\left(1+\frac{2}{\gamma M^2}+\frac{1}{M_{\rm A}^2}\right)+(\gamma+1)=0 \tag{VII.2.40}$$

for $M^2 < (2/\gamma)\beta^{-1}$. Being a quadratic, this equation admits two solutions for R, which are precisely the two (red and blue) solutions in the plot above at $\theta_2 = 0$ and $\theta_1 \simeq 0.13\pi$ ($N \simeq 0.83$). Graphically:

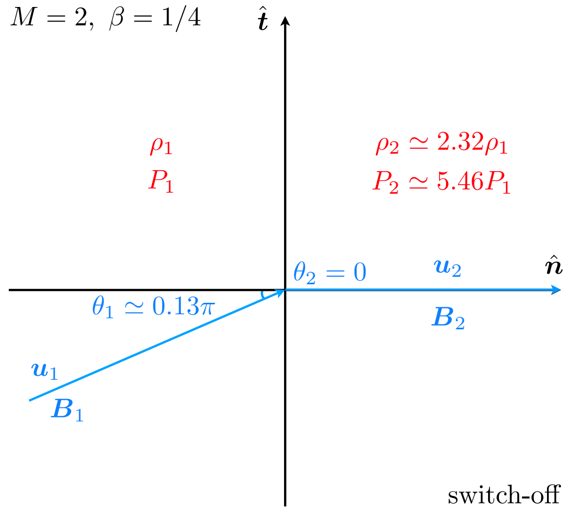

Solutions also allow for the reverse of this situation, called a "switch-on shock." In this case, a fluid with neither magnetic field nor flow velocity tangential to the shock front nevertheless acquires tangential components downstream of the shock, i.e., $B_{t2}, u_{t2} \neq 0$ even though $B_{t1}, u_{t1} = 0$. With $T = 0$ ($N = 1$), the momentum and induction equations provide

$$1+\frac{1}{\gamma M^2}=\frac{1}{R}+\frac{1}{\gamma M^2}\frac{P_2}{P_1}+\frac{1}{2M_{\rm A}^2}\frac{B_{t2}^2}{B_1^2}, \quad \frac{\boldsymbol{B}_{t2}}{B_1}=R\frac{\boldsymbol{u}_{t2}}{u_1}, \quad \text{and} \quad R=M_{\rm A}^2. \tag{VII.2.41}$$

Because R must be greater than one for a true shock solution, the shock must be super-Alfvénic for a switch-on solution to exist. The total energy equation in this situation may be solved for the pressure ratio:

$$\frac{P_2}{P_1}=(\gamma-1)\left[M_{\rm A}^2\left(\frac{M^2}{2}+\frac{1}{\gamma-1}\right)-\frac{M^2}{2M_{\rm A}^2}\left(1+\frac{B_{t2}^2}{B_1^2}\right)\right]. \tag{VII.2.42}$$

Substituting this expression back into (VII.2.41) yields

$$\frac{B_{t2}^2}{B_1^2} = (M_{\rm A}^2 - 1)\left[(\gamma+1) - (\gamma-1)M_{\rm A}^2 - \frac{2M_{\rm A}^2}{M^2}\right]. \tag{VII.2.43}$$

Note that the right-hand of this expression must be positive, corresponding to the tangential components "switching on", if

$$(M_{\rm A}^2 - 1)\left[(\gamma+1) - (\gamma-1)M_{\rm A}^2 - \frac{2M_{\rm A}^2}{M^2}\right] > 0. \tag{VII.2.44}$$

For $M^2 > 1$, this is satisfied provided that

$$1 < M_{\rm A}^2 < \frac{(\gamma+1)M^2}{(\gamma-1)M^2+2}, \quad \text{or} \quad \frac{2/\gamma}{M^2} < \beta < \frac{2(1+1/\gamma)}{(\gamma-1)M^2+2}. \tag{VII.2.45}$$

For $\gamma = 5/3$, this is a fairly narrow range of Alfvén Mach numbers. An example of a switch-off shock is shown in the figure below for $\gamma = 5/3$, $M = 2$, and $\beta = 1/2$:

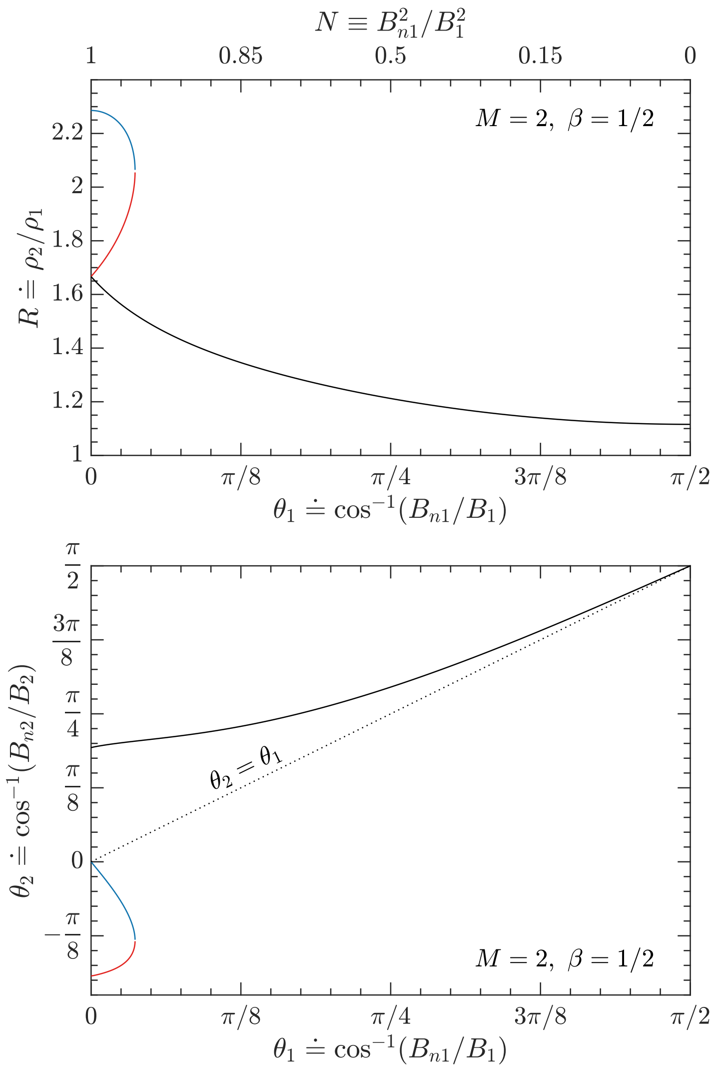

Notice that the roots traced by the black and red lines have non-zero θ_2 even when $\theta_1 = 0$, thus, switch-on shocks. These solutions stem from a degenerate root at $R = M_\mathrm{A}^2$, which separates as θ_1 becomes non-zero (as shown in the figure). Indeed, one may calculate a correction to the switch-off solution at small but non-zero $T = \epsilon \ll 1$ by writing $R = M_\mathrm{A}^2(1 + \epsilon^{1/2}\mathscr{z})$, expanding (VII.2.21) out to $\mathcal{O}(\epsilon)$, and solving for $\mathscr{z}$. The result is that

$$R = M_\mathrm{A}^2\left(1 + T^{1/2}\mathscr{z}\right) \quad \text{with} \quad \mathscr{z} = \pm\sqrt{\frac{M_A^2 - 1}{\gamma + 1 - M_\mathrm{A}^2(\gamma - 1 + 2/M^2)}}. \tag{VII.2.46}$$

With the factor in the square root being positive, R remains real and splits into two solutions, one $>M_\mathrm{A}^2$ and one $<M_\mathrm{A}^2$. Graphically:

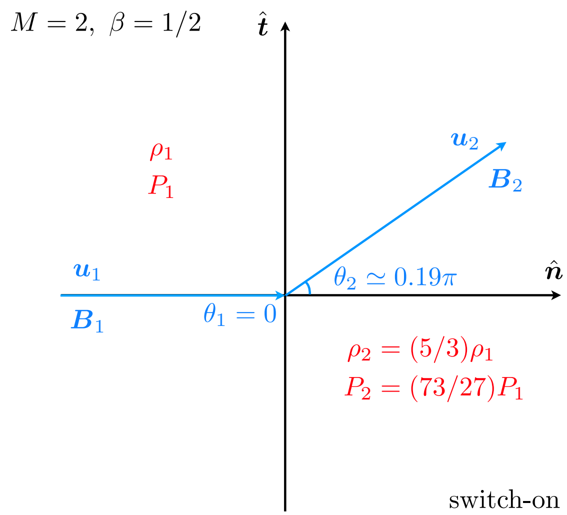

VII.2.6. *Radiative shocks*

$$\boldsymbol{\nabla}\boldsymbol{\cdot}\left[\left(\frac{1}{2}\rho u^2 + \frac{\gamma P}{\gamma - 1} + \frac{B^2}{4\pi}\right)\boldsymbol{u} - \frac{(\boldsymbol{B}\boldsymbol{\cdot}\boldsymbol{u})\boldsymbol{B}}{4\pi}\right] = -\rho\mathcal{L} \tag{VII.2.47}$$

[in progress]

VII.2.7. *Two-fluid shocks*

In a partially ionized gas, the ion-electron plasma and the neutrals can be considered as independent fluids coupled through a drag term representing collisions. The ion-electron plasma (subscript "i") therefore obeys the MHD equations,

$$\frac{\partial \rho_\mathrm{i}}{\partial t} + \boldsymbol{\nabla}\boldsymbol{\cdot}(\rho_\mathrm{i}\boldsymbol{u}_\mathrm{i}) = 0, \tag{VII.2.48}$$

$$\rho_\mathrm{i}\left(\frac{\partial}{\partial t} + \boldsymbol{u}_\mathrm{i}\boldsymbol{\cdot}\boldsymbol{\nabla}\right)\boldsymbol{u}_\mathrm{i} = -\boldsymbol{\nabla}P_\mathrm{i} + \frac{(\boldsymbol{\nabla}\times\boldsymbol{B})\times\boldsymbol{B}}{4\pi} - \alpha\rho_\mathrm{i}\rho_\mathrm{n}(\boldsymbol{u}_\mathrm{i} - \boldsymbol{u}_\mathrm{n}), \tag{VII.2.49}$$

$$\frac{\partial \boldsymbol{B}}{\partial t} = \boldsymbol{\nabla}\times(\boldsymbol{u}_\mathrm{i}\times\boldsymbol{B}), \tag{VII.2.50}$$

while the neutrals (subscript "n") obey the equations of hydrodynamics,

$$\frac{\partial \rho_{\rm n}}{\partial t} + \boldsymbol{\nabla \cdot} (\rho_{\rm n} \boldsymbol{u}_{\rm n}) = 0, \tag{VII.2.51}$$

$$\rho_{\rm n} \left(\frac{\partial}{\partial t} + \boldsymbol{u}_{\rm n} \boldsymbol{\cdot \nabla} \right) \boldsymbol{u}_{\rm n} = -\boldsymbol{\nabla} P_{\rm n} - \alpha \rho_{\rm i} \rho_{\rm n} (\boldsymbol{u}_{\rm n} - \boldsymbol{u}_{\rm i}). \tag{VII.2.52}$$

The ions and neutrals are coupled via a linear drag force, whose amplitude we quantify by introducing the collisional coupling parameter α. Note that the drag force satisfies Newton's third law, appearing with opposite signs in the momentum equations (VII.2.49) and (VII.2.52). These "two-fluid" equations admit a special kind of shock solution, called a C-type shock or a *C-shock* ("C" for "continuous"), in which there are no discontinuities in the hydrodynamical variables. This solution was discovered by Prof. Bruce Draine in the context of the partially ionized, radiative gas that comprises the cold phase of the interstellar medium, which he presented in what is now a classic paper in theoretical astrophysics (Draine 1980).

For simplicity, let us assume the plasma to be radiative, such that the pressures both upstream and downstream of the shock front satisfy $P_{\rm i} = \rho_{\rm i} C^2$ and $P_{\rm n} = \rho_{\rm n} C^2$, where C is the isothermal sound speed. We additionally take α to be constant. Following the convention in the rest of this Part, we orient our coordinate system such that the shock transition occurs at $x = 0$, with the far-upstream ($x \rightarrow -\infty$) pre-shock ions and neutrals being uniform in density ($\rho_{\rm i0}$ and $\rho_{\rm n0}$, respectively) and sharing a constant, steady flow $\boldsymbol{u}_{\rm i0} = \boldsymbol{u}_{\rm n0} \doteq U \hat{\boldsymbol{x}}$. A uniform magnetic field is oriented perpendicular to this flow, $\boldsymbol{B}_0 = B_{0y} \hat{\boldsymbol{y}}$, setting up conditions for a perpendicular shock.

Assuming steady state ($\partial/\partial t = 0$) and one-dimensional (x) structure, the continuity equations and the induction equation become, respectively,

$$\frac{\mathrm{d}}{\mathrm{d}x} (\rho_{\rm n} u_{{\rm n}x}) = 0 \quad \Longrightarrow \quad \rho_{\rm n} u_{{\rm n}x} = \rho_{\rm n0} U \quad \Longrightarrow \quad u_{{\rm n}x} = U \frac{\rho_{\rm n0}}{\rho_{\rm n}}, \tag{VII.2.53}$$

$$\frac{\mathrm{d}}{\mathrm{d}x} (\rho_{\rm i} u_{{\rm i}x}) = 0 \quad \Longrightarrow \quad \rho_{\rm i} u_{{\rm i}x} = \rho_{\rm i0} U \quad \Longrightarrow \quad u_{{\rm i}x} = U \frac{\rho_{\rm i0}}{\rho_{\rm i}}, \tag{VII.2.54}$$

$$\frac{\mathrm{d}}{\mathrm{d}x} (u_{{\rm i}x} B_y) = 0 \quad \Longrightarrow \quad u_{{\rm i}x} B_y = U B_{0y} \quad \Longrightarrow \quad B_y = B_{0y} \frac{\rho_{\rm i}}{\rho_{\rm i0}}. \tag{VII.2.55}$$

Using (VII.2.53)–(VII.2.55) in the neutral and ion-electron momentum equations,

$$\frac{\mathrm{d}}{\mathrm{d}x} (\rho_{\rm n} u_{{\rm n}x}^2 + \rho_{\rm n} C^2) = -\alpha \rho_{\rm i} \rho_{\rm n} (u_{{\rm n}x} - u_{{\rm i}x}),$$

$$\frac{\mathrm{d}}{\mathrm{d}x} \left(\rho_{\rm i} u_{{\rm i}x}^2 + \rho_{\rm i} C^2 + \frac{B_y^2}{8\pi} \right) = -\alpha \rho_{\rm i} \rho_{\rm n} (u_{{\rm i}x} - u_{{\rm n}x}),$$

gives

$$\frac{\mathrm{d}}{\mathrm{d}x} \left(\frac{\rho_{\rm n0}^2 U^2}{\rho_{\rm n}} + \rho_{\rm n} C^2 \right) = -\alpha \rho_{\rm i0} \rho_{\rm n0} U \left(\frac{\rho_{\rm i}}{\rho_{\rm i0}} - \frac{\rho_{\rm n}}{\rho_{\rm n0}} \right), \tag{VII.2.56}$$

$$\frac{\mathrm{d}}{\mathrm{d}x} \left(\frac{\rho_{\rm i0}^2 U^2}{\rho_{\rm i}} + \rho_{\rm i} C^2 + \frac{B_{0y}^2}{8\pi} \frac{\rho_{\rm i}^2}{\rho_{\rm i0}^2} \right) = -\alpha \rho_{\rm i0} \rho_{\rm n0} U \left(\frac{\rho_{\rm n}}{\rho_{\rm n0}} - \frac{\rho_{\rm i}}{\rho_{\rm i0}} \right). \tag{VII.2.57}$$

Introducing $\mathcal{I} \doteq \rho_{\rm i}/\rho_{\rm i0}$ and $\mathcal{N} \doteq \rho_{\rm n}/\rho_{\rm n0}$, and defining the dimensionless free parameters $M \doteq U/C$, $M_{\rm A} \doteq v_{\rm A,n}/C \doteq B_{0y}/\sqrt{4\pi \rho_{\rm n0} C^2}$, and $\chi_{\rm i} \doteq \rho_{\rm i0}/\rho_{\rm n0}$, equations (VII.2.56) and

(VII.2.57) become

$$\frac{\mathrm{d}}{\mathrm{d}\xi}\left(\frac{M^2}{\mathcal{N}}+\mathcal{N}\right)=-MM_{\mathrm{A}}(\mathcal{I}-\mathcal{N}), \tag{VII.2.58}$$

$$\frac{\mathrm{d}}{\mathrm{d}\xi}\left(\frac{M^2}{\mathcal{I}}+\mathcal{I}+\frac{M_{\mathrm{A}}^2}{2\chi_{\mathrm{i}}}\mathcal{I}^2\right)=-\frac{MM_{\mathrm{A}}}{\chi_{\mathrm{i}}}(\mathcal{N}-\mathcal{I}), \tag{VII.2.59}$$

where $\xi \doteq x/\ell_{\mathrm{ni}}$ and the neutral-ion collision length $\ell_{\mathrm{ni}} \doteq v_{\mathrm{A,n}}/\alpha\rho_{\mathrm{i0}}$. In terms of these variables, $u_{\mathrm{n}x}/C = M/\mathcal{N}$, $u_{\mathrm{i}x}/C = M/\mathcal{I}$, and $B_y/B_{y0} = \mathcal{I}$. Note that ℓ_{ni} is the distance an Alfvén wave would travel in the neutral fluid in the time it takes momentum to be transferred collisionally from the ions to the neutrals. If an Alfvénic disturbance in the magnetic field has wavelength $\lambda \lesssim \pi\ell_{\mathrm{ni}}$, it diffuses before collisions between neutrals and ions have time to transmit to the neutrals the magnetic force (e.g., Kulsrud & Pearce 1969, Appendix; also, Mouschovias 1991).

Numerically integrating (VII.2.58) and (VII.2.59) with $M = 100$, $M_{\mathrm{A}} = 10$, and $\chi_{\mathrm{i}} = 10^{-3}$ using a Runge–Kutta solver results in the figure below:

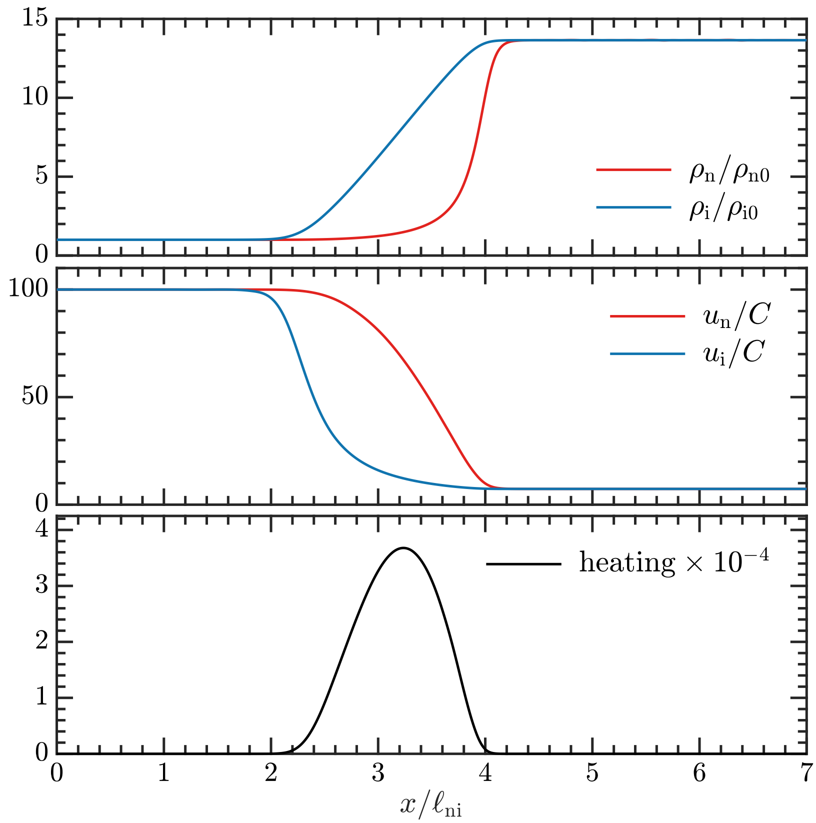

Note the presence of a "magnetic precursor" in the ionized plasma. Quoting from the abstract of Draine (1980), this precursor "heats and compresses the medium ahead of the front where the neutral gas undergoes a discontinuous change of state... Within this 'magnetic precursor' both ions and electrons stream through the neutral fluid with velocities which may be a significant fraction of the shock speed."

We may obtain the maximum possible jump in the density for a poorly ionized fluid as follows. Adding (VII.2.58) and $\chi_{\rm i}$ × (VII.2.59) gives

$$\frac{\mathrm{d}}{\mathrm{d}\xi}\left[\frac{M^2}{\mathcal{N}}+\mathcal{N}+\frac{M_{\rm A}^2}{2}\mathcal{I}^2+\chi_{\rm i}\left(\frac{M^2}{\mathcal{I}}+\mathcal{I}\right)\right]=0. \tag{VII.2.60}$$

In the far downstream $\xi\to\infty$, we have $\mathcal{N}=\mathcal{I}$. With $\chi_{\rm i}\ll 1$, equation (VII.2.60) implies

$$\frac{M^2}{\mathcal{N}}+\mathcal{N}+\frac{M_{\rm A}^2}{2}\mathcal{I}^2\approx\frac{M^2}{\mathcal{N}}+\mathcal{N}+\frac{M_{\rm A}^2}{2}\mathcal{N}^2\approx\text{const}. \tag{VII.2.61}$$

The constant can obtained in the far upstream, $\xi=0$, where it is equal to $M^2+1+M_{\rm A}^2/2$. Assuming $M\gg 1$, the largest terms in (VII.2.61) are then $(M_{\rm A}^2/2)\mathcal{N}^2\approx M^2$. Thus, $\mathcal{N}\approx\sqrt{2}(M/M_{\rm A})$, or

$$\frac{\rho_{\rm n}}{\rho_{\rm n0}}\approx\sqrt{2}\,\frac{U}{v_{\rm A,n}}. \tag{VII.2.62}$$

More information on the MHD dynamics of partially ionized plasmas is deferred to §X.

PART VIII

Resistive MHD

VIII.1. Ohmic resistivity

Up to now, we have assumed that the plasma is infinitely conducting, i.e., the magnetic field is frozen into the plasma flow. We now relax that assumption by introducing a finite conductivity σ that relates the current density $\boldsymbol{j}$ to the electric field $\boldsymbol{E}'$ in the rest frame of the plasma:

$$\boldsymbol{j} = \sigma \boldsymbol{E}' \doteq \sigma\left(\boldsymbol{E} + \frac{\boldsymbol{u}}{c} \times \boldsymbol{B}\right). \tag{VIII.1.1}$$

Finite σ implies finite resistivity η, which in a collisional plasma is driven by the friction force between the ions and electrons:

$$\begin{aligned} 0 \approx \boldsymbol{R}_{\rm ei} - en_{\rm e}\boldsymbol{E}' = \frac{m_{\rm e}n_{\rm e}}{\tau_{\rm ei}}(\boldsymbol{u}_{\rm i} - \boldsymbol{u}_{\rm e}) - en_{\rm e}\boldsymbol{E}' = \frac{m_{\rm e}n_{\rm e}}{\tau_{\rm ei}}\frac{\boldsymbol{j}}{en_{\rm e}} - en_{\rm e}\boldsymbol{E}' \\ \Longrightarrow \quad \boldsymbol{j} = \frac{e^2 n_{\rm e}\tau_{\rm ei}}{m_{\rm e}}\boldsymbol{E}' \doteq \sigma\boldsymbol{E}' \doteq \frac{1}{\eta}\boldsymbol{E}'. \end{aligned} \tag{VIII.1.2}$$

Using Ampére's law, the non-ideal induction equation then reads

$$\frac{\partial \boldsymbol{B}}{\partial t} = \boldsymbol{\nabla} \times (\boldsymbol{u} \times \boldsymbol{B}) - \boldsymbol{\nabla} \times \left(\frac{c^2\eta}{4\pi}\boldsymbol{\nabla} \times \boldsymbol{B}\right). \tag{VIII.1.3}$$

The first term is the familiar advection term. The second term might look more familiar to you if we take the resistivity to be spatially uniform and use $\boldsymbol{\nabla} \times (\boldsymbol{\nabla} \times \boldsymbol{B}) = -\nabla^2\boldsymbol{B}$ to obtain

$$\frac{\partial \boldsymbol{B}}{\partial t} = \boldsymbol{\nabla} \times (\boldsymbol{u} \times \boldsymbol{B}) + \frac{c^2\eta}{4\pi}\nabla^2\boldsymbol{B},$$

in which case the resistive term leads to a diffusion equation with diffusion coefficient $c^2\eta/4\pi$. Because this factor of $c^2/4\pi$ is often a nuisance to carry around, I will henceforth absorb this factor into the definition of the resistivity and regard η as a diffusion coefficient (with units of length^2 per time).

The relative importance of the advection and diffusion terms in (VIII.1.3) is quantified using the dimensionless *magnetic Reynolds number*,

$$\mathrm{Rm} \doteq \frac{UL}{\eta}, \tag{VIII.1.4}$$

where U and L are characteristic scales for the flow velocity and spatial gradients, respectively. For example,

$$\begin{aligned} \text{liquid metals in industrial contexts: } & \mathrm{Rm} \sim 10^{-3}\dots 10^{-1}, \\ \text{laboratory plasma-astrophysics experiments: } & \mathrm{Rm} \sim 1\dots 100 \text{ (and growing)}, \\ \text{planetary interiors: } & \mathrm{Rm} \sim 100\dots 300, \\ \text{solar convective zone: } & \mathrm{Rm} \sim 10^{6}\dots 10^{9}, \\ \text{warm phase of the interstellar medium: } & \mathrm{Rm} \sim 10^{18}, \\ \text{intracluster medium of galaxy clusters: } & \mathrm{Rm} \sim 10^{29}. \end{aligned}$$

But be careful: even in situations with $\mathrm{Rm} \ggg 1$ on the macroscopic scales, resistivity may still be important if sufficiently small spatial scales are produced, say, by a turbulent cascade or in a forming current sheet. For now, let's take a quick look at linear theory.

VIII.1.1. *Wave-driven Ohmic dissipation*

Regarding the linear theory of waves on a static, homogeneous background, there is nothing particularly special about the Ohmic decay of Alfvén waves versus the Ohmic decay of magnetosonic waves. Because the diffusion operator is isotropic, all modes suffer the same rate of magnetic diffusion, dependent only upon the magnitude of the wavenumber. Indeed, the linearized induction equation is

$$-\mathrm{i}\omega\delta\boldsymbol{B} = \mathrm{i}\boldsymbol{k}\cdot\boldsymbol{B}_0\delta\boldsymbol{u} - \boldsymbol{B}_0\mathrm{i}\boldsymbol{k}\cdot\delta\boldsymbol{u} - k^2\eta\delta\boldsymbol{B}. \tag{VIII.1.5}$$

For a shear Alfvén wave with $\delta\boldsymbol{u} = -(\boldsymbol{k}\cdot\boldsymbol{B}_0/\omega)(\delta\boldsymbol{B}/4\pi\rho)$, equation (VIII.1.5) becomes

$$\left[\omega(\omega + \mathrm{i}k^2\eta) - k_\parallel^2 v_\mathrm{A}^2\right]\delta\boldsymbol{B} = 0, \tag{VIII.1.6}$$

whose solutions satisfy

$$\omega = -\mathrm{i}\frac{k^2\eta}{2} \pm k_\parallel v_\mathrm{A}\sqrt{1 - \left(\frac{k^2\eta}{2k_\parallel v_\mathrm{A}}\right)^2}. \tag{VIII.1.7}$$

For $\mathrm{Rm} \sim v_\mathrm{A}/(k\eta) \gg 1$, these solutions become $\omega \approx \pm k_\parallel v_\mathrm{A} - \mathrm{i}k^2\eta/2$, i.e., weakly damped shear-Alfvén waves. Magnetic-field fluctuations produce currents, currents are associated with drifts between the charged species, and these interspecies drifts are damped by collisional friction.

VIII.1.2. *Ohmic dissipation heats plasma*

Think back to grade-school physics when you played with circuits... power is current squared times resistance, $P = RI^2$. In the language of non-ideal MHD, $\boldsymbol{j}\cdot\boldsymbol{E}' = \eta|\boldsymbol{j}|^2$. It is straightforward to show by dotting (VIII.1.3) with $\boldsymbol{B}/4\pi$ that this is precisely the rate at which the total magnetic energy decays:

$$\frac{\mathrm{d}}{\mathrm{d}t}\int \mathrm{d}V\,\frac{B^2}{8\pi} = \underbrace{-\int \mathrm{d}V\,\boldsymbol{u}\cdot\left(\frac{\boldsymbol{j}}{c}\times\boldsymbol{B}\right)}_{\substack{\text{minus the work of the}\\ \text{Lorentz force on the flow}}} - \underbrace{\frac{c}{4\pi}\oint \mathrm{d}\boldsymbol{S}\cdot(\boldsymbol{E}\times\boldsymbol{B})}_{\text{Poynting flux}} - \underbrace{\int \mathrm{d}V\,\eta|\boldsymbol{j}|^2}_{\substack{\text{Ohmic}\\ \text{dissipation}}}. \tag{VIII.1.8}$$

This liberated magnetic energy must go somewhere, of course, and it does:

$$\frac{P}{\gamma-1}\frac{\mathrm{D}}{\mathrm{D}t}\ln\frac{P}{\rho^\gamma} = \eta|\boldsymbol{j}|^2, \tag{VIII.1.9}$$

Voila. Joule heating.

VIII.2. Magnetic reconnection

Magnetic reconnection refers to the topological rearrangement of magnetic-field lines that converts magnetic energy to plasma energy. In these lecture notes, we will assume that such a rearrangement is facilitated by a spatially constant Ohmic resistivity, as might occur in a well-ionized collisional fluid:

$$\frac{\partial\boldsymbol{B}}{\partial t} = \boldsymbol{\nabla}\times(\boldsymbol{u}\times\boldsymbol{B}) + \eta\nabla^2\boldsymbol{B}.$$

This assumption is obviously not warranted in hot, dilute astrophysical systems, such as the collisionless solar wind, or in poorly ionized systems, like molecular clouds and pre-stellar cores. But let us assume this anyhow, knowing that (i) the physics of reconnection in even the simplest of systems is surprisingly rich and complex, and (ii) there is a huge amount of literature on all aspects of magnetic reconnection in a wide variety of environments. This part of the lecture notes is not intended as a replacement of that literature, nor a synopsis of current research in the field (particularly in the laboratory and the Earth's magnetosheath). What follows is an incomplete presentation of a few key highlights in the theory of magnetic reconnection, which will hopefully provide enough pedagogical value and inspiration to encourage you to dig into the literature further. For that, I recommend that you start with the excellent review articles by Zweibel & Yamada (2009), Yamada *et al.* (2010), and Loureiro & Uzdensky (2016).

VIII.3. Tearing instability

VIII.3.1. *Formulation of the problem*

We begin by analyzing the stability of a simple stationary equilibrium in which the magnetic field reverses across $x = 0$:

$$\boldsymbol{B}_0 = B_y(x)\hat{\boldsymbol{y}} + B_{\rm g}\hat{\boldsymbol{z}}, \qquad \text{(VIII.3.1)}$$

where $B_y(x)$ is an odd function and $B_{\rm g} = \text{const}$ denotes the guide field. A oft-employed profile for $B_y(x)$ is the Harris (1962) sheet:

$$B_y(x) = B_{\rm r}\tanh\left(\frac{x}{a}\right), \qquad \text{(VIII.3.2)}$$

where $B_{\rm r}$ is the asymptotic value of the reconnecting field and a is the characteristic scale length of the current sheet. Its profile, and the associated current density $j_z = (B_{\rm r}/a)\,\text{sech}^2(x/a)$, are shown in the figure below:

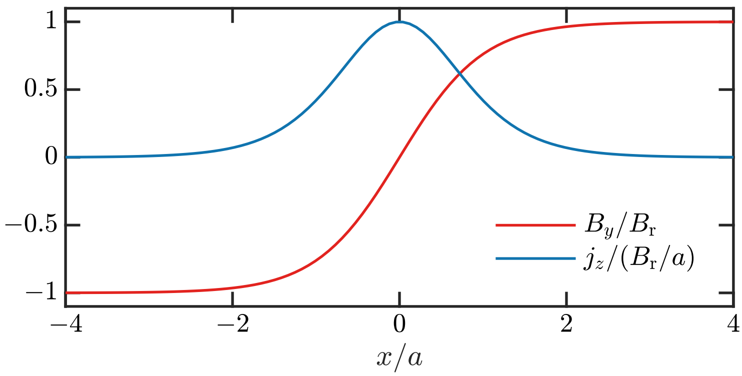

To have a stationary equilibrium, we require something to balance the magnetic pressure gradient implied by (VIII.3.1). One option is to allow the thermal pressure in the background to vary so that $P(x) + B_y^2(x)/8\pi = \text{const}$. Another option is to make the guide field also depend upon x and arrange for the total magnetic-field strength to be constant; for example, if the reconnecting field satisfies (VIII.3.2), then the guide field should satisfy $B_{\rm g}(x) = B_{\rm r}\,\text{sech}(x/a)$. Either way, the total pressure $P + B^2/8\pi$ in the equilibrium should be constant. We might consider allowing the background magnetic pressure gradient to be unbalanced, which would be fine if the tearing instability were to grow much faster than the current sheet would evolve globally from being initialized out of equilibrium. But the latter would occur on the Alfvén-crossing time of the sheet, $\sim a/v_{\rm A,r}$, which we will find is actually *shorter* than the characteristic growth time of the fastest-growing tearing mode. Many presentations of the tearing instability conveniently omit this point.

We start by linearizing the momentum and non-ideal induction equations about the x-dependent, pressure-balanced equilibrium (cf. (VI.2.1)):

$$\rho\frac{\partial\delta\boldsymbol{u}}{\partial t} = -\boldsymbol{\nabla}\left(\delta P + \frac{B_{\rm g}\delta B_z}{4\pi} + \frac{B_y\delta B_y}{4\pi}\right) + \frac{B_{\rm g}}{4\pi}\frac{\partial\delta\boldsymbol{B}}{\partial z} + \frac{B_y}{4\pi}\frac{\partial\delta\boldsymbol{B}}{\partial y} + \frac{{\rm d}B_y}{{\rm d}x}\frac{\delta B_x}{4\pi}\hat{\boldsymbol{y}}, \tag{VIII.3.3a}$$

$$\frac{\partial\delta\boldsymbol{B}}{\partial t} = -\delta u_x\frac{{\rm d}B_y}{{\rm d}x}\hat{\boldsymbol{y}} + B_{\rm g}\frac{\partial\delta\boldsymbol{u}}{\partial z} + B_y\frac{\partial\delta\boldsymbol{u}}{\partial y} + \eta\nabla^2\delta\boldsymbol{B}. \tag{VIII.3.3b}$$

Here we have taken the plasma to be incompressible, $\boldsymbol{\nabla\cdot}\delta\boldsymbol{u} = 0$; note further that the mass density ρ in (VIII.3.3a) refers only to its time-independent background value. As a result, we don't need the continuity equation to close our system of equations, and the energy equation is replaced by the requirement that the divergence of $(1/\rho)\times$(VIII.3.3a) vanish (which constrains δP). We have also ignored resistive diffusion of the background current-sheet profile, which should be fine as long as the growth rate of the tearing mode is $\gg \eta/a^2$; this will amount to the condition that the Lundquist number of the current sheet, $S_a \doteq v_{\rm A,r}a/\eta$ where $v_{\rm A,r} \doteq B_{\rm r}/\sqrt{4\pi\rho_0}$ is the Alfvén speed associated with the reconnecting field and ρ_0 is the mass density at the center of the reconnecting layer $(x=0)$, satisfies $S_a^{1/2} \gg 1$.

The next step, which is not at all necessary but is standard and simplifies this first pass through the analysis, is to assume that the perturbations have no z component and do not vary in the z direction, thereby reducing the problem completely to 2D. In this case, the guide field $B_{\rm g}$ disappears from the analysis, and incompressibility and the solenoidality constraint on the magnetic field allow us to write the perturbed velocity and magnetic field in terms of scalar potentials whose gradients lie in the x-y plane:

$$\delta\boldsymbol{u} = \hat{\boldsymbol{z}}\times\boldsymbol{\nabla}\phi, \quad \frac{\delta\boldsymbol{B}}{\sqrt{4\pi\rho_0}} = \hat{\boldsymbol{z}}\times\boldsymbol{\nabla}\psi, \tag{VIII.3.4}$$

Likewise, we may associate the background reconnecting field B_y with a scalar potential: $B_y(x)/\sqrt{4\pi\rho_0} = \varPsi'(x)$, where the prime denotes differentiation with respect to x. For example, if B_y is taken to be the Harris-sheet profile (VIII.3.2), then $\varPsi(x) = v_{\rm A,r}a\ln[\cosh(x/a)]$. Making these simplifications in (VIII.3.3), substituting in (VIII.3.4), and simplifying leads to

$$\frac{\partial}{\partial t}\left(\frac{\rho}{\rho_0}\hat{\boldsymbol{z}}\times\boldsymbol{\nabla}\phi\right) = -\boldsymbol{\nabla}\left(\frac{\delta P}{\rho_0} + \varPsi'\frac{\partial\psi}{\partial x}\right) + \varPsi'\frac{\partial}{\partial y}\hat{\boldsymbol{z}}\times\boldsymbol{\nabla}\psi - \varPsi''\frac{\partial\psi}{\partial y}\hat{\boldsymbol{y}}, \tag{VIII.3.5a}$$

$$\hat{\boldsymbol{z}}\times\boldsymbol{\nabla}\frac{\partial}{\partial t}\psi = \hat{\boldsymbol{z}}\times\boldsymbol{\nabla}\left(\varPsi'\frac{\partial\phi}{\partial y} + \eta\nabla^2\psi\right). \tag{VIII.3.5b}$$

We may remove the $\hat{\boldsymbol{z}}\times\boldsymbol{\nabla}$ from both sides of the latter equation without consequence. Finally, to eliminate $\boldsymbol{\nabla}\delta P$ from (VIII.3.5a), we take the curl of (VIII.3.5a) and use $\boldsymbol{\nabla}\times\boldsymbol{\nabla} = 0$. After the use of some vector identities and rearranging, our final equations are

$$\frac{\rho}{\rho_0}\frac{\partial}{\partial t}\left(\nabla^2\phi + \frac{{\rm d}\ln\rho}{{\rm d}x}\frac{{\rm d}\phi}{{\rm d}x}\right) = \varPsi'\frac{\partial}{\partial y}\nabla^2\psi - \varPsi'''\frac{\partial\psi}{\partial y}, \tag{VIII.3.6a}$$

$$\frac{\partial\psi}{\partial t} - \varPsi'\frac{\partial\phi}{\partial y} = \eta\nabla^2\psi. \tag{VIII.3.6b}$$

The former equation describes the evolution of the fluid vorticity, $\boldsymbol{\nabla}\times\boldsymbol{u} = \hat{\boldsymbol{z}}\nabla^2\phi$.

Because (VIII.3.6) are linear in the perturbation amplitudes, and because the background only depends upon x, we are allowed to adopt the solutions

$$\psi(t,x,y) = \psi(x)\,\mathrm{e}^{\mathrm{i}ky+\gamma t} \qquad \text{and} \qquad \phi(t,x,y) = \phi(x)\,\mathrm{e}^{\mathrm{i}ky+\gamma t}, \tag{VIII.3.7}$$

where k is the wavenumber and γ is the rate at which the perturbations will grow or decay. In this case, $\partial/\partial t \to \gamma$ and $\partial/\partial y \to \mathrm{i}k$, leaving us with

$$\gamma\frac{\rho}{\rho_0}\left(\frac{\mathrm{d}^2}{\mathrm{d}x^2} - k^2 + \frac{\mathrm{d}\ln\rho}{\mathrm{d}x}\frac{\mathrm{d}}{\mathrm{d}x}\right)\phi = \mathrm{i}k\varPsi'\left(\frac{\mathrm{d}^2}{\mathrm{d}x^2} - k^2\right)\psi - \mathrm{i}k\varPsi'''\psi, \tag{VIII.3.8a}$$

$$\gamma\psi - \mathrm{i}k\varPsi'\phi = \eta\left(\frac{\mathrm{d}^2}{\mathrm{d}x^2} - k^2\right)\psi. \tag{VIII.3.8b}$$

The trick to solving this set of equations is to realize that, as η tends towards zero, the derivative on the right-hand side of (VIII.3.8b) must grow to balance the terms on the left-hand side. In other words, a boundary layer forms about $x = 0$, outside of which the system satisfies the ideal-MHD equations and inside of which the resistivity is important. The width of this boundary layer is customarily denoted δ_{in}, and much of reconnection theory rests on determining its size given the various attributes of the host plasma. To do so, we will first solve (VIII.3.8a) and (VIII.3.8b) in the "outer region", where the resistivity is negligible and the system behaves as though it were ideal. Then they will be solved in the "inner region", where the resistivity dominates and $k \sim a^{-1} \ll \mathrm{d}/\mathrm{d}x \sim \delta_{\mathrm{in}}^{-1}$. The two solutions must asymptotically join onto one another; this matching, along with boundary conditions at $x = 0$ and $\pm\infty$, will determine the full solution.

Before proceeding with this program, it will be advantageous to define the resistive and Alfvén timescales,

$$\tau_\eta \doteq \frac{a^2}{\eta} \quad \text{and} \quad \tau_{\mathrm{A}} \doteq \frac{1}{ka\varPsi_0''(0)} = \frac{1}{kv_{\mathrm{A,r}}}, \tag{VIII.3.9}$$

respectively. We further assume $\tau_\eta^{-1} \ll \gamma \ll \tau_{\mathrm{A}}^{-1}$, i.e. the tearing mode grows faster than it takes for the entirety of the current sheet to resistively diffuse but slower than it takes for an Alfvén wave to cross k^{-1}. Physically, this implies that the outer solution results from neglecting the plasma's inertia and Ohmic resistivity.

VIII.3.2. *Outer equation*

Adopting the ordering $\tau_\eta^{-1} \ll \gamma \ll \tau_{\mathrm{A}}^{-1}$, equations (VIII.3.8$a$) and (VIII.3.8$b$) reduce to

$$0 = \left(\frac{\mathrm{d}^2}{\mathrm{d}x^2} - k^2 - \frac{\varPsi'''}{\varPsi'}\right)\psi_{\mathrm{out}} \quad \text{and} \quad \phi_{\mathrm{out}} = \frac{\gamma}{\mathrm{i}k\varPsi'}\psi_{\mathrm{out}}. \tag{VIII.3.10}$$

Note that $\varPsi'''/\varPsi' = B_y''/B_y$ measures the gradient of the current density, and so different current-sheet profiles will result in different solutions to (VIII.3.10). Regardless of the exact current-sheet profile, however, both ϕ_{out} and ψ_{out} must tend to zero as $x \to \pm\infty$. Also, since the y-component of the perturbed magnetic field must reverse direction at $x = 0$, ψ_{out} must have a discontinuous derivative there, corresponding to a singular current. Indeed, it is this discontinuity that characterizes the free energy available to reconnect, quantified by the tearing-instability parameter

$$\varDelta' \doteq \frac{1}{\psi_{\mathrm{out}}(0)}\frac{\mathrm{d}\psi_{\mathrm{out}}}{\mathrm{d}x}\bigg|_{-0}^{+0}, \tag{VIII.3.11}$$

and that ultimately warrants consideration of a resistive inner layer.

VIII.3.3. *Inner equation*

In the inner region where $k \ll \mathrm{d}/\mathrm{d}x \sim \delta_{\rm in}^{-1}$, the dominant terms in (VIII.3.8*a*) and (VIII.3.8*b*) are

$$\gamma \frac{\rho}{\rho_0} \frac{\mathrm{d}^2\phi_{\rm in}}{\mathrm{d}x^2} = \mathrm{i}k\Psi' \frac{\mathrm{d}^2\psi_{\rm in}}{\mathrm{d}x^2}, \tag{VIII.3.12}$$

$$\gamma\psi_{\rm in} - \mathrm{i}k\phi_{\rm in}\Psi' = \eta \frac{\mathrm{d}^2\psi_{\rm in}}{\mathrm{d}x^2}. \tag{VIII.3.13}$$

Note that ρ, whose gradient length scale is a, may be taken as constant over the inner-layer thickness $\delta_{\rm in} \ll a$, and so the pre-factor ρ/ρ_0 in (VIII.3.12) is $\simeq$1. These equations may be solved analytically provided some amenable form of Ψ'. Because we are deep within the current sheet, the leading-order term in a Taylor expansion will suffice, *viz.*, $\Psi' \approx \Psi''(0)x = v_{\rm A,r}(x/a)$. Then (VIII.3.12) and (VIII.3.13) may be straightforwardly combined to obtain

$$\frac{\mathrm{d}^2\psi_{\rm in}}{\mathrm{d}x^2} = -\left[\frac{\gamma}{k\Psi''(0)}\right]^2 \frac{1}{x}\frac{\mathrm{d}^2}{\mathrm{d}x^2}\left[\frac{1}{x}\left(1 - \frac{\eta}{\gamma}\frac{\mathrm{d}^2}{\mathrm{d}x^2}\right)\psi_{\rm in}\right]. \tag{VIII.3.14}$$

With some effort, this equation can actually be solved for $\psi_{\rm in}$ analytically. I'll show you how below. But even without that effort, equation (VIII.3.14) may be used to estimate the width of the boundary layer, $\delta_{\rm in}$:

$$1 \sim (\gamma a \tau_{\rm A})^2 \frac{\eta}{\gamma\delta_{\rm in}^4} \quad \Longrightarrow \quad \frac{\delta_{\rm in}}{a} \sim \left(\frac{\gamma\tau_{\rm A}^2}{\tau_\eta}\right)^{1/4}. \tag{VIII.3.15}$$

Note that $\delta_{\rm in}$ depends on k – each tearing mode k has a different boundary-layer width; because of this, each k will correspond to a different Δ'.

Normalizing lengthscales to $\delta_{\rm in}$ by introducing $\xi \doteq x/\delta_{\rm in}$, equation (VIII.3.14) may be written as

$$\frac{\mathrm{d}^2\psi_{\rm in}}{\mathrm{d}\xi^2} = -\frac{1}{\xi}\frac{\mathrm{d}^2}{\mathrm{d}\xi^2}\left[\frac{1}{\xi}\left(\Lambda - \frac{\mathrm{d}^2}{\mathrm{d}\xi^2}\right)\psi_{\rm in}\right], \tag{VIII.3.16}$$

where the eigenvalue $\Lambda \doteq \gamma^{3/2}\tau_{\rm A}\tau_\eta^{1/2} = \gamma\delta_{\rm in}^2/\eta$ is the growth rate of the tearing mode normalized by the rate of resistive diffusion across a layer of width $\delta_{\rm in}$. Provided we can solve (VIII.3.16), the solution $\psi_{\rm in}$ must be matched onto the outer solution $\psi_{\rm out}$. This is done by equating the discontinuity in $\psi_{\rm out}$, quantified by Δ' (see (VIII.3.11)), to the total change in $\mathrm{d}\psi_{\rm in}/\mathrm{d}x$ across the inner region, *viz.*,

$$\Delta' = \frac{2}{\delta_{\rm in}}\int_0^1 \mathrm{d}\xi\, \frac{1}{\psi_{\rm in}(0)}\frac{\mathrm{d}^2\psi_{\rm in}}{\mathrm{d}\xi^2}.$$

(The factor of 2 is because the solution is odd, and so the total change across the $x = 0$ surface is twice the change measured for $x > 0$.) The upper limit on the integral can be extended to $+\infty$ by committing only a $\sim$10% error:

$$\Delta' = \frac{2}{\delta_{\rm in}}\int_0^\infty \mathrm{d}\xi\, \frac{1}{\psi_{\rm in}(0)}\frac{\mathrm{d}^2\psi_{\rm in}}{\mathrm{d}\xi^2}. \tag{VIII.3.17}$$

So, find $\psi(\xi)$ by solving the inner equation (VIII.3.16), compute the integral in (VIII.3.17), and invert the answer to obtain the growth rate in terms of Δ'.

Before carrying out that program, it will be useful to further simply (VIII.3.16) by introducing

$$\chi(\xi) \doteq \xi^2 \frac{\mathrm{d}}{\mathrm{d}\xi}\left[\frac{\psi_{\rm in}(\xi)}{\xi}\right], \tag{VIII.3.18}$$

so that

$$\frac{\mathrm{d}}{\mathrm{d}\xi}\left[\frac{\mathrm{d}}{\mathrm{d}\xi}\left(\frac{1}{\xi^2}\frac{\mathrm{d}\chi}{\mathrm{d}\xi}\right)-\left(1+\frac{\Lambda}{\xi^2}\right)\chi\right]=0. \tag{VIII.3.19}$$

Integrating this equation once and, for reasons that will eventually become apparent, setting the integration constant to $-\chi_\infty$, we find

$$\xi^2\frac{\mathrm{d}}{\mathrm{d}\xi}\left(\frac{1}{\xi^2}\frac{\mathrm{d}\chi}{\mathrm{d}\xi}\right)-\left(\xi^2+\Lambda\right)\chi=-\chi_\infty\xi^2. \tag{VIII.3.20}$$

Once this equation is solved, the inner solution is obtained using (cf. (VIII.3.18))

$$\psi_{\mathrm{in}}(\xi)=-\xi\int_\xi^\infty \mathrm{d}x\,\frac{\chi(x)}{x^2}=-\xi\int_\xi^\infty \mathrm{d}x\,\frac{\chi'(x)}{x}-\chi(\xi), \tag{VIII.3.21}$$

which may then be plugged into (VIII.3.17) to compute Δ'.

VIII.3.4. *Approximate solutions*

There are a few ways to solve (VIII.3.10) and (VIII.3.20), none of which are particularly obvious. However, it's possible to obtain scaling laws for Δ' and the tearing-mode growth rate γ without actually doing so. In fact, the answers obtained in this way differ from those obtained by a more mathematically rigorous solution (see §VIII.3.5) by only order-unity coefficients. Nice.

We start with (VIII.3.10), the outer equation. With some knowledge that the fastest-growing modes occur at long wavelengths ($ka \ll 1$), we can make some progress by simply dropping the middle term in (VIII.3.10). Then, so long as B_y varies faster within $|x| \lesssim a$ than it does at $|x| \gg a$, we can estimate

$$\Delta' \sim \frac{1}{ka^2}. \tag{VIII.3.22}$$

(This scaling is exact for the Harris-sheet profile, solved for in §VIII.3.5.) One may formalize this estimate somewhat (Loureiro *et al.* 2007, 2013) by quantifying what "varies faster within $|x| \lesssim a$ than it does at $|x| \gg a$" means, but not much is gained intuitively by going that route, and the estimate (VIII.3.22) will suffice.

As for the inner equation (VIII.3.16), we know from (VIII.3.20) that, whatever its solution, $\psi_{\mathrm{in}}(\xi)$ only depends on the parameter Λ. Thus, equation (VIII.3.17) may be written as

$$\Delta'\delta_{\mathrm{in}} = f(\Lambda) \tag{VIII.3.23}$$

for some function $f(\Lambda)$. Combining (VIII.3.22) and (VIII.3.23) yields an expression for the growth rate, provided we can invert $f(\Lambda)$. Fortunately, we can, at least in certain limits.

The first limit is the so-called "constant-ψ approximation" or "FKR regime", which corresponds to $f(\Lambda) \sim \Lambda \ll 1$ (Furth *et al.* 1963). Then (VIII.3.23) gives $\Delta'\delta_{\mathrm{in}} \sim \Lambda$, so that

$$\boxed{\gamma_{\mathrm{FKR}} \sim \tau_{\mathrm{A}}^{-2/5}\tau_\eta^{-3/5}(\Delta' a)^{4/5}, \quad \frac{\delta_{\mathrm{in}}}{a} \sim \left(\frac{\tau_{\mathrm{A}}}{\tau_\eta}\right)^{2/5}(\Delta' a)^{1/5}} \tag{VIII.3.24}$$

With $\Delta' \sim 1/ka^2$ (see (VIII.3.22)), these become

$$\frac{\gamma_{\mathrm{FKR}}}{v_{\mathrm{A,r}}/a} \sim (ka)^{-2/5} S_a^{-3/5}, \quad \frac{\delta_{\mathrm{in}}}{a} \sim (ka)^{-3/5} S_a^{-2/5}, \tag{VIII.3.25}$$

where we have introduced the *Lundquist number*

$$S_a \doteq \frac{a v_{\mathrm{A,r}}}{\eta}. \tag{VIII.3.26}$$

Note that longer wavelengths have faster growth rates (the divergence as $k \to 0$ will be cured in the "Coppi" regime, in which the small-Δ' assumption breaks down – see below). This approximation results from setting $\psi_{\mathrm{in}} = \psi_{\mathrm{in}}(0)$ on the left-hand side of (VIII.3.13), so that the inner equation (VIII.3.13) becomes

$$\gamma\psi_{\mathrm{in}}(0) - \mathrm{i}k\phi_{\mathrm{in}}\Psi_0''(0)x = \eta\frac{\mathrm{d}^2\psi_{\mathrm{in}}}{\mathrm{d}x^2}, \tag{VIII.3.27}$$

and so (cf. (VIII.3.20))

$$\xi^2\frac{\mathrm{d}}{\mathrm{d}\xi}\left(\frac{1}{\xi^2}\frac{\mathrm{d}\chi}{\mathrm{d}\xi}\right) - \xi^2(\chi - \chi_\infty) = -\Lambda\psi_{\mathrm{in}}(0). \tag{VIII.3.28}$$

In effect, we are assuming that the resistive diffusion time across the inner-layer thickness is much shorter than the instability growth time, i.e., $\gamma \ll \eta/\delta_{\mathrm{in}}^2$, so that ψ_{in} can be approximated as constant on the dynamical time scale. Using (VIII.3.25) in this inequality requires $S_a \gg (\Delta' a)^4$. This is sometimes called the "small-Δ' regime".

The second limit is the "Coppi regime" or "large-Δ' regime", in which the constant-ψ approximation breaks down and $\gamma \sim \eta/\delta_{\mathrm{in}}^2$. This occurs for $\Lambda \sim 1^-$, at which $f(\Lambda) \to \infty$. The growth rate then becomes independent of Δ' and we have

$$\boxed{\gamma_{\mathrm{Coppi}} \sim \tau_{\mathrm{A}}^{-2/3}\tau_\eta^{-1/3}, \quad \frac{\delta_{\mathrm{in}}}{a} \sim \left(\frac{\tau_{\mathrm{A}}}{\tau_\eta}\right)^{1/3}} \tag{VIII.3.29}$$

In terms of the tearing-mode wavenumber k and the Lundquist number S_a,

$$\frac{\gamma_{\mathrm{Coppi}}}{v_{\mathrm{A,r}}/a} \sim (ka)^{2/3}S_a^{-1/3}, \quad \frac{\delta_{\mathrm{in}}}{a} \sim (ka)^{-1/3}S_a^{-1/3}. \tag{VIII.3.30}$$

In this limit, the shorter wavelengths have faster growth rates, opposite to the FKR scaling (VIII.3.25). This suggests a maximally growing mode, whose growth rate $\gamma_{\max}$ and wavenumber $k_{\max}$ may be estimated by matching the FKR solution (VIII.3.25) to the Coppi one (VIII.3.30):

$$\gamma_{\mathrm{FKR}} \sim \gamma_{\mathrm{Coppi}} \quad \Longrightarrow \quad k_{\max}a \sim S_a^{-1/4}, \quad \frac{\gamma_{\max}}{v_{\mathrm{A,r}}/a} \sim S_a^{-1/2}, \quad \frac{\delta_{\mathrm{in}}}{a} \sim S_a^{-1/4}. \tag{VIII.3.31}$$

Note that the FKR (Coppi) regime corresponds to $k > k_{\max}$ ($k < k_{\max}$).

Of course, all of these scalings make sense only if the modes can fit into the current sheet, i.e., $kL \gtrsim 1$, where L is the length of the current sheet. For the maximally growing mode to be viable thus requires a current-sheet aspect ratio of $L/a \gtrsim S_a^{1/4}$. If this inequality is not satisfied, then the fastest-growing mode will be the FKR mode (VIII.3.25) with the smallest possible allowed wavenumber, $kL \sim 1$. Thus, low-aspect-ratio sheets with $L/a \ll S_a^{1/4}$ will develop tearing perturbations comprising just one or two islands; the high-aspect-ratio sheets, in which the Coppi regime is accessible, will instead spawn whole chains comprising $\sim k_{\max}L$ islands.

VIII.3.5. *Exact solution for a Harris sheet*

This is **optional** material detailing a more rigorous derivation of the tearing-mode dispersion relation.

The solutions obtained in the last section should suffice for this course. But with some (read: a lot of) effort, one can be more precise. For that task, let us adopt the equilibrium flux function $\varPsi_0 = a v_{\mathrm{A,r}} \ln[\cosh(x/a)]$, corresponding to the Harris-sheet profile (VIII.3.2). Then (VIII.3.10) becomes

$$\left[\frac{\mathrm{d}^2}{\mathrm{d}x^2} - k^2 + \frac{2}{a^2}\operatorname{sech}^2\!\left(\frac{x}{a}\right)\right]\psi_{\mathrm{out}} = 0 \quad \text{and} \quad \phi_{\mathrm{out}} = -\mathrm{i}\gamma\tau_{\mathrm{A}}\coth\!\left(\frac{x}{a}\right)\psi_{\mathrm{out}}. \tag{VIII.3.32}$$

The former equation can be solved by changing variables to $\mu = \tanh(x/a)$, so that $\operatorname{sech}^2(x/a) = (1-\mu^2)^{-1}$ and

$$\frac{\mathrm{d}}{\mathrm{d}x} = \frac{1-\mu^2}{a}\frac{\mathrm{d}}{\mathrm{d}\mu}, \qquad \frac{\mathrm{d}^2}{\mathrm{d}x^2} = \frac{1-\mu^2}{a}\frac{\mathrm{d}}{\mathrm{d}\mu}\frac{1-\mu^2}{a}\frac{\mathrm{d}}{\mathrm{d}\mu}.$$

Then (VIII.3.32) becomes

$$\left[\frac{\mathrm{d}}{\mathrm{d}\mu}(1-\mu^2)\frac{\mathrm{d}}{\mathrm{d}\mu} + 2 - \frac{k^2a^2}{1-\mu^2}\right]\psi_{\mathrm{out}} = 0 \quad \text{and} \quad \phi_{\mathrm{out}} = -\mathrm{i}\gamma\tau_{\mathrm{A}}\frac{\psi_{\mathrm{out}}}{\mu}, \tag{VIII.3.33}$$

the first of which you might recognize as the associated Legendre equation

$$\left[\frac{\mathrm{d}}{\mathrm{d}\mu}(1-\mu^2)\frac{\mathrm{d}}{\mathrm{d}\mu} + \ell(\ell+1) - \frac{m^2}{1-\mu^2}\right]P_\ell^m(\mu) = 0$$

with $\ell = 1$ and $m = ka$. Transforming the boundary conditions $\psi(\pm\infty) = 0$ into $\psi(\mu = \pm 1) = 0$ and enforcing $\psi(\mu) = \psi(-\mu)$, the solution to (VIII.3.33) is thus

$$\psi_{\mathrm{out}} = C_{1m}P_1^m(\mu), \tag{VIII.3.34}$$

with $C_{1m} = \text{const}$. If you can't picture in your head what the first associated Legendre polynomial with non-integer m looks like – I know I can't – you may like to know that the outer solution may be equivalently written as

$$\psi_{\mathrm{out}}(x) = C'_{1m}\mathrm{e}^{-kx}\left[1 + \frac{1}{ka}\tanh\!\left(\frac{x}{a}\right)\right] \tag{VIII.3.35}$$

for $\xi \geqslant 0$, where $C'_{1m} = \text{const}$. (Note that $\psi_{\mathrm{out}}(-\xi) = \psi_{\mathrm{out}}(\xi)$.) Visually:

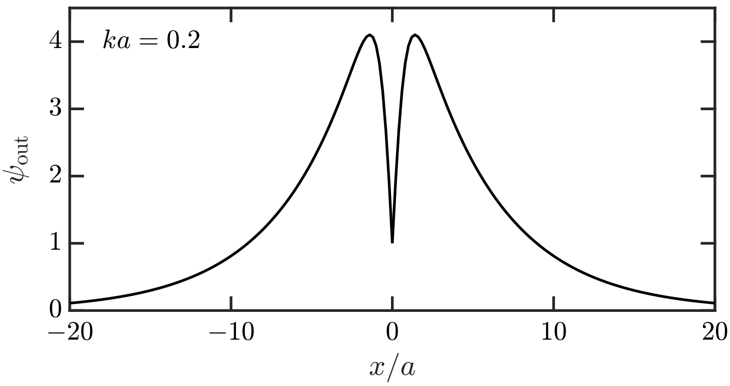

Recall that Δ' measures the discontinuity of $\mathrm{d}\psi_{\mathrm{out}}/\mathrm{d}x$ at $x = 0$ (see (VIII.3.11)). Restoring the $\cos(ky)$ dependence of ψ_{out} provides the following isocontours of ψ_{out}, which are equivalently the magnetic-field lines:

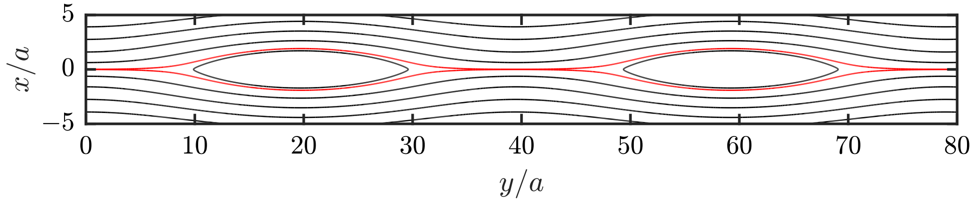

For ease of visualization, I plotted two y wavelengths using $ka = (2\pi)^{-1}$ and set the tearing-mode amplitude to 0.2 (which in a realistic system would be well outside of the linear regime). The red line is called the *separatrix*; it serves as the boundary between the inside of each magnetic island and the surrounding field lines, and runs through the "X-points" that lie at $y = 0, 2\pi/k, 4\pi/k$, etc. To determine the island width w, we follow the isocontour that starts from the X-point at, say, $(x, y) = (0, 0)$ and set its x location when $y = \pi/k$ equal to the half-width $w/2$:

$$\cancelto{0}{\Psi(0)} + \underbrace{\psi(0,0)}_{=\,\psi_{\rm out}(0)} = \Psi(w/2) + \psi(w/2, \pi/k) \approx \frac{1}{2}\Psi''(0)\frac{w^2}{4} + \underbrace{\psi(w/2,\pi/k)}_{=\,-\psi_{\rm out}(w/2)},$$

where we've used $\cos(\pi) = -1$ and approximated $\Psi(x)$ a distance x away from the neutral line by its Taylor expansion, $(1/2)\Psi''(0)x^2$. If we then take ψ to be approximately constant within the island, *viz.* $\psi_{\rm out}(w/2) \approx \psi_{\rm out}(0)$, we find that island width satisfies

$$w \approx 4\sqrt{\frac{\psi(0)}{\Psi''(0)}}.$$

Note that $\Psi''(0) = v_{\rm A,r}/a$ for the Harris-sheet profile. Solving for the mode amplitude C_{1m} (or C'_{1m}) requires matching onto the inner solution, but even before doing that we can compute Δ' using $\psi_{\rm out} \propto P_1^m(\mu)$ in (VIII.3.11):[10]

$$\begin{aligned}\Delta' a &= \frac{1}{P_1^m(0)}\frac{{\rm d}P_1^m}{{\rm d}\mu}\bigg|_{-0}^{+0} = \frac{2}{P_1^m(0)}\frac{{\rm d}P_1^m}{{\rm d}\mu}\bigg|_{\mu=0} = 2\left(\frac{1}{m} - m\right) \\ &= 2\left(\frac{1}{ka} - ka\right).\end{aligned} \tag{VIII.3.36}$$

Note that $\Delta' > 0$ requires $ka < 1$ – any unstable mode must have an extent at least as large as the current-sheet thickness. This places an upper limit on the wavenumber of the FKR modes (VIII.3.25).

As for the inner equation, let us use its compact form (VIII.3.20), repeated here for convenience:

$$\xi^2\frac{\rm d}{{\rm d}\xi}\left(\frac{1}{\xi^2}\frac{{\rm d}\chi}{{\rm d}\xi}\right) - \left(\xi^2 + \Lambda\right)\chi = -\chi_\infty\xi^2, \tag{VIII.3.37}$$

where $\Lambda \doteq \gamma^{3/2}\tau_{\rm A}\tau_\eta^{1/2}$. There are a few ways to solve (VIII.3.37), none of which are particularly obvious. One way, explained in Appendix A of Ara *et al.* (1978), is as follows. Write

$$\chi = \chi_\infty \sum_{n=0}^{\infty} a_n L_n^{(-3/2)}(\xi^2)\,{\rm e}^{-\xi^2/2}, \tag{VIII.3.38}$$

[10]See `https://dlmf.nist.gov/14.5` for information on $P_\ell^m(0)$ and ${\rm d}P_\ell^m/{\rm d}\mu|_{\mu=0}$.

where $L_n^\alpha(z)$ are the associated Laguerre (or "Sonine") polynomials satisfying

$$z\frac{\mathrm{d}^2 L_n^{(\alpha)}}{\mathrm{d}z^2} + (\alpha+1-z)\frac{\mathrm{d}L_n^{(\alpha)}}{\mathrm{d}z} + nL_n^{(\alpha)} = 0. \tag{VIII.3.39}$$

Substitute this decomposition into (VIII.3.20) and use the recursion relations

$$\frac{\mathrm{d}L_n^\alpha}{\mathrm{d}z} = -L_{n-1}^{\alpha+1}(z) \text{ if } 1 \leqslant n \ (= 0 \text{ otherwise}),$$
$$nL_n^{(-3/2)}(z) = -\left(z+\frac{1}{2}\right)L_{n-1}^{(-1/2)}(z) - zL_{n-2}^{(1/2)}(z),$$

to obtain

$$\sum_{n=0}^{\infty} a_n\,\xi^{-2}\,\mathrm{e}^{-\xi^2/2}L_n^{(-3/2)}(\xi^2)\big(4n+\Lambda-1\big) = 1. \tag{VIII.3.40}$$

Multiply this by $\mathrm{e}^{-\xi^2/2}\xi^{-1}L_m^{-3/2}$, integrate, and use the orthogonality relation

$$\int_0^\infty \mathrm{d}z\,\mathrm{e}^{-z}z^\alpha L_m^\alpha L_n^\alpha = \delta_{mn}\frac{\Gamma(n+\alpha+1)}{\Gamma(n+1)}$$

to find that

$$\begin{aligned}
a_n\frac{(n-3/2)!}{n!}(4n+\Lambda-1) &= \int_0^\infty \mathrm{d}z\,z^{-1/2}\mathrm{e}^{-z/2}L_n^{-3/2} \\
&= \int_0^\infty \mathrm{d}z\,z^{-1/2}\mathrm{e}^{-z/2}(L_n^{-1/2} - L_{n-1}^{-1/2}) \\
&= \sqrt{2}(-1)^n\left[\frac{\Gamma(n+1/2)}{\Gamma(n+1)} + \frac{\Gamma(n-1/2)}{\Gamma(n)}\right] \\
\implies \quad a_n &= \frac{(-1)^n}{\sqrt{2}}\frac{4n-1}{4n+\Lambda-1}.
\end{aligned}$$

Thus, equation (VIII.3.38) becomes[11]

$$\chi = \frac{\chi_\infty}{\sqrt{2}}\,\mathrm{e}^{-\xi^2/2}\sum_{n=0}^{\infty}(-1)^n L_n^{-3/2}(\xi^2)\frac{4n-1}{4n+\Lambda-1} = \xi^2\frac{\mathrm{d}}{\mathrm{d}\xi}\frac{\psi_{\mathrm{in}}}{\xi}, \tag{VIII.3.41}$$

which may be solved for ψ_{in} following (VIII.3.21).

Actually doing so and plugging the solution into (VIII.3.17) to compute Δ' ain't easy, as it involves a lot of non-standard math. I may LaTeX those steps up one day, but, for now, I'll just skip to the answer:

$$\Delta'\delta_{\mathrm{in}} = f(\Lambda) \doteq \frac{\pi}{2}\frac{\Gamma[(\Lambda+3)/4]}{\Gamma[(\Lambda+5)/4]}\frac{\Lambda}{1-\Lambda}. \tag{VIII.3.42}$$

This is an implicit equation for Γ, which may be solved numerically (see figure below). But it's possible to recover our approximate results (VIII.3.24) and (VIII.3.29) in their respective limits. For $\Lambda \ll 1$,

$$f(\Lambda) \approx \frac{\pi}{2}\frac{\Gamma(3/4)}{\Gamma(5/4)}\Lambda \simeq 2.124\,\Lambda \quad \implies \quad \gamma \approx 0.547\,\tau_{\mathrm{A}}^{-2/5}\tau_\eta^{-3/5}(\Delta' a)^{4/5}. \tag{VIII.3.43}$$

Our approximate result for this FKR regime, equation (VIII.3.24), is off by only a factor

[11] Note that we cannot use the expansion (VIII.3.38) if $\Lambda = 1$.

of 0.547 – not too bad. For $\Lambda = 1^-$,

$$f(\Lambda) \approx \frac{\pi}{2}\frac{\Gamma(1)}{\Gamma(3/2)}\frac{1}{1-\Lambda} = \frac{\sqrt{\pi}}{1-\Lambda} \quad \Longrightarrow \quad \gamma \approx \tau_{\rm A}^{-2/3}\tau_\eta^{-1/3} - \mathcal{O}\left(\frac{kv_{\rm A,r}}{\Delta' a}\right). \qquad \text{(VIII.3.44)}$$

This matches our Coppi-regime estimate, (VIII.3.29). These asymptotic solutions actually do rather well across the full range of wavenumbers:

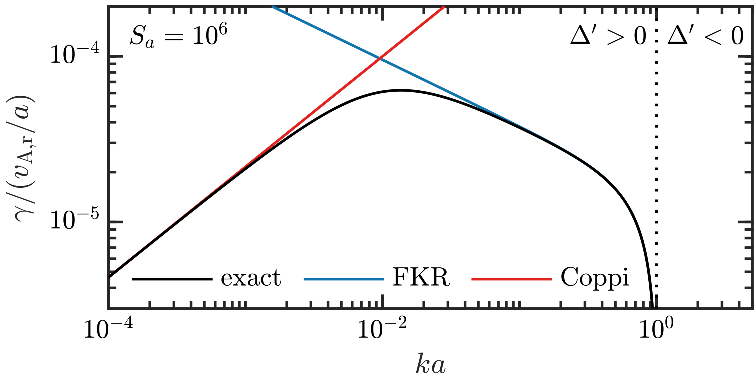

It also appears that we are well justified in estimating the maximally growing mode by matching the FKR and Coppi expressions (as in (VIII.3.31)). These regimes also occur where we anticipated, with $f(\Lambda) = \Delta'\delta_{\rm in}$ being $\ll 1$ ($\gg 1$) in the FKR (Coppi) regime:

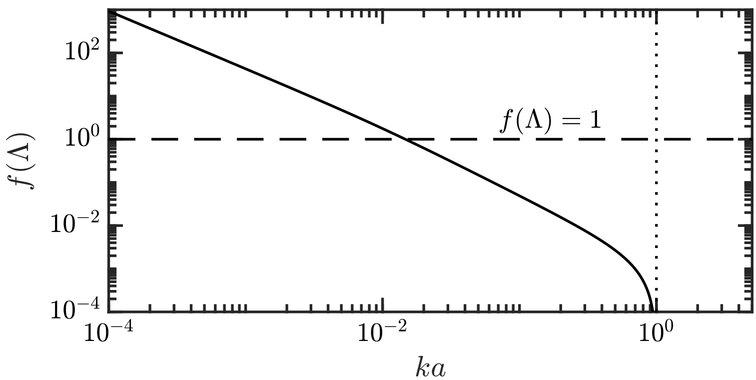

Thus the "small-Δ'" / "large-Δ'" phraseology.

VIII.3.6. *Nonlinear evolution and X-point collapse*

How long does this linear phase, in which the tearing modes grow exponentially, last? That depends on the Δ' of the mode. If the Coppi regime is accessible – i.e., if the maximally growing wavenumber $k_{\max}$ (see (VIII.3.31)) that results in $\Delta'\delta_{\rm in} \gtrsim 1$ also satisfies $k_{\max}a < 1$ – then X-point collapse is essentially instantaneous once the width $w = 4\sqrt{-\psi(0)/\Psi_0''(0)}$ of the exponentially growing island reaches $\delta_{\rm in}$. At this moment, $w\Delta'$ is also $\sim$1, and so the deformations of the current sheet by the nonlinear islands have driven the regions between the X-points to marginal stability. If the fastest-growing available modes are instead FKR-like, then there is a gap between when the nonlinear regime begins ($w \sim \delta_{\rm in}$) and when it ends ($w\Delta' \sim 1$). In between occurs a period of secular growth called the Rutherford (1973) stage, in which $\dot{w} \sim \eta\Delta'(w)$, the argument of Δ' indicating that the logarithmic derivative of $\psi_{\rm out}$ is to be taken across the island (rather than across the inner-layer width).[12] During this slow growth stage, the initially unstable current profile flattens and conditions are set up for the collapse of the inter-island X points (Waelbroeck 1993; Loureiro *et al.* 2005). The figure below, adapted from Loureiro *et al.* (2005), shows contours of ψ at the beginning of X-point collapse (left) and the formation of an embedded, high-aspect ratio current sheet (right):

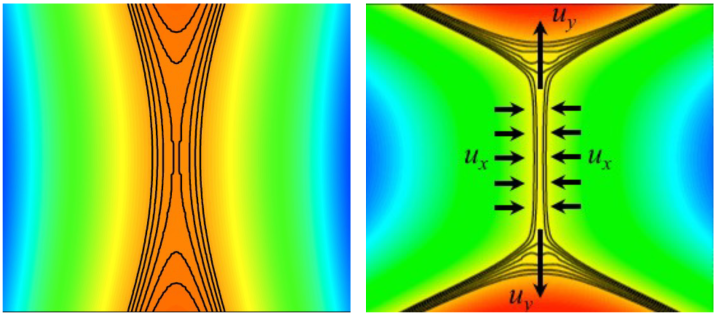

This current sheet is reminiscent of the now-famous Sweet–Parker configuration.

VIII.4. Sweet–Parker reconnection

Peter Sweet (Sweet 1958) and Eugene Parker (Parker 1957) provided the first quantitative model of magnetic reconnection, envisioning it to be a steady-state process in which a two-dimensional, incompressible flow advects magnetic flux into a current sheet of length L and thickness $\delta_{\mathrm{SP}} \ll L$. It is through the latter dimension that plasma, accelerated in the direction along the current sheet by magnetic tension, is expelled in the form of an outflow:

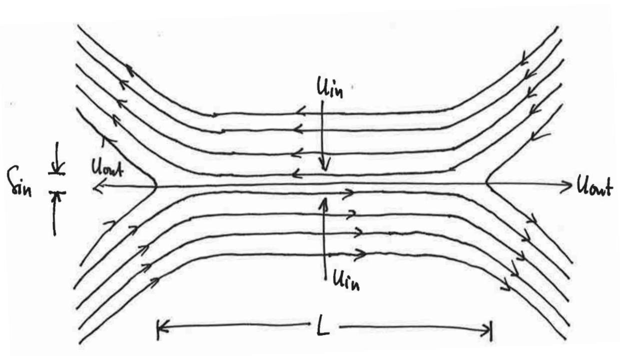

Steady state is achieved by (i) balancing the inflow velocity u_{in} and the outflow velocity u_{out} using mass conservation, $u_{\mathrm{in}} L \sim u_{\mathrm{out}} \delta_{\mathrm{SP}}$; (ii) balancing the advective and resistive electric fields so that all the inflowing magnetic flux is resistively destroyed, $u_{\mathrm{in}} v_{\mathrm{A,r}} \sim \eta j_z \sim \eta v_{\mathrm{A,r}}/\delta_{\mathrm{SP}}$; and (iii) stipulating that the outflows are Alfvénic, $u_{\mathrm{out}} \sim v_{\mathrm{A,r}}$. (This final ingredient follows from conservation of energy, with the magnetic energy flux into

[12] Rutherford (1973) did not predict a saturation amplitude for the algebraically growing nonlinear tearing mode. Subsequent papers by Militello & Porcelli (2004) and Escande & Ottaviani (2004) ("POEM") derived a modified equation for the Rutherford stage, $\dot{w} \sim \eta(\Delta' - \alpha w/a^2)$ with α being a constant dependent upon the initial current-sheet geometry, thus predicting a saturated amplitude $w \sim \Delta' a^2$.

the sheet balancing the kinetic energy flux out of the sheet.) The result is

$$\frac{u_{\rm in}}{v_{\rm A,r}} \sim \frac{\delta_{\rm SP}}{L} \sim \left(\frac{v_{\rm A,r}L}{\eta}\right)^{-1/2} \doteq S^{-1/2}, \tag{VIII.4.1}$$

where S is the Lundquist number (using the current-sheet length L as the normalizing lengthscale). In the solar corona, $S \sim 10^{12}$–10^{14}; in the Earth's magnetotail, $S \sim 10^{15}$–10^{16}; and in a modern tokamak like JET, $S \sim 10^{6}$–10^{8}. You can see that $S^{-1/2}$ is typically a very small number, and so Sweet–Parker (SP) reconnection is *slow* – not as slow as pure resistive diffusion, but slow in the sense that the reconnection rate $\tau_{\rm r}^{-1} \doteq u_{\rm in}/L \sim (v_{\rm A,r}/L)\, S^{-1/2}$ tends towards zero as $S \to \infty$. For example, the SP model predicts that a reconnection-driven solar flare in a $S \sim 10^{14}$ part of the solar corona should last $\sim$2 mths; instead, flares are observed to last between 15 min and 1 hr. Not good.

This mismatch between theory and observation was immediately appreciated, and spawned several attempts to formulate a model in which fast reconnection occurs. The culprit is the smallness of the resistive layer: the fact that it must be thin enough to make the current density large also means that the outflowing mass must pass through too small of an opening. One particularly notorious attempt to circumvent this constraint was proposed by Petschek (1964) (later revisited and amended by Kulsrud (2001)), in which the current-sheet length L was shortened at the expense of introducing four standing slow-mode shocks emanating from a central diffusion region:

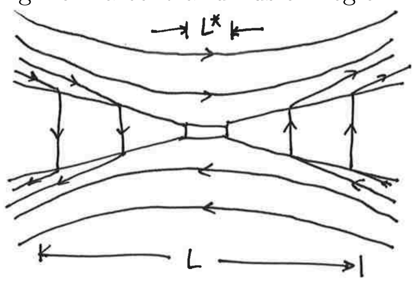

The result is a logarithmic dependence of the reconnection rate on S, $\tau_{\rm r}^{-1} \sim (v_{\rm A,r}/L) \ln S$. Unfortunately, no convincing evidence for this type of reconnection has been found (Park *et al.* 1984; Biskamp 1986; Uzdensky & Kulsrud 2000; Malyshkin *et al.* 2005; Loureiro *et al.* 2005), even when Petschek's solution is used as an initial condition (Uzdensky & Kulsrud 2000).[13]

It is worth emphasizing that the failure of the SP model to explain magnetic reconnection as it occurs in nature is not due to any shortcoming of the theory itself. There are no obvious mistakes in the theory, which has been put on a rigorous footing (e.g., Uzdensky & Kulsrud 2000). Indeed, both numerical simulations (e.g., see figure 4(b) of Loureiro *et al.* 2005) and laboratory experiments (e.g., Ji *et al.* 1998) have measured reconnection rates in excellent agreement with the SP scalings (VIII.4.1). What, then, is the issue?

VIII.5. Plasmoid instability

Let us suspend judgement for the meantime and suppose that the SP model is correct. With tearing-mode theory in hand, let us ask the intriguing question of whether or not the steady-state SP current sheet is stable to tearing instabilities. One could of course

[13]Petschek-like configurations do emerge when strongly localized (anomalous) resistivity profiles are used (Malyshkin *et al.* 2005; Sato & Hayashi 1979; Ugai 1995; Scholer 1989; Erkaev *et al.* 2000, 2001; Biskamp & Schwarz 2001), as might occur under collisionless conditions.

go the route of rigorously doing the linear tearing theory using the SP solution as the background state, as Loureiro *et al.* (2007) did in a now-classic paper, but for our purposes it will be sufficient to simply replace the current-sheet thickness a in the tearing-mode theory of §VIII.3 with $\delta_{\rm SP} \sim S^{-1/2}L$ (Tajima & Shibata 1997; Bhattacharjee *et al.* 2009; Loureiro *et al.* 2013). Focusing on the maximally growing tearing mode (VIII.3.31),

$$k_{\max}L \sim \frac{L}{a}S_a^{-1/4} \longrightarrow \frac{L}{\delta_{\rm SP}}\left(\frac{v_{\rm A,r}\delta_{\rm SP}}{\eta}\right)^{-1/4} \sim S^{3/8}, \tag{VIII.5.1a}$$

$$\frac{\gamma_{\max}}{v_{\rm A,r}/L} \sim \frac{L}{a}S_a^{-1/2} \longrightarrow \frac{L}{\delta_{\rm SP}}\left(\frac{v_{\rm A,r}\delta_{\rm SP}}{\eta}\right)^{-1/2} \sim S^{1/4}, \tag{VIII.5.1b}$$

$$\frac{\delta_{\rm in}}{L} \sim \frac{a}{L}S_a^{-1/4} \longrightarrow \frac{\delta_{\rm SP}}{L}\left(\frac{v_{\rm A,r}\delta_{\rm SP}}{\eta}\right)^{-1/4} \sim S^{-5/8}. \tag{VIII.5.1c}$$

This is the *plasmoid instability* – essentially, the tearing instability of a SP current layer. Of course, the situation in question is very different than that obtained using the stationary equilibrium Harris sheet, perhaps most obviously because the former has background flows. These flows can be stabilizing in the tearing calculation, a possibility we have ignored in making the estimates in (VIII.5.1). This may be circumvented, however, by demanding that $\gamma \gg v_{\rm A,r}/L$, $k_{\max}L \gg 1$, and $\delta_{\rm in}/\delta_{\rm SP} \ll 1$ – demands that may be satisfied if $S \gtrsim 10^4$. Indeed, it is at this critical Lundquist number that the plasmoid instability is (now routinely) observed to occur in numerical simulations of reconnection (e.g., Samtaney *et al.* 2009; Daughton *et al.* 2009; Bhattacharjee *et al.* 2009; Ni *et al.* 2010; Huang & Bhattacharjee 2010; Loureiro *et al.* 2012, 2013). The example below is taken from a resistive-MHD numerical simulation by Samtaney *et al.* (2009), showing the evolution of the current density (color) in the central $x = [-\delta_{\rm SP}, \delta_{\rm SP}]$ region of a SP current sheet with $S = 10^7$:

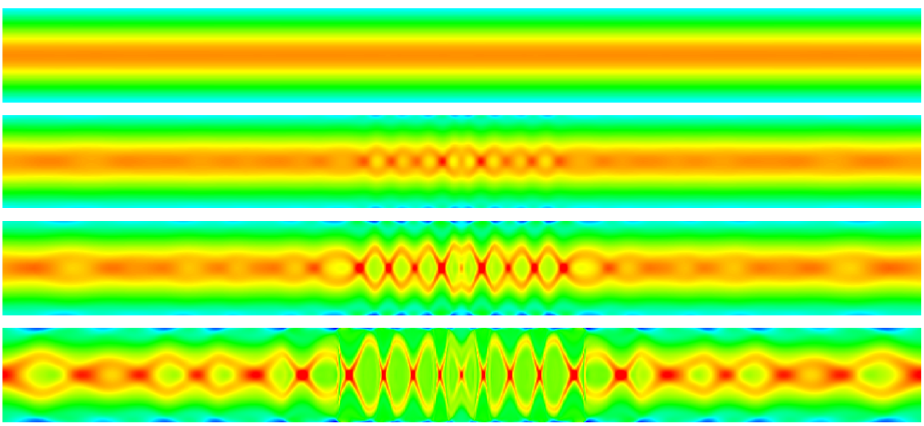

Below is another example, taken from Bhattacharjee *et al.* (2009) using $S = 2\pi \times 10^5$:

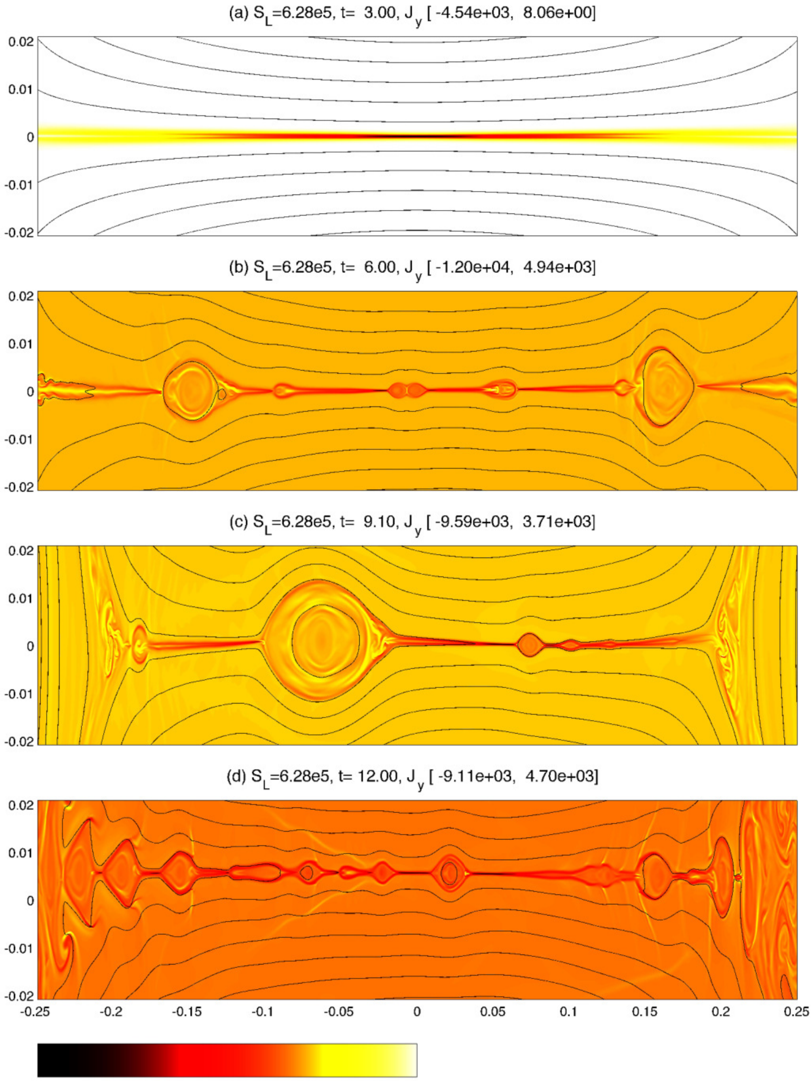

Since then, simulations of plasmoid-dominated reconnection has become an industry.

Given that large-aspect-ratio SP current sheets are violently unstable to the plasmoid instability, it is worth asking whether we should expect them to exist in nature at all. Indeed, Lundquist numbers of typical space and astrophysical plasmas are absurdly large, with $S \sim 10^{13}$ or so in the solar corona implying a plasmoid-instability time scale less than 0.06% of the dynamical time scale. Why would a nice SP current sheet ever be realized under these conditions? See Pucci & Velli (2014) and Uzdensky & Loureiro (2016) for more.[14]

[14]You may also wish to see Alt & Kunz (2019) and Winarto & Kunz (2022) for reasons why a relatively large-scale, smoothly varying current layer (e.g., a Harris sheet) should not be expected to occur in a weakly collisional, high-β plasma.

PART IX

Turbulence and dynamo

IX.1. Kolmogorov–Obukhov theory of hydrodynamic turbulence

This is simple. Like all simple things, it resulted from a stroke of genius (Kolmogorov 1941; Obukhov 1941), one which everyone now says is obvious. It's *just* dimensionless analysis!

Suppose energy is being pumped into some fluid at large scales at a rate ε, which is fixed. At scales small enough that the system is locally homogeneous but not so small that viscosity (or whatever dissipative effect there are) is unimportant – the so-called "inertial range" – this ε is passed along conservatively, scale by scale: a constant energy flux. Assuming this "passing" of energy is local, the energy spectrum is, by dimensional analysis,

$$\boxed{E(k) \sim \varepsilon^{2/3} k^{-5/3}} \tag{IX.1.1}$$

It cannot be any different under these assumptions:

$$[\varepsilon] = \frac{U^3}{L} \qquad \left[\int \mathrm{d}k\, E(k)\right] = U^2,$$

and that's it. There is one timescale – L/U, the eddy turnover time at the outer scale L where the velocity is U. (Density is taken to be constant, which becomes a better assumption the further down the cascade you go where the motions become more and more subsonic.) This also implies that the typical velocity increment between points separated by a distance λ is

$$\boxed{\delta u_\lambda \sim (\varepsilon\lambda)^{1/3}} \tag{IX.1.2}$$

The corresponding scale-dependent rate of strain is $\delta u_\lambda/\lambda \sim \epsilon^{1/3}\lambda^{-2/3}$. Thus, the fastest eddies are the ones at the viscous scale, $\delta u_{\lambda_\nu}/\lambda_\nu \propto \lambda_\nu^{-2/3}$, where the kinetic energy is ultimately thermalized as heat.

One could go on from here to some other Kolmogorovian things, but I won't.

IX.2. Iroshnikov–Kraichnan theory of MHD turbulence

Now suppose that fluid were conducting and threaded by a magnetic field. The problem with just using Kolmogorov may be stated in two ways. First, the homogeneous assumption in the Kolmogorov treatment is similar to saying that, at sufficiently small scales (but still those above the dissipative scales), the fluctuations on those scales are independent of any large-scale structure or features of the "background" in which they reside. This is obviously *not* true when there is a magnetic field: all scales feel that magnetic field, even if it is only at large scales.[15] Secondly, dimensional analysis is no longer enough, as now there are two speed, U and $v_\mathrm{A} \doteq B/\sqrt{4\pi\rho}$, and a directionality imposed by $\boldsymbol{B}$. One way of dealing with the latter – the route taken by Iroshnikov (1963) and Kraichnan (1965) – is to assume isotropy in the Kolmogorovian way, even at small scales: there is no $k_\parallel$ and $k_\perp$, there is only k. Their way of dealing with the former was to give special prominence to the Alfvén time, $\tau_\mathrm{A} \sim \lambda/v_\mathrm{A}$ – the time for an Alfvén wave to cross the scale λ. The nonlinear cascade time that goes into $\varepsilon = \text{const} \sim \delta u_\lambda^2/\tau_\lambda$ is obtained by asking how long must one wait for a wave packet to be sufficiently

[15] Equivalently, a uniform magnetic field cannot be removed by a Galilean transform.

distorted. You see, MHD turbulence has Alfvén-wave packets as its building blocks, not hydrodynamic eddies. From the RMHD equations written in terms of Elsässer potentials (V.5.18), it is clear that only oppositely propagating Alfvén-wave packets interact, and that the change in δu_λ of one packet due to the nonlinear interaction with another in a crossing time τ_A is $\sim(\delta u_\lambda^2/\lambda)\times(\lambda/v_\mathrm{A})$ – the nonlinearity times the characteristic timescale. In "weak" turbulence, this gives only a small change. So, one requires many collisions to distort a wave packet by an amount equal to itself. If these collisions add up randomly, we get the random-wave scaling

$$N_\mathrm{collisions}^{1/2}\mathit{\Delta}(\delta u_\lambda)\sim\delta u_\lambda \quad\Longrightarrow\quad N_\mathrm{collisions}\sim\left[\frac{\delta u_\lambda}{\mathit{\Delta}(\delta u_\lambda)}\right]^2\sim\left(\frac{v_\mathrm{A}}{\delta u_\lambda}\right)^2.$$

The energy transfer time is then $N_\mathrm{collisions}\tau_\mathrm{A}\sim\tau_\lambda$, so

$$\tau_\lambda\sim\left(\frac{v_\mathrm{A}}{\delta u_\lambda}\right)^2\frac{\lambda}{v_\mathrm{A}}\sim\frac{v_\mathrm{A}\lambda}{\delta u_\lambda^2}.$$

Combining these relations yields

$$\varepsilon\sim\frac{\delta u_\lambda^2}{\tau_\lambda}\sim\delta u_\lambda^2\frac{\delta u_\lambda^2}{v_\mathrm{A}\lambda}=\mathrm{const}\quad\Longrightarrow\quad\boxed{\delta u_\lambda\sim(\varepsilon v_\mathrm{A}\lambda)^{1/4}} \tag{IX.2.1}$$

Accordingly,

$$\int_{1/\lambda}^{\infty}\mathrm{d}k\,E(k)\sim\delta u_\lambda^2\quad\Longrightarrow\quad E(k)\sim(\varepsilon v_\mathrm{A})^{1/2}k^{-3/2} \tag{IX.2.2}$$

(Note: Since $\tau_\lambda\gg\lambda/v_\mathrm{A}$, a wave packet must undergo many uncorrelated interactions with oppositely moving wave packets before energy is transferred to small scales.)

This picture held for 30 years.[16]

IX.3. Goldreich–Sridhar theory of MHD turbulence

Isotropy can't be right. Again, a simple statement that is obvious in retrospect. (This was realized relatively early on from tentative experimental and numerical evidence, e.g., Montgomery & Turner (1981) and Shebalin *et al.* (1983).) But it took until 1995 to be worked into a predictive theory (Goldreich & Sridhar 1995). The idea is that perturbations with $k_\parallel\ll k_\perp$ are more natural in a magnetic field that is hard to bend but has little qualms with small-scale structure perpendicular to itself. The problem is to determine how $k_\parallel/k_\perp$ scales. This is provided by *critical balance*: the linear and nonlinear timescales are comparable at all scales.[17] Thus,

$$\tau_\mathrm{A}=\frac{\ell}{v_\mathrm{A}}\sim\tau_\lambda\sim\frac{\lambda}{\delta u_\lambda}, \tag{IX.3.1}$$

where now λ denotes a perpendicular scale and ℓ denotes a parallel scale. Proceeding as in Kolmogorov,

$$\varepsilon\sim\frac{\delta u_\lambda^2}{\tau_\lambda}\sim\frac{\delta u_\lambda^3}{\lambda}\quad\Longrightarrow\quad E(k_\perp)\sim\varepsilon^{2/3}k_\perp^{-5/3}. \tag{IX.3.2}$$

---

[16]I learned from Alex Schekochihin that Iroshnikov (1963) was largely unnoticed at the time and "he disappeared into Soviet obscurity." Apparently, he worked at the Institute of Oceanology in later years and died in 1991 at the age of 54.

[17]That $\tau_\mathrm{A}/\tau_\lambda$ is scare invariant has only been found recently by Mallet *et al.* (2015), who dubbed this "refined critical balance".

A Kolmogorov spectrum, but one in the direction across the field. Along the field,

$$\ell \sim \lambda \frac{v_{\mathrm{A}}}{\delta u_\lambda} \quad \Longrightarrow \quad \frac{\ell}{\lambda} \sim v_{\mathrm{A}}(\varepsilon\lambda)^{-1/3}, \tag{IX.3.3}$$

and so the anisotropy *increases* at smaller scales. We have

$$\delta u_\lambda \sim (\varepsilon\lambda)^{1/3} \quad \text{and} \quad \delta u_\ell \sim (\varepsilon\ell/v_{\mathrm{A}})^{1/2},$$

so that $E(k_\parallel) = E(k_\perp)(\mathrm{d}k_\perp/\mathrm{d}k_\parallel) \propto k_\parallel^{-2}$. Physically, the critical balance ban be argued from causality (e.g. Boldyrev 2005; Nazarenko & Schekochihin 2011): ℓ is the distance an Alfvénic pulse travels along the field at speed v_{A} in a time τ_λ – this is the maximum distance over which the fluctuation can remain correlated.

These (predicted!) scalings have been since measured in numerical simulations and in the solar wind. For the latter, the figure on the left below shows the parallel ($P_\parallel$) and perpendicular ($P_\perp$) spectra (Fourier and wavelet) of the magnetic fluctuations in the solar wind, measured by the *Ulysses* spacecraft and computed by Wicks *et al.* (2010). (The spacecraft-measured frequencies have been converted to wavenumbers k using the Taylor hypothesis.) An earlier (and first ever) result – the spectral index as a function of the angle to the local mean magnetic field θ_B – is shown on the right (Horbury *et al.* 2008). Note that both are in agreement with the GS scalings, $E(k_\perp) \propto k_\perp^{-5/3}$ and $E(k_\parallel) \propto k_\parallel^{-2}$.

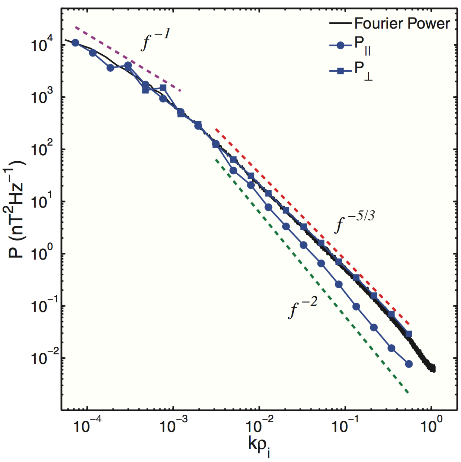

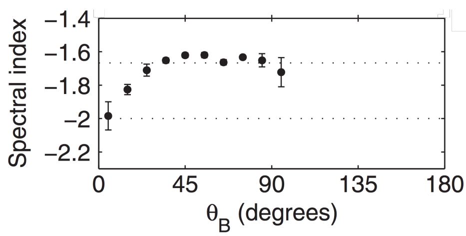

One slight issue is that simulations, while confirming the $\ell \sim \lambda^{2/3}$ scaling (e.g., Cho & Vishniac 2000; Maron & Goldreich 2001), instead find a $-3/2$ spectrum (rather than $-5/3$). This led Boldyrev (2006) to propose a correction to the theory dubbed *dynamical alignment*.

IX.4. Boldyrev's dynamical alignment

[in preparation]

Argued that the filament-like eddies implied by the GS95 picture are not realizable; that, instead, fluctuations are three-dimensionally anisotropic. This anisotropy is due to an angular alignment of magnetic-field and velocity-field polarizations – essentially, the turbulence wants to be as "Alfvénic" as possible, with $\boldsymbol{u}_\perp$ and $\boldsymbol{B}_\perp$ the same. ((Matthaeus *et al.* 2008) identified the dynamical tendency for the velocity and magnetic field to align locally in patches in numerical simulations.) Of course, this alignment cannot be precise, or else the nonlinear interaction between counterpropagating Alfvén-wave packets would be turned off. Instead, Boldyrev (2006) argued that, at each scale λ, the alignment of fluctuations should attain the maximal level consistent with a constant energy flux through that scale. This implies an alignment angle $\theta_\lambda \propto \lambda^{1/4}$, so that the magnetic-field and velocity-field fluctuations become increasingly aligned at smaller and smaller scales, i.e., the dynamic alignment is *scale dependent*. This progressively weakens the nonlinear interaction. The end result is a perpendicular energy spectrum $E(k_\perp) \propto k_\perp^{-3/2}$, consistent with multiple numerical simulations of MHD turbulence.

rephrased: minimal degree of misalignment is set by a kind of uncertainty principle: direction of local magnetic field can only be defined with a small angle $\theta_\lambda \sim \delta B_\lambda / B_0 \ll 1$, and so the fluctuations cannot be aligned any more precisely than this.

Boldyrev:

$$\boldsymbol{z}_\perp^\pm \boldsymbol{\cdot} \boldsymbol{\nabla} \boldsymbol{z}_\perp^\mp \sim \theta_\lambda \frac{\delta u_\lambda^2}{\lambda} \quad \Longrightarrow \quad \ell \sim \frac{v_{\rm A}\lambda}{\theta_\lambda \delta u_\lambda}$$

$$\tau_\lambda \sim \frac{\ell}{v_{\rm A}} \sim \frac{\lambda}{\theta_\lambda \delta u_\lambda}$$

$$\frac{\delta u_\perp^2}{\tau_\lambda} = \text{const} \quad \Longrightarrow \quad \delta u_\lambda \propto (\lambda/\theta_\lambda)^{1/3} \sim (\varepsilon v_{\rm A} \lambda)^{1/4} \quad \Longrightarrow \quad E(k_\perp) \sim (\varepsilon v_{\rm A})^{1/2} k_\perp^{-3/2}.$$

Looks like IK spectrum but is anisotropic with critical balance: $\ell \sim v_{\rm A}^{3/2} \varepsilon^{-1/2} \lambda^{1/2}$. Parallel spectrum is the same as in GS95.

adapted from Boldyrev (2006):

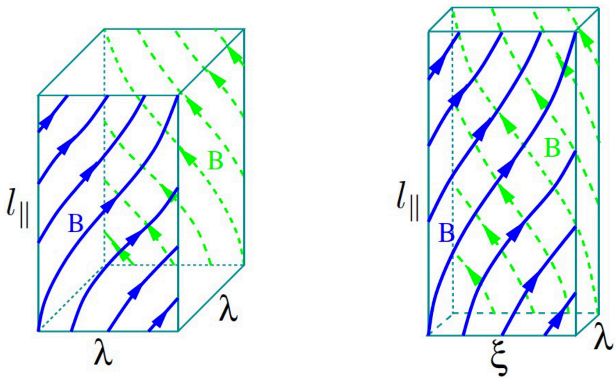

See Mason *et al.* (2006, 2008, 2011, 2012); Perez *et al.* (2012, 2014)

Beresnyak (2011): in RMHD limit, $\delta B_\lambda / B_0$ is an arbitrarily small quantity and thus so must be θ_λ. This means nonlinearity would disappear from RMHD ordering. Only way to keep nonlinearity is to order $\theta_\lambda \sim 1$ wrt RMHD ordering, i.e., it cannot scale with ϵ. Thus, you can't have $\ell / v_{\rm A} \propto \lambda^{1/2}$. This, even though aligned MHD turbulence has been measured in RMHD simulations.

Chandran *et al.* (2015); Mallet *et al.* (2015); Mallet & Schekochihin (2017): alignment between $\boldsymbol{u}_\perp$ and $\boldsymbol{B}_\perp$ not, mathematically, the same as alignment between $\boldsymbol{z}_\perp^+$ and $\boldsymbol{z}_\perp^-$. Found that alignment angle between the Elsasser fields at any given scale is *anticorrelated* with their amplitudes. Intermittency matters: how is λ, ξ, and ℓ distributed in a turbulent MHD system?

For many more details (especially concerning weak turbulence and the most recent explorations of the connection between turbulence and the disruption of current sheets by tearing instability), see the excellent recent review of MHD turbulence by Alex Schekochihin (Schekochihin 2022).

IX.5. Zel'dovich's fluctuation dynamo

What if we now have hydrodynamic turbulence sitting in a conducting fluid hosting a weak zero-net-flux magnetic field (i.e., no imposed field)? Let us set aside the question of what the turbulence looks like and ask a simpler question: under what conditions will this "seed" magnetic field be amplified? This is the problem of *small-scale* or *fluctuation dynamo*. It's not easy, and has only been solved under specific conditions.

As a first step, suppose we have a planar flow field $\boldsymbol{u} = u_x(t,x,y,z)\hat{\boldsymbol{x}} + u_y(t,x,y,z)\hat{\boldsymbol{y}}$, with $\boldsymbol{\nabla\cdot u} = 0$ but otherwise arbitrary. The z-component of the resistive-MHD induction equation with constant η,

$$\frac{\partial \boldsymbol{B}}{\partial t} = \boldsymbol{\nabla}\times(\boldsymbol{u}\times\boldsymbol{B}) + \eta\nabla^2\boldsymbol{B}, \tag{IX.5.1}$$

is then

$$\frac{\partial B_z}{\partial t} + \boldsymbol{u\cdot\nabla} B_z = \eta\nabla^2 B_z. \tag{IX.5.2}$$

Multiplying (IX.5.2) by $2B_z$ and integrating over the volume of the plasma, we find

$$\frac{\partial\langle B_z^2\rangle}{\partial t} = -2\eta\langle|\boldsymbol{\nabla}B_z|^2\rangle, \tag{IX.5.3}$$

and so B_z resistively decays to 0. If $B_z = 0$, then the solenoidality constraint on the magnetic field becomes $\partial B_x/\partial x + \partial B_y/\partial y = 0$ and so the planar components of the magnetic field may be written in terms of a vector potential, $\boldsymbol{B} = \boldsymbol{\nabla}\times(A\hat{\boldsymbol{z}})$. The latter satisfies the un-curled induction equation,

$$\frac{\partial A}{\partial t} + \boldsymbol{u\cdot\nabla}A = \eta\nabla^2 A \quad\Longrightarrow\quad \frac{\mathrm{d}}{\mathrm{d}t}\langle A^2\rangle = -2\eta\langle|\boldsymbol{\nabla}A|^2\rangle. \tag{IX.5.4}$$

Again, the magnetic field decays resistively. Thus, no dynamo can be maintained by a planar flow (Zel'dovich 1957). This is referred to as *Zel'dovich's anti-dynamo theorem.* There are other "anti-dynamo theorems", one of which will be proven below (§IX.7), but let us explore the fluctuation dynamo a bit further.

The simplest approach is to consider the zero-net-flux magnetic field to be so weak energetically that it exerts no dynamical effect on the fluid flow, i.e., the Lorentz force is negligible on all scales of interest. This is the *kinematic* limit, in which the velocity field can be prescribed without regard for the evolution of the magnetic field. Also, we'll take $\mathrm{Pm} \doteq \nu/\eta = \mathrm{Rm}/\mathrm{Re} \gg 1$.[18] This causes the viscous scale λ_ν, at which $\boldsymbol{u\cdot\nabla u} \sim \nu\nabla^2\boldsymbol{u}$, to be much larger than the resistive scale λ_η, at which $\boldsymbol{B\cdot\nabla u} \sim \eta\nabla^2\boldsymbol{B}$. The former may be estimated using

$$\boldsymbol{u\cdot\nabla u} \sim \frac{\delta u_{\lambda_\nu}^2}{\lambda_\nu} \sim \varepsilon^{2/3}\lambda_\nu^{-1/3} \quad\text{and}\quad \nu\nabla^2\boldsymbol{u} \sim \nu\frac{\delta u_{\lambda_\nu}}{\lambda_\nu^2} \sim \nu\varepsilon^{1/3}\lambda_\nu^{-5/3}.$$

Matching these gives

$$\lambda_\nu \sim \nu^{3/4}\varepsilon^{-1/4} \sim L\,\mathrm{Re}^{-3/4} \quad\text{and}\quad \delta u_{\lambda_\nu} \sim \nu^{1/4}\varepsilon^{1/4} \sim U\,\mathrm{Re}^{-1/4}, \tag{IX.5.5}$$

where $\mathrm{Re} \doteq UL/\nu$. To estimate the latter (the resistive scale), note that

$$\frac{\partial\boldsymbol{B}}{\partial t} = \boldsymbol{\nabla}\times(\boldsymbol{u}\times\boldsymbol{B}) \quad\Longrightarrow\quad \frac{\mathrm{d}B^2}{\mathrm{d}t} = 2\boldsymbol{BB}\boldsymbol{:}\boldsymbol{\nabla u} \quad\Longrightarrow\quad \frac{\mathrm{d}\ln B}{\mathrm{d}t} = \hat{\boldsymbol{b}}\hat{\boldsymbol{b}}\boldsymbol{:}\boldsymbol{\nabla u} \tag{IX.5.6}$$

for an incompressible velocity field. Thus, because velocity gradients are what grow the

[18] $\mathrm{Pm} \simeq 2.6\times10^{-5}T^4/n$ in fully ionized plasmas, which is $\sim\!10^{29}$ in the ICM and $\sim\!10^{11}$ in the warm phase of the ISM.

field, the viscous-scale eddies, where the stretching rate $\delta u_\lambda/\lambda \sim \varepsilon^{1/3}\lambda^{-2/3}$ is fastest, will be the most important. Accordingly, $\boldsymbol{\nabla u} \sim \delta u_{\lambda_\nu}/\ell_\nu \sim (U/L)\,\mathrm{Re}^{1/2}$; balancing this with $\eta\lambda_\eta^2$ at the resistive scale leads to

$$\lambda_\eta \sim L\,\mathrm{Re}^{-1/4}\,\mathrm{Rm}^{-1/2} \sim \lambda_\nu\,\mathrm{Pm}^{-1/2} \ll \lambda_\nu. \tag{IX.5.7}$$

Graphically,

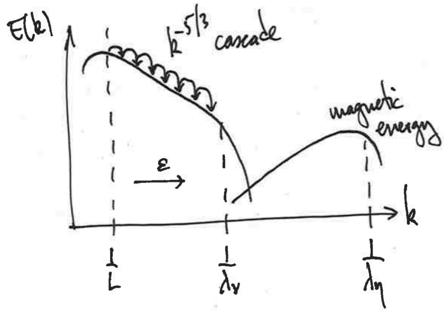

Now then, because $\delta u_{\lambda_\nu} \sim (\varepsilon/\nu)^{1/2}\lambda_\nu \propto \lambda_\nu$, the viscous-scale motions are smooth and Taylor-expandable. The turbulence looks like a succession of random-in-time linear shears, and the magnetic field becomes arranged in folds with field reversals on the resistive scale (see Schekochihin & Cowley 2007, for a review):

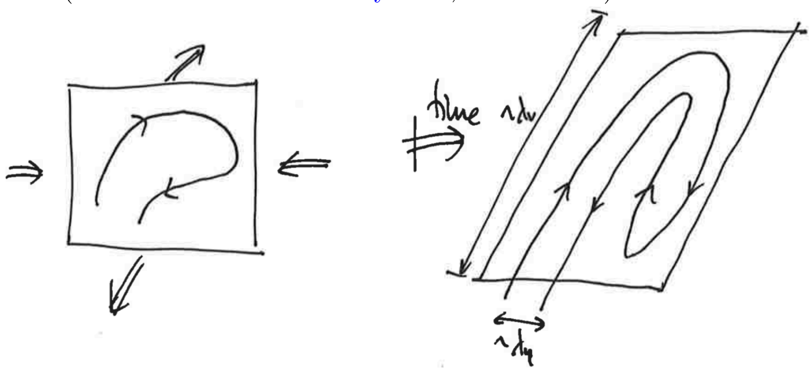

It is in this configuration that the mean magnetic-field strength becomes amplified by the chaotic flows, a point we now prove following the arguments in Zel'dovich *et al.* (1984).

Because the viscous-scale velocity fluctuations $\delta u_{\ell_\nu} \propto \ell_\nu$ are smooth, we can write the velocity field as a Taylor expansion about some point $\boldsymbol{r} = \boldsymbol{0}$:

$$u^\ell(t,\boldsymbol{r}) = u^\ell(t,\boldsymbol{0}) + \sigma^\ell_m(t) r^m + \dots, \tag{IX.5.8}$$

where summation over repeated indices is implied. Of course, we have the freedom to set $u^i(t,\boldsymbol{0}) = 0$ by moving to that frame of reference. Then, the jth component of the resistive-MHD induction equation (IX.5.1) is

$$\frac{\partial B^j}{\partial t} + \sigma^\ell_m(t) r^m \frac{\partial B^j}{\partial r^\ell} = B^m \sigma^j_m(t) + \eta\nabla^2 B^j. \tag{IX.5.9}$$

We seek a solution as a sum of plane waves with time-dependent wavevector $\boldsymbol{k} = \boldsymbol{k}(t)$:

$$B^j(t,\boldsymbol{r}) = \int \mathrm{d}^3\boldsymbol{k}_0\, B^j(t,\boldsymbol{k}_0) \exp\bigl[\mathrm{i}k_n(t,\boldsymbol{k}_0) r^n\bigr], \tag{IX.5.10}$$

where $\boldsymbol{k}(t,\boldsymbol{k}_0)$ is the time-dependent wavenumber whose value at $t = 0$ is $\boldsymbol{k}_0$. (Thus, $k_n(0,\boldsymbol{k}_0) = k_{0n}$.) This works nicely because (IX.5.9) is linear, so that each $\boldsymbol{k}$ is a solution. Substituting (IX.5.10) into (IX.5.9) and examining each Fourier component independently,

$$\begin{aligned}\frac{\partial}{\partial t}\Big[B^j(t,\boldsymbol{k}_0)\mathrm{e}^{\mathrm{i}k_n(t,\boldsymbol{k}_0)r^n}\Big] &= \mathrm{e}^{\mathrm{i}k_n(t,\boldsymbol{k}_0)r^n}\left[\frac{\partial B^j(t,\boldsymbol{k}_0)}{\partial t} + \mathrm{i}B^j(t,\boldsymbol{k}_0)r^m\frac{\partial k_m(t,\boldsymbol{k}_0)}{\partial t}\right]\\ &= \mathrm{e}^{\mathrm{i}k_n(t,\boldsymbol{k}_0)r^n}\Big[-\sigma^\ell_m(t)r^m\,\mathrm{i}k_\ell(t,\boldsymbol{k}_0)B^j(t,\boldsymbol{k}_0)\\ &\qquad + B^m(t,\boldsymbol{k}_0)\sigma^i_m(t) - \eta k^2(t,\boldsymbol{k}_0)B^j(t,\boldsymbol{k}_0)\Big],\end{aligned} \tag{IX.5.11}$$

Equation (IX.5.11) must be satisfied at each $\boldsymbol{r}$, and so

$$\frac{\partial B^j(t,\boldsymbol{k}_0)}{\partial t} = -\eta k^2(t,\boldsymbol{k}_0)B^j(t,\boldsymbol{k}_0) + B^m(t,\boldsymbol{k}_0)\sigma^j_m(t), \tag{IX.5.12a}$$

$$\frac{\partial k_m(t,\boldsymbol{k}_0)}{\partial t} = -k_\ell(t,\boldsymbol{k}_0)\sigma^\ell_m(t), \tag{IX.5.12b}$$

with the initial conditions $B^j(0,\boldsymbol{k}_0) = B^j_0(\boldsymbol{k}_0)$ and $k_m(0,\boldsymbol{k}_0) = k_{0m}$.

To go any further, we require a model $\sigma^\ell_m(t)$ tensor. There are a few options, but the following is the simplest:

$$\boldsymbol{\sigma} = \begin{bmatrix}\lambda_1 & 0 & 0\\ 0 & \lambda_2 & 0\\ 0 & 0 & \lambda_3\end{bmatrix} \tag{IX.5.13}$$

with $\mathrm{tr}(\boldsymbol{\sigma}) = \lambda_1+\lambda_2+\lambda_3 = 0$ (incompressibility). We may arrange the coordinate system such that

$$\underbrace{\lambda_1}_{\text{stretching}} > \underbrace{\lambda_2}_{\text{“null”}} > \underbrace{\lambda_3}_{\text{compression}} \quad \text{and} \quad \lambda_1 > 0,\ \lambda_3 < 0. \tag{IX.5.14}$$

Then (IX.5.12) becomes

$$\frac{\partial B^j(t,\boldsymbol{k}_0)}{\partial t} = -\eta k^2(t,\boldsymbol{k}_0)B^j(t,\boldsymbol{k}_0) + B^j(t,\boldsymbol{k}_0)\lambda_j, \tag{IX.5.15a}$$

$$\frac{\partial k_m(t,\boldsymbol{k}_0)}{\partial t} = -k_\ell(t,\boldsymbol{k}_0)\lambda^\ell, \tag{IX.5.15b}$$

whose solutions are

$$B^j(t,\boldsymbol{k}_0) = B^j_0(\boldsymbol{k}_0)\,\mathrm{e}^{\lambda_j t - \eta\int_0^t \mathrm{d}t'\,k^2(t',\boldsymbol{k}_0)}, \tag{IX.5.16a}$$

$$k_m(t,\boldsymbol{k}_0) = k_{0m}\,\mathrm{e}^{-\lambda_m t}. \tag{IX.5.16b}$$

Note that some components of $\boldsymbol{k}(t,\boldsymbol{k}_0)$ decay (k_1) while others grow (k_3); thus, stretching (along $\hat{\boldsymbol{e}}_1$) and compression (along $\hat{\boldsymbol{e}}_3$). We now ask whether or not this leads to a net amplification of the mean magnetic energy:

$$\begin{aligned}
\langle B^2\rangle &\doteq \int \mathrm{d}^3\boldsymbol{r}\,|\boldsymbol{B}(t,\boldsymbol{r})|^2 \\
&= \int \mathrm{d}^3\boldsymbol{r} \int \mathrm{d}^3\boldsymbol{k}_0 \int \mathrm{d}^3\boldsymbol{k}_0'\, B_j(t,\boldsymbol{k}_0) B^j(t,\boldsymbol{k}_0')\,\mathrm{e}^{\mathrm{i}[k_n(t,\boldsymbol{k}_0)+k_n(t,\boldsymbol{k}_0')]r^n} \\
&= \int \mathrm{d}^3\boldsymbol{k}_0 \int \mathrm{d}^3\boldsymbol{k}_0'\, B_j(t,\boldsymbol{k}_0) B^j(t,\boldsymbol{k}_0')\,(2\pi)^3\, \underbrace{\delta\big[\boldsymbol{k}(t,\boldsymbol{k}_0)+\boldsymbol{k}(t,\boldsymbol{k}_0')\big]}_{\substack{=\delta\left[(\boldsymbol{k}_0+\boldsymbol{k}_0')_n\,\mathrm{e}^{-\lambda_n t}\right] \\ =\delta(\boldsymbol{k}_0+\boldsymbol{k}_0')\left[\det\left(\mathrm{e}^{-\boldsymbol{\sigma}t}\right)\right]^{-1} \\ =\delta(\boldsymbol{k}_0+\boldsymbol{k}_0')\,\mathrm{e}^{-\mathrm{tr}(\boldsymbol{\sigma})t} \\ =\delta(\boldsymbol{k}_0+\boldsymbol{k}_0')\ \text{since}\ \mathrm{tr}(\boldsymbol{\sigma})=0}}\,, \\
&= \int \mathrm{d}^3\boldsymbol{k}_0\,(2\pi)^3\, B_j(t,\boldsymbol{k}_0) B^j(t,-\boldsymbol{k}_0), \\
&= \int \mathrm{d}^3\boldsymbol{k}_0\,(2\pi)^3\,|\boldsymbol{B}(t,\boldsymbol{k}_0)|^2,
\end{aligned}$$

which is just Parseval's theorem, i.e., the energy of the field is the sum of the energies of the plane waves. So we must calculate the energy of each mode using (IX.5.16):

$$\begin{aligned}
|\boldsymbol{B}(t,\boldsymbol{k}_0)|^2 &= \mathrm{e}^{-2\eta\int_0^t \mathrm{d}t'\,k^2(t',\boldsymbol{k}_0)}\Big[\underbrace{|B_{01}(\boldsymbol{k}_0)|^2\,\mathrm{e}^{2\lambda_1 t}}_{\substack{\text{exponentially larger} \\ \text{than the rest,} \\ \text{since } \lambda_1>\lambda_2>\lambda_3}} + |B_{02}(\boldsymbol{k}_0)|^2\,\mathrm{e}^{2\lambda_2 t} + |B_{03}(\boldsymbol{k}_0)|^2\,\mathrm{e}^{2\lambda_3 t}\Big] \\
&\approx |B_{01}(\boldsymbol{k}_0)|^2\,\mathrm{e}^{2\lambda_1 t - 2\eta\int_0^t \mathrm{d}t'\,k^2(t',\boldsymbol{k}_0)}.
\end{aligned}$$

The time integral in the exponential is

$$\begin{aligned}
\int_0^t \mathrm{d}t'\,k^2(t',\boldsymbol{k}_0) &= \int_0^t \mathrm{d}t'\left(k_{01}^2\,\mathrm{e}^{-2\lambda_1 t} + k_{02}^2\,\mathrm{e}^{-2\lambda_2 t} + k_{03}^2\,\mathrm{e}^{-2\lambda_3 t}\right) \\
&= \frac{k_{01}^2}{2\lambda_1}(1-\mathrm{e}^{-2\lambda_1 t}) + \frac{k_{02}^2}{2\lambda_2}(1-\mathrm{e}^{-2\lambda_2 t}) \underbrace{- \frac{k_{03}^2}{2|\lambda_3|}(1-\mathrm{e}^{2|\lambda_3|t})}_{\text{since }\lambda_3<0} \\
&\approx \frac{k_{01}^2}{2\lambda_1} + \frac{k_{02}^2}{2\lambda_2} + \frac{k_{03}^2}{2|\lambda_3|}\mathrm{e}^{2|\lambda_3|t},
\end{aligned}$$

with the final line following after assuming $\lambda_2 > 0$ (as it usually is in real turbulence). Thus,

$$|\boldsymbol{B}(t,\boldsymbol{k}_0)|^2 \approx |\boldsymbol{B}_{01}(\boldsymbol{k}_0)|^2\,\exp\left[2\lambda_1 t - \eta\left(\frac{k_{01}^2}{\lambda_1} + \frac{k_{02}^2}{\lambda_2} + \frac{k_{03}^2}{|\lambda_3|}\,\mathrm{e}^{2|\lambda_3|t}\right)\right]. \tag{IX.5.17}$$

For most modes, the energy decays super-exponentially. But there is a subset of modes, those satisfying

$$\frac{k_{01}^2}{2\lambda_1^2 t/\eta} + \frac{k_{02}^2}{2\lambda_1\lambda_2 t/\eta} + \frac{k_{03}^2}{2\lambda_1|\lambda_3|t\,\mathrm{e}^{-2|\lambda_3|t}/\eta} \lesssim 1, \tag{IX.5.18}$$

which actually grows. Within this ellipsoidal volume of size

$$\sim \lambda_1^2(\lambda_2|\lambda_3|)^{1/2}\left(\frac{t}{\eta}\right)^{3/2}\mathrm{e}^{-|\lambda_3|t},$$

the mean magnetic energy satisfies

$$\begin{aligned}\frac{\langle B^2\rangle}{(2\pi)^3} &= \int \mathrm{d}^3\boldsymbol{k}_0\,|\boldsymbol{B}(t,\boldsymbol{k}_0)|^2\\ &\sim \lambda_1^2(\lambda_2|\lambda_3|)^{1/2}\left(\frac{t}{\eta}\right)^{3/2}|B_{01}(\boldsymbol{k}_0)|^2\ \underbrace{\mathrm{e}^{2\lambda_1 t-|\lambda_3|t}}_{\substack{=\mathrm{e}^{(\lambda_1-\lambda_2)t}\\ \text{since }\mathrm{tr}(\boldsymbol{\sigma})=0}}\\ &\propto t^{3/2}\,\mathrm{e}^{(\lambda_1-\lambda_2)t},\end{aligned} \tag{IX.5.19}$$

which increases in time because $\lambda_1>\lambda_2$. Therefore, dynamo works in 3D for certain $\boldsymbol{k}_0$.

What if $\lambda_2<0$? In this case, the growing modes occur within the volume

$$\frac{k_{01}^2}{2\lambda_1^2 t/\eta}+\frac{k_{02}^2}{2\lambda_1|\lambda_2|t\,\mathrm{e}^{-2|\lambda_2|t}/\eta}+\frac{k_{03}^2}{2\lambda_1|\lambda_3|t\,\mathrm{e}^{-2|\lambda_3|t}/\eta}\lesssim 1,$$

and one can show that

$$\langle B^2\rangle\sim\lambda_1^2(|\lambda_2||\lambda_3|)^{1/2}\left(\frac{t}{\eta}\right)^{3/2}B_{02}^2\ \underbrace{\mathrm{e}^{(\lambda_1-2|\lambda_2|)t}}_{=\mathrm{e}^{(|\lambda_3|-|\lambda_2|)t}}.$$

Thus, the mean magnetic energy grows at rate set by $|\lambda_3|-|\lambda_2|$.

Physically, what's going on is the following. During stretching, the magnetic field aligns with $\hat{\boldsymbol{e}}_1$ (i.e., $\boldsymbol{B}\sim B_{01}\,\mathrm{e}^{\lambda_1 t}\hat{\boldsymbol{e}}_1$). The wavevector mostly wants to align with the compression direction (i.e., $\boldsymbol{k}\sim k_{03}\,\mathrm{e}^{|\lambda_3|t}\hat{\boldsymbol{e}}_3$), which makes most modes decay super-exponentially. The only modes that don't decay are those that had $\boldsymbol{k}_0$ almost perpendicular to $\hat{\boldsymbol{e}}_3$ to begin with (i.e., $k_{03}\lesssim(\dots)\,\mathrm{e}^{-|\lambda_3|t}$ – see (IX.5.18)). Since $\boldsymbol{k}_0\perp\boldsymbol{B}_0$, this means that the growing modes mostly have $\boldsymbol{k}_0\sim k_{02}\hat{\boldsymbol{e}}_2$. Again, the picture is

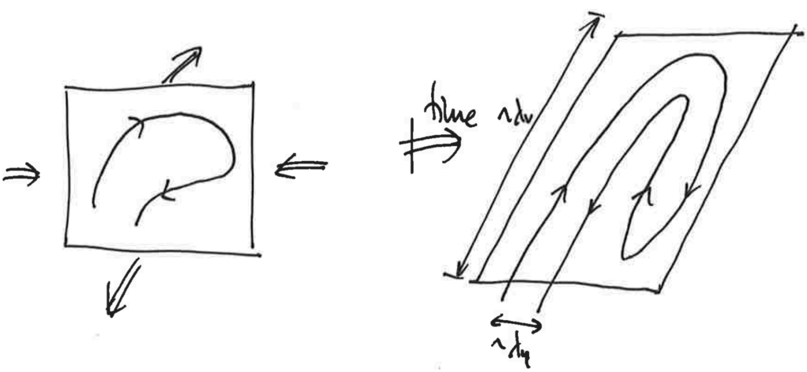

And the winning configuration is

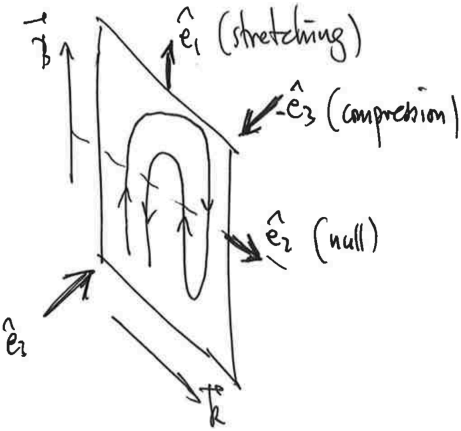

Any other configuration means that each time you stretch, you also compress – then antiparallel field lines are brought together and B^2 decays resistively.[19]

Zel'dovich showed that such a dynamo won't work in 2D. Can we show that using his model? First, in 2D we have $\lambda_1 + \lambda_2 = 0$. Without loss of generality, assume $\lambda_1 > 0$, so that $\hat{\boldsymbol{e}}_1$ is the "stretching" direction and $\hat{\boldsymbol{e}}_2$ is the "compressing" direction. Equations (IX.5.16) then imply

$$\begin{aligned} |\boldsymbol{B}(t,\boldsymbol{k}_0)|^2 &= \mathrm{e}^{-2\eta\int_0^t \mathrm{d}t'\,k^2(t',\boldsymbol{k}_0)}\Big[|B_{01}(\boldsymbol{k}_0)|^2\mathrm{e}^{2\lambda_1 t} + |B_{02}(\boldsymbol{k}_0)|^2\mathrm{e}^{-2\lambda_1 t}\Big], \\ &\approx |B_{01}(\boldsymbol{k}_0)|^2\,\mathrm{e}^{2\lambda_1 t\,-\,2\eta\int_0^t \mathrm{d}t'\,k^2(t',\boldsymbol{k}_0)}, \end{aligned} \tag{IX.5.20}$$

where the time integral in the exponential is

$$\begin{aligned} \int_0^t \mathrm{d}t'\,k^2(t',\boldsymbol{k}_0) &= \int_0^t \mathrm{d}t'\,\Big(k_{01}^2\,\mathrm{e}^{-2\lambda_1 t} + k_{02}^2\,\mathrm{e}^{2\lambda_1 t}\Big) \\ &= \frac{k_{01}^2}{2\lambda_1}(1-\mathrm{e}^{-2\lambda_1 t}) - \frac{k_{02}^2}{2\lambda_1}(1-\mathrm{e}^{2\lambda_1 t}) \\ &\approx \frac{k_{01}^2}{2\lambda_1} + \frac{k_{02}^2}{2\lambda_1}\mathrm{e}^{2\lambda_1 t}. \end{aligned} \tag{IX.5.21}$$

Thus, growth is only possible for those modes satisfying

$$\frac{k_{01}^2}{2\lambda_1^2 t/\eta} + \frac{k_{02}^2}{2\lambda_1^2 t\,\mathrm{e}^{-2\lambda_1 t}/\eta} \lesssim 1, \tag{IX.5.22}$$

which constitutes an ellipsoidal area of size

$$\sim \lambda_1^2\left(\frac{t}{\eta}\right)\mathrm{e}^{-\lambda_1 t}. \tag{IX.5.23}$$

The problem is that, with $k_2(t)$ increasing exponentially, the only modes with the potential for growth must have $\boldsymbol{k}_0$ almost perpendicular to $\hat{\boldsymbol{e}}_2$. But, because $\boldsymbol{k}_0\cdot\boldsymbol{B}_0(\boldsymbol{k}_0) = 0$ via the divergence-free constraint on the magnetic field, the initial field must then be largely in the $\hat{\boldsymbol{e}}_2$ direction:

$$B_{01}(\boldsymbol{k}_0) = -\frac{k_{02}}{k_{01}}B_{02}(\boldsymbol{k}_0) \sim -\mathrm{e}^{-\lambda_1 t}B_{02}(\boldsymbol{k}_0), \tag{IX.5.24}$$

[19] I learned all this stuff from Alex Schekochihin.

the final step following from (IX.5.22). Then the mean magnetic energy satisfies

$$\begin{aligned}\frac{\langle B^2\rangle}{(2\pi)^2} &= \int \mathrm{d}^2\boldsymbol{k}_0\,|\boldsymbol{B}(t,\boldsymbol{k}_0)|^2 \\ &\sim \lambda_1^2\left(\frac{t}{\eta}\right)\mathrm{e}^{-\lambda_1 t}\,|B_{01}(\boldsymbol{k}_0)|^2\,\mathrm{e}^{2\lambda_1 t} \\ &\sim \lambda_1^2\left(\frac{t}{\eta}\right)|B_{02}(\boldsymbol{k}_0)|^2\,\mathrm{e}^{-\lambda_1 t}. \end{aligned} \tag{IX.5.25}$$

Thus, the fluctuation dynamo is impossible in 2D. Physically, the difficulty is that the only way to avoid bringing oppositely oriented magnetic fields together in a 2D incompressible flow, and thereby avoid super-exponential resistive damping, is to orient the initial magnetic field across the stretching direction rather than along it. But this stretching then dilutes (rather than increases) the field strength, leading to exponential decay. The difference between 2D and 3D is that, in the latter case, the compression direction, to which the wavevector would want to align exponentially, can be avoided by starting with modes whose $\boldsymbol{k}_0$ initially lies in the third ("null") direction. Otherwise, every time you stretch, you also compress, and antiparallel field lines are brought together.

IX.6. Kazantsev–Kraichnan model of the fluctuation dynamo

This is **optional** material and is not written pedagogically.

We start with the evolution equations (IX.5.12), repeated here for convenience:

$$\begin{aligned}\frac{\partial B^i(t,\boldsymbol{k}_0)}{\partial t} &= -\eta k^2(t,\boldsymbol{k}_0)B^i(t,\boldsymbol{k}_0) + B^m(t,\boldsymbol{k}_0)\sigma^i_{\ m}(t), \\ \frac{\partial k_m(t,\boldsymbol{k}_0)}{\partial t} &= -k_i(t,\boldsymbol{k}_0)\sigma^i_{\ m}(t).\end{aligned}$$

The first step is to split the magnetic field into its scalar strength and its unit-vector direction: $\boldsymbol{B} = B\hat{\boldsymbol{b}}$, so that $B^i = Bb^i$. Substituting this decomposition into the above equations, and henceforth suppressing the argument $(t,\boldsymbol{k}_0)$, yields

$$\begin{aligned}\frac{\partial B}{\partial t} &= -\eta k^2 B + b^i b^m \sigma^i_{\ m} B, \\ \frac{\partial b^i}{\partial t} &= b^m\sigma^i_{\ m} - b^\ell b^m \sigma^\ell_{\ m} b^i, \\ \frac{\partial k_m}{\partial t} &= -k_i\sigma^i_{\ m}\end{aligned}$$

The next step is to adorn all of these variables with tildes, which will denote that they are *random* variables. We are about to engage in a statistical calculation, which is quite different than what was done in the previous section. In this case, all random variables are distributed according to a joint probability density function, $\mathcal{P}(t;B,\boldsymbol{k},\hat{\boldsymbol{b}})$, and the tildes will remind us that the field strength, field direction, and wavenumber that we are carrying around in our equations are not *the* field strength, field direction, and wavenumber. So,

$$\frac{\partial \tilde{B}}{\partial t} = -\eta \tilde{k}^2 \tilde{B} + \tilde{b}^i \tilde{b}^m \tilde{\sigma}^i_m \tilde{B}, \tag{IX.6.1a}$$

$$\frac{\partial \tilde{b}^i}{\partial t} = \tilde{b}^m \tilde{\sigma}^i_m - \tilde{b}^\ell \tilde{b}^m \tilde{\sigma}^\ell_m \tilde{b}^i, \tag{IX.6.1b}$$

$$\frac{\partial \tilde{k}_m}{\partial t} = -\tilde{k}_i \tilde{\sigma}^i_m \tag{IX.6.1c}$$

The rate-of-strain tensor $\tilde{\sigma}^\ell_m \doteq \partial_m \tilde{u}^\ell$ is taken to have the two-time correlation function

$$\overline{\tilde{\sigma}^i_m(t)\tilde{\sigma}^j_n(t')} = \mathit{\Gamma}^{ij}_{mn}(t)\delta(t-t'), \tag{IX.6.2}$$

where the overline denotes the statistical ensemble average and

$$\mathit{\Gamma}^{ij}_{mn}(t) = \kappa_2 \Big[\delta^{ij}\delta_{mn} + a(\delta^i_m \delta^j_n + \delta^i_n \delta^j_m)\Big]. \tag{IX.6.3}$$

Here, κ_2 is the second-order coefficient in the Taylor expansion of the velocity correlation tensor

$$\overline{\tilde{u}^i(t,\boldsymbol{r})\tilde{u}^j(t',\boldsymbol{r}')} = \delta(t-t')\kappa^{ij}(\boldsymbol{r}-\boldsymbol{r}'), \tag{IX.6.4}$$

where

$$\kappa^{ij}(\boldsymbol{y}) = \kappa_0 \delta^{ij} - \frac{1}{2}\kappa_2 \Big[y^2 \delta^{ij} + 2a y^i y^j\Big] + \dots. \tag{IX.6.5}$$

The constant a parametrizes the rate of strain; its value is fixed by assuming an incompressible flow, $\mathit{\Gamma}^{ij}_{in} = 0$ and $\mathit{\Gamma}^{ij}_{mj} = 0$, giving

$$a = -\frac{1}{1+d} \tag{IX.6.6}$$

in d dimensions. The tensors $\mathit{\Gamma}^{ij}_{mn}$ and κ^{ij} are related in Fourier space by

$$\mathit{\Gamma}^{ij}_{mn}(t) = \int \frac{\mathrm{d}^d \boldsymbol{k}}{(2\pi)^d}\, k_m k_n \kappa^{ij}(\boldsymbol{k}). \tag{IX.6.7}$$

Our ultimate goal here is to obtain an evolution equation for the magnetic-energy spectrum $M(k)$. This can be done by first deriving an evolution equation for the joint probability density function of the magnetic field $\boldsymbol{B}$ and its wavenumber $\boldsymbol{k}$,

$$\mathcal{P}(t; B, \boldsymbol{k}, \hat{\boldsymbol{b}}) = \overline{\tilde{\mathcal{P}}} \doteq \overline{\delta(B - \tilde{B}(t))\delta(k_m - \tilde{k}_m(t))\delta(b^i - \tilde{b}^i(t))}, \tag{IX.6.8}$$

and then taking the appropriate moments; to wit,

$$M(t,k) = \int \mathrm{d}\mathit{\Omega}_{\boldsymbol{k}}\, k^2 \int \mathrm{d}^3 \hat{\boldsymbol{b}} \int \mathrm{d}B\, B^2 \mathcal{P}(t; B, \boldsymbol{k}, \hat{\boldsymbol{b}}), \tag{IX.6.9}$$

where $\mathrm{d}\mathit{\Omega}_{\boldsymbol{k}}$ is an element of solid angle in wavenumber space. Taking the time derivative of (IX.6.8) and using (IX.6.1), we get

$$
\begin{aligned}
\frac{\partial \mathcal{P}}{\partial t} = \overline{\frac{\partial \tilde{\mathcal{P}}}{\partial t}} &= \overline{\left[-\frac{\partial \tilde{B}(t)}{\partial t}\frac{\partial}{\partial B} - \frac{\partial \tilde{k}_m(t)}{\partial t}\frac{\partial}{\partial k_m} - \frac{\partial \tilde{b}^i(t)}{\partial t}\frac{\partial}{\partial b^i}\right]\tilde{\mathcal{P}}} \\
&= -\overline{\left[\tilde{b}^i(t)\tilde{b}^m(t)\tilde{\sigma}^i_m(t)\tilde{B}(t)\frac{\partial}{\partial B} - \eta\tilde{k}^2(t)\tilde{B}(t)\frac{\partial}{\partial B} - \tilde{\sigma}^i_m(t)\tilde{k}_i(t)\frac{\partial}{\partial k_m}\right.} \\
&\qquad \overline{\left. + \tilde{\sigma}^i_m(t)\tilde{b}^m(t)\frac{\partial}{\partial b^i} - \tilde{\sigma}^l_m(t)\tilde{b}^l(t)\tilde{b}^m(t)\tilde{b}^i(t)\frac{\partial}{\partial b^i}\right]\tilde{\mathcal{P}}} \\
&= -\hat{L}^m_i\overline{\tilde{\sigma}^i_m(t)\tilde{\mathcal{P}}} + \eta k^2\frac{\partial}{\partial B}B\mathcal{P}, \qquad \text{(IX.6.10)}
\end{aligned}
$$

where

$$\hat{L}^m_i \doteq \frac{\partial}{\partial B}Bb^ib^m - \frac{\partial}{\partial k_m}k_i + \frac{\partial}{\partial b^i}b^m - \frac{\partial}{\partial b^l}b^lb^ib^m. \qquad \text{(IX.6.11)}$$

To arrive at the final line of (IX.6.10), the identity $a\,\delta(a-b) = b\,\delta(a-b)$ was used. Note that everything in the square brackets in the final line is non-random. To perform the remaining ensemble average, we make use of the Furutsu–Novikov formula (Furutsu 1963; Novikov 1965), which generalizes Gaussian splitting to functions:

$$\overline{\tilde{\sigma}^i_m(t)\tilde{\mathcal{P}}(t)} = \int_0^t \mathrm{d}t'\,\overline{\tilde{\sigma}^i_m(t)\tilde{\sigma}^j_n(t')}\,\overline{\frac{\delta\tilde{\mathcal{P}}(t)}{\delta\tilde{\sigma}^j_n(t')}}. \qquad \text{(IX.6.12)}$$

The functional derivative with respect to $\tilde{\sigma}^j_n(t')$ can be calculated by formally integrating $\partial\tilde{\mathcal{P}}(t)/\partial t$ with respect to time:

$$
\begin{aligned}
\frac{\delta\tilde{\mathcal{P}}(t)}{\delta\tilde{\sigma}^j_n(t')} &= -\hat{L}^m_i\int_0^t \mathrm{d}t''\,\frac{\delta\tilde{\sigma}^i_m(t'')}{\delta\tilde{\sigma}^j_n(t')}\tilde{\mathcal{P}}(t'') - \int_0^t \mathrm{d}t''\,\left(\hat{L}^m_i\tilde{\sigma}^i_m(t'') - \eta k^2\frac{\partial}{\partial B}B\right)\cancel{\frac{\delta\tilde{\mathcal{P}}(t'')}{\delta\tilde{\sigma}^j_n(t')}} \\
&= -\hat{L}^n_j\int_0^t \mathrm{d}t''\,\delta(t'-t'')\tilde{\mathcal{P}}(t'') = -\hat{L}^n_j\tilde{\mathcal{P}}(t'). \qquad \text{(IX.6.13)}
\end{aligned}
$$

The last term in first line is dropped because it disappears when $t = t'$, owing to causality (i.e., $\tilde{\mathcal{P}}$ cannot depend on future values of $\tilde{\sigma}$). Using this result in (IX.6.12) alongside (IX.6.2), we find

$$\overline{\tilde{\sigma}^i_m(t)\tilde{\mathcal{P}}(t)} = -\frac{1}{2}\hat{L}^n_j\mathit{\Gamma}^{ij}_{mn}\overline{\tilde{\mathcal{P}}(t)} = -\frac{1}{2}\hat{L}^n_j\mathit{\Gamma}^{ij}_{mn}\mathcal{P}(t). \qquad \text{(IX.6.14)}$$

The result of these manipulations is a closed equation for the joint probability density function:

$$\frac{\partial\mathcal{P}}{\partial t} = \frac{1}{2}\hat{L}^m_i\hat{L}^n_j\mathit{\Gamma}^{ij}_{mn}\mathcal{P} + \eta k^2\frac{\partial}{\partial B}B\mathcal{P}. \qquad \text{(IX.6.15)}$$

Equation (IX.6.15) can be greatly simplified by noting that $\mathcal{P}(B,\boldsymbol{k},\hat{\boldsymbol{b}})$ must have the following factorization:

$$\mathcal{P}(B,\boldsymbol{k},\hat{\boldsymbol{b}}) = \delta(|\hat{\boldsymbol{b}}|^2 - 1)\delta(\hat{\boldsymbol{b}}\cdot\boldsymbol{k})\widehat{P}(B,k). \qquad \text{(IX.6.16)}$$

The two delta functions result, respectively, from $\hat{\boldsymbol{b}}$ being a unit vector and from the solenoidality constraint $\hat{\boldsymbol{b}}\cdot\boldsymbol{k} = 0$. The remaining factor in (IX.6.16), $\widehat{P}(B,k)$, is a result of the statistics being homogeneous and the relative alignment of $\hat{\boldsymbol{b}}$ and $\boldsymbol{k}$ being fixed.[20]

[20] $\widehat{P}(B,k)$ receives proper normalization below in (IX.6.24), after which its ornamental hat is dropped.

In order to express (IX.6.15) in terms of $\widehat{P}$, we use the chain rule to write

$$\hat{L}_j^n = -k_j\frac{\partial}{\partial k_n} + \left(b^n\frac{\partial}{\partial b^j} - b^j b^n b^q\frac{\partial}{\partial b^q}\right) + b^j b^n\left(\frac{\partial}{\partial B}B - d - 2\right), \tag{IX.6.17}$$

where d is the dimensionality of the system, and then calculate the combination $\hat{L}_j^n\Gamma^{ij}_{mn}\mathcal{P}(B,\boldsymbol{k},\hat{\boldsymbol{b}})$. For any function f,

$$\begin{aligned}\hat{L}_j^n\delta(\hat{\boldsymbol{b}}\cdot\boldsymbol{k})f &= \delta(\hat{\boldsymbol{b}}\cdot\boldsymbol{k})\hat{L}_j^n f - k_j b^n\delta'(\hat{\boldsymbol{b}}\cdot\boldsymbol{k})f + (b^n k_j - b^j b^n\hat{\boldsymbol{b}}\cdot\boldsymbol{k})\delta'(\hat{\boldsymbol{b}}\cdot\boldsymbol{k})f\\ &= \delta(\hat{\boldsymbol{b}}\cdot\boldsymbol{k})\hat{L}_j^n f - b^j b^n(\hat{\boldsymbol{b}}\cdot\boldsymbol{k})\delta'(\hat{\boldsymbol{b}}\cdot\boldsymbol{k})f\\ &= \delta(\hat{\boldsymbol{b}}\cdot\boldsymbol{k})(\hat{L}_j^n + b^n b^j)f,\end{aligned} \tag{IX.6.18}$$

where we have used $x\delta'(x) = -\delta(x)$ to obtain the final equality. Similarly,

$$\hat{L}_j^n\delta(|\hat{\boldsymbol{b}}|^2-1)f = \delta(|\hat{\boldsymbol{b}}|^2-1)(\hat{L}_j^n + 2b^n b^j)f. \tag{IX.6.19}$$

Combining (IX.6.18) and (IX.6.19) leads to

$$\begin{aligned}\hat{L}_j^n\Gamma^{ij}_{mn}\mathcal{P} &= \delta(\hat{\boldsymbol{b}}\cdot\boldsymbol{k})\delta(|\hat{\boldsymbol{b}}|^2-1)(\hat{L}_j^n + 3b^n b^j)\Gamma^{ij}_{mn}\widehat{P}(B,k)\\ &= \delta(\hat{\boldsymbol{b}}\cdot\boldsymbol{k})\delta(|\hat{\boldsymbol{b}}|^2-1)\left[-\frac{k_j k_n}{k^2}\Gamma^{ij}_{mn}k\frac{\partial}{\partial k} + b^j b^n\Gamma^{ij}_{mn}\left(\frac{\partial}{\partial B}B - d + 1\right)\right]\widehat{P}(B,k).\end{aligned} \tag{IX.6.20}$$

Taking into account the solenoidality constraint $\hat{\boldsymbol{b}}\cdot\boldsymbol{k} = 0$ imposed by the prefactor in (IX.6.20), the following combinations in (IX.6.20) may be calculated:

$$\frac{k_j k_n}{k^2}\Gamma^{ij}_{mn} = \kappa_2\left[a\delta^i_m + (a+1)\frac{k_i k_m}{k^2}\right], \tag{IX.6.21a}$$

$$b^j b^n\Gamma^{ij}_{mn} = \kappa_2\big[a\delta^i_m + (1+a)b^i b^m\big]. \tag{IX.6.21b}$$

Using these formulae in (IX.6.20) gives

$$\begin{aligned}\hat{L}_j^n\Gamma^{ij}_{mn}\mathcal{P} = \kappa_2\delta(\hat{\boldsymbol{b}}\cdot\boldsymbol{k})\delta(|\hat{\boldsymbol{b}}|^2-1)\bigg\{&-\left[a\delta^i_m + (a+1)\frac{k_i k_m}{k^2}\right]k\frac{\partial}{\partial k}\\ &+ \big[a\delta^i_m + (1+a)b^i b^m\big]\frac{\partial}{\partial B}B - a(d-1)\delta^i_m - (1+a)(d-1)b^i b^m\bigg\}\widehat{P}(B,k).\end{aligned} \tag{IX.6.22}$$

Further applying the operator $\hat{L}_i^m$ and expending much effort along the same lines gives us the expression for the first term in (IX.6.15):

$$\begin{aligned}\hat{L}_i^m\hat{L}_j^n\Gamma^{ij}_{mn}\mathcal{P} = \bigg\{&(2a+1)k^2\frac{\partial^2}{\partial k^2} + (1+2a)\frac{\partial}{\partial B}B\frac{\partial}{\partial B}B\\ &- 2a\frac{\partial}{\partial B}Bk\frac{\partial}{\partial k} + \big[d + (3d-1)a\big]k\frac{\partial}{\partial k}\\ &- (1+3a)(d-1)\frac{\partial}{\partial B}B + a(d-1)^2\bigg\}\widehat{P}(B,k).\end{aligned} \tag{IX.6.23}$$

Normalizability of the PDF requires that

$$\begin{aligned}1 &= \int \mathrm{d}^d\hat{\boldsymbol{b}}\,\delta(|\hat{\boldsymbol{b}}|^2-1)\int \mathrm{d}^d\boldsymbol{k}\,\delta(\hat{\boldsymbol{b}}\cdot\boldsymbol{k})\int \mathrm{d}B\,\widehat{P}(B,k)\\ &= \frac{S_{d-1}S_{d-2}}{2}\int_0^\infty \mathrm{d}k\,k^{d-2}\int \mathrm{d}B\,\widehat{P}(B,k),\end{aligned} \tag{IX.6.24}$$

where S_n is the surface area of unit n-sphere (e.g., $S_1 = 2\pi$, $S_2 = 4\pi$). Taking this normalization into consideration, we define $P(B,k) \doteq S_{d-1}S_{d-2}k^{d-2}\widehat{P}(B,k)/2$ and use

$$k^{d-2}k\frac{\partial}{\partial k}\frac{1}{k^{d-2}}P = \left[k\frac{\partial}{\partial k} - (d-2)\right]P, \tag{IX.6.25a}$$

$$k^{d-2}k^2\frac{\partial^2}{\partial k^2}\frac{1}{k^{d-2}}P = \left[k^2\frac{\partial^2}{\partial k^2} - 2(d-2)k\frac{\partial}{\partial k} + (d-2)(d-1)\right]P \tag{IX.6.25b}$$

to turn (IX.6.15) into

$$\begin{aligned}\frac{\partial P}{\partial t} = \frac{1}{2}\kappa_2\bigg\{&(1+2a)\frac{\partial}{\partial k}k^2\frac{\partial}{\partial k} + (1+2a)\frac{\partial}{\partial B}B\frac{\partial}{\partial B}B \\ &- 2a\frac{\partial}{\partial B}B\frac{\partial}{\partial k}k - \big[(d-2)+(d-3)a\big]\frac{\partial}{\partial k}k \\ &- (1+a)(d-1)\frac{\partial}{\partial B}B\bigg\}P + \eta k^2\frac{\partial}{\partial B}BP.\end{aligned} \tag{IX.6.26}$$

We now enforce incompressibility. Substituting (IX.6.6) into (IX.6.26) leads to the final form of the evolution equation of the joint PDF:

$$\begin{aligned}\frac{\partial P}{\partial t} = \frac{\kappa_2}{2(d+1)}\bigg[&(d-1)\frac{\partial}{\partial k}k^2\frac{\partial}{\partial k} + (d-1)\frac{\partial}{\partial B}B\frac{\partial}{\partial B}B + 2\frac{\partial}{\partial B}B\frac{\partial}{\partial k}k \\ &- (d-1)^2\frac{\partial}{\partial k}k - d(d-1)\frac{\partial}{\partial B}B\bigg]P + \eta k^2\frac{\partial}{\partial B}BP.\end{aligned} \tag{IX.6.27}$$

The magnetic-energy spectrum is $M(k) = (1/2)\int_0^\infty \mathrm{d}B\, B^2 P(B,k)$. Taking the B^2 moment of (IX.6.27) leads to

$$\frac{\partial M}{\partial t} = \frac{\overline{\gamma}}{d+2}\frac{\partial}{\partial k}\left[k^2\frac{\partial}{\partial k} - \left(\frac{4}{d-1} + d - 1\right)k\right]M + 2\overline{\gamma}M - 2\eta k^2 M, \tag{IX.6.28}$$

where

$$\overline{\gamma} \doteq \kappa_2\frac{(d-1)(d+2)}{2(d+1)}. \tag{IX.6.29}$$

It is straightforward to show by changing variables using $z = \ln k$ that equation (IX.6.28) is a diffusion equation with constant coefficients. In fact, it is in the form of a Fokker–Planck equation, with diffusion of the magnetic energy through k-space (the term in brackets), growth of the magnetic energy via stretching at a rate $2\overline{\gamma}$, and diffusion of the magnetic field via resistivity at a rate $2\eta k^2$.

In three dimensions ($d = 3$), equation (IX.6.28) becomes

$$\frac{\partial M}{\partial t} = \frac{\overline{\gamma}}{5}\frac{\partial}{\partial k}\left(k^2\frac{\partial}{\partial k} - 4k\right)M + 2\overline{\gamma}M - 2\eta k^2 M, \quad \text{with} \quad \overline{\gamma} = \kappa_2\frac{5}{4}. \tag{IX.6.30}$$

This equation has the following solution when $\eta = 0$:

$$M(t,k) = \mathrm{e}^{(3/4)\overline{\gamma}t}\int_0^\infty \frac{\mathrm{d}k'}{k'}\,M_0(k')\frac{1}{\sqrt{\pi\kappa_2 t}}\left(\frac{k}{k'}\right)^{3/2}\mathrm{e}^{-[\ln(k/k')]^2/\kappa_2 t}, \tag{IX.6.31}$$

which you can verify by substitution; here, $M_0(k)$ is the initial spectrum of the magnetic energy. Thus, the magnetic energy grows exponentially and exhibits a power spectrum $\propto k^{3/2}$ – the *Kazantsev spectrum*. The peak wavenumber moves exponentially fast towards smaller scales until resistivity becomes important, at which time the following approximate solution holds:

$$M(k) \approx k^{3/2} \mathrm{e}^{(3/4)\overline{\gamma}t} K_0(k/k_\eta), \tag{IX.6.32}$$

where K_0 is the zeroth-order modified Bessel function of the second kind ("MacDonald function") and $k_\eta = \sqrt{\overline{\gamma}/10\eta} \gg k_\nu$ is the resistive scale. Such a spectrum is shown in the figure below:

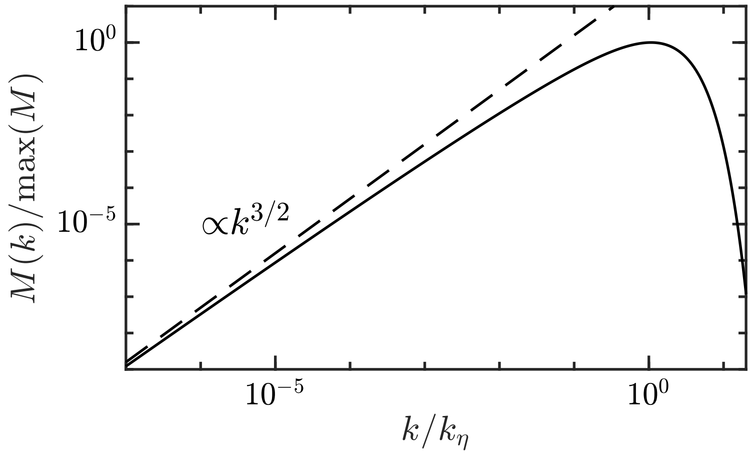

Read more in Kulsrud & Anderson (1992) and Schekochihin *et al.* (2002).

IX.7. Cowling's anti-dynamo theorem

Zel'dovich's anti-dynamo theorem is just one of many anti-dynamo theorems, all of which involve some constraints on the allowed symmetries of the velocity fields that can act as dynamos or of the magnetic fields that can be generated by dynamo action. Their essence can be summarized in three words: "symmetry is bad". (There is another type of constraint on dynamo action concerning the minimum Rm below which field amplification is hampered by resistivity, but I won't cover that here.) Perhaps the most well-known of these is the Cowling (1933) anti-dynamo theorem, which states that an axisymmetric magnetic field (that vanishes at infinity) cannot be maintained by dynamo action. (Wikipedia adds "by an axially symmetric current", but this qualifier is unnecessary. A non-axisymmetric flow always creates a non-axisymmetric field. The converse is not true, however: an axisymmetric flow can create a non-axisymmetric magnetic field, e.g., the Ponomarenko dynamo.) From Cowling's seminal paper on magnetic fields in sunspots:

> A similar argument shows that a field which resembles an axially symmetric field in certain respects cannot, in general, be maintained by the currents it itself sets up. For example, suppose that the lines of force are closed curves all threading a limiting closed curve, and threading it in the same direction. Then the currents required to maintain the field will, near the limit curve, have a component in the direction of the curve which is at all points directed in the same sense round the curve. This component is not due to electrostatic fields, which can only make currents flow from points of high potential to points of low potential, and cannot cause them to flow round a circuit: equally it cannot be due to electromagnetic induction, by an argument similar to the above. Hence such a field cannot be self-maintained...
>
> Since, then, fields possessing a general similarity to an axially symmetric field cannot be self-maintained, we are led to conclude that the magnetic field of a

sunspot is not self-maintained. For the same reason the general magnetic fields of the Sun and the Earth cannot be self-maintained, as was suggested by Larmor.[21]

The proof goes as follows. Consider an axisymmetric magnetic field in cylindrical coordinates (R, φ, z) of the form $\boldsymbol{B} = B_\varphi(R,z)\hat{\boldsymbol{\varphi}} + \boldsymbol{B}_\mathrm{p}(R,z)$, where B_φ is the toroidal (azimuthal) component and $\boldsymbol{B}_\mathrm{p} = \boldsymbol{\nabla}\times(A\hat{\boldsymbol{\varphi}})$ is the poloidal (radial and axial) component. The fluid flow is, by necessity, axisymmetric as well: $\boldsymbol{u} = u_\varphi(R,z)\hat{\boldsymbol{\varphi}} + \boldsymbol{u}_\mathrm{p}(R,z)$, with $\boldsymbol{\nabla}\cdot\boldsymbol{u}_\mathrm{p} = 0$ assumed. Substituting these fields into the resistive-MHD induction equation (IX.5.1) leads to

$$\frac{\partial B_\varphi}{\partial t} + R\boldsymbol{u}_\mathrm{p}\cdot\boldsymbol{\nabla}\frac{B_\varphi}{R} = \eta\left(\nabla^2 - \frac{1}{R^2}\right)B_\varphi + R\boldsymbol{B}_\mathrm{p}\cdot\boldsymbol{\nabla}\frac{u_\varphi}{R}, \tag{IX.7.1}$$

$$\frac{\partial A}{\partial t} + \frac{1}{R}\boldsymbol{u}_\mathrm{p}\cdot\boldsymbol{\nabla}(RA) = \eta\left(\nabla^2 - \frac{1}{R^2}\right)A. \tag{IX.7.2}$$

These are the cylindrical analogues of (IX.5.2) and (IX.5.4), respectively. The important term here is the final one in (IX.7.1); with $u_\varphi = R\Omega(R,z)$, it constitutes a source term that produces a toroidal magnetic field by the shearing of a poloidal one – the so-called "Ω effect". While this can transiently make a strong toroidal field, it does not constitute a dynamo. The reason why is that this term relies on the longevity of the poloidal field, whose evolution is governed through (IX.7.2). It is this equation that dooms the poloidal field to resistive decay. To see this, define the flux function $\psi \doteq RA$; then (IX.7.2) may be written as

$$\frac{\partial \psi}{\partial t} + \boldsymbol{u}_\mathrm{p}\cdot\boldsymbol{\nabla}\psi = \eta R\left(\nabla^2 - \frac{1}{R^2}\right)\frac{\psi}{R}.$$

Multiplying this equation through by 2ψ and re-arranging terms,

$$\frac{\partial \psi^2}{\partial t} + \boldsymbol{\nabla}\cdot(\boldsymbol{u}_\mathrm{p}\psi^2) = 2\eta\boldsymbol{\nabla}\cdot\left(\psi^2\,\boldsymbol{\nabla}\ln\frac{\psi}{R}\right) - 2\eta|\boldsymbol{\nabla}\psi|^2.$$

Integrating over space leaves

$$\frac{\mathrm{d}\langle\psi^2\rangle}{\mathrm{d}t} = -2\eta\langle|\boldsymbol{\nabla}\psi|^2\rangle,$$

and so the poloidal component of the magnetic field decays resistively. With no source term in (IX.7.1), the toroidal component shares the same fate.

IX.8. Mean-field dynamos

In the fluctuation dynamo, a zero-net-flux magnetic field is amplified by a chaotic flow. The resulting field generally has its power on the smallest available scales. There is another kind of dynamo in which both the magnetic and velocity fields have mean components – one which generically leads to the growth of large-scale magnetic fields. While

[21] Sir Joseph Larmor (1919) at a meeting of the British Association for the Advancement of Science asked "How could a rotating body such as the Sun become a magnet? . . . Such internal motion induces an electric field acting on the moving matter: and if any conducting path around the Solar axis happens to be open, an electric current will flow round it, which may in turn increase the inducing magnetic field. In this way it is possible for the internal cyclic motion to act after the manner of the cycle of a self-exciting dynamo, and maintain a permanent magnetic field from insignificant beginnings, at the expense of some of the energy of the internal circulation."

an active topic of research concerns the interplay between the small-scale fluctuation dynamo and this "mean-field dynamo", here I will focus exclusively on the latter.[22]

The basic idea is to split the magnetic and velocity fields into their mean and fluctuating parts:

$$\boldsymbol{B} = \langle \boldsymbol{B} \rangle + \delta \boldsymbol{B} \quad \text{and} \quad \boldsymbol{u} = \langle \boldsymbol{u} \rangle + \delta \boldsymbol{u}. \tag{IX.8.1}$$

Note that $\langle \delta \boldsymbol{B} \rangle = \langle \delta \boldsymbol{u} \rangle = 0$ by definition. The evolution of the volume-averaged quantities $\langle \boldsymbol{B} \rangle$ and $\langle \boldsymbol{u} \rangle$ will depend upon quantities quadratic in the fluctuations, *viz.* $\langle \delta \boldsymbol{B}\, \delta \boldsymbol{B} \rangle$, $\langle \delta \boldsymbol{B}\, \delta \boldsymbol{u} \rangle$, $\langle \delta \boldsymbol{u}\, \delta \boldsymbol{B} \rangle$, and $\langle \delta \boldsymbol{u}\, \delta \boldsymbol{u} \rangle$. These quadratic quantities will then depend on cubic terms, and the cubic terms on quartic terms, and on. It is the business of mean-field theory to close this hierarchy and thereby obtain a closed equation for the time evolution of $\langle \boldsymbol{B} \rangle$ and $\langle \boldsymbol{u} \rangle$. This proceeds as follows.

Assuming that our averaging procedure commutes with differentiation, the averaged resistive-MHD induction equation (see (IX.5.1)) is

$$\frac{\partial \langle \boldsymbol{B} \rangle}{\partial t} = \boldsymbol{\nabla} \times \langle \boldsymbol{u} \times \boldsymbol{B} \rangle + \eta \nabla^2 \langle \boldsymbol{B} \rangle. \tag{IX.8.2}$$

The term of interest is, of course, the inductive term, which may be expanded using (IX.8.1):

$$\langle \boldsymbol{u} \times \boldsymbol{B} \rangle = \langle \boldsymbol{u} \rangle \times \langle \boldsymbol{B} \rangle + \langle \delta \boldsymbol{u} \times \delta \boldsymbol{B} \rangle \doteq \langle \boldsymbol{u} \rangle \times \langle \boldsymbol{B} \rangle + \boldsymbol{\mathcal{E}}, \tag{IX.8.3}$$

where we have defined the *mean electro-motive force* (emf) $\boldsymbol{\mathcal{E}}$. Equation (IX.8.2) then becomes

$$\boxed{\frac{\partial \langle \boldsymbol{B} \rangle}{\partial t} = \boldsymbol{\nabla} \times \big(\langle \boldsymbol{u} \rangle \times \langle \boldsymbol{B} \rangle \big) + \boldsymbol{\nabla} \times \boldsymbol{\mathcal{E}} + \eta \nabla^2 \langle \boldsymbol{B} \rangle} \tag{IX.8.4}$$

It is this mean emf that spoils Cowling's theorem. As I foreshadowed, one cannot write down a closed-form expression for $\boldsymbol{\mathcal{E}}$ without approximation, but let us feign ignorance and carry on regardless.

The equation governing the magnetic-field fluctuations may be obtained by further subtracting (IX.8.4) from (IX.5.1). Introducing the vector $\boldsymbol{\mathcal{G}} \doteq \delta \boldsymbol{u} \times \delta \boldsymbol{B} - \langle \delta \boldsymbol{u} \times \delta \boldsymbol{B} \rangle$ and re-arranging terms, the result is

$$\frac{\partial \delta \boldsymbol{B}}{\partial t} - \boldsymbol{\nabla} \times \big(\langle \boldsymbol{u} \rangle \times \delta \boldsymbol{B} \big) - \boldsymbol{\nabla} \times \boldsymbol{\mathcal{G}} - \eta \nabla^2 \delta \boldsymbol{B} = \boldsymbol{\nabla} \times \big(\delta \boldsymbol{u} \times \langle \boldsymbol{B} \rangle \big). \tag{IX.8.5}$$

Note that all terms on the left-hand side of this equation are linear in $\delta \boldsymbol{B}$, at least to the extent that $\boldsymbol{u}$ is independently prescribed. The right-hand side, however, is a source term; physically, it represents the creation of a fluctuating magnetic field by the fluctuating velocity shearing and tangling the mean magnetic field. It is at this point that most discussions state that the resulting linear relation between $\delta \boldsymbol{B}$ and $\langle \boldsymbol{B} \rangle$ implies a linear relation between $\boldsymbol{\mathcal{E}}$ and $\langle \boldsymbol{B} \rangle$, and that relation is simply written down as if it fell from heaven above. I don't buy it, so perhaps it is worthwhile to actually calculate the

[22]You can find a nice review article on mean-field dynamos and their history here: http://www.aip.de/People/khraedler/HIST_MHD_06_Rae.pdf

contribution to $\boldsymbol{\mathcal{E}}$ from that source term:

$$\begin{aligned}
\boldsymbol{\mathcal{E}}_{\text{source}}(t) &= \left\langle \delta\boldsymbol{u}(t) \times \int^t \mathrm{d}t' \left. \frac{\partial \delta\boldsymbol{B}(t')}{\partial t'} \right|_{\text{source}} \right\rangle \\
&= \left\langle \delta\boldsymbol{u}(t) \times \int^t \mathrm{d}t'\, \boldsymbol{\nabla} \times \bigl[\delta\boldsymbol{u}(t') \times \langle \boldsymbol{B}(t')\rangle\bigr] \right\rangle \\
&= \int^t \mathrm{d}t' \left\langle \bigl[\boldsymbol{\nabla}(\delta\boldsymbol{u}(t') \times \langle\boldsymbol{B}(t')\rangle)\bigr] \boldsymbol{\cdot} \delta\boldsymbol{u}(t) - \delta\boldsymbol{u}(t) \boldsymbol{\cdot} \boldsymbol{\nabla}\bigl[\delta\boldsymbol{u}(t') \times \langle\boldsymbol{B}(t')\rangle\bigr] \right\rangle \\
\implies \quad \mathcal{E}^i_{\text{source}}(t) &= \int^t \mathrm{d}t' \, (\epsilon_{j\ell m}\delta_{ik} - \epsilon_{jim}\delta_{\ell k}) \\
&\quad \times \left[\left\langle \delta u^\ell(t) \frac{\partial \delta u^m(t')}{\partial r^k} \right\rangle \langle B^j(t')\rangle + \langle \delta u^\ell(t) \delta u^m(t')\rangle \frac{\partial \langle B^j(t')\rangle}{\partial r^k} \right] \\
&\doteq \int^t \mathrm{d}t' \left[\alpha_{ij}(t-t')\langle B^j(t')\rangle + \beta_{ijk}(t-t') \frac{\partial\langle B^j(t')\rangle}{\partial r^k} \right]. \qquad \text{(IX.8.6)}
\end{aligned}$$

In the final step, we have introduced the $\boldsymbol{\alpha}(\tau)$ and $\boldsymbol{\beta}(\tau)$ tensors, which are related to correlations between the velocity fluctuations separated in time by an interval τ. Notably, $\boldsymbol{\alpha}$ says something about the correlation between the velocity fluctuations and their vorticity, $\delta\boldsymbol{\omega} \doteq \boldsymbol{\nabla} \times \delta\boldsymbol{u}$. If the turbulence is homogeneous and isotropic, then $\alpha_{ij}(\tau) = \alpha(\tau)\delta_{ij}$ and $\beta_{ijk}(\tau) = \beta(\tau)\epsilon_{ijk}$, and (IX.8.6) becomes

$$\boldsymbol{\mathcal{E}}_{\text{source}} = \int^t \mathrm{d}t' \, \bigl[\alpha(t-t')\langle\boldsymbol{B}(t')\rangle - \beta(t-t')\boldsymbol{\nabla} \times \langle\boldsymbol{B}(t')\rangle\bigr], \qquad \text{(IX.8.7)}$$

where

$$\alpha(t-t') = -\frac{1}{3}\langle \delta\boldsymbol{u}(t) \boldsymbol{\cdot} \delta\boldsymbol{\omega}(t')\rangle \quad \text{and} \quad \beta(t-t') = \frac{1}{3}\langle\delta\boldsymbol{u}(t) \boldsymbol{\cdot} \delta\boldsymbol{u}(t')\rangle. \qquad \text{(IX.8.8)}$$

The combination $\boldsymbol{u} \boldsymbol{\cdot} \boldsymbol{\omega}$ is known as the *kinetic helicity*; it is zero if the velocity field is on the average mirror symmetric. If the flow has a vanishing correlation time relative to the growth/decay time of the magnetic field, then it is said to be "delta-correlated" and (IX.8.7) becomes

$$\boldsymbol{\mathcal{E}}_{\text{source}} \simeq \alpha\langle\boldsymbol{B}\rangle - \beta\boldsymbol{\nabla} \times \boldsymbol{B}. \qquad \text{(IX.8.9)}$$

In this case, the final (β) term acts as a turbulent diffusivity, supplementing the resistive diffusivity: $\eta\nabla^2\langle\boldsymbol{B}\rangle$ in (IX.8.4) becomes $(\eta+\beta)\nabla^2\langle\boldsymbol{B}\rangle$.

The α and β terms are usually argued to represent not only the source term on the right-hand side of (IX.8.5) but also all the other emf-like terms on its left-hand side. Let us follow this assumption and adopt (IX.8.9) as an approximation for the total mean emf and see what it implies for dynamo action. Equation (IX.8.4) then reads

$$\frac{\partial\langle\boldsymbol{B}\rangle}{\partial t} = \boldsymbol{\nabla} \times \bigl(\langle\boldsymbol{u}\rangle \times \langle\boldsymbol{B}\rangle\bigr) + \alpha\boldsymbol{\nabla} \times \langle\boldsymbol{B}\rangle + (\eta+\beta)\nabla^2\langle\boldsymbol{B}\rangle. \qquad \text{(IX.8.10)}$$

We consider two limits of this equation. First, assume $\langle\boldsymbol{u}\rangle = 0$, so that the mean-field inductive term vanishes and we have

$$\frac{\partial\langle\boldsymbol{B}\rangle}{\partial t} = \alpha\boldsymbol{\nabla} \times \langle\boldsymbol{B}\rangle + (\eta+\beta)\nabla^2\langle\boldsymbol{B}\rangle.$$

Adopting plane-wave solutions $\sim\exp(\gamma t + \mathrm{i}\boldsymbol{k} \boldsymbol{\cdot} \boldsymbol{r})$, it is straightforward to show that the growth/decay rate γ satisfies

$$\gamma = \pm k\alpha - k^2(\eta+\beta), \qquad \text{(IX.8.11)}$$

where the upper (lower) sign corresponds to negative (positive) magnetic helicity. The growing solution is called an "α^2 dynamo". For $k > 0$, the α term generates $\langle B_y \rangle$ from $\langle B_x \rangle$, and then further uses that $\langle B_y \rangle$ to amplify the original $\langle B_x \rangle$. Note that the signs of the kinetic and magnetic helicities must be alike. If, for some reason α were to depend on $\langle \boldsymbol{B} \rangle$ in such a way that it decreases as the mean magnetic-field strength increases (e.g., via back-reaction from the Lorentz force), then this dynamo will eventually shut off – an effect referred to as "α quenching".

Now restore the $\langle \boldsymbol{u} \rangle \times \langle \boldsymbol{B} \rangle$ term and suppose $\langle \boldsymbol{u} \rangle = -\omega x \hat{\boldsymbol{y}}$, where $\omega > 0$ is the characteristic frequency of the flow shear. Then (IX.8.10) becomes

$$\left(\frac{\partial}{\partial t} - \omega x \frac{\partial}{\partial y} \right) \langle \boldsymbol{B} \rangle = -\omega \langle B_x \rangle \hat{\boldsymbol{y}} + \alpha \boldsymbol{\nabla} \times \langle \boldsymbol{B} \rangle + (\eta + \beta) \nabla^2 \langle \boldsymbol{B} \rangle.$$

Note that the gradient in the fluid flow generates $\langle B_y \rangle$ by shearing $\langle B_x \rangle$ into the stream-wise direction. If the α term is such that this generated field is re-oriented into the x direction, then the mean field will grow – a process known as the "α-ω dynamo". So long as $\boldsymbol{k} \cdot \hat{\boldsymbol{y}} = 0$, plane-wave solutions satisfy

$$\gamma = \pm \sqrt{k_z \alpha (\mathrm{i}\omega + k_z \alpha)} - k^2 (\eta + \beta). \tag{IX.8.12}$$

Clearly, there must be a component of $\boldsymbol{k}$ in the $\hat{\boldsymbol{y}} \times \boldsymbol{\nabla} |\langle \boldsymbol{u} \rangle|$ direction. But it also must have the correct sign for growth. This is complicated by the i that accompanies ω: the growth rate is complex, and so these *dynamo waves* propagate. To figure this out, let us assume $|k_z \alpha| \ll \omega$, so that the α^2 component of the dynamo expressed in (IX.8.12) is sub-dominant to the α-ω component. Then

$$\gamma \approx \pm \sqrt{\mathrm{i} k_z \alpha \omega} - k^2 (\eta + \beta).$$

Suppose that $\mathrm{Re}(\gamma) > 0$, so that we have growth. Recalling $\sqrt{\mathrm{i}} = \pm(1+\mathrm{i})/\sqrt{2}$, we require $k_z \alpha \omega = \boldsymbol{k} \cdot (\hat{\boldsymbol{y}} \times \boldsymbol{\nabla} |\langle \boldsymbol{u} \rangle|) > 0$. In this case, $\gamma \approx k_z \alpha \omega (1 + \mathrm{i})/\sqrt{2}$ and so the mode grows and propagates along the trajectory $\dot{z} = -\alpha\omega/\sqrt{2}$, i.e., in the $-\alpha \hat{\boldsymbol{y}} \times \boldsymbol{\nabla} |\langle \boldsymbol{u} \rangle|$ direction. Note further that the fastest-growing mode has $\boldsymbol{k}$ exactly parallel to $\hat{\boldsymbol{y}} \times \boldsymbol{\nabla} |\langle \boldsymbol{u} \rangle|$.

This kind of mean-field dynamo is important in the differentially rotating solar convective zone, in which the resulting dynamo waves have been conjectured to cause the observed 22-year period of sunspot activity (Parker 1955). (In spherical geometry with φ replacing y and (r, θ) replacing (x, z), the growing dynamo mode propagates in the $-\alpha \hat{\boldsymbol{\varphi}} \times \boldsymbol{\nabla} \mathit{\Omega}$ direction, where $\mathit{\Omega}(r, \theta)$ is the angular velocity.) The idea is that the Solar dynamo is of the α-ω type, with $\alpha > 0$ (< 0) in the northern (southern) hemisphere and $\partial \mathit{\Omega} / \partial r < 0$ throughout the convection zone. This combination gives the correct equator-ward migration of sunspots (e.g. Moffatt 1978; Parker 1979; Krause & Raedler 1980).

One could write a lot more about dynamo theory, experiment, and observation, but these course notes are not really the place for that. If you'd like to learn more, you can start with the excellent reviews by Childress & Gilbert (1995), Gilbert (2003), and Rincon (2019).

PART X
Beyond MHD

[in progress]

PART XI

Problem sets

REFERENCES

Alt, A. & Kunz, M. W. 2019 Onset of magnetic reconnection in a collisionless, high-β plasma. *J. Plasma Phys.* **85** (1), 764850101.

Ara, G., Basu, B., Coppi, B., Laval, G., Rosenbluth, M. N. & Waddell, B. V. 1978 Magnetic reconnection and m = 1 oscillations in current carrying plasmas. *Annals of Physics* **112**, 443–476.

Balbus, Steven A. 1988 On Thermal Instability and Hydrostatic Equilibrium in Cooling Flows. *Astrophys. J.* **328**, 395.

Balbus, S. A. 2003 Enhanced Angular Momentum Transport in Accretion Disks. *Ann. Rev. Astron. Astrophys.* **41**, 555–597.

Balbus, Steven A. & Soker, Noam 1989 Theory of Local Thermal Instability in Spherical Systems. *Astrophys. J.* **341**, 611.

Beresnyak, A. 2011 Spectral Slope and Kolmogorov Constant of MHD Turbulence. *Physical Review Letters* **106** (7), 075001.

Bernstein, I. B. 1983 The variational principle for problems of ideal magnetohydrodynamic stability. In *Basic Plasma Physics: Selected Chapters, Handbook of Plasma Physics, Volume 1* (ed. A. A. Galeev & R. N. Sudan), p. 199.

Bernstein, I. B., Frieman, E. A., Kruskal, M. D. & Kulsrud, R. M. 1958 An Energy Principle for Hydromagnetic Stability Problems. *Proc. Roy. Soc. London Ser. A* **244** (1236), 17–40.

Bhattacharjee, A., Huang, Y.-M., Yang, H. & Rogers, B. 2009 Fast reconnection in high-Lundquist-number plasmas due to the plasmoid Instability. *Phys. Plasmas* **16** (11), 112102.

Bhattacharjee, A., Ng, C. S. & Spangler, S. R. 1998 Weakly Compressible Magnetohydrodynamic Turbulence in the Solar Wind and the Interstellar Medium. *Astrophys. J.* **494**, 409–418.

Biskamp, D. 1986 Magnetic reconnection via current sheets. *Physics of Fluids* **29**, 1520–1531.

Biskamp, D. & Schwarz, E. 2001 Localization, the clue to fast magnetic reconnection. *Physics of Plasmas* **8**, 4729–4731.

Blackman, Eric G. 2004 How spectral shapes of magnetic energy and magnetic helicity influence their respective decay timescales. *Plasma Phys. Controlled Fusion* **46** (2), 423–430.

Boldyrev, S. 2005 On the spectrum of magnetohydrodynamic turbulence. *Astrophys. J.* **626**, L37.

Boldyrev, Stanislav 2006 Spectrum of magnetohydrodynamic turbulence. *Phys. Rev. Lett.* **96**, 115002.

Bondi, H. 1952 On spherically symmetrical accretion. *Mon. Not. R. Astron. Soc.* **112**, 195.

Braginskii, S. I. 1965 Transport Processes in a Plasma. *Reviews of Plasma Physics* **1**, 205.

Chandran, B. D. G., Schekochihin, A. A. & Mallet, A. 2015 Intermittency and Alignment in Strong RMHD Turbulence. *Astrophys. J.* **807**, 39.

Chandrasekhar, S. & Kendall, P. C. 1957 On Force-Free Magnetic Fields. *Astrophys. J.* **126**, 457.

Childress, S. & Gilbert, A. D. 1995 *Stretch, Twist, Fold: The Fast Dynamo*. Springer-Verlag.

Cho, J. & Vishniac, E. T. 2000 The Anisotropy of Magnetohydrodynamic Alfvénic Turbulence. *Astrophys. J.* **539**, 273–282.

Cowling, T. G. 1933 The magnetic field of sunspots. *Mon. Not. R. Astron. Soc.* **94**, 39–48.

Daughton, W., Roytershteyn, V., Albright, B. J., Karimabadi, H., Yin, L. & Bowers, K. J. 2009 Transition from collisional to kinetic regimes in large-scale reconnection layers. *Physical Review Letters* **103** (6), 065004.

De Hoffmann, F. & Teller, E. 1950 Magneto-hydrodynamic shocks. *Phys. Rev.* **80**, 692–703.

Draine, B. T. 1980 Interstellar shock waves with magnetic precursors. *Astrophys. J.* **241**, 1021–1038.

Elsasser, W. M. 1950 The hydromagnetic equations. *Phys. Rev.* **79**, 183.

Erkaev, N. V., Semenov, V. S., Alexeev, I. V. & Biernat, H. K. 2001 Rate of steady-state reconnection in an incompressible plasma. *Physics of Plasmas* **8**, 4800–4809.

Erkaev, N. V., Semenov, V. S. & Jamitzky, F. 2000 Reconnection Rate for the Inhomogeneous Resistivity Petschek Model. *Physical Review Letters* **84**, 1455–1458.

Ertel, H. 1942 Ein neuer hydrodynamischer Wirbelsatz. *Meteorol. Z.* **59** (9), 277–281.

Escande, D. F. & Ottaviani, M. 2004 Simple and rigorous solution for the nonlinear tearing mode. *Physics Letters A* **323**, 278–284.

Freidberg, Jeffrey P. 2014 *Ideal MHD*.

Frieman, E. & Rotenberg, M. 1960 On Hydromagnetic Stability of Stationary Equilibria. *Rev. Mod. Phys.* **32** (4), 898–902.

Furth, H. P. 1965 Toroidal magnetic field configurations and finite resistivity. In *Lectures presented at the Trieste Seminar on Plasma Physics*, p. 391.

Furth, H. P., Killeen, J. & Rosenbluth, M. N. 1963 Finite-Resistivity Instabilities of a Sheet Pinch. *Physics of Fluids* **6**, 459–484.

Furutsu, K. 1963 On the statistical theory of electromagnetic waves in a fluctuating medium (I). *J. Res. NBS* **67D**, 303.

Gilbert, A. D. 2003 Dynamo theory. In *Handbook of mathematical fluid dynamics, Volume 2* (ed. S. Friedlander & D. Serre), pp. 355–441. Elsevier Science BV.

Goldreich, P. & Sridhar, S. 1995 Toward a theory of interstellar turbulence. 2: Strong alfvenic turbulence. *Astrophys. J.* **438**, 763–775.

Goldreich, P. & Tremaine, S. 1979 The excitation of density waves at the Lindblad and corotation resonances by an external potential. *Astrophys. J.* **233**, 857–871.

Goldreich, P. & Tremaine, S. 1980 Disk-satellite interactions. *Astrophys. J.* **241**, 425–441.

Greene, J. M. & Johnson, J. L. 1968 Interchange instabilities in ideal hydromagnetic theory. *Plasma Phys.* **10** (8), 729–745.

Hain, K. & Lüst, R. 1958 Zur Stabilität zylindersymmetrischer Plasmakonfigurationen mit Volumenströmen. *Zeitschrift Naturforschung Teil A* **13** (11), 936–940.

Harris, E. G. 1962 On a plasma sheath separating regions of oppositely directed magnetic field. *Il Nuovo Cimento* **23**, 115–121.

Helander, P. 2014 Theory of plasma confinement in non-axisymmetric magnetic fields. *Rep. Prog. Phys.* **77** (8), 087001.

Horbury, T. S., Forman, M. & Oughton, S. 2008 Anisotropic Scaling of Magnetohydrodynamic Turbulence. *Physical Review Letters* **101** (17), 175005.

Huang, Y.-M. & Bhattacharjee, A. 2010 Scaling laws of resistive magnetohydrodynamic reconnection in the high-Lundquist-number, plasmoid-unstable regime. *Physics of Plasmas* **17** (6), 062104–062104.

Iroshnikov, P. S. 1963 Turbulence of a Conducting Fluid in a Strong Magnetic Field. *Astronomicheskii Zhurnal* **40**, 742.

Ji, H., Yamada, M., Hsu, S. & Kulsrud, R. 1998 Experimental Test of the Sweet-Parker Model of Magnetic Reconnection. *Physical Review Letters* **80**, 3256–3259.

Kadomtsev, B. B. & Pogutse, O. P. 1974 Nonlinear helical perturbations of a plasma in the tokamak. *Soviet Journal of Experimental and Theoretical Physics* **38**, 283–290.

Kolmogorov, A. 1941 The Local Structure of Turbulence in Incompressible Viscous Fluid for Very Large Reynolds' Numbers. *Akademiia Nauk SSSR Doklady* **30**, 301–305.

Kraichnan, R. H. 1965 Inertial-Range Spectrum of Hydromagnetic Turbulence. *Physics of Fluids* **8**, 1385–1387.

Krause, F. & Raedler, K.-H. 1980 *Mean-field magnetohydrodynamics and dynamo theory*. Pergamon.

Kulsrud, R. & Pearce, W. P. 1969 The Effect of Wave-Particle Interactions on the Propagation of Cosmic Rays. *Astrophys. J.* **156**, 445.

Kulsrud, R. M. 2001 Magnetic reconnection: Sweet-Parker versus Petschek. *Earth, Planets, and Space* **53**, 417–422.

Kulsrud, Russell M. & Anderson, Stephen W. 1992 The Spectrum of Random Magnetic Fields in the Mean Field Dynamo Theory of the Galactic Magnetic Field. *Astrophys. J.* **396**, 606.

Loureiro, N. F., Cowley, S. C., Dorland, W. D., Haines, M. G. & Schekochihin, A. A. 2005 X-Point Collapse and Saturation in the Nonlinear Tearing Mode Reconnection. *Phys. Rev. Lett.* **95** (23), 235003.

Loureiro, N. F., Samtaney, R., Schekochihin, A. A. & Uzdensky, D. A. 2012 Magnetic reconnection and stochastic plasmoid chains in high-Lundquist-number plasmas. *Physics of Plasmas* **19** (4), 042303–042303.

Loureiro, N. F., Schekochihin, A. A. & Cowley, S. C. 2007 Instability of current sheets and formation of plasmoid chains. *Phys. Plasmas* **14** (10), 100703–100703.

Loureiro, N. F., Schekochihin, A. A. & Uzdensky, D. A. 2013 Plasmoid and Kelvin-Helmholtz instabilities in Sweet-Parker current sheets. *Phys. Rev. E* **87** (1), 013102.

Loureiro, N. F. & Uzdensky, D. A. 2016 Magnetic reconnection: from the Sweet-Parker model to stochastic plasmoid chains. *Plasma Phys. Controlled Fusion* **58** (1), 014021.

Lundquist, S. 1951 On the stability of magneto-hydrostatic fields. *Phys. Rev.* **83**, 307.

Mallet, A. & Schekochihin, A. A. 2017 A statistical model of three-dimensional anisotropy and intermittency in strong Alfvénic turbulence. *Mon. Not. R. Astron. Soc.* **466**, 3918–3927.

Mallet, A., Schekochihin, A. A. & Chandran, B. D. G. 2015 Refined critical balance in strong Alfvénic turbulence. *Mon. Not. R. Astron. Soc.* **449**, L77.

Malyshkin, L. M., Linde, T. & Kulsrud, R. M. 2005 Magnetic reconnection with anomalous resistivity in two-and-a-half dimensions. I. Quasistationary case. *Physics of Plasmas* **12** (10), 102902–102902.

Manheimer, W. M. & Lashmore-Davies, C. 1984 MHD instabilities in simple plasma configuration.

Maron, J. & Goldreich, P. 2001 Simulations of Incompressible Magnetohydrodynamic Turbulence. *Astrophys. J.* **554**, 1175–1196.

Marsh, G. E. 1996 *Force-Free Magnetic Fields: Solutions, Topology and Applications*. Singapore: World Scientific.

Mason, J., Cattaneo, F. & Boldyrev, S. 2006 Dynamic Alignment in Driven Magnetohydrodynamic Turbulence. *Physical Review Letters* **97** (25), 255002.

Mason, J., Cattaneo, F. & Boldyrev, S. 2008 Numerical measurements of the spectrum in magnetohydrodynamic turbulence. *Phys. Rev. E* **77** (3), 036403.

Mason, J., Perez, J. C., Boldyrev, S. & Cattaneo, F. 2012 Numerical simulations of strong incompressible magnetohydrodynamic turbulence. *Physics of Plasmas* **19** (5), 055902–055902.

Mason, J., Perez, J. C., Cattaneo, F. & Boldyrev, S. 2011 Extended Scaling Laws in Numerical Simulations of Magnetohydrodynamic Turbulence. *Astrophys. J. Lett.* **735**, L26.

Matthaeus, W. H., Pouquet, A., Mininni, P. D., Dmitruk, P. & Breech, B. 2008 Rapid Alignment of Velocity and Magnetic Field in Magnetohydrodynamic Turbulence. *Physical Review Letters* **100** (8), 085003.

Mikhailovskii, A. B. & Tsypin, V. S. 1971 Transport equations and gradient instabilities in a high pressure collisional plasma. *Plasma Phys.* **13** (9), 785–798.

Mikhailovskii, A. B. & Tsypin, V. S. 1984 Transport equations of plasma in a curvilinear magnetic field. *Beiträge aus der Plasmaphysik* **24** (4), 335–354.

Militello, F. & Porcelli, F. 2004 Simple analysis of the nonlinear saturation of the tearing mode. *Physics of Plasmas* **11**, L13–L16.

Moffatt, H. K. 1978 *Magnetic field generation in electrically conducting fluids*. Cambridge University Press.

Montgomery, D. & Turner, L. 1981 Anisotropic magnetohydrodynamic turbulence in a strong external magnetic field. *Phys. Fluids* **24**, 825.

Mouschovias, T. C. 1991 Magnetic braking, ambipolar diffusion, cloud cores, and star formation - Natural length scales and protostellar masses. *Astrophys. J.* **373**, 169–186.

Nazarenko, S. V. & Schekochihin, A. A. 2011 Critical balance in magnetohydrodynamic, rotating and stratified turbulence: towards a universal scaling conjecture. *J. Fluid Mech.* **677**, 134.

Newcomb, W. A. 1962 Lagrangian and Hamiltonian methods in magnetohydrodynamics. *Nucl. Fusion Suppl.* **2**, 451–463.

Ni, L., Germaschewski, K., Huang, Y.-M., Sullivan, B. P., Yang, H. & Bhattacharjee, A. 2010 Linear plasmoid instability of thin current sheets with shear flow. *Physics of Plasmas* **17** (5), 052109.

Novikov, E. A. 1965 Functionals and the random-force method in turbulence theory. *J. Exp. Theor. Phys.* **20**, 1290.

Obukhov, A. M. 1941 On the distribution of energy in the spectrum of turbulent flow. *Akademiia Nauk SSSR Doklady* **32**, 19.

Oughton, S., Dmitruk, P. & Matthaeus, W. H. 2003 Coronal Heating and Reduced MHD. In *Turbulence and Magnetic Fields in Astrophysics* (ed. E. Falgarone & T. Passot), *Lecture Notes in Physics, Berlin Springer Verlag*, vol. 614, pp. 28–55.

Park, W., Monticello, D. A. & White, R. B. 1984 Reconnection rates of magnetic fields including the effects of viscosity. *Physics of Fluids* **27**, 137–149.

Parker, E. N. 1955 Hydromagnetic Dynamo Models. *Astrophys. J.* **122**, 293.

Parker, E. N. 1957 Sweet's Mechanism for Merging Magnetic Fields in Conducting Fluids. *J. Geophys. Res.* **62**, 509–520.

Parker, E. N. 1979 *Cosmical magnetic fields: Their origin and their activity*. Oxford University Press.

Perez, J. C. & Chandran, B. D. G. 2013 Direct Numerical Simulations of Reflection-driven, Reduced Magnetohydrodynamic Turbulence from the Sun to the Alfvén Critical Point. *Astrophys. J.* **776**, 124.

Perez, J. C., Mason, J., Boldyrev, S. & Cattaneo, F. 2012 On the Energy Spectrum of Strong Magnetohydrodynamic Turbulence. *Physical Review X* **2** (4), 041005.

Perez, J. C., Mason, J., Boldyrev, S. & Cattaneo, F. 2014 Scaling Properties of Small-scale Fluctuations in Magnetohydrodynamic Turbulence. *Astrophys. J. Lett.* **793**, L13.

Petschek, H. E. 1964 Magnetic Field Annihilation. *NASA Special Publication* **50**, 425.

Pucci, F. & Velli, M. 2014 Reconnection of Quasi-singular Current Sheets: The "Ideal" Tearing Mode. *Astrophys. J. Lett.* **780**, L19.

Rayleigh, J. W. S. 1880 On the stability, or instability, of certain fluid motions. *Proc. London Math. Soc.* **11**, 57.

Rincon, François 2019 Dynamo theories. *Journal of Plasma Physics* **85** (4), 205850401.

Rutherford, P. H. 1973 Nonlinear growth of the tearing mode. *Phys. Fluids* **16**, 1903–1908.

Samtaney, R., Loureiro, N. F., Uzdensky, D. A., Schekochihin, A. A. & Cowley, S. C. 2009 Formation of Plasmoid Chains in Magnetic Reconnection. *Physical Review Letters* **103** (10), 105004.

Sato, T. & Hayashi, T. 1979 Externally driven magnetic reconnection and a powerful magnetic energy converter. *Physics of Fluids* **22**, 1189–1202.

Schekochihin, Alexander A. 2022 MHD turbulence: a biased review. *J. Plasma Phys.* **88** (5), 155880501.

Schekochihin, Alexander A., Boldyrev, Stanislav A. & Kulsrud, Russell M. 2002 Spectra and Growth Rates of Fluctuating Magnetic Fields in the Kinematic Dynamo Theory with Large Magnetic Prandtl Numbers. *Astrophys. J.* **567** (2), 828–852.

Schekochihin, A. A. & Cowley, S. C. 2007 Turbulence and Magnetic Fields in Astrophysical Plasmas. In *Magnetohydrodynamics: Historical Evolution and Trends* (ed. S. Molokov, R. Moreau & H. K. Moffatt), p. 85. Springer.

Scholer, M. 1989 Undriven magnetic reconnection in an isolated current sheet. *J. Geophys. Res.* **94**, 8805–8812.

Shebalin, J. V., Matthaeus, W. H. & Montgomery, D. 1983 Anisotropy in MHD turbulence due to a mean magnetic field. *J. Plasma Phys.* **29**, 525–547.

Solov'ev, L. S. 1968 The Theory of Hydromagnetic Stability of Toroidal Plasma Configurations. *J. Exp. Theor. Phys.* **26**, 400.

Strauss, H. R. 1976 Nonlinear, three-dimensional magnetohydrodynamics of noncircular tokamaks. *Phys. Fluids* **19**, 134–140.

Strauss, H. R. 1977 Dynamics of high beta Tokamaks. *Phys. Fluids* **20**, 1354–1360.

Sturrock, P. A. 1994 *Plasma Physics: An Introduction to the Theory of Astrophysical, Geophysical and Laboratory Plasmas*, 1st edn. New York: Cambridge University Press.

Sweet, P. A. 1958 The Neutral Point Theory of Solar Flares. In *Electromagnetic Phenomena in Cosmical Physics* (ed. B. Lehnert), *IAU Symposium*, vol. 6, p. 123.

Tajima, T. & Shibata, K., ed. 1997 *Plasma astrophysics*.

Taylor, J. B. 1986 Relaxation and magnetic reconnection in plasmas. *Rev. Mod. Phys.* **58**, 741–763.

Ugai, M. 1995 Computer studies on powerful magnetic energy conversion by the spontaneous fast reconnection mechanism. *Physics of Plasmas* **2**, 388–397.

Uzdensky, D. A. & Kulsrud, R. M. 2000 Two-dimensional numerical simulation of the resistive reconnection layer. *Physics of Plasmas* **7**, 4018–4030.

Uzdensky, D. A. & Loureiro, N. F. 2016 Magnetic Reconnection Onset via Disruption of a Forming Current Sheet by the Tearing Instability. *Phys. Rev. Lett.* **116** (10), 105003.

Waelbroeck, F. L. 1993 Onset of the sawtooth crash. *Phys. Rev. Lett.* **70**, 3259–3262.

Wicks, R. T., Horbury, T. S., Chen, C. H. K. & Schekochihin, A. A. 2010 Power and spectral index anisotropy of the entire inertial range of turbulence in the fast solar wind. *Mon. Not. R. Astron. Soc.* **407**, L31–L35.

Wicks, R. T., Roberts, D. A., Mallet, A., Schekochihin, A. A., Horbury, T. S. & Chen, C. H. K. 2013 Correlations at large scales and the onset of turbulence in the fast solar wind. *Astrophys. J.* **778**, 177 [erratum: *Astrophys. J.* **782**, 118 (2014)].

Winarto, H. W. & Kunz, M. W. 2022 Triggering tearing in a forming current sheet with the mirror instability. *J. Plasma Phys.* **88** (2), 905880210.

Yamada, M., Kulsrud, R. & Ji, H. 2010 Magnetic reconnection. *Rev. Mod. Phys.* **82**, 603–664.

Zank, G. P. & Matthaeus, W. H. 1992*a* The equations of reduced magnetohydrodynamics. *J. Plasma Phys.* **48**, 85.

Zank, G. P. & Matthaeus, W. H. 1992*b* Waves and turbulence in the solar wind. *J. Geophys. Res.* **97**, 17189.

Zel'dovich, Ya. B. 1957 The Magnetic Field in the Two-Dimensional Motion of a Conducting Turbulent Liquid. *Soviet Journal of Experimental and Theoretical Physics* **4**, 460.

Zel'dovich, Y. B., Ruzmaikin, A. A., Molchanov, S. A. & Sokolov, D. D. 1984 Kinematic dynamo problem in a linear velocity field. *Journal of Fluid Mechanics* **144**, 1–11.

Zweibel, E. G. & Yamada, M. 2009 Magnetic Reconnection in Astrophysical and Laboratory Plasmas. *Ann. Rev. Astron. Astrophys.* **47**, 291–332.